



HAL
open science

**Molecular dynamic of the methionyl-tRNA synthetase
and its novel non-canonical functions in the yeast *S.
cerevisiae***

Sylvain Debard

► **To cite this version:**

Sylvain Debard. Molecular dynamic of the methionyl-tRNA synthetase and its novel non-canonical functions in the yeast *S. cerevisiae*. Genomics [q-bio.GN]. Université de Strasbourg, 2019. English. NNT : 2019STRAJ057 . tel-03270763

HAL Id: tel-03270763

<https://theses.hal.science/tel-03270763>

Submitted on 25 Jun 2021

HAL is a multi-disciplinary open access archive for the deposit and dissemination of scientific research documents, whether they are published or not. The documents may come from teaching and research institutions in France or abroad, or from public or private research centers.

L'archive ouverte pluridisciplinaire **HAL**, est destinée au dépôt et à la diffusion de documents scientifiques de niveau recherche, publiés ou non, émanant des établissements d'enseignement et de recherche français ou étrangers, des laboratoires publics ou privés.

ÉCOLE DOCTORALE DES SCIENCES DE LA VIE ED414



| **UMR7156 Dynamiques & Plasticité des Synthétases** |

THÈSE

présentée par :

Sylvain DEBARD

soutenue le **27 septembre 2019**

pour obtenir le grade de

DOCTEUR DE L'UNIVERSITÉ DE STRASBOURG

Discipline : **Sciences du Vivant**

Spécialité : **Aspects Moléculaires et Cellulaires de la Biologie**

Dynamique moléculaire de la méthionyl-ARNt synthetase et ses nouvelles fonctions non-canoniques chez la levure *S. cerevisiae*.

THÈSE dirigée par :

Pr. BECKER Hubert

Professeur des Universités, Université de Strasbourg, France

RAPPORTEURS :

Pr. IBBA Michael

Professeur, Ohio State University, USA

Pr. STATHOPOULOS Constantinos

Professeur, University of Patras, Grèce

EXAMINATEUR :

Pr. DUCHENE Anne-Marie

Professeur des Universités, Université de Strasbourg

DOCTORAL SCHOOL OF LIFE AND HEALTH SCIENCES ED414



| UMR7156 Dynamic & Plasticity of Synthetases |

THESIS

presented by :

Sylvain DEBARD

defended on **september 27th, 2019**

for the degree of

DOCTOR OF STRASBOURG UNIVERSITY

Discipline : **Life Sciences**

Option : **Molecular and Cellular Biology**

Molecular dynamic of the methionyl-tRNA synthetase and its novel non-canonical functions in the yeast *S. cerevisiae*

THESIS supervisor :

Pr. BECKER Hubert

Professor, Strasbourg University, France

REFEREES :

Pr. IBBA Michael

Professor, Ohio State University, USA

Pr. STATHOPOULOS Constantinos

Professor, University of Patras, Greece

EXAMINER :

Pr. DUCHENE Anne-Marie

Professor, Strasbourg University

Table of contents

Table of contents	iii
List of Figures	x
List of Tables	xiv
List of abbreviations	xvi
Amino acids and aaRS nomenclature	xviii
About this manuscript	xix



01 General introduction 21

I. Eukaryotic cytosolic translation	23
I.1. Genetic code	23
I.2. The major actors of protein synthesis	25
I.2.1. The eukaryotic ribosomal particle	25
I.2.2. The messenger RNA	27
I.2.3. Protein translation factors	29
I.2.4. Amino acids	29
I.2.5. tRNAs : the “adaptor” molecules	33
I.2.5.1. tRNAs structure	33
I.2.5.2. Maturation of pre-tRNAs	35
I.3. The three (or four) steps translation process	39
I.3.1. The initiation: search for the AUG start codon	41
I.3.2. Elongation: synthesis of the peptide chain	43
I.3.3. Termination and recycling	43
II. The aminoacyl-tRNA synthetases (aaRSs) family	47
II.1. The canonical function of aaRSs	47
II.2. aaRSs are divided into two classes	47
II.2.1. Class I aaRSs	49
II.2.2. Class II aaRSs	49
II.3. Translational fidelity and quality control	51
II.3.1. tRNA identity	53
II.3.2. aaRS proofreading of misacylated tRNAs	53
II.3.3. Beneficial misacylation	55
II.4. Incorporation of non-standard aa and indirect pathways	57
II.4.1. The two non-standard aa incorporation	57

II.4.2. Indirect pathways of aa-tRNA biosynthesis	59
II.5. Acquisition of new appended domains and formation of multi-synthetase complexes	61
II.5.1. Acquisition of new aaRSs domains throughout evolution	61
II.5.2. Multi-aminoacyl-tRNA synthetase complexes (MSCs) formation and evolution	67
II.6. aaRSs relocation and associated nontranslational functions	71
II.7. The yeast AME complex	71
II.7.1. Structure and organization of the AME complex	71
II.7.2. Arc1 protein: more than a binding partner	73
II.7.2.1. An aaRS cofactor enhancing aminoacylation efficiency	73
II.7.2.2. An anchoring platform for the cytosolic aaRSs	75
III. The methionine system and complexity	79
III.1. Methionine metabolism and redox functions	79
III.1.1. Biosynthesis of methionine and methionine derivatives in yeast	79
III.1.2. Redox system and methionine as antioxidant	81
III.1.2.1. Definition of oxidative stress	81
III.1.2.2. Mitochondria as major source of ROS	83
III.1.2.3. Oxidative stress response and the methionine system	85
III.2. The tRNA substrates for MetRS	87
III.2.1. The tRNA ^{Met} identity determinants for the yeast MetRS	87
III.2.2. One enzyme but two tRNA substrates	89
III.3. Modular organization of the yeast MetRS	93
III.3.1. Conservation and evolution of MetRS sequences	93
III.3.2. Sequence and structure of the yeast MetRS	93
III.4. Features of MetRSs across the tree of life	97
III.4.1. Methionine mischarging and adaptative translation	97
III.4.1.1. Methods used for detection of Met mistranslation	97
III.4.1.2. Misacylation properties of MetRS and consequences of mismethionylation	99
III.4.2. Nuclear relocation and additional function	101
III.4.3. Cleavage of bacterial and human MetRS orthologs	103
IV. Purpose of my thesis work	105
Appendices	106



02 Results & Discussion

113

I. Development of a fluorescent reporter to monitor Met misincorporation in <i>S. cerevisiae</i>	115
I.1. Context of the study	115
I.2. Use of fluorescence to assess Met misincorporation	115
I.3. Design of the bifluorescent protein reporter	117
I.4. Procedure of cell selection for suitable FBP expression	121
I.5. Proof of concept for BFP reporter	121
I.6. Quantification of Met misincorporation in basal condition	123
I.6.1. Design and optimization of the quantification protocol	123
I.6.2. Met misincorporation without stress	125
I.7. Deletion of Arc1 enhances global Met misincorporation	125
I.8. Development of the BFP system for use in oxidative conditions	129
I.8.1. Setting oxidative stress conditions	129
I.8.2. Adapting the BFP system to oxidative stress	133
I.8.3. First results show oxidant-mediated mismethionylation	135
I.9. Discussion	135
I.9.1. Confirmation of mismethionylation by mass spectrometry	135
I.9.2. Met misincorporation at Leu position	137
I.9.3. Multiple use for the BFP system	139
I.9.4. Met misincorporation and surface exposed defence	141
I.9.5. Concluding remarks	143
II. Study of a newly characterized truncated form of yeast MetRS	145
II.1. Context of the study	145
II.2. General characterization of the proteolytic cleavage	147
II.2.1. Design of <i>ex vivo</i> cleavage protocol and role of Rim13 protease	147
II.2.2. Chemical and physical properties of the MetRS processing protease	149
II.3. The Arc1 protein acts as MetRS protector from proteolytic cleavage	151
II.4. Searching for the MetRS specific protease	153
II.5. Identification of the proteolytic cleavage site	159
II.6. Finding a non-cleavable mutant of MetRS	161
II.6.1. Analysis of MetRS substitution mutants around the cleavage site	161
II.6.2. The proteolytic cleavage is not sequence dependent	163
II.7. Determining the role of MetRS(Δ 132)	165
II.7.1. Production of the truncated MetRS(Δ 132) is enhanced in thermal or nutritional stresses	165

II.7.2. The cleaved isoform constitutes the nuclear pool of MetRS	167
II.7.3. Pep4 relocalizes in the vicinity of nucleus under heat stress	169
II.7.4. Cleavage of MetRS prevents its precipitation at high temperature	169
II.8. Discussion and preliminary results	171
II.8.1. MetRS cleavage and cellular compartmentalization	171
II.8.2. Cleavage complexity and other proteases	175
II.8.3. Cleavage of MetRS is fluctuant depending on yeast clones	175
II.8.4. Clarifying the role of the truncated MetRS	177
II.8.5. Truncated MetRS and mismethionylation	179
II.8.6. Concluding remarks	180

III. Study of the mitochondrial role of Arc1 protein **183**

III.1. Context of the study	183
III.2. Arc1 is dual-localized in the cytosol and mitochondria	183
III.3. Respiratory deficiency can be suppressed spontaneously	185
III.4. Identification of the suppressive mutation in <i>arc1Δ</i> SUP genome	189
III.5. Discussion: Arc1 as a co-folding partner for mitochondrial relocalization?	189

IV. General conclusion **193**

Supplemental figures and tables **196**



03 Material & Methods **219**

I. Molecular biology for gene amplification and cloning **221**

I.1. Bacterial strains	221
I.2. Bacterial growth media	221
I.3. Calcium chloride competent cell protocol	221
I.4. Bacterial cell transformation	221
I.5. Plasmid extraction from bacterial cell	223
I.6. PCR amplification of DNA fragments	223
I.7. DNA visualisation under UV light	223
I.8. PCR DNA clean up and gel extraction	223
I.9. Enzymatic restriction of plasmids	225
I.10. Cloning strategies	225
I.10.1. Traditional cloning	225
I.10.2. Gateway™ cloning	225
I.10.3. Gibson assembly	227
I.11. Plasmid sequence verification	227

II. Procedures used for <i>S. cerevisiae</i> cells	229
II.1. Yeast growth media	229
II.2. Yeast growth phases and OD monitoring	229
II.3. Yeast transformation	231
II.4. Serial dilution spotting assay	231
II.5. Yeast mating procedure	231
II.5.1. Mating on agar plate	231
II.5.2. Mating in liquid medium	233
II.5.3. Selection of diploids and/or mating type selection	233
II.6. Diploid sporulation and tetrad dissection	235
II.7. Fluorescence microscopic observations	235
II.8. Yeast protein extract preparation	237
II.8.1. Total protein extract	237
II.8.2. Soluble protein extract	237
II.8.3. Subcellular fractionation	237
III. Biochemistry and biophysical techniques	239
III.1. Protein electrophoresis and immunoblotting	239
III.2. tRNA synthesis by <i>in vitro</i> transcription	241
III.2.1. Purification of recombinant T7 RNA polymerase	241
III.2.2. Design of the DNA template used for transcription	241
III.2.3. <i>In vitro</i> transcription of tRNAs	243
III.2.4. Purification of <i>in vitro</i> transcripts by gel electrophoresis	243
III.3. Purification of MBP-MetRS enzymes	245
III.3.1. Overexpression and enrichment of MBP-MetRS with amylose beads	245
III.3.2. Cleavage of MBP with factor Xa	247
III.3.3. FPLC purification of MetRS for enzymatic characterisation	247
III.3.3.1. Heparin chromatography	247
III.3.3.2. Gel filtration protocol	249
III.3.4. Sample dialysis and determination of protein concentration	249
III.4. Aminoacylation assay	251
III.5. MetRS immunoprecipitation	251
III.6. Mass spectrometry analyses	251
III.6.1. Procedure for co-immunoprecipitated MetRS interactants	251
III.6.2. TMPP protocol for N-terminus characterization and MetRS cleavage site identification	253
III.6.2.1. TMPP protein labelling	253
III.6.2.2. LC-MS/MS and data analysis	254

Lists of primers, plasmids and yeast strains	257
I.1. Tables of primers	257
I.2. Tables of plasmids	259
I.3. Tables of yeast strains	267



04 Publications & Posters **275**

Publication 1: Debard *et al*, 2017, *Methods* **276**

Publication 2: Yakobov *et al*, 2018, *BBA* **292**

Poster 1: 26th tRNA conference, September 4-8 2016, Jeju, South Korea **308**

Poster 2: 11th aaRS meeting, Oct. 29th-Nov. 2nd 2017, Clearwater beach, Florida **310**

Poster 3: 27th tRNA conference, September 23-27 2018, Strasbourg, France **312**



05 Bibliography **315**

I. Text references **316**

II. Figures and tables references **340**

List of Figures

General introduction

Figure I-1: Standard genetic code table and deviation to the standard code	22
Figure I-2: Major actors of protein synthesis and importance of RNA molecules	24
Figure I-3: Biosynthesis of amino acids from glucose and ammonia in <i>S. cerevisiae</i>	30
Figure I-4: tRNA structures	34
Figure I-5: tRNA maturation steps in <i>S. cerevisiae</i>	36
Figure I-6: Yeast tRNA nucleotide modifications pattern	38
Figure I-7: Modifications of the wobble position in yeast tRNAs	38
Figure I-8: The initiation steps of yeast translation and recycling of initiation factors	40
Figure I-9: Elongation steps of translation	42
Figure I-10: Termination and recycling steps	44
Figure I-11: The aminoacylation reaction proceeds through two steps	46
Figure I-12: Crystal structure and organization of aaRSs and their interaction with tRNA and ATP	48
Figure I-13: General modular organization of the aaRSs from the two classes and subclasses	50
Figure I-14: aaRS editing process	54
Figure I-15: The 21 st and 22 nd genetically encoded amino acids	58
Figure I-16: Indirect pathways of aa-tRNA biosynthesis	58
Figure I-17: Modular composition of the <i>E. coli</i> , <i>S. cerevisiae</i> and human 20 aaRSs and of the yeast and metazoan aaRS-associated protein	62
Figure I-18: Known structures of additional aaRS domains	64
Figure I-19: Composition and architecture of characterized MSCs	68
Figure I-20: The yeast AME complex: composition and structure	72
Figure I-21: Secondary structure organization of the N-termini of the three AME proteins	72
Figure I-22: Arc1 protein as an aaRS cofactor	74
Figure I-23: Subcellular relocation of AME components	76
Figure I-24: General sulfur metabolism in yeast and generation of the two sulfur-containing aa Met and Cys	78
Figure I-25: Redox reactions and ROS generation	80
Figure I-26: Mitochondria and formation of superoxide in yeast	82
Figure I-27: Cellular defences against ROS	84
Figure I-28: Methionine oxidation by ROS and recycling by Msr enzymes	84

Figure I-29: tRNA _i ^{Met} transcript mutants and determination of identity elements	88
Figure I-30: Secondary structures of yeast initiator and elongator tRNA ^{Met}	90
Figure I-31: Structures of MetRS enzymes in the tree of life	92
Figure I-32: Structural features of yeast MetRS and localization of essential residues	94
Figure I-33: Met misincorporation during protein synthesis and oxidative stress response	96
Figure I-34: Mismethionylated tRNAs identified by tRNA microarrays	98
Figure I-35: Growth conditions and MetRS features that enhance tRNA mismethionylation in <i>E. coli</i> , <i>S. cerevisiae</i> and in human cells	100
Figure I-36: Nuclear relocation mechanisms of human and yeast MetRS	102
Figure I-37: Localisation of protease cleavage sites identified on human and bacterial MetRS	102
Appendix 1: Relative growth of <i>S. cerevisiae</i> on various sole nitrogen sources	106
Appendix 2: Chromosomal organization of the <i>S. cerevisiae</i> genome	107
Appendix 3: Nucleotide modifications of yeast tRNAs with the associated modifying enzymes and their role in tRNA metabolism and regulation	108
Appendix 4: Chemical structures of yeast nucleotide modifications found in tRNAs	109
Appendix 5: Superimposition of the two eukaryotic MetRS structures	110
 Results and discussion	
Figure R-1: Method used to identify misacylated tRNAs with Met	114
Figure R-2: Structures of the mRuby and EGFP fluorescent proteins	114
Figure R-3: Design of the dual fluorescent reporter used in this study	116
Figure R-4: Choice of yeast vectors for bifluorescent reporter expression	118
Figure R-5: Number of cycles during PCR is crucial for accurate mutagenesis	118
Figure R-6: Heterogeneity in BFP expression for clones derived from same transformation experiment	120
Figure R-7: Several steps are needed to select clones suitable for fluorescence quantification	120
Figure R-8: Loss of red fluorescence for all BFP mutants but BFP(Gln)	122
Figure R-9: Correlation between expression and green fluorescence emission of the BFP reporters	124
Figure R-10: Quantification of Met misincorporation through Correlated Total Cell Fluorescence	124
Figure R-11: Met misincorporation for all 61 BFP variants expressed in WT strain grown in rich medium	126
Figure R-12: Met misincorporation increases in <i>arc1Δ</i> background	127
Figure R-13: Validation of the implication of Arc1 in Met misincorporation	128

Figure R-14: Effects of oxidants on yeast cell growth and protein synthesis	130
Figure R-15: Engineering of BFP constructs under the control of promoters of genes whose expressions are induced by oxidative stress	132
Figure R-16: Oxidative stress increases Met misincorporation	134
Figure R-17: Design of the BFP reporter suitable for mass spectrometry analyses	136
Figure R-18: Sequence comparison of tRNA ^{Met} with tRNA ^{Leu} (CUU,CUC) and tRNA ^{Leu} (UUA)	138
Figure R-19: Yeast strain expressing human MetRS presents a different Met misincorporation profile	140
Figure R-20: Summary of results found on cleavage of yeast MetRS	144
Figure R-21: <i>Ex vivo</i> cleavage of recombinant purified yeast MetRS	146
Figure R-22: Characterisation of the MetRS protease using <i>ex vivo</i> assay	148
Figure R-23: Arc1 protein inhibits MetRS cleavage both <i>ex vivo</i> and <i>in vivo</i>	150
Figure R-24: Purification of the yeast MetRS protease by sequential chromatographies	152
Figure R-25: Proteins found in the active Superdex 200 fractions analysed by 14 % SDS-PAGE and silver staining	154
Figure R-26: The vacuolar Pep4 protease is involved in MetRS cleavage	156
Figure R-27: Identification of MetRS cleavage site between Y132 and A133 residues	158
Figure R-28: Inhibiting proteolytic cleavage by mutating the MetRS	160
Figure R-29: Chimeric mutant of MetRS fused to N-ter of GluRS are still cleaved	162
Figure R-30: The cleavage of MetRS is enhanced in thermal and nutritional stresses	164
Figure R-31: The cleaved MetRS(Δ 132) is dual-localized in nucleus and cytosol	166
Figure R-32: Pep4 relocates into cytoplasm during oxidative and thermal stress	168
Figure R-33: MetRS(Δ 132) is more stable at higher temperature than the MetRS(WT)	170
Figure R-34: Complexity of the MetRS cleavage	172
Figure R-35: Isolation of a genetic mutant exhibiting low level of MetRS(Δ 132)	174
Figure R-36: Clones expressing MetRS(Δ 132)-V5 as the sole MetRS isoform displayed slow growth phenotype	176
Figure R-37: Strains expressing MetRS(Δ 132) presents higher Met misincorporation levels than the WT strains	178
Figure R-38: The <i>arc1</i> Δ strain displays a growth phenotype	182
Figure R-39: Dual-localization of Arc1 both in cytosol and mitochondria	184
Figure R-40: Spontaneous growth of <i>arc1</i> Δ strains on respiratory medium	186
Figure R-41: The <i>arc1</i> SUP strain contains a single substitution in <i>HAS1</i> gene	188
Figure R-42: Loss of interaction with GluRS and MetRS induces deficient respiratory growth	190

Figure R-43: Summary of results found in my thesis projects	192
Figure R-44: Vacuolar MetRS(WT) and yeast growth deficiency	194
Supplemental S1: Selection of BFP clones to create the BFP strain library	197
Supplemental S2: Effect of oxidants on yeast growth on solid medium	198
Supplemental S3: Using flow cytometry to monitor Met misincorporation with the BFP system	199
Supplemental S4: Absence of Arc1 does not prevent MetRS aggregation	201
Supplemental S5: Sequence comparison of N-terminal domains of the yeast MetRS and GluRS	201
Supplemental S6: MetRS(Δ 132) does not interact with Arc1	202
Supplemental S7: Growth and survival phenotype of strains in different stress conditions	203
Supplemental S8: Time course of aminoacylation of yeast tRNA by the recombinant yeast MetRS(WT) and MetRS(Δ 132)	204
Supplemental S9: Confirmation of the deletion of <i>ARC1</i> gene in the <i>arc1</i> SUP strains	205
Supplemental S10: Growth of several <i>arc1</i> Δ strains (SUP strains) on various respiratory media	205
Supplemental S11: Overexpression of MetRS in <i>arc1</i> Δ strain restores growth in respiratory medium	206
Supplemental S12: Chromosomes segregation during sporulation and spores viability	207
 Material & Methods	
Figure MM-1: Schematic representation of the different cloning strategies used	224
Figure MM-2: Yeast growth curve and the different growth phases	230
Figure MM-3: Protocol for yeast spotting assay	230
Figure MM-4: Yeast mating in liquid medium	232
Figure MM-5: Diploid sporulation and tetrad dissection	234
Figure MM-6: Preparation of yeast protein extracts	236
Figure MM-7: Engineering of tRNA expression plasmid for T7 in vitro transcription	242
Figure MM-8: Purification of in vitro transcripts	244
Figure MM-9: Purification of recombinant MetRS	246
Figure MM-10: FPLC purification of recombinant MetRS	248
Figure MM-11: Preparation of the aminoacylation reaction mixture with [³⁵ S]Met	276
Figure MM-12: TMPP reaction performed at pH 8.2 to specifically target the N-termini amines of proteins	252

List of Tables

General introduction

Table I-1: Yeast translation factors and their role in protein synthesis	28
Table I-2: tRNA sequences alignment from <i>S. cerevisiae</i> and features of tRNA genes	32
Table I-3: Standard classification and features of aaRSs based on structural and chemical properties	48
Table I-4: Yeast tRNA identity elements and anti-determinants	52
Table I-5: Errors made by the translation machinery and description of techniques used to study mistranslation	56
Table I-6: Description of the two-step pathway of aa-tRNA synthesis	60
Table I-7: Association of aaRS with one accessory protein and subsequent location and role	70
Table I-8: Yeast MetRS catalytic constants for tRNA _f ^{Met} with or without Arc1	74
Table I-9: Studies of Msr mutants and their phenotype related to oxidative stress	86
Table I-10: Techniques used to monitor mismethionylation and identify mismethionylated tRNA species	96

Results and discussion

Table R-1: List of yeast proteins found in all active Superdex 200 fractions	154
Table R-2: Sequence alignment of MetRS residues around the cleavage site present in MetRSs from various phylogenetic origins	158
Table R-3: Kinetic parameter (K_m) of tRNA ^{Met} transcripts for aminoacylation by MetRS isoforms	178
Table S1: Description and photophysical properties of some fluorescent proteins (FPs)	196
Table S2: Protein interactants found only in the MetRS(WT)-V5 (upper table) and only in the MetRS(Δ 132)-V5 (lower table) co-IP experiments	198
Table S3: List of genes found as copy number variants (CNVs) in strains MetRS(Δ 132) and MetRS(Δ 132) SUP	202
Dissection tables	208-216

Material & Methods

Table MM-1: <i>E. coli</i> competent strains used for cloning strategies	220
Table MM-2: Media for bacterial culture and antibiotic concentration used for selection	220
Table MM-3: PCR protocol details according to the kit used	222
Table MM-4: Composition of the 1 × Gibson assembly buffer	226

Table MM-5: Composition of yeast rich media	228
Table MM-6: Composition of yeast synthetic media	228
Table MM-7: Composition of yeast specific media	228
Table MM-8: List of antibodies used for immunoblotting	238
Table MM-9: <i>E. coli</i> strain used for recombinant protein overexpression	246
Table MM-10: Primers used for gene amplification on DNA genome	257
Table MM-11: Primers used for plasmid sequencing	258
Table MM-12: BFP plasmids library	259
Table MM-13: Mutated or modified BFP plasmids	261
Table MM-14: Plasmids for <i>E. coli</i> overexpression	261
Table MM-15: Plasmid vectors for Gateway cloning	262
Table MM-16: Plasmids with fluorescent tag	263
Table MM-17: Plasmids with cMyc tag	263
Table MM-18: Plasmids with HA tag	264
Table MM-19: Plasmids with V5 tag	265
Table MM-20: WT haploid yeast strains and genetic background	267
Table MM-21: Haploid yeast strains	268
Table MM-22: Diploid yeast strains	271

List of abbreviations

aa-AMP: aminoacyl-adenylate	EMAPII: Endothelial Monocyte-Activating Polypeptide
aa-tRNA^{Aaa}: aminoacyl-tRNA ^{Aaa}	eRF: eukaryotic release factor
aa: amino acid	FA: Formic Acid
aaRS: aminoacyl-tRNA synthetase	g, L, h, min, s: gram, liter, hour, minute, second
ABD: Anticodon Binding Domain	g: gravitational force
AC: anticodon	GDP: guanosine diphosphate
ADP: adenosine diphosphate	GFP: Green Fluorescent Protein
AdT: amidotransferase	GST: Glutathion S-transferase
AIMP: aaRS complex Interacting Multifunctional Protein	GTP: guanosine triphosphate
AME: Arc1•MRS•ERS	H₂O₂: hydrogen peroxyde
AMP: adenosine monophosphate	Hs: <i>Homo sapiens</i>
Amp: Ampicilline	IB: Immuno Blot
ATP: adenosine triphosphate	kb: kilo base pairs
BFP: Bi-Fluorescent Protein	K_d: dissociation constant
bp: base pair	kDa: kilodalton
C-ter/Cter: C-terminal	K_m: Michaelis constant
Co-IP: co-immunoprecipitation	LB: Lysogeny Broth
CP1: Connective Peptide 1	LZ: leucine zipper
cpm: count per minute	M: molar
DIC: Differential interference Contrast	MARS: multi-aminoacyl-tRNA synthetase complex
DNA: desoxyribonucleic acid	Met: methionine
E. coli/Ec: <i>Escherichia coli</i>	MetO: Methionine Sulfoxide
eEF: eukaryotic elongation factor	mRNA: messenger RNA
(E)GFP: (Enhanced) Green Fluorescent Protein	MS: Mass Spectrometry
eIF: eukaryotic initiation factor	

MSC: MultiSynthetase Complex	ROS: Reactive Oxygen Species
Msr: Methionine Sulfoxide Reductase	rRNA: ribosomal RNA
MTS: Mitochondrial Targetting Signal	S: Svedberg
N-ter/Nter: N-terminal	<i>S. cerevisiae/Sce:</i> <i>Saccharomyces cerevisiae</i>
ncRNA: non-coding RNA	SDS: Sodium DodecylSulfate
ND: Non-Discriminant	Sec: Selenocysteine
NES: Nuclear Export Signal	SOD: Superoxide Dismutase
NLS: Nuclear Localization Signal	TCA: trichloroacetic acid
O/N: Overnight	TMPP: TriMethoxyPhenyl Phosphonium
OB: oligonucleotide/oligosaccharide-binding	TRBD: tRNA-binding domain
OD: Optical Density	tRNA: transfert RNA
PAGE: PolyAcrylamide Gel Electrophoresis	UNE: Unique Element
PCR: Polymerase Chain Reaction	v/v: volume/volume
pdb: Protein DataBase	W/V: weight/volume
PI3P: Phosphatidyl Inositol 3 Phosphate	WB: Western Blot
PIC: Pre-initiation Complex	WT: Wild Type
PP_i: pyrophosphate	YPD: Yeast extract Peptone Dextrose
Pyl: Pyrrolysine	μ-, n-, m-: micro-, nano-, milli-
RNA: ribonucleic acid	° C: degree Celsius

Amino acids and aaRS nomenclature

Amino acids			aminoacyl-tRNA synthetases		
Name	Three letters	One letter	Standard name	Short names	
Alanine	Ala	A	Alanyl-tRNA-synthetase	AlaRS	ARS
Cysteine	Cys	C	Cysteinyl-tRNA-synthetase	CysRS	CRS
Aspartate	Asp	D	Aspartyl-tRNA-synthetase	AspRS	DRS
Glutamate	Glu	E	Glutamyl-tRNA-synthetase	GluRS	ERS
Phenylalanine	Phe	F	Phenylalanyl-tRNA-synthetase	PheRS	FRS
Glycine	Gly	G	Glycyl-tRNA-synthetase	GlyRS	GRS
Histidine	His	H	Histidyl-tRNA-synthetase	HisRS	HRS
Isoleucine	Ile	I	Isoleucyl-tRNA-synthetase	IleRS	IRS
Lysine	Lys	K	Lysyl-tRNA-synthetase	LysRS	KRS
Leucine	Leu	L	Leucyl-tRNA-synthetase	LeuRS	LRS
Methionine	Met	M	Methionyl-tRNA-synthetase	MetRS	MRS
Asparagine	Asn	N	Asparaginyl-tRNA-synthetase	AsnRS	NRS
Proline	Pro	P	Prolyl-tRNA-synthetase	ProRS	PRS
Glutamine	Gln	Q	Glutaminyl-tRNA-synthetase	GluRS	QRS
Arginine	Arg	R	Arginyl-tRNA-synthetase	ArgRS	RRS
Serine	Ser	S	Seryl-tRNA-synthetase	SerRS	SRS
Threonine	Thr	T	Threonyl-tRNA-synthetase	ThrRS	TRS
Valine	Val	V	Valyl-tRNA-synthetase	ValRS	VRS
Tryptophane	Trp	W	Tryptophanyl-tRNA-synthetase	TrpRS	WRS
Tyrosine	Tyr	Y	Tyrosyl-tRNA-synthetase	TyrRS	YRS

About this manuscript

I have been working in the lab "Dynamic and Plasticity of Synthetases" for four years, studying the dynamic of the methionyl-ARNt synthetase (MetRS) in the yeast *S. cerevisiae*. The MetRS belongs to the aminoacyl-tRNA synthetases (aaRS) family, ubiquitous enzymes essential for cell life and catalyzing the aminoacylation of tRNAs. Despite its well known function in protein synthesis, I have studied the potential non-canonical features and functions of the yeast MetRS. To present my work during the last four years, this manuscript contains:

- a general introduction, starting with a description of the eukaryotic translation to introduce all molecular actors, and essentially the tRNA molecules. Then the aaRSs family will be described in more details, before focusing on the methionine system and its complexity in the third part. For this introduction, all figures and tables have been created during my PhD to illustrate and supplement the text blocks.
- The results of my research, subdivided in three parts. Each part contains a detailed presentation of the results and a discussion about the results and the perspectives.
- The material and the methods used in the laboratory. The primers used and all the plasmids and yeast strains engineered are listed in this section.
- The scientific productions made in the laboratory, including scientific reviews and posters.
- The bibliography subdivided in two categories: the references found in the text blocks (sorted by alphabetical order) and the references found in the figures and/or tables (sorted by numbers).



GENERAL

INTRODUCTION

- I** EUKARYOTIC CYTOSOLIC TRANSLATION **23**
- II** THE AMINOACYL-tRNA SYNTHETASES FAMILY **47**
- III** THE METHIONINE SYSTEM AND COMPLEXITY **79**
- IV** PURPOSE OF MY THESIS WORK **105**

- APPENDICES** **106**



UUU	Phe	UCU		UAU	Tyr	UGU	Cys
UUC		UCC	Ser	UAC		UGC	
UUA	Leu	UCA		UAA	<i>Gln Tyr</i> <i>Tyr Glu</i> <i>Glu</i>	UGA	<i>Trp Sec Trp</i> <i>Cys Gly</i> STOP
UUG		UCG		UAG	<i>Leu Glu Ala</i> <i>Gln Pyl Leu</i> <i>Tyr Tyr</i>	UGG	Trp
CUU	<i>Thr</i> <i>Ala</i>	CCU		CAU	His	CGU	<i>gly</i>
CUC	<i>Thr</i>	CCC	Pro	CAC		CGC	<i>gly</i>
CUA	<i>Thr</i> <i>Ala</i>	CCA		CAA	Gln	CGA	<i>gly</i>
CUG	<i>Ser Thr</i> <i>Ala</i>	CCG		CAG		CGG	<i>gly</i>
AUU		ACU		AAU	Asn	AGU	Ser
AUC	Ile	ACC	Thr	AAC		AGC	
AUA	<i>Met</i>	ACA		AAA	<i>Asn</i>	AGA	<i>Ser Gly</i> Arg
AUG	Met	ACG		AAG	Lys	AGG	<i>Ser Gly</i> <i>Lys</i>
GUU		GCU		GAU	Asp	GGU	
GUC		GCC	Ala	GAC		GGC	Gly
GUA	Val	GCA		GAA		GGA	
GUG		GCG		GAG	Glu	GGG	

Caption

R = NC(=O)C(R)O

● Codon reassigned as stop codon in organelles

Figure I-1: Standard genetic code table and deviation to the standard code. Representation of the standard codon table. Three code letters is used for aa, and the chemical structure of each of the 20 standard aa is shown. Codons with known reassignment are in pink boxes. Names of new aa assigned to these codons are written in italic, in black for bacterial or eukaryotic nuclear genomes, and in red for organellar genomes (mitochondria or plastids). Data compiled come from [Ambrogelly et al, 2007](#); [Sengupta and Higgs, 2015](#); [Mukai et al, 2017](#).

I. Eukaryotic cytosolic translation

Translation, such as replication and transcription, is an essential process and represents the final step of protein synthesis. Several steps are required to decode mRNA codons (triplets of nucleotides) into their corresponding amino acids (aa), leading to the synthesis of a protein chain composed of a mixture of the 20 classical aa residues, if the organism uses the standard genetic code. However, in addition to these 20 classical aa, two additional aa can be incorporated during protein synthesis: selenocysteine (Sec) and pyrrolysine (Pyl) known as the 21st and 22nd genetically-encoded aa, respectively (Böck *et al.*, 1991; Hao *et al.*, 2002). Since Sec is only incorporated in a specific subset of proteins (25 selenoproteins in human proteome, but no selenoprotein in Fungi) and Pyl is used in only methanogenic archaea and few bacteria (Zhang and Gladyshev, 2007; Prat *et al.*, 2012), I will mainly focus on the 20 classical ones in this chapter, but Sec and Pyl incorporation will be discussed later (§ II.4.1, page 57). Since translation is evolutionary well conserved and has extensively been studied in yeast, the next sections will essentially focus on translation-related mechanisms in the yeast model *S. cerevisiae*.

I.1. Genetic code

For each organism, the genetic code describes the connection between the information contained into the mRNA molecule (encoded in nucleotide triplets called codons) and the composition of proteins (build from amino acid residues during protein synthesis). This genetic code is roughly universal among living species, so that the vast majority of organisms associates the same aa to the same corresponding codon or set of codons. This genetic code is represented in its classical codon table view in **Figure I-1**. With the 4 bases present in the mRNA molecule (A, U, G and C), there are 64 (= 4³) codons for only 20 common proteogenic aa, meaning that some aa are encoded by several synonymous codons, a feature of the genetic code also known as the genetic code degeneracy. Among the 64 codons, 61 are encoding aa (called sense codons) and 3 direct termination of translation (nonsense or stop codons). Two aa are encoded by a single codon (Met and Trp) whereas 3 others are specified by 6 synonymous codons (Leu, Arg and Ser); and the rest of aa are encoded by 4 codons (4-codon boxes). Most of the time, a change in the third base of the codon does not change the aa identity: thus it is likely that the genetic code evolved to minimize deleterious effects of mutations. In agreement with this observation, a change of U to C in third position always specifies the same aa, and same for A to G except for Trp(UGG) and Met(AUG), the two one-box codons. This codon

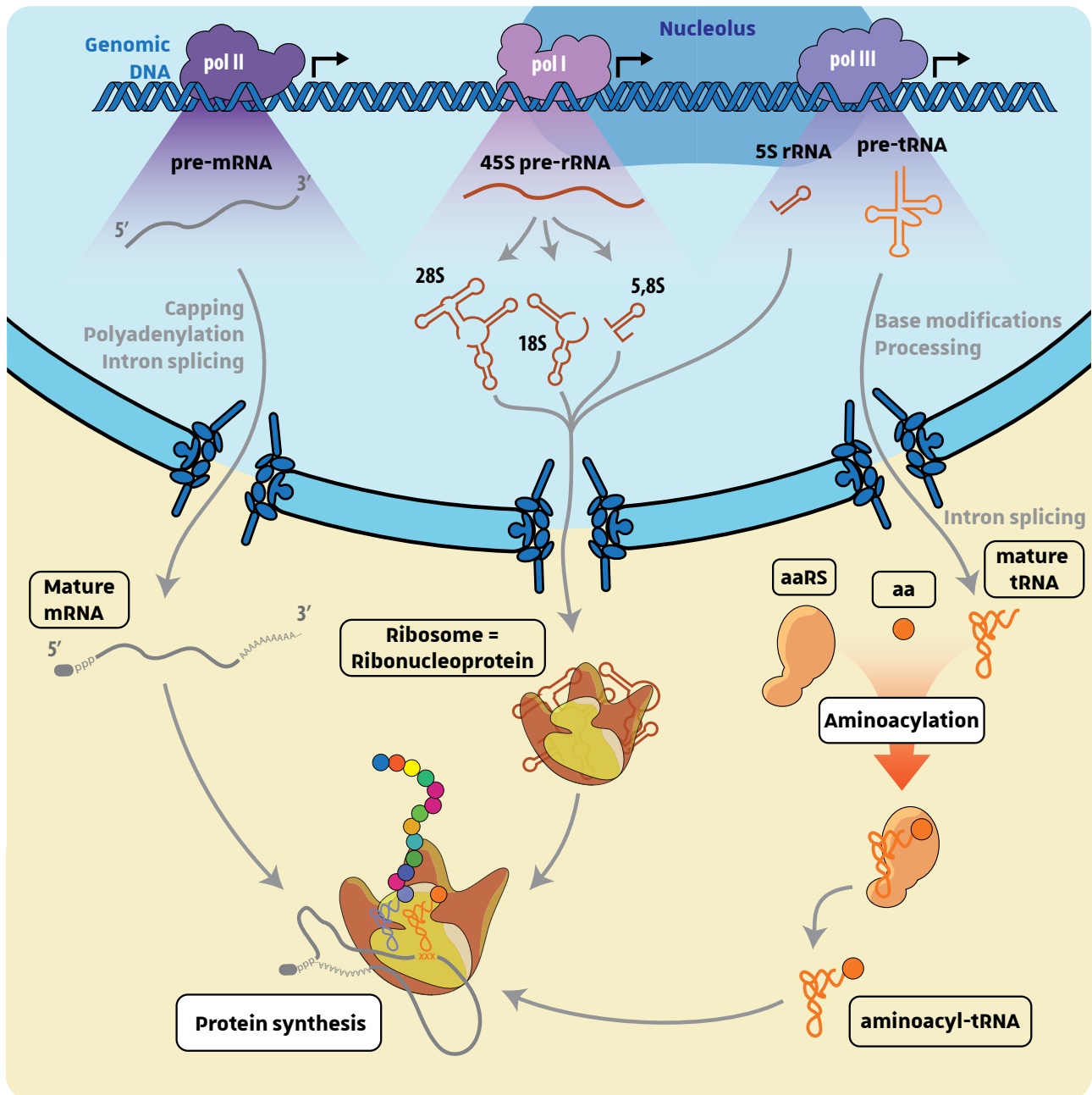


Figure I-2: Major actors of protein synthesis and importance of RNA molecules. Protein synthesis requires a large diversity of molecules and macromolecules. RNAs are essential, from the template messenger RNA (mRNA) transcribed by the RNA polymerase II (pol II) to the ribosomal RNAs (rRNAs) transcribed by the pol I and III. Aminoacyl-tRNAs (aa-tRNAs) are synthesized by aminoacyl-tRNA-synthetases (aaRSs) by attaching an amino acid (aa) to its cognate transfer RNA (tRNA).

assignment was thought to be universal in all three kingdoms of life, but studies have shown that some deviations were present in some bacterial, eukaryotic nuclear or organellar genomes. For example, mitochondria of vertebrate code Met from AUA codon (instead of AUG) and Trp from UGA (usually a stop codon). All reassignments referenced in the literature are noted in **Figure I-1**: majority of deviations are found for the stop codons since only one such codon is found per gene, so their reassignment would not cause too many troubles to the proteome (Mukai *et al.*, 2017). Within the nuclear genome of *S. cerevisiae*, the genetic code does not deviate from the standard code, although there are some deviations among fungi (Krassowski *et al.*, 2018).

I.2. The major actors of protein synthesis

Cells need to synthesize a large amount of proteins in a short time lapse to be able adapt their metabolism to the changing environment. For example, on rich medium, yeast cells are rapidly dividing and require the synthesis of $\approx 13,000$ proteins per second (von der Haar, 2008). The fact that a single yeast cell needs nearly 200,000 ribosomes to translate 60,000 mRNA molecules (Zenklusen, Larson and Singer, 2008; Firczuk *et al.*, 2013) and almost 10^6 translation elongation factors molecules (making them the most abundant proteins in a cell) illustrates the essentiality of protein synthesis. This part will describe the major components of translation which are summarized in **Figure I-2**.

I.2.1. The eukaryotic ribosomal particle

The ribosome represents a platform for the binding of other partners, like aminoacylated tRNAs and the mRNA, and is responsible for the translation of mRNA into proteins. Indeed, the production of proteins in logarithmically growing yeast cells would only be limited by the availability of free ribosomes (Shah *et al.*, 2013). A ribosome is a large ribonucleoparticle (RNP) (around 4 MDa in eukaryotes, about 40% larger than bacterial ribosome, with a sedimentation coefficient of 80S consisting of two unequal subunits, a large (60S) and a small (40S), with distinct compositions (Wilson and Doudna Cate, 2012). The small 40S subunit of the yeast consists of 33 ribosomal proteins and only one rRNA called 18S rRNA, whereas the large 60S subunit contains 46 proteins and three rRNAs called 28S, 5.8S and 5S. This structurally complex RNP exerts multiple functions:

- binding of the mRNA and aminoacyl-tRNA (aa) or tRNA molecules,
- decoding of mRNA codons (small subunit),

- interaction with nonribosomal protein factors,
- catalysis of peptide bond formation (large subunit),
- sliding through the mRNA molecule to translate continuously the open reading frame.
- translocation inside endoplasmic reticulum (through Signal Recognition Particle; for synthesis of membrane proteins),

The rRNAs are more than essential, they not only have a scaffolding role, but they also carry the ribosomal catalytic activity. Indeed, the peptidyl transferase activity necessitates the correct positioning of the A-site aa-tRNA and P-site peptidyl-tRNA that solely depends on 28S rRNA, making the ribosome a ribozyme. These rRNAs are first transcribed as a 35S pre-rRNA within the nucleolus by the RNA polymerase prior to processing that yield 5.8S, 18S and 25S rRNAs. The last rRNA, 5S rRNA, is transcribed by RNA polymerase III.

1.2.2. The messenger RNA

Messenger RNAs, also called “coding RNAs”, are single stranded ribonucleic acids composed of the succession of ribonucleotides linked by phosphodiester bonds, and transcribed by RNA polymerase II within the nucleoplasm. Discovered in 1961 by Jacob and Monod while studying the lactose operon of *Escherichia coli* (Jacob and Monod, 1961), these ubiquitous molecules serve as templates to encode the aa sequence in protein. In eukaryotes, once co- or post-transcriptionally modified (5' capped, 3' polyadenylated and spliced for intron-containing genes), mature mRNAs are exported through the nuclear pores and participate to the translation as a substrate for the ribosomal machinery. One can note that splicing in yeast is a rare event, since the genome of *S. cerevisiae* only contains 296 introns spanned in 283 genes (about 5% of the yeast genes) (Parenteau *et al.*, 2008), with a vast majority of intron-containing genes coding for ribosomal proteins (Ares *et al.*, 1999). Surprisingly, one-third of these introns are not essential for growth, and the majority of introns can be removed without major consequences on growth (Parenteau *et al.*, 2008). Another type of post-transcriptional modification found in all domain of life, called RNA editing, consists of base substitutions and short insertions or deletions within an mRNA, leading to proteome diversification (mostly when the base edition occurs within the mRNA coding region). However, this process has only recently been revealed in fungi, and no such modifications have been described, so far, in *S. cerevisiae* (Teichert, 2018). Once exported in the cytosol, this mature mRNA binds several translation initiation factors, allowing physical communication between the 5' cap structure and the

Table I-1: Yeast translation factors and their role in protein synthesis (inspired from [Dever, 2016](#))

Factor name	Gene (Subunit)	Systematic name	Length (aa)	Role(s)	
eIF1	<i>SUI1</i>	YNL244c	108	Promotes stable 43S PIC complex and start AUG recognition	
eIF1A	<i>TIF11</i>	YMR260c	153	Promotes stable 43S PIC complex and start AUG recognition. Prevent Met-tRNA _{Met} binding to the A-site.	
eIF2	<i>SUI2</i> (α)	YJR007w	304	The GTP-bound form of eIF2 binds to MettRNA _{Met} and promote the binding of the charged initiator tRNA Met to the 40S ribosome.	
	<i>SUI3</i> (β)	YPL237w	285		
eIF2B	<i>GCD11</i> (γ)	YER025w	527	Converts eIF2•GDP released from the 48S PIC to an active GTP-bound form through its guanine nucleotide exchange activity.	
	<i>GCN3</i> (α)	YKR026c	305		
	<i>GCD7</i> (β)	YLRYL291c	381		
	<i>GCD1</i> (γ)	YOR260w	578		
	<i>GCD2</i> (δ)	YGR083c	651		
	<i>GCD6</i> (ϵ)	YDR211w	712		
eIF3	<i>RPG1/TIF32</i> (α)	YBR079c	964	Stimulates recruitment of the ternary complex and mRNA to the 40S small ribosomal subunit	
	<i>PRT1</i> (β)	YOR361c	763		
	<i>NIP1</i> (γ)	YMR309c	812		
	<i>TIF35</i> (δ)	YDR429c	274		
	<i>TIF34</i> (ϵ)	YMR146c	347		
eIF4A	<i>HCR1</i> (ζ)	YLR192c	265		
	<i>TIF1</i>	YKR059w	395		
	<i>TIF2</i>	YJL138c	395		
eIF4B	<i>TIF3</i>	YPR163c	436	Binds to mRNA, alters the structure of the mRNA entry channel on the 40S ribosome. Enhance eIF4A helicase activity	
eIF4E	<i>CDC33</i>	YOL139c	213	m ⁷ G mRNA cap-binding protein, binds eIF4G to mediate mRNA circularization with Pab1 interaction.	
eIF4G	<i>TIF4631</i>	YGR162w	952	Binds the mRNA and bridges interaction between eIF4E and Pab1, mediates mRNA circularization. Recruit the 43S PIC through interaction with eIF5.	
	<i>TIF4632</i>	YGL049c	914		
eIF5	<i>TIF5</i>	YPR041w	405	Stimulates the GTPase activity of eIF2, and bridges interaction between eIF2 and eIF1/3.	
eIF5B	<i>FUN12</i>	YAL035w	1002	Promotes ribosomal 60S subunit joining to the PIC complex.	
eEFs	eEF1A (EF1 α)	<i>TEF1</i>	YPR080w	458	Provides aa-tRNA delivery to the 80S ribosome.
		<i>TEF2</i>	YBR118w	458	
	eEF1B (EF1B $\alpha\gamma$)	<i>TEF5</i>	YAL003w	206	Converts eEF1A•GDP released from the 48S PIC to an active GTP-bound form through its guanine nucleotide exchange activity.
		<i>TEF4</i>	YKL081w	412	
	eEF2	<i>CAM1</i>	YPL048w	415	Promotes the translocation of the mRNA and the peptidyl-tRNA from the A site to the P site of the 80S ribosome.
		<i>EFT1</i>	YOR133w	842	
	eEF3	<i>EFT2</i>	YDR385w	842	Facilitates release of deacylated tRNA from the E site.
<i>TEF3</i>		YLR249w	1044		
eIF5A	<i>HEF3</i>	YNL014w	1044	Promotes peptide bond formation by aa-tRNA rearrangement.	
	<i>HYP2</i>	YEL034w	157		
	<i>ANB1</i>	YJR047c	157	ANB1 is expressed specifically in anaerobic conditions.	
eRFs	eRF1	<i>SUP45</i>	YBR143c	437	Stop codons recognition. Promotes hydrolysis of the aminoacyl bond to release the polypeptide from the peptidyl-tRNA.
	eRF3	<i>SUP35</i>	YDR172w	685	Critical for stop codons recognition and discrimination, and accelerates peptide release.
	Rli1 (ABCE1)	<i>RLI1</i>	YDR091c	608	Promotes eRF1-mediated hydrolysis and release of the polypeptide. Also promotes release of the 60S subunit by ATP hydrolysis.

3' poly(A) tail and enhancing the mRNA translation by circularization of the mature transcript (Iizuka *et al.*, 1994; Tarun and Sachs, 1995; Wells *et al.*, 1998). This mature mRNA carries information from DNA in a three-letter genetic code and represents the matrix that is decoded by the ribosome, one codon representing one aa after decoding.

I.2.3. Protein translation factors

Translation, like transcription, can be divided into three phases: initiation, elongation and termination. Each phase of translation requires specific protein factors. Initiation Factors (IF) will be used during initiation, Elongation Factors (EF) during elongation and Release Factors (RF) during termination. These factors display multiple functions like:

- bringing substrates to the ribosome in the right place,
- switching from one state to another by cycling between a GTP-bound form and a GDP-bound form,
- translocation of the mRNA and of the aa- or peptidyl-tRNAs within the ribosome,
- release of the neosynthesized protein, of the mRNA and recycling of the ribosome

For each phase, specific factors are involved: 11 translation IFs encoded by 24 independent genes, 6 EFs (11 genes) and 3 RFs (3 genes). All the factors and their specific role are listed in **Table I-1**. The contribution of each translation factor will be detailed in the next section.

I.2.4. Amino acids

Amino acids are essential for life since they are the building blocks of proteins and have a central role in general metabolism. Amino acids metabolism is relatively complex but well known in yeast: as catabolic substrates, they constitute a broad source of carbon and nitrogen, and they participate to anabolic reactions such as biosynthesis of nucleotides. Yeast differs from mammals in aa biosynthesis, since mammals are not able to synthesize *de novo* the complete pool of proteinogenic aa: mammals must obtain some aa (called essential aa) from their diet. The yeast *S. cerevisiae* is able to grow on a medium with ammonium as the sole nitrogen source, meaning that all the aa are synthesized *de novo* in yeast anabolism. All aa carbon skeletons (α -keto acids) derive from the glucose catabolic pathway, and the α -amino group usually comes from the glutamate or glutamine, the two amino acids that constitute a storage form of free ammonia through two anabolic reactions:

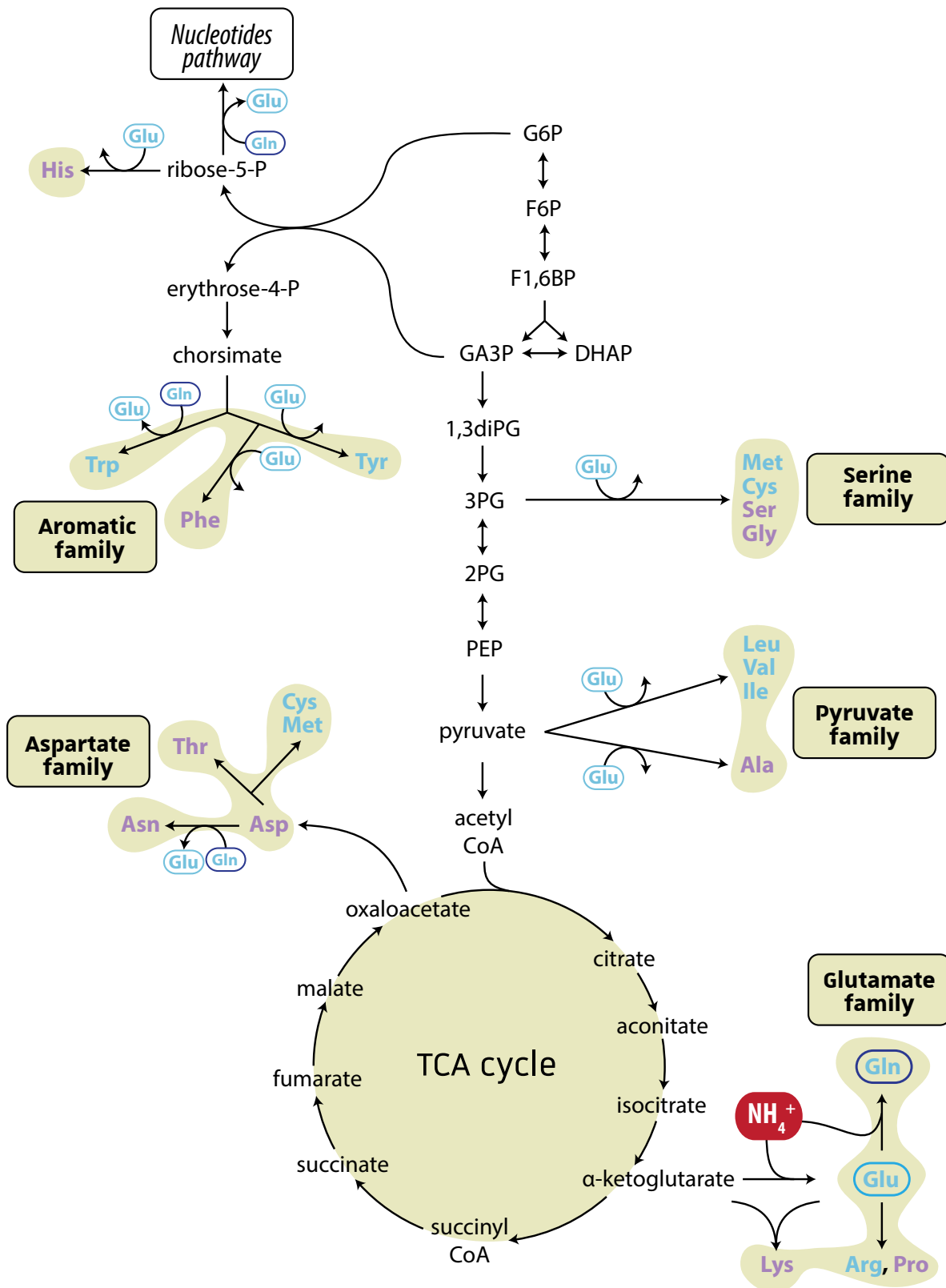


Figure I-3: Biosynthesis of amino acids from glucose and ammonia in *S. cerevisiae* (inspired from Ljungdahl and Daignan-Fornier, 2012). The amino acids are grouped by family according to their origin or their chemical properties, and are colored according to the class of their associated aaRS: blue for class I and purple for class II. G6P: Glucose-6-phosphate; F6P: fructose-6-phosphate; F1,6BP: fructose-1,6-bisphosphate; DHAP: dihydroxyacetone phosphate; GA3P: glyceraldehyde-3-phosphate; 1,3diPG: 1,3-bisphosphoglycerate; 3PG: 3-phosphoglycerate; 2PG: 2-phosphoglycerate; PEP: phosphoenolpyruvate; CoA: coenzyme A.

synthesis of Glu from ammonium and α -ketoglutarate by the NADPH-dependent glutamate dehydrogenase (*GDH1*), and synthesis of Gln from ammonium and glutamate by the glutamine synthetase (*GLN1*) (see **Figure I-3**). In their natural environment, yeast cells need to adapt their nitrogen assimilation according to the nitrogen content, by controlling both the uptake of ammonia and its metabolism. In addition to assimilate free ammonia, they can grow on different media with only one aa as sole source of nitrogen (with the exception of Lys, His and Cys). However, the growth rate is highly dependent on the nature of aa as nitrogen source, leading to aa classified as preferred or non-preferred (Watson, 1976; Niederberger, Miozzari and Hütter, 1981; Cooper, 1982; Godard *et al.*, 2007; Ljungdahl and Daignan-Fornier, 2012; results compiled in **Appendix 1**, page 106)

Once the pool of all aa is generated within the cell, free aa can be found in several compartments: the cytosolic fraction, mitochondria (to sustain the mitochondrial translation), the nucleus and the vacuole. The latter, similar to mammalian lysosome, is not only a turgor organelle nor a simple detoxifying compartment, but is also the major storage compartment for aa, phosphate, Ca^{2+} , and metal ions (Klionsky, Herman and Emr, 1990; Li and Kane, 2009). Among the aa families, the basic and neutral aa are the most representative families stored in the vacuole, and the acidic ones are mostly cytosolic (Wiemken and Dürr, 1974; Messenguy, Colin and Have, 1980; Kitamoto *et al.*, 1988). Storage of basic aa is actually a strategy to improve the storage of nitrogen, since basic aa have one or two more nitrogen atom in their chemical structure, making them a powerful nitrogen source. All these aa need to cross the vacuolar membrane through membrane transport systems, among which a lot are using the proton-driving force (energized by the $\text{V}_0\text{V}_1 \text{H}^+$ -ATPase) through antiport or symport system (reviewed in Li and Kane, 2009; Ljungdahl and Daignan-Fornier, 2012). Upon nitrogen starvation, expression of all these aa transporters needs to be upregulated to adequately maintain the amount of free nitrogen source, and same is true for expression of plasma membrane-localized transporters to facilitate the uptake of aa into the cell (Ljungdahl, 2009) and to allow assimilation of nitrogen and incorporation of all these aa during translation. However, even if we know that aa are known regulators of cellular signalling, little is known about how they are sensed directly within the cell. The indirect signal of aa (or nitrogen) starvation is the sensing of uncharged tRNA molecules by Gcn2 pathway that prevents initiation of translation (Dong *et al.*, 2000).

I.2.5. tRNAs : the “adaptor” molecules

The last (but not least!) actor of protein synthesis listed in this manuscript is the tRNA molecule: this small RNA (54 to 100 nucleotides across organisms and depending on tRNA species) is the key to deciphering the codons in mRNA since it allows the cell to convert ribonucleotide sequence language into the corresponding aa sequence language (polypeptides) (Nirenberg and Matthaei, 1961; Nirenberg, Matthaei and Jones, 1962). Indeed, each aa is carried to elongating ribosomes by a specific subset of isoaccepting cognate tRNAs . They are brought to the growing end of the polypeptide chain within the ribosome in the form of aminoacyl-tRNA (aa-tRNA) which correspond to tRNA-attached aa that are generated by the aaRS family of enzymes. In *S. cerevisiae*, there are 43 tRNA species (or isodecoders families) encoded by 274 genes. All these tRNA genes are dispersed throughout the genome (composed of 16 chromosomes (see **Appendix 2**, page 107), and each tRNA isodecoder consists of 1 to 16 copies (see **Table I-2**). These tRNA genes are transcribed by the RNA polymerase III in the nucleolus, a nuclear subcompartment not enveloped by a membrane and containing dense DNA regions (Thompson *et al.*, 2003).

I.2.5.1. tRNAs structure

This ubiquitous RNA molecule folds into a specific secondary structure that was determined for the first time in 1965 for the 77 nt-long yeast tRNA^{Ala} (Holley *et al.*, 1965). Within three years, twelve different tRNAs had been sequenced, and they all could be folded into the same secondary structure termed “cloverleaf structure”. Watson-Crick base pairing enables the sequence to fold into a structure containing four hairpin helices (or stem) and four major loops (**Figure I-4**):

- the acceptor stem, a 7-base pair helix prolonged at the 3'end by a single stranded nucleotide called the discriminator base (position 73) followed by the strictly conserved CCA sequence which is added by the tRNA nucleotidyl transferase in eukaryotes (Chen *et al.*, 1990). This stem is called “acceptor” because the aa will covalently be attached to the 3'- or 2'-OH group of the terminal adenine (position 76).
- The D-arm containing a 4-bp stem and a 6- to 11-bp loop with usually a dihydrouridine (D), explaining the name D-arm for this element.
- The anticodon arm, with a 5-bp stem ending in a 7-bp loop that contains the central triplet of nucleotides called anticodon that will base pair with the corresponding mRNA codon in

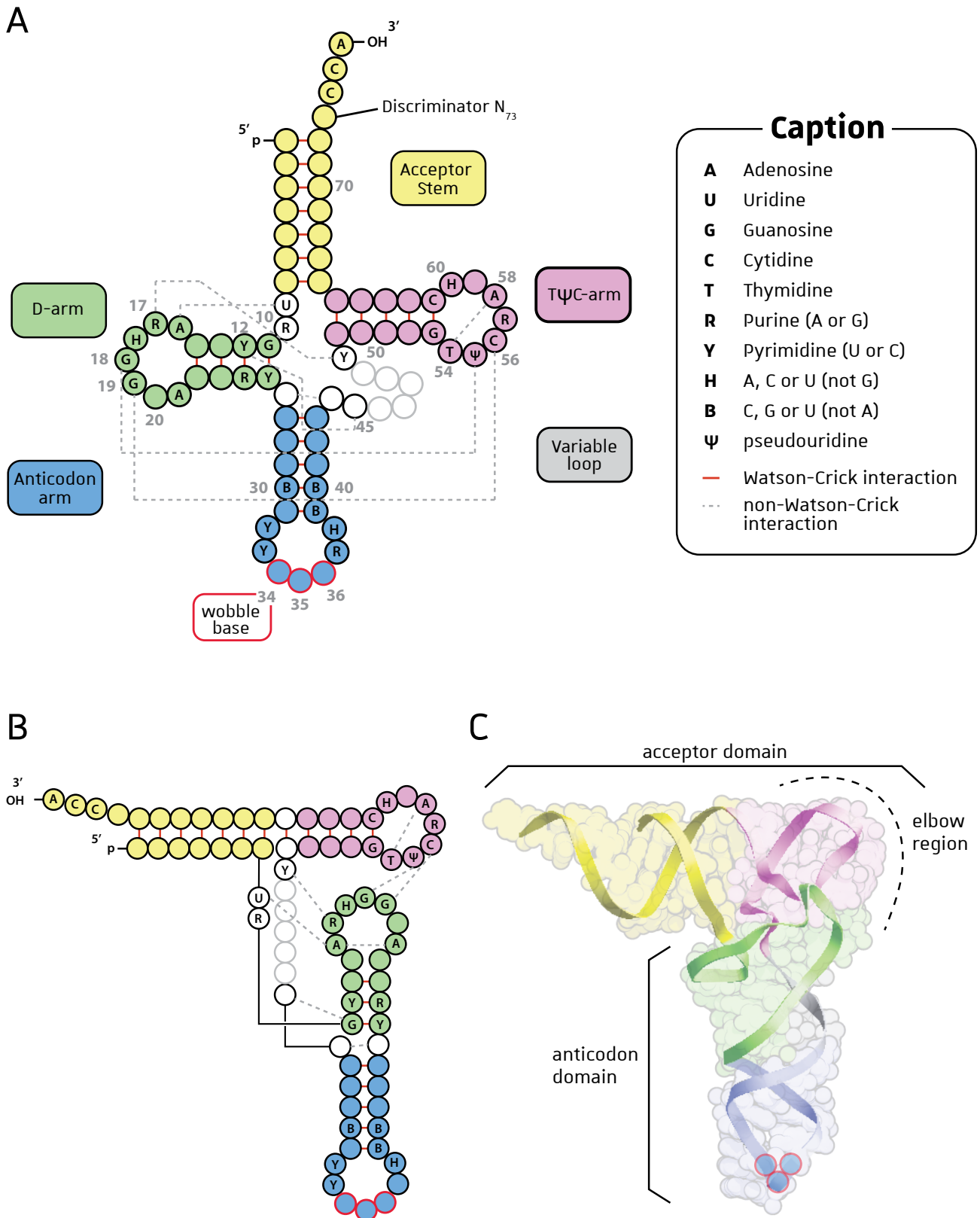


Figure I-4: tRNA structures (inspired from Enkler, 2014). **A.** The class 1 tRNA cloverleaf structure and the consensus sequence of tRNAs from *S. cerevisiae* (from Marck *et al*, 2002). **B.** Same secondary structure with L-shape folding to minimize distance for non-Watson-Crick interactions. **C.** Three-dimensionnall structure of yeast tRNA^{Phe} (pdb 1TRA).

ribosomes.

- The TΨC arm (or T arm) with a 5-bp stem and a 7-bp loop usually containing the TΨC sequence.

An extra fourth loop called the variable loop or variable region (V-loop) is present between the anticodon and the TΨC stems and is made of 3 to 15 nucleotides in *S. cerevisiae* tRNAs. The size of this variable loop specifies the class of tRNA: class 1 tRNAs present a small variable loop, whereas class 2 tRNAs have a longer variable region that usually folds into a hairpin structure (tRNAs^{Ser} and tRNAs^{Leu} since tRNAs^{Tyr} is a class 1 tRNA in *Sce* and there is no tRNAs^{Sec}) (**Table I-2**, page 32). For tRNA^{His} species, an extra 5' nucleotide is present in the position -1 (G₋₁) (see **Table I-2**) that base pairs the discriminatory base. Even if this cloverleaf secondary structure is simple to understand and to draw on paper, this is not the actual three-dimensional structure. In the early 70's, the first 3D-structure of a tRNA has been solved at 4 Å resolution, once more on a yeast tRNA: tRNA^{Phe} (Kim *et al.*, 1973). This crystal structure revealed an L-shaped folding composed of two perpendicular helices: one formed by the acceptor stem and the TΨC hairpin stacking together (called the acceptor domain) and the second by the D-arm and the anticodon hairpin (called the anticodon domain) (**Figure I-4**). This remarkable folding is stabilized by non-Watson-Crick interactions, especially between the D and T loops, allowing the formation of the elbow region. This L-shaped folding is extremely important since it allows more than 70 Å distance between the 3'-terminal acceptor residue and the anticodon sequence, these two regions present in opposite corners of the molecule. This distance is adequate with mRNA codons interacting with the tRNA anticodon in the small ribosomal subunit, and binding of the 3'-aminoacylated CCA end of the tRNA in the peptidyl transferase located in the large ribosomal subunit. All these characteristics make tRNA the bridging molecule between the nucleotidic and the peptidic language.

I.2.5.2. Maturation of pre-tRNAs

After transcription by the RNA polymerase III, tRNA genes give rise to non-mature tRNAs called pri-tRNAs ("pri" stands for primary). These pri-tRNAs possess a 5' leader and a 3' trailer sequence (of about 12 nt) that are removed in the mature tRNAs sequence (**Figure I-5**). Also, unlike prokaryotic tRNA genes the eukaryotic tRNA genes do not encode the 3' terminal CCA sequence (unlike prokaryotes). Therefore, these larger precursors need to be processed to yield pre-tRNAs that will be further matured. For almost all organisms, the tRNA 5' leader is removed in one step by the ribonuclease P (RNase P), an ubiquitous endoribonuclease composed of nine protein subunits

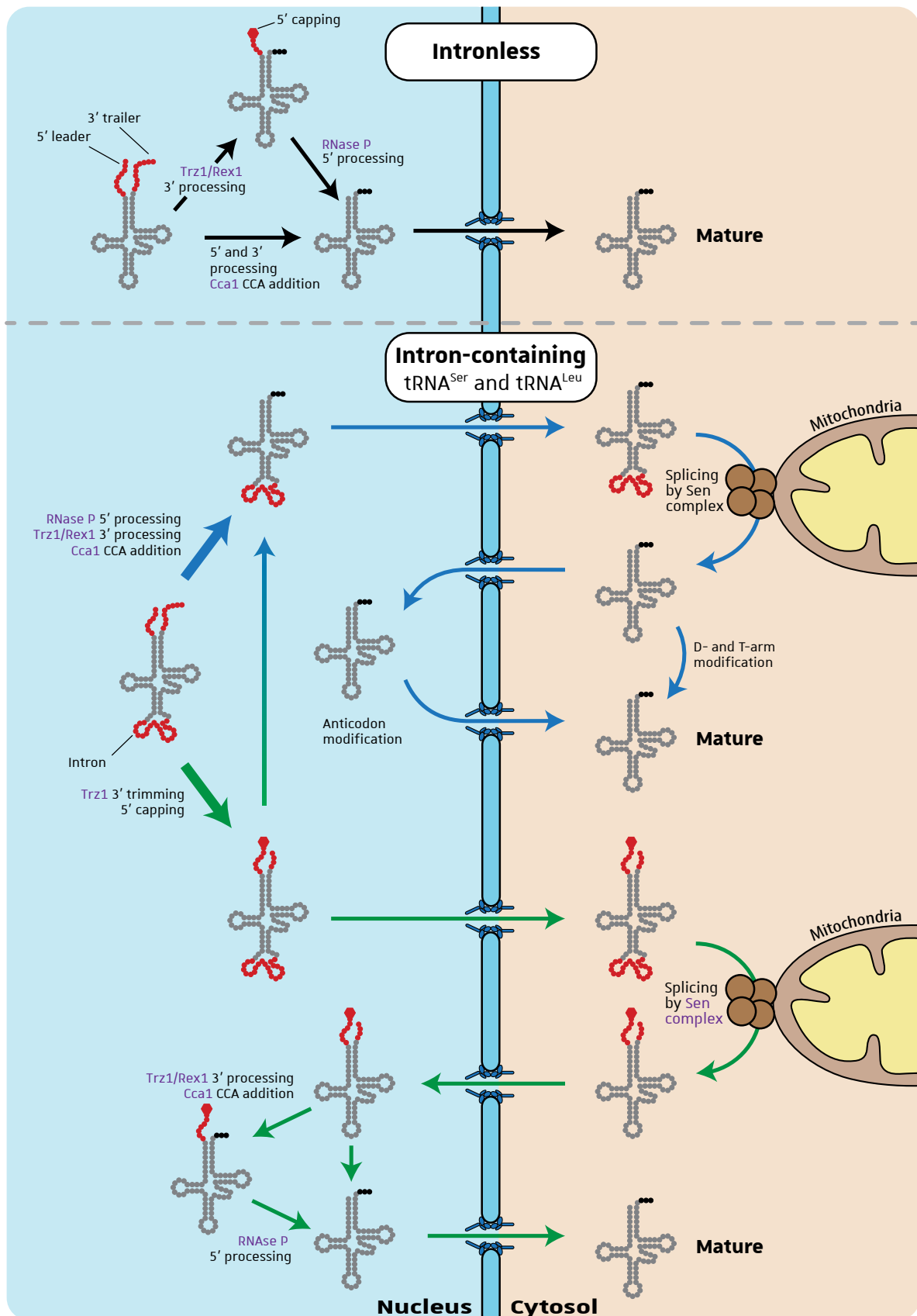


Figure I-5: tRNA maturation steps in *S. cerevisiae* (inspired from Ohira and Suzuki, 2016). pre-tRNAs transcribed by the RNA polymerase III can be subdivided in two subclasses, intronless and intron-containing tRNAs. For both subclasses, pre-tRNAs are end matured in the nucleus and exported to the cytosol. For intron-containing tRNA, the intron splicing step occurs in the cytosol by the mitochondrial-associated Sen complex. Extra sequences of each precursor are shown in red and black dots indicate CCA sequence.

and one catalytic RNA in eukaryotes (Evans, Marquez and Pace, 2006). It has been shown that before 5' processing, tRNAs can harbour methylguanosine cap structure at their 5' terminus and be protected from 5'-exonucleolytic degradation during the tRNA maturation process (Ohira and Suzuki, 2016). For tRNA^{His}, the addition of the extra 5'G is catalyzed by Thg1, adding the 5'G in the 3' to 5' direction (Gu *et al.*, 2003). The 3' end maturation is more complex and involves both endo- and exonucleolytic activities, with the addition of the terminal CCA (Mörl and Marchfelder, 2001). In *S. cerevisiae*, 3' trailer is removed by the tRNase Z endonuclease, called Trz1, and 3' trimming is carried out by the 3'-5' Rex1 exoribonuclease, in association with the nuclear-specific Rrp6 exosome component (Skowronek *et al.*, 2014). Despite a well characterisation of all these maturation events, the temporality of each step is still unclear. The post-transcriptional addition of the 3' terminal CCA sequence is catalyzed by the yeast tRNA nucleotidyl transferase Cca1 (Chen *et al.*, 1990).

Among the 274 tRNA genes in *S. cerevisiae*, 59 genes (20 %) code for intron-containing tRNA (Chan and Lowe, 2009). In yeast, there is only one intron per tRNA between positions 37 and 38 in the anticodon loop, with size varying from 14 bp for tRNA^{Trp(CCA)} to 60 bp for tRNA^{Ile(UAU)} (see **Table I-2**, page 32). All these intron-containing tRNAs have to be processed to excise the intron and form pre-tRNA. The yeast tRNA splicing endonuclease was the first tRNA splicing complex identified and is composed of four subunits Sen2, Sen15, Sen34 and Sen54 (Rauhut, Green and Abelson, 1990; Trotta *et al.*, 1997). It allows the cleavage of both 5'- and 3'-splice sites of the intron by phosphoester transfer, and the two subsequent tRNA exons are joined by the yeast tRNA ligase Trl1, the first 5'-phosphate ligase identified (Phizicky, Schwartz and Abelson, 1986). This yeast splicing complex is localized on the mitochondrial outer membrane, leading to tRNA splicing in the cytosol and sometimes retrograde transport into the nucleus to complete the maturation process (**Figure I-5**).

During post-transcriptional maturation, pre-tRNAs undergo various base modifications within their sequence at different stages of tRNA biogenesis (Phizicky and Hopper, 2010). In the yeast *S. cerevisiae*, 26 chemically distinct modifications have been identified within the sequenced cytoplasmic tRNAs, with an average of 12-13 modifications per tRNA (Limbach, Crain and McCloskey, 1994; Sprinzl *et al.*, 1998). All yeast tRNA modifications are depicted in **Appendix 3 and 4**, page 108 and page 109. According to their position inside the tRNA sequence, tRNA nucleoside modifications can carry different functions, but most of them are important for three-dimensional integrity and stabilization of the L-shaped structure (**Appendix 3**, page 108). Some modifications are also crucial for aaRS recognition or discrimination (called determinant or antideterminant) and

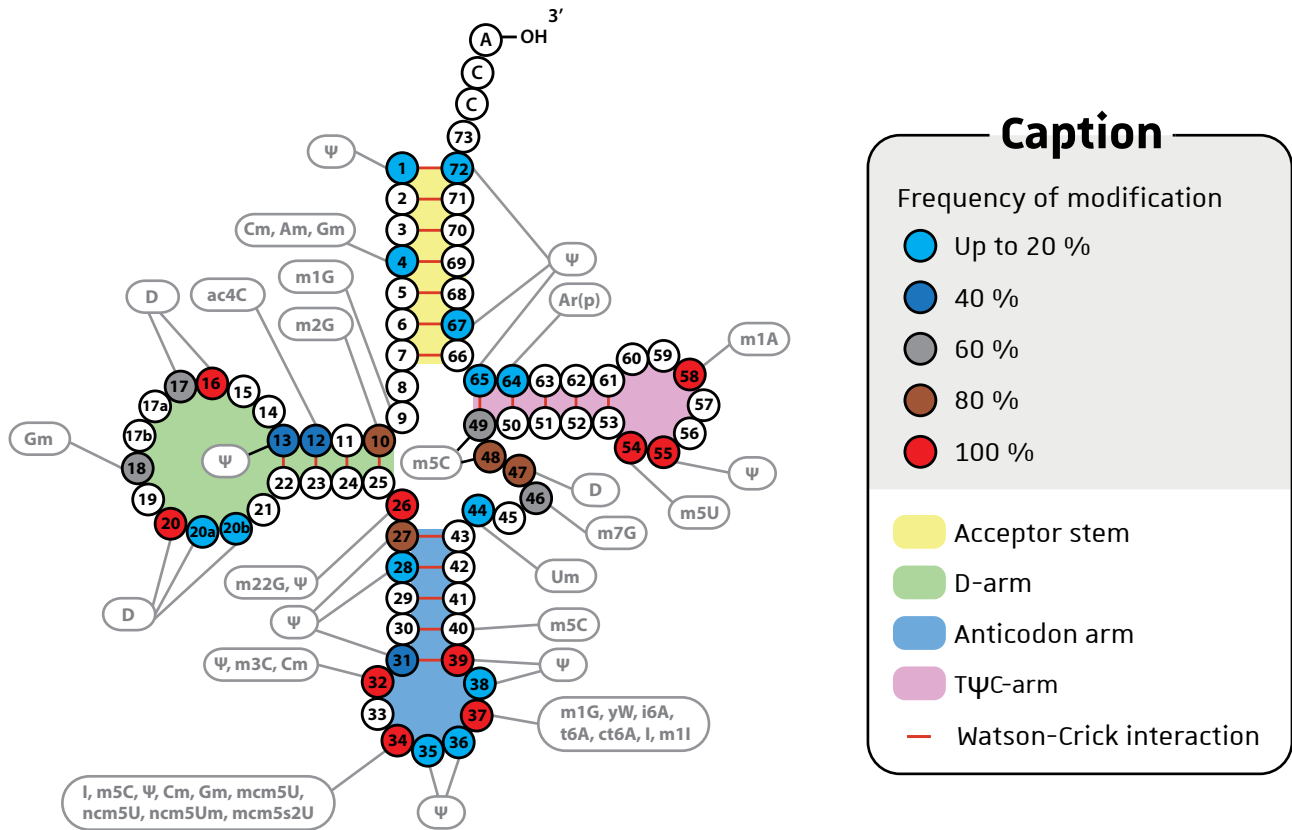


Figure I-6: Yeast tRNA nucleotide modifications pattern. All tRNA nucleoside modifications known in yeast are depicted with their position in the tRNA sequence. Their name and functions are listed in Appendix 3, and chemical representation of each modification is found in **Appendix 4**. Frequency of modification comes from [Mohler and Ibbá, 2017](#).

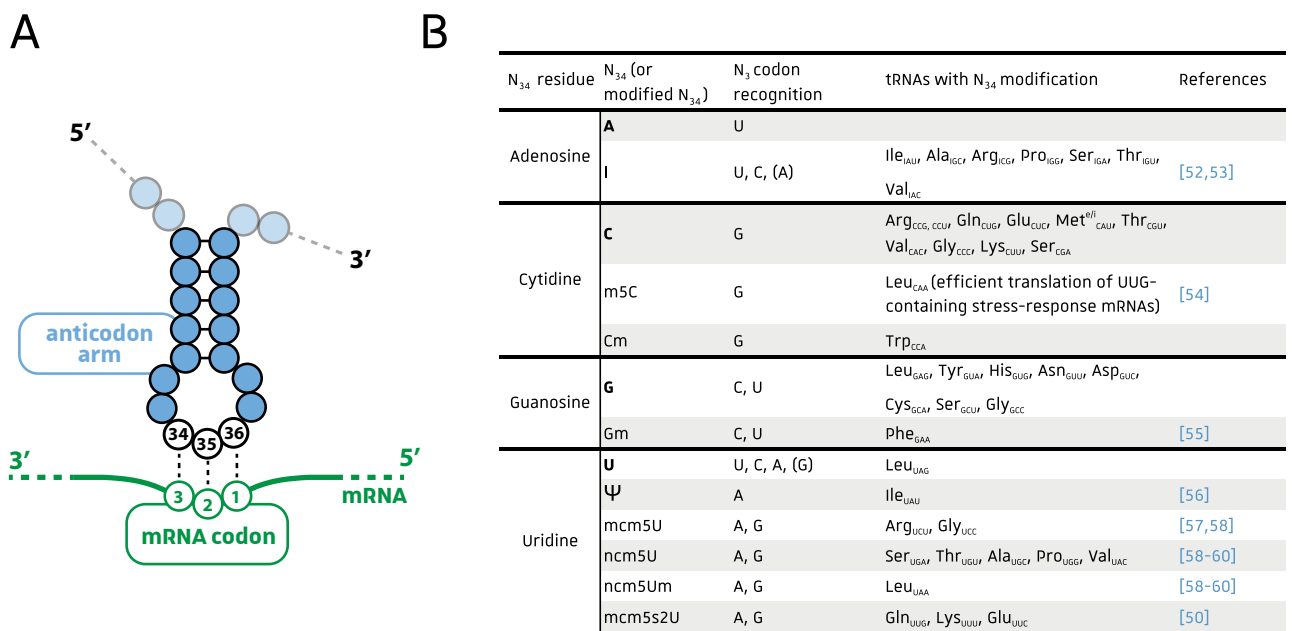


Figure I-7: Modifications of the wobble position in yeast tRNAs. **A.** Representation of the anticodon arm facing the mRNA sequence. tRNA residue N_{34} , called wobble residue, faces the residue N_3 of the mRNA codon. **B.** Modification of N_{34} residue allows recognition of specific N_3 codon residue.

others are required for additional modification (Cm in position 32 of tRNA^{Phe} is required for the modification of G₃₇ in wybutosine yW₃₇). All tRNA modifying enzymes are known in yeast and are listed in **Appendix 3**, page 108. Some are really specific for one individual modification at one particular position, whereas others are responsible for the modification of a single nucleoside but at different positions of the tRNA molecule (Trm4 methylates cytidine at 4 different positions). Some, however, can modify different types of nucleosides like Trm13 that adds 2'-O-methyl on either A, C or G. Another striking observation is the number of modifications (in terms of variety and density) found in the AC-stem. Indeed, 16 out of 26 modifications are found in the AC-stem, with 11 residues potentially modified by the most elaborate modifications (**Figure I-6** and **Appendix 3**, page 108). Furthermore, several modifications are found in the AC-loop containing the anticodon triplet, with the majority of modifications found in positions 34 and 37 (and **Figure I-6**). The N₃₄ nucleotide pairs with the third mRNA codon base, and is called the 'wobble' position. Most of the time, the first two base-pairs between tRNA(N₃₆)-codon(N₁) and tRNA(N₃₅)-codon(N₂) are canonical (Watson-Crick type), but the third base-pair at the wobble position can be canonical as well as nonstandard, allowing either the expansion or the restriction of the repertoire of codons that a single tRNA can recognize during protein synthesis (Crick, 1966; Lim and Curran, 2001; Jackman and Alfonzo, 2013). These non-Watson-Crick interactions often involve a modified N₃₄ within the tRNA sequence (Varian *et al.*, 2002). The most characterized N₃₄ modification is the A₃₄ to I₃₄ by N6-deamination by the yeast Tad2/3 complex (**Appendix 3 and 4**, page 108). This modification allows I₃₄ to base-pair with A, U and C, according to Crick's wobble hypothesis (Crick, 1966, and **Figure I-7**). This modification allows I₃₄-containing tRNAs to base pair with 3 codons instead of 2. We can notice on **Table I-2 and I-3** that all yeast tRNAs containing A₃₄ possess the I₃₄ modification.

I.3. The three (or four) steps translation process

Protein synthesis can be divided into three (or four) major steps: the initiation, elongation, termination, and the ribosome recycling. This process relies on accurate incorporation, from the N-terminus to the C-terminus, of aa during peptide chain elongation (Dintziz, 1961) catalyzed by the ribosome reading the messenger RNA from its 5' to 3'-end direction. All the actors listed previously play an important role for each step of ribosomal translation.

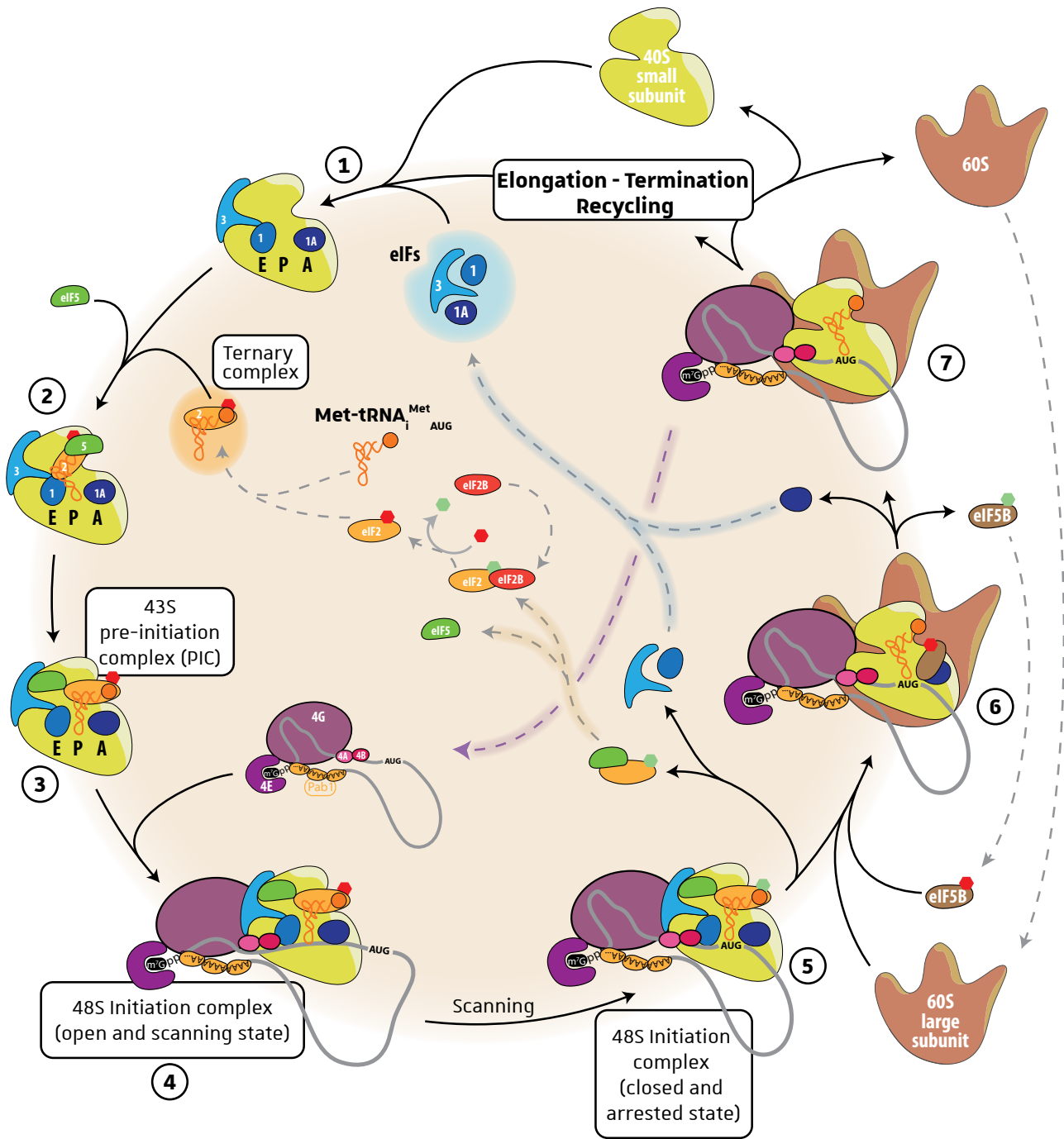


Figure I-8: The initiation steps of yeast translation and recycling of initiation factors. ① ② and ③ The initiation relies on pre-formation of the ternary complex that binds to the small ribosomal subunit and its associated initiation factors (eIFs) to form the 43S PIC complex. ④ This complex binds to mRNA (gray) complexed with initiation factors complex eIF4F (purple) to form the 48S initiation complex. ⑤ ⑥ and ⑦ After AUG recognition and GTP hydrolysis, the ribosomal 60S large subunit joins the mRNA complex to form the elongating complex. ● GDP, ● GTP.

I.3.1. The initiation: search for the AUG start codon

Translation initiation is the most complex step of protein synthesis and has undergone massive changes during evolution since bacterial initiation requires only three initiation factors IF1/2/3 (Laursen *et al.*, 2005) compared to 11 initiation factors (and 24 independent genes) in yeast (Table I-1, page 28). The initiation starts with the formation of the 43S Pre-Initiation Complex (PIC) and is completed when the 40S small ribosomal subunit stalls at the start codon and the 60S large ribosomal subunit joins it to form the 80S elongating ribosome particle. This 43S PIC is composed of the small ribosomal subunit bound to the methionylated initiator $\text{tRNA}_i^{\text{Met(AUG)}}$ ($\text{Met-tRNA}_i^{\text{Met(AUG)}}$) and to eIF1/1A/2/3/5 initiation factors (Figure I-8). The $\text{Met-tRNA}_i^{\text{Met(AUG)}}$ binds the small ribosomal subunit as a ternary complex involving GTP-bound eIF2 (Algire *et al.*, 2002). This ternary complex is then binding to the 40S ribosome together with eIF1/1A/3 and eIF5 that facilitate this interaction (Majumdar, Bandyopadhyay and Maitra, 2003). Once formed, the 43S complex is competent to interact with the mRNA molecule which is circularized through the interaction between the cap-binding complex eIF4F (made by eIF4A/B/E/G bound to the capped 5'-end) and the polyA-binding protein Pab1 bound to mRNA 3'-end polyA tail (Tarun and Sachs, 1995). The next step is the recruitment of the 43S PIC near the 5'-end of the mRNA complex mediated by the interaction between eIF4G and eIF5 (Asano *et al.*, 2001) and the helicase activity of eIF4A that unwinding secondary structure elements on the mRNA sequence on which the 43S PIC will bind. The 43S PIC in an open, scanning-competent state moves along the mRNA leader in 3' direction searching for a AUG start codon in a suitable sequence context called the Kozak sequence (Kozak, 1986). This Kozak sequence varies across organisms both in length and sequence (Cavener, 1987), but the consensus Kozak sequence in yeast is rich in adenine and poor in guanine, and was determined to be $(A_{50}/U_{50})A(A_{50}/C_{50})A_{100}(A_{50}/C_{33})A_{89}\text{AUGU}_{38}C_{52}(U_{50}/C)$ (Hamilton, Watanabe and de Boer, 1987).

The anticodon of the $\text{Met-tRNA}_i^{\text{Met}}$ (which is located into the 40S ribosomal P site) scans the mRNA and select the AUG start codon by Watson-Crick base interaction (Cigan, Feng and Donahue, 1988). This codon-anticodon base pairing triggers conformational changes of several initiation factors and eIF2-mediated GTP to GDP + P_i hydrolysis inducing its release together with eIF1 (Algire, Maag and Lorsch, 2005). Binding of $\text{Met-tRNA}_i^{\text{Met(AUG)}}$ to eIF2•GDP is much weaker than to eIF2•GTP (K_d of 150 nM and 10 nM, respectively), allowing release of eIF2•GDP from the P site after start codon selection (Kapp and Lorsch, 2004). Further dissociation of eIF2•GDP complex, eIF5 and eIF3 induce the PIC conformational change to a closed, scanning-arrested state. At this stage, eIF5B•GTP

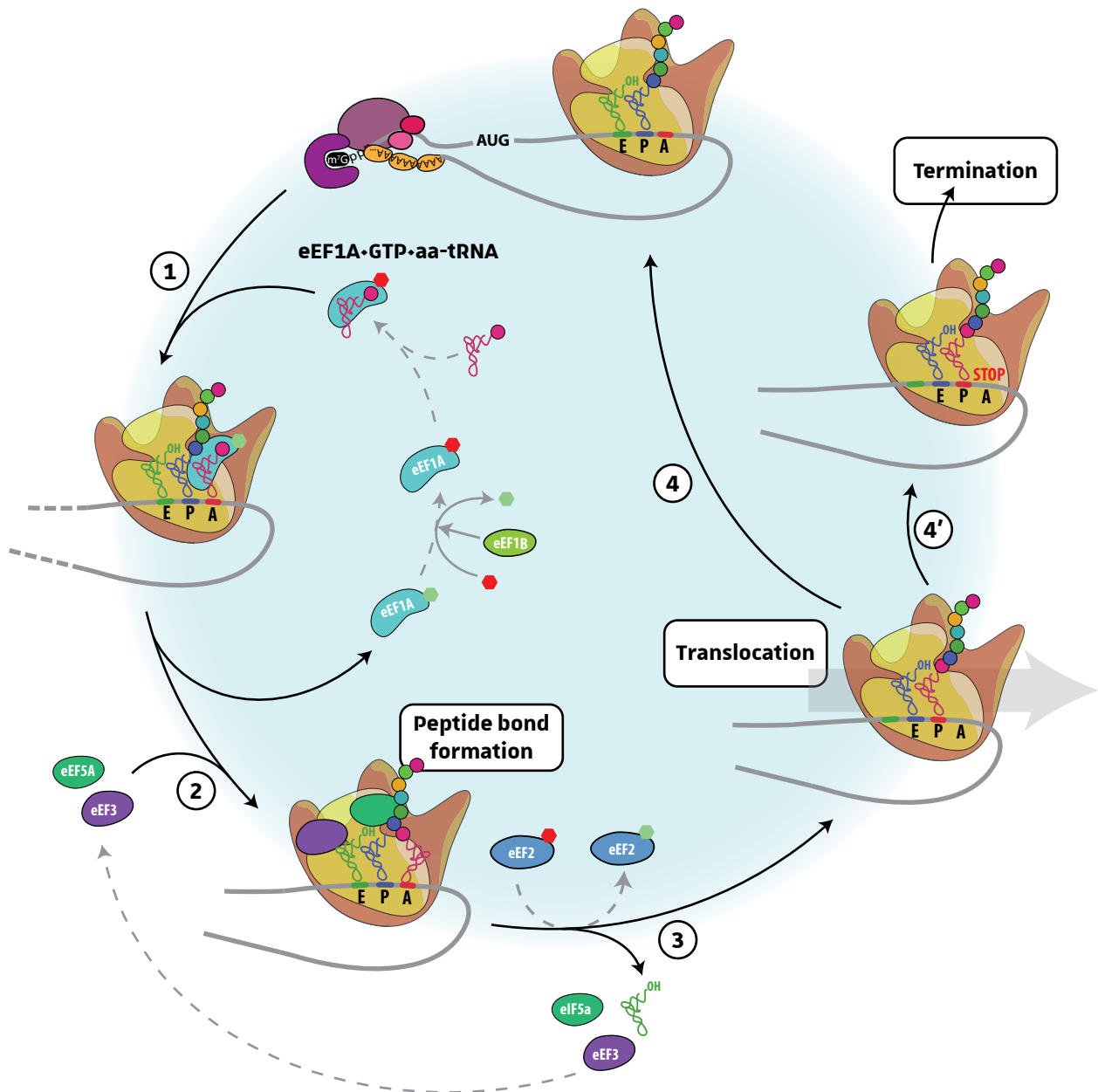


Figure I-9: Elongation steps of translation. ① The aa-tRNA cargo in complex with eEF1A•GTP is delivered to the A site of the elongating 80S ribosome. Codon-anticodon base pairing induces GTP hydrolysis and the release of eEF1A•GDP and subsequent binding of eEF5A and eEF3. ② Peptide bond formation is catalysed by the ribosome, and GTP hydrolysis by eEF2 induces the release of eEF5A and eEF3, and ③ the translocation of the mRNA and shift of the peptidyl-tRNA from A- to P-site. The A site is free to accept a new aa-tRNA to pursue elongation ④ or a termination factor, if a stop codon is positioned in the A-site ④'.

promotes binding of the 60S ribosomal subunit and formation of the 80S ribosome (Pestova *et al.*, 2000). In the 80S particle, eIF1A is bound in the A site but hydrolysis of the GTP molecule of eIF5B•GTP through its GTPase activity will promote its release from the 80S ribosome together with eIF1A (Acker *et al.*, 2009). The initiation ends when the 80S ribosome only contains the Met-tRNA_i^{Met} in its P site and an empty A site free to accept an elongator aa-tRNA.

I.3.2. Elongation: synthesis of the peptide chain

Translation elongation is well conserved between eukaryotes and bacteria and consists in polymerization of aa in the N-terminus to C-terminus direction (Rodnina and Wintermeyer, 2009). Similar to eIF2, the eEF1A•GTP binary elongator factor complex binds to an elongator aminoacyl-tRNA (aa-tRNA) to form a ternary complex that will deliver its aa-tRNA cargo to the A site of the elongating 80S ribosome (Mateyak and Kinzy, 2010, **Figure I-9**). GTP hydrolysis and release of eEF1A•GDP is induced by the codon-anticodon base pairing. Binding of eEF3 and eEF5A to the ribosome induces a conformation rearrangement of the aa-tRNA within the A-site, moving the aa carried by the A-site tRNA closer to the aa or peptide carried by the P-site tRNA, and facilitating the transpeptidase reaction. eEF3 has been proposed to promote the release of the deacylated tRNA from the E site (Triana-Alonso, Chakraborty and Nierhaus, 1995; Andersen *et al.*, 2006). After peptide bond formation, eEF2•GTP binds to the 80S ribosome, and subsequent GTP hydrolysis induces translocation of the mRNA and shift of the peptidyl-tRNA from the A- to P-site (Ling and Ermolenko, 2016), leaving the A-site free to accept a new aa-tRNA molecule.

I.3.3. Termination and recycling

Termination begins when, after translocation, one of the three stop codons (UGA, UAA or UAG) is located in the A-site of an elongating 80S ribosome. Each of these 3 stop codons will be recognized by the N-terminal domain of the eRF1 release factor that binds in the A-site occupied by a stop codon. Binding of eRF1 in the A-site is made possible because this factor adopts a three dimensional structure that mimics the L-shaped structure of a tRNA (Bertram *et al.*, 2000). Then, eRF3•GTP binds tightly to eRF1 and promotes stop codon recognition and discrimination (Wada and Ito, 2014). Upon GTP hydrolysis, eRF3•GDP dissociates and the Rli1 factor binds to eRF1 and promotes hydrolysis of the ester bond linking the protein to the P-site tRNA and subsequent release of the neo-synthesized protein (Khoshnevis *et al.*, 2010; Shoemaker and Green, 2011) (**Figure I-10**).

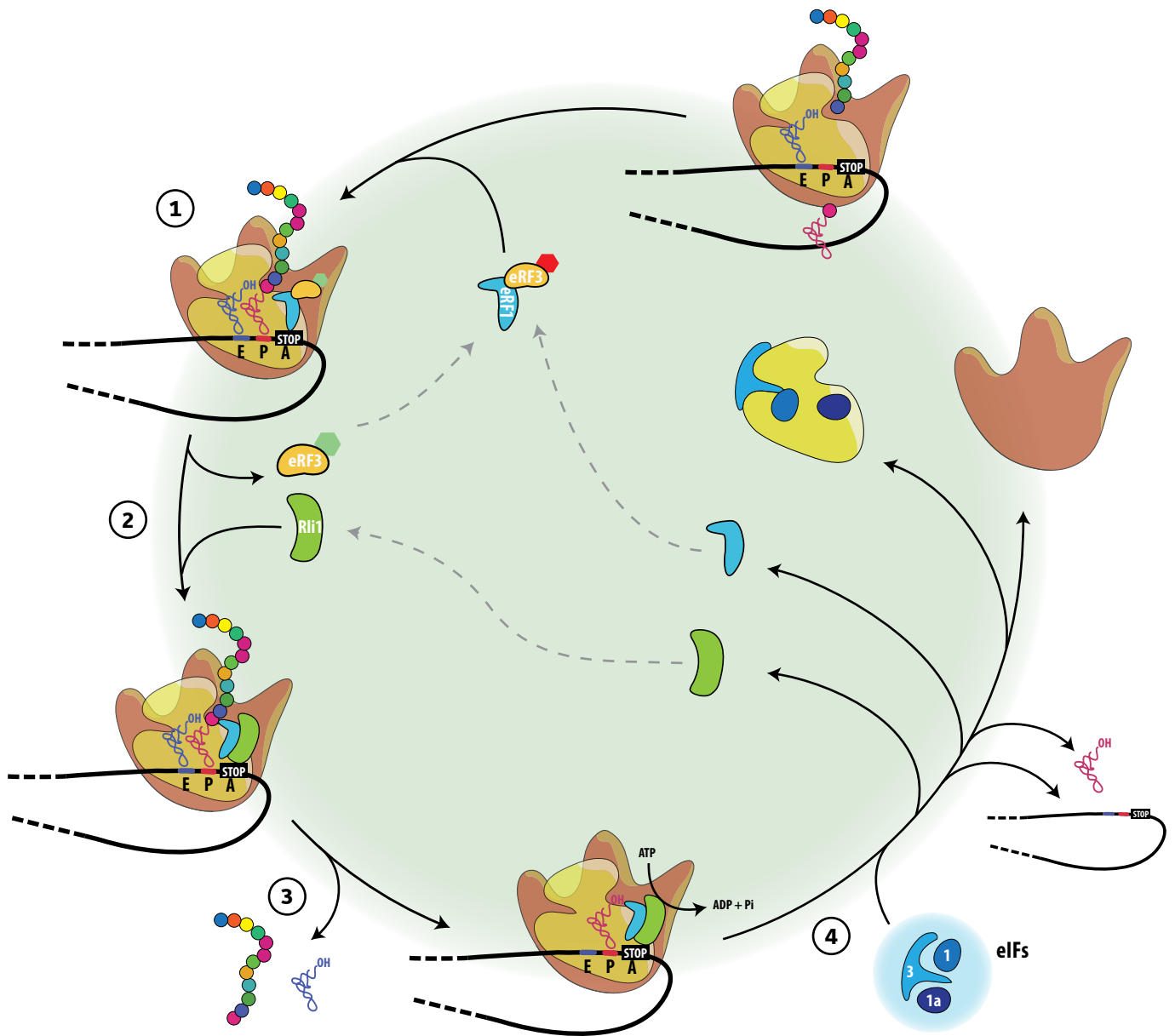


Figure I-10: Termination and recycling steps. ① The release factor eRF1 binds to eRF3•GTP and recognizes the stop codon in the A-site. ② GTP hydrolysis by eRF3 induces its release and the binding of Rli1 to eRF1, promoting hydrolysis of the ester bond and subsequent release of the neo-synthesized protein ③. ATPase activity of Rli1 promotes 80S ribosome dissociation and release of the deacylated tRNA and mRNA ④. These molecules can be recycled for another round of initiation.

The last step of translation, ribosome recycling, is crucial for ribosomal subunit dissociation prior to their participation in a new round of translation initiation. At this stage, the 80S ribosome is bound to the mRNA, the deacylated tRNA is in the P-site and eRF1•GTP•Rli1 complex is located in the A-site. The ATPase activity of Rli1 is important for this recycling since it promotes 80S ribosome dissociation into 60S and 40S subunits complexed with the deacylated tRNA and the mRNA (Pisarev *et al.*, 2010; Young *et al.*, 2015). The separated subunits are then bound by free initiation factors that can initiate translation on the same AUG start codon facilitated by the mRNA circularization, or on a different mRNA molecule. In few cases, reinitiation can occur significantly at a downstream start site of uORF of up to 35 codons (Rajkowitsch *et al.*, 2004).



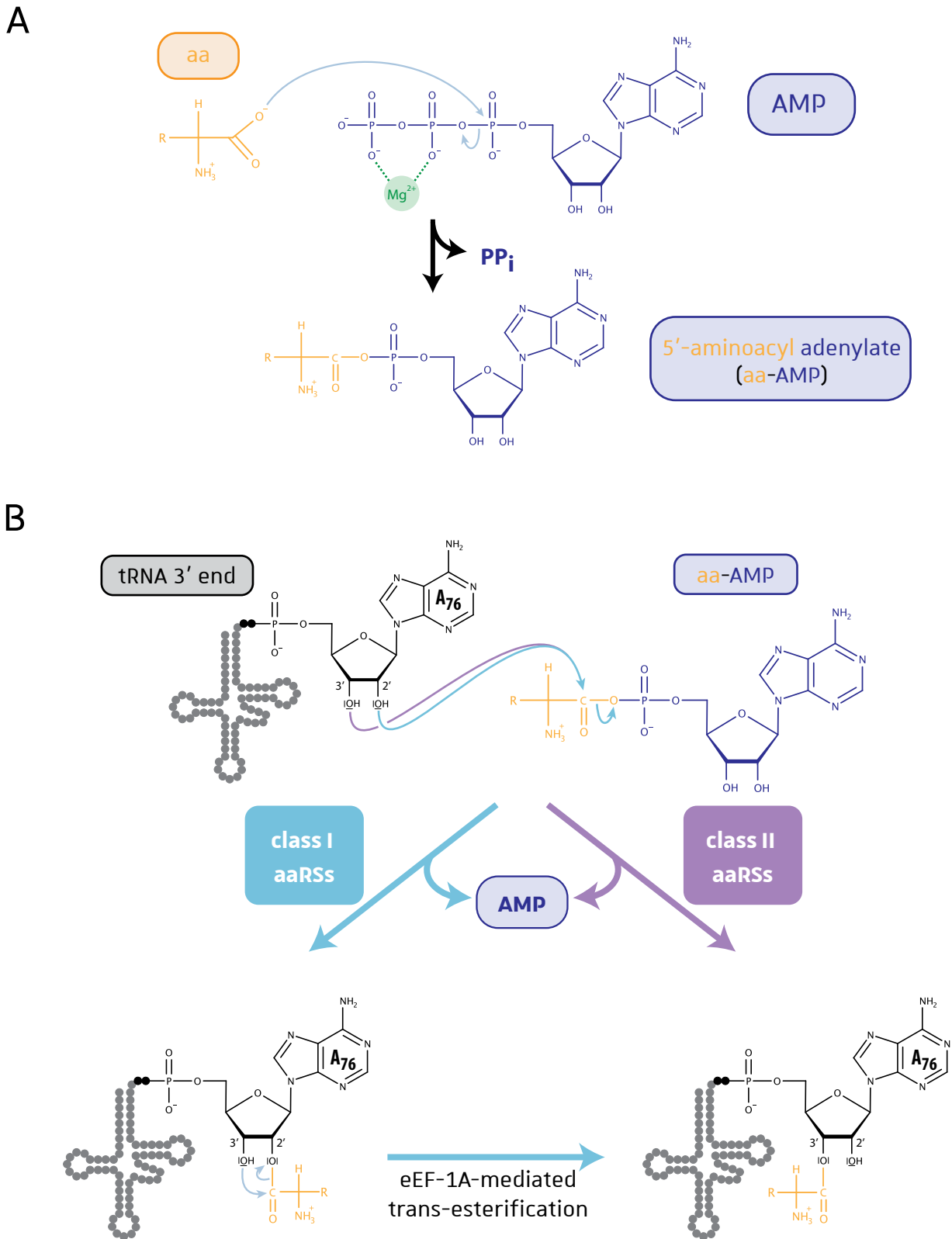


Figure I-11: The aminoacylation reaction proceeds through two steps. A. First step is the aa activation with ATP (stabilized with Mg^{2+}) to form the 5'-aminoacyl adenylate (aa-AMP). **B.** Second step is the aa attachment onto the 3' end of tRNA. According to the class of the aaRS, tRNA can be charged either on its 3'-OH end (class II) or on its 2'-OH end (class I). For the latter case, rapid trans-esterification occurs to charge tRNA in 3'-OH end.

II. The aminoacyl-tRNA synthetases (aaRSs) family

II.1. The canonical function of aaRSs

Aminoacyl-tRNA synthetases (aaRSs) constitute an ancient family of ubiquitous enzymes essential for life since they catalyse aminoacylation (or charging) of tRNAs (Fournier *et al.*, 2011). This reaction involves the attachment of an aa to its cognate tRNA in two sequential steps: the activation of the aa followed by its attachment onto an hydroxyl group of the terminal adenosine of the CCA sequence found at the 3' end of all tRNAs (Figure I-11). Activation of the aa requires ATP (stabilized with Mg^{2+} cation) to form an enzyme-bound intermediate: the 5'-aminoacyl adenylate or aminoacyl-AMP (aa-AMP) by formation of the mixed anhydride linkage between the aa carboxylic group and the α -phosphate of ATP (Figure I-11A). This reaction can occur in the absence of the cognate tRNA for all aaRSs except for ArgRS (Mitra and Mehler, 1966; Mehler and Mjtra, 1967), GluRS (Wen Lee, Ravel and Shive, 1967; Kern and Lapointe, 1979; Sekine *et al.*, 2006), GlnRS (Ravel *et al.*, 1965; Hong *et al.*, 1996) and class I LysRS (Ibba *et al.*, 1999). The mixed anhydride aa-AMP product then reacts with tRNA to form the aminoacyl-tRNA (aa-tRNA). The tRNA can be charged either on its 2'-OH of the terminal A_{76} by the class I enzymes or the 3'-OH of its terminal A_{76} by class II aaRSs (Arnez and Moras, 1997) (Figure I-11B). Since the final form of aa-tRNA bound to eEF1A is the one for which its terminal 3'-OH is esterified by the aa carboxylic group, and that the 3'-aminoacyl isomer is thermodynamically more stable than the 2'-isomer, a rapid trans-esterification occurs to charge tRNA in 3'-OH (Taiji, Yokoyama and Miyazawa, 1983). The overall aminoacylation reaction is thermodynamically driven to completion by the hydrolysis of the pyrophosphate (PP_i) formed and released during the aa activation step. The final aa-tRNA product is suitable for aa incorporation during protein synthesis.

II.2. aaRSs are divided into two classes

Most cells possess one cytosolic aaRS specific for each of the 20 standard proteinogenic aa. They all catalyse the same aminoacylation reaction using Mg^{2+} and ATP, an L-shaped tRNA and an aa. All these common features would suggest a common ancestor for these aaRSs, and the entire set of these enzymes should be structurally related. However, the analysis of aaRSs sequences, 3D structures and oligomerization states shows large differences within this family of enzymes (Eriani *et al.*, 1990; Ibba, Curnow and Söll, 1997). Actually, aaRSs do not show vertical inheritance from a

Table I-3: Standard classification and features of aaRSs based on structural and chemical properties

		Class I	Class II
Catalytic domain features	Structure	Rossmann nucleotide-binding fold (5 parallel β -strands with separated α -	7 anti-parallel β -strands flanked by α -helices
	Conserved signature sequence motifs	HIGH (His-Ile-Gly-His) KMSKS (Lys-Met-Ser-Lys-Ser)	Motif 1: +G Φ XX Φ X Λ P Φ Φ Motif 2: ++ Φ X Φ Λ XXFRXEX...(n = 4-12)...+ Φ XXFXX Φ Motif 3: Λ X Φ G Φ G Φ G Φ ER Φ Φ Φ Φ
Mechanistic features	tRNA 3' end hydroxyl group acceptor	2'OH	3'OH
	tRNA acceptor stem binding	Via the minor groove side of the helix	Via the major groove side of the helix
	ATP conformation when bound to aaRS	Straight conformation	Bent conformation
	Terminal tRNA CCA	Hairpin (bent) conformation	Extended conformation
	Rate-limiting step	Release of aminoacyl-tRNA	Amino acid activation and/or transfer on tRNA
		aaRS Oligomerization Edited aa	aaRS Oligomerization Edited aa
aaRS subclasses	Subclass a	MetRS α Hcy	SerRS α 2 Thr, Cys
		ValRS α Thr, Abu	ThrRS α 2 Ser
		IleRS α Val, Cys	AlaRS α 2 Ser, Gly
		LeuRS α Nva, Ile	GlyRS α 2
		CysRS α	ProRS α 2 Ala, Cys
	Subclass b	ArgRS α	HisRS α 2
		GluRS α	AspRS α 2
		GlnRS α	AsnRS α 2
	Subclass c	LysRS α	LysRS α 2 Orn, Hcy, Hse
TyrRS α 2		PheRS ($\alpha\beta$)2 Tyr, Ile	
TrpRS α 2		SepRS α 4	
		PylRS α 2	

Table designed with data from Ribas de Pouplana and Schimmel, 2001; Perona and Hadd, 2012; Perona and Gruic-Sovulj, 2013. In bold, aaRS catalysing the tRNA-dependent aa activation. Underlined: 2'OH attachment +: basic; Φ : hydrophobic; Λ small aa; X:any aa.

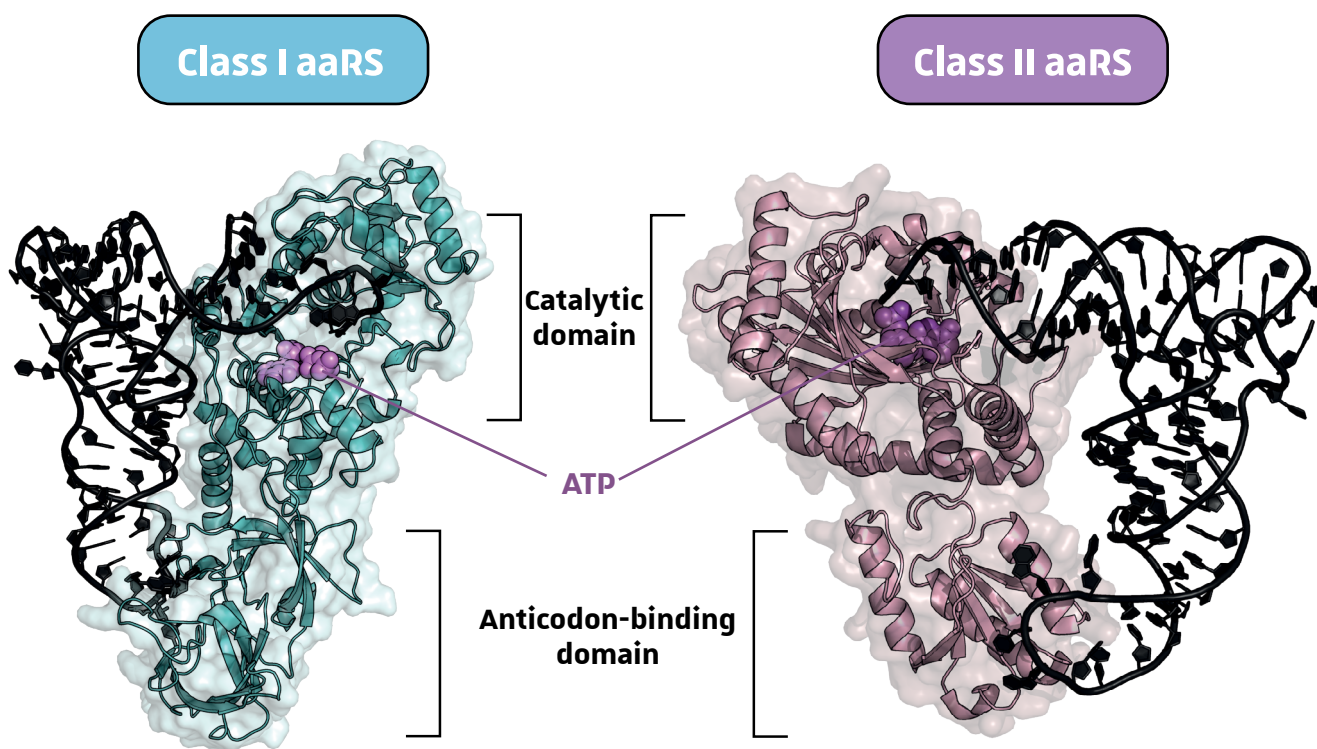


Figure I-12: Crystal structure and organization of aaRSs and their interaction with tRNA and ATP. Class I aaRSs (left) recognize tRNA via the minor groove, and bent the terminal CCA end, whereas class II aaRSs (right) bind the major groove side of tRNA. Class I aaRS structure: *E. coli* GlnRS (pdb 1GTR); Class II aaRS structure: *E. coli* ThrRS (pdb 1QF6).

common ancestral enzyme and are divided into two distinct evolutionarily unrelated classes that differ on the basis of their structural motifs, anticodon recognition, site of aminoacylation and aa specificity (Ribas de Pouplana and Schimmel, 2001; Perona and Hadd, 2012) **Table I-3**). Each aa is specified by a class I or class II aaRS, with the exception of LysRS that can only be found as a class II enzyme in eukaryotes, in majority of bacteria and a small number of archaea, and as a class I aaRS in most archaea and few bacteria (Ambrogelly, Korencic and Ibba, 2002).

II.2.1. Class I aaRSs

The aa for which the class I aaRSs are specific tend to be larger and more hydrophobic than those of the other class II. Class I aaRSs are subdivided in three subclasses. These enzymes are mostly monomeric, except for the two Ic aaRS subclasses, TyrRS and TrpRS, which are catalytically active only as homodimer (Beikirch, von der Haar and Cramer, 1972; Hossain and Kallenbach, 1974). All eleven class I aaRSs share two conserved sequence motifs for which the consensus sequence is HIGH and KMSKS and possess a catalytic domain based on the Rossmann nucleotide-binding fold. These two HIGH and KMSKS motifs form the ATP-binding site, essential for aa activation, that binds ATP in an extended conformation (Rould *et al.*, 1989). This catalytic domain is split in two halves by an inserted domain called CP1 (Connective Polypeptide 1), which binds the tRNA 3'-single stranded end (containing the CCA) in a bent conformation. However, for the homodimeric TrpRS and TyrRS, this inserted domain constitutes the dimer interface (Doubl   *et al.*, 1995) and for LeuRS, IleRS and ValRS the CP1 domain is a hydrolytic editing domain that ensures aa fidelity (Betha, Williams and Martinis, 2007). Class I aaRSs bind the tRNA acceptor-stem *via* the minor groove side through their C-terminal anticodon-binding domain (ABD), orienting the terminal A₇₆ 2'-OH group for attachment of aa (Sprinzl and Cramer, 1975) (**Figure I-12**).

II.2.2. Class II aaRSs

This class contains ten aaRSs for the standard aa, but recently 2 additional aaRSs that structurally belong to class II enzymes were added to the subclass IIc: the O-phosphoserylRS (SepRS) and the pyrrolysylRS (PylRS) that are mostly found in methanogenic archaea. All class II aaRSs are either homodimers (α_2 or α_4) or heterotetramer ($(\alpha\beta)_2$ for PheRS). Class II enzymes share three consensus sequence motifs in their catalytic domain called motif 1, 2 and 3 (Cusack *et al.*, 1990), see detailed sequences in **Table I-3**). Most of the time, the dimer interface includes motif 1, and motifs 2 and 3

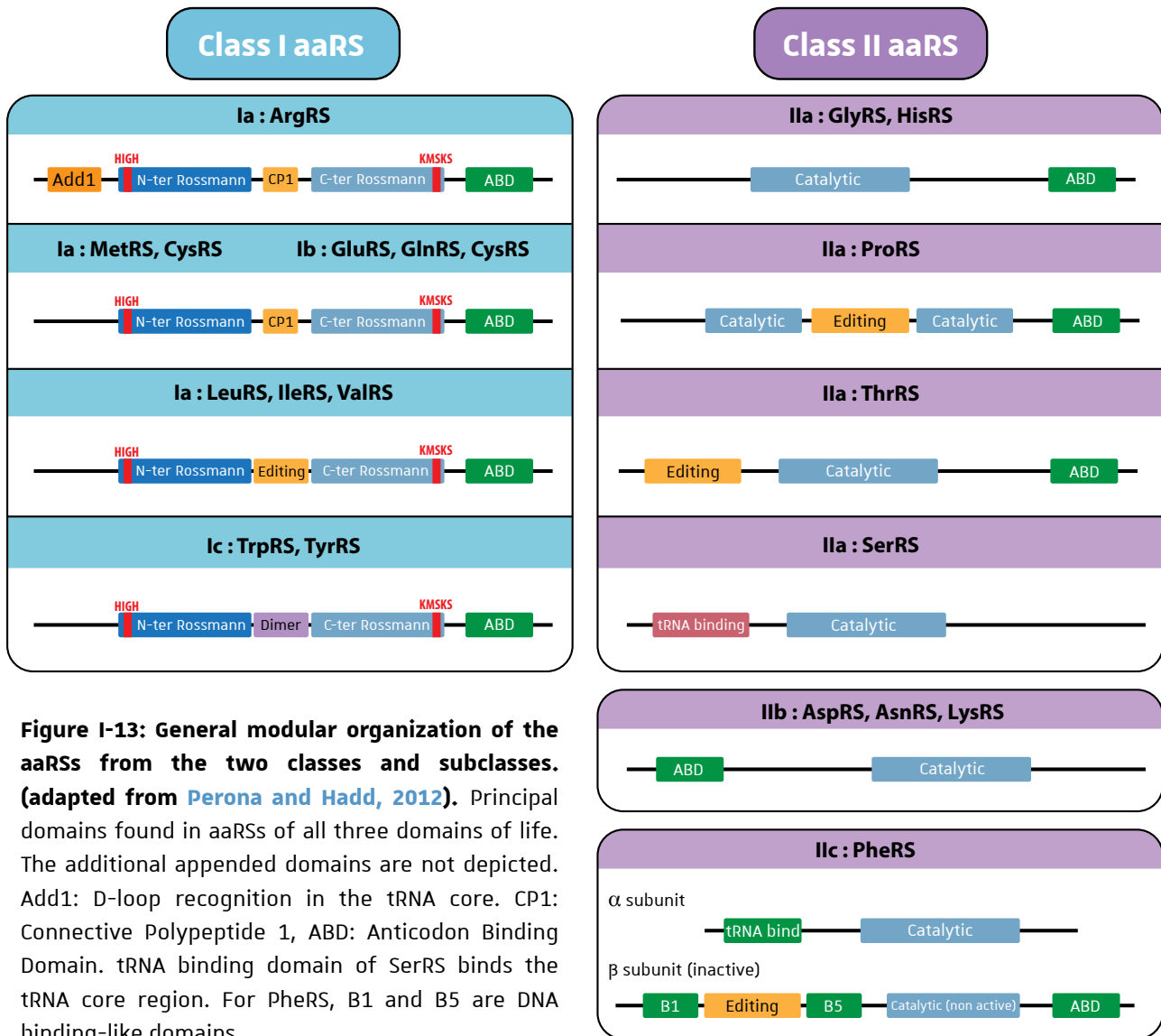


Figure I-13: General modular organization of the aaRSs from the two classes and subclasses. (adapted from Perona and Hadd, 2012). Principal domains found in aaRSs of all three domains of life. The additional appended domains are not depicted. Add1: D-loop recognition in the tRNA core. CP1: Connective Polypeptide 1, ABD: Anticodon Binding Domain. tRNA binding domain of SerRS binds the tRNA core region. For PheRS, B1 and B5 are DNA binding-like domains.

are both part of the catalytic site. These aaRSs bind ATP in a bent conformation and bind the tRNA acceptor-stem *via* the major groove side resulting in 3'-OH charging, except for PheRS (2'-OH) and AsnRS (both 2'-OH and 3'-OH) (Sprinzl and Cramer, 1973; Sprinzl, 2006). Differential binding of tRNA by the two aaRS classes has consequences on the solvent exposition of the tRNA domains: variable loop of tRNA recognized by class I aaRSs is exposed to the solvent, whereas it faces the enzyme for class II aaRSs (Figure I-12). Class II aaRSs are also subdivided in three subclasses. aaRSs from subclass IIa are specific for hydrophobic and small polar aa (Table I-3). Their ABD domain is also localized at the C-terminus, with the exception of SerRS that does not use the anticodon-stem to discriminate its cognate tRNA but rather the acceptor- and D-stem (Figure I-13, Normanly, Ollick and Abelson, 1992). One feature of subclass IIb is that they all bind a tRNA with a central uridine 35 base (U_{35}) in the anticodon loop. This subclass is specific for charged and large polar aa (Asn, Asp and Lys) and present a N-terminally-located ABD adopting an OB-fold (Figure I-13). The PheRS is the "standard" aaRS present in the subclass IIc and is active as a $(\alpha\beta)_2$ heterotetramer. The α subunit catalyses the two-step aminoacylation reaction, and the tRNA binding site is located across both α and β subunits. Two other aaRSs (PylRS and SepRS) belong to this subclass IIc but are present only in methanogens and few bacteria (Kavran *et al.*, 2007; Hauenstein, Hou and Perona, 2008). The PylRS charges pyrrolysine onto a suppressor tRNA^{pyl} to incorporate this aa at UAG stop codon (Srinivasan, James and Krzycki, 2002), whereas the SepRS incorporates the nonstandard aa phosphoserine onto tRNA^{Cys} to generate the Cys-tRNA^{Cys} by a two-step tRNA-dependent aa modifying pathway.

II.3. Translational fidelity and quality control

The fidelity of translation relies on several steps, from the association between an aa and its cognate tRNA to the accurate base pairing of the aa-tRNA anticodon with the mRNA codon. Even though normal cellular functions would need absolute accuracy, translation appears to be the most error prone process with 10^{-4} error rate, compared to replication (10^{-8}) and transcription (10^{-5}) (Rosenberger and Hilton, 1983; Kunkel and Bebenek, 2000). A big part of the translation fidelity relies on the accuracy of the aminoacylation reaction: charging the wrong aa onto a tRNA (or the right aa on the wrong tRNA) would result in aa misincorporation inside proteins, even if there is a perfectly accurate codon-anticodon pairing inside the ribosome A-site. Thus, aminoacylation is of first importance for maintenance of the genetic code integrity and relies on quality control steps made by aaRSs that target both the aa activation step and the aa-tRNA prior its release from the enzyme.

Table I-4: Yeast tRNA identity elements and anti-determinants

	tRNA	Identity elements	Anti-determinants (aaRS blocked)	Identity elements position on tRNA structure
Class I	Arg	C35, G/U36	C6-G67 (AspRS)	
	Trp	A73, C34, C35	U28-A42, A37 (mammalian TrpRS)	
	Ile	I/Ψ34, A35, U36	U30-G40 (GlnRS, LysRS) U34 (MetRS)	
	Leu	A73, A35, G37, V-loop	V-loop (?)	
	Met	A73, C32, U33, C34, A35, U36, A37, A38, D-arm		
	Cys	U73, G34, C35, A36		
	Tyr	A73, C1-G72, G34, Ψ35, A36		
	Val	A73, A35		
	Glu			
Gln				
Class II	Ser	A-stem, V-loop	G37 (LeuRS)	
	Asp	G73, G34, U35, C36, C38, G10-U25	m ⁷ G37 (ArgRS)	
	Ala	G3-U70	G3-U70 (ThrRS)	
	Thr	G1-C72, G35, U36		
	Gly	A73, C2-G71, G3-C70, C35, C36		
	His	A73, (5'p)G-1, G34, U35		
	Phe	A73, G34, A35, A36, G20		
	Lys			
	Asn			
Pro				

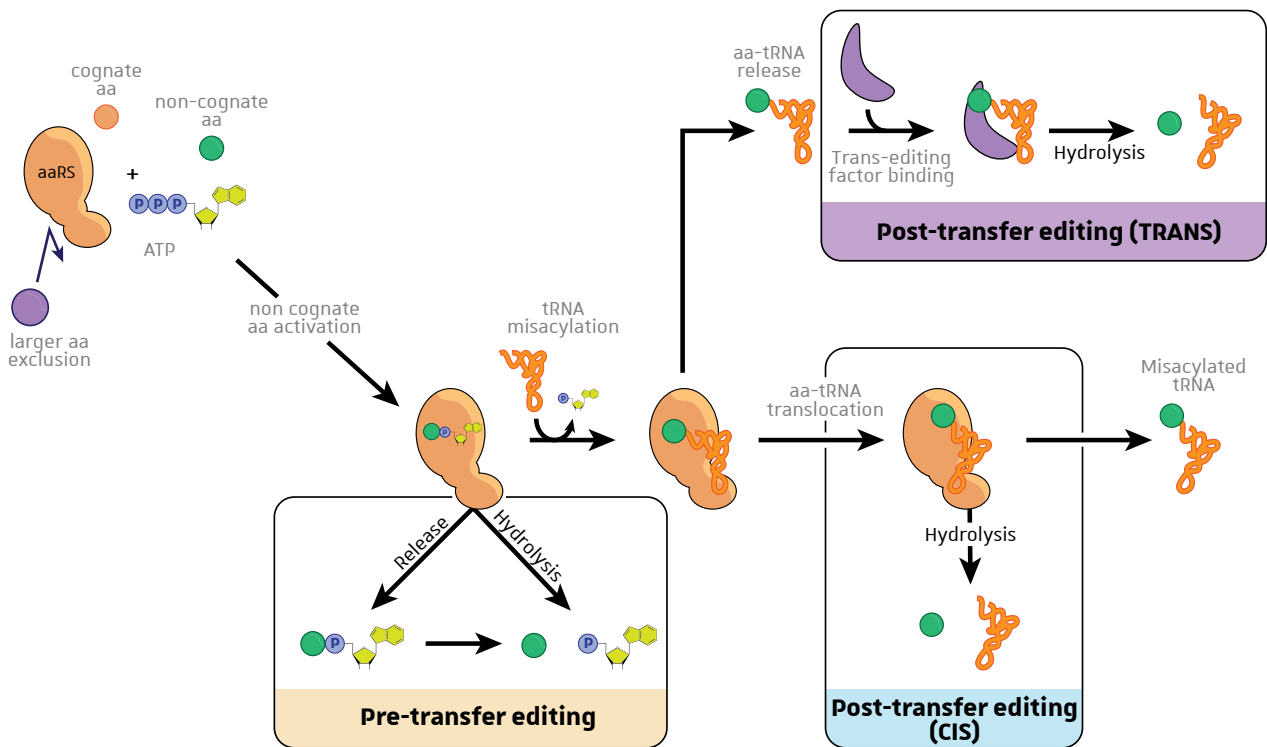
Adapted from Giegé, Sissler and Florentz, 1998 and Vasil'eva and Moor, 2007. Color used are same as Figure I-4 and Table I-2.

II.3.1. tRNA identity

As described previously, all tRNAs share common features in terms of three-dimensional structure (L-shaped) and length. As a rule, each aaRS needs to bind and charge specifically its corresponding set of tRNAs, called isoacceptor tRNAs. According to yeast tRNA sequences alignment (**Table I-2**, page 32), some regions like D- and T-hairpins are more conserved and are not considered as specificity determinants. However, isoacceptor tRNAs share common features mostly found in the acceptor-stem and the anticodon region. In a tRNA, nucleotides whose mutations are accompanied by a loss of tRNA aminoacylation efficiency by their cognate aaRSs are designated as identity elements or identity determinants, and are preferentially positioned in the anticodon loop and acceptor-stem ([Giegé, Sissler and Florentz, 1998](#); [Vasil'eva and Moor, 2007](#)). Common identity elements are the anticodon triplet positions (mostly nucleotides 35 and 36, as nucleotide 34 is the wobble position) and the nucleotide 73 also called "discriminator base". In addition to these nucleotides, variable loops for tRNA^{Leu} and tRNA^{Ser} would likely participate to the accuracy of aminoacylation through steric hindrance. Moreover, some nucleotides prevent tRNA recognition by nonspecific aaRS and are called anti-determinants. All known positive and negative signals in yeast are listed in **Table I-4**. It is not surprising that the vast majority of tRNA determinants are located within the acceptor-stem, D-arm and anticodon loop since these residues are usually in close contact with aaRSs during aminoacylation (**Table I-4** (right part) and **Figure I-12**, page 48). As we saw previously, tRNAs undergo numerous post-transcriptional modifications that can be altered during a cellular stress. Some of these modifications can play an important role in tRNA recognition to prevent misselection and would represent stress-sensitive determinants for aminoacylation accuracy.

II.3.2. aaRS proofreading of misacylated tRNAs

Even though tRNA mischarging is mostly prevented by tRNA identity signals and the diversity of tRNA sequences, it is more difficult for an aaRS to select its cognate aa from the 19 remaining ones (in standard genetic code) since 2 different aa can differ by only one methyl group (Cys and Met) or one hydroxyl group (Phe and Tyr). Thus, aa misactivation is a not rare and needs to be corrected. AaRSs that have a tendency to misactivate near-cognate aa have editing domains that will proofread the mischarged tRNA formed after aa misactivation ([Ling, Reynolds and Ibba, 2009](#)). The first sieve preventing non-cognate aa binding is the active site structure and size that enables binding of cognate and smaller aa, but excludes the larger ones. However, if a non-cognate aa is



Pre-transfer editing aaRSs	Pre & Post-transfer editing aaRSs	Trans-editing factors
MetRS <i>Hcy, Nle</i>	LeuRS <i>Met, Val, Ile, Nva, Hcy, Nle</i>	YbaK <i>Cys-tRNA^{Pro}</i>
SerRS <i>Thr, Cys, SerHX</i>	IleRS <i>Val, Cys, Thr, Leu, Hcy, Nle, Abu</i>	ProX <i>Ala-tRNA^{Pro}</i>
LysRS <i>Met, Leu, Cys, Hcy, Hse, Orn, Nle, Nva</i>	ValRS <i>Thr, Cys, Ala, Abu, Hcy, Nle</i>	AlaX <i>Ser-tRNA^{Ala} Gly-tRNA^{Ala}</i>
	ThrRS <i>Ser</i>	
	PheRS <i>Tyr, Ile</i>	
	ProRS <i>Ala, Cys, 4hPro</i>	
	AlaRS <i>Gly, Ser</i>	

Figure I-14: aaRS editing process (inspired from Ling, Reynolds and Ibba, 2009). The editing aaRSs with their corresponding edited aa are listed in the lower panel, as well as trans-editing factors with their associated edited aa-tRNA.

activated this misactivated aminoacyl-adenylate can be first hydrolysed by the enzyme prior to transfer of the aminoacyl moiety to the 3' end of tRNA: this process is called pre-transfer editing. This intermediate can be either hydrolysed directly within the active site, or can translocate to the editing site before hydrolysis. Alternatively, it can be released from the aaRS into solution and spontaneously hydrolysed (**Figure I-14**). Moreover, if the misactivated aa is transferred to the tRNA, the resulting misacylated tRNA can also be proofread in a separate editing domain through translocation and hydrolysis of the ester bond, a process called post-transfer editing (**Figure I-14**). All these editing activities act in "cis" meaning that they are catalyzed by a separate domain but physically attached to the same aaRS that synthesizes the misacylated tRNA. However, post-transfer editing can also occur after release of the final misacylated tRNA by autonomous trans-editing factors specific for misacylated tRNA^{Pro} and tRNA^{Ala} (list **Figure I-14**).

II.3.3. Beneficial misacylation

Despite all these editing processes, mischarging of tRNAs can occur inside cells. In some cases and some organisms, misacylation is even beneficial for cells because the mischarged tRNA is an obligatory intermediate in the formation of an aa-tRNA. Indeed the synthesis of some aa-tRNA species is made by a two steps pathway that requires first misacylation of a non-cognate tRNA by a non-discriminating aaRS and then tRNA-dependent conversion of the aa moiety (see §II.4). Besides this particular case, misacylation leads to challenging of the genetic code integrity during ribosomal translation that results in the so-called mistranslation. These errors of mRNA decoding were thought to be highly disadvantageous for cells, and that highly accurate proteome was required to support life (Orgel, 1963; Crick, 1968). Previous studies have shown that mistranslation was not a rare event and that several organisms could tolerate a relatively high level of aa misincorporation (Drummond and Wilke, 2009; Kramer *et al.*, 2010). For example, it has been shown that *E. coli* can grow similarly to wild type with 10 % Asp misincorporated instead of Asn by activating a compensatory heat shock response to discard misfolded proteins (Ruan *et al.*, 2008). Although mistranslation is generally considered as deleterious, it can be beneficial for cells under specific conditions: oxidative stress (Wiltrout *et al.*, 2012), antibiotics, immunoresistance and antifungal resistance (Meyerovich, Mamou and Ben-Yehuda, 2010), usually by creating cell surface variation (Miranda *et al.*, 2013). Obviously, most of mistranslated proteins appear during stress or because growth conditions varied, and it is often difficult to establish if mistranslation is only a consequence of this stress or an adaptation to increase cell survival. Since the beginning of the 60's, several studies have reported mistranslation

Table 1-5: Errors made by the translation machinery and description of techniques used to study mistranslation

aa (codon) misread	aa replaced	Error rates	Organism	Description of the technique used in the study	Condition of the experiment	Reference
Radio-labelled methods						
Ile	Val/Leu	0.03 %	Chicken (oviduct)	Ovalbumin sequence analysis with radioactive Val, Leu and Ile	Basal	[61]
Ile	Val	0.01 %	Rabbit (reticulocytes)	Rabbit hemoglobin sequence analysis with radioactive Val	Basal	[62]
Arg(CGU/C)	Cys	0.001-0.01 %	<i>E. coli</i>	35S-Cys labelling and purification of flagellin (do not contain Cys residue)	Basal and antibiotic stress	[63]
Asn(AAU/AAC)	Lys	0.001-0.01 %	<i>E. coli</i>	Isoelectric focusing pattern analysis with radioactive Met, Pro or Leu	Asn or Lys starvation in relA strain	[64]
Arg/Trp	Cys	0.1 %	<i>E. coli</i>	Radioactive labelling with 35S-Cys followed by proteolytic cleavage of ribosomal proteins L7/L12 and S6.	Basal	[65]
UGA readthrough		1%	<i>E. coli</i>	3H-Leu labelling of bacterial cells infected with Qbeta phage and SDS-PAGE analysis	Infected <i>E. coli</i> cells with phage	[66]
Global	His/Trp	0.1-1 %	<i>E. coli</i>	14C-His or 14C-Trp labelling of <i>E. coli</i> infected with Qbeta phage, SDS-PAGE and band excision	Infected <i>E. coli</i> cells with phage	[66]
Phe	Leu	1-5 %	<i>S. solifataricus</i>	Poly(U) derived cell free polypeptide system with radioactive Phe and Leu	Aminoglycoside antibiotics	[67]
Mass spectrometry methods						
Arg(AGA)	Lys	40%	<i>E. coli</i>	MS analysis on well expressed protein.	Basal	[68]
Asn	Asp	10%	<i>E. coli</i>	MS analysis on DHFR(S3N) protein	Basal condition with D. radiodurans ND-AsPRS expression	[69]
Ser(CUG)	Leu	3-5 %	<i>C. albicans</i>	Purification of PKG modified reporter and mass spectrometry peptide analysis	Basal, H2O2, pH or T° changing	[70]
Many aa		0.001-0.1 %	Mammalian (CHO cells)	MS on recombinant IgG2 in mammalian cells and recombinant protein in <i>E. coli</i> .	Basal	[71]
			<i>E. coli</i>	MS on purified human serum albumin		
Phe	Tyr	8%	<i>S. cerevisiae</i>	MS on reporter elastin-like polypeptide sequence	Minimal medium or with excess of Tyr. in WT or phePS editing deficient strains	[72]
Protein reporter based methods						
Gly(GGC)	Ser	0.1 %	<i>E. coli</i>	Beta-lactamase (S68G) reporter activity	Basal and for WT, rpsD and rpsL strains	[73]
Ala(GCU)	His	0.002 %	<i>S. cerevisiae</i>	Catalytic reporter CATIII(H195A) assay	Basal	[74]
Tyr(UAC)	His	0.0005 %	<i>S. cerevisiae</i>	Catalytic reporter CATIII(H195Y) assay	Basal and paromomycin treatment	[74]
UGA readthrough		5%	<i>B. subtilis</i>	LacI gene with non-sense mutation and LacZ gene activity reading	Basal on WT and rpsL mutant	[75]
Val	Thr	15%	Human (NH/3T3 cells)	GFP(T65V) reporter	Basal with editing deficient VALRS	[76]
24 codons	Lys	0.01 %	<i>E. coli</i>	Dual reporter Fireflies Luciferase(K529X)-Renilla Luciferase, measure of luciferase activity	Basal and antibiotic stress	[77]
UAA/JUGA readthrough	ND	0.4 %	<i>B. subtilis</i>	Fluorescent GFP reporter with non-sense mutation	Basal, stationary phase, different temperatures	[78]
Asn	Asp	0.8 %	<i>M. smegmatis</i>	Dual reporter Renilla Luciferase(D120N or E144Q)-Firefly Luciferase, measure of luciferase activity	Log and stationary phase, low pH	[79]
Gln	Glu	0.2 %	<i>M. smegmatis</i>	mCherry(M72X)-GFP reporter	Basal - Oxidative conditions	[79]
Glu	Met	1-10 %	Human (HEK cells)			[80]
Pro	Ala	2.8 %	<i>S. cerevisiae</i>	GFP(D129P) reporter	Basal condition	[81]
		8.9 %		tRNA ^{Pro} G3:U70 overexpressed		
Pro	Ala	2-5 %	Human (HEK cells)	GFP(D129P) reporter	tRNA ^{Pro} G3:U70 overexpressed	[82]

Similar tables found in [Ou et al, 2019](#); [Mohler and Ibba, 2017](#).

cases, either in basal conditions or in stress-induced cells, and methods have evolved to be more precise and accurate, from radioactive labelling to new enzymatic or fluorescent reporter systems (listed in **Table I-5**).

II.4. Incorporation of non-standard aa and indirect pathways

II.4.1. The two non-standard aa incorporation

In addition to the 20 standard genetically-encoded proteinogenic aa, two additional aa have been found to be genetically encoded in some genomes: selenocysteine (Sec) and pyrrolysine (Pyl), respectively known as the 21st and 22nd genetically encoded aa. The latter is a modified lysine with a 4-methylpyrroline-5-carboxylate group linked by an amide to the Nε (**Figure I-15A**) and was first discovered in 2002 in methanogenic archaea of the *Methanosarcinaceae* family and later in bacteria ([Hao et al., 2002](#); [Zhang and Gladyshev, 2007](#)). In these methanogenic archaea, genes encoding methylamine methyltransferases (enzymes essential to generate methane) contain an in-frame UAG amber stop codon that is read through by the ribosome and translated by pyrrolysyl residue. This residue appears to be crucial for the enzyme activity. Pyrrolysyl-tRNA^{Pyl} is made by direct attachment of Pyl to this amber suppressor tRNA^{Pyl(CUA)} by the class IIc PylRS ([Blight et al., 2004](#)). The structure of tRNA^{Pyl} differs from the classical tRNA structure since it displays a D-loop with only 5 nucleotides, an AC-stem with 6 bp, and a TΨC-loop without these three residues sequence. The mRNA sequence context is also important for Pyl insertion since a specific Pyl Insertion (PYLIS) element next to the UAG Pyl codon of the mRNAs of methylamine methyltransferases has been shown to promote Pyl insertion ([Théobald-Dietrich, Giegé and Rudinger-Thirion, 2005](#)). Pyl incorporation has become the first known example so far, of direct aminoacylation of a tRNA with a nonstandard aa. Indeed, incorporation of the 21st aa, Sec, discovered in 1986 both in mammals and bacteria ([Chambers et al., 1986](#); [Zinoni et al., 1986](#)) has been shown to proceed *via* two consecutive steps ([Lee et al., 1989](#)) (**Figure I-15B**). Sec residue can be found in the active sites of selenoproteins (25 genes encoding selenoproteins in mammals, none in fungi and higher plant) mostly to perform catalytic redox reactions ([Arnér, 2010](#)). This aa is generated by tRNA-dependent modification of a precursor aa attached to the opal suppressor tRNA^{Sec}. First tRNA^{Sec} is charged with Ser by the SerRS to form Ser-tRNA^{Sec}. This is possible because tRNA^{Sec} resembles tRNA^{Ser} in such an extent that it can be recognized by SerRS. However, since tRNA^{Sec} presents a longer acceptor stem and D-stem, a long variable arm and usually a shorter TΨC-loop, the misacylated Ser-tRNA^{Sec} is not able to bind EF-Tu,

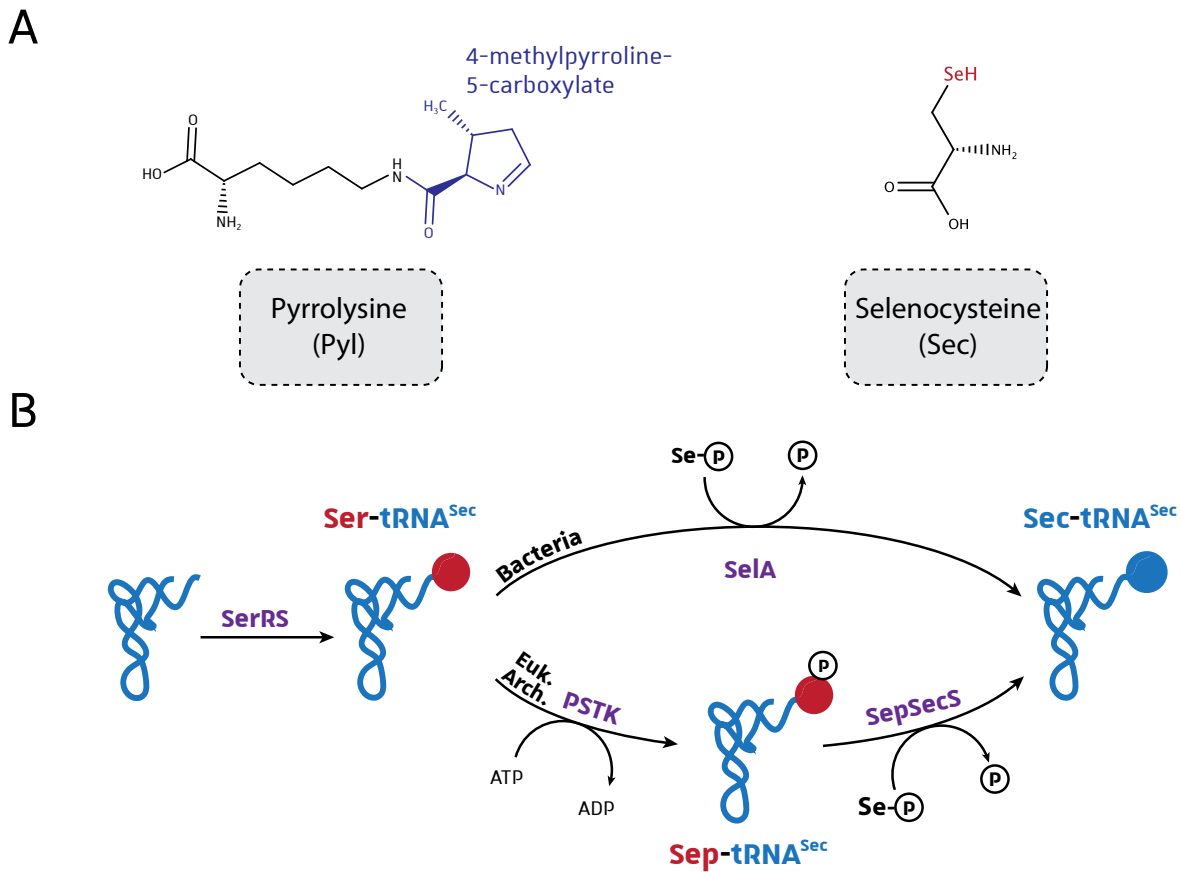


Figure I-15: The 21st and 22nd genetically encoded amino acids. **A.** Chemical structure of pyrrolysine (Pyl) and selenocysteine (Sec). **B.** Two-step pathway of $\text{Sec-tRNA}^{\text{Sec}}$ synthesis in bacteria and three step pathway in eukarya (Euk.) and archaea (Arch.). Se-P , selenophosphate; Sep, O-phosphoseryl. Adapted from Yuan *et al*, 2008.

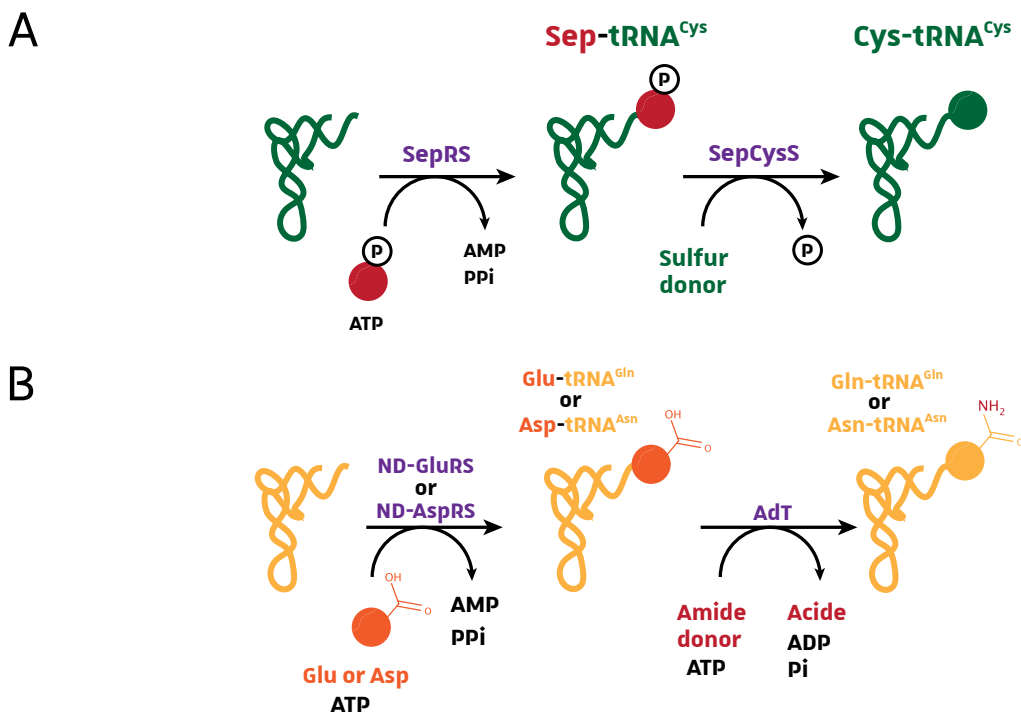


Figure I-16: Indirect pathways of aa-tRNA biosynthesis (Adapted from Yuan *et al*, 2008). **A.** Lack of CysRS in some archaea is counterbalanced by a two-step pathway. **B.** Two-step pathway for amide aa-tRNA synthesis in some archaea and in eukaryotic organelles.

preventing the misincorporation of Ser (Hubert *et al.*, 1998). After serylation of tRNA^{Sec}, the seryl residue is either (i) directly selenylated by Sela to form Sec-tRNA^{Sec} like in bacteria (Leinfelder *et al.*, 1988), or (ii) is phosphorylated by *O*-phosphoseryl-tRNA-kinase (PSTK) to form *O*-phosphoseryl-tRNA^{Sec} (Sep-tRNA^{Sec}) and subsequently selenylated by the SepSecS enzyme in eukaryotes and archaea (Yuan *et al.*, 2006). Both Sela and SepSecS are PLP-dependent enzymes and use selenophosphate as selenium donor (**Figure I-15B**). The subsequent Sec-tRNA^{Sec} is then brought to elongating ribosomes by specific elongation factors: SelB in bacteria and the eEFSec•SBP2 complex in eukaryotes (Forchhammer, Leinfelder and Böck, 1989; Copeland *et al.*, 2000; Fagegaltier *et al.*, 2000). These factors bring the aminoacyl-tRNA to the ribosome to recode the UGA “opal” stop codon present in a *cis*-acting stem loop structure called SECIS usually found in the 3'-UTR of selenoprotein complex mRNAs (Low and Berry, 1996).

II.4.2. Indirect pathways of aa-tRNA biosynthesis

We have seen that Sec incorporation required more steps than the classical aminoacylation mechanism used for the standard aa. However, for some organisms this indirect pathway is also needed to aminoacylate tRNAs with standard aa. For the majority of eukaryotes and very few bacterial species, the 20 different types of standard aa-tRNA are catalyzed by a full and unique set of the 20 different aaRSs. But in the majority of bacteria and all archaea, one or more aaRSs genes are missing, suggesting that aminoacylation of the corresponding orphan tRNAs is made by a non-conventional route. The best example to illustrate this case is the genome of the archaeon *Methanocaldococcus jannaschii* sequenced in 1996 and lacking three expected aaRS genes: those encoding CysRS, AsnRS and GlnRS (Bult *et al.*, 1996). It was shown that in these archaea, the lack of CysRS is compensated by a tRNA^{Cys}-dependent two-step pathway analogue to Sec-tRNA^{Sec} formation in bacteria (**Figure I-16A**). In this pathway, tRNA^{Cys} is first mischarged by the SepRS with Sep, then the Sep moiety is tRNA-dependently converted into Cys by the SepCysS enzyme (Sauerwald *et al.*, 2005). AsnRS and GlnRS specific for amide aa (Gln and Asn) are also often missing in archaea (all are missing GlnRS), most bacteria, and organelles (only for GlnRS), meaning that classical tRNA charging with these two aa cannot be made directly. Instead, the metabolic precursors of Gln and Asn, Glu and Asp, are first attached to the non-cognate tRNA^{Gln/Asn} by a non-discriminating (ND) aaRS (ND-GluRS/ND-AspRS) (Lapointe, Duplain and Proulx, 1986; Becker *et al.*, 1997) (**Figure I-16B**). The misacylated Glu/Asp-tRNA^{Gln/Asn} is then amidated into the correct amide aa-tRNA by a tRNA-dependent amidotransferase (AdT) called GatCAB (bacteria, archaea and organelles) or GatDE

Table I-6: Description of the two-step pathways of aa-tRNA synthesis

aa incorporated	Organism	First step		Second step		Elongation factor
		aaRS	aa-tRNA	Modifying enzyme	Final product	
Non standard aa	Bacteria	SerRS	Ser-tRNA ^{Sec}	SelA	Sec-tRNA ^{Sec}	SelB
	Eukaryotes*, archaea	SerRS	Ser-tRNA ^{Sec}	(1) PSTK (2) SepSecS	(1) Sep-tRNA ^{Sec} (2) Sec-tRNA ^{Sec}	eEFSec•SBP2
Classical aa	Methanogenic archaea	SepRS	Sep-tRNA ^{Cys}	SepCysS	Cys-tRNA ^{Cys}	eEF1A, EF-Tu
	Archaea, bacteria	ND-AspRS	Asp-tRNA ^{Asn}	Asp-AdT Archaea : GatCAB Bacteria : GatCAB	Asn-tRNA ^{Asn}	eEF1A, EF-Tu
	Mitochondria, chloroplasts, archaea, bacteria	ND-GluRS	Glu-tRNA ^{Gln}	Glu-AdT Yeast mito : GatFAB Archaea : GatDE Bacteria : GatCAB	Gln-tRNA ^{Gln}	eEF1A, EF-Tu

* No Sec incorporation in Fungi

(only archaea) (Curnow *et al.*, 1997; Becker and Kern, 1998). So far, four types of tRNA-dependant amidotransferases are known: the heterotrimeric GatCAB and GatFAB, and the heterodimeric GatDE and GatAB. The GatCAB has been found in both archaea and bacteria, but functions as an Asp-AdT in archaea, and also as a dual Asp-AdT and/or Glu-AdT in bacteria (Sheppard *et al.*, 2008; **Table I-6**). The heterodimeric GatDE is archaea-specific and is a specific Glu-AdT (Tumbula *et al.*, 2000). In eukaryotic organelles such as mitochondria and chloroplasts, the organellar GlnRS is absent and the indirect pathway involving the GatCAB Glu-AdT enzyme generates the organellar Gln-tRNA^{Gln} (Pujol *et al.*, 2008; Nagao *et al.*, 2009). More recently, the new homodimeric GatAB complex has been found in the apicoplast of the human parasite *Plasmodium falciparum* with a Glu-AdT activity (Mailu *et al.*, 2015). The last heterotrimeric Gat complex has been found in the yeast mitochondria for the formation of the mitochondrial Gln-_mtRNA^{Gln}. In yeast, the ND-GluRS appears to be the cytosolic GluRS, which is imported into mitochondria to mischarge the _mtRNA^{Gln} (Frechin *et al.*, 2009). The subsequent amidation of the Glu moiety of Glu-_mtRNA^{Gln} is performed by the heterotrimer GatFAB. The only difference between GatCAB and GatFAB is the GatF subunit which is homolog to the GatC but possesses an additional N-terminal extension that plays a role in catalysis (Araiso *et al.*, 2014).

II.5. Acquisition of new appended domains and formation of multi-synthetase complexes

During evolution, aaRSs acquired additional nontranslational activities through recruitment of new structural domains while preserving their essential aminoacylation activity. From prokaryotes to higher eukaryotes, most of the aaRSs acquired specific domains that allow them to interact with new protein or nucleic acid partners, to enhance the aminoacylation activity, to regulate their subcellular localization and to carry new non-canonical functions.

II.5.1. Acquisition of new aaRSs domains throughout evolution

When we compare the protein sequences of eukaryotic cytoplasmic aaRSs with their prokaryotic counterparts, we clearly see that the protein size has increased during evolution, except for AlaRS (Guo and Yang, 2014; Mirande, 2017), **Figure I-17**). This increase in size of the eukaryotic aaRSs originates from acquisition of novel structural domains. Some of these domains are homologous to well-known structural modules found in other families of proteins such as the **G**lutathione **S**-**T**ransferase (GST) domain and the **L**eucine-**Z**ipper (LZ) domain, whereas other domains like the















aaRS	Extra domain	aaRS domains	Role of the appended domain	Ref.
AlaRS	∅	 Ec, Sc, Hs		
AspRS	Lys Rich	 Ec Sc, Hs	<ul style="list-style-type: none"> • Non specific tRNA binding • Facilitation of aa-tRNA transfer to eEF1γ 	[83-85]
LysRS	Lys Rich	 Ec Sc, Hs	<ul style="list-style-type: none"> • Enhances tRNA^{Lys} binding affinity • Delivering of tRNA^{Lys3} into the HIV virion • Interaction with 67LR laminin receptor 	[86,87] [88] [89]
AsnRS	Lys Rich	 Ec Sc, Hs	<ul style="list-style-type: none"> • tRNA^{Asn} binding (hypothetical) 	
ArgRS	Leu Zip.	 Ec, Sc Hs	<ul style="list-style-type: none"> • Interaction with p43/AIMP1, LeuRS and IleRS in the MSC 	[90]
ValRS	Lys Rich	 Ec Sc	<ul style="list-style-type: none"> • Non specific tRNA binding activity 	[91]
	GST	 Hs	<ul style="list-style-type: none"> • Interaction with elongation factor EF1-H 	[92]
GlyRS	WHEP	 Ec, Sc Hs	<ul style="list-style-type: none"> • Regulator of dynamic structure and activity of GlyRS 	[93,94]
HisRS	WHEP	 Ec, Sc Hs	<ul style="list-style-type: none"> • Stimulating antigen in idiopathic myositis (targeted by autoantibodies) 	[95,96]
TrpRS	WHEP	 Ec, Sc Hs	<ul style="list-style-type: none"> • Interactions with DNA-PK and PARP-1 to activate p53 • Avoid angiostatic activity of the enzyme 	[97] [98]
MetRS	Trbp111	 Ec	<ul style="list-style-type: none"> • Facilitation of tRNA binding ; MetRS dimerization 	[99]
	GST	 Sc	<ul style="list-style-type: none"> • Interaction within the MSC 	[100, 101]
	WHEP	 Hs	<ul style="list-style-type: none"> • Binding of tRNA and facilitates Met-tRNA transfer to eEF-1α 	[102]
CysRS	GST	 Ec Sc, Hs	<ul style="list-style-type: none"> • Interaction with eEF-1γ 	[103]

Figure I-17: Modular composition of the *E. coli* (Ec), *S. cerevisiae* (Sc) and human (Hs) 20 aaRSs and of the yeast and metazoan aaRS-associated protein. The aaRSs are listed by their appended domain composition. Core domain (catalytic and tRNA-binding domains) is colored in blue for class I aaRSs and in purple for class II aaRSs. New appended domains are in yellow. Adapted from Guo and Yang, 2014; Guo et al, 2009; Mirande, 2017

GluRS & ProRS	GST		<ul style="list-style-type: none"> Interaction with Arc1 in yeast [100]
	WHEP		<ul style="list-style-type: none"> Fusion of GluRS and ProRS [104] Formation of the GAIT complex [105] Binding of 5'-UTR of target mRNAs [105] Interaction with IleRS and ArgRS [106]
GlnRS	UNE-Q		<ul style="list-style-type: none"> Essential for correct yeast cell growth and complementarity for Gln and tRNA^{Gln} [107,108]
ThrRS	UNE-T		<ul style="list-style-type: none"> Undefined
PheRS α	UNE-F		<ul style="list-style-type: none"> Binding of tRNA^{Phe} [109] Potential binding to dsDNA or dsRNA [109]
TyrRS	EMAPII		<ul style="list-style-type: none"> Cytokine activity [110] Masks ELR cytokine motif in TyrRS sequence [111]
SerRS	UNE-S		<ul style="list-style-type: none"> NLS embedded for nuclear localization, essential for vascular development [112,113]
IleRS	UNE-I2 R R		<ul style="list-style-type: none"> Retains IleRS in the MSC through interaction with WHEP domains of EPRS [114]
LeuRS	UNE-L		<ul style="list-style-type: none"> Leucine-dependent interaction with the RagD GTPase of mTORC1 [115,116]
	LZ binding		<ul style="list-style-type: none"> Binding to the LZ domain of ArgRS [117]

AIMP	Extra domain	AIMP domains	Role of the appended domain	Ref.
p43/ AIMP1	Leu Zip.		<ul style="list-style-type: none"> Interaction with ArgRS and p38 in the MSC [90] 	[90]
	EMAPII		<ul style="list-style-type: none"> Interaction with ArgRS in the MSC [118] 	[118]
p38/ AIMP2	Leu Zip.		<ul style="list-style-type: none"> Interaction with p43 in the MSC [101] 	[101]
	GST		<ul style="list-style-type: none"> Interaction with IleRS, LysRS and GluProRS in the MSC [101,119] 	[101,119]
p18/ AIMP3	GST		<ul style="list-style-type: none"> Interaction with MetRS in the MSC [101,120] Tumor suppressor activity through ATM interaction [121] 	[101,120] [121]
Arc1p	GST		<ul style="list-style-type: none"> Interaction with both MetRS and GluRS [122] 	[122]
	EMAPII		<ul style="list-style-type: none"> Enhances catalytic activities of MetRS/GluRS [123,124] Maintain MetRS and GluRS in the cytosol [123,124] 	[123,124]

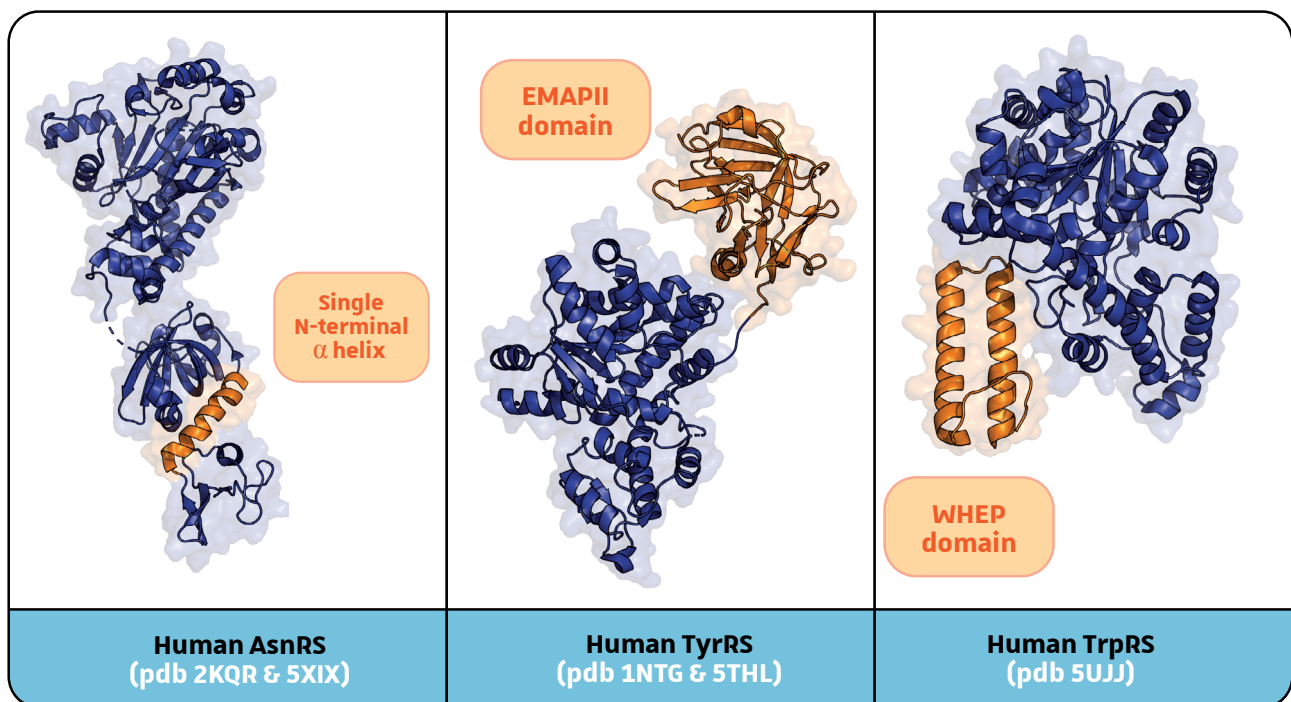


Figure I-18: Known structures of additional aaRS domains. Core of the aaRS is colored in blue, and additional domains are in orange/yellow. For human AsnRS and TyrRS, structures combine two different pdb format, and the domain assembly has been done manually and does not represent the natural 3D structure.

WHEP domain or the EMAPII domain, are only found within the aaRSs family. Unique domains found in only one aaRS member are called UNE-X domains, where X represents the aa-specificity of the aaRS (Guo, Schimmel and Yang, 2010). All the following new appended domains found in aaRSs are illustrated together with their roles (when known) in **Figure I-17**.

The smallest appended domain of aaRSs is a single N-terminal α -helix which is found in the eukaryotic subclass IIb aaRSs AspRS, LysRS and AsnRS. These aaRSs acquired a 30-50 aa-long helix in their N-terminal domain, next to the OB-fold ABD (**Figure I-18**). These three aaRSs have never been crystallized with this N-terminal extension, but NMR spectroscopy studies confirmed the single α -helix conformation (Cheong *et al.*, 2003; Crepin *et al.*, 2011). This helix appears to be amphiphilic, with positively charged residues allowing the binding to charged nucleic acids like tRNAs. Indeed, these N-terminal helices enhance the tRNA binding affinities of these aaRSs, and most of the time these interactions are not specific for the cognate tRNA, but for several tRNAs (Frugier, Moulinier and Giegé, 2000; Francin *et al.*, 2002; Ryckelynck, Giegé and Frugier, 2003).

An original motif only found in the aaRS family is a domain highly homologous to a cytokine called **Endothelial Monocyte-Activating Polypeptide II** (EMAPII) (Kao *et al.*, 1992). The N-terminal portion of this domain is homologous to the Trbp111 domain found in bacterial MetRS as a C-terminal extension involved in dimerization and tRNA-binding (**Figure I-18**; Swairjo *et al.*, 2000). The EMAP-II like domain is always found at the C-terminal domain of proteins and is present in metazoan TyrRS and *C. elegans* MetRS, but also in aaRS-interacting proteins like p43/AIMP1 in metazoan and the yeast Arc1p protein. This domain forms a compact structure with an N-terminal open β -barrel surrounded by small helices (**Figure I-18**; Renault *et al.*, 2001). In the human TyrRS, the EMAPII domain appears to be dispensable for aminoacylation, but its removal through proteolysis is associated with apparition of a cytokine activity mediated by both the released EMAPII domain and the N-terminal part called mini-TyrRS (Wakasugi and Schimmel, 1999; Lee *et al.*, 2012). In aaRS-interacting proteins, this domain is essential for their interaction with aaRSs to form **MultiSynthetase Complexes** (MSC) (**Figure I-17**; Ahn, Kim and Lee, 2003; Simader *et al.*, 2006). Another appended domain found only in some human aaRSs is the WHEP domain. This domain name, WHEP, comes from the fact that it has originally been found in human TrpRS (W), HisRS (H) and GluProRS (EP). Later it was shown that human MetRS and GlyRS also present this ~50 aa residues long domain (**Figure I-17**). Located either in C-terminus (MetRS), N-terminus (GlyRS, TrpRS, HisRS) or in the middle of GluProRS, this domain adopts an antiparallel helix-turn-helix structure with a positively-charged region dedicated

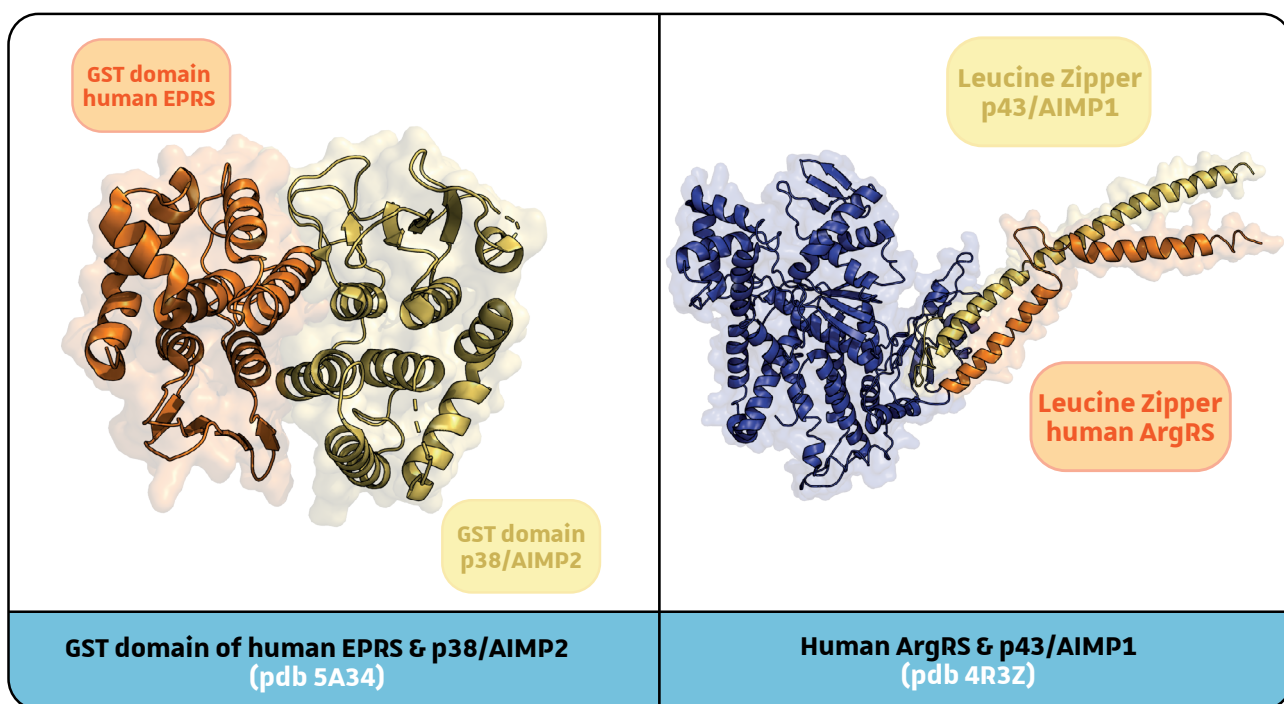


Figure I-18(bis): Known structures of additional aaRS domains. Core of the aaRS is colored in blue, and additional domains are in orange/yellow.

to non-specific RNA-binding (**Figure I-18**; Cahuzac *et al.*, 2000). In addition to this binding property, WHEP domains are dedicated to a myriad of different functions, such as interactions with protein (DNA-PK and PARP1 for TrpRS; Sajish *et al.*, 2012) or RNA partners (binding of mRNA for GluProRS; Jia *et al.*, 2008).

Two other common protein domains found in the aaRS family and which act as protein-protein interaction modules for higher eukaryotes mostly are the GST and LZ domains. As a consequence, the aaRSs and aaRS interacting proteins that display these domains will form MSCs. The GST-like domain, found only in N-terminus of aaRSs, is formed by α -helices bundle that allows formation of a dimeric interface which mediate higher-order interactions between aaRSs and their interacting proteins (**Figure I-18(bis)**). This domain is found in two mammalian aaRS complex-interacting multifunctional protein (AIMPs) p38/AIMP2 and p18/AIMP3 that interact with several GST domain-containing aaRSs of the MSC (**Figure I-17**). More interestingly, GST-like domains are also found in eukaryotic elongation factors eEF-1 γ and eEF-1 β , suggesting possible interactions between these factors and aaRSs to provide tRNA channelling during protein synthesis (Koonin *et al.*, 1994; Negrutskii *et al.*, 1999; Kaminska, Shalak and Mirande, 2001). In addition to higher eukaryote aaRSs, the GST-like domain is also found in yeast MetRS, GluRS and Arc1p that, accordingly, form the unique yeast MSC called AME (see next section). Similarly, the helical motif LZ domain found in ArgRS of higher eukaryotes allows interaction with p43/AIMP1 in the MSC by hydrophobic interaction between the two LZ domains (Fu *et al.*, 2014).

The unique appended domains found in single aaRS are less well characterized but present a plurality of functions, including tRNA binding for UNE-F (Finarov *et al.*, 2010), protein interaction for UNE-I2 and UNE-L (Rho *et al.*, 1996; Min Han *et al.*, 2012) or nuclear localization signal for UNE-S associated with vascular development (Fukui, Hanaoka and Kawahara, 2009; Xu *et al.*, 2012).

II.5.2. Multi-aminoacyl-tRNA synthetase complexes (MSCs) formation and evolution

As mentioned in the previous section, the recruitment of new appended domains in the aaRS scaffold often enables interaction with new partners (**Figure I-17**). This new interaction network appears to be essential for higher eukaryotes, since it has been established for several years that cellular and organismal complexity did not always correlate with the expansion of protein-coding genes number. Instead of increasing the number of genes, organism evolved to expand macromolecular

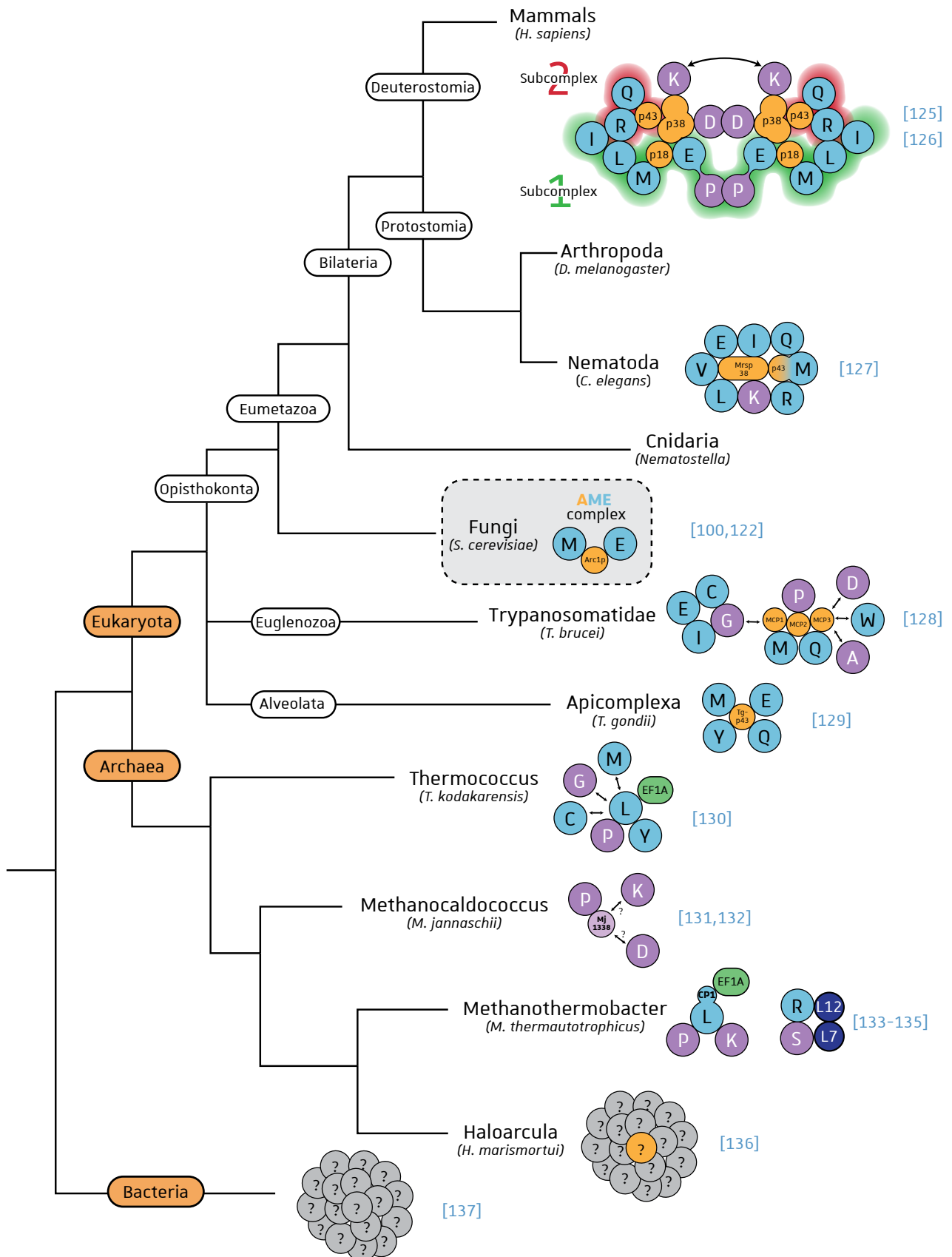


Figure I-19: Composition and architecture of characterized MSCs. This phylogenetic tree illustrates MSCs identified in various organisms belonging to different clades. The one-letter code is used for each aaRS. Class I and class II aaRSs are colored in blue and purple, respectively. The aaRS-associated proteins are colored in yellow. This figure is inspired from Havrylenko and Mirande, 2015 and Laporte *et al*, 2014. The MARS complex found in human is modeled according to Cho *et al*, 2015.

interactions, and this phenomenon is clearly observed within the aaRS family. Even though these enzymes are essential and ubiquitous, their potential to assemble into MSCs has been mostly shown in higher organisms and are admitted to provide a role of dynamical platforms for subcellularly relocating aaRSs. Since the vast majority of prokaryotes present a single compartment, the absence of well characterized MSCs correlates with the absence of aaRSs relocation, with the exception of cyanobacteria and their subcellular compartmentalization. The only potential bacterial MSC has been reported in *E. coli* as a ~ 400-1000 kDa complex with extremely weak interactions between the protein partners (Harris, 1987). The existence of this complex is still under debate since this study is the only one reporting such bacterial MSC.

In archaea, small MSCs have been characterized in different organisms and are often interacting with translation factors such as eEF1A or directly with the ribosome through interaction with L7/L12 ribosomal proteins (Figure I-19; Raina *et al.*, 2012; Godinic-Mikulcic *et al.*, 2014). These interactions would suggest a role in aa-tRNA channelling from aa-tRNAs synthesis to their delivery to translating ribosomes. For the majority of the archaeal MSCs, no additional AIMP s have been described, since complex formation is mediated mostly by aaRSs and translation factors. Moreover, Figure I-19 shows that archaeal MSCs contains often more class II aaRSs (purple) than class I (blue), whereas in eukaryotes class I aaRSs are the most abundant and the assembly is mediate by additional specific AIMP s.

The smallest MSC found in eukaryotes is the yeast AME complex, containing the anchor protein Arc1p and the two aaRSs MetRS and GluRS (Figure I-19). This complex is one of the most studied MSC and will be analysed into more detailed in the next section §III. The MSC from vertebrates has been the first one that was isolated from rat liver in the 70's (Bandyopadhyay and Deutscher, 1971), and observed in several subsequent studies in different type of cells such as rabbit reticulocytes, human placenta cells or mammalian cells in culture, but also in the arthropod *Drosophila melanogaster* that contains a similar MSC composition (Kerjan *et al.*, 1994). This high molecular weight complex of ~1.5 MDa contains nine aaRS activities and the three AIMP1/2/3 auxiliary proteins (Figure I-19). The class II aaRSs are present as dimers (LysRS, AspRS and bi-functional GluProRS). The five other class I aaRSs are monomeric but present in two copies within the complex (Cho *et al.*, 2015), as well as the three AIMP s that constitute an anchoring platform to retain all these aaRSs in the MSC. The central AIMP2/p38 scaffold protein that has no homologs in bacteria, archaea and lower eukaryotes, stably maintains this symmetrical and long complex, and allows the association in two subcomplexes (Figure I-19).

Table I-7: Association of aaRS with one accessory protein and subsequent location and role
(inspired from Hausmann and Ibba, 2008)

Species	aaRS	Subsequent relocalization	New interactant	Cellular signal	Impact on aaRS (or AIMP)	Role	Reference	
Bacteria	<i>E. coli</i>	ProRS	None	YbaK	None	None	Editing of Cys-tRNA ^{Pro}	[138-140]
	<i>M. tuberculosis</i>	LysRS-MprF	Plasma membrane	Plasma membrane lipids	None	None	Lysination of PG, resistance towards antimicrobial peptides	[141]
	<i>T. thermophilus</i>	AspRS	None	Amidotransferase	None	None	Enhance indirect synthesis of Asn-tRNA ^{Asn}	[142]
	<i>D. radiodurans</i>	TrpRS II	None	Nitric oxide synthase	None	None	Synthesis of 4-nitro-Trp in response to radiation damage	[143]
	<i>Anabaena</i>	ValRS	Thylakoid membrane	FoF1 ATP synthase complex	Differentiation of heterocysts	None	Thylakoid shaping and heterocyst differentiation	[144,145]
Archaea	<i>M. janaschii</i>	ProRS	None	Mj1338	None	None	Link between energy production and translation?	[131]
	<i>M. thermoaut.</i>	LeuRS	None	EF-1A	None	None	Enhanced aminoacylation	[134]
Eukaryotes	<i>S. cerevisiae</i>	SerRS	None	Pex21	Constitutive	None	Pex21 enhances the binding of tRNA ^{Ser} to SerRS	[146-148]
		TyrRS	None	Knr4	Yeast sporulation	None	Potential role in cell wall biosynthesis during sporulation	[149,150]
		LeuRS (mito)	None	mRNA bi4 maturase	None	None	Alternative splicing of group I introns	[151,152]
		LeuRS	None	Gtr1-TORC1	Leucine availability	None	Leucine signalling to TORC1	[115]
		AspRS	Nuclear	AspRS mRNA	High amount of AspRS	NLS in N-terminal extension	Inhibition of AspRS expression	[153,154]
		GlyRS	Nuclear	3' end of mRNA	None	None	Transcription termination	[155,156]
		MetRS	Nuclear	Nuclear components	Diauxic shift (respiratory)	Downregulation of Arc1	Transcription regulation of Atp1 subunit	[157]
		GluRS	Mitochondrial	GatFAB	Diauxic shift (respiratory)	Downregulation of Arc1	Mitochondrial Gln-tRNA ^{Gln} formation	[158]
Vertebrates	ThrRS	Nuclear	n.d	Constitutive	None	Regulation of angiogenesis	[159,160]	
	SerRS	Nuclear	VEGFA promoter and SIRT2; YY1	Constitutive relocation through UNE-S domain	None	Repression of VEGFA expression and vascular development	[112,113,161-163]	
	mini-TyrRS	Extracellular	CXCR1 receptor	TNF alpha stimulation	Proteolytic cleavage, C-terminus removal	Cytokine activity, cell migration and angiogenesis	[110,164,165]	
	mini-TrpRS	Extracellular	VE-cadherin	IFN gamma stimulation	Alternative splicing, N-terminus removal	Inhibition of angiogenesis	[165-167]	
	<i>H. sapiens</i>	ValRS						[92]
AspRS							[85]	
LysRS		Cytosol	EF-1A	None	None	Delivery of aa-tRNA to the ribosome	[169]	
TrpRS						Enhanced aminoacylation	[169]	
MetRS							[102]	
GlnRS		Cytosol	ASK1	Fas-mediated apoptosis	Gln-dependent interaction	Prevention of apoptosis	[170]	
MetRS (nucleolar)		Nuclear	n.d.	Cell growth signal (EGF, insulin...)	None	Synthesis of rRNA	[171]	
TyrRS		Nuclear	Nuclear TRIM28 and HDAC1	Oxidative stress, angiogenin, nicotinamide	Acetylation of Lys244	Prevention of DNA damages	[172-174]	
TrpRS		Nuclear	PARP1 and DNA-PKc	IFN-gamma stimulation	Conformational change	p53 activation and apoptosis	[97,175]	
LysRS		Nuclear	Nuclear MITF	Allergen recognition by mast cell and MAPK pathway	Ser207 phospho.	Upregulation of gene transcription in mast cells	[176-178]	
		Cytoplasmic membrane	67LR laminin receptor	Binding of laminin to integrins and MAPK activation	Thr52 phospho.	Inhibition of 67LR ubiquitination and promotion of metastasis	[89]	
		Exosome - extracellular	Syntenin	Starvation conditions and TNF alpha	N-terminus proteolytic cleavage (Δ1-12)	Triggers inflammatory response	[179,180]	
GlyRS		Extracellular	Extracellular domain of CDH6 (K-cadherin)	Fas-ligand released from tumor cells	None	Defense against Erk-activated tumor formation	[181]	
LeuRS		Lysosomal	Vps34	Amino acids concentration	Leucine binding	Stimulation of Vps34 kinase activity	[182]	
		Lysosomal	RagD (mTORC1)	Intracellular leucine concentration	Leucine binding	mTORC1 activation	[116]	
	Plasma membrane	FATP1	Insulin stimulation of adipocytes	Ser999 phospho.	Induce long chain fatty acids uptake	[183]		
EPRS	Cytosol	GAIT complex (NSAP1•GAPDH•L13a)	IFN-gamma stimulation	Ser886 and Ser999 phospho.	mRNA silencing of ceruloplasmin in myeloid cells	[184-186]		
	Cytosol	PCBP2	Viral infection	Ser990 phospho.	Prevents MAVS ubiquitination to block virus replication	[187]		
LysRS	HIV encapsidation	Gag virion protein	HIV infection	Ser207 phospho.	Packaging of HsLysRS and its cognate tRNA ^{Lys} into the HIV-1 virion	[188-191]		

II.6. aaRSs relocation and associated nontranslational functions

The proposed function of MSCs was first tRNA channelling during protein biosynthesis, since these MSCs but also individual aaRS have been found to interact with other components of the protein synthesis machinery like eEF1A or the ribosome (**Figure I-19** and **Table I-7**). In addition to this tRNA channelling role during translation, MSCs were more recently considered as retention platforms allowing accretion of several aaRSs that can be released under specific physiological conditions to exert a non-translational activity either in the cytosol or in a new compartment that they relocate to. In general, relocation relies on aaRS post-translational modification, proteolytic cleavage of a domain or changing concentration of a binding partner. These modifications can expose to solvent a localization signal sequence targeting the aaRS to the corresponding new compartment (nucleus, mitochondria, plasma membrane or extracellular matrix). Obviously, all these new relocations and new binding partners are often related to new unexpected functions that are listed in **Table I-7**. This table shows correlation between new binding partners, new relocating compartment and the new characterized functions of the aaRSs. When available, the aaRS modification and the cellular signal responsible for this relocation is indicated. These new non-canonical and fascinating roles for aaRSs are more and more discussed in the literature, and during my PhD I published two reviews on aaRSs relocation and their associated non-canonical functions ([Debard *et al.*, 2016](#), page 276; [Yakobov *et al.*, 2018](#), page 292).

II.7. The yeast AME complex

The smallest MSC known so far is composed of the two class I cytosolic aaRSs MetRS and GluRS in complex with a single AIMP protein called Arc1 (or Arc1p). This minimal MSC called AME (for **Arc1•MRS•ERS**) is found in all fungi studied so far, and the yeast *S. cerevisiae* has been the best model to understand the role of this trimeric complex. This section will describe into details the structure and dynamics of yeast AME complex, with an analysis of the new functions exerted by yeast MetRS and GluRS.

II.7.1. Structure and organization of the AME complex

The Arc1 anchor protein is a 42 kDa protein (376 aa) that binds tightly the yeast MetRS and GluRS, thereby ensuring their cytosolic localization ([Simos *et al.*, 1996](#); [Galani *et al.*, 2001](#)). This protein, first discovered for binding to G4 nucleic acids (or G-quadruplex) found in guanine-rich nucleic

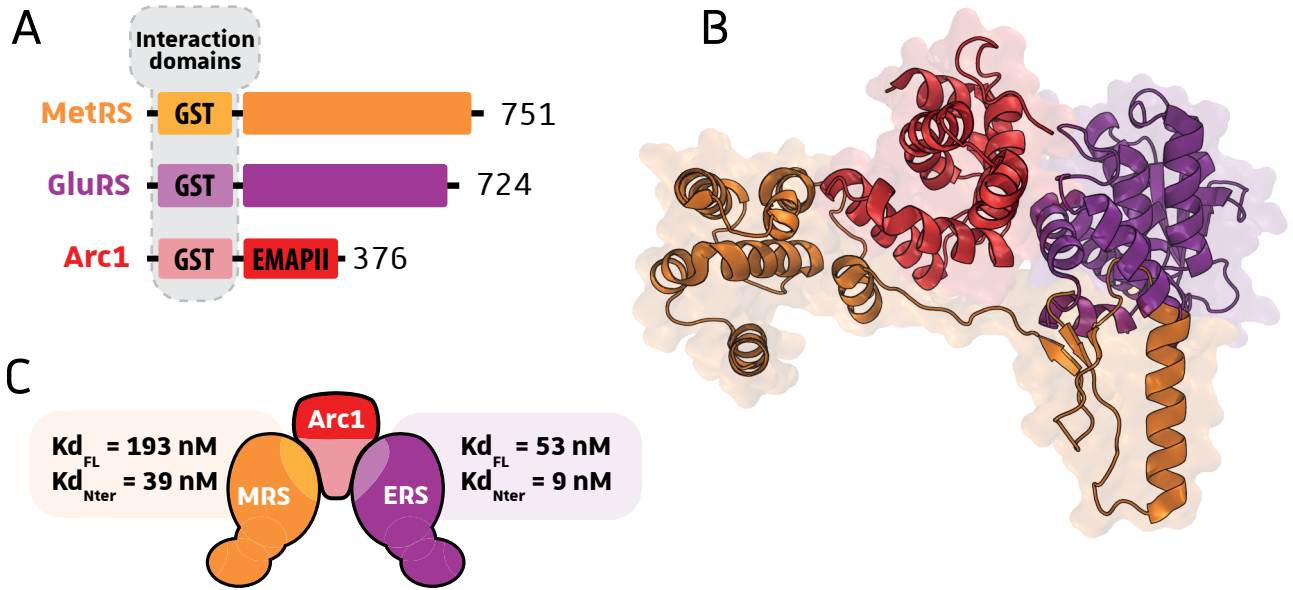


Figure I-20: The yeast AME complex: composition and structure. **A.** The three proteins interact through their N-terminal GST-like domains. **B.** Superimposition model of the two binary complexes Arc1•GluRS (pdb 2HRK) and Arc1•MetRS (pdb 2HSN). **C.** Affinities of MetRS (orange), GluRS (purple) and their respective N-terminal domains for Arc1, determined by SPR (from Karanasios *et al*, 2007).

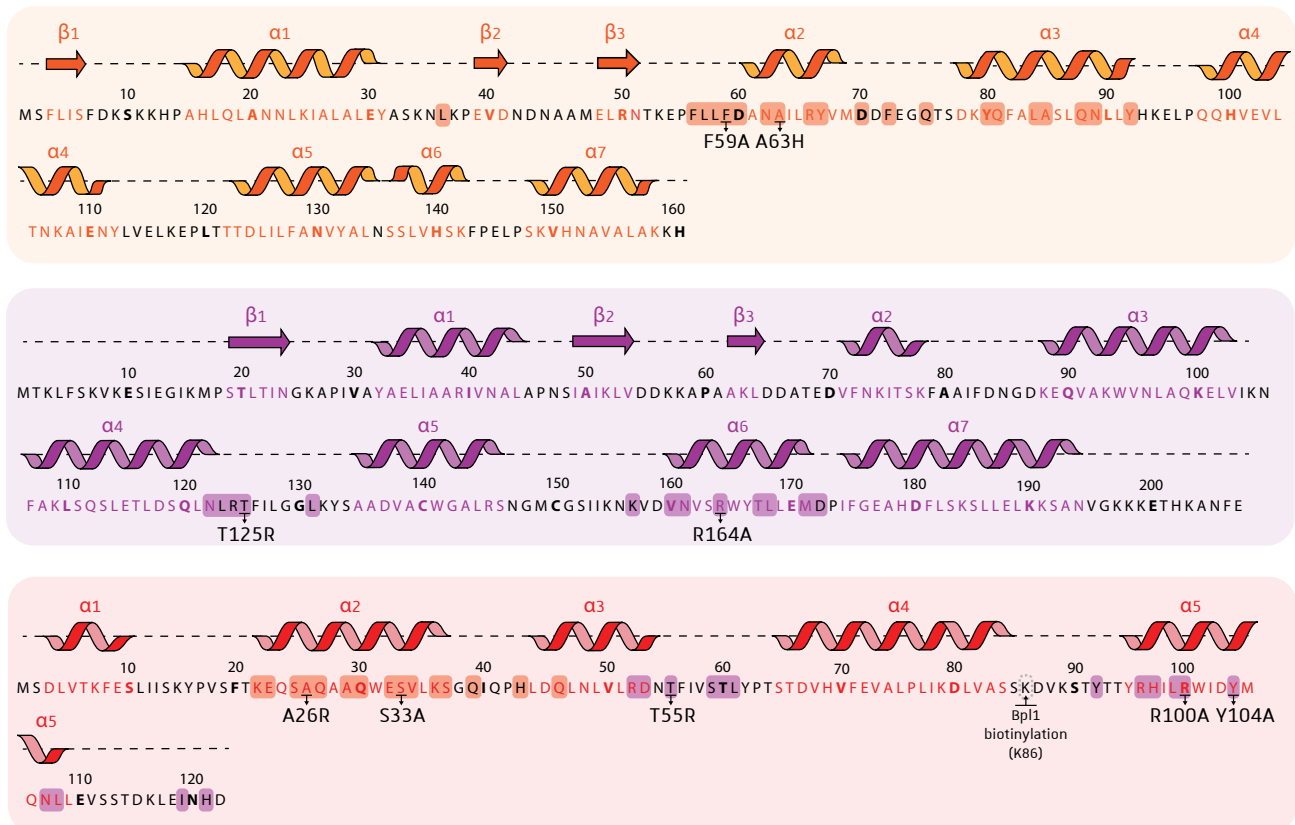


Figure I-21: Secondary structure organization of the N-termini of the three AME proteins. The sequence of each protein is shown below the modular structure, with residues belonging to helix or strand colored in orange (MetRS), purple (GluRS) or red (Arc1). The residues involved in protein interaction are highlighted in the corresponding color. For Arc1 sequence, residues highlighted in orange and purple are involved in interaction with MetRS and GluRS, respectively. Mutations that have been shown to disrupt the interaction with the corresponding protein are indicated below the residue (Karanasios *et al*, 2007).

acids was called G4p1 or p42 (Frantz and Gilbert, 1995) and is the platform protein homologous to the mammalian AIMP1/p43. The GST-like domain located in N-terminus of all the three partners mediates interactions between Arc1 and the two aaRSs. Crystallographic structures of the two binary complexes of the N-terminal GST-like domains of Arc1 complexed to GluRS (pdb 2HRK) and to MetRS (pdb 2HSN) have been solved (Simader *et al.*, 2006). N-terminal domains of the two aaRSs share a common secondary structure with three small β -strands and seven α -helices, whereas Arc1 N-terminus is composed of five α helices only. Superimposition of the Arc1 GST-like domain complexed to the GST-like domain of GluRS and MetRS is represented in **Figure I-20B** and shows dual interactions between two adjacent but non-overlapping Arc1 interfaces and each aaRS: 15 residues inside the region encompassing residues 22-46 of Arc1 are contacting the two α -helices α 1 and α 2 of the MetRS, whereas interaction with GluRS involves 16 residues inside regions 52-61 and 92-121 of Arc1 (**Figure I-21**). Affinity analysis by surface plasmon resonance (SPR) revealed equilibrium dissociation constants (K_d) for this trimer which is in the nanomolar range (Karanasios *et al.*, 2007). However, N-terminal domains of the two aaRSs display greater affinity for the GST-like domain of Arc1 than the full-length enzymes, suggesting that catalytic domains of the two aaRSs decrease the interaction strength of the heterotrimeric AME complex (**Figure I-20C**).

II.7.2. Arc1 protein: more than a binding partner

Despite its small molecular weight (42 kDa), several roles have been suggested and demonstrated for this protein, including that of a cytosolic anchoring platform or cofactor for the two-associated aaRSs. Since deletion of Arc1 gene in yeast is not lethal, studies on Arc1 deletion strains gave new insight about its potential new functions. A review written by my host laboratory describes into details all the roles that have been attributed to Arc1 (Frechin *et al.*, 2010). The following section will focus more about the impact of Arc1 on the dynamics of the AME complex.

II.7.2.1. An aaRS cofactor enhancing aminoacylation efficiency

In addition to its N-terminal domain (N domain) involved in aaRSs interactions, Arc1 sequence exhibits an intermediate domain (called Middle or M domain) rich in alanyl- and lysyl- residues dedicated to non-specific RNA binding through phosphate backbone interactions, and a specific C-terminal tRNA-binding domain (C domain) (Simos *et al.*, 1996, 1998). Note that the M domain is similar in sequence to nuclear H1 histone (34 % identity). Both M and C domains are forming the

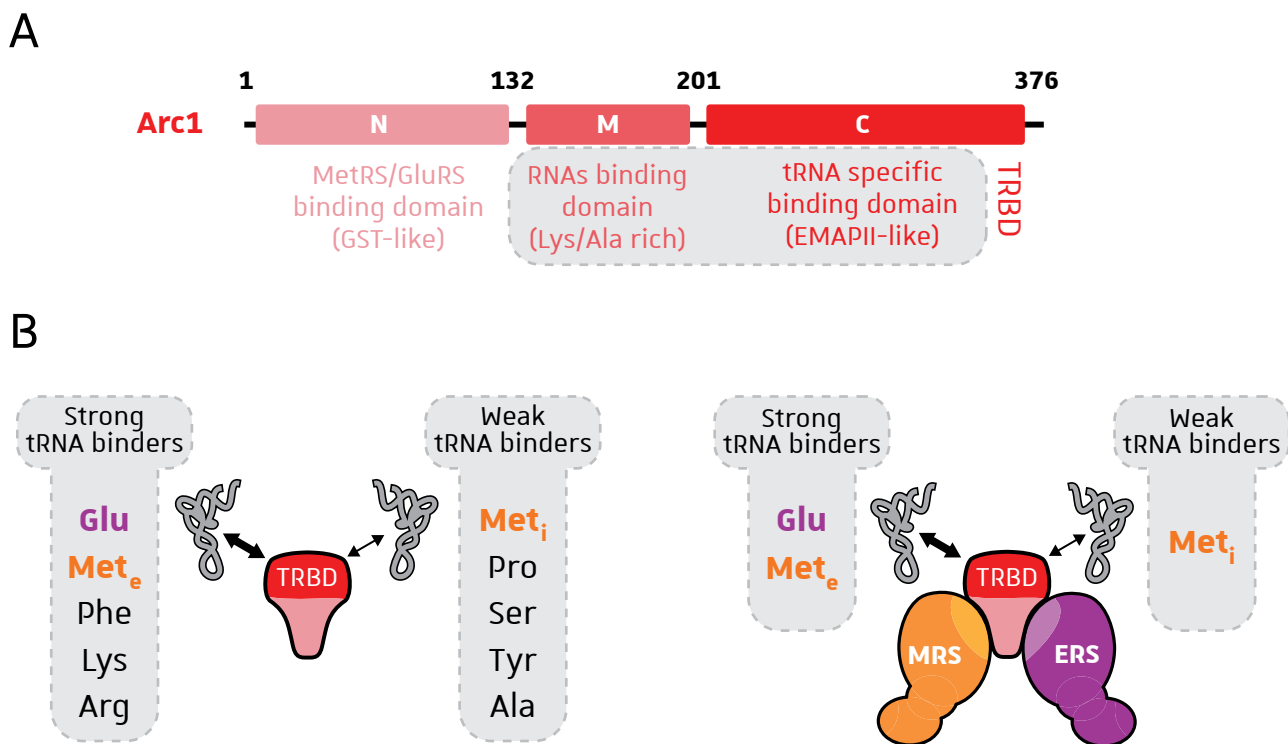


Figure I-22: Arc1 protein as an aaRS cofactor. A. Modular organization of Arc1. **B.** Free Arc1 binds several tRNAs species with various affinities, whereas Arc1 complexed to the two aaRSs selectively binds tRNAs Met and Glu with high affinities (Deinert *et al*, 2001).

Table I-8: Yeast MetRS catalytic constants for tRNA_i^{Met} with or without Arc1
(data from Simos *et al*, 1996, 1998)

	Purified MetRS and Arc1 proteins				Crude extracts		Purified MetRS	
	MetRS	MetRS + Arc1	MetRS + Arc1-ΔM	MetRS + Arc1-ΔC	<i>arc1Δ</i> strain	ARC1 strain	- Arc1	+ Arc1
K_m (μM)	6-14	< 0.1	5-8	0.66	8.3	< 1	6.6	≤ 0.1
k_{cat} (min^{-1})	1.3	6.3	1.8	6	16	40	1.3	6.3
k_{cat}/K_m^*	1	500	2	70	1	> 80	1	> 300

* The catalytic efficiency k_{cat}/K_m is relative to the one obtained for MetRS alone

tRNA-binding domain (TRBD) of Arc1 (**Figure I-22A**). This TRBD, containing an OB-fold motif found in some aaRSs (Swairjo *et al.*, 2000), is able to non-specifically bind RNAs like 5S RNA and several tRNAs, among which tRNA^{Glu}, the elongator and initiator tRNAs^{Met} and other different tRNA species (Phe, Lys, Arg...) (Deinert *et al.*, 2000; **Figure I-22B**). Interestingly, when Arc1 is engaged into the AME complex, the tRNA binding is more specific and only tRNA^{Glu} and tRNA^{Met} are strongly bound to the complex, and in much less extent tRNA^{Met} (**Figure I-22B**). It is important to notice that individual MetRS does not efficiently bind its cognate tRNAs *in vitro*, whereas the GluRS is able to interact with its cognate tRNA^{Glu} (Deinert *et al.*, 2001). These interactions are consistent with an involvement of Arc1 in the tRNA channelling that would facilitate the delivery of aa-tRNAs to the two aaRSs by creating a high local tRNA concentration in proximity of their catalytic sites. Moreover, Arc1 could facilitate the tRNA orientation and thus correctly position the aa-tRNA inside the catalytic domain of the enzymes. In agreement with this channelling function, Arc1 is an enzymatic cofactor able to increase the catalytic efficiency of both MetRS and GluRS. It has been shown that the catalytic efficiency of Arc1-bound MetRS increases almost 500-fold. This increase is essentially due to an effect of Arc1 on the affinity of MetRS for its tRNA (Simos *et al.*, 1996, 1998 and **Table I-8**). For the GluRS, no quantitative catalytic parameters have been obtained due to the unavailability of purified post-transcriptionally-modified tRNA^{Glu}, but the presence of Arc1 clearly enhance the aminoacylation activity of GluRS in a total tRNA extract or in a tRNA^{Glu}-enriched counter-current fraction (Graindorge *et al.*, 2005).

II.7.2.2. An anchoring platform for the cytosolic aaRSs

Besides its role as cofactor for aminoacylation, Arc1 is also a structural platform that maintains the two aaRSs into the cytosol. Indeed, Arc1 fused to the fluorescent protein GFP is found exclusively in the cytosol and excluded from nucleus (Galani *et al.*, 2001). Nuclear exclusion of Arc1p is mediated by a strong nuclear export signal (NES) present in its sequence and recognize by the nuclear exportin Xpo1 (homologous to the mammalian Crm1) (Galani, Hurt and Simos, 2005). However, intermittent nuclear localisation of Arc1 would be essential for its participation to tRNA nuclear export that needs binding of Arc1 to non-aminoacylated tRNAs, mediated by its TRBD domain, inside the nucleus (Simos *et al.*, 1996; Grosshans, Hurt and Simos, 2000). The cytosolic location of Arc1 allows the two associated aaRSs to be anchored into the cytosol through interactions of their GST-domain. As a consequence, interactions with the two aaRSs are lost when N-terminal domain of Arc1 is partially or totally deleted (**Figure I-23A**; Galani *et al.*, 2001). Same results are obtained with point

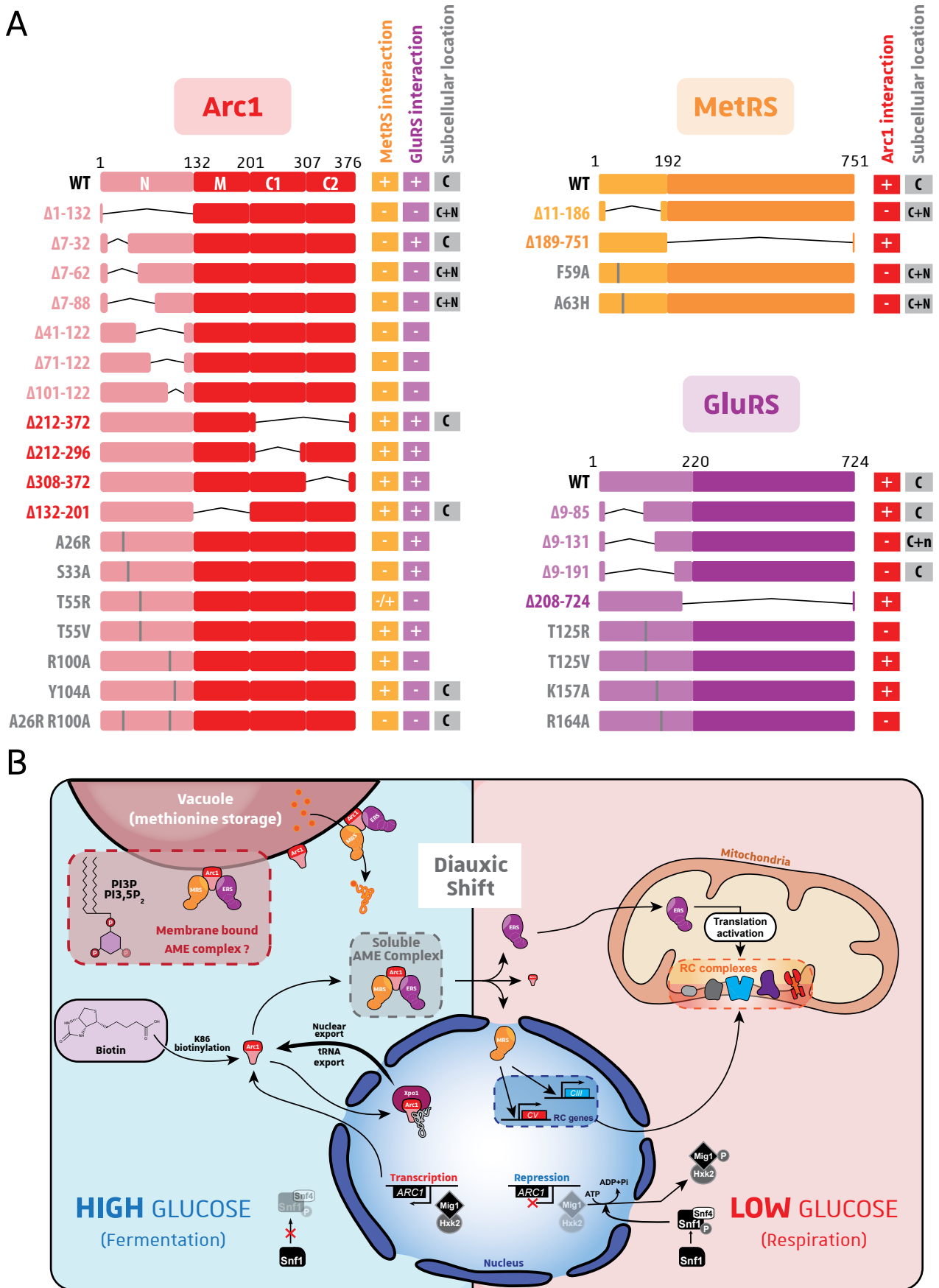


Figure I-23: Subcellular relocation of AME components. **A.** Analysis of *in vitro* interactions and subcellular localization of several mutants of Arc1 (red), MetRS (orange) and GlURS (purple). C: cytosolic; C+N: cytosolic and nuclear. Data from [Deinert et al, 2001](#); [Galani et al, 2001](#); [Karanasios et al, 2007](#). **B.** Summary of AME complex dynamic and protein relocation according to the cellular metabolism.

mutations on Arc1 residues that contact residues of the GST-like domains of the aaRSs (**Figure I-23A**; Karanasios *et al.*, 2007). Along the same line, MetRS appears to be both cytosolic and nuclear when released from the AME complex by deletion of its N-terminus or point mutations, whereas the GluRS was never found in the nucleus even when dissociated from the AME complex (except for the $\Delta 9-131$ mutant where a weaker nuclear signal was observed by fluorescence and confocal microscopy (**Figure I-23A**, Galani *et al.*, 2001)). Recent studies, achieved in the lab, have shown a more complex dynamics for the yeast MSC: during the transition between fermentation to respiration (called the diauxic shift), the release of the two aaRSs from the AME complex allows the synchronization of the nuclear transcription and the mitochondrial translation through aaRSs relocation (Frechin *et al.*, 2014). Indeed, the Snf1/4 glucose-sensing pathway is activated upon respiration (low glucose concentration) and downregulates transcription of *ARC1*. The subsequent decrease of Arc1 leads to the release of both aaRSs and their relocation to nucleus (for MetRS) and to mitochondria (for GluRS). The released cytosolic GluRS has been shown to relocate into mitochondria to regulate translation of one subunit of the F_1F_0 ATP synthase through the synthesis of Glu-tRNA^{Gln}, essential for the formation of mitochondrial Gln-tRNA^{Gln} by the indirect transamidation pathway (Frechin *et al.*, 2009). On the other hand, nuclear relocation of the cytosolic MetRS regulates transcription of another subunit of the F_1F_0 ATP synthase and also of other genes of the mitochondrial electron transport chain (ETC) that encode subunits of complex III (Frechin *et al.*, 2014, **Figure I-23B**).

In addition to this cytosolic anchoring platform, surprising features have been discovered about Arc1. First, it has been shown that Arc1 is able to bind phospholipids, and essentially the phosphatidylinositol molecules PI3P and PI(3,5)P₂ (Fernández-Murray and McMaster, 2006). This interaction with lipids would suggest some sort of affinity of Arc1 to membranes, and more specifically the vacuolar membrane since these types of phospholipids are enriched in this membrane (Obara *et al.*, 2008; Takatori and Fujimoto, 2016). The AME complex would then relocalize to the surface of the vacuole and might represent a sensor for Met stored inside this compartment (**Figure I-23B**). Finally, Arc1 also is post-translationally modified by Bpl1, the biotin protein ligase that adds a biotin group to the ϵ -amino group of Lys86 located in the N-terminal domain that binds both aaRSs (K86, **Figure I-23B**; Kim *et al.*, 2004). Even if this modification is present in the region in close contact with GluRS (**Figure I-21**, page 72), it does not interfere with aaRS interaction, but seems to have a crucial role for thermal adaptation (Chang *et al.*, 2016).

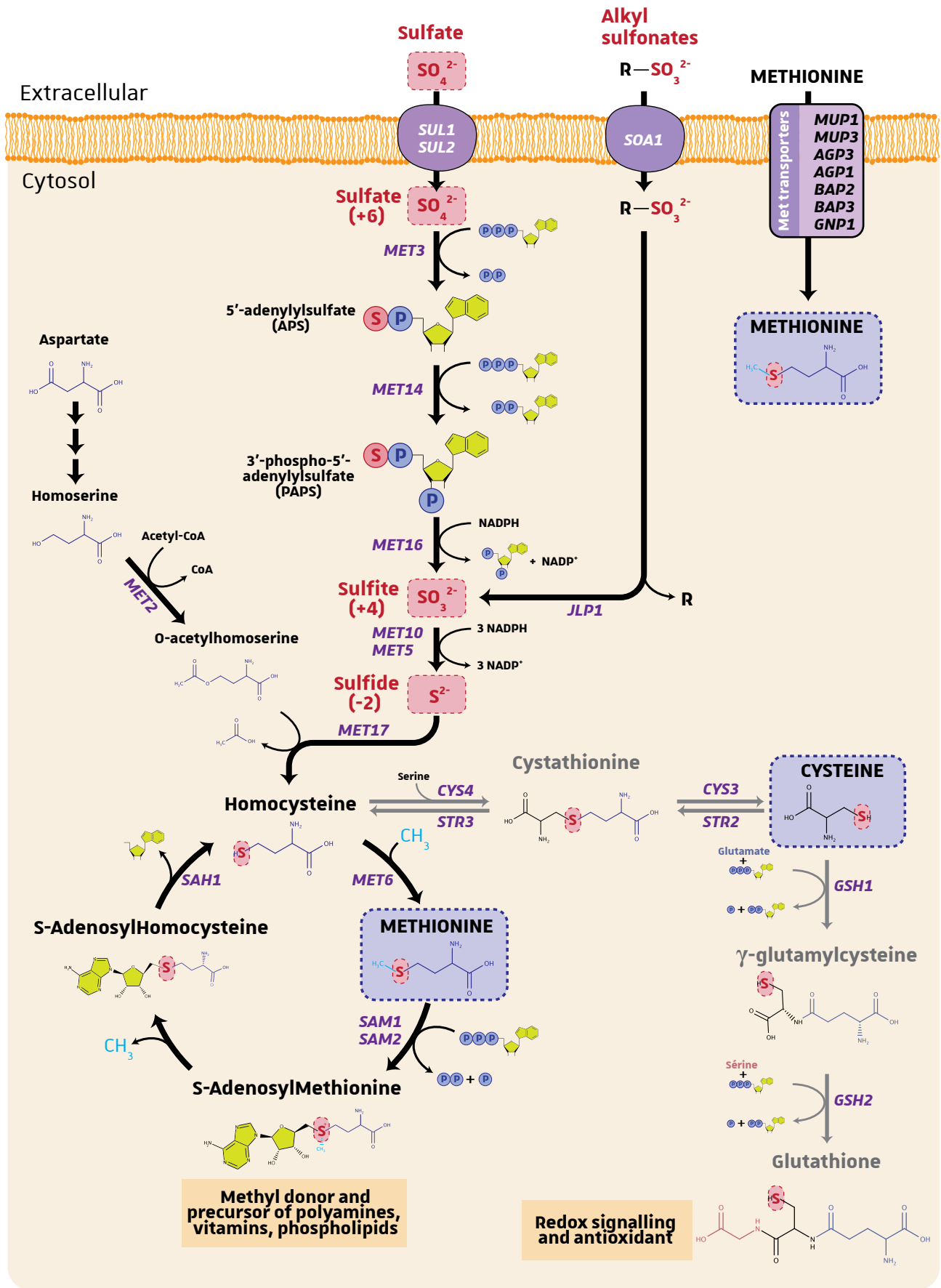


Figure I-24: General sulfur metabolism in yeast and generation of the two sulfur-containing aa Met and Cys. All yeast enzymes known in this metabolism are indicated in purple. Inorganic sulfur molecules are written in red, with the sulfur oxidation state when known. The most common transporters are indicated.

III. The methionine system and complexity

The Met molecule (or 2-amino-4-(methylthio)butanoic acid) is an essential non polar sulfur-containing aa incorporated into protein chains through the enzymatic action of the MetRS and the ribosome. This aa is the first aa incorporated into the polypeptide chain at an initiator AUG codon, but is also incorporated during the elongation at elongator AUG codons. The specificity of the MetRS and the two tRNAs substrates will be discussed in this section after an introduction about the Met metabolism and its role in yeast cell.

III.1. Methionine metabolism and redox functions

III.1.1. Biosynthesis of methionine and methionine derivatives in yeast

Unlike mammals where methionine is a dietary essential aa, yeast is able to synthesis *de novo* the sulfur-containing aa from sulfate or alkylsulfonates aa after their uptake through the plasma membrane (**Figure I-24**). However, yeast is also able to directly uptake Met from the environment through general and more specific aa transporter (**Figure I-24**). The sulfate ion (SO_4^{2-}), which contains a sulfur atom with an oxidation number of +6, undergoes several reduction reactions catalyzed by redox enzymes that finally give rise to the sulfide (S^{2-}) with an oxidation number of -2. Sulfide is then incorporated by the *O*-acetylhomoserine sulfhydrylase enzyme Met17 into a four-carbon chain yielding homocysteine at the end of the sulfate assimilation pathway (**Figure I-24**). A methyl group (originating from 5-methyl-tetrahydrofolate) is then added to homocysteine by the homocysteine methyltransferase Met6 to form Met through the transmethylation pathway. Note that the vast majority of the genes coding for Met metabolism enzymes are positively regulated by Met4/Met28 transcription factors that are induced under sulfur-limiting condition. Methionine can be transformed into *S*-adenosylmethionine (SAM) by the two enzymes Sam1/Sam2. SAM is used in a plethora of reactions due to its electron-deficient trivalent sulfur atom: it represents the best methyl group donor to modify nucleic acids, proteins or lipids, it also functions as an amino donor and as a propylamine donor for spermidine and spermine synthesis. SAM demethylation generate *S*-adenosylhomocysteine (SAH) that can be turned back to homocysteine and the new synthesis of Met: this cycle of reactions involving Met biosynthesis is called the methyl cycle. The other sulfur-containing aa, cysteine, is also synthesized from homocysteine but through another pathway: the transsulfuration pathway involving cystathionine as intermediate. The latter pathway is also the

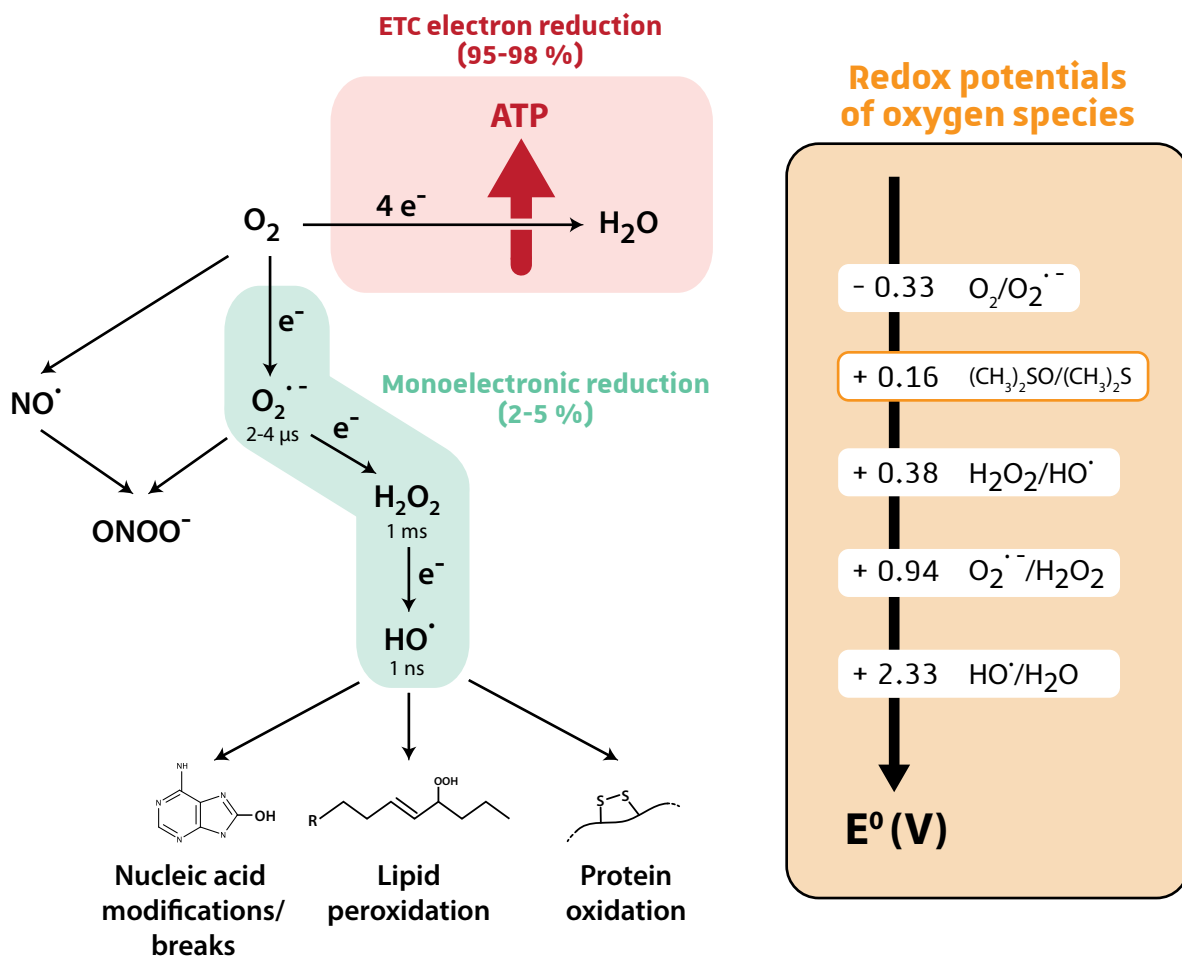


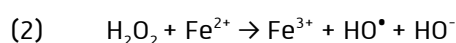
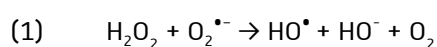
Figure I-25: Redox reactions and ROS generation . ROS formation from single electron transfer to molecular oxygen. Monoelectronic reduction occurs several times to generate diverse ROS, with HO^{\cdot} as the most harmful radical. Redox potential for oxygen species are given from Ilan, Czapski and Meisel, 1976; da Silva *et al*, 2013. Redox potential of dimethyl sulfoxide/dimethyl sulfide is shown in orange and was obtained in Wood, 1981.

entry point for the production of glutathione (GSH), a cysteine-containing tripeptide playing a role in redox signalling and acting as a general antioxidant. Thus, Met metabolism is involved in wide range of cellular sulfide processes, and more generally the sulfur metabolism is of great importance since Met, cysteine and their derivatives play critical roles in cell metabolism beyond their primary role in protein synthesis.

III.1.2. Redox system and methionine as antioxidant

III.1.2.1. Definition of oxidative stress

An oxidation-reduction (redox) reaction is a chemical reaction that involves electron transfer from a reducer (electron donor) to an oxidizer (electron acceptor). Thus, during this reaction, the reducer is oxidized and the oxidizer is reduced. This type of reaction is present in a variety of functions including respiration, photosynthesis in plants and photosynthetic microorganisms, and metabolic reactions such as β -oxidation. Even if all these cellular reactions are tightly regulated, they can generate highly reactive by-products that can have deleterious effects on cells. The most commonly studied cellular oxidants are the reactive oxygen species (ROS) or the nitrogen reactive species (RNS). All these reactive agents contain oxygen, a highly electronegative atom found in cell in its O_2 form called molecular oxygen. In the O_2 molecule, oxygen has two unpaired electrons in two different orbitals and is susceptible to free radical formation through reduction with one or three electrons to form superoxide ($O_2^{\bullet -}$) or the extremely reactive hydroxyl radical (HO^\bullet), respectively. Production of superoxide is not spontaneous (endergonic) since the redox potential of $O_2/O_2^{\bullet -}$ is negative (-0.36 V, **Figure I-25**) and the required energy mostly comes from enzymatic activities. However, the following single-electron reduction into hydrogen peroxide (H_2O_2) is spontaneous (exergonic), thus the half-life of superoxide is extremely short (2 to 4 μs) and highly reactive. On the other hand, hydrogen peroxide is relatively long-living (1 ms) and more stable, so it is able to diffuse across cellular membranes and reach distant molecules. The most harmful ROS is the hydroxyl radical HO^\bullet produced by the Haber-Weiss reaction (1) or the Fenton reaction (2) catalyzed by Fe^{2+} (or Cu^+):



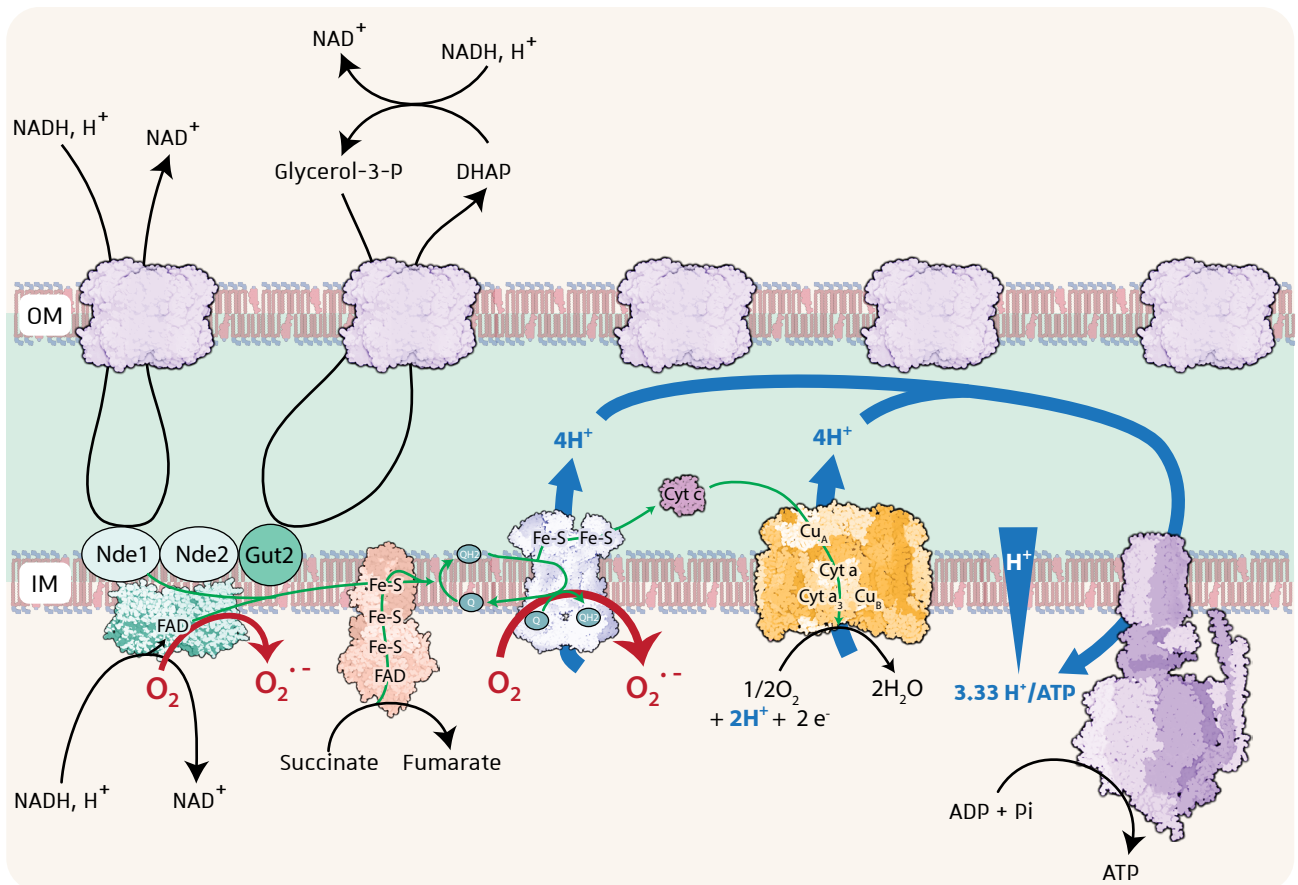


Figure I-26: Mitochondria and formation of superoxide in yeast. Formation of superoxide (in red) occurs mainly on Ndi1 protein and complex III (blue). Electron flow along the inner membrane is shown in green. Complex identification: OM protein (pink, pdb 2K4T), Ndi1 (green, pdb 4G9K), complex II (dark orange, 3AE1), complex III (blue, pdb 3CXH), cytochrome c (dark pink, pdb 1HRC), complex IV (orange, pdb 3X2Q), ATP synthase (purple, pdb 4B2Q). OM: Outer membrane; IM: Inner membrane.

Hydroxyl radical is thus highly reactive (half-life of 1 ns) and deleterious for cells. These free radicals are more reactive due to their single unpaired electron (they do not follow the octet rule) and can further oxidize lipids, proteins or nucleic acids and cause damages (**Figure I-25**). The imbalance between oxidants and reducing agent levels in favour of pro-oxidant activity is called oxidative stress. This stress can arise from antioxidants deficiency and/or increased levels of oxidants through exogenous routes like ionizing radiation, UV exposure and environmental toxins or endogenous cellular activity like by-products of peroxisomal metabolism or mitochondrial activity; the latter being considered as the major source of ROS production (Finkel and Holbrook, 2000). Oxidative stress has been extensively studied for its implication in human diseases like inflammatory diseases, neurodegenerative diseases (Parkinson, ALS, Alzheimer...) and in aging (Berlett and Stadtman, 1997; Finkel and Holbrook, 2000; Muller, Laboratory and Kramer, 2000).

III.1.2.2. Mitochondria as major source of ROS

Within mitochondria, the electron transport chain is the place of oxidative ATP phosphorylation through electrons transport from electron donors (NADH, H⁺, succinate or Glycerol-3-phosphate) to molecular oxygen reduced by two electrons into a water molecule (**Figure I-26**). However, since the transport of the two electrons is sequential, molecular oxygen is prone to single electron reduction by radical by-products, leading to superoxide formation (Inoue *et al.*, 2003; Turrens, 2003). Indeed, 2 to 5 % of the total molecular oxygen is not totally reduced into water during respiration but is reduced by only one electron diverted from the flow to form superoxide and further reduced forms. Whereas there are up to eleven potential mitochondrial sources of superoxide identified so far, respiratory chain complex I (Ndi1 for yeast) and complex III are considered to be major contributors (Starkov, 2008; Wong *et al.*, 2017). Indeed, reverse electron transport at complex I due to a highly reduced coenzyme Q (QH₂) or electron transfer from the free radical semiquinone anion Q^{•-} generated in complex III are the major sources of molecular oxygen reduction into superoxide (**Figure I-26**; Robb *et al.*, 2018).

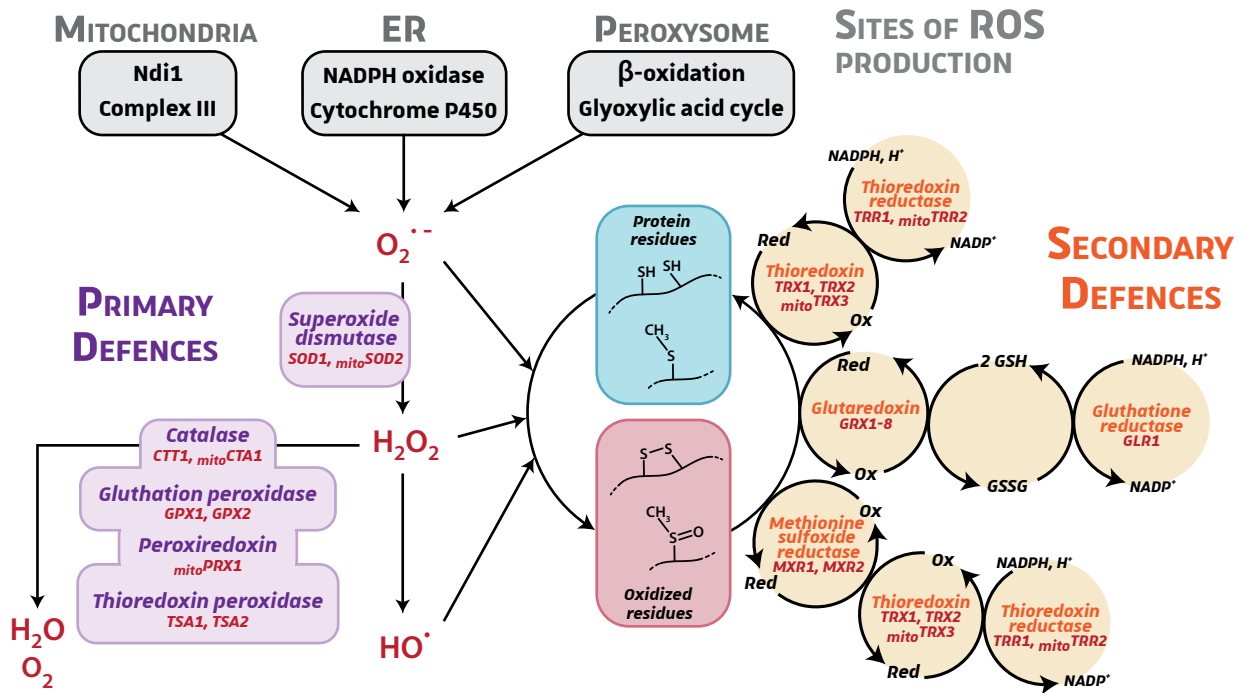


Figure I-27: Cellular defences against ROS. Primary defences act directly on inorganic ROS, whereas secondary defences modify oxidized proteins. Names of yeast enzymes are colored in red.

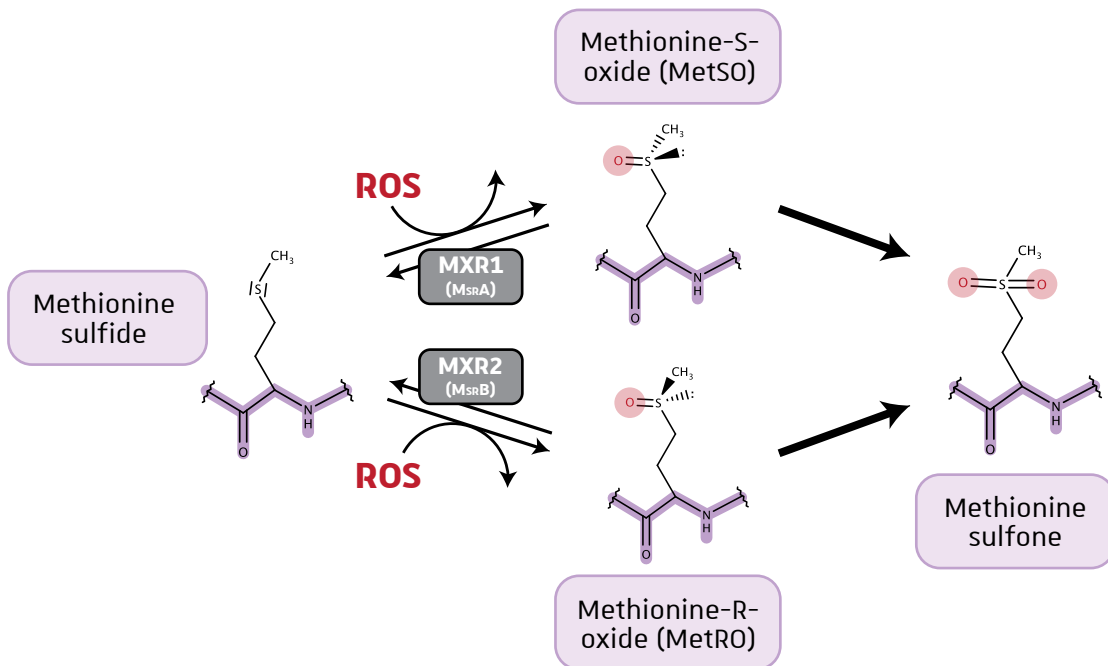


Figure I-28: Methionine oxidation by ROS and recycling by Msr enzymes. The methionine sulfide group can be oxidized by ROS forming either S- or R- methionine oxide epimers. These molecules can be either reduced back to methionine sulfide by Msr enzymes or be irreversibly further oxidized into methionine sulfone.

III.1.2.3. Oxidative stress response and the methionine system

Organisms have evolved several complex antioxidant defences to minimize oxidative damages to proteins and other macromolecules. Detoxification of oxidant species involves both enzymatic and non-enzymatic reactions that lower the oxidative balance. The enzymatic pathway is more often induced under oxidative burst and involves several redox enzymes like superoxide dismutase (SOD), catalase, peroxidase or peroxiredoxin (**Figure I-27**). SOD catalyses conversion of superoxide into hydrogen peroxide (H_2O_2), then catalase, peroxidase or peroxiredoxin convert the H_2O_2 into water before obtaining the harmful hydroxyl radical. These enzymes are part of the primary defences since they eliminate the primary inorganic oxidant molecules before they damage cellular compounds. However, secondary defence systems also exist to repair oxidative damages done on DNA, lipids and proteins. In proteins, the main residues altered by oxidative stress are the two sulfur-containing residues: cysteine and methionine. Oxidized cysteine residues form disulfide bonds that can disorganize the protein folding because they can create covalent links between proteins. However, cysteine residues have a pKa around 8.5, making them difficult to be oxidized spontaneously at physiological pH. Methionine is also subjected to oxidation by ROS to form methionine-S/R-oxide epimers according to the stereochemistry (**Figure I-28**). Spontaneous (non-enzymatic) oxidation of methionine is more efficient than of cysteine since it is independent of the pH ([Peskin and Winterbourn, 2001](#)). Moreover, the redox potential of dimethyl sulfoxide/dimethyl sulfide couple is + 0,16 V, below all redox potentials of ROS, so the sulfide group of Met is suitable for ROS oxidation ([Wood, 1981](#); **Figure I-25**). This oxidation is reversible and reduction is catalyzed, in *S. cerevisiae*, by 2 methionine sulfoxide reductases (or MetO reductases), MsrA (*MXR1* gene) and MsrB (*MXR2* gene), each of them specific for one stereoisomer (**Figure I-27 and I-28**, [Black et al., 1960](#); [Brot and Weissbach, 1983](#); [Lim et al., 2011](#)). These MetO reductases (Msrs) are found in all organisms from bacteria to mammals (essentially in aerobic organisms), showing the importance of this enzyme family and of this antioxidant protection system ([Weissbach, Resnick and Brot, 2005](#)). Through this redox cycling, Met residues are able to act as both a repair system to reverse damage proteins whose Met residues had been oxidized and as antioxidant “pumps” to play an important role in ROS detoxification ([Levine et al., 1996](#); [Stadtman et al., 2002](#); [Luo and Levine, 2009](#)). This antioxidant system may be even more efficient with surface-exposed Met residues which are more accessible to redox reaction with ROS and the Msrs ([Levine et al., 1996](#); [Tarrago et al., 2012](#)). Methionine residues have been shown to be more prone to oxidation compare to other residues, since Met is one of

Table I-9: Studies of Msr mutants and their phenotype related to oxidative stress

	Organism	Phenotype of Msr mutant cells	Ref.
Msr downregulation	<i>M. genitalium</i>	Hypersensitivity to H ₂ O ₂ , virulence is reduced	[192]
	<i>B. cereus</i>	Accumulation of high level of Met(O) exoproteins in the growth medium	[193]
	<i>S. aureus</i>	Increased sensitivity to H ₂ O ₂ and HOCl induced oxidative stress	[194]
	<i>S. aureus</i>	Increased susceptibility to H ₂ O ₂ compared to WT	[195]
	<i>E. coli</i>		
	<i>N. gonorrhoeae</i>	Show altered adherence patterns though adhesin deficiency	[196]
	<i>S. pneumoniae</i>		
	<i>E. coli</i>	More sensitive to H ₂ O ₂ stress in disk assay on solid plate	[197]
	<i>E. coli</i>	Highly sensitive to H ₂ O ₂ and reactive nitrogen intermediates (nitrite and GSNO)	[198]
	<i>S. cerevisiae</i>	Growth of mutant delayed for 4-5 h with 1 mM H ₂ O ₂	[199]
	<i>S. cerevisiae</i>	More Met oxidation (free or protein-borne) in the mutant with 1 mM H ₂ O ₂	[200]
	<i>S. cerevisiae</i>	More sensitive to NaOCl (20 μM)	[200]
	Mouse	Shorter life span, more sensitive to hyperoxia induced oxidative stress, neurological defect	[201]
	Mouse	Increased sensitivity to paraquat induced oxidative stress	[202]
	Mouse (kidney)	Enhances kidney inflammatory response and oxidative stress after ischemia	[203]
	Monkey (retina cells)	Loss of viability and resistance to oxidative stress induced by TCHP (Tertiary-butyl hydroxyperoxide)	[204]
	<i>H. sapiens</i> (lens cell)	More sensitive to H ₂ O ₂ treatment	[205]
	<i>H. sapiens</i> (lens cell)	Loss of mitochondrial membrane potential and increased ROS production	[206]
Msr overexpression	<i>S. cerevisiae</i>	Increased viability to NaOCl treatment (40 μM)	[200]
	<i>S. cerevisiae</i>	Better resistance to 2 mM H ₂ O ₂ toxicity compared to WT	[207]
	<i>D. melanogaster</i> (neurons)	Extended life span, higher resistance to paraquat	[208]
	<i>Rattus</i> (PC12 cells)	Lower ROS concentration during hypoxia and/or reoxygenation	[209]
	<i>Rattus</i> (cardiac myocytes)	MsrA overexpression prevents apoptotic cell death	[209]
	<i>Rattus</i> (cardiac myocytes)	Protection from oxydative stress induced by hypoxia	[210]
	<i>H. sapiens</i> (lens cell)	More resistant to H ₂ O ₂ (from 800 μM to 950 μM) compared to WT	[205]
	<i>H. sapiens</i> (fibroblasts)	Increased survival after H ₂ O ₂ oxidative stress (250-750 μM)	[211]

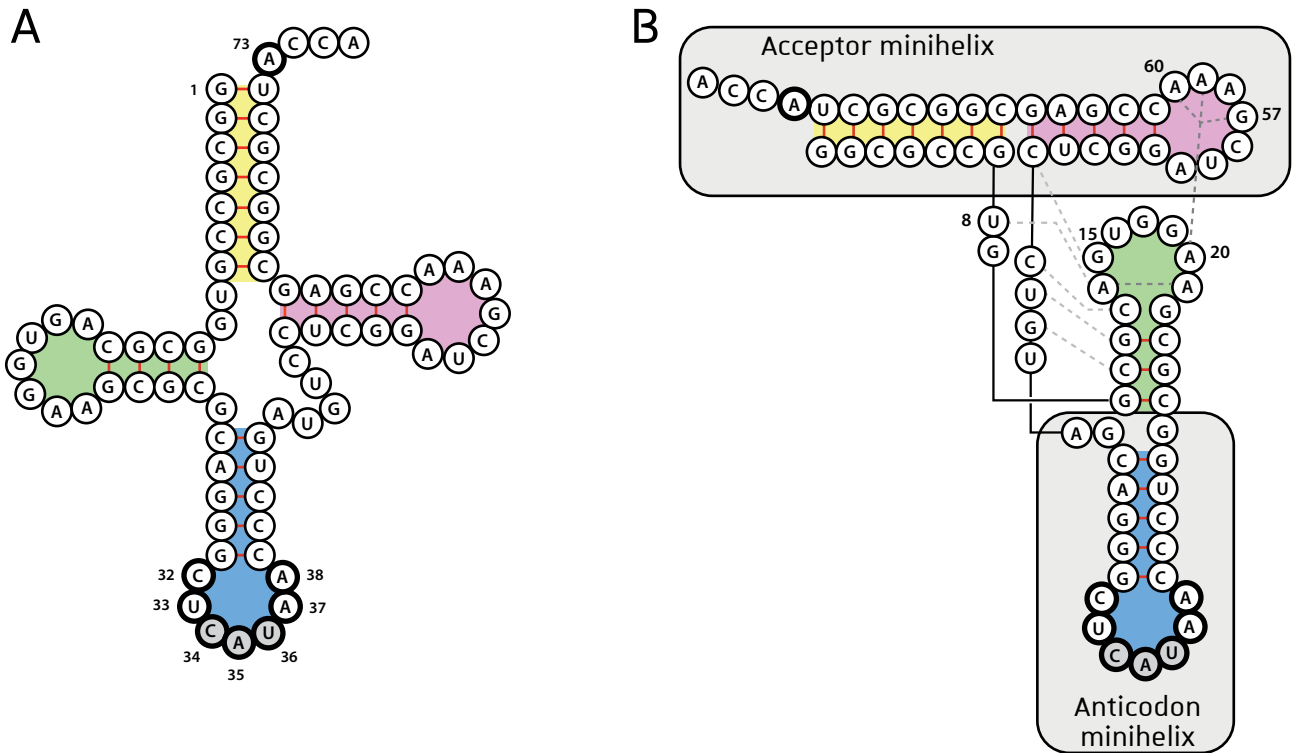
the first to be oxidized after treatment with chloramine-T, and prevent enzymatic inactivation by protecting surrounding residues (Shechter, Burstein and Patchornik, 1975; Reddy *et al.*, 1994). In addition to these results, previous studies have shown that this redox cycling between Met and MetO residues is crucial for ROS scavenging through Met replacement with the isosteric norleucine (carbon analogue to Met, Luo and Levine, 2009) or through Msrs mutated cell phenotypes showing variable sensitivity to ROS (summarized in **Table I-9**, reviewed in Lourenço Dos Santos, Petropoulos and Friguet, 2018). The robustness of this system is even more important, considering the local concentration of Met residues that a protein would constitute, since it has been established that surface-exposed Met residues of proteins provide high concentrations of antioxidant with 100 mM effective concentration for eight Met residues within the protein sequence (Levine *et al.*, 1996). This aspect is found in mitochondria, the major cellular ROS source, where it has been observed that increase of Met residues in mitochondrial proteins correlates with the mass-specific metabolic rates. For this reason, there is an accumulation of surface exposed Met residues in animals with high metabolic rate that, consequently, produce higher levels of ROS (Schindeldecker and Moosmann, 2015). Another striking evidence for Met residue as antioxidant is the evolution of the mitochondrial genetic code in some organisms where AUA codon specifies Met instead of leucine (Bender, Hajjeva and Moosmann, 2008). In such mitochondria the average Met content reaches 6 % in protein sequence, 3 times more than in non-recoded mitochondria, and these additional Met residues appear to be also surface exposed in mitochondrial proteins.

III.2. The tRNA substrates for MetRS

Methionine incorporation is crucial for protein synthesis since it is the first aa incorporated in the polypeptide chain during eukaryotic translation (**Figure I-8**, page 40). Moreover, Met can also be incorporated later on during elongation. Thus it appears that the Met-tRNA^{Met} is the only aminoacyl-tRNA to be recognized by both initiation and elongation factors. To specify each step of translation, cells have developed two tRNAs^{Met}, each one dedicated for a translation step. In this section, we will analyse the tRNAs determinants for the yeast MetRS, then compare the two tRNAs^{Met} sequences.

III.2.1. The tRNA^{Met} identity determinants for the yeast MetRS

To discriminate the two tRNAs^{Met} from the other non-specific tRNA species, the MetRS needs to recognize specific determinants present on its cognate tRNAs. As seen in **Table I-4** page 52, aaRSs



	Transcript	Anticon loop sequence						N ₇₃	Relative loss of efficiency	
		32	33	34	35	36	37			38
tRNA ^{Met} substitution mutants		C	U	C	A	U	A	A	A	1
		C	U	C	A	U	A	A	G	40
		C	U	G	A	U	A	A	A	> 1700
		C	U	U	A	U	A	A	A	> 500
		C	U	A	A	U	A	A	A	> 1700
	tRNA ^{Met} (with G ₁)	C	U	C	C	U	A	A	A	140
		C	U	C	G	U	A	A	A	> 500
		C	U	C	U	U	A	A	A	> 1700
		C	U	C	A	C	A	A	A	> 1700
		C	U	C	A	G	A	A	A	55
		C	U	C	A	A	A	A	A	> 1700
		U	U	C	A	U	A	C	A	170
		U	U	C	A	U	A	C	G	> 1700
Chimeric non-cognate tRNAs	tRNA ^{Asp}	U	U	G	U	C	G	C	A	> 1700
		U	U	C	A	U	G	C	A	> 1700
		U	U	C	A	U	G	C	G	140
		C	U	C	A	U	A	A	G	80
		C	U	C	A	U	A	A	A	3
	tRNA ^{Val}	U	U	U	A	C	A	C	A	> 1700
		U	U	C	A	U	A	C	A	52
		U	U	C	A	U	A	C	G	> 1700
		C	U	C	A	U	A	A	G	9
		C	U	C	A	U	A	A	A	1

tRNA ^{Met} variant	K _i (μM)	Relative loss of efficiency
Anticodon minihelix		
Anticodon CAU	40	
Anticodon GAU	> 1000	
Acceptor minihelix		
Acceptor A73	> 1000	n.m
Acceptor G73	n.m	
Tertiary mutant transcripts		
U ₈ → C ₈		> 1000
G ₁₅ → A ₁₅		470
A ₂₀ G ₅₇ A ₆₀ → U ₂₀ A ₅₇ G ₆₀		> 1000
Hybrid transcripts		
ΔT-arm		10
ΔD-arm		> 300

Figure I-29: tRNA^{Met} transcript mutants and determination of identity elements (from Senger *et al*, 1996; Despons *et al*, 1992). **A.** Sequence of the tRNA^{Met} transcript used for aminoacylation assay (upper), and results of the assay with different tRNA mutants (lower). **B.** Structure and composition of minihelices designed in the study (upper) and results of catalytic analyses for the minihelices or substitution and deletion mutants (lower). n.m. not measurable

use predominantly nucleotidic bases from the acceptor stem and the anticodon region to achieve specific tRNA recognition and discrimination. Bacterial determinants for MetRS relies mostly on the anticodon recognition since CAU anticodon replacement in other tRNA species made them aminoacylated by the *E. coli* MetRS (Schulman and Goddard, 1973; Schulman and Pelka, 1983, 1988). The yeast Met identity system, however, appears to be more complicated. Studies using yeast purified recombinant MetRS have shown that CAU anticodon replacement was not sufficient to charge non-cognate tRNAs (tRNA^{Asp} and tRNA^{Val}) and that nucleotide A₇₃ is crucial for tRNA^{Met} recognition (Senger *et al.*, 1992). Establishment of kinetic parameters of MetRS for several yeast tRNA_i^{Met} mutants and various hybrid tRNAs (deletion of D-arm or T-arm, use of individual minihelices) have shown that tRNA^{Met} identity was a mix of primary, secondary and tertiary structure features (**Figure I-29**). In fact, determinants of yeast tRNA^{Met} are the A₇₃ discriminatory base, the all anticodon loop and the D-arm essential for aminoacylation by MetRS (Senger and Fasiolo, 1996; results summarized in **Figure I-29**). These identity elements correlate with the fact that they are all present in both initiator and elongator tRNAs^{Met}: the D-arm is relatively well conserved, the anticodon loop is exactly the same sequence and the A₇₃ discriminator is conserved (**Figure I-30**)

III.2.2. One enzyme but two tRNA substrates

The incorporation of Met into proteins is mediated by the production of Met-tRNA^{Met} by the MetRS enzyme. As we have seen previously, 10 genes coding for tRNA^{Met} are present in yeast genome: 5 coding for the initiator tRNA_i^{Met} (called IMT genes for initiator methionine tRNA) and the same number of genes code for the elongator tRNA_e^{Met} (EMT genes) (**Table I-2**, page 32). Initiator tRNA is used to incorporate Met at the AUG start codon during initiation of translation whereas the elongator tRNA^{Met} brings the elongating Met to decode internal AUG codons (Housman *et al.*, 1970; Smith and Marcker, 1970).

Concentrations of these two tRNA need to be finely tuned in the cell. A two-fold decrease in tRNA_i^{Met} expression in yeast increases significantly the doubling time (Francis and Rajbhandary, 1990). The sequence of tRNA_i^{Met} gene is the most conserved among those of all tRNA species, in all three kingdoms of life (Sprinzl *et al.*, 1998; Marck and Grosjean, 2002). Since these two tRNA^{Met} have to fulfil different functions during translation, each displays specific attributes that helps the translation machinery to distinguish them (reviewed in Kolitz and Lorsch, 2010). To identify critical determinants for each tRNA^{Met}, swapping nucleotides between the two tRNAs has been used and

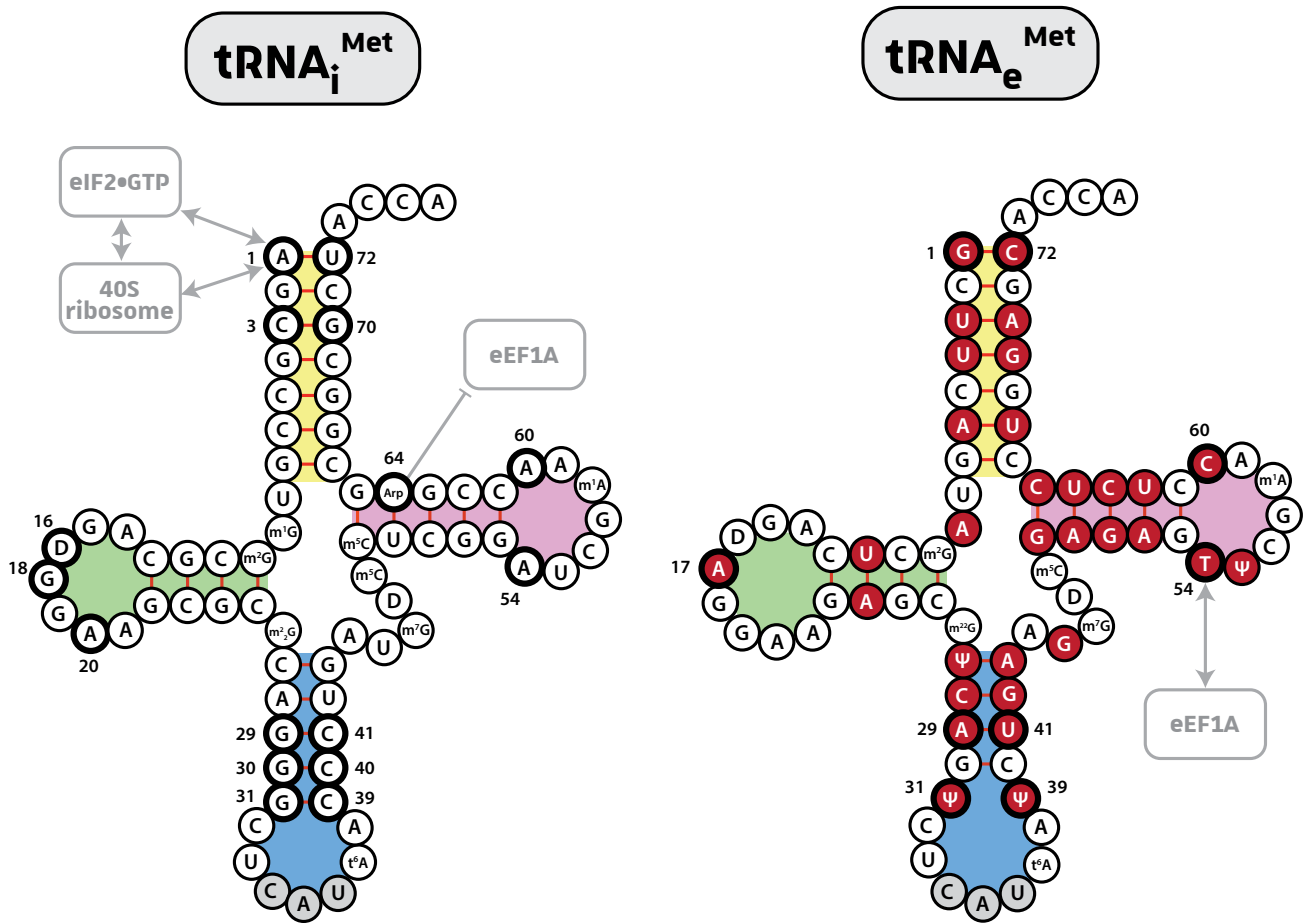


Figure I-30: Secondary structures of yeast initiator (left) and elongator (right) tRNA^{Met}. Positions with numbers are nucleotides previously found to be important to distinguish the initiator from the elongator (identity elements). Red nucleotides are those differing between the two tRNAs. Corresponding names and structures of post-transcriptionally modified nucleotides are found in **Appendix 3** and **Appendix 4**, respectively. Enzymes responsible for these modifications are also found in **Appendix 3**.

Caption

- Nucleotide in tRNA^{Met} different from initiator sequence
- Identity element
- Anticodon nucleotide
- Acceptor stem
- D-arm
- Anticodon arm
- TψC-arm
- Watson-Crick interaction

tested in cells deleted in all initiator/elongator tRNA genes.

- The elongator is longer by one more base pair and has an additional A₁₇ in its D-loop (**Figure I-30**).
- The base pair 1:72 in the acceptor stem is different between the two tRNAs^{Met} and has an important role in initiator/elongator discrimination. It has been shown that yeast tRNA_i^{Met} with G₁:C₇₂ instead of A₁:U₇₂ could act as an elongator tRNA, whereas tRNA_e^{Met} with A₁:U₇₂ is less efficient for elongation (Åström, von Pawel-Rammingen and Byström, 1993). Moreover, this A₁:U₇₂ base pair is important for binding to initiation factor eIF2 (Farruggio *et al.*, 1996).
- The yeast tRNA_i^{Met} is the only one tRNA who lacks the T₅₄-Ψ₅₅ within the T-loop (**Table I-2**) which is replaced by A₅₄-U₅₅ instead. The T₅₄ present in tRNA_e^{Met} is an important elongator determinant for eEF1A recognition, since function of yeast tRNA_e^{Met} with A₅₄ is compromised unless eEF1A is overexpressed (Åström, von Pawel-Rammingen and Byström, 1993). Same is true for A₅₄ in the initiator tRNA: substitution by U₅₄ in yeast is lethal in an initiator null-strain (Pawel-Rammingen, Åström and Byström, 1992).

Post-transcriptional nucleotides modifications are also important in the two tRNAs^{Met}, with initiator tRNA especially sensitive because it carries 11 different modified nucleotides (**Figure I-30**), but most of them are non-essential. Among these modifications, m¹A₅₈ appears to be important for initiator maturation since loss of the methylation impairs translation initiation (Anderson *et al.*, 1998). Another important determinant for the initiator tRNA^{Met} is the 2-O-ribosylphosphate modification on A₆₄ (Arp₆₄) of the T-stem. This modification act as anti-elongator determinant since loss of Arp₆₄ by a deletion of the catalysing enzyme Rit1, allows the initiator tRNA to function in elongation and triggers survival of cells lacking the elongator tRNA (Åström and Byström, 1994). Its position within the T-stem would interfere for binding to eEF1A through steric exclusion, whereas eIF2 only bind the Met residue and acceptor stem of Met-tRNA_i^{Met} (Shin *et al.*, 2011).

Of course, all identity elements act synergistically and in combination to ensure specificity for each tRNA^{Met}. For example, introduction of A₁:U₇₂ and G₃₁:C₃₉ into tRNA_e^{Met} increased its affinity for eIF2-GTP, as well as introduction of A₅₄ and A₆₀ in the T-loop (Kapp, Kolitz and Lorsch, 2006; Dong *et al.*, 2014).

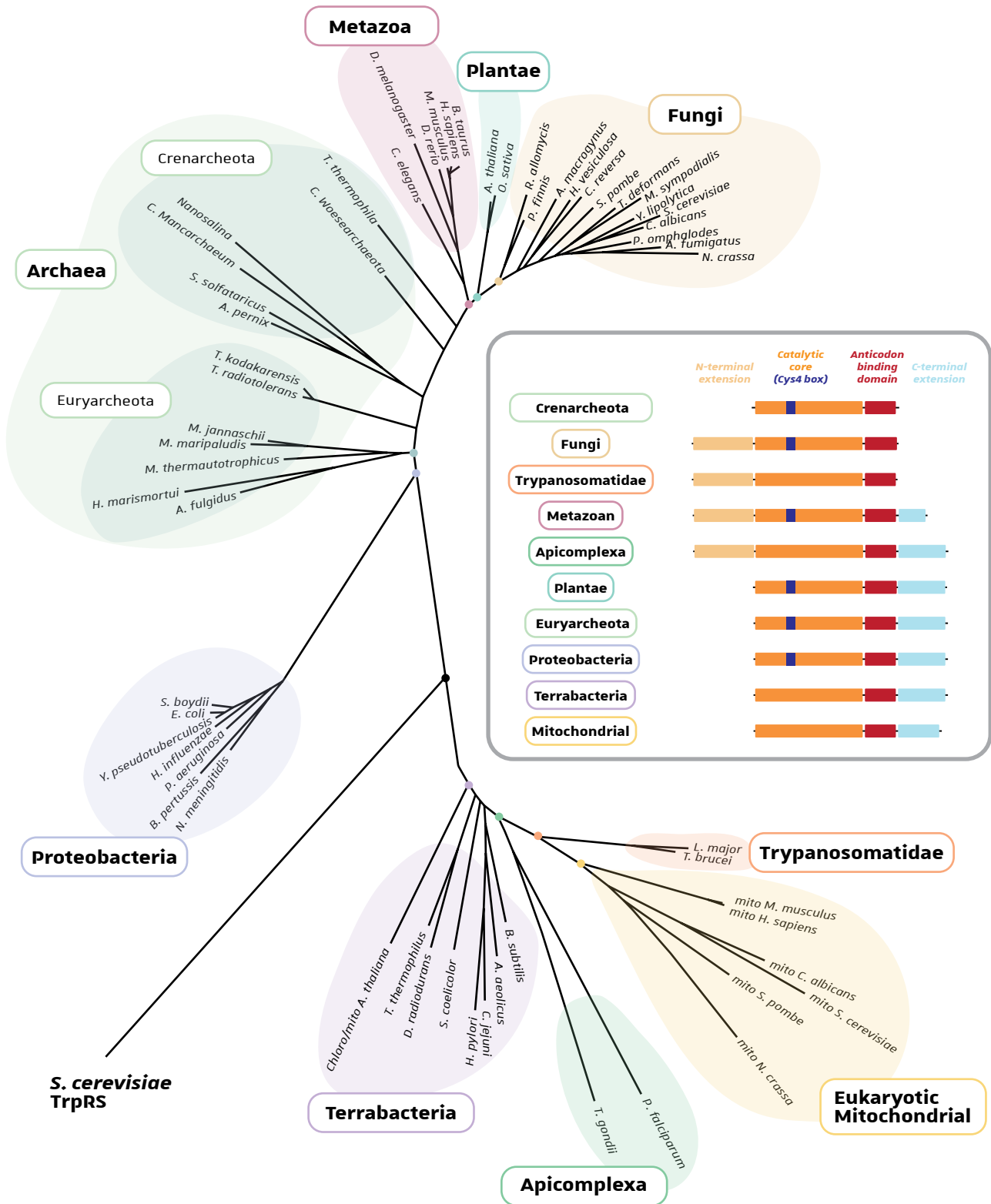


Figure I-31: Structures of MetRS enzymes in the tree of life. Sixty polypeptide sequences of MetRS in eucaryotic and procaryotic organisms, as well as organellar MetRSs sequences have been aligned and a phylogenetic tree has been established from this protein alignment. The *S. cerevisiae* TrpRS is used as an outgroup to place the root of the tree. MAFFT online service was used for protein sequence alignment; and phylogenetic tree was generated with IQ-TREE web server and visualized with FigTree. The modular organizations of those MetRSs according to their phylogenetic origins are displayed in the inset.

III.3. Modular organization of the yeast MetRS

III.3.1. Conservation and evolution of MetRS sequences

The MetRSs from the three kingdoms of life have distinct structural features but share a common minimal core enzyme essential for the enzymatic activity (catalytic core and anticodon binding domain (ABD), dark orange and red in **Figure I-31**). Sequence alignments of several MetRSs belonging to organisms from different kingdoms, show that MetRSs can be divided into four modular groups (**Figure I-31**):

- The minimal catalytic (catalytic core and ABD) core found mostly in *Crenarcheota*.
- The minimal core and an additional N-terminal domain for MetRS from *Fungi* and *Trypanosomatidae*. As seen previously, this N-terminal extension mediates association with Arc1 in *S. cerevisiae*.
- The minimal core and an additional C-terminal domain in MetRSs from Plants, *Euryarcheota*, bacteria and the mitochondrial counterpart of cytosolic eukaryotic MetRSs. This domain is essential for *E. coli* MetRS' dimerization and binds non-specifically to tRNAs (Mellot *et al.*, 1989).
- Metazoan and Apicomplexa possess both an additional C- and N-terminal domains, allowing plethora of new interactions (Yakobov *et al.*, 2018).

III.3.2. Sequence and structure of the yeast MetRS

Cytosolic MetRS is a class I aaRS belonging to the subclass Ia and contains a Rossmann fold catalytic core with the HLGK and KFSKS signature motifs essential for its aminoacylation activity (Schmitt *et al.*, 1994, **Figure I-32A and 32C**). Inside this catalytic core, a connective polypeptide CP1 is inserted and contains a zinc-binding site between residues 337–353 (called Cys4 box). This domain has been shown to bind zinc ions (1:1 stoichiometry) and to participate to tRNA-independent homocysteine editing (Senger *et al.*, 2001; **Figure I-32A**). A difficulty in MetRS analysis is the lack of available three-dimensional structures in the databases. Even if the structure of the full-length bacterial MetRS has been solved almost 30 years ago (Brunie, Zelwer and Risler, 1990), it took a long time for resolving the first eukaryotic MetRS structure and, still, the eukaryotic MetRS structures that were solved are those of the parasite *Leishmania major* and of the human enzymes (Larson

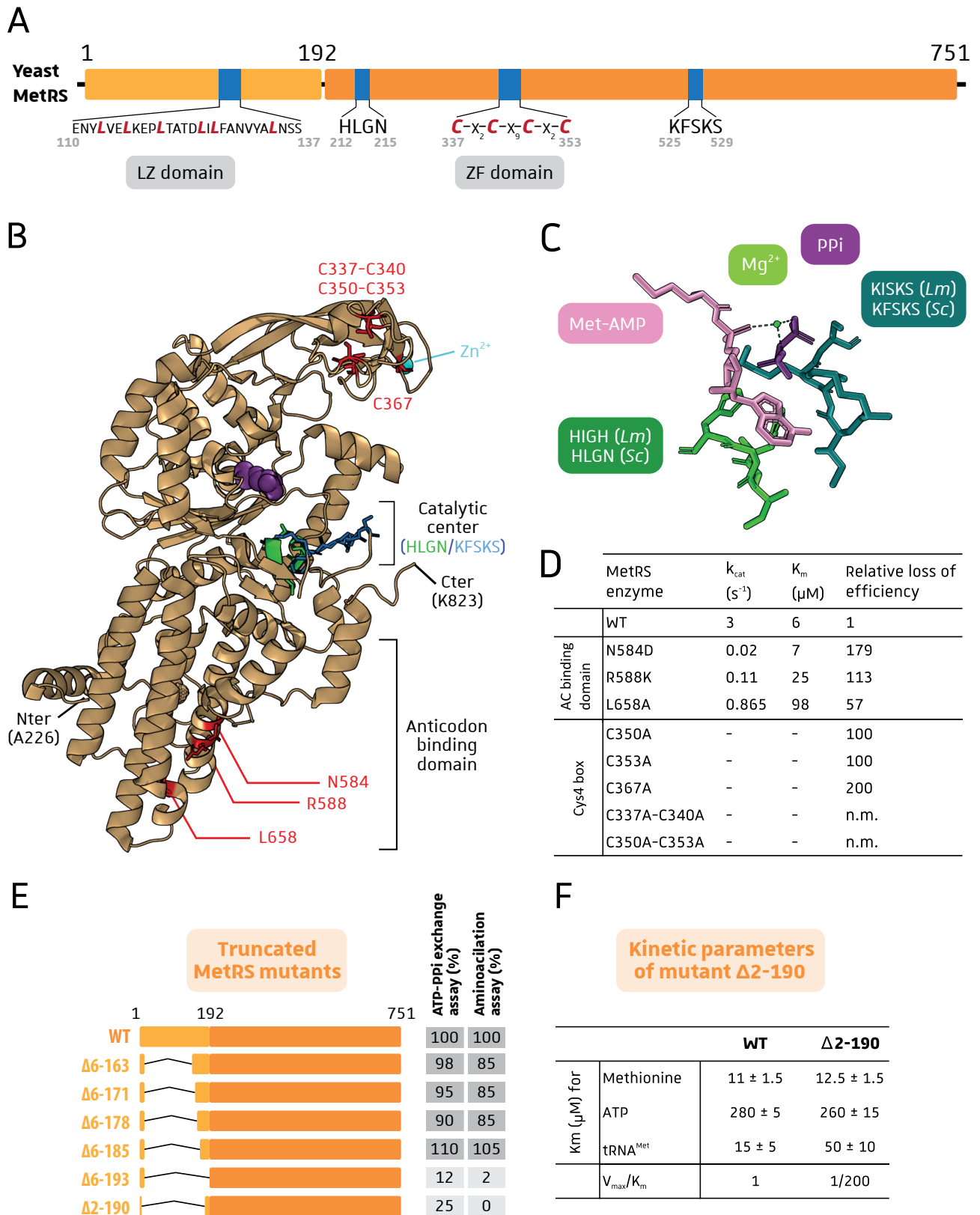


Figure I-32: Structural features of yeast MetRS and localization of essential residues. **A.** Modular organization of the yeast MetRS sequence. LZ: Leucine Zipper, ZF: Zinc Finger. **B.** Three-dimensional structure of yeast MetRS. Since no structure for yeast MetRS has been resolved so far, here is shown the crystal structure of human MetRS (pdb 5GOY) with Met (spheres in purple) and Zn^{2+} . Residues in red have been mutated in yeast MetRS to analyse their importance in catalysis in D. **C.** Structure of the *L. major* MetRS catalytic center with the two signature motifs (pdb 3KFL). **D.** Kinetic properties for aminoacylation of various yeast MetRS mutants. n.m.: not measurable (Senger et al, 2001, Despons et al, 1992, Despons et al, 1991). **E.** Enzymatic parameters of WT and N-terminally truncated MetRSs, in percentage relative to the WT (Results summarized from Walter et al, 1989). **F.** Kinetic parameters of the mutant $\Delta 2-190$ displaying a severe loss of activity.

et al., 2011 (pdb 3KFL); Lee, Cho and Kang, to be published (pdb 5GOY)) correspond to N-terminally truncated forms. In addition, the structure of yeast N-terminal GST-like domain of yeast MetRS part complexed to the corresponding Arc1 domain has been solved (Simader *et al.*, 2006; **Figure I-20B**, page 72) but not the core of the yeast MetRS. As shown in **Figure I-32B**, the sequence of the human MetRS crystallized starts at residue A226, and the *L. major* MetRS at K206 even if many attempts to crystallize the full-length protein were unsuccessfully made (Larson *et al.*, 2011). Even if the structure of yeast MetRS is still not available, we can easily predict that its structure would be similar to the human and parasite homologues, since they share 36.5 % and 22 % identity (50 % and 36 % similarity) respectively. Besides, the superimposition of the two solved protein structures shows high structural similarities (see **Appendix 5A**, page 110). Same is true with the superimposition of bacterial MetRS with the human MetRS (**Appendix 5B**, page 110). Based on structural models, several residues have been shown to be important for aminoacylation: some residues (N584, R588 and L658) within the anticodon binding domain and the cysteine residues forming the zinc-binding site (**Figure I-32B and 32D**, Despons *et al.*, 1991; Senger *et al.*, 2001). This reveals that this Cys4 box domain is important for the maintenance of the active site and might position the tRNA correctly due to its position above the catalytic center through structural flexibility.

In contrast to its bacterial counterpart, eukaryotic MetRS is a monomeric enzyme since it lacks the Trbp111-like C-terminal domain that mediates dimerization of the bacterial enzyme (**Figure I-17**, page 62). This 133 aa-long C-terminal extension appeared to be essential for dimerization but not for aminoacylation (Cassio and Waller, 1971). However, an N-terminal GST-like domain extension of 192 aa residues is found in *S. cerevisiae* MetRS (Walter *et al.*, 1983). It appeared that this domain is not entirely essential for the aminoacylation efficiency (Walter *et al.*, 1989). Truncation of the first 185 aa residues did not affect drastically neither the activity nor the stability of the mutants since they were well expressed (western blot analysis) in yeast cells and showed almost unmodified aminoacylation activity *in vitro* (**Figure I-32E**). However, deletion of additional five residues resulted in drastic loss of activity for tRNA aminoacylation due mainly to an impact on the V_{max} since K_m for each substrate are not really impaired, except K_m for tRNA which increases three-fold (**Figure I-32F**). Thus, this eukaryote-specific N-terminal domain is dispensable for aminoacylation, but remains important for alternative functions like interaction within an MSC (AME for yeast and MARS for human) (**Figure I-17**, page 62).

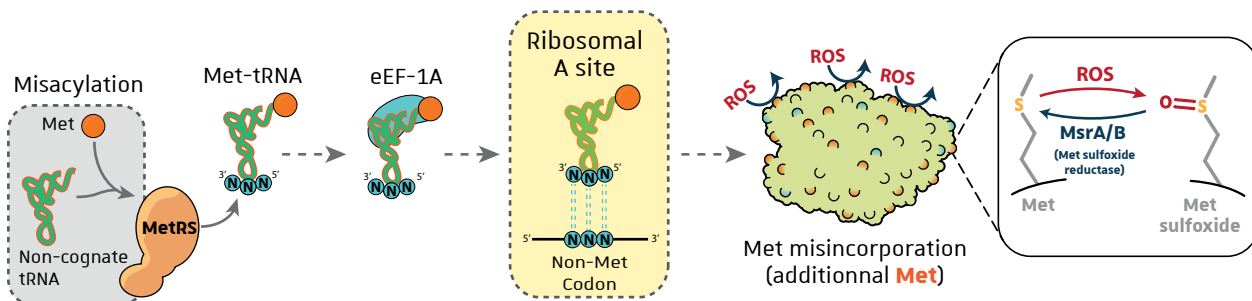


Figure I-33: Met misincorporation during protein synthesis and oxidative stress response. MetRS is able to misacylate non-cognate tRNAs with Met, resulting in Met misincorporation at non-Met position during translation elongation. These additional Met residues are expected to buffer ROS through oxidation of the reactive sulphur group into sulfoxide and subsequent catalytic reduction of sulfoxide with sulfur by Msr enzymes.

Table I-10: Techniques used to monitor mismethylation and identify mismethylated tRNA species

	Organism	Technique	Enzyme and tRNA used	Environmental conditions	tRNAs misacylated with Met	Ref.
Bacteria	<i>E. coli</i>	FB-AA tRNA microarrays	tRNA <i>in vitro</i> transcripts Purified MetRS and total tRNAs	<i>In vitro</i>	Thr(CGU) Arg(CCU)	[212]
	<i>E. coli</i>	FB-AA Mass spectrometry	Purified MetRS (WT and K362E, K388E mutants)	Anaerobic conditions and antibiotic exposure	Many tRNAs	[213]
	Mouse gut microbiom	tRNA microarrays	<i>In vivo</i> cell pulse labelling	Anaerobic conditions	Variable according to the mouse and the microorganism	[214]
Archaea	<i>A. pernix</i>	tRNA microarrays Mass spectrometry	<i>In vivo</i> cell pulse labelling and purified MetRS	Low growth temperatures (75 °C)	Leu(BAG) Leu(YAA)	[215]
Yeast	<i>S. cerevisiae</i>	tRNA microarrays FB-AA Mass spectrometry	<i>In vivo</i> cell pulse labelling and with purified AME complex	Basal or yeast in stationary phase	Many tRNAs	[216]
Human	Human (HeLa cells)	tRNA microarrays Mass spectrometry	<i>In vivo</i> cell pulse labelling and purified MetRS	Virus infection, TLR ligand, oxidative stress	Many tRNAs	[217]
	Human (HEK293T)	Reporter mCherry-GFP tRNA microarrays	<i>In vivo</i>	Basal and arsenite treatment	Glu(UUC) Glu(CUC)	[80]
	Human (HEK293T)	Reporter RFP FB-AA Mass spectrometry	<i>In vivo</i> RFP reporter Purified MetRS WT and S209D/S825D mutant)	Basal, arsenite treatment and MetRS mutant S209D/S825D	Lys(CUU), Ala(AGC), Gly(GCC), His(GUG), Leu(CAG)	[218]
	Human (HEK293T)	tRNA microarrays Mass spectrometry	<i>In vivo</i> cell pulse labelling	Addition of Ca ²⁺ in growth medium	Tyr, Glu, Asp, Val, Phe	[219]

FB-AA = Filter-based aminoacylation assay; B = C, G or U; Y = C or U

III.4. Features of MetRSs across the tree of life

As we have seen in the previous sections, aaRSs carry out additional nontranslational functions. The MetRS does not escape to this rule, since this synthetase displays several features *in vivo* found in bacteria and eukaryotes. All these new characteristics have been studied during my thesis.

III.4.1. Methionine mischarging and adaptative translation

III.4.1.1. Methods used for detection of Met mistranslation

We have seen in previous sections that Met can play a major role in oxidative stress response by reducing harmful oxidants in a reversible way, catalyzed by Msr reductase enzymes. Cells are able to temporarily increase the content of Met residues in proteins during oxidative stress to enhance ROS remediation (Wang and Pan, 2016). They do so by misacylation of non-methionyl-tRNAs by the MetRS: the result is a misacylated Met-tRNA that can be used during elongation and direct incorporation of Met residues at non-Met position (Figure I-33). Since tRNA misacylation can rapidly be induced (no transcription factors and new gene expression needed), this mechanism would constitute an immediate extra-genetic system providing protection against oxidative damages without gene expression requirement. Such phenomenon has been shown in bacteria, archaea, yeast and mammalian cells and several techniques are used to reveal this tRNA mismethionylation and subsequent misincorporation of Met (Table I-10). Several approaches are possible to identify misacylated tRNA species, and usually new studies start with a tRNA microarray that allow simultaneous detection of several tRNA species (Netzer *et al.*, 2009; Jones, Alexander and Pan, 2011; Schwartz *et al.*, 2016). This technique relies on [³⁵S]-Met pulse-radiolabelling of cells followed by total RNA extraction and hybridization to tRNA microarrays. These microarrays are made of oligonucleotides DNA probes complementary to all tRNA species from the organism being studied and enable detection of mismethionylated tRNAs with a 0.1 % detection limit. This method allows detection of numerous tRNA species being misacylated (see Figure I-34) and needs to be carefully interpreted, since false positive results might contaminate the microarray. To confirm some misacylated tRNAs, the classical filter-based *in vitro* aminoacylation assay can be used on tRNA transcript synthesized from *in vitro* transcription and methionylated with purified MetRS (Jones, Alexander and Pan, 2011; Wiltout *et al.*, 2012; Schwartz *et al.*, 2016). In some cases, the *in vitro* aminoacylation assay does not correlate with tRNA microarrays. Indeed, the *E. coli* tRNA^{Thr(CGU)}

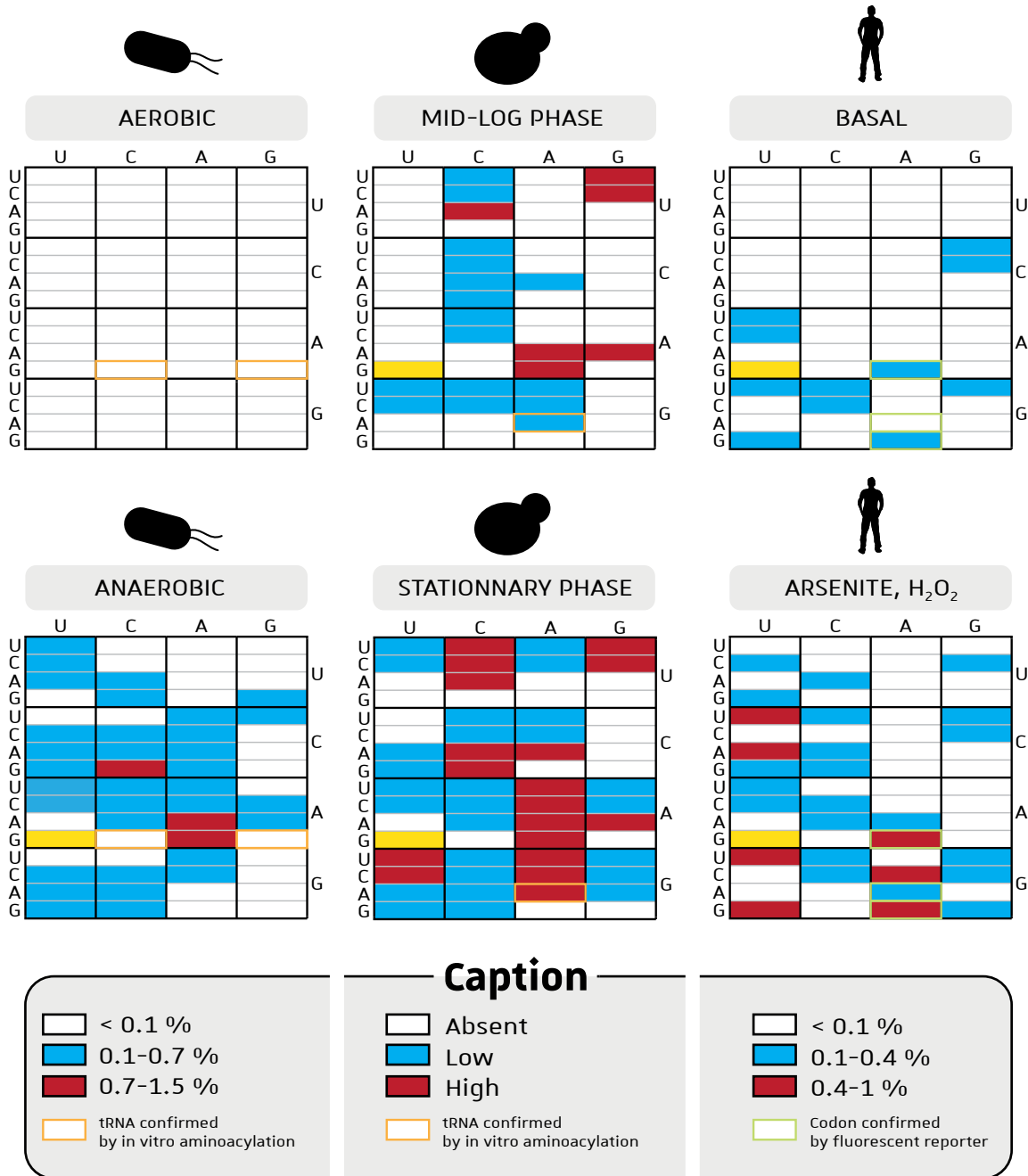


Figure I-34: Mismethionylated tRNAs identified by tRNA microarrays. Results are shown with the standard table of the genetic code: when a tRNA is found mismethionylated, the corresponding codon read by this tRNA is colored in either blue or red according the signal intensity ($[^{35}\text{S}]$ -signal relative to all tRNAs^{Met}). Met codon is highlighted in yellow. Data used for this figure come from [Schwartz et al, 2016](#) and [Jones et al, 2011](#) for *E. coli*; [Wiltrout et al, 2012](#) for *S. cerevisiae*; [Netzer et al, 2009](#) and [Gomes et al, 2016](#) for mammals.

and tRNA^{Arg(CCU)} have been found to be misacylated in a first tRNA microarray experiment (Jones, Alexander and Pan, 2011) and even confirmed *in vitro* by aminoacylation assay, but these exact same bacterial tRNAs were then not found to be mismethionylated in a second tRNA microarray, even in anaerobic conditions that are supposed to enhance Met misacylation (Schwartz *et al.*, 2016) **Figure I-34**). Usually, these tRNA microarrays enable detection of lots of misacylated tRNAs which, if used for protein synthesis, would result in high proteome variation even in basal conditions (**Figure I-34**). One might remember that this misacylated tRNAs are not used equally in protein elongation since eEF1A (or bacterial EF-Tu) binds poorly some misacylated tRNA and thus does not deliver them to ribosome which improves translation accuracy (LaRiviere, Wolfson and Uhlenbeck, 2001; Asahara and Uhlenbeck, 2005). To assess mistranslation level in proteins, mass spectrometry can be used to detect low frequency aa substitutions in purified protein of interest or in the whole proteome. Other method relies on quantification of Met incorporation using a fluorescent reporter that has a Met residue critical for fluorescence emission. The codon of this essential Met is mutated but the reporter can still emit a fluorescent signal if the mutated codon is mistranslated by Met, in other words if a mismethionylated tRNA is used during translation (Lee *et al.*, 2014; Gomes *et al.*, 2016; **Table I-10**). This fluorescence-based approach relies on a case-by-case analysis of each codon and is often used as confirmation of previous result obtained by the tRNA microarray techniques. During my PhD, I developed such a fluorescent reporter device to analyse Met misincorporation for almost all coding codons in yeast.

III.4.1.2. Misacylation properties of MetRS and consequences of mismethionylation

All previous studies on mismethionylation have found lots of misacylated tRNA in various organisms (**Table I-8** and **Figure I-34**). Conditions used to study mismethionylation vary according to the organism that was studied and the physiological conditions or stress: anaerobiosis and antibiotic exposure for bacteria, thermal stress in archaea, growth phase in yeast cells or oxidative stress and innate immune response in mammals (**Table I-10** and **Figure I-34** and **I-35**). All these stresses might result in tRNA modifications and/or MetRS modification to allow mischarging of non-cognate tRNAs. In bacteria, the WT MetRS was shown to aminoacylate various tRNA species in anaerobic conditions (Schwartz *et al.*, 2016; **Figure I-34**). Directed mutagenesis of some aa residues of the bacterial MetRS have revealed their importance for MetRS accuracy. Indeed, substitution of some residues increased the mischarging of tRNA^{Arg(CCU)} and tRNA^{Thr(CGU)} (Q211, Q213, C477, T489 and Y490),





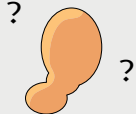
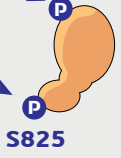
Organism			
Stress	Anaerobiosis	Stationnary phase Oxidative stress	Oxidative stress Innate immune
MetRS features	<div style="display: flex; justify-content: space-around; align-items: center;"> <div style="border: 1px solid red; padding: 5px; color: red; text-align: center;"> Accuracy increased F277L W221A D369A W461D </div> <div style="text-align: center;">  </div> <div style="border: 1px solid blue; padding: 5px; color: blue; text-align: center;"> MisMet increased Q211A Q213A C477S T489A Y490A </div> </div>		<div style="text-align: center;">  </div> <div style="display: flex; justify-content: center; margin-top: 10px;"> <div style="border: 1px solid blue; border-radius: 10px; padding: 5px; margin-right: 10px;">ERK kinase</div> <div style="margin-right: 10px;">→</div> <div style="border: 1px solid blue; border-radius: 10px; padding: 5px; margin-right: 10px;">MisMet increased</div> </div>

Figure I-35: Growth conditions and MetRS features that enhance tRNA mismethionylation in *E. coli*, *S. cerevisiae* and in human cells. In *E. coli*, mutations of MetRS have been shown either to increase (red) or decrease (blue) tRNA charging accuracy. In human, ERK kinase is responsible of MetRS phosphorylation which decreases its fidelity during oxidative stress or innate immune repsonse.

whereas other substitutions were shown to increase the accuracy of MetRS (F277, W221, D369 and W461, see **Figure I-35**), indicating that all these residues play a role (negative or positive) in the accuracy of tRNA methionylation. All these residues are dispersed across the protein sequence, showing the important role of both the anticodon-binding domain and the catalytic domain for tRNA discrimination.

A modified promiscuous MetRS has been found in human cells (Lee *et al.*, 2014). During oxidative stress, ERK1/2 phosphorylates the human MetRS at position S209 and S825 located in the GST-like domain and in the anticodon-binding domain, respectively. These two phosphorylated residues enhance the mischarging of Met on non-methionyl tRNAs (tRNA^{Lys} has been used in this study). This Met mischarging was shown to reduce intracellular ROS levels and protect cells from oxidative damages (Lee *et al.*, 2014). In yeast, no protein modifications are known to enhance mismethionylation, though we know that binding of MetRS to Arc1 should increase fidelity of aminoacylation since Arc1 binds tightly the tRNA_e^{Met} inside the AME complex. However, no differences of mismethionylated tRNAs were found in an *arc1Δ* strain compare to the wild-type (Wiltrout *et al.*, 2012). With our fluorescent reporter we have been able to see differences between these two strains, highlighting the role of Arc1 in MetRS accuracy (see **Results Project I**, page 115).

III.4.2. Nuclear relocation and additional function

The majority of the MetRS localizes in the cytosol which is the compartment in eukaryotes where translational machinery resides. However, some studies have shown that this aaRS could be imported into the nucleus both in yeast and in human cells. Indeed, we bioinformatically identified a putative NLS in the cytosolic human and yeast MetRS sequences (Debard *et al.*, 2016). In general, nuclear aaRSs are thought to aminoacylate tRNAs inside the nucleus and this nuclear aminoacylation serves as a proofreading step that ensures that tRNA was correctly processed prior to its export (Lund and Dahlberg, 1998; Sarkar, Azad and Hopper, 1999; Grosshans, Hurt and Simos, 2000). Moreover, nuclear aminoacylation might provide aa-tRNA to the nuclear ribosomal machinery since nuclear protein synthesis has been reported in some studies (McLeod *et al.*, 2014). In addition to these potential roles, the human MetRS was found in nucleolus of cells treated with mitogenic signals like EGF, PDGF and insulin (Ko *et al.*, 2000; Gunasekera *et al.*, 2004). This nucleolar relocation may have a role in ribosomal biogenesis as cells incubated with anti-MetRS antibodies have decreased amount of newly synthesized rRNAs (Ko *et al.*, 2000; **Figure I-36**). How the MetRS translocates into

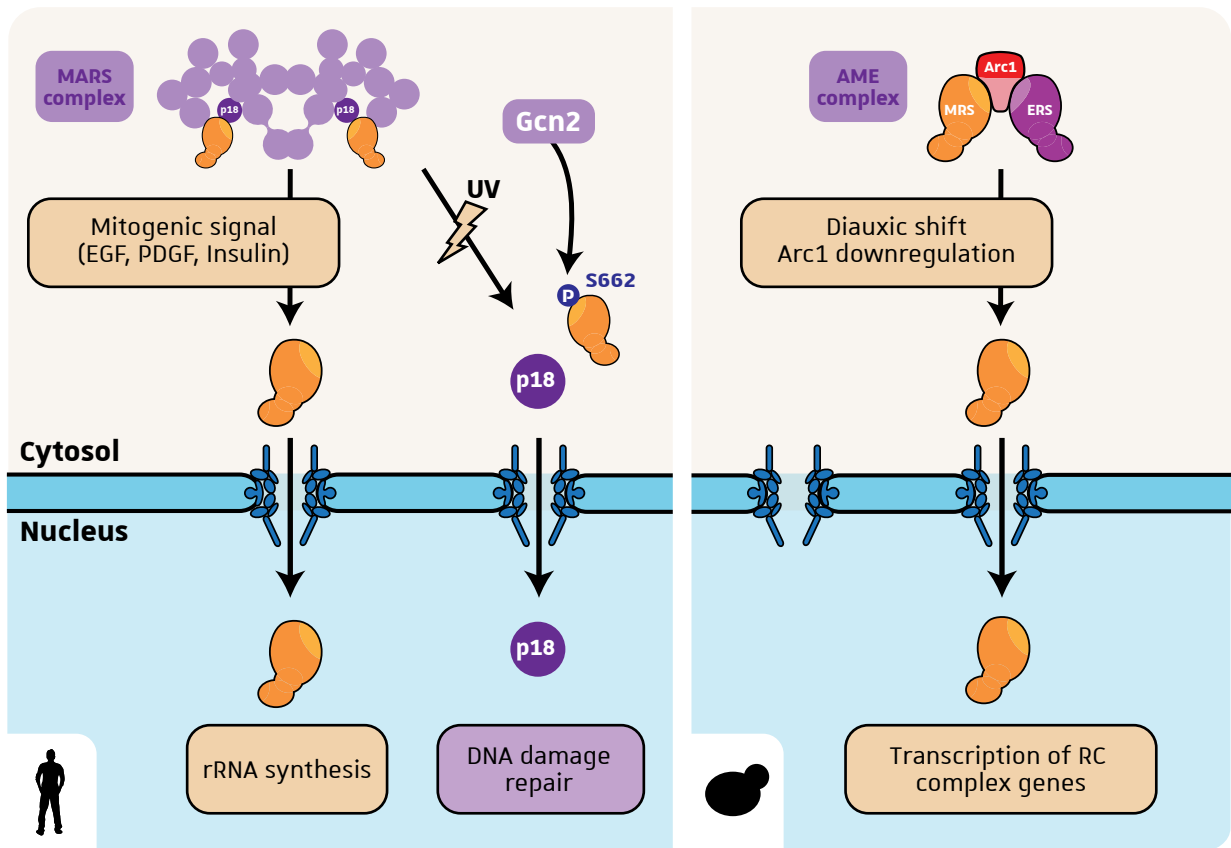


Figure I-36: Nuclear relocation mechanisms of human (left) and yeast (right) MetRS. In human, nuclear relocation of MetRS is triggered during mitogenic signal causing dissociation from the MARS complex. p18 protein relocates into the nucleus through UV treatment and subsequent phosphorylation of MetRS by Gcn2, inducing p18 translocation. In yeast, the diauxic shift induces arc1 downregulation and subsequent release of MetRS from the AME complex.

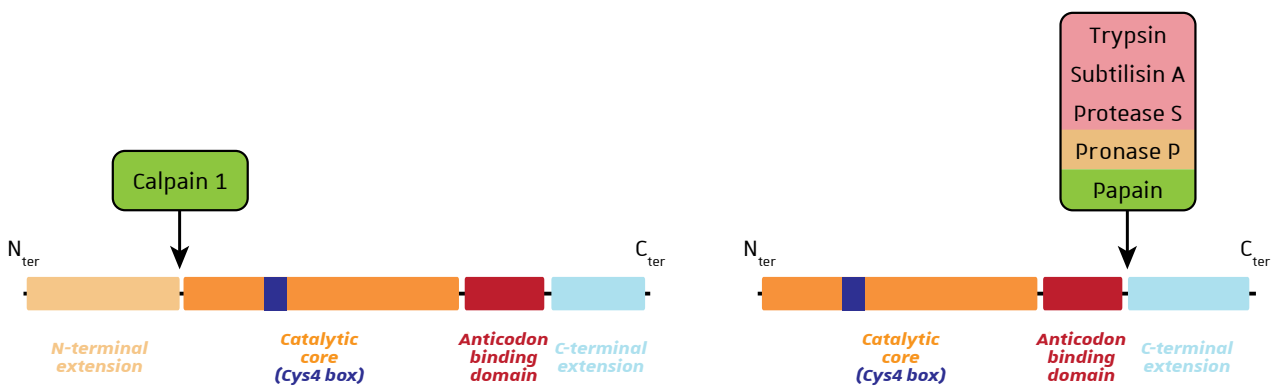


Figure I-37: Localisation of protease cleavage sites identified on human (left) and bacterial (right) MetRS. The proteases involved are indicated above the MetRS modular organization, and are colored according to their catalytic residues (caption).

Caption
 Catalytic residue
 Serine
 Serine / Metal
 Cysteine

the nucleus and how it interacts with RNA polymerase I remains unclear. The associated protein AIMP3/p18 is also translocated into the nucleus to mediate DNA damage repair caused by UVs. This translocation event is activated through GCN2-mediated phosphorylation of MetRS on its Ser662 residue, destabilizing the interaction with p18 and causing its dissociation from the human MSC also called the MARS complex (**Figure I-36**). In yeast, relocation has been seen in respiration after the diauxic shift that triggers decrease of Arc1 concentration and thus release of MetRS ([Frechin *et al.*, 2014](#); **Figure I-23B**, page 76). This relocation is Arc1-dependent since deletion of the N-terminal Arc1-binding domain of MetRS enables translocation of the enzyme into the nucleus ([Galani *et al.*, 2001](#); **Figure I-23A**, page 76). Yeast nuclear MetRS was shown essential for synchronous expression of proteins from the respiratory chain complex and growth of yeast cells in respiratory medium ([Frechin *et al.*, 2014](#)). However, like in human cells, the molecular mechanism of nuclear MetRS regulation is not fully understood.

III.4.3. Cleavage of bacterial and human MetRS orthologs

During evolution, we have seen that extra domains were added to the MetRS protein essentially at the N-terminus part (**Figure I-31**, page 92). Additional domains are not always essential for aminoacylation activity. Indeed, studies show that yeast MetRS was still active after deletion of the 185 first residues (**Figure I-32E**, page 94). Several aaRSs were found cleaved in cells and truncated forms can harbour different functions. For example, IFN- γ induces N-terminus removal of TrpRS in vertebrates, generating a shorter form called mini-TrpRS that exerts an anti-angiogenic action through secretion in the extracellular matrix and new interaction with VE-cadherin ([Zeng *et al.*, 2011](#)). Interestingly, naturally occurred truncated forms of MetRS have been found in both bacteria and human ([Cassio and Waller, 1971](#); [Lei *et al.*, 2015](#)). First observation was conducted in *E. coli* where purified bacterial MetRS showed time-dependent proteolytic cleavage after addition of trypsin, pronase P, protease S, papain or subtilisin A (**Figure I-37**). These endopeptidases have different catalytic types and show similar pattern for MetRS cleavage ([Cassio and Waller, 1971](#)). The newly characterized truncated form showed similar enzymatic activity but increased stability against heat inactivation compared to the native enzyme. Thus, removal of approximately quarter of its size allows the bacterial MetRS to be more resistant on thermal stress. This bacterial truncated form might be the result of C-terminal domain removal since the essential catalytic HIGH signature motif is present close to the N-terminus and its removal would have resulted in loss of enzymatic activity. Same observation has been conducted in human cells with cleavage of purified aaRSs

from the MSC component. It has been shown that several MARS complex components were cleaved by calpain protease added on purified aaRSs (Lys-, Asp-, Gln-, Arg-, Met-, GluPro-, Leu- and IleRS). Identification of the cleavage sites for human GlnRS and ArgRS has been validated by N-terminal protein sequencing (Thr199 and Ala64, respectively) (Lei *et al.*, 2015), but the N-terminal of the truncated MetRS was not identified. Calpain digestion of MetRS produced deletion fragment of about 20 kDa and was predicted to be the removal of the N-terminal GST domain since the C-terminal hexahistidine tag was still present in the truncated form (**Figure I-37**). Since this GST-like domain is supposed to interact with the MSC component p18, removal of this N-terminal domain should release the human MetRS from the MSC, but this has never been demonstrated.

These cleavages were all found *in vitro* with addition of a purified protease or of a cytosolic extract to the purified MetRS. However, it has not been established if these truncated forms of MetRS were actually present *in vivo* and if they had a significant role in the cells.

IV. Purpose of my thesis work

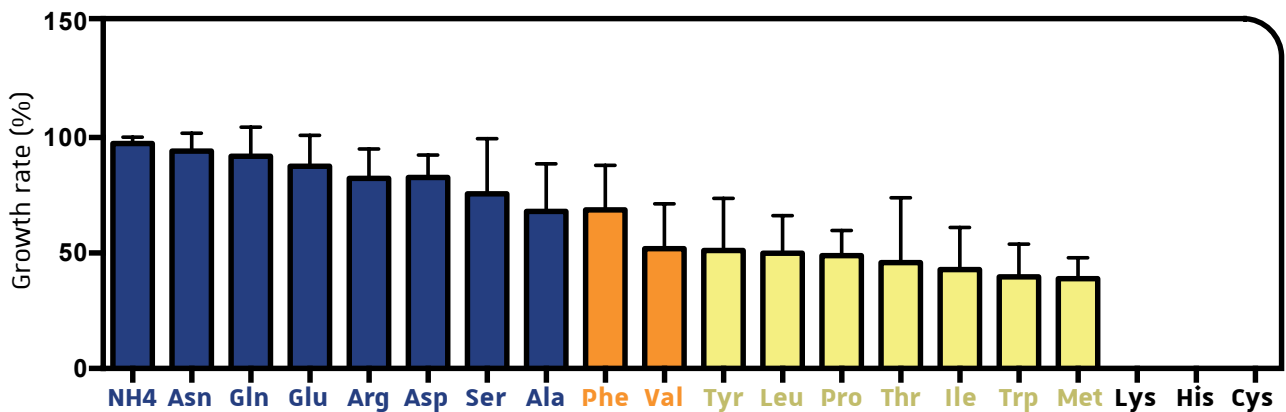
In the team “Dynamics and plasticity of synthetases”, I mainly worked on the molecular dynamics of the AME complex by focusing on the yeast MetRS functions. I started my PhD in 2015 working on tRNA mismethionylation events and subsequent Met misincorporation into proteins. Indeed, a lot of data were available concerning the mismethionylated tRNA species found in bacteria (Jones, Alexander and Pan, 2011; Schwartz and Pan, 2016), yeast (Wiltrout *et al.*, 2012) or human cells (Netzer *et al.*, 2009; Gomes *et al.*, 2016) (Figure I-35, page 100), but we had no information about the real incorporation of these mischarged Met residue into protein synthesis. Hence the objective was to engineer and use a molecular tool to determine and also quantify Met misincorporation using yeast as a model organism (Project I, page 115). I initiated this project, and several Master students I supervised during my PhD were also involved (Anne-Marie Lobstein, Master 1; Marion Wendenbaum, Master 2).

In addition to this project, a previous PhD student in the lab, Dr. Daphné Laporte, had observed the presence of a truncated MetRS in yeast. This observation was the first *in vivo* discovery of a shorter MetRS isoform in *S. cerevisiae*, since shorter form of MetRS were always obtained by *in vitro* cleavage on purified MetRS in both *E. coli* and human cells (Cassio and Waller, 1971; Lei *et al.*, 2015). A better characterisation of this truncated MetRS, along with the regulation of the cleavage were the objectives for this second project that I started during my second year of PhD (Project II, page 145).

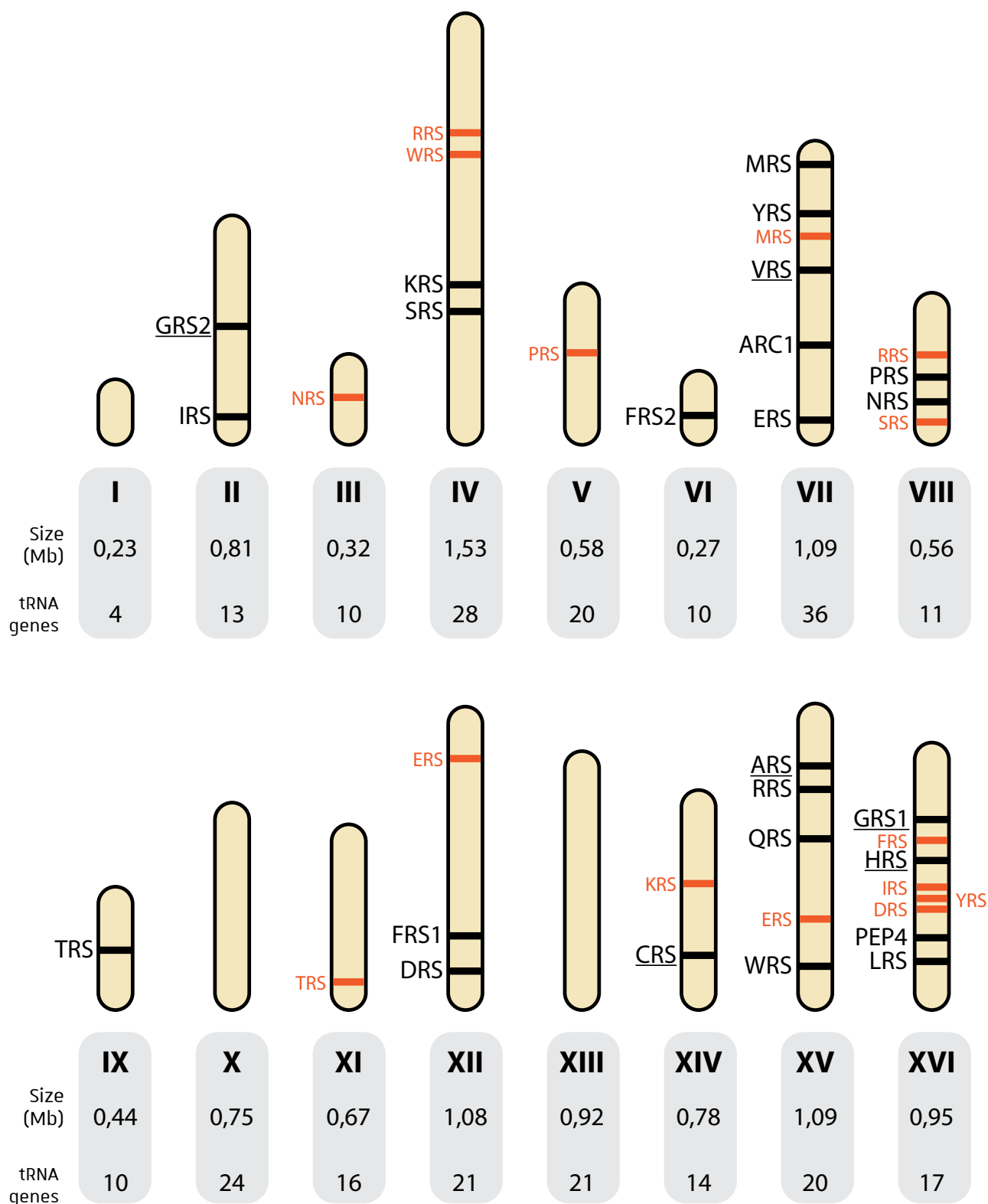
The last study described in this manuscript is the characterisation of a new mitochondrial role for Arc1. Indeed, I observed a respiratory growth deficiency for strains deleted for *ARC1* gene. Such a phenotype had never been described in the literature, and I wanted to understand more the role of the pool of Arc1 capable of relocating to the mitochondria. Results have shown that Arc1 is actually a dual localized protein present in both the cytosol and mitochondria, which plays an important role for the viability of *S. cerevisiae* in respiratory conditions (Project III, page 183).



Appendices



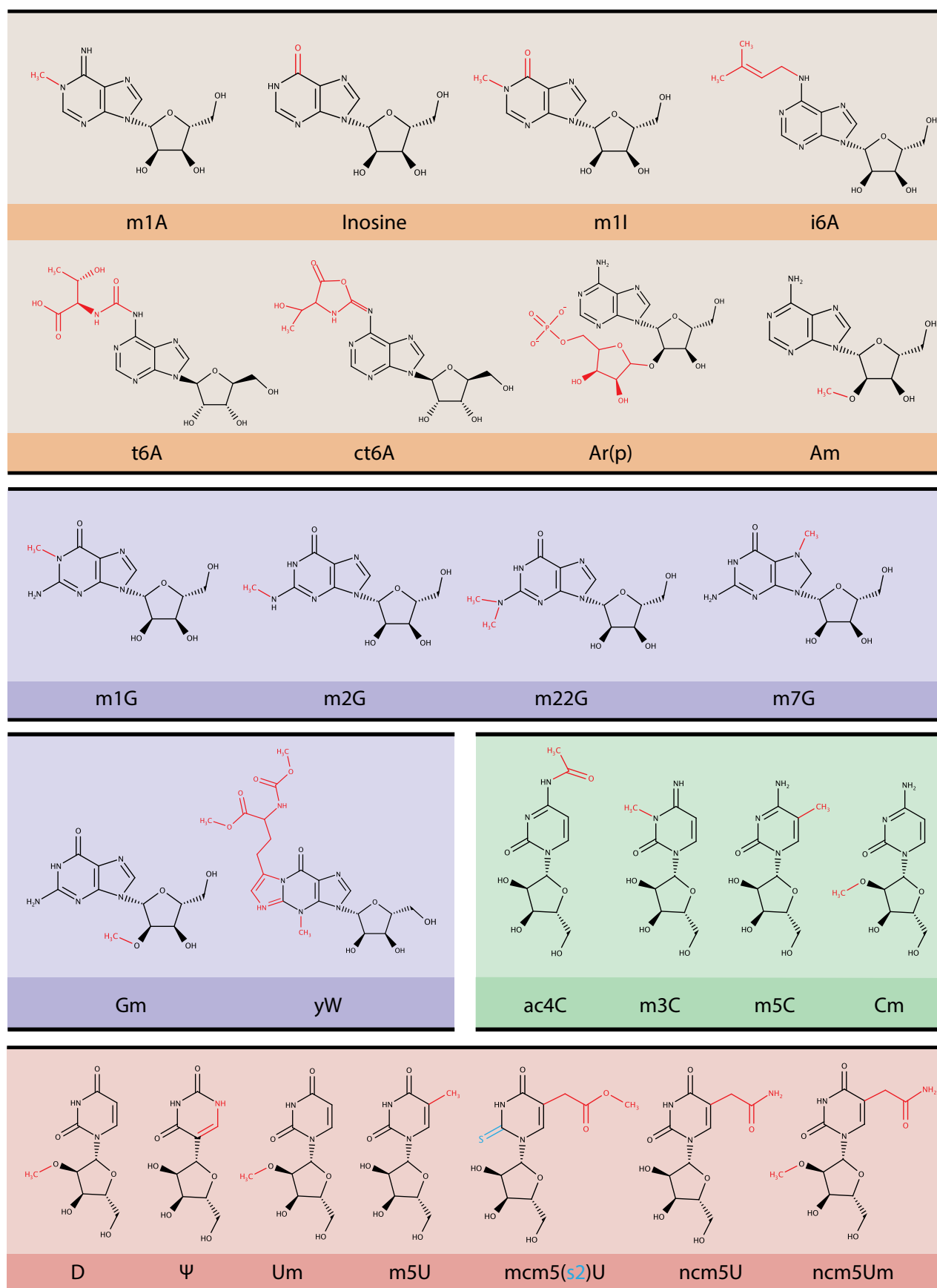
Appendix 1: Relative growth of *S. cerevisiae* on various sole nitrogen sources. This graph is a compilation of results found in [Godard *et al*, 2007](#); [Cooper, 1982](#); [Niederberger *et al*, 1981](#); [Watson, 1976](#), and rewied in [Ljungdahl and Daignan-Fornier, 2012](#). All aa, with the exception of Lys, His and Cys, can support yeast growth as sole nitrogen source, with different efficiency. Blue aa are called preferred aa, whereas yellows are non-preferred aa showing limiting growth rate. For each individual study, 100 % growth rate reffers to the lowest dividing time found for the strain used in this study.



Appendix 2: Chromosomal organization of the *S. cerevisiae* genome. The 16 yeast chromosomes are illustrated with length proportional to their nucleotides size. Number of tRNA genes is indicated below each chromosomes. Position of each aaRS genes is indicated with an horizontal bar (black for cytosolic aaRSs genes, orange for mitochondrial aaRSs genes). aaRSs underlined are synthetases without known mitochondrial gene. Chromosomal localization of *ARC1* and *PEP4* genes are also displayed.

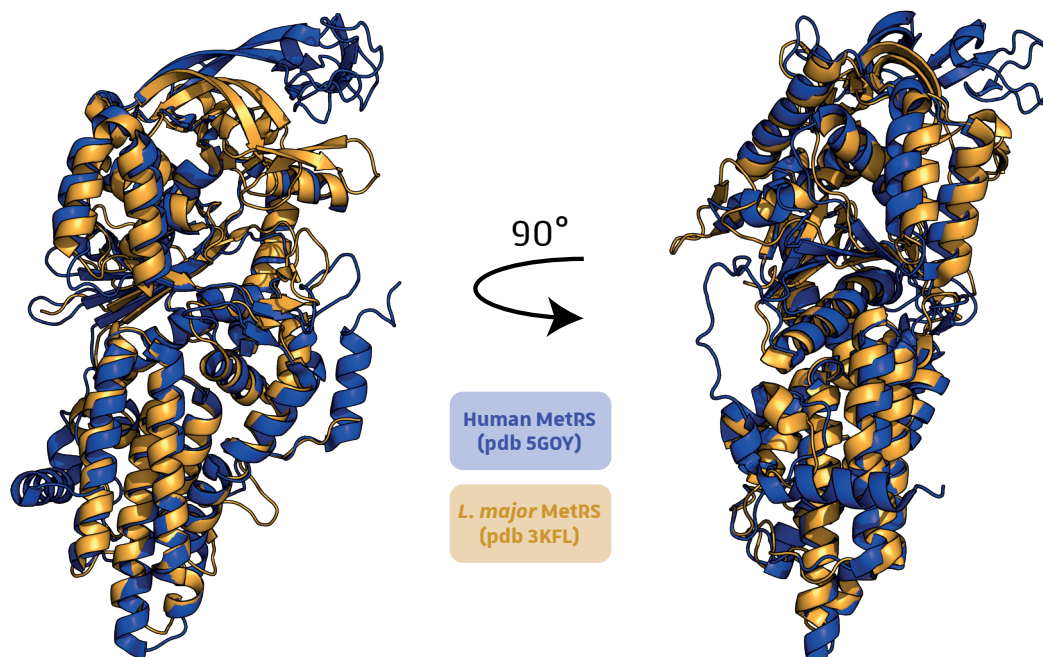
Appendix 3: Nucleotide modifications of yeast tRNAs with the associated modifying enzymes and their role in tRNA metabolism and regulation.

TRNA modif.	Standard chemical name	Modifying enzyme(s)	Modified nucleotide(s)	Function/role or comment	References
Modified Adenosine	m ¹ A	Trm6/Trm61	m ¹ A ₆₉	Prevents tRNA ^{Met} polyadenylation and degradation by nuclear surveillance pathway. Stabilization of the T-loop structure.	[1,2]
	I	Tad2/Tad3	I ₃₄	Determinant of tRNA ^{Met} for IleRS	[3]
	m ¹ I	Tad1 & Trm5	m ¹ I ₃₇	Mostly present in tRNA ^{Met}	[4,5]
	i ¹ A	Mod5	i ¹ A ₃₇	Increases fidelity to cognate codons. Stabilization of the AC loop.	[6]
	t ¹ A	KEOPS complex	t ¹ A ₃₇	Efficient decoding during translation, and accurate start-codon selection. Determinant of tRNA ^{Met} for IleRS.	[7-10]
	ct ¹ A	Sua5	ct ¹ A ₃₇	Decoding ANN codons (including initiator AUG)	[11]
	Ar(p)	Rit1	Ar(p) ₃₄	Identity element: tRNA ^{Met} with Ar(p) ₃₄ does not interact with eEF1α but eIF2	[12,13]
	Am	Trm13	Am ₄	Stabilization of aminoacyl stem?	[14,15]
	ac ¹ C	Tan1	ac ¹ C ₃₂	tRNA ^{Met} and tRNA ^{Met} temperature resistant	[16]
	m ¹ C	Trm140	m ¹ C ₃₂	Stabilization of the anticodon loop?	[17,18]
Modified Cytidine	m ¹ C	Trm4	m ¹ C ₅₄ , m ¹ C ₆₀ , m ¹ C ₆₈ , m ¹ C ₆₉	Enhance Mg ²⁺ binding of tRNA ^{Phe}	[19,20]
	Cm	Trm13	Cm ₄	Stabilization of aminoacyl stem?	[14,15]
		Trm7	Cm ₃₂ , Cm ₃₄	Stabilization of the anticodon loop. Cm ₃₂ in tRNA ^{Phe} is required for Ym ₃₇	[21,22]
	m ¹ G	Trm10	m ¹ G ₆	Antideterminant in tRNA ^{Arg} prevent recognition by ArgRS	[23]
Modified Guanosine	m ¹ G	Trm5	i ¹ G		[24]
	m ² G	Trm11/12 complex	m ² G ₅₉		[25]
	m ² G	Trm1	m ² G ₆₆	Stabilization of the L-shaped structure?	[26,27]
	m ¹ G	Trm8/Trm82	m ¹ G ₆₆	tRNA ^{Met} temperature resistant	[28]
	Gm	Trm13	Gm ₄	Stabilization of D-arm and T-arm interaction	[14,15]
		Trm3	Gm ₁₉	Improves codon anticodon interaction Gm ¹⁹ in tRNA ^{Phe} is required for Ym ¹⁹ modification	[29]
		Trm7	Gm ₃₄	Prevents -1 frameshifting. Determinant of tRNA ^{Phe} for PheRS. Stabilisation of the anticodon loop	[20,21]
Modified Uridine	D	Trm5, Tyw1/2/3/4	Ym ₃₇		[5,18,30,31]
		Dus1	D ₁₆ , D ₁₇		[32]
		Dus2	D ₂₀		[33,34]
		Dus3	D _{20a} , D _{20b}	All D nucleosides promote structural flexibility and dynamic motion	[33]
		Dus4	D ₄₇		[33]
		Pus1	Ψ ₁ , Ψ ₂₆ , Ψ ₂₇ , Ψ ₃₄ , Ψ ₃₈ , Ψ ₆₅	Ψ ₃₆ determinant of tRNA ^{Met} for IleRS	[3,35]
		Pus2 ^{min}	Ψ ₆₇		[36]
		Pus3	Ψ ₂₇ , Ψ ₂₈ , Ψ ₇₂	Structural role (Ψ ₃₉)	[37]
		Pus4	Ψ ₃₈ , Ψ ₃₉		[38]
		Pus6	Ψ ₃₅		[39]
		Pus7	Ψ ₃₁		[40,41]
		Pus8/Pus9	Ψ ₁₃ , Ψ ₃₂ , Ψ ₃₅	Ψ ₃₅ determinant of tRNA ^{Tyr} for TyrRS	[42]
	Um	Trm44	Um ₄₄	tRNA ^{Met} and tRNA ^{Met} temperature resistant	[43]
m ¹ U	Trm2	m ¹ U ₅₄	Stabilization of tRNA ^{Met} . Reverse Hoogsteen base pairing with A ₆₉ .	[44]	
mcm ¹ U	Elp1-6, Trm9/12	mcm ¹ U ₃₄	Efficient decoding during translation, restriction of wobble base pairing	[45,46]	
ncm ¹ U	Elp1-6	ncm ¹ U ₃₄	Efficient decoding during translation, restriction of wobble base pairing	[45,46]	
ncm ¹ Um	Trm7	ncm ¹ Um ₃₄	Efficient decoding during translation, restriction of wobble base pairing	[21,47]	
mcm ¹ sU	Elp1-6, Trm9-112, Kti11-14, Urm1	mcm ¹ sU ₃₄	Efficient decoding during translation, enhances stability of the stacking of the triplet	[48-51]	

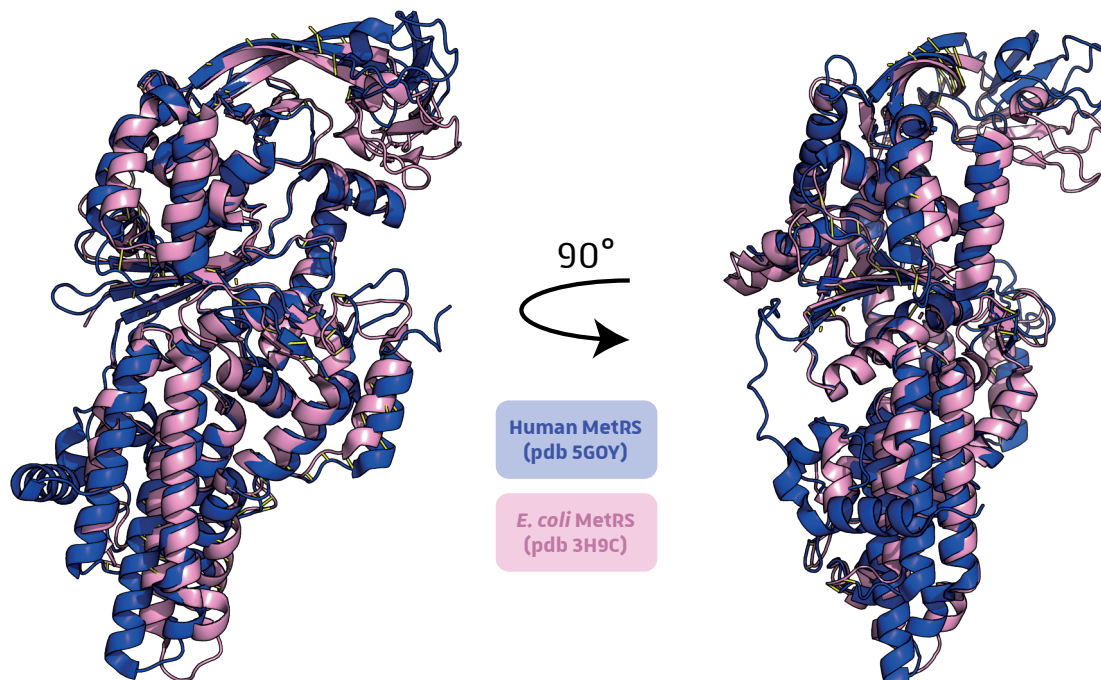


Appendix 4: Chemical structures of yeast nucleotide modifications found in tRNAs. Chemical structures of modified adenosines, guanosines, cytidines and uridines are respectively on orange, purple, green and red backgrounds. Each modification is added in red (and blue for s2U) and are abbreviated by their short name according to the nomenclature (Boccaletto *et al*, 2018).

A



B



Appendix 5: Superimposition of the two eucaryotic MetRS structures. A and B. The superimposition shows high similarities between the human MetRS (in blue, pdb 5GOY) and the *L. major* MetRS (A) (in orange, pdb 3KFL) and the human MetRS (in blue, pdb 5GOY) and the *E. coli* MetRS (B) (in pink, pdb 3H9C). All MetRSs share the same modular composition and the same secondary structures.



RESULTS & DISCUSSION

- I DEVELOPMENT OF A FLUORESCENT REPORTER TO MONITOR Met MISINCORPORATION IN *S. CEREVISIAE*** 115
- II STUDY OF A NEWLY CHARACTERIZED TRUNCATED FORM OF YEAST MetRS** 145
- III STUDY OF THE MITOCHONDRIAL ROLE OF Arc1 PROTEIN** 183
- IV GENERAL DISCUSSION** 192
- SUPPLEMENTAL FIGURES** 197



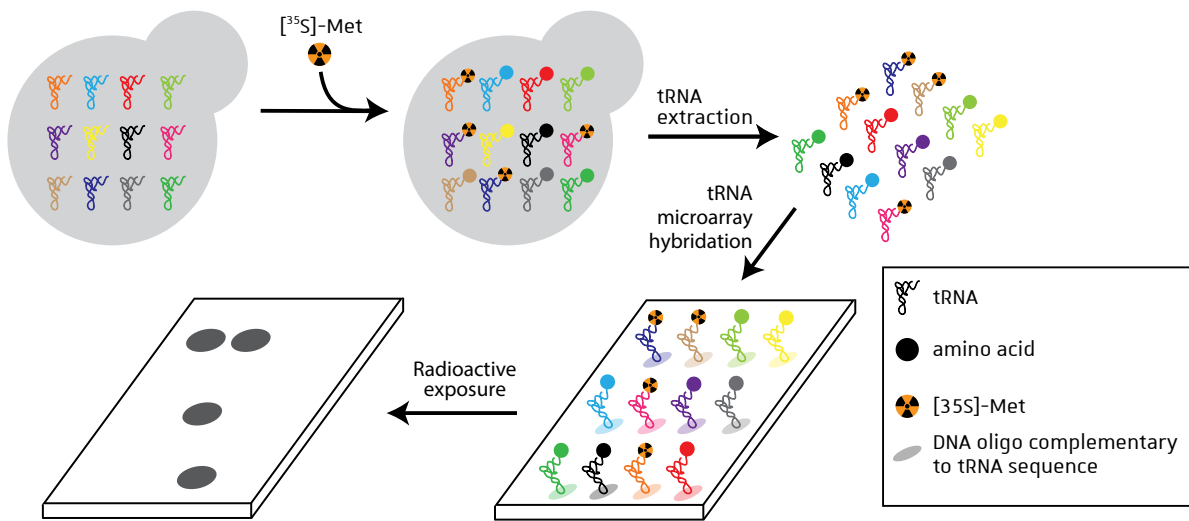


Figure R-1: Method used to identify misacylated tRNAs with Met. Yeast cells are cultured with $[^{35}\text{S}]\text{-Met}$ in the medium, total aa-tRNAs are extracted and incubated on a tRNA microarray spotted with oligonucleotides complementary and specific to all tRNA species. Radioactive signal is then observed and the associated misacylated tRNAs are identified because each oligo is spotted at a particular location on the microarray.

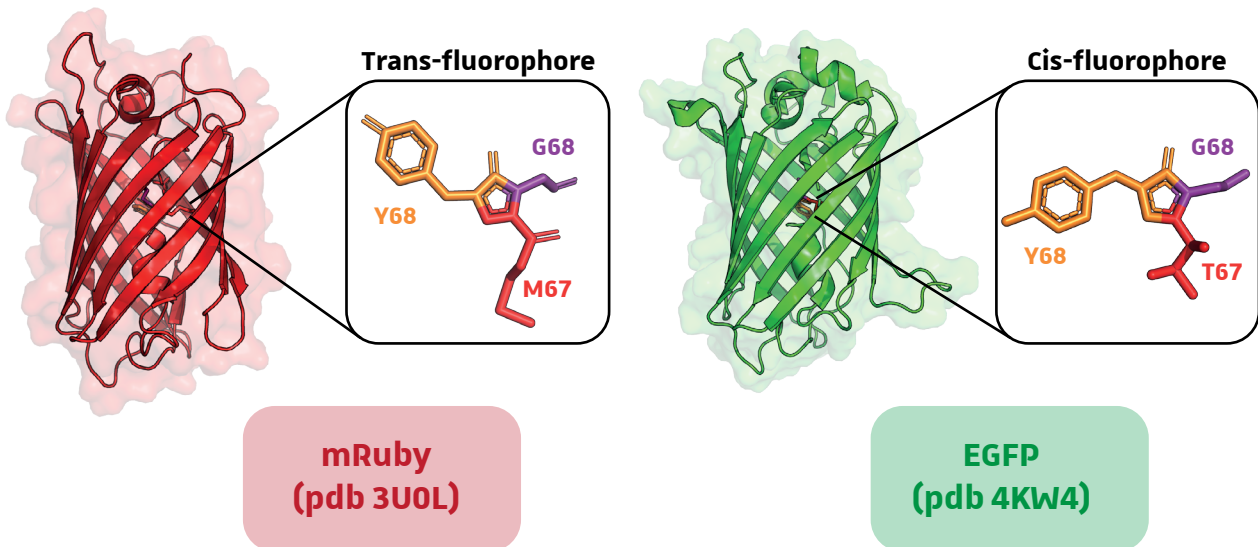


Figure R-2: Structures of the mRuby and EGFP fluorescent proteins. aa residues constituting the fluorophores are highlighted in squares. The tyrosyl residue orientation defines the trans- or cis-fluorophore conformation: mRuby2 fluorophore $\text{M}_{67}\text{-Y}_{68}\text{G}_{69}$ is in trans-conformation, whereas the EGFP fluorophore $\text{T}_{65}\text{-Y}_{66}\text{G}_{67}$ presents a cis-conformation.

I. Development of a fluorescent reporter to monitor Met misincorporation in *S. cerevisiae*

I.1. Context of the study

Several studies have been working on mistranslation into the proteome (see **Table I-5**, page 56), and most of the techniques used were adapted to study a single aa misread. For methionine misincorporation, majority of the studies did not analysed Met misincorporation into proteins but were constrained to identify the misacylated tRNAs with Met, and extrapolation was done to assess Met misincorporation. These studies all used cells pulse labelling with [³⁵S]-Met followed by tRNA microarrays (**Figure R-1**; [Netzer et al., 2009](#); [Jones, Alexander and Pan, 2011](#); [Wiltrout et al., 2012](#)). The results obtained with this method are somewhat unusual since plenty of tRNA species are found misacylated in each study (**Figure I-34**, page 98), and it is difficult to conceive that such high mischarging is compatible with cell survival, especially in basal condition. An explanation could be that majority of these tRNAs won't be used by the ribosomal machinery since eEF1A should not bind these misacylated tRNAs ([LaRiviere, Wolfson and Uhlenbeck, 2001](#)). Therefore, we wanted to create a strategy allowing us to determine and ideally quantify tRNA mismethionylation and Met misincorporation level in the yeast *S. cerevisiae*. We needed to design a protein reporter that would tells us if a methionine has been misincorporated instead of another aa at a specific position. Among these reporters, the protein should have in its sequence a methionine residue essential for its activity, either enzymatic, colorimetric or fluorescent. Finally, the protein activity has to be detected easily with a standard assay.

I.2. Use of fluorescence to assess Met misincorporation

As discussed in the introduction, several studies developed colorimetric or fluorescent tools to monitor mistranslation. No enzyme with colorimetric activity (like luciferase) was found with a known essential Met residue. However, some fluorescent proteins (FPs) harbour a Met residue crucial for their fluorescence capacity. The GFP protein from *Aequorea victoria* and its derivatives are popular but do not possess an essential Met residue (**Table S1**, page 196). However, another family of red fluorescent proteins (RFPs) has been discovered in *Anthozoa* species ([Matz et al., 1999](#)). It was previously shown that Met misincorporation was detectable using a Red Fluorescent Protein (RFP) derivative protein ([Lee et al., 2014](#)). The first RFP discovered was the commercially

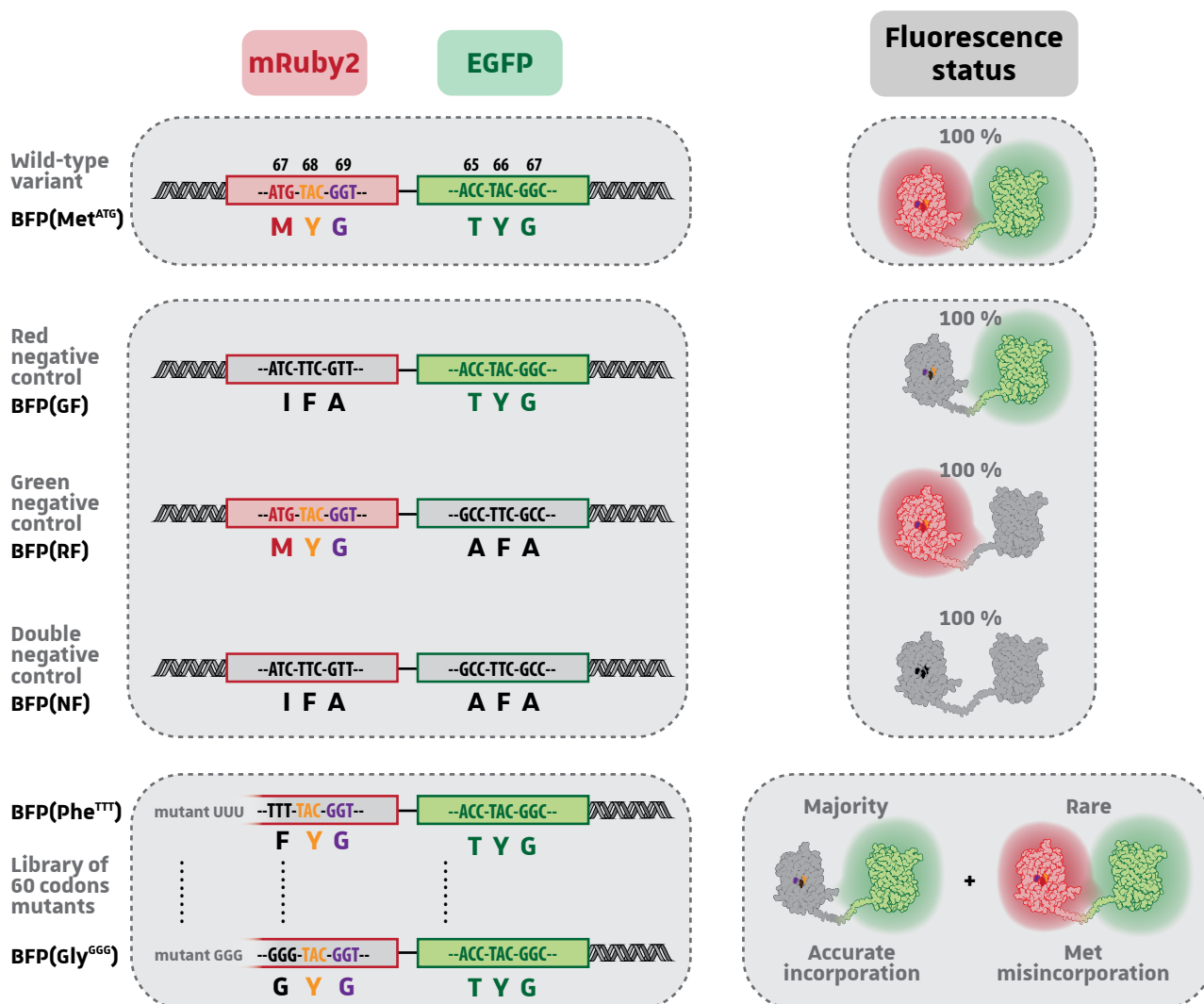


Figure R-3: Design of the dual fluorescent reporter used in this study. The tandem fluorescent reporter relies on the fusion of the mRuby2 (fluorophore M₆₇Y₆₈G₆₉) to the EGFP (fluorophore T₆₅Y₆₆G₆₇) called Bifluorescent reporter (BFP). Cells expressing the wild-type variant BFP(Met^{ATG}) are both red (100 % signal for quantification) and green fluorescent. The red negative control BFP(GF) has a degenerated mRuby2 fluorophore and represents the 0 % of red signal. EGFP fluorophore is degenerated in the green negative control BFP(RF), and both fluorophores are mutated in the BFP(NF). Library of the 60 codon mutants (M67 substitution) for mRuby2 has been engineered, and each mutant is called BFP(aa^{XXX}), with aa corresponding to the residue that substitutes M67, and XXX the codon coding for this residue. Cells expressing each BFP variant might present a faint red signal due to Met misincorporation at position 67 in the mRuby2 sequence.

known DsRed, with the fluorophore sequence QYG, and present slow maturation of the fluorophore, tetrameric oligomerization and tendency to aggregate. Screening of new naturally occurring RFPs led to the discovery of eqFP611 from *Entacmaea quadricolor* with MYG fluorophore (**Figure R-2** and **Table S1**, page 196). This protein presents faster maturation and reduced oligomerization tendency compared to DsRed (Wiedenmann *et al.*, 2002). Engineering from this protein sequence allowed design of mRuby2, a monomeric RFP with improved brightness and photostability (**Table S1**; Lam *et al.*, 2012). Since Met misincorporation and misincorporation is a relatively rare event in cells, I needed enough brightness to be able to detect Met misincorporation. All these fluorescent properties for mRuby2 (mRuby3 has been engineered later during my PhD) led me to choose this red fluorescent protein to visualize and quantify Met misincorporation.

1.3. Design of the bifluorescent protein reporter

We wanted to use this fluorescent protein in a way similar to the one used in a previous work to identify a promiscuous MetRS in human (Lee *et al.*, 2014). The red fluorescent protein used in this study (TagRFP) contains an essential Met in its fluorophore, just like mRuby2. The aim was to mutate this Met₆₇ residue by replacing the corresponding ATG₆₇ codon with AAG₆₇ (coding for Lys) to turn off the fluorescence signal, except if Met is misincorporated and thus restores red fluorescence. This fluorescent-based technique presumes a case-by-case analysis of each codon, using a collection of plasmid bearing each codon combination at position 67. All previous studies have investigated only few codons essentially because generating mutant in human cells is time-consuming. With mRuby2 as fluorescent reporter, we took advantage of the yeast *S. cerevisiae* to generate a collection of 61 mutants carrying single codon substitution at position 67, each for every 61 sense codons (**Figure R-3**). Using such “all-or-nothing” fluorescent reporter involves the use of an internal control to assess intrinsic variations in protein expression and to be able to quantify and normalize the red fluorescent signal. Thus, I fused in the 3' end part of the mRuby2 gene the wild-type EGFP gene to (i) be sure that the tandem fluorescent probe is well expressed in cells, since all positive cells would present green fluorescence in microscopy or flow cytometry, and (ii) to normalize the red signal observed with the green fluorescence to quantify Met misincorporation. Thus, each construct is called BFP(aa^{xxx}), where BFP stands for BiFluorescent Protein and (XXX) is the mRuby2 codon in position 67 coding for the corresponding aa (**Figure R-3**). To be more precise in red signal quantification, I also designed control vectors: a “green fluorescent only” vector (BFP(GF)) with the whole mRuby2 fluorophore aa triad mutated into isosteric aa residues (IFA instead of MYG), an

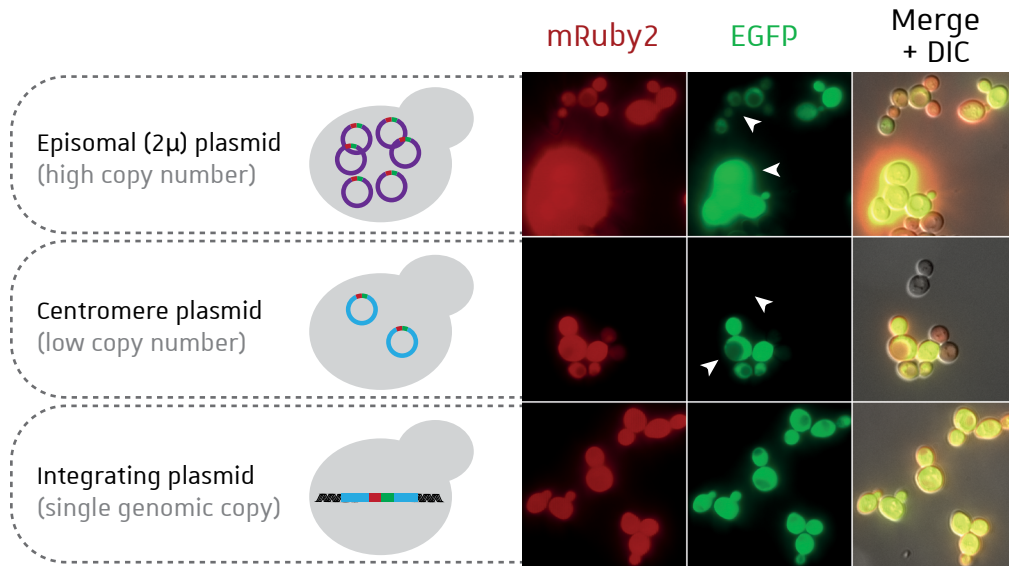


Figure R-4: Choice of yeast vectors for bifluorescent reporter expression. Observation by epifluorescence microscopy of yeast cells carrying episomal (pAG424), centromeric (pAG414) or integrated (pAG304) plasmids expressing BFP(Met^{ATG}). High fluorescent heterogeneity (white arrowheads) is observed for episomal and centromeric vectors, but not for integrating plasmid.

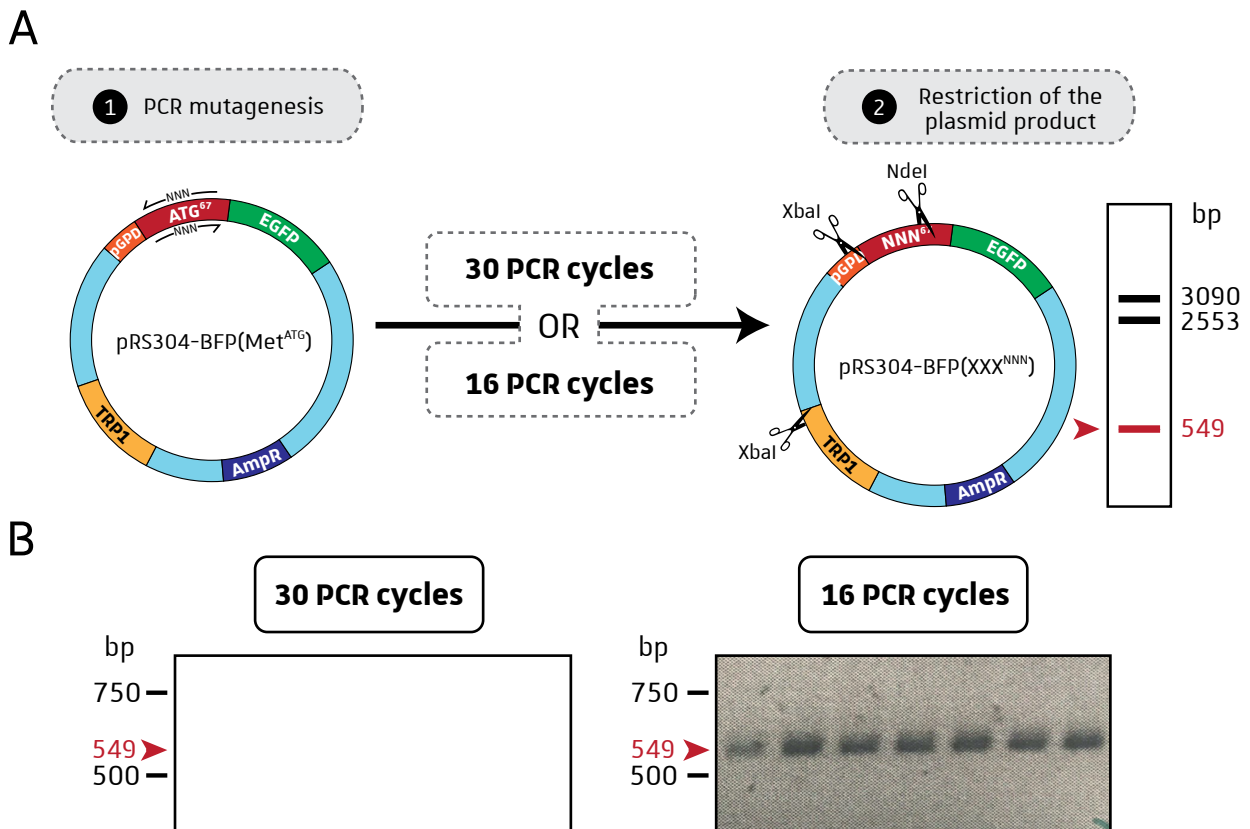


Figure R-5: Number of cycles during PCR is crucial for accurate mutagenesis. **A.** Protocol for PCR mutagenesis using overlapping primers and 30 or 16 PCR cycles. The resulting mutated plasmids are digested with NdeI and XbaI restriction enzymes, leading to three DNA fragments. The smallest fragment of 549 bp (red arrowhead) contains the mutated sequence. **B.** Analysis by electrophoresis on 2 % agarose of the PCR bands obtained after restriction by XbaI/NdeI of several plasmid products after 30 or 16 PCR cycles. Insertions into the fragment are observed when 30 cycles are programmed during PCR (fragments with a size above 549 bp, left panel).

EGFP-mutated plasmid to form the “red fluorescent only” vector (BFP(RF)) and the combination of the two degenerated fluorophores to obtain a non-fluorescent vector (BFP(NF)) (**Figure R-3**).

Observing rare event like Met misincorporation raises several questions about the yeast promoter that should be used to have enough protein expression, and about the nature of the expression system. Yeast vectors usually contain standard promoters: some are constitutively active, whereas others can be activated by metabolic changes or metabolites. In the same way, some promoting sequences are considered strong promoters and allow high gene expression. For our bifluorescent protein reporter, I have used the promoter of the *TDH3* gene (also called *GAPDH* or *GPD*) coding for the glyceraldehyde-3-phosphate dehydrogenase involved in glycolysis. This *pGPD* is considered as a strong promoter and is constitutively expressed in cells (Bitter and Egan, 1984). Another aspect of the plasmid that was used, was the choice of the origin of replication determining the plasmid copy number. In yeast, commonly used vectors are either high copy number (episomal or 2 μ plasmid, p42x series) or low copy number (centromere or CEN/ARS plasmid, p41x series). Quantification of the number of copies for these plasmids showed that 2 μ plasmid copy number varied between 15 and 35 copies per cell, and CEN/ARS plasmids ranged from 2 to 5 copies (Karim, Curran and Alper, 2013). This heterogeneity in copy number for the same cell population would have been a problem for microscopy analyses since some single cells will have a strong fluorescent signal compare to others with weak or no signal at all (**Figure R-4**). More surprisingly, some cells were heterogeneous for green and red fluorescence with these types of vectors, which should not be the case since parameters were chosen to have red and green equivalent signals. I thus decided to clone the BFP construct into an integrating plasmid (p30X series). This type of yeast plasmid lacks yeast-specific origin of replication and must be integrated into the yeast chromosome by homologous recombination. Integration of the vector occurs only once in a single specific locus, thus only a single copy of the construct is present in each cell, allowing a homogeneous expression of the BFP reporter in all cells derived from a single clone (**Figure R-4**). Another advantage of using integrative plasmid is possibility to store yeast stains at -80 °C without any fluorescence loss which can occur with non-integrative plasmids. Indeed, strain selection is time consuming (see next session) and storage of fluorescent strains allows faster analyses without having to do yeast transformation and selection before quantification analyses.

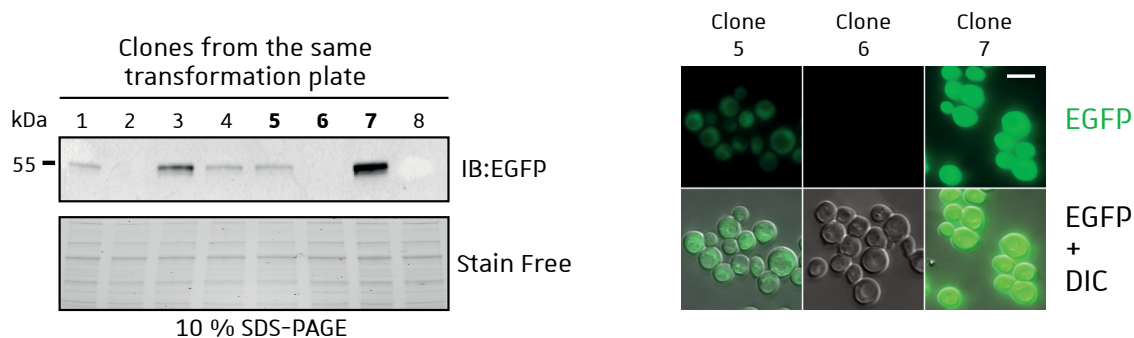


Figure R-6: Heterogeneity in BFP expression for clones derived from same transformation experiment. BY4742 cells have been transformed with a BFP plasmid and grown on selective medium. Individual clones were analysed by western blotting (left) and epifluorescence microscopy (right). Scale bar, 10 μ m.

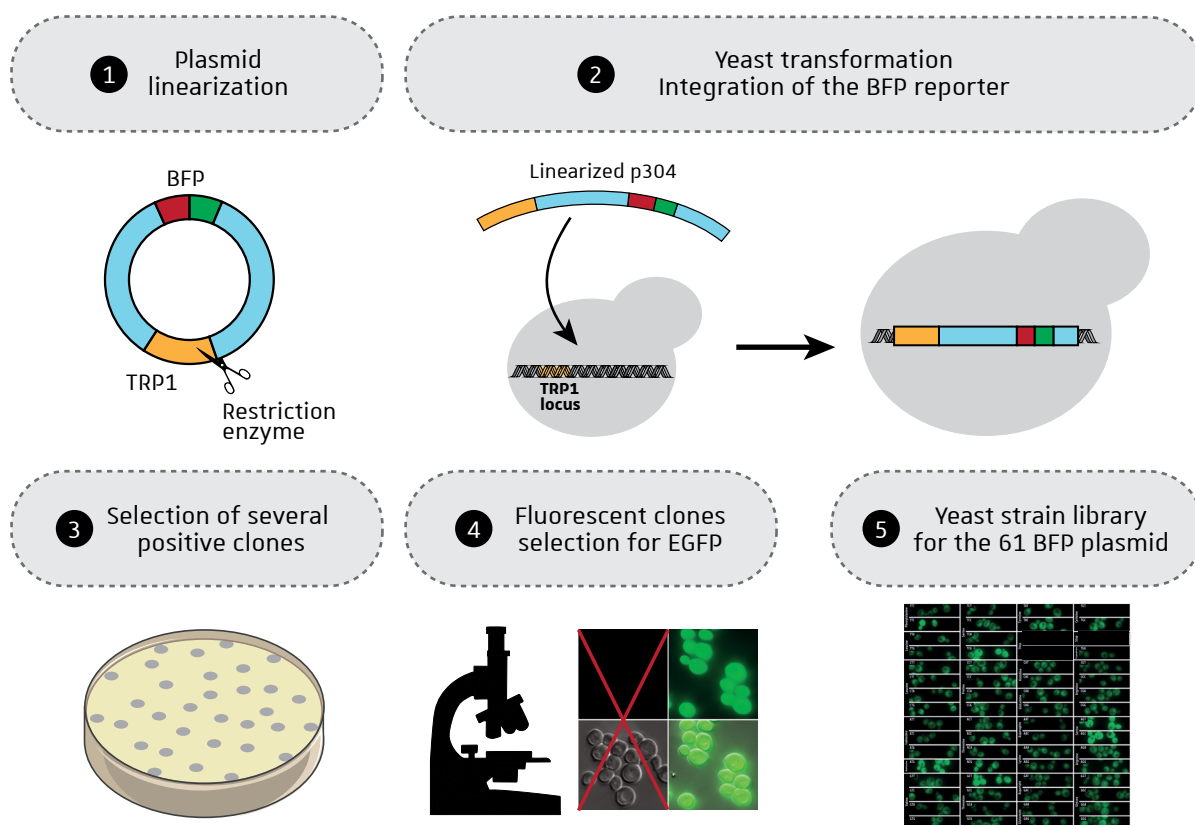


Figure R-7: Several steps are needed to select clones suitable for fluorescence quantification. Integrative plasmid p304-BFP has to be linearized by restriction enzyme into the auxotroph marker *TRP1* (PmlI or AccI). The linearized plasmid is transformed into yeast cells and integrated by homologous recombination. Several positive clones are picked onto selective plates and analysed by epifluorescence microscopy. Only clones with suitable EGFP expression are kept in the yeast strain codon library.

I.4. Procedure of cell selection for suitable FBP expression

Since integrating vectors gave a homogeneous signal of fluorescence for both green and red signals with the native BFP(Met^{ATG}), I decided to create the strain collection with the integrative pRS304 vector expressing the BFP reporter and carrying the auxotrophic marker *TRP1* gene. I started by the mutagenesis of the pRS304-BFP(Met^{ATG}) to obtain the set of all 61 plasmids. The strategy used was PCR-mutagenesis with overlapping primers to change only the codon sequence. A set of 120 (60 forward and 60 reverse) primers has been ordered, each primer differing only in the codon 67 of the mRuby2 gene coding for Met₆₇ residue (see page 258 for primers sequence). Classical PCR protocol with 30 cycles was not appropriate for this PCR mutagenesis since the PCR product had internal insertions probably due to multiple-primer insertions. Reducing to 16 the number of PCR cycles was enough to obtain the desired PCR product (**Figure R-5**).

After yeast transformation, the pRS304-BFP vector allows selection of positive clones on selective minimal medium lacking tryptophan (see **Mat&Met**, page 228). Clones growing on this medium were collected and analysed both by Western blotting of total cell extract and by epifluorescence microscopy. For the same plasmid used, positive clones (supposed to carry single copy of the BFP reporter and the *TRP1* marker) expressed the reporter with high heterogeneity among the clones that were selected (**Figure R-6**). This was surprising since all clones should have expressed the BFP reporter under control of the strong and constitutive *pGPD* promoter. Thus, the reporter integration at *TRP1* locus might interfere with protein expression in some cases. For microscopic quantification of fluorescence, I needed suitable expression of the reporter (signal between clone 5 and 7, **Figure R-6**). Thus, selection of each positive clone from the whole bank of plasmids was required before fluorescence quantification and further analyses. After each yeast transformation, several clones had to be analysed by epifluorescence microscopy to select one clone with suitable EGFP expression and was kept to build the FBP reporter yeast strain library (**Figure R-7** and **Supplemental S1**).

I.5. Proof of concept for BFP reporter

Once the yeast strains harbouring the whole plasmid library were obtained, it was necessary to confirm the loss of red fluorescence for each BFP mutant to ensure that Met misincorporation by red fluorescence recovery was indeed possible. All 61 BFP yeast clones have been observed by microscopy for detection of the red signal and results are shown in **Figure R-8**. The mRuby2 signal is

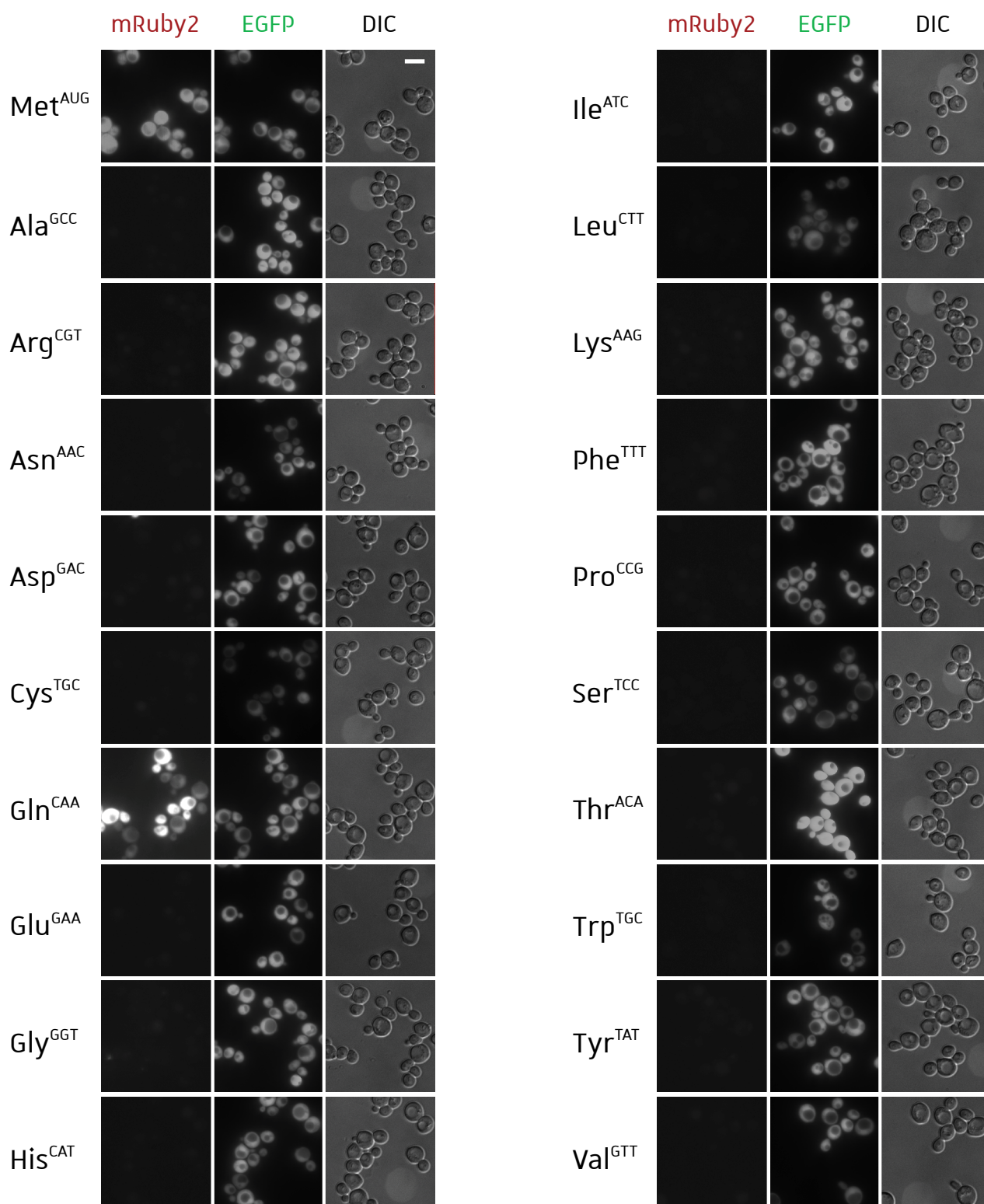


Figure R-8: Loss of red fluorescence for all BFP mutants but BFP(Gln). The whole BFP yeast strain library has been analysed by epifluorescence microscopy to observe the loss of red fluorescence due to mRuby2 Met67 substitution. Only one codon for each BFP mutant is shown. Red fluorescence is lost for all BFP construct except BFP(Gln^{CAA}). The BFP(Gln^{CAG}) mutant shows also remaining red fluorescence (not shown). Scale bar, 10 μ m.

actually lost for all BFP mutants, except for BFP(Gln^{CAA} and Gln^{CAG}) for which the red fluorescence is closely equivalent to native BFP(Met^{ATG}) with, however, some heterogeneity in the red signal among cells from the same clone. This strong and heterogeneous red signal is unlikely reflecting the Met misincorporation, which should constitute a rare event, suggesting that the Gln67 substitution might be able to form an active fluorophore. Such fluorophore (Gln67, Tyr68 and Gly69) is actually present in other RFP like DsRed and mRFP1 (**Table S1**, page 196), and this substitution reconstitutes the red fluorescence in BFP(Gln). Thus, using our BFP reporter, we could identify and quantify of Met misincorporation at all coding codons with the exception of the CAA and CAG codons coding for Gln.

For quantification of Met misincorporation, we wanted to normalize the red signal with the expression level of each BFP reporter. As seen in **Figure R-8**, there are some variations in EGFP signal for the different BFP reporters that were analysed, and these variations should be proportional to the expression level for all BFP reporters. A second possibility would be that substitution of Met67 on mRuby2 sequence results in perturbation in EGFP emission. To assess that BFP expression level correlates with green signal, we chose eight different yeast strains carrying BFP reporters and assess in parallel BFP expression level by western blotting using anti-GFP antibodies, and the EGFP green signal by microscopy (**Figure R-9**). Overall, there is a good correlation between BFP expression and EGFP emission (**Figure R-9B**).

1.6. Quantification of Met misincorporation in basal condition

1.6.1. Design and optimization of the quantification protocol

The method used to quantify Met misincorporation was really important step to ascertain that there was no bias that was introducing in the imaging and calculation. Selecting strains with similar BFP expression was the first restricting criteria we imposed to be sure that all green fluorescent images had similar intensities. This was crucial, since high intensity can saturate the camera sensor, with some pixels exceeding the dynamic range of the camera and resulting in distorted results. In the same way, it allows working with the same excitation exposure for all samples, so that the fluorescent intensity (green and red) is proportional to protein amounts. After setting up these parameters, we composed a script in collaboration with Dr. J. Mutterer (IBMP, Strasbourg) to assess mRuby2 signal and quantify Met misincorporation. This script enables localization of individual cells through EGFP signal, then transfers cell pattern to the red signal picture (since misincorporation

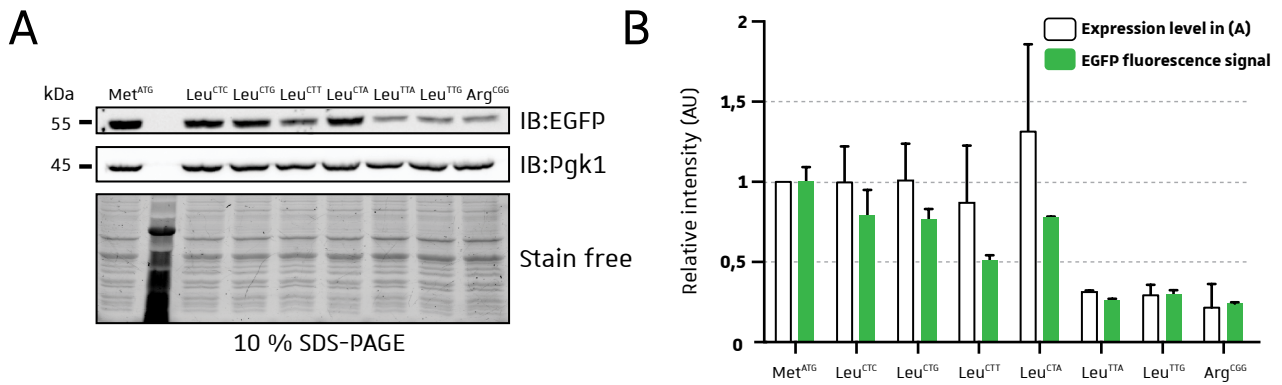


Figure R-9: Correlation between expression and green fluorescence emission of the BFP reporters. Eight different BFP reporters strains have been chosen to assess in parallel **(A)** the expression level of BFP proteins by western blotting and **(B)** the EGFP fluorescent signal by microscopy. The relative expression level of BFP (white bars) and EGFP signal (green bars) are compared in **B** (n = 2).

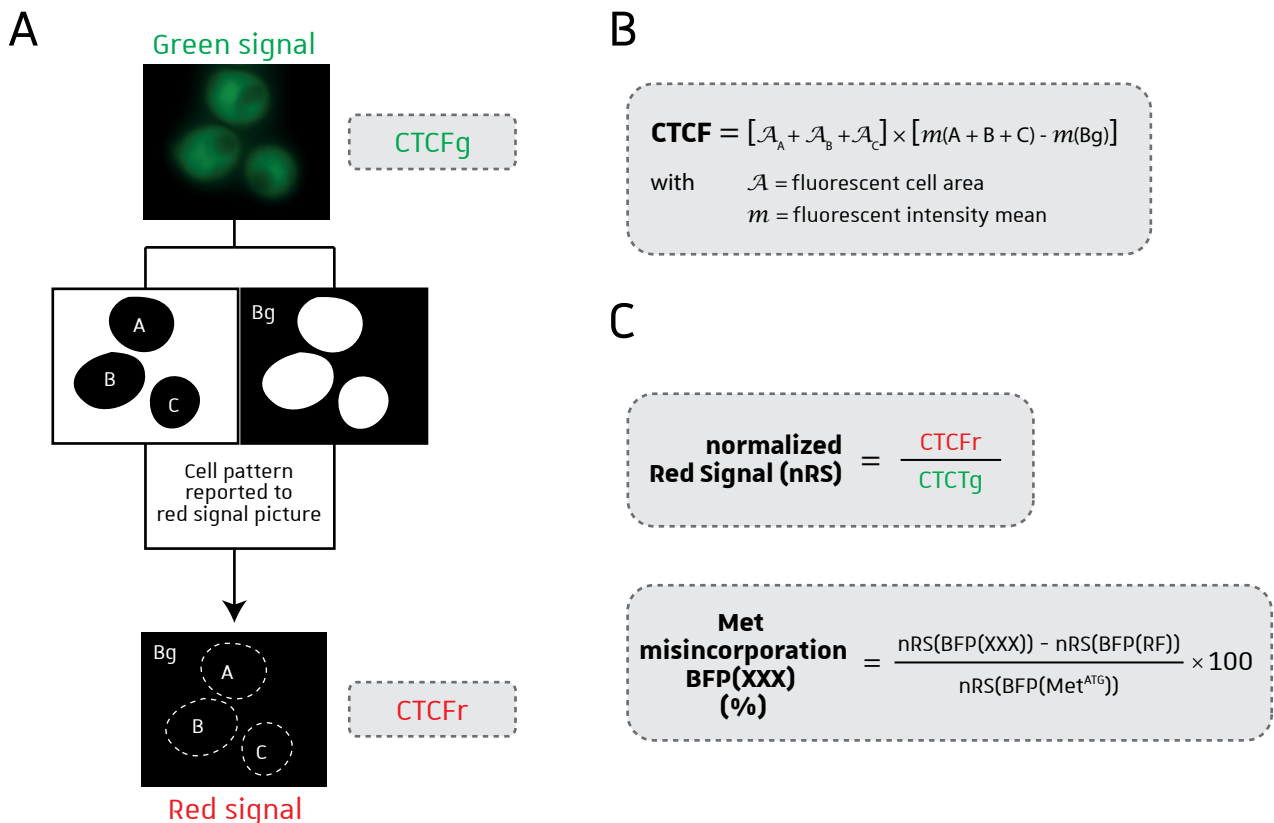


Figure R-10: Quantification of Met misincorporation through Correlated Total Cell Fluorescence (CTCF). **A.** The program used to quantify Met misincorporation analyses each green positive cells (A, B and C) and extracts the background (Bg). Area and fluorescence intensity means are calculated for each component (cells and background) and the CTCF is obtained in the two fluorescent canals (green and red). **B.** CTCF reveals total fluorescence of the cells without any fluorescence noise due to the background. **C.** Finally, the CTCFr/CTCFg ratio normalizes the red fluorescent signal with protein expression (nRS), and Met misincorporation is obtained by subtraction of the negative control BFP(RF) and divided by the positive BFP(Met^{ATG}) to get the percentage of misincorporation.

of Met is a rare event, the red signal is more often faint and not observable by eyes). After object selection in both fluorescent canals, the correlated total cell fluorescence (CTCF) is obtained for red and green fluorescence signals (**Figure R-10A**). This CTCF parameter reflects the fluorescent intensity with background signal subtraction (**Figure R-10B**). The ratio between the two CTCF values results in the normalized red signal (nRS) for each image, and the Met incorporation for a strain is obtained by deducting the nRS of the red negative control (BFP(RF), to set the 0 % of Met misincorporation) subdivided by the positive control nRS (BFP(Met^{ATG}) which is set to 100 % Met “misincorporation”) (**Figure R-10C**). All these steps are performed for each BFP strain, with ten acquisitions per strain and more than 100 cells imaged in total.

1.6.2. Met misincorporation without stress

The complete BFP yeast strain library in the WT RS453 genetic background was obtained and assessed for Met misincorporation without any cellular stress to estimate the basal level of Met misincorporation. All BFP strains were cultured in rich medium and harvested in logarithmic phase before microscopy analyses. Results obtained are shown in genetic code table format, each codon corresponding to a BFP strain (**Figure R-11A**). As expected, red signals for all strains were very low except for BFP(Gln) reporters. For majority of BFP strains, no significant Met misincorporation into mRuby2 fluorophore is observed (**Figure R-11A**). However, misincorporation is measurable for all six BFP(Leu) strains that display 0.52 % to 1.49 % Met misincorporation, and in BFP(Lys^{AAA}) that yields 0.8 % Met incorporation. In a lesser extent, some other strains are showing positive misincorporation signal (Thr^{ACC}, Asn^{AAC}, the four codon Arg^{CGA, CGG, AGA, AGG}, Ser^{AGC} and Gly^{GGG}). These first results suggest that yeast MetRS mischarges all tRNAs able to decode these codons, and the corresponding mischarged Met-tRNAs are used for protein synthesis.

1.7. Deletion of Arc1 enhances global Met misincorporation

As I mentioned in the introduction, Arc1 is a major cofactor of yeast MetRS and GluRS that enhances the catalytic efficiency of the enzyme mainly by increasing their binding efficiency to tRNA^{Met} and tRNA^{Glu} (**Figure I-22**, page 74 and **Table I-8**, page 74). Absence of Arc1 protein might thus result in lowering the local tRNA^{Met} concentration in close proximity to MetRS, and would possibly increase tRNA mischarging. To test this hypothesis, *ARC1* was deleted in the WT RS453 strain and a collection of BFP *arc1Δ* strains was made to monitor Met misincorporation in the absence of Arc1. After

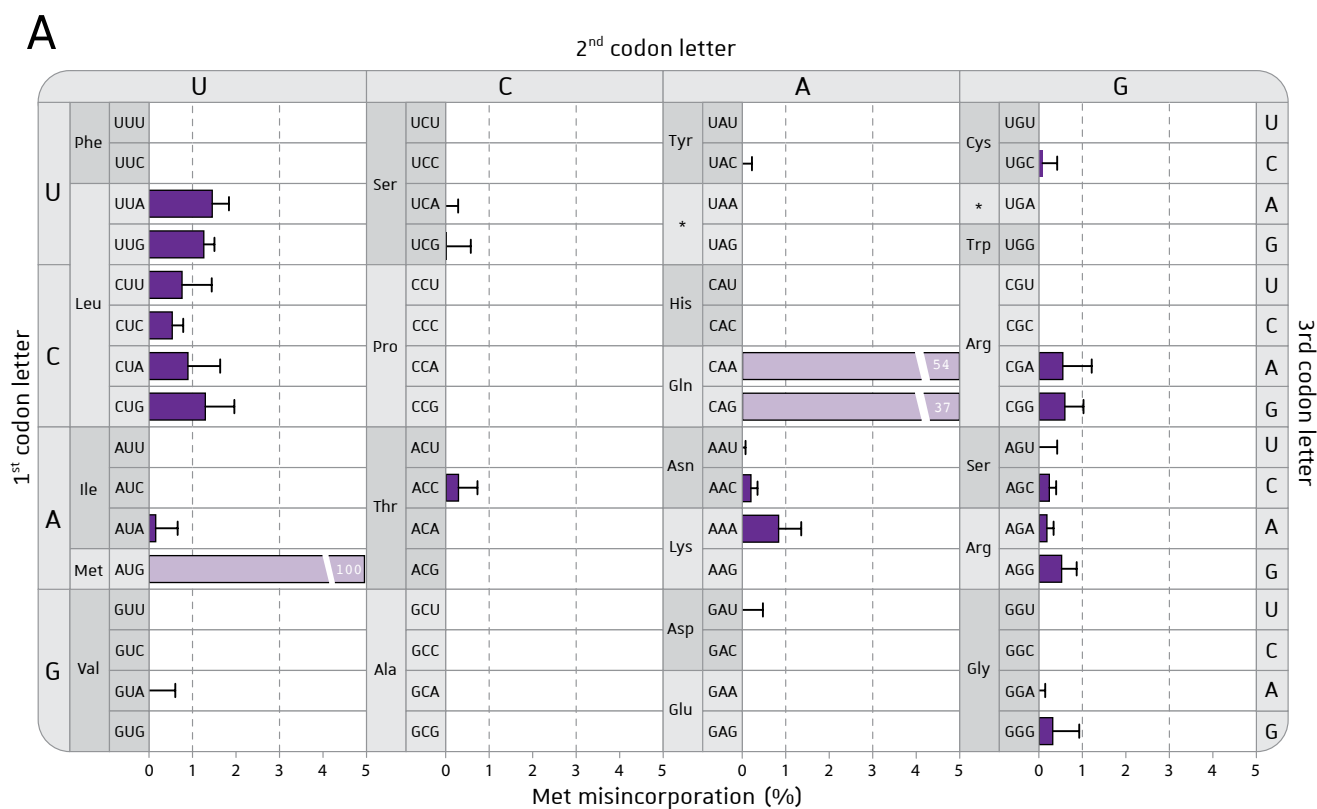
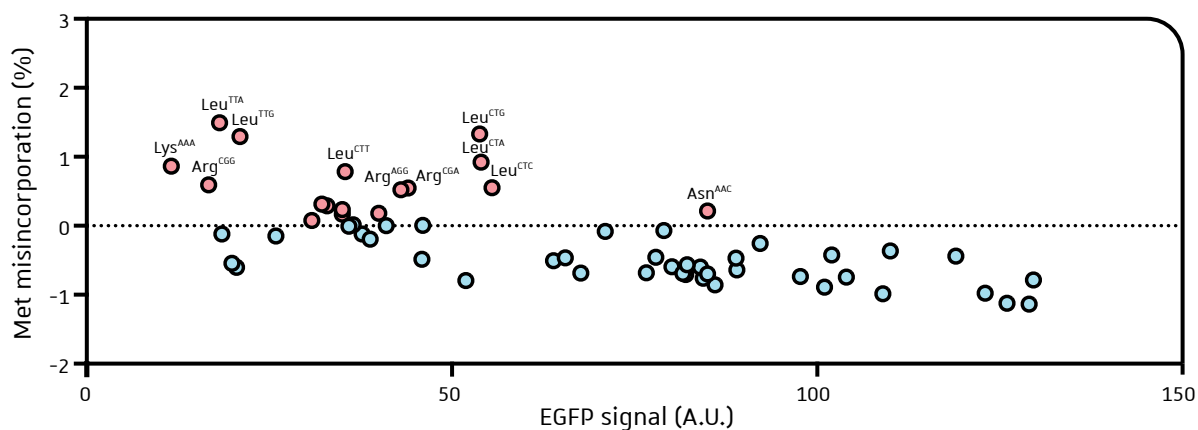
**B**

Figure R-11: Met misincorporation for all 61 BFP variants expressed in WT strain grown in rich medium. The entire BFP library in WT RS453 genetic background was analysed by epifluorescence microscopy. Yeast cells were grown in rich YPD medium and harvested in logarithmic phase before observation under the microscope. Quantification is performed as described in **Figure R-10. A.** Results for BFP(Gln) and BFP(Met) are indicative since they do not represent actual misincorporation (light purple with % indicated in white). Means and standard deviations are obtained on more than 100 cells analysed (n=1). **B.** Misincorporation of Met is analysed according to the EGFP expression.

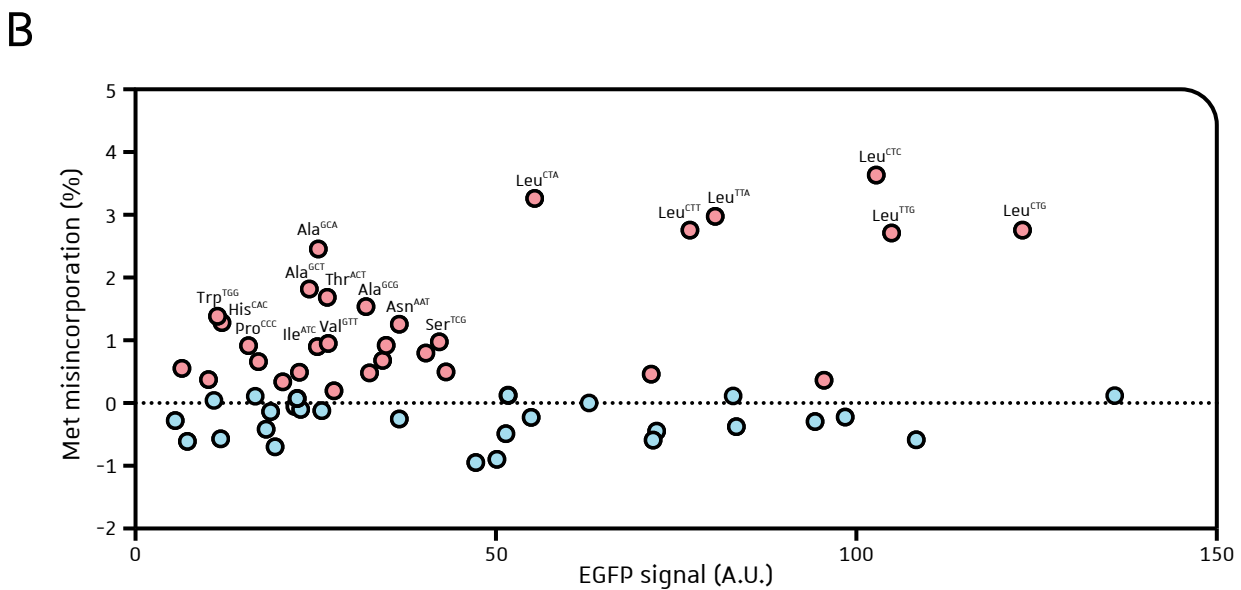
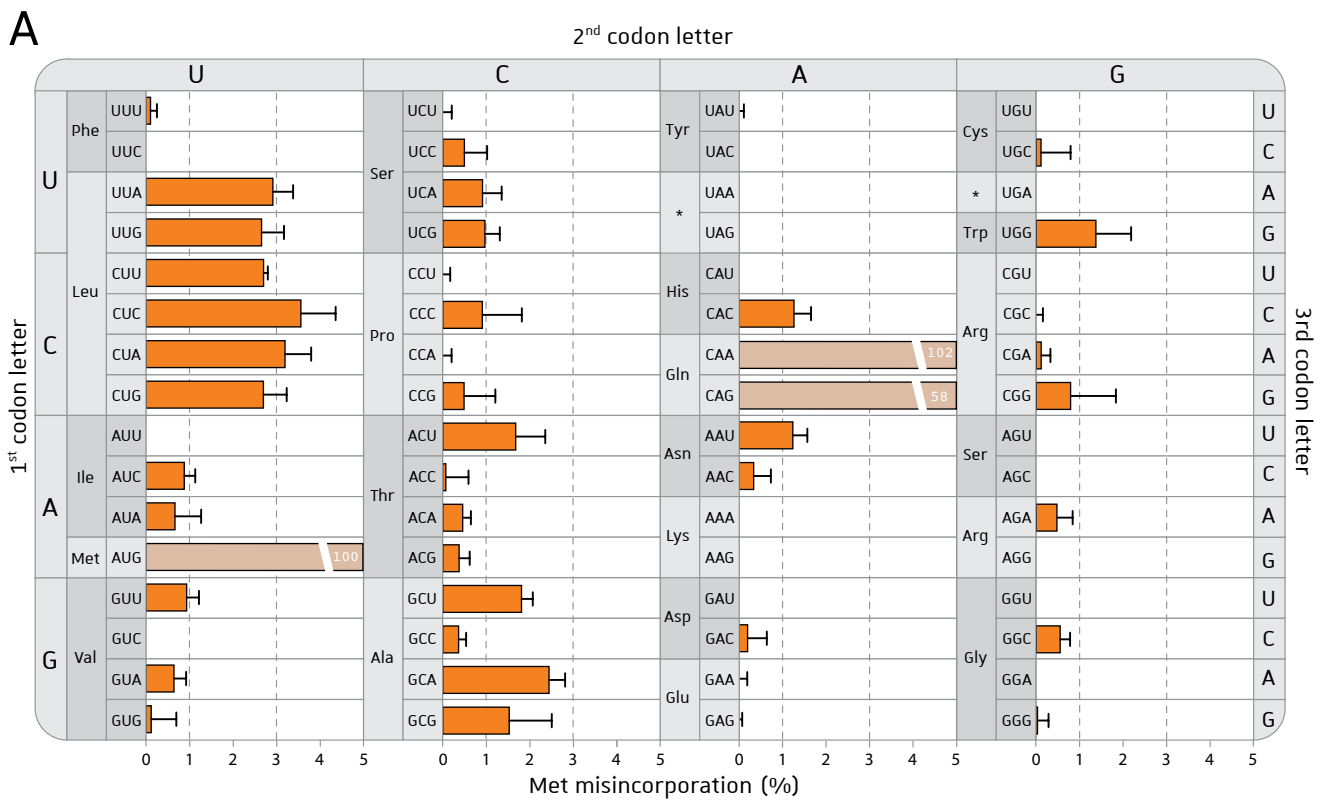


Figure R-12: Met misincorporation increases in *arc1Δ* background. The BFP library was generated in a *arc1Δ* RS453 genetic background and was analysed by epifluorescence microscopy. Cells were grown in rich YPD medium and harvested in logarithmic phase before observation under the microscope. Quantification is performed as described in **Figure R-10**. **A.** Results for BFP(Gln) and BFP(Met) are indicative since they do not represent actual misincorporation (light orange with % indicated in white). Means and standard deviations are obtained on more than 100 cells analysed ($n=1$). **B.** Misincorporation of Met is analysed according to the EGFP expression.

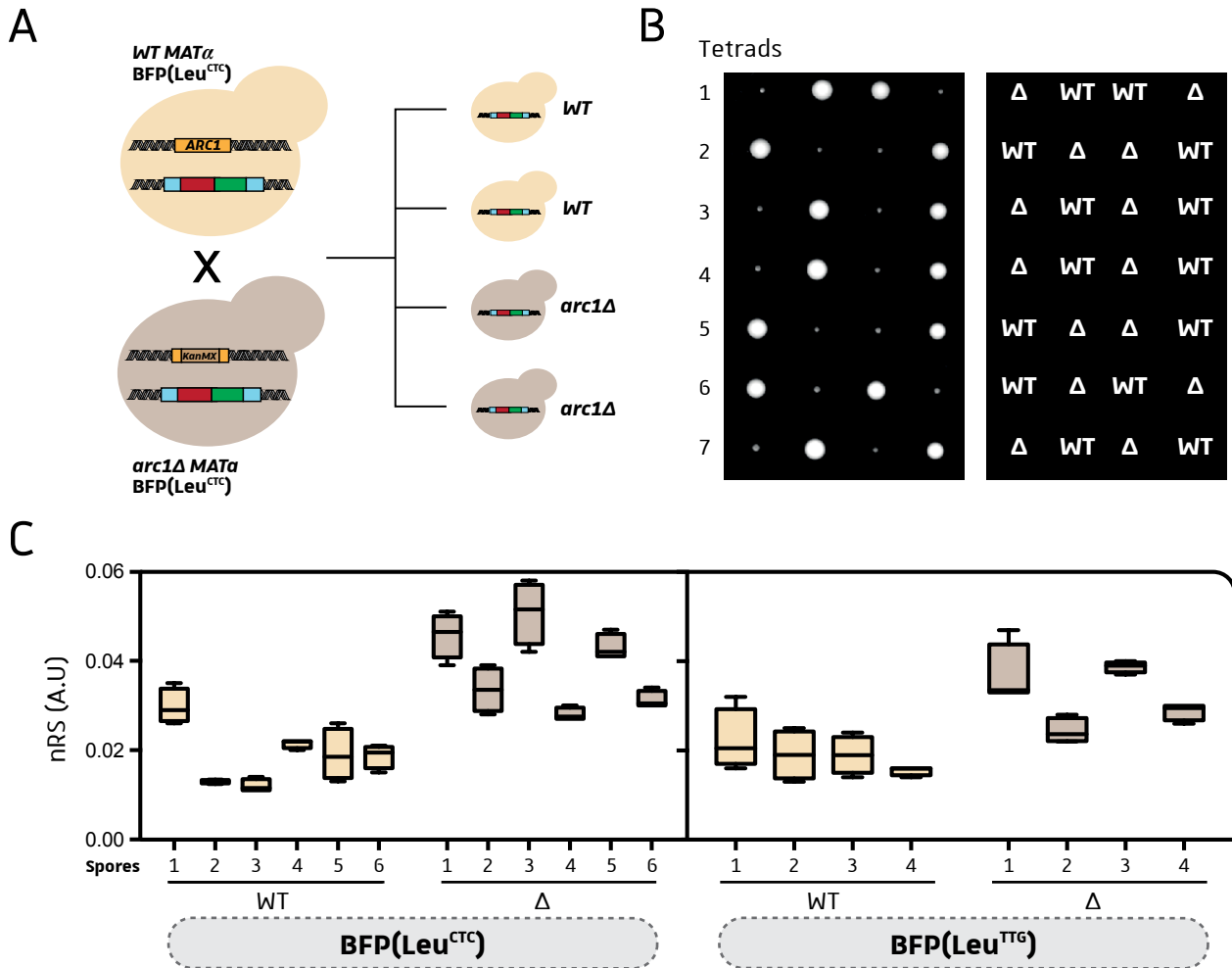


Figure R-13: Validation of the implication of Arc1 in Met misincorporation. **A.** The two BFP(Leu) WT and *arc1Δ* strains were crossed. Sporulation of the diploïde generates tetrades with four spores: two WT and two *arc1Δ*. **B.** Result of the dissection showing *arc1Δ* spores with slow growth (small colonies) and WT phenotype with no impact on growth. **C.** Several spores have been observed by epifluorescence microscopy and the normalized red signal (nRS) was quantified for each colony. For both BFP(Leu) strains, deletion of *ARC1* results in higher Met misincorporation than in WT strains.

quantification in the same conditions than in **Figure R-11**, misincorporation is observed in much more BFP *arc1Δ* strains than in BFP WT strain (**Figure R-12**). Indeed, twenty BFP strains show significant Met misincorporation only in the absence of Arc1. Similarly, all six BFP(Leu) strains display high signal, with misincorporation levels around three times higher than in WT strains (**Figure R-12A**). Again, all positive strains present high heterogeneity in reporter expression and do not correspond to bias in quantification (**Figure R-12B**). This result shows, for the first time, implication of Arc1 in MetRS aminoacylation fidelity. Indeed, previous work showed that deletion of Arc1 had no impact on mismethionylation profile (Wiltrout *et al.*, 2012). To confirm that the result in Figure R11 was not due to another mutation present in the RS453 *arc1Δ* strain's genome, I crossed BFP(Leu^{CTC}) WT strain with BFP(Leu^{CTC}) *arc1Δ* to analyse the Met misincorporation repartition in spores (**Figure R-13A**). If the absence of Arc1 is responsible of the misincorporation phenotype found in Figure R-11B, all spores with *ARC1* deletion should all have more normalized red signal (nRS) than the WT spores. All *arc1Δ* spores present typical slow growth and small colonies on agar plates (**Figure R-13B**). Analysis of the nRS for each individual colony shows that deletion of *ARC1* induces higher signal for all six *arc1Δ* spores compared to WT (**Figure R-13C, left part**). I obtained the same result with the BFP(Leu^{T66}) strains (**Figure R-13C, right part**). Thus, the higher misincorporation signal observed in the *arc1Δ* is not due to difference in genomic background but is correlated with the absence of the Arc1 cofactor.

I.8. Development of the BFP system for use in oxidative conditions

As discussed in the introduction, tRNA mismethionylation by yeast MetRS and subsequent Met misincorporation into proteins might prevent oxidative damages through reversible redox reactions. Hence it was necessary to adapt the tandem fluorescent probe for use in oxidative conditions and to compare our results with the ones obtained in previous studies of yeast mismethionylation (Wiltrout *et al.*, 2012).

I.8.1. Setting oxidative stress conditions

In the literature, oxidants and their working concentrations are extremely diverse, and depend on the yeast strain used in the study and the growth conditions (rich or minimal medium, in liquid or solid medium). In a first attempt to assess oxidative stress effects on mismethionylation, we wanted to grow the BFP strains in rich liquid medium (no nutritional deficiency) with oxidant added at a

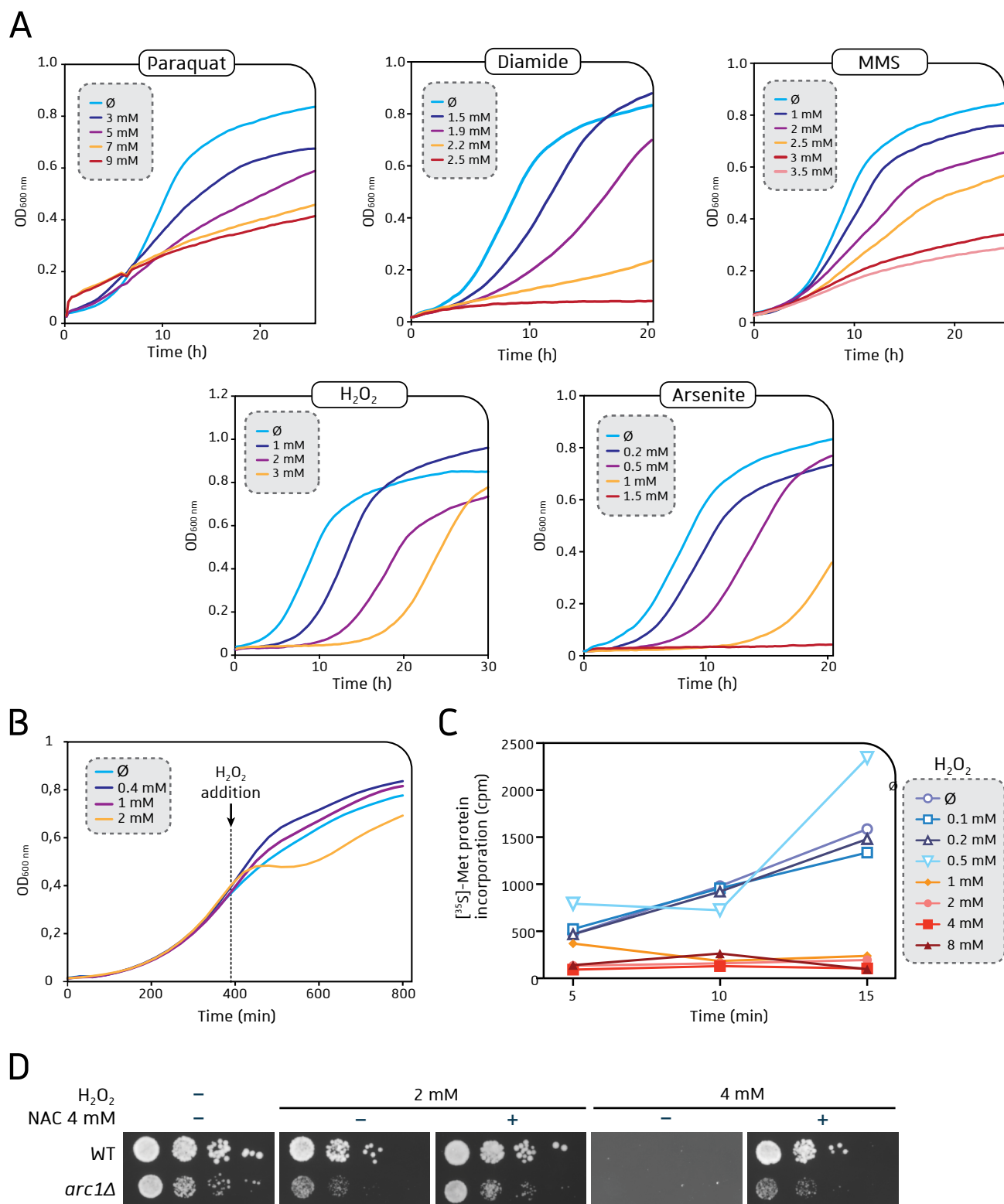


Figure R-14: Effects of oxidants on yeast cell growth and protein synthesis. A. Growth curves of RS453 strain grown in YPD rich medium at 30 °C with indicated concentration of oxidants. **B.** Growth curves of RS453 strain grown in YPD rich medium at 30 °C supplemented with H₂O₂ at the indicated concentration after 6h30 of incubation. **C.** Monitoring of the rate of protein synthesis by [³⁵S]-Met incorporation. Yeast cells are grown at 30 °C until mid-log phase is reached, then H₂O₂ is added together with [³⁵S]-Met. Cells are incubated at 30 °C and collected after 5, 10 and 15 min, and total protein extract are prepared. Incorporation of [³⁵S]-Met is quantified by liquid scintillation counting. **D.** Yeast spotting assay of WT or *arc1Δ* strains on YPD rich agar plate in absence or presence of H₂O₂ and N-acetylcysteine (NAC) as reductant.

non-lethal dose. To improve our chances to observe mismethionylation, I tested several classical ROS-generating chemicals used in oxidative stress assay:

- hydrogen peroxide (H_2O_2), a physiological oxidant relatively unreactive as is but acts as a superoxide precursor (**Figure I-25**, page 80),
- sodium arsenite (AsO_3^{3-}), a toxic metalloid with high toxicity associated with elevated levels of intracellular ROS (Wu, Yi and Zhang, 2013),
- diamide, a sulfhydryl reagent which oxidizes thiols in proteins into disulfides (Kosower and Kosower, 1995),
- paraquat dichloride (methyl viologen), a redox-cycling xenobiotic that stimulates superoxide production by accepting electrons from the NADPH coenzyme (Bus and Gibson, 1984).
- **Methyl MethaneSulfonate (MMS)**, a DNA alkylating reagent that enhances ROS production (Salmon *et al.*, 2004).

These oxidative chemicals were added to the rich liquid growth medium and yeast growth was monitored (**Figure R-14A**). Surprisingly, the effects on yeast growth were different according to the oxidizing chemical used. For some oxidants, increased concentrations did affect the growth rate, switching from exponential to linear growth with higher generation time (**Figure R-14A**, growth curves with Paraquat, diamide and MMS), but for both H_2O_2 and arsenite no effects on growth rates were observed. Instead of reducing the yeast growth rate, increased amount of these two chemicals induced a delay in the logarithmic growth, but once the cells started to divide no growth lowering was observed. This longer lag phase might be due to oxidative cell adaptation for a certain time, or might reflect the time needed for yeast to detoxify all the amount of oxidant. These first growth assays allowed us to monitor the working concentrations in liquid medium of paraquat (5 mM), diamide (2 mM) and MMS (2 mM). For H_2O_2 and arsenite these results did not enable to estimate the non-lethal concentrations.

Following these oxidative growth assays, more adjustments were needed. Indeed, we wanted to read mismethionylation after a specific time of incubation with the oxidant (from 1 h to several hours). This condition supposed adding the oxidant while the BFP strain was in logarithmic growth phase. Thus we started culture of the strain, and added H_2O_2 after around 6 hours ($\text{OD}_{600\text{nm}}$

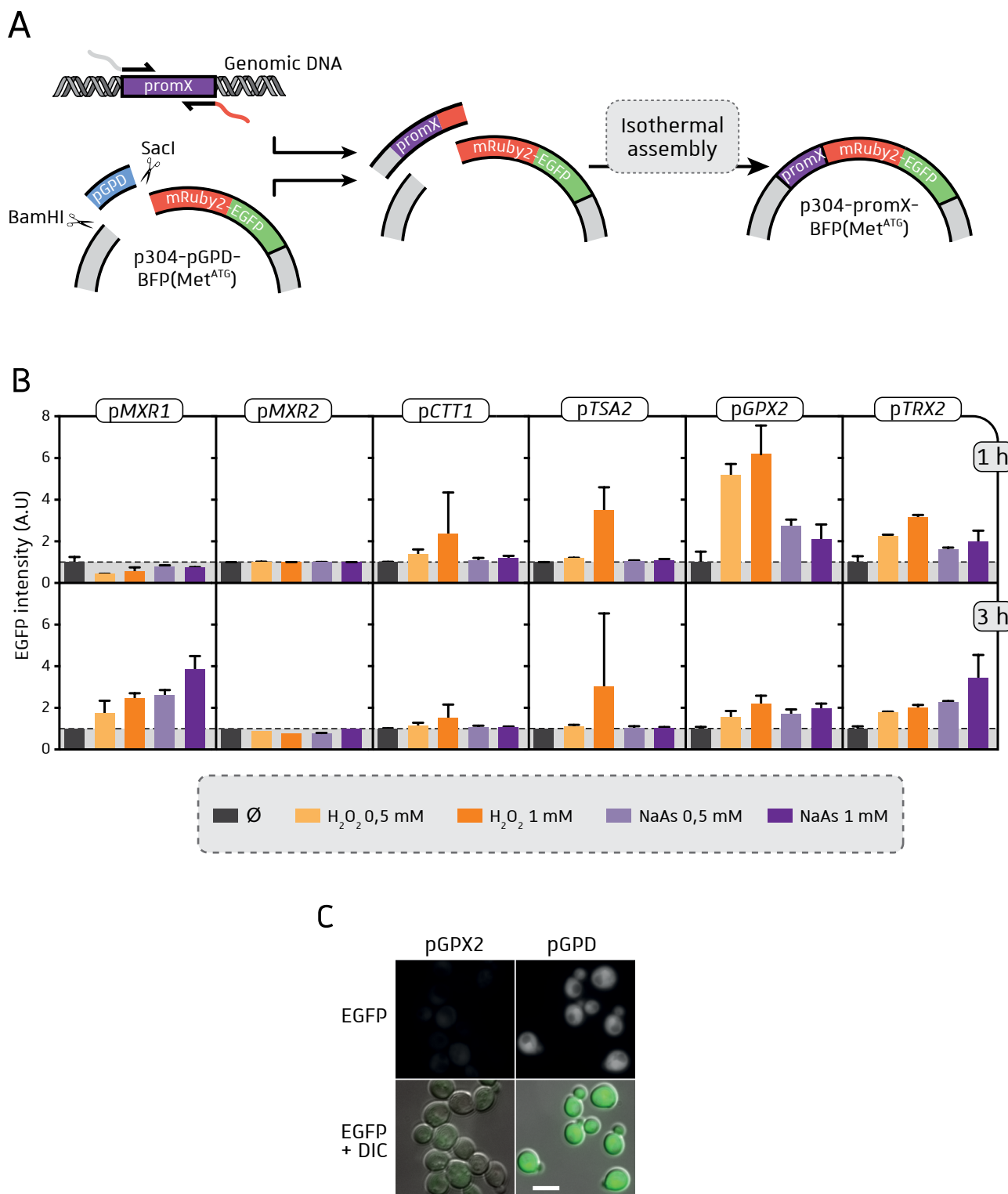


Figure R-15: Engineering of BFP constructs under the control of promoters of genes whose expressions are induced by oxidative stress. A. Description of the cloning method used to switch the *GPD* promoter (*pGPD*) by a specific promoter (*promX*). **B.** Quantification of the green fluorescent signal of cells expressing BFP(Met^{ATG}) under control of the indicated promoter. Cells were cultured at 30 °C in YPD rich medium, or in YPD with H₂O₂ (orange) or arsenite (NaAs, purple) at the indicated concentration. Cells were harvested after 1 h (upper panel) or 3 h (lower) incubation at 30 °C. **C.** Imaging of cells expressing the BFP(Met^{ATG}) under the control of the *pGPX2* after 3 h treatment with 1 mM H₂O₂ (left panel). Imaging of the BFP(Met^{ATG}) strain with *pGPD* promoter grown in rich medium is shown on the right for comparison. Scale bar, 10 μm.

at 0.4) (**Figure R-14B**). While adding 1 mM H₂O₂ on cells did not significantly affect the growth rate, 2 mM H₂O₂ seemed to stop cell division for a while (around 2 hours) and lost its inhibitory effect thereafter. We assumed this lag effect might be due to ROS-dependent inhibition of protein synthesis, since such translational effect had previously been described (Shenton *et al.*, 2006). Inhibition of translation by oxidants was an issue for our BFP system since production of the tandem fluorescent probe relies on protein synthesis to monitor mismethionylation. We tested the effect of H₂O₂ treatment on protein synthesis by pulse labelling with [³⁵S]Met and measurements of radiolabelled Met incorporation in total protein extract (**Figure R-14C**). We indeed found that H₂O₂ concentrations above 1 mM inhibit the aa incorporation during protein synthesis after 15 min of incubation. However this inhibitory effect was analysed only for 15 min and further analysis should determine if this effect is lost after few hours, since addition of 1 mM of H₂O₂ on cells did not show effect on growth curve (**Figure R-14B**). Similar growth studies have also been carried on solid medium, and inhibitory concentrations appeared to be higher for cells growing on agar plates (**Figure R-14D** and **Supplemental S2**, page 198). The specific oxidative effect was inhibited by adding reducing N-acetyl cysteine (NAC) to the solid medium before plating.

I.8.2. Adapting the BFP system to oxidative stress

Since action of ROS had a general impact on translation, it was crucial to adapt our BFP system to be well expressed under oxidative conditions. Since the *GPD* promoter (*pGPD*) upstream the BFP coding sequence is a constitutive promoter, we wanted to use a promoter specifically activated under oxidative stress. We took advantage of previous studies performed on yeast to identify genes up-regulated by ROS (Shenton *et al.*, 2006; Morano, Grant and Moye-Rowley, 2012). Obviously, the majority of the proteins up-regulated in response to ROS exposure were identified as protective enzymes involved in ROS primary and secondary defences (**Figure I-27**, page 84). Among these genes, we selected the promoters of the two Msrs enzymes Mxr1/Mxr2, the catalase Ctt1, the peroxiredoxin Tsa2, the glutathione peroxidase Gpx2 and the thioredoxin Trx2. We thus amplified these associated promoters (1,000 bp upstream the coding sequence) by PCR and cloned each promoting sequence upstream the BFP(Met^{ATG}) reporter by removing *pGPD* in parallel (**Figure R-15A**). We then expressed each BFP construct into a WT RS453 strain and analysed the BFP expression by assessing EGFP fluorescence. As expected, all BFP strains displayed no observable green fluorescence in basal conditions (YPD, rich medium). We then treated cells with either H₂O₂ or arsenite to observe gene expression activation and subsequent EGFP fluorescence after 1 h or 3 h

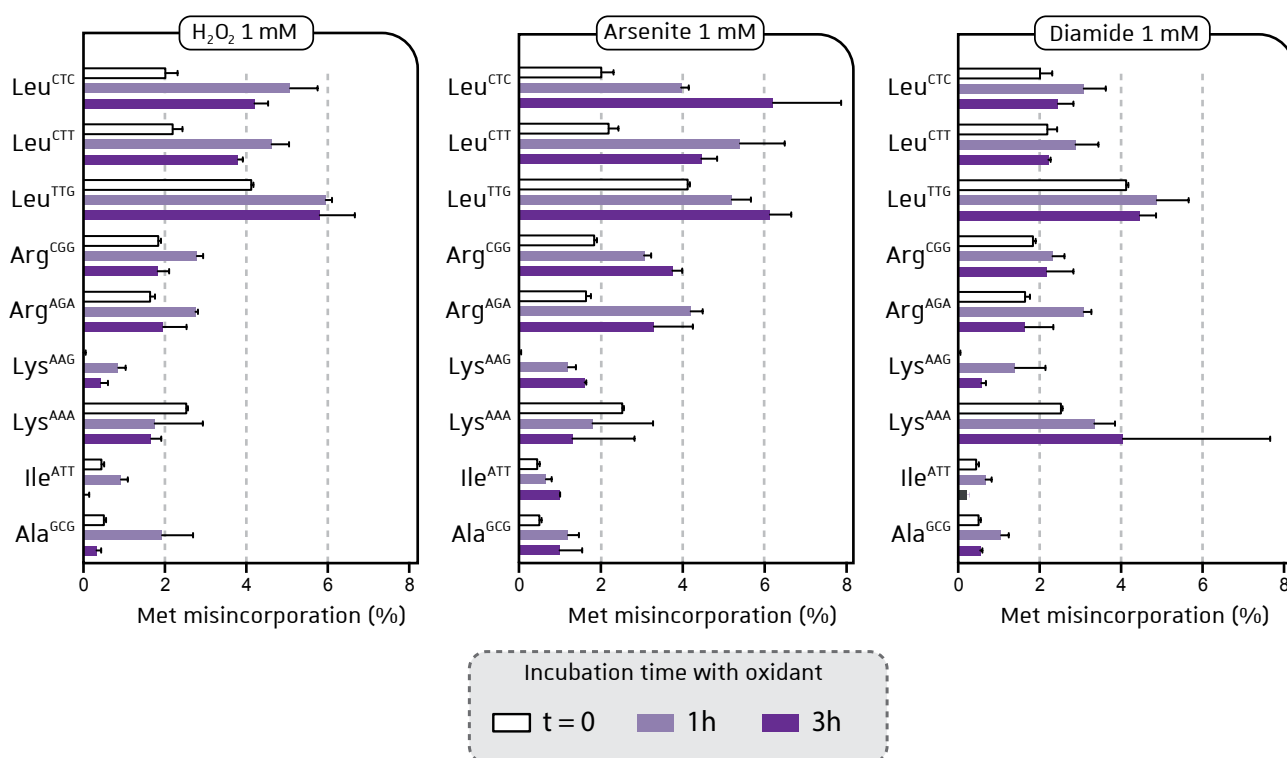


Figure R-16: Oxidative stress increases Met misincorporation. Yeast BFP WT strain library (RS453 genetic background) was analysed by epifluorescence microscopy. WT yeast cells were grown in rich YPD medium at 30 °C until mid-log phase was reached, then 1 mM H₂O₂, 1 mM arsenite or 1 mM diamide was added to the cells and grown again at 30 °C. Cells were harvested after either 1 h (light purple) or 3 h (dark purple) before observation under the microscope. Quantification is performed as described in Figure R-10.

treatment. Results in **Figure R-15B** show that promoters did not respond equally to oxidative stress: some allow gene expression after 1 h (p*GPX2*), after 3 h (p*MXR1*), or both (p*TRX2*). Intriguingly, p*MXR2* was not activated in all oxidative conditions that were tested, and p*TSA2* showed lower BFP expression only with 1 mM H₂O₂. Thus, only p*GPX2* gave us expected results with H₂O₂ treatment, but this gene activation was too low to be used for fluorescence quantification since the EGFP signal did not reach more than 20 % of that obtained with the GPD promoter (**Figure R-15C**).

I.8.3. First results show oxidant-mediated mismethionylation

Since we did not find suitable promoters to use in oxidative conditions, we used the BFP strains with the GPD promoter to assess oxidant-mediated mismethionylation rate. Cells were grown in rich medium until logarithmic phase and oxidants (H₂O₂, arsenite or diamide) were added to the culture for 1h or 3 h incubation. Fluorescence and resulting Met misincorporation were quantified for only 11 BFP strains: the controls BFP(Met^{ATG}) and BFP(GF), and 9 different BFP strains shown in **Figure R-16**. First observations show that all three oxidants used in this assay gave significant global increase in mismethionylation after 1 h or 3 h of treatment, with lower effects for diamide that might be due to a low working concentration (1 mM used, whereas 2 mM seemed more appropriate according to **Figure R-14A**, page 130). Interestingly, the three BFP(Leu^{CTC}, ^{CTT} and ^{TTG}) strains used show high impact of H₂O₂ or arsenite on Met misincorporation, with a 2- to 3-fold increase after 3 h treatment for BFP(Leu^{CTC}) and BFP(Leu^{CTT}), and to a lesser extent for BFP(Leu^{TTG}). Again, this study revealed strong mismethionylation at Leu codons induced by oxidative stress, but also at additional codon positions in a lesser extent. Hence, this preliminary result suggests that Met misincorporation might constitute a specific defence against oxidative stress, with a preference for mismethionylation at Leu codons.

I.9. Discussion

I.9.1. Confirmation of mismethionylation by mass spectrometry

Results of mismethionylation obtained in rich medium gave us unexpectedly results since the potentially mismethionylated tRNAs by the MetRS appeared to be essentially the tRNA^{Leu} species. These tRNAs were not found particularly mismethionylated in yeast, except maybe for tRNA^{Leu}(UUC) and tRNA^{Leu}(AUC) in oxidative conditions (**Figure I-34**, page 98, [Wiltrout et al., 2012](#)). Since it is the first time that such a tandem fluorescent reporter is used in yeast to analyse mismethionylation at

A

aa	Molecular weight (g/mol)	Density (g/mol)	pI	Dipole moment (D)	Hydrophobicity	Side-Chain flexibility
Methionine	149.2	1.30	5.7	1.80	0.811	High
Leucine	131.2	1.20	6.0	0.09	0.918	Moderate

B

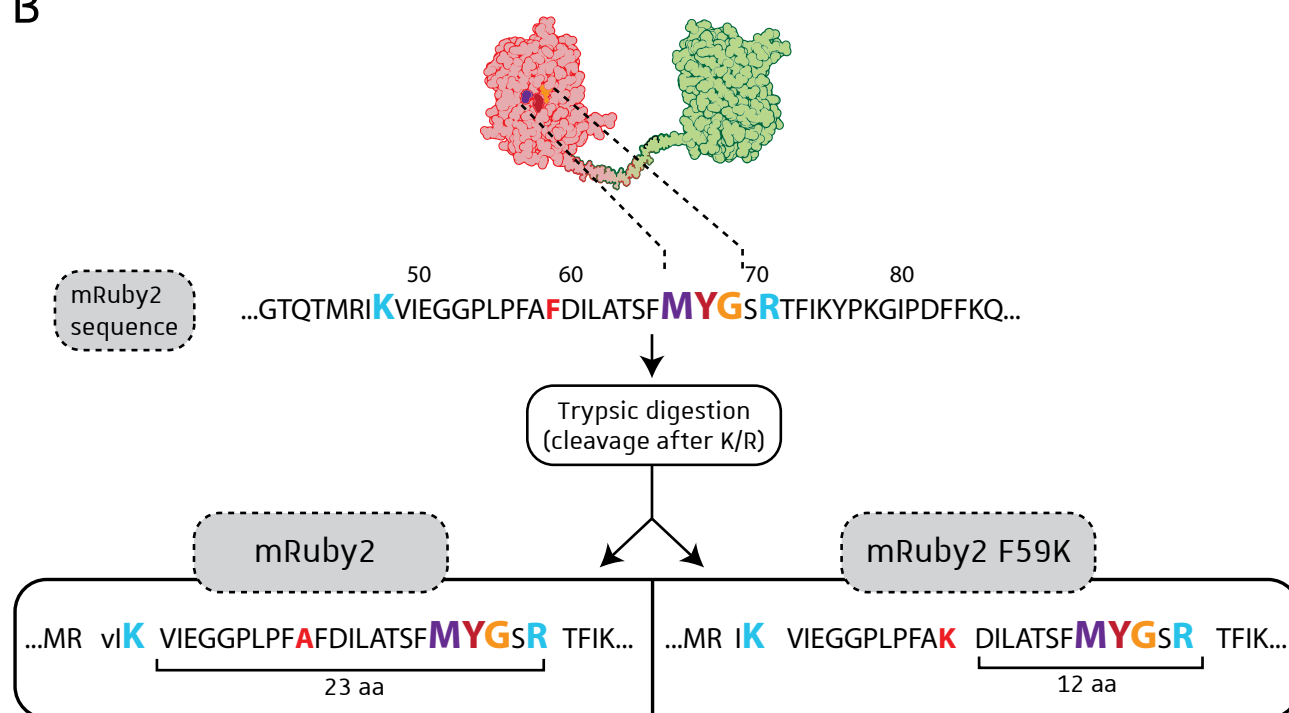


Figure R-17: Design of the BFP reporter suitable for mass spectrometry analyses. **A.** Physical and chemical properties of Met and Leu residues (from [Forney-Stevens, Bogner and Pikal, 2016](#)). **B.** Each BFP reporter from the library was mutated at position 59 to obtain F59K substitution. This mutant reporter gives rise to a 12 aa-long peptide after trypsin digestion containing the fluorophore triad. This peptide has a mass allowing its detection in a trypsin digested total protein extract of each of the F59K BFP variant.

all coding codon positions, we needed to confirm these results by mass spectrometry as a proof of concept. Indeed, the remaining red fluorescence found for the six BFP(Leu) strains could either be (i) a signal caused by few mismethionylation events at Leu codons in yeast or (ii) a faint signal caused by the leucyl residue accurately incorporated in position 67 of the mRuby2 sequence, without any mismethionylation event. This latter assumption could be explained by a similar size and properties shared by leucine and methionine (**Figure R-17A**) residues. Therefore, the conformation of leucyl residue in the mRuby2 fluorophore could partly restore red fluorescence signal without any Met misincorporation event. To confirm our microscopic observation, we designed the mRuby2 sequence to be analysed by mass spectrometry (MS). In its present sequence, after trypsin digestion (required for MS analysis), the mRuby2 fluorophore is located in a 23 residues-long peptide with a spectrum not detectable by MS (**Figure R-17B**). Hence, we created the complete collection of mRuby2 F59K (^{F59K}BFP) mutants with a 12 residues-long peptide suitable for MS analysis. Unfortunately the F59K mutant lost its red fluorescence properties (data not shown) and cannot be used for microscopic quantifications. We sent total protein extracts from strains expressing the ^{F59K}BFP constructs (^{F59K}BFP(Met,Leu, Arg, Lys and Gln)) to MS analysis, but no peptide corresponding to misincorporation events have been observed in the samples we submitted to MS analyses. Absence of detection might be explained by a two weak sensitivity of the technique. Since there are only few events of Met misincorporation, the number of peptides with Met67 is too small to be detected in a total protein extract. To increase our chances to observe misincorporation events, we will prepare pure BFP protein extract by co-immunoprecipitation of the tandem fluorescent reporter with anti-GFP antibodies and purification on magnetic beads.

I.9.2. Met misincorporation at Leu position

Our results are divergent from previous studies and can be explained by the fact that we are using a different method. All studies aiming at identifying mismethionylated tRNAs were done using [³⁵S]-Met incubation followed by tRNA microarrays but not by checking Met misincorporation during protein synthesis. This might explain the high rate of mismethionylation observed in all these studies in *E. coli*, *S. cerevisiae* and human (**Figure I-34**, page 98). These studies did not take into consideration the potential editing effect of the elongation factor eEF1A (EF-Tu in bacteria) that binds poorly some acylated tRNA and thus does not deliver them to ribosome ([LaRiviere, Wolfson and Uhlenbeck, 2001](#); [Asahara and Uhlenbeck, 2005](#)). Even if we also identified Met misincorporation at Lys(AAA) and Arg(AGA) codons which are decoded by tRNAs that were previously

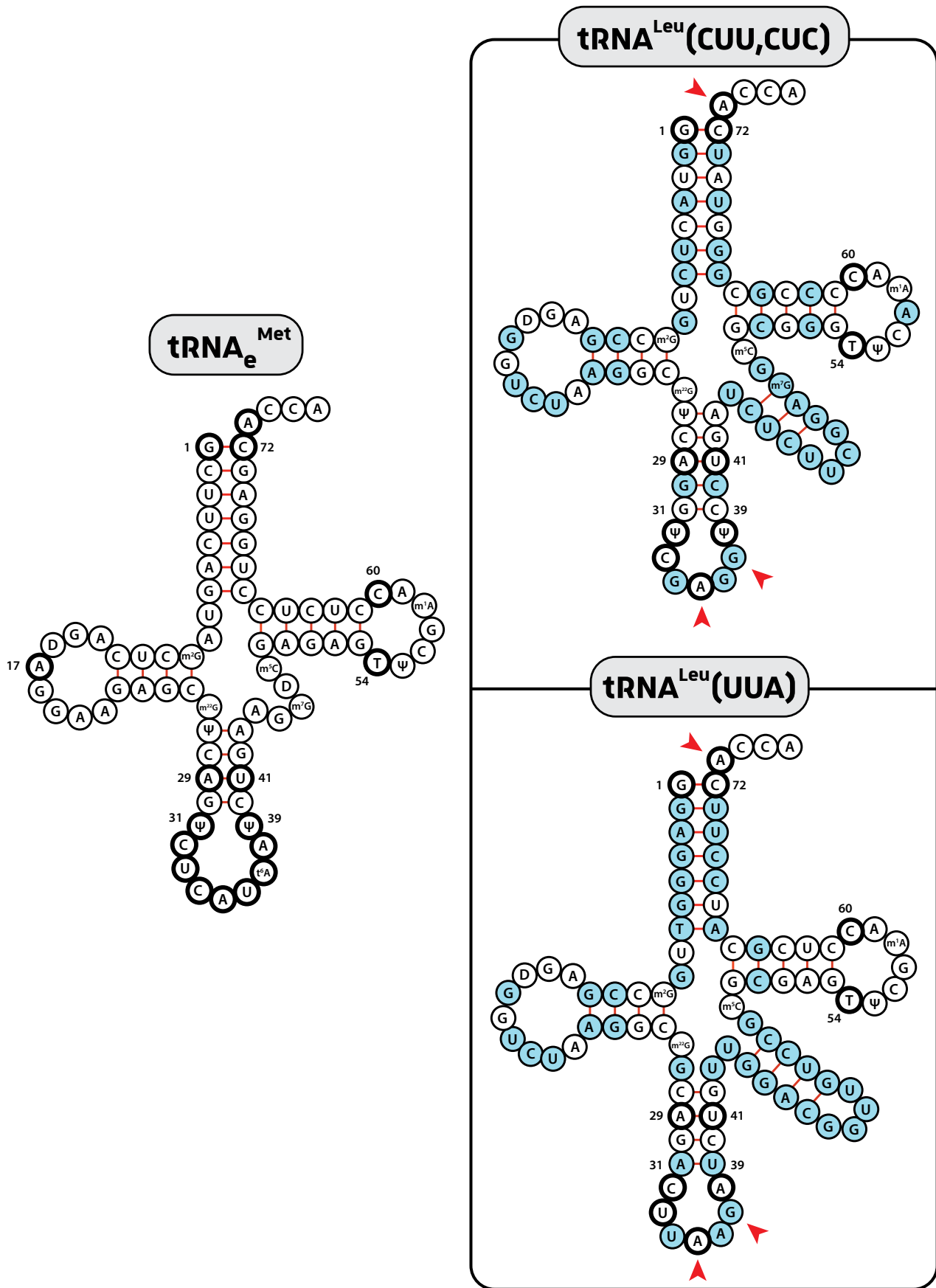


Figure R-18: Sequence comparison of tRNA_e^{Met} with tRNA^{Leu}(CUU,CUC) and tRNA^{Leu}(UUA). Nucleotides in bold circles are identity elements for tRNA_e^{Met} reviewed in Figure 27 and 28. Blue nucleotides are those differing for Leu tRNAs compared to tRNA_e^{Met}. Red arrowheads highlight the identity element for LeuRS aminoacylation (A₃₄, G₃₇ and A₇₃).

found as highly mismethionylated in yeast (Wiltout *et al.*, 2012), our BFP system also identified the entire set of Leu codons and with high rate of Met misincorporation. Replacement of Leu by Met seems a logical strategy at first sight since (i) Leu is one of the most abundant aa found in proteins, representing 32 % of all aa residues along with Ser, Lys and Glu, and is present in all proteins (Wu, 2013). Hence mismethionylation can occur at multiple positions in the proteome. Moreover, (ii) Leu is a hydrophobic residue with a neutral lateral chain, and is nearly isosteric with Met, meaning that replacement by Met would not alter drastically the protein structure. However, Leu is found preferentially buried in low accessibility regions into proteins (Mer and Andrade-Navarro, 2013), so Met misincorporation in such locations would limit encounters with ROS for further detoxification. Comparisons between tRNAs^{Met} and tRNAs^{Leu} also show that (iii) tRNAs^{Leu} are sharing most of the identity elements essential for MetRS recognition (Table I-2, page 32 for sequences alignment, and Figure R-18). If Met misincorporation at Leu position really occurs in cells, we cannot exclude the other possibility which would be that leucyl-tRNA synthetase (LeuRS) misactivates Met and transfers Met onto tRNAs^{Leu}, leading to the same misincorporation event. But it is unlikely that LeuRS misactivates Met since catalytic efficiency of LeuRS for Met activation was very low with a discrimination factor of $2 \cdot 10^4$ compared to Leu activation (Cvetesic *et al.*, 2016). In addition, yeast tRNA^{Leu} identity is composed of A₃₅, G₃₇ and A₇₃ only, and tRNA^{Met} does not have G₃₇ (Figure R-18). All these observations are in agreement with a tRNA^{Leu} misacylated by the MetRS, and we are currently testing *in vitro* aminoacylation of tRNAs^{Leu} transcripts by the recombinant MetRS to confirm our BFP observations.

I.9.3. Multiple use for the BFP system

Now that the collection of the 61 BFP plasmids is available, the system can be expressed in various strains to analyse the effects of some genes that could be involved in Met mistranslation. We already have the whole collection in the WT RS453, BY4742 and W303 yeast backgrounds, and their respective *arc1Δ* strains. To get more information about Met misincorporation across species, we could consider the possibility to perform heterologous expression of the human MetRS in *S. cerevisiae*. Indeed, the yeast *mes1Δ* strain is rescued by a plasmid overexpressing the human MetRS (Figure R-19A). Thus, I engineered a yeast strain expressing only the human ortholog MetRS-cMyc (Figure R-19B) and I tested this strain for Met misincorporation on some BFP constructs (Figure R-19C). It appeared that the humanized *S. cerevisiae* strain presents a different Met misincorporation profile, with a significant signal for BFP(Ile^{ATT}) and BFP(Ala^{GCG}) that is never

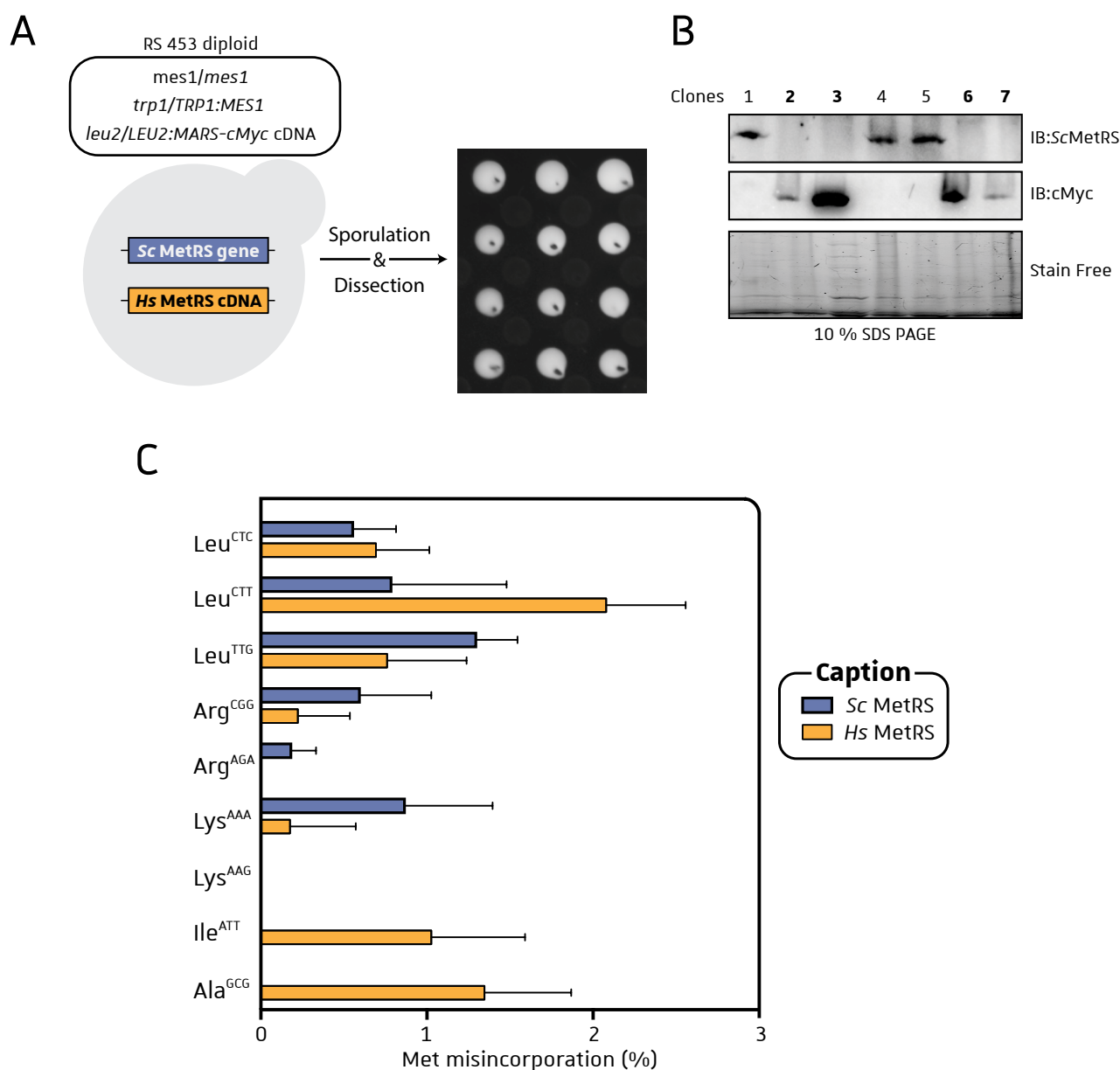


Figure R-19: Yeast strain expressing human MetRS presents a different Met misincorporation profile. A. Sporulation and dissection of a diploid strain expressing one copy of the yeast MetRS gene (*MES1*) and one copy of the human MetRS gene cDNA (*MARS*, tagged with cMyc). Genotype of each spores was determined, and analysed in B. **B.** Immunoblotting of total protein extracts from spores obtained in A. Some clones expressed only the yeast MetRS (recognized by the ScMetRS antibody), whereas others were living with the sole human MetRS-cMyc (in bold). **C.** Yeast BFP strains (RS453 genetic background) were analysed by epifluorescence microscopy. Cells expressing yeast MetRS (Sc MetRS) or human ortholog (*Hs* MetRS) were grown in rich YPD medium and harvested in logarithmic phase before observation under microscope. Quantification is performed as described in **Figure R-10**. Means and standard deviations are obtained on more than 100 cells analysed.

observed for yeast MetRS. Even expressed in a heterologous system, our BFP system might be attractive to study the whole Met misincorporation pattern of orthologous MetRSs. We can also test myriads of conditions in which Met misincorporation could be either enhanced or reduces. I have started to analyse BFP strains grown in glycerol, a respiratory medium where mitochondria are highly active and supposed to produce high quantity of ROS (**Figure I-26**, page 82), but preliminary results did not show significant enhancement of Met incorporation.

All the Met misincorporation results shown in this thesis have been obtained by imaging cells with an epifluorescence microscope. It allows analysis of single cells but imaging several cells might be time consuming if one wants to be statistically relevant. Indeed, imaging more than hundreds of cells cannot be performed in a reasonable time. Therefore, during my time in the lab, I tried to analyse BFP strains using flow cytometry. This technique allows the analysis of thousands of cells in less than a minute. By using flow cytometry, we were able to see the increase of Met misincorporation for BFP(Leu^{CTC}) strain after treatment with 5 mM paraquat (**Supplemental S3**, page 199). In the future, both microscopy and flow cytometry could be complementary methods to monitor Met misincorporation.

I.9.4. Met misincorporation and surface exposed defence

The Met misincorporation in proteins is thought to play an important role in ROS scavenging, since deletion of the methionine sulfoxide reductases (Msrs) is deleterious for cells surviving (**Table I-9**, page 86). However, this system might be robust only if these misincorporated Met residues were accessible by the ROS and the Msrs enzymes, meaning that they are surface-exposed in the protein structures ([Levine et al., 1996](#); [Tarrago et al., 2012](#)). If such a system exists, the translation machinery should misincorporate Met in precise position along the mRNA sequence. Our hypothesis was as followed: we assumed that the tRNAs that are the most mismethionylated (or the most mismethionylated tRNA isoacceptors) would translate an mRNA codon coding for an aa often found exposed at the surface of protein structures. With such a system, the Met misincorporation would not be a random mechanism and the additional Met residues would statistically be more present on protein surface. Hence, we were interested in the correlation between position of an aa residue in the protein structure and its corresponding codon in the mRNA sequence to see if there was some sort of codon usage bias for surface-exposed residues. We started a bioinformatics study in collaboration with Dr. Olivier Poch and Dr. Luc Moulinier (ICube, UMR CNRS 7357, Strasbourg). The aim

of this work was to download all existing yeast protein structures, dissociate the surface exposed residues from the buried residues, and recover their corresponding coding codon in the mRNA sequence. At the end, we should have a list of each 61 coding codon sorted by their exposed/buried ratio of the associated corresponding aa residue. With this study, we wanted to know whether some codons (Leu codons?) are more prone to code for surface-exposed residues. It would also be interesting to analyse this result with respect to synonymous codons since we found different Met misincorporation rates depending on the synonymous codon analysed.

1.9.5. Concluding remarks

This project still needs improvements in the methodology. To study more precisely the effects of oxidative stress, we need to find an adequate promoter strongly induced by oxidants. Moreover, if we want to study Met misincorporation in a shorter time lapse, we would need to change the red fluorescent protein, since maturation time of mRuby2 is too long for observation after shorter times (150 min for mRuby2, 40 min for mCherry). Despite some adjustments in the technique, we already have plenty of constructs to efficiently study Met misincorporation in yeast. The first data have already shown interesting results, with Met misincorporation at some codon that had never been identified before, and for the first time we have seen the impact of Arc1 in MetRS accuracy. Altogether, the results from this project will allow us to elucidate some of the molecular aspects of the adaptative translation in yeast.



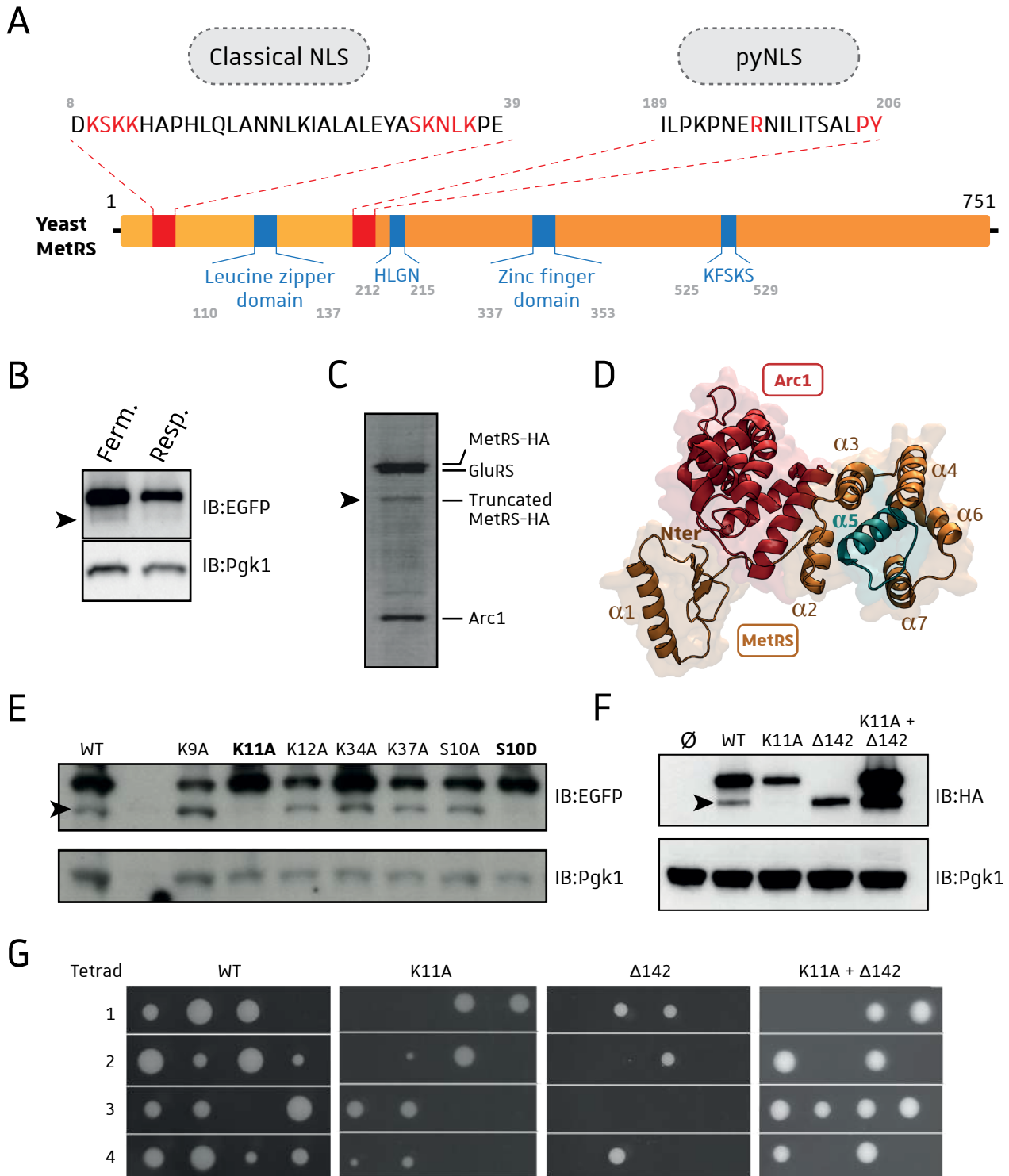


Figure R-20: Summary of results found on cleavage of yeast MetRS (Results B, C, E, F and G from [D. Laporte thesis, 2016](#)). **A.** Sequence of yeast MetRS shows two NLSs confirmed by mutagenesis and EGFP-tagged MetRS localization. **B.** Truncated form of MetRS (arrow) is observed by anti-EGFP immunoblotting in fermentation condition. **C.** Immunoprecipitation of MetRS-HA reveals co-IP of the AME complex component (Arc1 and GluRS) and IP of the truncated MetRS. **D.** Mass spectrometry analysis of the immunoprecipitated truncated MetRS-HA identified the cleavage site between residues 114 and 132, within the $\alpha 5$ helix (blue). **E.** Analysis of different NLS mutants for MetRS shows absence of cleavage for K11A and S10D mutants. **F.** Expression of mutants in diploides strains carrying endogenous MetRS and tagged mutants. **G.** Spores distribution of the dissected tetrads of sporulated diploides shown in F. Coexpression of both constructs restores cell viability.

II. Study of a newly characterized truncated form of yeast MetRS

II.1. Context of the study

Several previous studies have identified truncated forms of eukaryotic aaRSs (Wakasugi and Schimmel, 1999; Park *et al.*, 2005; Zeng *et al.*, 2011; **Table I-7**, page 70) and have shown their crucial roles in extracellular signalling in mammals. We have seen that the MetRS was found to be processed in *E. coli* and human cells through proteolytic cleavage (**Figure I-37**, page 102). However, the role for these shorter MetRS forms, if any, is still speculative since the cleavage was observed exclusively *in vitro* or *ex vivo*. Indeed, the MetRS was purified from *E. coli* or HeLa cells and then proteolysis was carried out by adding purified enzymes or a total cell extract (Cassio and Waller, 1971; Lei *et al.*, 2015). Thus, relevance of the existence of a truncated MetRS has never been ascertained *in vivo* in any organism, and as such, truncation has never been reported for yeast MetRS either.

Few years ago, a former PhD student in the lab, Dr. Daphné Laporte, observed the presence of a truncated form for yeast cytosolic MetRS. In the meantime, identification of two nuclear localization signals (NLSs) in the N-terminus of MetRS revealed the importance for the cytosolic MetRS to be nuclear (**Figure R20-A**). Indeed, in addition to a first classical bi-partite NLS identified within residues 8-39, a pyNLS was characterized just upstream of the catalytic residues HLGK. This second NLS is present at the end of the N-terminal Arc1-binding domain and explains the nuclear localization of the deletion mutant $\Delta 11-186$ (**Figure I-23A**, page 76). The truncated form was visualized by western blot analyses of cells expressing C-terminal EGFP-tagged MetRS (**Figure R-20B**). Surprisingly, cleavage happens in fermentation but not in respiration. The shortened form was also evidenced by immunoprecipitation of HA-tagged MetRS (**Figure R-20C**) followed by mass spectrometry analyses on this co-purified truncated form that identified the cleavage site which is located in the $\alpha 5$ helix between residues 114 and 132 (**Figure R-20D**). Studying mutation of the NLS residues led to the finding of two mutants that were not cleaved anymore (mutant S10D and K11A, **Figure R-20E**). This discovery raised the question of potential essentiality of this MetRS cleavage for yeast's survival? To answer this question, a diploid strain carrying only one copy of the endogenous MetRS was transformed with only the K11A mutant or the truncated MetRS isoform: MetRS($\Delta 142$). Tetrad dissection and analyses showed a 2:2 segregation, demonstrating the non-

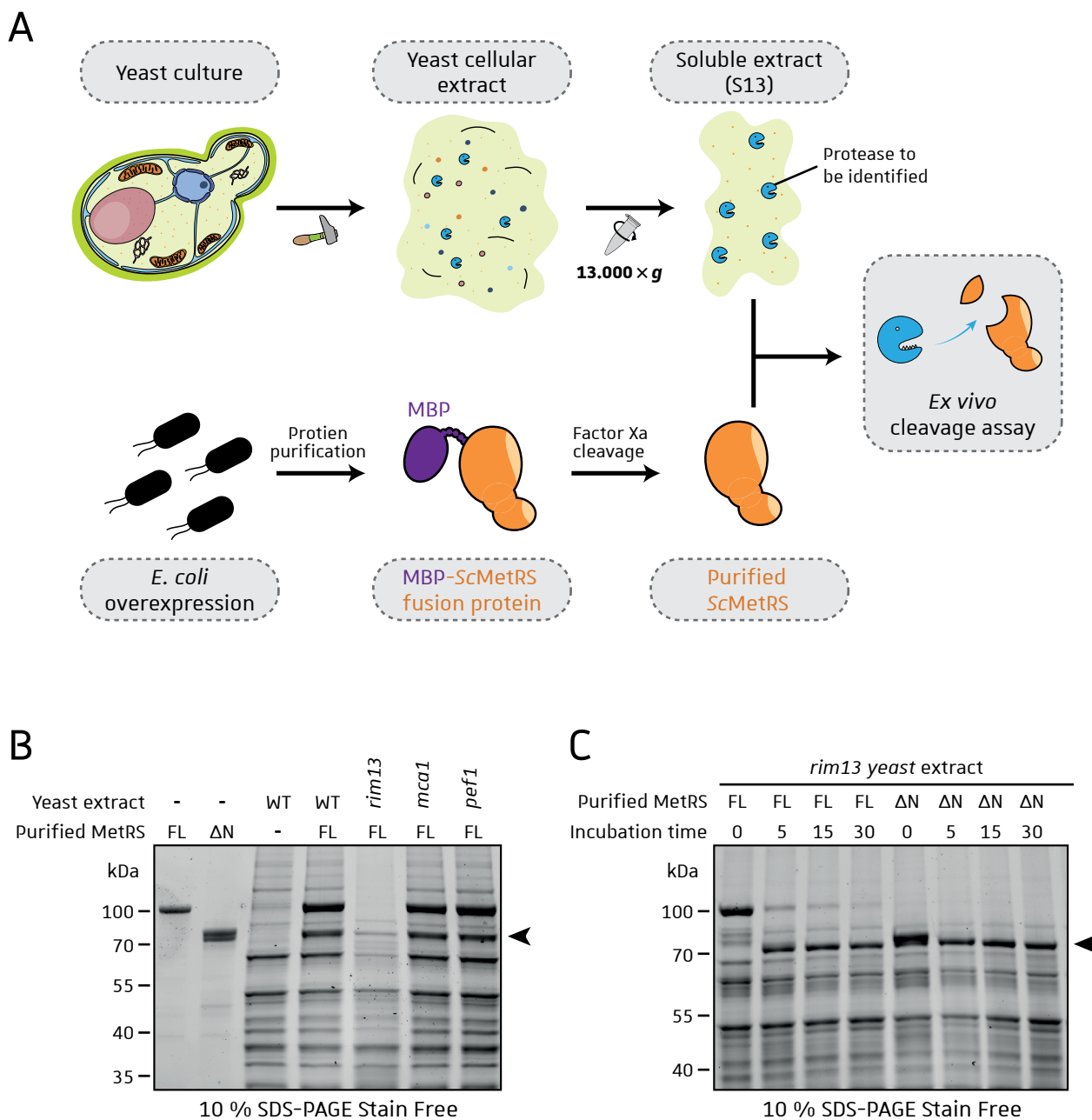


Figure R-21: Ex vivo cleavage of recombinant purified yeast MetRS. **A.** Schematic protocol of ex vivo cleavage experiment. Soluble yeast extract is obtained by yeast cell breakage and centrifugation of the lysate at $13.000 \times g$ to remove cell debris and heavy membranes. In parallel, recombinant yeast MetRS is purified from an *E. coli* overexpressing strain after removal of the N-terminal MBP-tag by factor Xa digestion. Both the yeast extract and the recombinant purified MetRS are incubated at $30^\circ C$ for 60 min and cleavage is observed by SDS-PAGE. **B.** Ex vivo cleavage of yeast MetRS after addition of yeast extract from WT strain or from strains deleted from given protease genes and 60 min incubation at $30^\circ C$. Position of truncated MetRS is indicated by a black arrow. FL: full length, ΔN : MetRS($\Delta 1-142$). **C.** Kinetic of MetRS clivage by yeast extract deleted for the from the Rim13 protease. Position of truncated MetRS is indicated by a black arrow. FL: full length, ΔN : MRS($\Delta 1-142$)

viability of spores carrying only the truncated form or the non-truncated form (**Figure R-20G**). In addition, transformation of the same diploid with both plasmid constructions led to tetrads with three or four viable spores, showing that co-expression of both forms of MetRS is essential for yeast survival. Thus, the cleavage of yeast MetRS appeared to be essential, and the aim of my project was to confirm and characterize into more details the role of this truncated and essential isoform of yeast MetRS.

II.2. General characterization of the proteolytic cleavage

II.2.1. Design of *ex vivo* cleavage protocol and role of Rim13 protease

To go further into details about the production of this truncated MetRS, we wanted to prove this shorter form was produced by endoproteolytic cleavage. We had previous evidence that this shorter form was not generated by translation at an alternative start codon but rather mediated by protease-specific cleavage ([Laporte, thesis, 2016](#)). However, no data were obtained concerning the regulation or the specificity of this cleavage. To answer these questions, I needed to develop an assay allowing the production of this truncated form, controlling in the same time the external parameters (temperature, buffer, chemicals...). Inspired by [Lei et al., 2015](#), I set up an *ex vivo* assay by adapting their experimental protocol to yeast cells. This assay requires purification of recombinant yeast MetRS in *E. coli* (source of MetRS to be cleaved) and preparation of a soluble yeast extract (source of the protease) (**Figure R-21A**). For recombinant MetRS purification, a protocol allowing purification of Maltose-Binding protein (MBP)-tagged MetRS had previously been developed in the lab (see **Mat&Met**, page 245). After cleavage by factor Xa to remove the MBP from the yeast MetRS, the soluble yeast extract is added onto the purified recombinant MetRS and the mixture is incubated at 30 °C to promote cleavage. Obviously, this assay relies on the presence of the unknown protease into the soluble fraction obtained after centrifugation of the cellular extract at 13.000 × *g*. **Figure R-21B** illustrates the result of such assay using recombinant MetRS and a yeast extract from WT BY4742 strain (Lanes 1-4). Incubation of the yeast extract with the recombinant MetRS for 60 min at 30 °C shows appearance of a 70 kDa protein band that was absent in both the yeast extract and the purified recombinant protein separately. This band has the same electrophoretic mobility in SDS-PAGE as the purified recombinant yeast MetRS(Δ 142), strongly suggesting that this band is likely the truncated form of yeast MetRS that can be isolated from fermenting yeast cells (**Figure R-21B**, lanes 2 and 4). Thus, this assay is suitable to observe the *ex vivo* truncation of the recombinant yeast MetRS, with a simple SDS-PAGE and gel staining analysis.

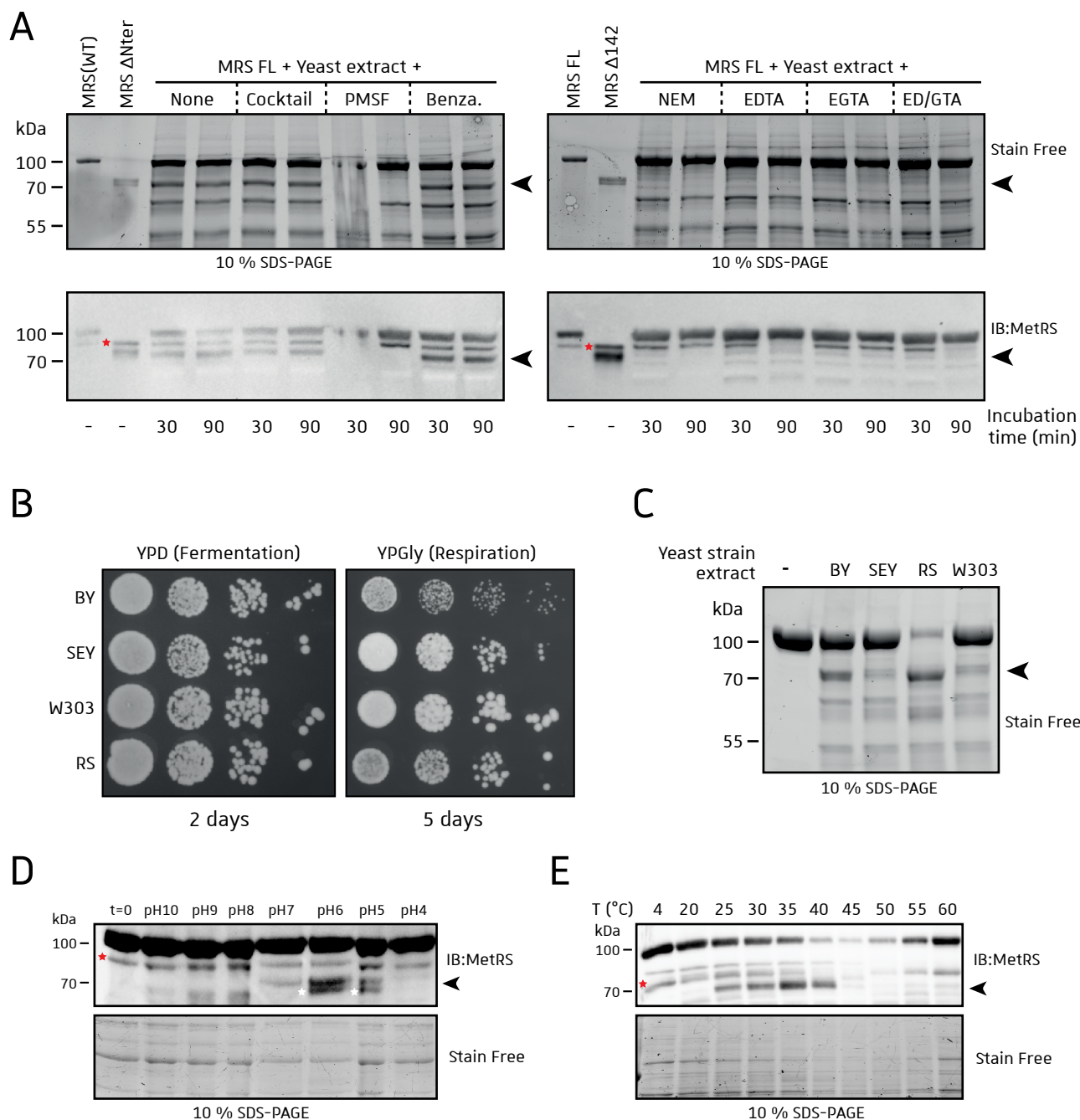


Figure R-22: Characterisation of the MetRS protease using *ex vivo* assay. **A.** *Ex vivo* cleavage assay using different protease inhibitors or chelators with WT yeast extract from BY4742 strain incubated for 30 min or 90 min at 30 °C. Cocktail: EDTA-free protease inhibitor cocktail from Roche, Benza: benzamidine, ED/GTA: EDTA and EGTA. All individual inhibitors or chelators were used at 10 mM. The red star indicates a non specific band revealed by anti-MetRS antibodies **B.** Yeast spotting assay of 4 different yeast strains used in the lab grown on rich medium with glucose (YPD) or glycerol (YPGly) as carbon source. **C.** Cleavage of recombinant MetRS using yeast extract from the strains analysed in B. **D.** *Ex vivo* cleavage at different pH using RS453 extracts, for 1 h at 30 °C. **E.** *Ex vivo* cleavage using WT RS453 strain and incubated at different temperatures indicated above.

Since the homologous human MetRS was found to be cleaved by calpain, a Ca^{2+} -dependent cysteine protease, I decided to test three different yeast strains deleted for such protease in an attempt to see abolition of MetRS cleavage. The deleted strain extracts I use were those of strains deleted from the yeast calpain-like Rim13, the penta EF-Hand protein Pef1 and the metacaspase Mca1 (**Figure R-21B**, lanes 5-7). After incubation of these extracts with recombinant MetRS, both *mca1Δ* and *pef1Δ* extracts still showed a proteolytic activity similar to WT strain, but *rim13Δ* strain showed a complete digestion of the FL-MetRS (lane 5). To be certain that the proteolytic cleavage mediated by the extract was specifically targeting MetRS, the activity of the *rim13Δ* extract was analysed with shorter incubation times, showing again almost fully cleavage of recombinant MetRS after 5 min (**Figure R-21C**, lane 1-4). Yet incubation of the recombinant MetRS Δ 142 isoform with *rim13Δ* extract did not show an additional degradation even after 30 min incubation, showing that this cleavage is really specific for the full-length yeast MetRS. However, the recombinant MetRS Δ 142 isoform seems to be shorter since the molecular weight (MW) of the band before incubation is slightly bigger than after 5 min incubation with the extract, suggesting that the truncated form is shorter than the MetRS Δ 142 isoform (lane 5 and 6).

II.2.2. Chemical and physical properties of the MetRS processing protease

The protease Rim13 might play a major role in regulating MetRS cleavage but is not the protease that cleaves MetRS. To go further in trying to identify the MetRS processing protease, the cleavage assay was performed using different protease inhibitors or divalent-cations chelators. Results in **Figure R-22A** show that MetRS cleavage was not inhibited by the EDTA-free protease inhibitor cocktail provided by Roche, which was a surprising result since these tablets contain several inhibitors targeting essentially serine and cysteine proteases. The two inhibitors with observable effects on cleavage were PhenylMethylSulfonyl Fluoride (PMSF) and N-EthylMaleimide (NEM). PMSF is known to inhibit serine proteases and papain, a cysteine protease, whereas NEM modifies cysteine residues and thus inhibits cysteine proteases. The two cations chelators: EDTA and EGTA, also inhibit the cleavage, showing that the protease might be dependent on divalent cations like Mg^{2+} or Ca^{2+} . Immunoblotting of the gel with anti-MetRS antibodies reveals an additional band that appears to be non-specific because this band is present in both purified MetRS enzymes isoforms (**Figure R-22A**, red star). The non-specific protein recognized by the antibodies is actually a bacterial contaminant which co-purified with recombinant MetRS given that blotting of *E. coli* extract with the antibodies

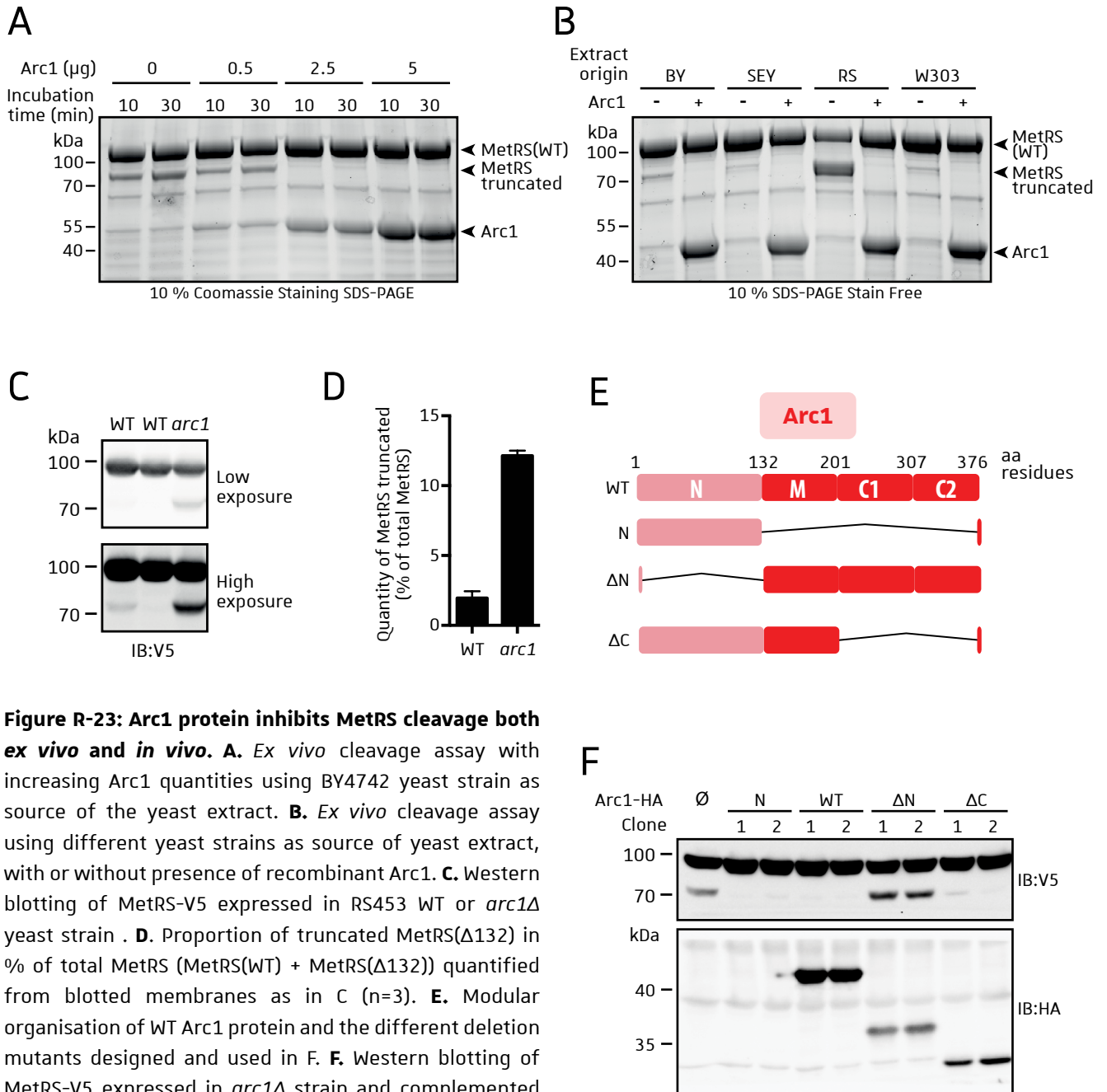


Figure R-23: Arc1 protein inhibits MetRS cleavage both *ex vivo* and *in vivo*. **A.** *Ex vivo* cleavage assay with increasing Arc1 quantities using BY4742 yeast strain as source of the yeast extract. **B.** *Ex vivo* cleavage assay using different yeast strains as source of yeast extract, with or without presence of recombinant Arc1. **C.** Western blotting of MetRS-V5 expressed in RS453 WT or *arc1Δ* yeast strain. **D.** Proportion of truncated MetRS(Δ 132) in % of total MetRS (MetRS(WT) + MetRS(Δ 132)) quantified from blotted membranes as in C (n=3). **E.** Modular organisation of WT Arc1 protein and the different deletion mutants designed and used in F. **F.** Western blotting of MetRS-V5 expressed in *arc1Δ* strain and complemented with Arc1-HA mutants described in E. The N mutant is not observed on the immunoblot due to its low molecular weight.

results in a strong signal at the same position on the membrane (result not shown). However, the band corresponding to cleaved MetRS is still observed on the immunoblot. Taken together, these results suggest that the unknown protease might be a serine or cysteine protease using cations.

During the development of this *ex vivo* assay I realised that the intensity of MetRS cleavage was different according to the yeast strain used to prepare soluble extract. I have started experiments with the yeast strain BY4742 since the deletion mutant collection that is available in the lab is in the BY background. We also work on different yeast strains like SEY6110, W303 or RS453 with different phenotypes according to the carbon source used (**Figure R-22B**). It appears that the RS453 background presents the most specific MetRS proteolytic activity, with more than 80 % of the recombinant MetRS truncated after 1 h incubation at 30 °C (**Figure R-22C**). For all other experiments designed to study MetRS cleavage, I have used the RS453, unless otherwise indicated.

Using this RS453 background, optimal pH and temperature have been tested for the protease (**Figure R-22D and 22E**). Although the temperature range for the activity is relatively usual (between 25 °C and 40 °C), the optimal pH appears to be slightly acid, with more activity at pH 5.0 and 6.0 than at neutral pH. Proteolytic activity for acidic pH seems to generate a second smaller truncated form not visible when the cleavage is made at neutral pH (**Figure R-22D**, white stars). So far, I haven't elucidated the presence of this additional band at acidic pH. However, the specific proteolytic activity for low pH strongly suggests that the unknown protease might be present in acidic compartment such as the vacuole or endosomes.

II.3. The Arc1 protein acts as MetRS protector from proteolytic cleavage

The cleavage site was predicted to be located between residue 121 and 132 in the N-terminal part of yeast MetRS. As seen before, the N-terminus of MetRS interacts with the N-terminal domain of Arc1 (**Figure R-20D**, page 144). Binding of Arc1 to the N-terminal part of MetRS might protect from cleavage through steric hindrance. To test this hypothesis, I added to the cleavage assay increasing concentrations of recombinant Arc1 protein. As the quantity of Arc1 increased, the cleavage was highly suppressed even after 30 min incubation (**Figure R-23A**). Same result was observed for the four yeast genetic backgrounds tested with or without presence of Arc1 (**Figure R-23B**). The RS453 strain still showed the strongest proteolytic activity, which was highly inhibited by addition of equimolar amounts of Arc1. To show the importance of such interaction with Arc1 *in vivo*, it was

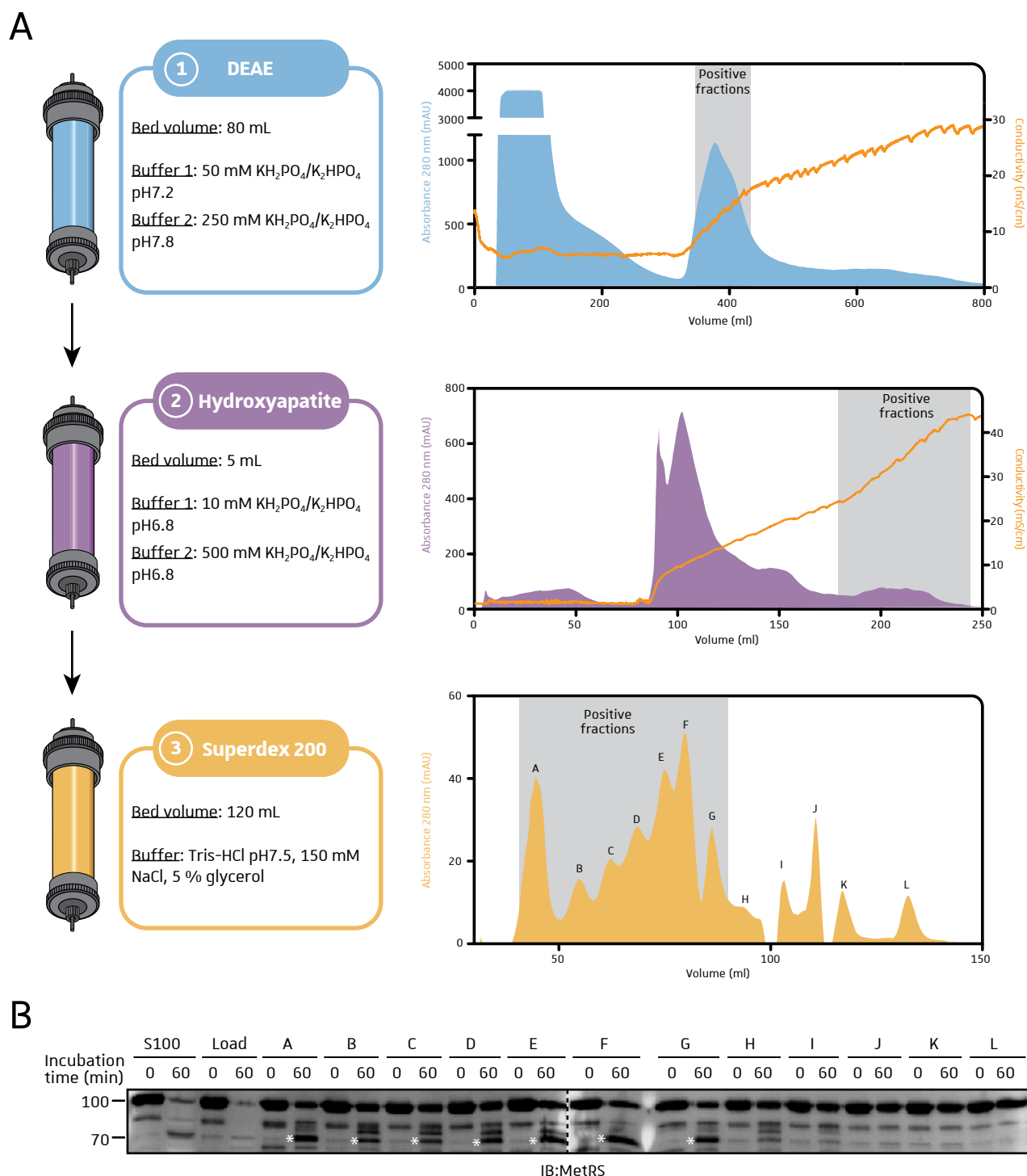


Figure R-24: Purification of the yeast MetRS protease by sequential chromatographies. **A.** Detailed chromatography conditions for all matrices is shown as well as the corresponding chromatograms. The grey zone on each chromatogram corresponds to the fractions presenting proteolytic activity on MetRS tested by *ex vivo* assay. These fractions were pooled and used as loading sample for the next column chromatography. **B.** *Ex vivo* cleavage assay of the fractions corresponding to peaks A to L from the size-exclusion chromatography (Superdex 200). «S100» corresponds to the initial soluble yeast extract, and «Load» fraction is the sample loaded onto the superdex 200 column (= positive fractions pooled after hydroxyapatite column).

necessary to identify the truncated form in total yeast extract by western blotting. Unfortunately, the anti-yeast MetRS antibodies developed in the lab were not enough sensitive to reveal the truncated form that represents a small fraction of total MetRS inside cells. Therefore, I tested different C-terminal tags on yeast MetRS to choose the most suitable couple tag/antibody to be able to observe and quantify the truncated form. It appears that the V5 epitope gave me the best signal with observable truncated form in immunoblot. As shown in **Figure R-23C**, the shorter form is not always properly observed in WT strain, but deletion of *ARC1* drastically enhances the proportion of cleaved MetRS, from 2 % in WT to 12 % in *ARC1* deleted strain (**Figure R-23D**). To show that the protection of Arc1 is mediated by the interaction with its N-terminal domain to Arc1, I used different Arc1 mutants: deleted in its C-terminal domain (ΔC), N-terminal domain (ΔN) or both C-terminal and middle domain resulting in only the N-terminal part (N) (**Figure R-23E**). All these mutants were expressed individually in *arc1 Δ* strain expressing the ectopic MetRS-V5 tagged enzyme. Results in **Figure R-23F** show that protection from cleavage is lost only when the N-terminal part of Arc1 is absent (mutant ΔN). This domain expressed alone within the cell is sufficient to bring MetRS protection against the cleavage. All these results show that Arc1 act as a molecular protector from the protease through binding with its N-terminal part to the yeast MetRS.

II.4. Searching for the MetRS specific protease

All the previous results regarding the MetRS cleavage properties led us to some assumptions about the protease that would be involved in MetRS maturation. However, since this cleavage seemed essential for yeast according to previous results (**Figure R-20G**, page 144), the deletion of the corresponding protease should, in principle, be lethal. Thus, testing several protease deletion strains by *ex vivo* cleavage assay for their ability to cleave the recombinant MetRS would be both time consuming and not relevant if this protease is essential for cell viability. The other strategy adopted was to take advantage of the *ex vivo* assay using a yeast extract fractionated by sequential preparative column chromatographies. The idea was to perform the *ex vivo* assay with individual fractions collected after each chromatographic step. After a the first step of chromatography, all positive fractions for MetRS cleavage were collected, pooled and subjected to an other chromatography column (**Figure R-24A**). Having no chemical information about the protease (size, isoelectric point, ...), I started with a weak anion exchanger using Diethylaminoethyl (DEAE) cellulose. After testing by *ex vivo* assay, the positive fractions appeared to represent proteins with moderate affinity to the column, which represent around 30 % of total proteins (**Figure R-24A**, upper part).

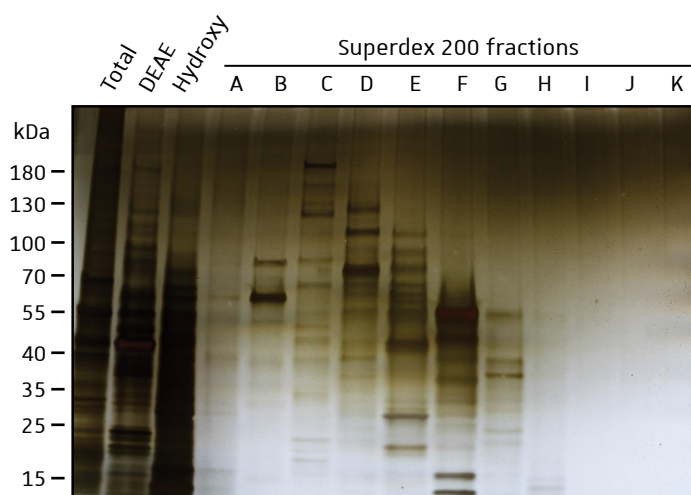


Figure R-25: Proteins found in the active Superdex 200 fractions analysed by 14 % SDS-PAGE and silver staining. Fractions of Superdex 200 chromatography were analysed by SDS-PAGE followed by silver staining. Crude extract before chromatography (Total), sample after DEAE column (DEAE) and after hydroxyapatite column (Hydroxy) were also analysed on gel.

Table R-1: List of yeast proteins found in all active Superdex 200 fractions (peaks A to G). Proteins related to protease activity are highlighted in orange.

Biological Function	Standard Name	UniProt Accession Number	Systematic Name	Protein Description	Molecular Size (kDa)
Oxides metabolism	ACC1	QD0955	YWR142	Acetyl-CoA carboxylase	250
	FBA1	P14540	YKL060C	Fructose 1,6-bisphosphate aldolase	40
	TPS2	P31688	YDR074W	Trehalose-6-phosphate synthase/phosphatase	103
	SEC53	P07283	YFL045C	Phosphomannomutase	29
	TSL1	P38427	YML100W	Trehalose synthase complex regulatory subunit TSL1	123
	TPS1	Q00764	YBR126C	Alpha trehalose-6-phosphate synthase/phosphatase	56
Lipid metabolism	FAS1	P07149	YKL182W	Fatty acid synthase subunit beta	229
	FAS2	P19097	YPL231W	Fatty acid synthase alpha subunit	207
	KES1	P35844	YPL145C	Oxysterol-binding protein homolog 4	49
aaRSs	FRS1	P15624	YLR060W	Cytoplasmic phenylalanine-tRNA ligase beta subunit	67
	VAS1	P07806	YGR094W	Mitochondrial valine-tRNA ligase	126
	ILS1	P09436	YBL076C	Cytoplasmic isoleucine-tRNA ligase	123
	KRS1	P15180	YDR037W	Lysine-tRNA ligase cytoplasmic	68
Protein translation	GCD11	P32481	YER025W	Eukaryotic translation initiation factor 2 γ -subunit	58
	YEF3	P16521	YLR249W	Translation elongation factor 3	116
	EFT1	P32324	YOR133W	Elongation factor 2	93
	DYS1	P38791	YHR068W	Deoxyhypusine synthase	43
Vacuolar ATPase	VMA1	P17255	YDL185W	V-type proton ATPase catalytic subunit A	119
	VMA13	P41807	YPR036W	V-type proton ATPase subunit H	54
Protease activity	PRB1	P09232	YEL060C	Cerevisin (vacuolar proteinase B)	70
	PEP4	P07267	YPL154C	Saccharopepsin (Vacuolar aspartyl protease)	44
	APE1	P14904	YKL103C	Vacuolar aminopeptidase 1	57
	RPN5	Q12250	YDL147W	26S proteasome regulatory subunit RPN5	52
	RPN9	Q04062	YDR427W	26S proteasome non ATPase regulatory subunit RPN9	46
	RPN3	P40016	YER021W	26S proteasome regulatory subunit RPN3	60
Other functions	OXR1	Q08952	YPL196W	Oxidation resistance protein 1	31
	SEY1	A6ZP10	YOR165W	Dynammin-like GTPase	89
	YDJ1	P25491	YNL064C	Type I HSP40 co-chaperone	45

The next chromatographic step was performed on a hydroxyapatite column, a general ion exchanger retaining both positively and negatively charge proteins. The fractions containing MetRS cleaving activity were found highly bound to the column since they eluted at high phosphate concentrations (**Figure R-24A**, middle part). These two sequential chromatographies enable to eliminate more than 95 % of the total proteins. A size-exclusion chromatography was then performed on the pooled positive fractions to sort protein according to their molecular size. The associated chromatogram showed twelve different elution peaks (**Figure R-24A**, lower part). All the associated fractions were then tested by *ex vivo* assay, and it appeared that seven fractions (A to G) were positive for MetRS cleavage (**Figure R-24B**).

All these fractions contained several proteins as observed in SDS-PAGE followed by silver staining (**Figure R-25**). It is likely that several proteins might be present in complexes since small proteins are present in fractions where protein with higher size are expected. Since fractions A to G were positive for cleavage, they all have been analysed by mass spectrometry, and proteins found in all seven fractions are reported in **Table R-1**. Various protein families were identified during the analysis, with protein related to energetic metabolism (osides and lipids) and protein synthesis (4 different aaRSs and translation factors). This study also identified six proteins having (or related to) proteolytic activities (highlighted in orange in **Table-R1**): three regulatory proteins of the 26S proteasome complex (Rpn3, Rpn5 and Rpn9) and three vacuolar proteases (Prb1, Pep4 and Ape1). The three Rpn proteins are part of the 19S regulatory particles (19S RP) that serves as proteasome activator and recognition of proteins marked by polyubiquitin chains (Tanaka, 2009). The only proteolytic activity of the Rpn proteins is removal of the ubiquitin chains from the captured substrate (deubiquitinase (DUB) activity). However, no such activity have been described for the three Rpn proteins identified in our MS analysis, and no deletion mutants for the associate genes are available in our collection strain, probably because of the lethality caused by their deletion.

The three vacuolar proteases identified in each fraction are endopeptidases that contribute to protein degradation into vacuole, a yeast compartment responsible for nutrient storage, protein homeostasis and detoxification. The *PEP4* gene codes for proteinase A, a monomeric aspartyl endoprotease that proteolytically activates itself (autoactivation) and Prb1 is also called proteinase B (Woolford *et al.*, 1986). Aspartyl proteases are characterized by two catalytic Asp residues mediating an acid-base hydrolysis reaction (Parr *et al.*, 2007). Prb1 is a serine endoprotease with a broad substrate specificity, and Ape1 (aminopeptidase I, also called Lap4) is a zinc-dependent

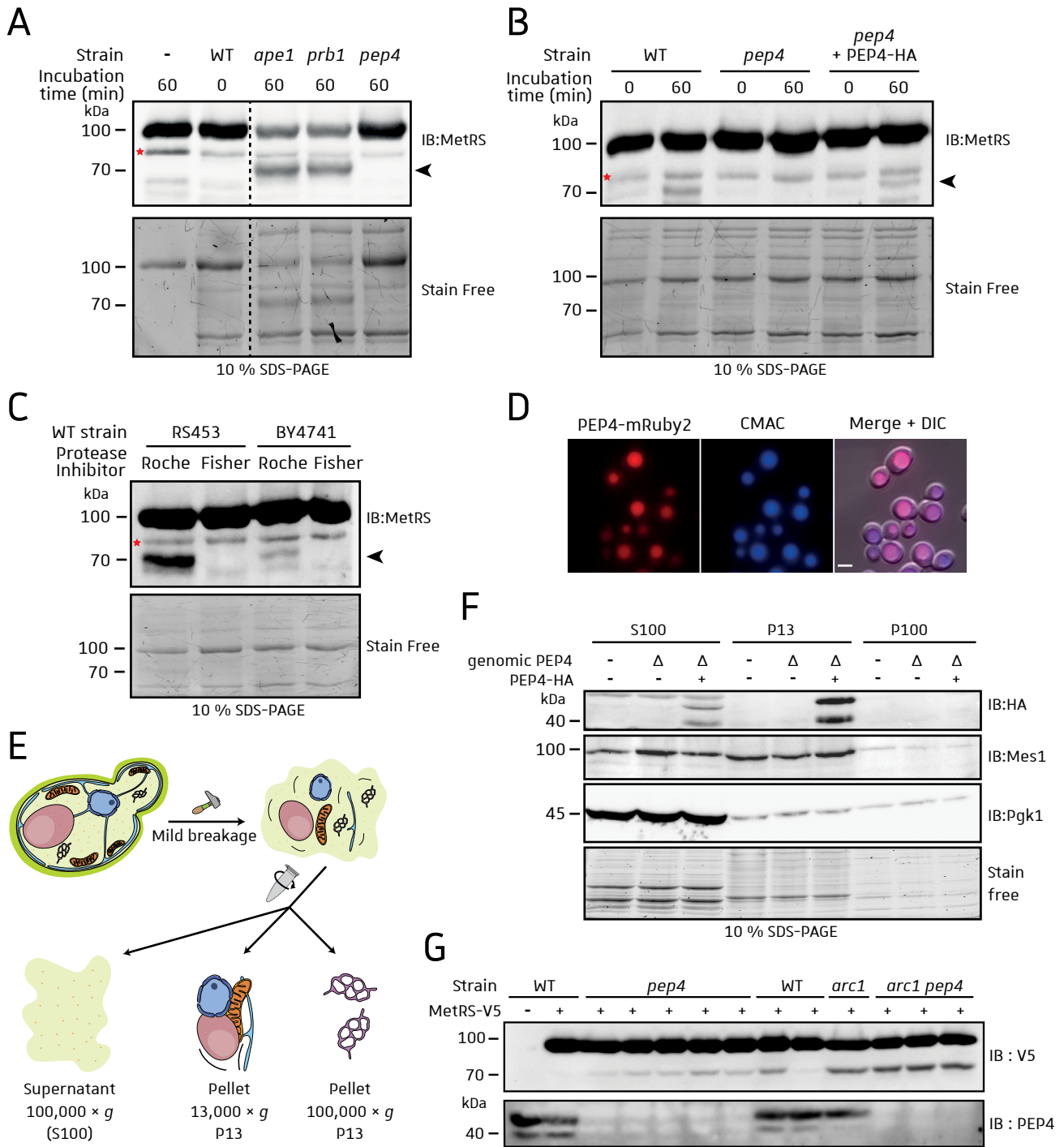


Figure R-26: The vacuolar Pep4 protease is involved in MetRS cleavage. **A.** *Ex vivo* cleavage assay with soluble extract of yeast strains deleted from genes encoding identified proteases in **Table R-1**. All strains are of the BY4742 genetic background. The red star indicates a non-specific band **B.** *Ex vivo* cleavage assay of RS453 strains deleted for *PEP4* and ectopically expressing Pep4-HA. **C.** Inhibition of the *ex vivo* cleavage by anti-potease cocktail from ThermoFisher (Fisher) but not from Roche. **D.** Subcellular localization of Pep4-mRuby2 fusion protein expressed in a *pep4Δ* strain and vacuolar staining with CMAC. Scale bar, 5 μm **E.** Schematic representation of the subcellular fractionation protocol enabling separation of soluble fraction (S100) from membranous fractions (P13 and P100). **F.** Western blot analysis of subcellular fractionation showing two forms for Pep4 and its organellar localization. **G.** Western blotting of MetRS-V5 expressed in RS453 yeast strain WT or deleted for *PEP4* gene (*pep4*), *ARC1* (*arc1*) or both (*arc1 pep4*).

metallo-aminopeptidase involved in glutathione degradation (Adamis *et al.*, 2009). Deletion mutant strains for each of these vacuolar protease were available in our lab collection (in the BY4742 genetic background) and cellular extracts have been prepared to test them in our *ex vivo* assay (**Figure R-26A**). Cleavage of recombinant MetRS was still present for extracts from *ape1Δ* and *prb1Δ* strains, but deletion of *PEP4* gene totally abolished the cleavage after 1 h incubation. To confirm the role of Pep4 in MetRS cleavage, deletion of the *PEP4* gene was performed in RS453 background strain, and Pep4-HA was cloned and ectopically expressed in a *pep4* strain. Results show confirmation of absence of cleavage in the *pep4Δ* RS453 strain (**Figure R-26B**). As expected, ectopic expression of Pep4 recovered the wild-type phenotype with cleavage of recombinant MetRS. These preliminary results strongly suggested the sole implication of Pep4 in the MetRS cleavage, and were also in agreement with the absence of inhibition by the protease cocktail inhibitors used in **Figure R-22A**, page 148. Indeed, the cocktail inhibitors (from Roche) used in the *ex vivo* assay did not contain a single chemical inhibiting aspartyl protease. When I tested a different anti-protease inhibitor (from ThermoFisher) containing a specific aspartyl protease inhibitor (pepstatin A), the inhibition was actually abolished (**Figure R-26C**). Similarly, pepstatin A alone inhibits the cleavage thereby confirming the role of Pep4 in MetRS cleavage. This protease is localized within the vacuolar lumen since fusion of mRuby2 fluorescent protein to Pep4 shows a clear vacuolar signal (**Figure R-26D**). Cellular fractionation of yeast cells also indicates that Pep4 is highly present into the membranous fraction in two different forms: a higher molecular form (inactive precursor or zymogen) of 52 kDa and a lower mature form of 42 kDa (**Figure R-26F**).

Implication of Pep4 in MetRS cleavage was only demonstrated through *ex vivo* assay with a recombinant MetRS used as substrate. It was necessary to show that deletion of Pep4 abolished the truncation *in vivo*. Strains expressing MetRS-V5 were deleted for *PEP4* gene and cleavage was analysed by western blotting (**Figure R-26G**). Unfortunately, despite confirmation that *PEP4* was indeed deleted deletion of Pep4 (no signal in blotting with anti-Pep4 antibody), the shorter form of MetRS was still observed in these *pep4Δ* strains. Additional deletion of *ARC1* gene also increased the amount of truncated MetRS despite the absence of Pep4. Hence, Pep4 has a proteolytic activity on recombinant MetRS but is probably not the only protease able to cleave the synthetase *in vivo*. Alternatively or additionally, posttranslational modifications of MetRS, not present in the recombinant MetRS overexpressed in *E. coli*, prevent cleavage by Pep4.

II.5. Identification of the proteolytic cleavage site

Since deletion of *PEP4* did not result in absence of MetRS cleavage, I was not able to have a strain that does not produce a truncated MetRS to analyse its phenotype and understand the role of the shorter form of MetRS. I thus tried to get information about the cleavage site position and residues in order to specifically mutate these residues and to obtain a non-truncated MetRS. Purification of the shorter MetRS followed by conventional mass spectrometry analysis gave only a partial result with cleavage site within the $\alpha 5$ helix (**Figure R-20D**, page 144). Difficulties for cleavage site identification were due to (i) a low concentration of truncated MetRS in the sample, (ii) a poor sequence coverage with only few digestion peptides analysed and (iii) N-terminal aa are rarely identified. Determining the N-terminal residue of the truncated MetRS proved to be challenging, and we needed new technical advances to elucidate the cleavage site. New methods for N-terminus characterization rely on N-terminal addition of a large molecule carrying a positive charge on the N-terminal amine group (Wagner *et al.*, 1991). We collaborated with the laboratory of Dr. Carapito that uses the TMPP reagent as derivative agent of the N-terminal function (Gallien *et al.*, 2009; Bertaccini *et al.*, 2013; see TMPP chemical structure and derivatization reaction in **Figure MM-12**, page 252). Adding this positively charged molecule enhances ionization efficiency and thus improves detection of low-abundant proteins. We analysed two types of sample with this method: the truncated recombinant MetRS obtained by *ex vivo* cleavage assay (**Figure R-27A**) and the shorter MetRS obtained by immunoprecipitation of cMyc tagged MetRS (**Figure R-27B**). Bands from the SDS-PAGE gel have been extracted, then reduced, alkylated and derivatized with TMPP before further tryptic digestion and nanoLC-MS/MS analysis. For both analyses, only one tryptic N-terminal peptide was obtained, with sequence residues ALNSSLVHSK (**Figure R-27C**). As expected, this peptide belongs to both MetRS $\alpha 5$ and $\alpha 6$ helices, and the N-terminal alanyl residue identified in position 133 is located downstream the tyrosyl residue Y132 (**Figure R-27D**). Hence the proteolytic cleavage of MetRS occurs both *in vitro* and *in vivo* between Y132 and A133 residues. When aligning residues around the cleavage site from several organisms, it appears that Y132 is relatively conserved across species, and A133 is more subjected to replacement with hydrophobic residues (**Table R-2**). At first sight, the region around these residues is mainly hydrophobic. This is consistent with a Pep4-mediated cleavage since early studies have shown that Pep4 preferentially cleaves substrates between two hydrophobic residues: Phe, Leu or Glu at P1 site (aa on the N-terminal side of the hydrolysed peptide) and Phe, Ile, Leu or Ala at P1' site (aa on the C-terminal side) (Dreyer, 1989; Kondo *et al.*, 1998).

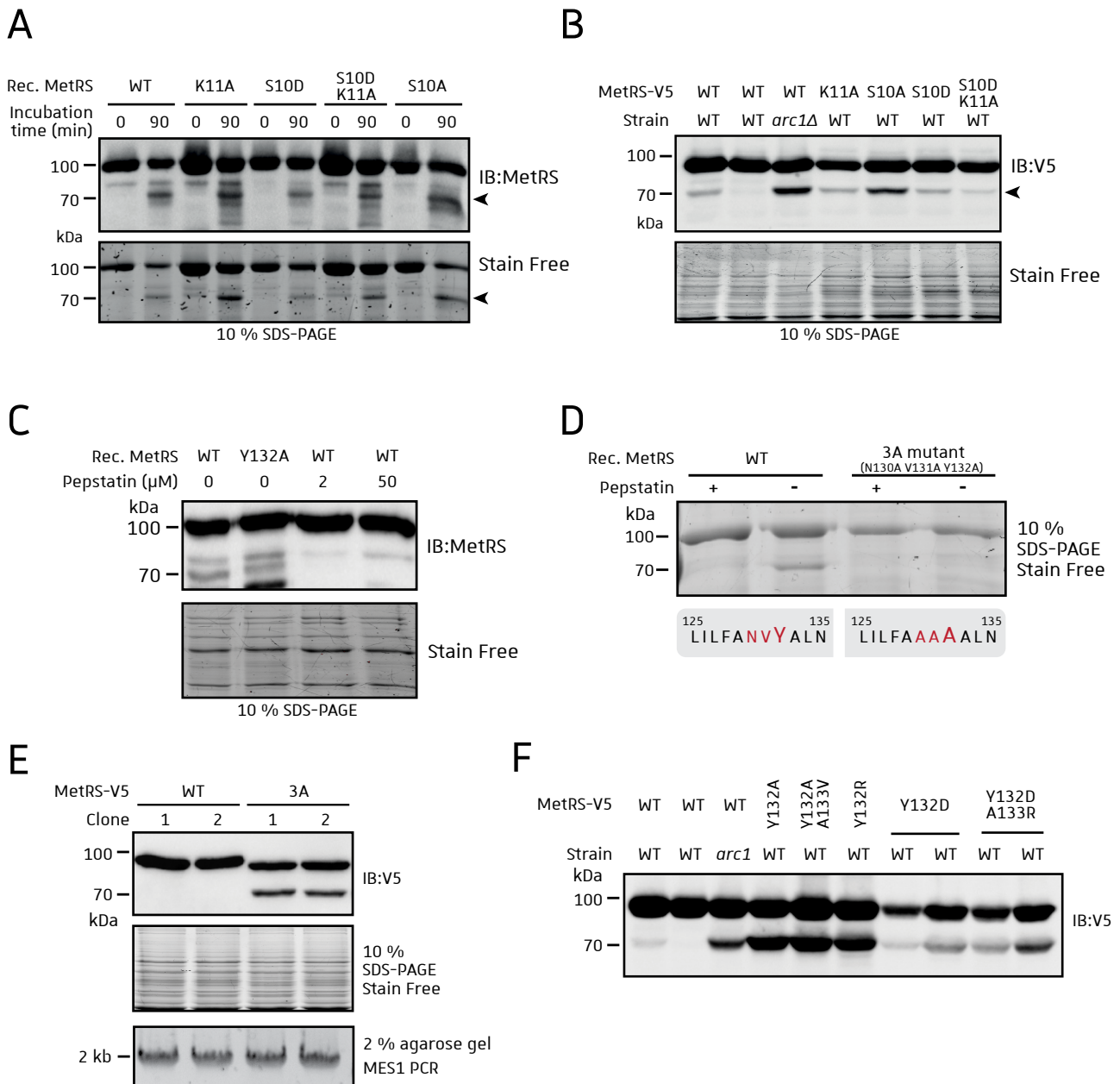


Figure R-28: Inhibiting proteolytic cleavage by mutating the MetRS. **A.** *Ex vivo* cleavage assay using different recombinant MetRS mutants. According to previous results obtained by Dr. D. laporte, these mutations were supposed to hinder cleavage. **B.** Western blotting of yeast protein total extract expressing MetRS-V5 (WT or mutated in the corresponding residues) with (WT) or without (*arc1Δ*) Arc1. **C.** *Ex vivo* assay cleavage of WT MetRS or the Y132A mutant with 60 min incubation at 30 °C. Pepstatin was used to totally inhibit the proteolytic activity. **D.** *Ex vivo* cleavage assay of WT MetRS or of the 3A mutant (N130A V131A Y132A) with 60 min incubation at 30 °C. Pepstatin was used to totally inhibit the proteolytic activity. **E.** Western blotting of yeast protein total extract expressing MetRS-V5 WT or 3A. PCR products of *MES1* gene amplification sent for sequencing are shown in the lower panel. **F.** Western blotting of yeast protein total extract expressing MetRS-V5 (WT or mutated in the corresponding residues) with (WT) or without (*arc1*) the presence of Arc1.

II.6. Finding a non-cleavable mutant of MetRS

II.6.1. Analysis of MetRS substitution mutants around the cleavage site

Since deletion of Pep4 did not totally inhibit the cleavage of MetRS, I tried to generate cleavage mutants with no ability to be processed. As discussed in §II.1, some mutants were previously found not cleavable with mutations in the first NLS (K11A and S10D mutations). Hence these recombinant mutants were produced and tested for their ability to be cleaved in the *ex vivo* cleavage assay. Results in **Figure R-28A** shows that all mutants were cleaved by the protease after 90 minutes of incubation at 30 °C, in similar proportion to WT recombinant MetRS. When expressed in yeast, these mutants of MetRS were also cleaved, with more proteolytic activity for the S10A mutant (**Figure R-28B**). This result was consistent with tetrad dissection analyses showing that all MetRS mutants tested were viable despite absence of the MetRS(WT) (**Dissection table 1 to 6**, page 208-page 213), and that the sole MetRS(Δ 132) was able to sustain yeast viability (**Dissection tables, 7 and 8**, page 214-215).

Determination of the cleavage site was helpful to design new cleavage mutants. Since the Y132 residue was rather conserved among Fungi and Metazoa (**Table R-2**, page 158), I first replaced this large tyrosyl residue by a small hydrophobic alanyl residue (mutation Y132A). The recombinant Y132A MetRS appeared to be still cleaved in the *ex vivo* assay (**Figure R-28C**) and its expression sustained yeast viability in absence of the MetRS(WT) (**Dissection 6**, page 213). Thus, I extended mutations to upstream residues: V131 and N130 to produce the recombinant 3A MetRS mutant (N130A/V131A/Y132A). *Ex vivo* cleavage assay of this recombinant mutant showed absence of processing (**Figure R-28D**), but expression in yeast revealed a strong cleavage (**Figure R-28E**). This last result was surprising, and to be sure that no recombination occurred during plasmid transformation, I sequenced the MetRS-V5 sequence in each yeast genomes. Sequencing results showed the expected MetRS-V5 sequences for these mutants, with only the three mutated residues. In an attempt to find a cleavage MetRS mutant, I designed other mutants for the cleavage site. Knowing that Pep4 (if Pep4 is really the protease acting *in vivo*) had preferences for hydrophobic residues, I made substitutions with positively charged residues (Y132R, Y132D or Y132D/A133R). Results in **Figure R-28F** shows the same cleavage effect of these mutations than for 3A mutant, with a high yield of cleavage, sometimes either higher than in an *arc1* Δ background.

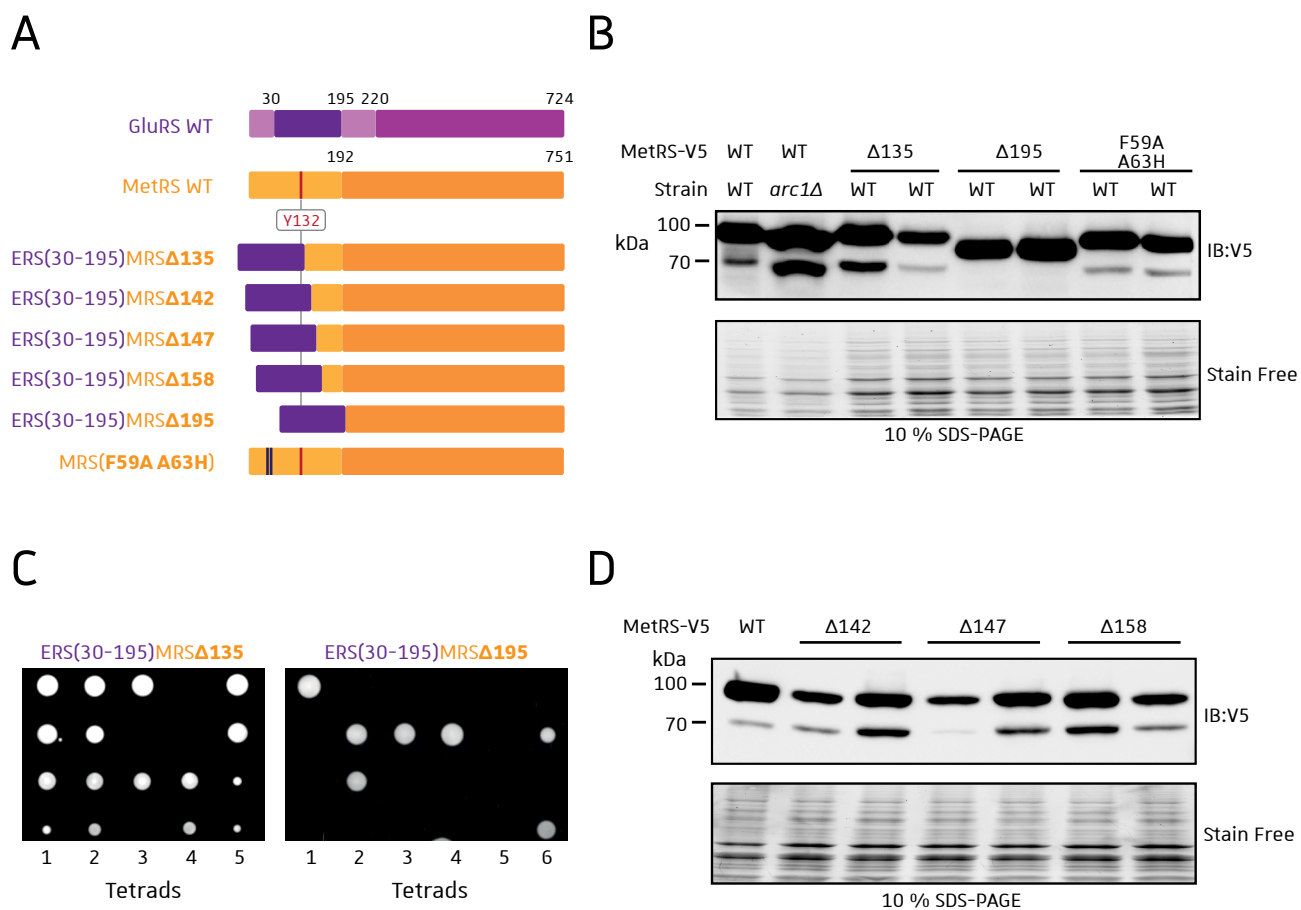


Figure R-29: Chimeric mutant of MetRS fused to N-ter of GluRS are still cleaved. **A.** Modular organization of the different chimeric mutant designed for the study. **B.** Western blotting of yeast protein total extract expressing MetRS-V5 (WT or chimeric mutants) with (WT) or without (*arc1Δ*) Arc1. **C.** Tetrad dissection plate of *MES1/mes1* diploids expressing either the mutant ERS(30-195)MRSΔ135 or ERS(30-195)MRSΔ195. **D.** Western blotting of WT yeast protein total extract expressing MetRS-V5 (WT or N-terminus truncated mutants).

II.6.2. The proteolytic cleavage is not sequence dependent

All the previous results seemed to show that the protease was not really specific for a particular sequence, and that any substitution around the cleavage site tended to enhance the processing rate of MetRS. To test the hypothesis that the cleavage is not dependent of the N-terminal protein sequence, I created a chimeric protein with the N-terminal part (N-ter) of the yeast GluRS fused to the MetRS truncated at different residues (**Figure R-29A**). This domain was suitable for cleavage analysis since no high sequence identity was present between the two N-ter of the aaRSs (**Supplemental S5**, page 201). The N-ter of GluRS was cut out of his first 30 residues since we identified in the lab presence of a Mitochondrial Targeting Signal (MTS) in these first residues. At the same time, I also tried to analyse the cleavage of the mutant F59A/A63H, which was supposed to lose its Arc1-binding capacity as discussed in the introduction (**Figure I-22**, page 74). First result showed that the ERS(30-195)MRS Δ 135 mutant (Δ 135 mutant), even with absence of conserved N-ter sequence and absence of the entire cleavage site, was still efficiently cleaved (**Figure R-29B**). However, replacing the complete N-ter domain of the MetRS (Δ 195) by the GluRS Nter abolished the truncation (**Figure R-29B**). This was encouraging, showing that the sequence directing the cleavage might be present between residues 136-195. This two mutant were tested for viability in yeast: dissection of a diploid strain *mes1/MES1* containing either the ERS(30-195)MRS Δ 135 or ERS(30-195)MRS Δ 195 showed viability for the first but lethality for the last (**Figure R-29C**), meaning that this non-truncated form of MetRS did not ensure the function of the WT MetRS. Nonetheless, this lack of viability might certainly be due to an excess of Nter MetRS deletion, since the MetRS mutants Δ 6-193 and Δ 2-190 displayed weak aminoacylation activity (Walter *et al.*, 1989, **Figure I-33E and 33F**, page 96). This prompted me to create other chimeric mutants with deletion of structural motifs (around α 7 helix) within the N-ter of MetRS without perturbing the 3D structure (**Figure R-29A**). Unfortunately the three chimeric mutants showed a cleavage by western blotting, even for the ERS(30-195)MRS Δ 158 mutant, meaning that cleavage recognition might be present between residues 159-195.

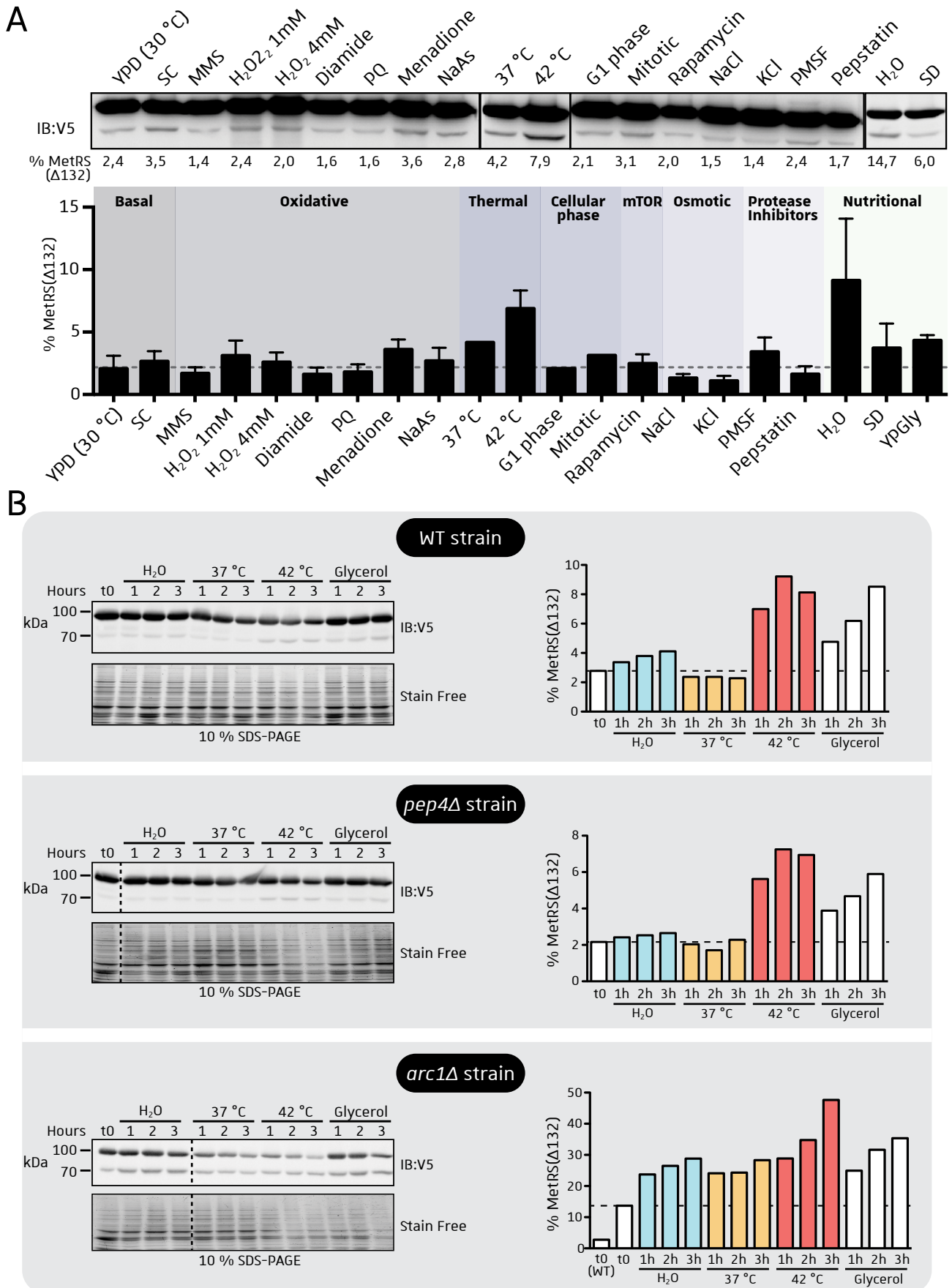


Figure R-30: The cleavage of MetRS is enhanced in thermal and nutritional stresses . A. Haploid *mes1Δ* strain expressing MetRS-V5 was cultured in rich medium (YPD) then submitted to several stresses for 3 h. The cleaved form of MetRS was quantified from anti-V5 western blotting (lower panel, n=3). **B.** Strains expressing MetRS-V5 were subjected to stresses in same condition than in A, for 1 h, 2 h or 3 h. Total protein extracts were blotted with anti-V5 and the cleaved form was quantified.

II.7. Determining the role of MetRS(Δ 132)

II.7.1. Production of the truncated MetRS(Δ 132) is enhanced in thermal or nutritional stresses

To understand the potential role of this truncated isoform of MetRS, it was essential to find conditions where truncation of MetRS was enhanced. Since the MetRS-V5 gave a good signal for quantification in western blot, I used a *mes1* Δ haploid strain expressing ectopic MetRS-V5. This strain was grown in rich medium (YPD) at 30 °C and stressed with several chemicals or nutritional deficits. Since we had no indication about induction of this cleavage, a large panel of stresses has been tested for 3 h (**Figure R-30A**): oxidative, thermal, osmotic and nutritional. I also tested the cleavage when cells were synchronized in G1 phase or in mitotic phase using α factor or when cells were treated with the mTOR pathway inhibitor, rapamycin, or when cells were exposed to protease inhibitors disrupting vacuolar and endosomal functions. Results in **Figure R-30A** show that cleavage of the MetRS is highly increased under thermal stress (from 2 % of truncated form at 30 °C to 7 % at 42 °C) and different nutritional conditions (absence of nutrients in water or diauxic shift from glucose to glycerol as sole carbon source). To get more details about the cleavage during these stresses, I tested three different strains expressing MetRS-V5: the WT strain, *pep4* Δ and *arc1* Δ deletion strains. The aim was to (i) observe the cleavage in a shorter time frame by analysis cells after 1, 2 or 3 h of stress, (ii) to check if cleavage properties are similar in the *pep4* Δ strain or if truncation is reduced due to *PEP4* gene deletion, and (iii) confirm that absence of Arc1 allowed more MetRS cleavage. Results in **Figure R-30B** show same tendency for each strain: except for the 37 °C stress, quantities of MetRS(Δ 132) is increasing with time, with thermal stress at 42 °C giving the highest amount of cleavage. As expected, *pep4* Δ strain exhibited a similar cleavage than the WT, but absence of Pep4 did not prevent the increase of the truncated form. However, the proportion of MetRS(Δ 132) compared to MetRS full-length was found always lower in the absence of Pep4 (around 20 % less), and this might reveal a partial role of the protease in MetRS cleavage (but quantification needs to be done with more data and biological replicates). Result with *arc1* Δ strain was remarkable, since all stresses raised a large amount of cleaved MetRS reaching 50 % of total MetRS after 3 hours at 42 °C (**Figure R-30B**, lower panel). Note that only the proportion of cleaved MetRS was quantified, not the absolute quantity: indeed this large increase at 42 °C is also due to apparent decrease of total MetRS, with the full-length form decreasing in higher proportion than the MetRS(Δ 132) isoform. This massive decreasing was not observed neither for the WT nor for the

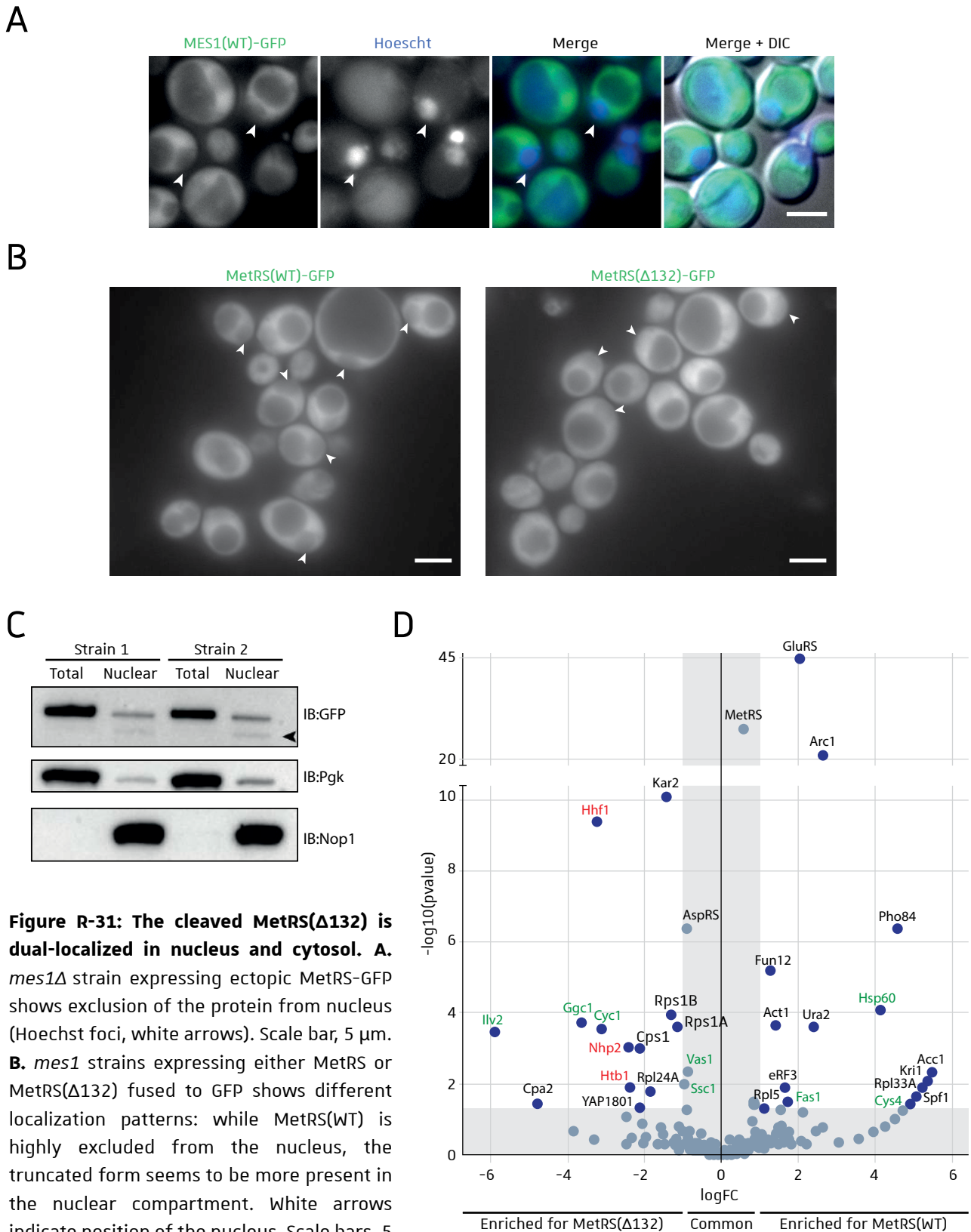


Figure R-31: The cleaved MetRS(Δ 132) is dual-localized in nucleus and cytosol.

A. *mes1* Δ strain expressing ectopic MetRS-GFP shows exclusion of the protein from nucleus (Hoechst foci, white arrows). Scale bar, 5 μ m.

B. *mes1* strains expressing either MetRS or MetRS(Δ 132) fused to GFP shows different localization patterns: while MetRS(WT) is highly excluded from the nucleus, the truncated form seems to be more present in the nuclear compartment. White arrows indicate position of the nucleus. Scale bars, 5 μ m.

C. Result from [D. Laporte, 2016](#). Purified nucleus from strain expressing MetRS-GFP blotted with anti-GFP, anti-Pgk (cytosolic control) and anti-Nop1 (nuclear control) antibodies. Sample from total or nuclear extract are visualized for two independent strains.

D. Volcano plot showing proteins identified during the MetRS-V5 co-immunoprecipitation on *mes1* Δ yeast extracts with strains expressing the MetRS(WT)-V5 or the MetRS(Δ 132)-V5. Hits found in the gray zone (light blue round) are not statistically significant to confirm enrichment in one IP. Hits with negative and positive logFC are enriched in the Met(Δ 132) IP and MetRS(WT) IP, respectively. Red: nuclear protein, Green: mitochondrial protein.

pep4 Δ strains, showing a role of Arc1 in MetRS' stability during stress exposure. Nonetheless, this truncated form stands for nearly half of the total MetRS at 42 °C in absence of Arc1, suggesting an important role of this shorter form in thermal stress.

II.7.2. The cleaved isoform constitutes the nuclear pool of MetRS

The majority of the cellular MetRS pool is cytosolic: the Arc1 anchoring protein act as a platform to retain the two cytosolic aaRSs (MetRS and GluRS) in the cytosol. However it was known that a part a MetRS was relocating into the nucleus, especially during the diauxic shift (Frechin *et al.*, 2014). However no cleaved form of the enzyme was observed in the nucleus by western blot, mostly due to a low sensitivity of the antibodies. When observing cells expressing GFP-tagged MetRS, the global localization appears to be cytosolic, with no vacuolar fraction of MetRS and partial exclusion of MetRS from the nucleus (**Figure R-31A**, see white arrows for nucleus exclusion). Fusion to GFP of the cleaved MetRS(Δ 132) form showed nearly the same profile, but with much less exclusion from the nuclear compartment. Indeed, nuclei are nearly unseen in the GFP channel (**Figure R-31A**, white arrows). These observations confirmed a previous result obtained by Dr. Laporte showing that the shorter MetRS form was predominantly present into the nucleus since MetRS(Δ 132) signal was increased in the purified nucleus fractions compared to total extract (**Figure R-31C**). Another evidence for nuclear localization of MetRS(Δ 132) was the result of a co-immunoprecipitation (co-IP) assay of each MetRS isoform followed by mass spectrometry analyses. The pairwise comparison of protein interactants first showed that Arc1 (and consequently GluRS) was not binding anymore to the MetRS(Δ 132) due to absence of the GST-like N-terminal domain of the MetRS(WT) (**Figure R-31D**). This loss of interaction with Arc1 was previously shown by co-IP and Immunoblotting (**Supplemental 5**), confirming the absence of AME complex formation when the MetRS is proteolytically cleaved, and emphasizing the nuclear translocation for the MetRS(Δ 132). A second observation was the presence of nuclear interactants identified only in the MetRS(Δ 132) co-immunoprecipitation experiment: the two histones H4 (HHF1) and H2B (HTB1), and the snoRNP subunit Nhp2 (**Figure R-31D**, red hits; complete list of interactants with description is given in **Table S2**, page 200). Interaction with histones is not entirely surprising since M domain of Arc1 is similar to histone H1 (33 % identity). These interactions are consistent with a privileged nuclear location of the truncated MetRS, and histone proteins interactions might reveal a possible DNA-binding activity, despite the absence of known DNA-binding domain in the MetRS sequence.

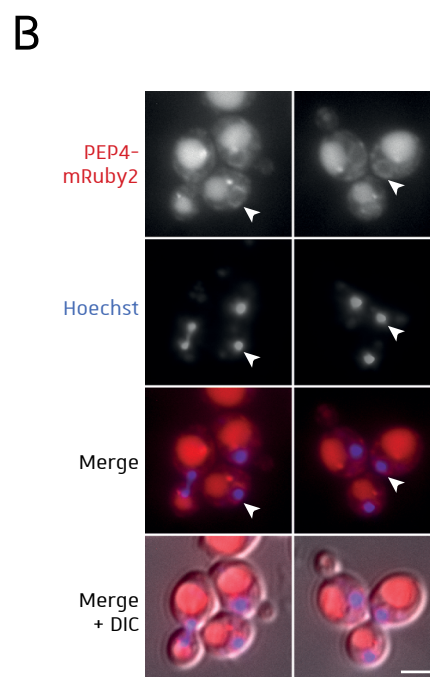
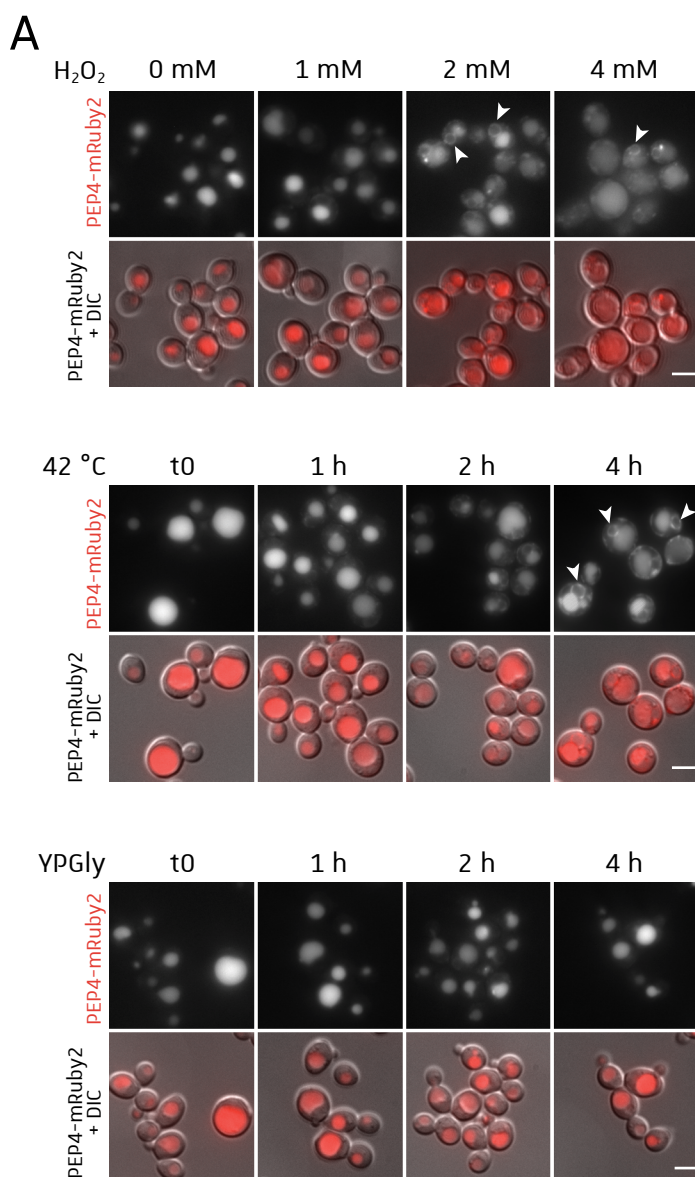


Figure R-32: Pep4 relocates into cytoplasm during oxidative and thermal stress. **A.** *pep4Δ* strain expressing Pep4-mRuby2 was incubated with H₂O₂ (lower panel) for 3 h at different concentrations, or incubated at 42 °C (middle) or at 30 °C in YPGlycerol (lower). Pep4 relocation from vacuole to cytoplasm is observed for H₂O₂ exposure and thermal stress at 42 °C, but not for YPGlycerol incubation. White arrow indicates a halo distribution of the protein. Scale bars, 5 μm. **B.** Same strain as in A incubated at 42 °C for 4 h and stained with Hoechst dye showing Pep4 location around the nuclear envelope. Scale bar, 5 μm.

II.7.3. Pep4 relocates in the vicinity of nucleus under heat stress

After observing that MetRS cleavage was enhanced at high temperature, I analysed the localization of the enzymes in basal condition and during stress exposure. Previous studies have shown that Pep4 was released from the vacuolar lumen into the cytoplasm in H₂O₂-treated cells (Mason *et al.*, 2005). Relocation of Pep4 was interesting since this relocating form would access more easily to the cytoplasmic MetRS than when sequestered into the vacuolar lumen. To identify the subcellular localization of the protease, a *pep4* Δ strain expressing ectopic Pep4-mRuby2 fusion fluorescent protein was used. Treatment of this strain with up to 2 mM of H₂O₂ for 3 h did induced relocation of Pep4 into the cytoplasm (Figure R-32A, upper). I also visualized its relocation during heat stress (Figure R-32A, middle) and during the metabolism switch from fermentation to respiration (Figure R-32A, lower). Same relocation was observed only at 42 °C after 2 h of incubation, with no observable cytoplasmic diffusion when cells were grown in glycerol for 4h. The cytoplasmic distribution of the protein in the cell after oxidative or heat stress exhibited a halo shape location (Figure R-32A, white arrows). By staining nuclei with hoechst dye, it appeared that this halo co-localized and surrounded the nucleus (Figure R-32B). Hence, Pep4 spatial distribution induced in heated cells is similar than the one observed for oxidative stress and allows the protease to reach the vicinity of the nucleus where the cleaved MetRS is more abundant.

II.7.4. Cleavage of MetRS prevents its precipitation at high temperature

Since the proportion of cleaved MetRS increases during heat stress, we needed to understand the function of the MetRS(Δ 132) during temperature increase. A recent study showed that aggregation of endogenous proteins occurred after a heat shock of 8 min at 46 °C in *S. cerevisiae* (Wallace *et al.*, 2015). This study particularly showed that yeast MetRS (as well as GluRS) formed cytosolic aggregates after heat stress, and *in vitro* reconstitution of AME complex aggregates revealed that the pelletable material was, surprisingly, still active for aminoacylation. Interestingly, in their SDS PAGE analysis the authors report presence of an additional band that they called "a minor soluble degradation product" which might correspond to the MetRS truncated form. This product appeared to be more soluble at 46 °C than the MetRS(WT). These *in vivo* and *in vitro* results strongly suggested that the MetRS(Δ 132) might be more soluble than the WT form at higher temperatures. To test this hypothesis, *mes1* Δ strains expressing either the WT or MetRS(Δ 132) fused to GFP were analysed by

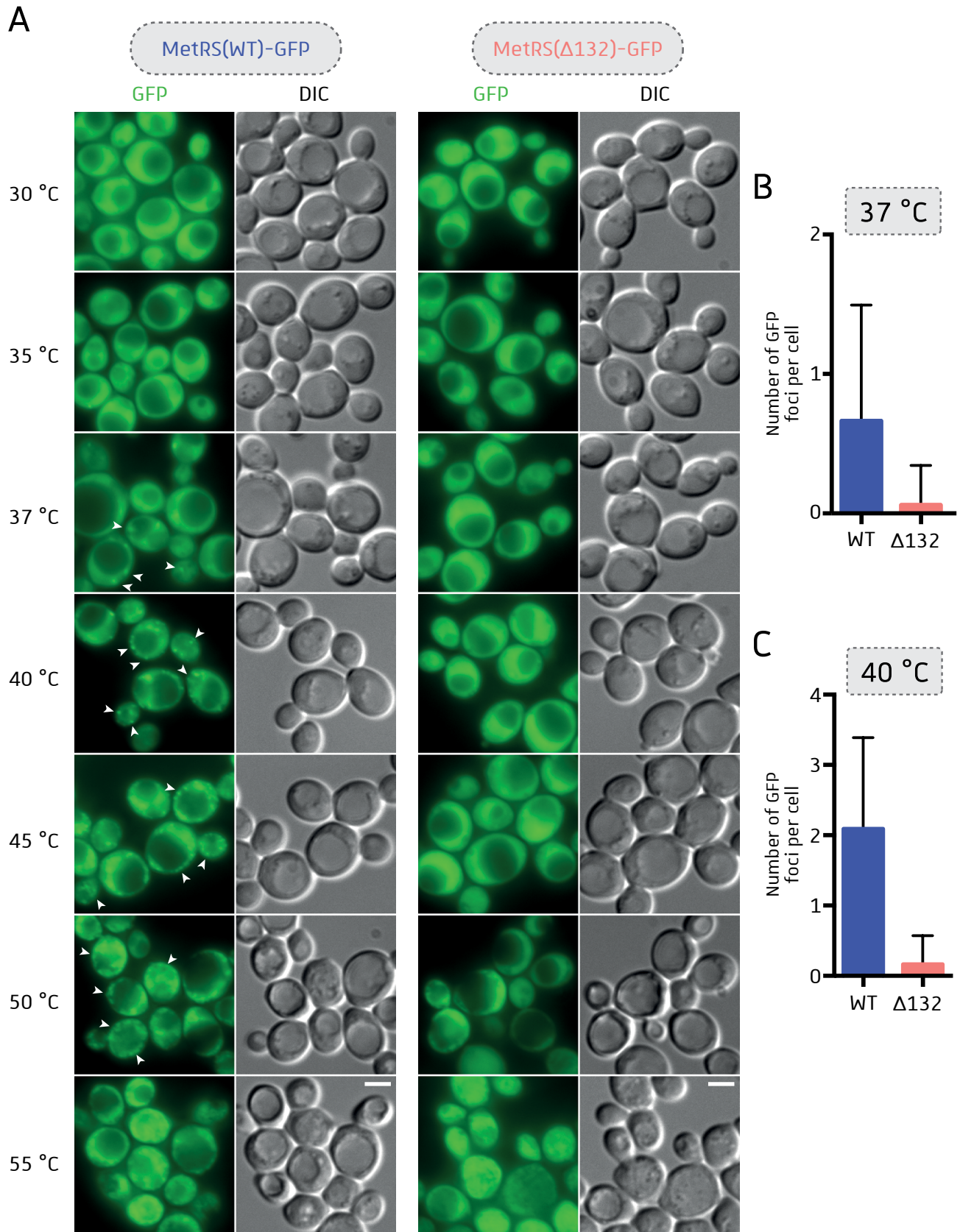


Figure R-33: MetRS(Δ 132) is more stable at higher temperature than the MetRS(WT). **A.** Haploid *mes1 Δ* strains expressing ectopic MetRS-GFP (WT or Δ 132) were imaged at 30 °C and after 9 min heat shock at different temperatures indicated on the left. Cytosolic foci are observed for MetRS(WT) from 37 °C to 50 °C (white arrowheads), whereas MetRS(Δ 132) remains soluble. Scale bar, 5 μ m. **B and C.** Number of GFP foci quantification per cell at 37 °C (B) and 40 °C (C) for each strain (n= 200 cells).

fluorescence microscopy after a 9 min of heat shocks at different temperatures (**Figure R-33A**). As in Wallace *et al.*, the MetRS(WT) formed cytosolic aggregates as temperature was raising. The GFP foci were observed from 37 °C to 50 °C and higher temperatures were damaging cells and compromised GFP localization. Formation of aggregates started at 37 °C, with on average 1 GFP foci per cell (**Figure R-33B**). Interestingly, deletion of the N-terminal domain of MetRS prevented the enzyme to precipitate even for the highest temperatures (**Figure R-33A**, MetRS(Δ 132)-GFP). When cells expressing MetRS(WT)-GFP presented two GFP foci per cell at 40 °C, almost all cells expressing MetRS(Δ 132)-GFP had no visible aggregates (**Figure R-33C**). Taken together, these observations showed that the truncated MetRS(Δ 132) is more stable at higher temperatures than its full-length counterpart.

Knowing the higher thermal stability of the cleaved MetRS, I was wondering if its solubility was intrinsic or due to the absence of Arc1. Indeed, the MetRS(WT) precipitation could be induced by Arc1 thermal denaturation and subsequent aggregation, and loss of Arc1 interaction might rescue the cleaved MetRS from aggregation. To test this possibility, the MetRS-GFP expressing strains were deleted for *ARC1* gene and observed as described above. Microscopy analyses of these strains showed that absence of Arc1 did not prevent aggregation of the MetRS(WT)-GFP (**Supplemental S4**, page 201). Thus, the higher solubility of the MetRS(Δ 132) is only due to the absence of its N-terminal part, and not because of its loss of interaction with Arc1.

II.8. Discussion and preliminary results

II.8.1. MetRS cleavage and cellular compartmentalization

Using the *ex vivo* cleavage assay led me to the identification of the Pep4 vacuolar protease, and deletion of *PEP4* gene totally abolished MetRS cleavage in this assay. However, *in vivo* observation showed that cleavage still occurred in a *pep4* Δ strain, and revealed a complex regulation in the yeast cell with very likely another (or several) protease(s) involved in the cleavage. One of the possible drawbacks of the experiments I did could originate from the way I prepare f my yeast extract samples used in the *ex vivo* assay. Indeed, the extract used (and supposed to contain the protease) is obtained by cell breakage and sequential centrifugations at 5,000 and 13,000 $\times g$ of the extract to get rid of cellular debris and heavy membranes (soluble fraction called S13). These centrifugations were also required to avoid clogging of the tubing during HPLC system chromatography. By using a

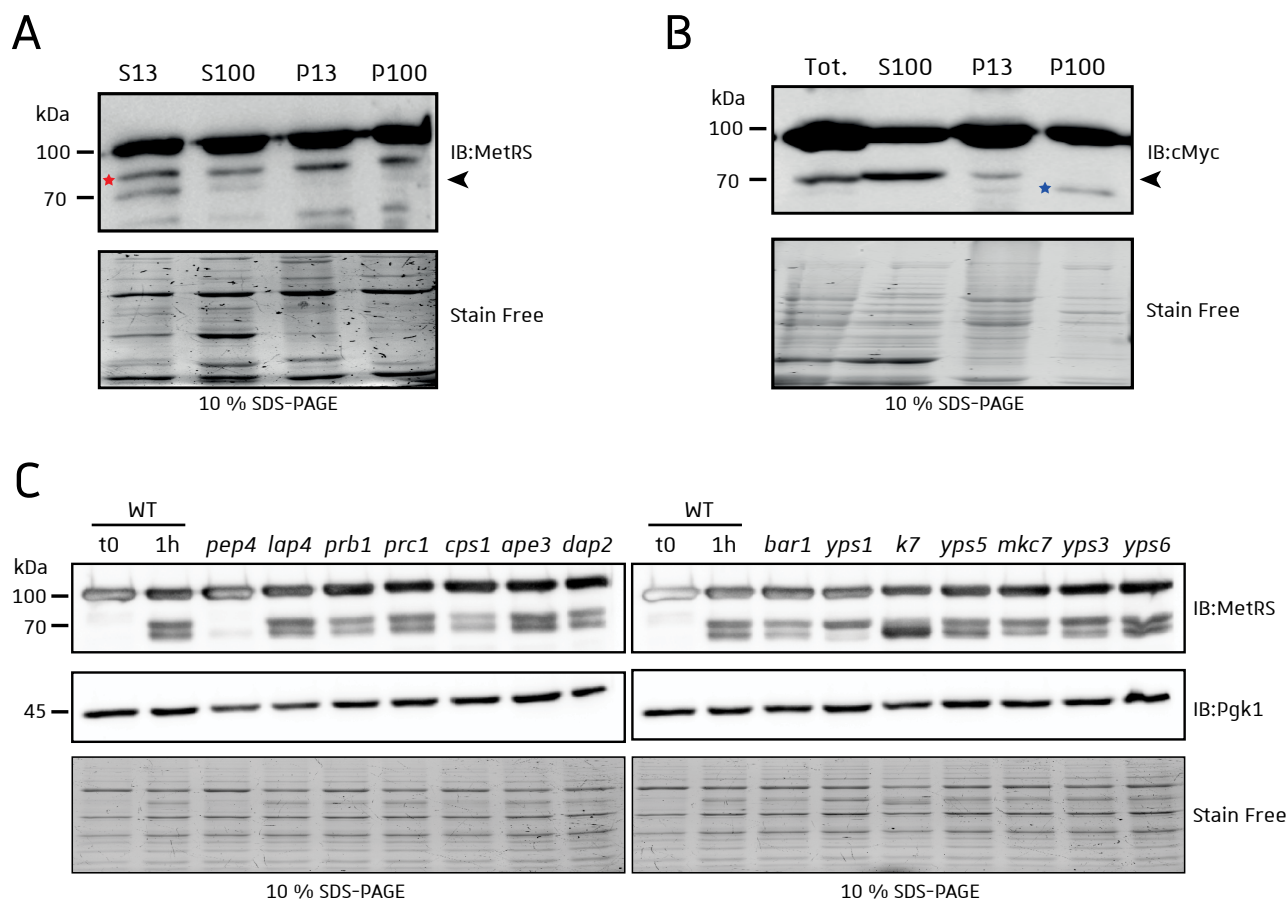


Figure R-34: Complexity of the MetRS cleavage. **A.** *Ex vivo* cleavage assay using different fractions of yeast extract: soluble fraction after $13,000 \times g$ (S13), $100,000 \times g$ (S100), and the respective pellet fractions (P13 and P100). Black arrowhead indicates position of the truncated MetRS($\Delta 132$), and red star indicates a protein from *E. coli* not specifically recognized by the antibodies. **B.** Western blotting of yeast total extract (Tot.) or of subcellular fractions (soluble S100, and pellets P13 and P100). Black arrowhead indicates position of the MetRS($\Delta 132$), and the blue star highlights a lower form of truncated MetRS. **C.** *Ex vivo* cleavage assay using extracts from several strains deleted from genes encoding proteases: either proteases known to be processed by Pep4 (left part) or other aspartic proteases (right part). Cleavage was performed at pH 6.5.

soluble protein extract, I inevitably exclude all integral membrane proteins and other membrane-associated proteins. Since Pep4 is localized in the vacuolar lumen, it is likely that a protease anchored to vacuolar membrane might play an additional role in MetRS cleavage. I have tried to use the yeast pellet fraction in the *ex vivo* cleavage assay. Interestingly, the S100 fraction (soluble fraction after centrifugation at $100,000 \times g$) displayed lower cleavage properties than the S13 fractions, showing that the protease activity I'm interested in might be present in membrane fractions that can be separated after centrifugation (**Figure R-34A**). However, protease activity was not recovered in the pelleted fractions (P13 and P100) compared to the S13 fraction. The activity might be lost when the protease is embedded into the pellet fraction. The fact that vacuolar Pep4 was identified was correlating with the potential vacuolar location of the MetRS. Indeed, the AME complex was found highly bound to the vacuolar membrane as shown by subcellular fractionation and immunoblotting (**Figure R-34B, Poster 1** page 308). High amount of MetRS is bound to membranes (more than 50%), so does Arc1 that was shown to interact with vacuolar membrane (PhD work of M. Hemmerlé; [Fernández-Murray and McMaster, 2006](#)). Interestingly, the truncated form of MetRS was highly soluble since large majority of the protein is present in the soluble (S100) fraction (**Figure R-34B**). Proteolytic cleavage in the vicinity of the vacuole by Pep4 (and other protease) and subsequent loss of interaction with Arc1 might release the MetRS(Δ 132) from the vacuolar membrane to the cytosol. Formation of MetRS(Δ 132) by the protease Pep4 is somewhat a novel concept since no such aspartic protease were found in *E. coli* or in human cells. The lysosomal Pep4 human ortholog cathepsin D (CatD) is involved in a number of neurodegenerative diseases when mutated since many proteins involved in pathologic disorders are substrates of this protease ([Vidoni et al., 2016](#); [Aufschnaiter et al., 2017](#)). Pep4 was described in the literature as enhancing H₂O₂ resistance and extending life span by anti-apoptotic and anti-necrotic actions ([Marques et al., 2006](#); [Carmona-Gutiérrez et al., 2011](#)), and is essential for vacuolar protein degradation. Indeed, deletion of Pep4 triggers accumulation of autophagic bodies in the vacuole ([Takeshige, 1992](#)). Since the yeast vacuole is a reservoir for neutral and sulfur-containing aa, Met concentration could be sensed by the vacuolar MetRS (through AME complex interaction) and cleavage of the MetRS would be a signal of Met (or nitrogen) starvation, and would explain the increase of MetRS cleavage with nutritional stress (culture in H₂O or minimal medium without nitrogen).

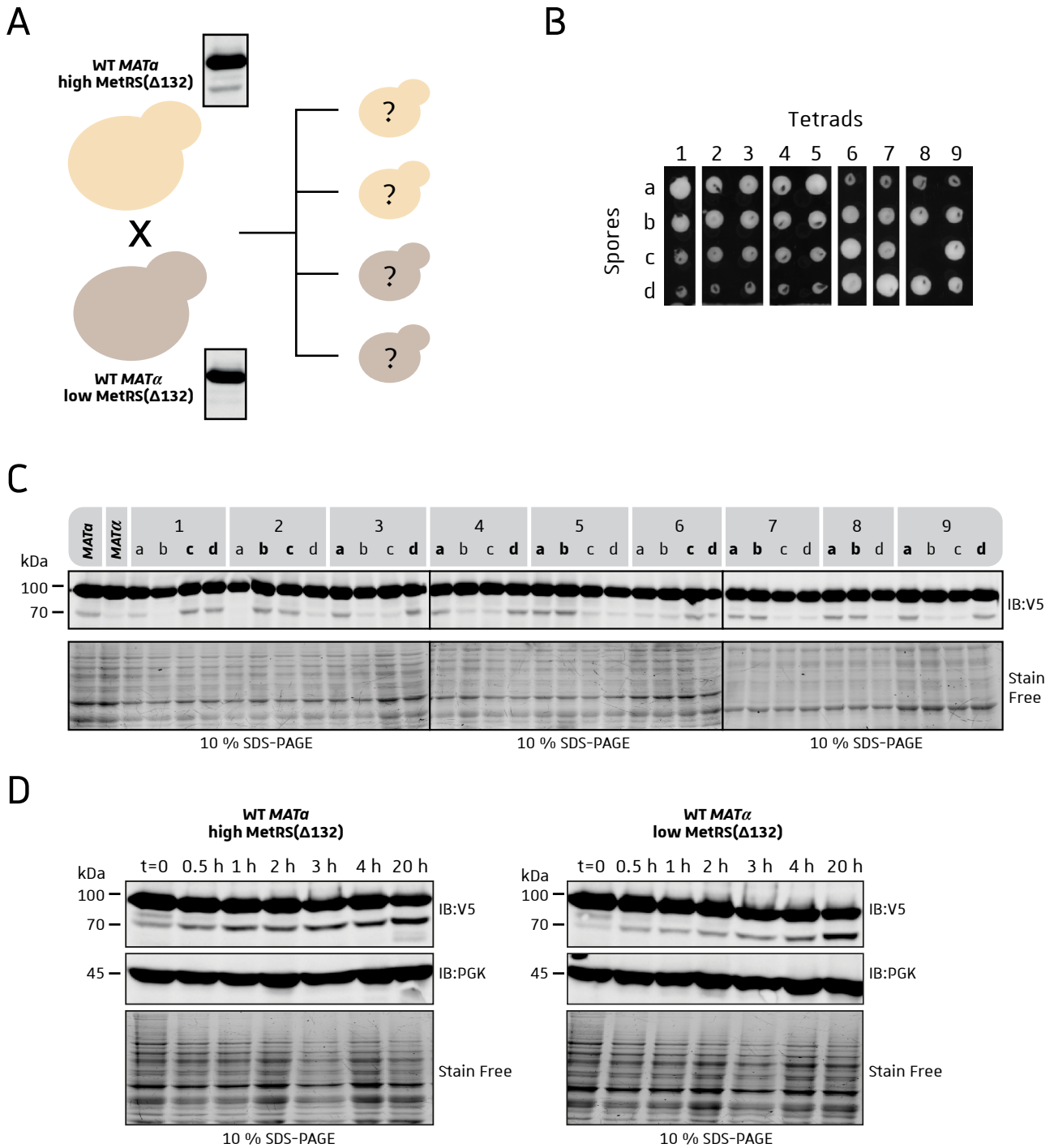


Figure R-35: Isolation of a genetic mutant exhibiting low level of *MetRS(Δ132)*. **A.** Cross between two strains expressing *MetRS-V5* and displaying either a high or low cleavage yield. Sporulation of the resulting diploid gave rise to 4 spores with cleavage yield determined in **C**. **B.** Dissection plate obtained from dissection of tetrads from the diploid from **A**. **C.** Western blotting of the spores from **B**, all expressing *MetRS-V5* with variable cleavage rates. *MATα* and *MATα* strains are the parental strains crossed to form the diploid. **D.** The two parental strains were incubated at 42 °C for the indicated time and total protein extracts were immunoblotted to observe *MetRS-V5* cleavage.

II.8.2. Cleavage complexity and other proteases

The cleavage of MetRS appears to be more complex since lower form of cleaved MetRS have been observed in Immunoblotting of membranous fractions (**Figure R-34B**, blue star). Other form of truncated MetRS appeared also when I was searching for other potential proteases implied in the cleavage (**Figure R-34C**). Since deletion of the *PEP4* gene was not enough to prevent cleavage *in vivo*, I tested with the *ex vivo* assay strains deleted for proteases known to be processed and matured by Pep4, or other vacuolar aspartic proteases. Note that the Cps1 protease (carboxypeptidase S) was identified to be a MetRS(Δ 132) interactant in the co-IP experiments (**Figure R-31D**, page 166). I have used a highly purified recombinant MetRS for this *ex vivo* assay, and slightly decreased the pH for the reaction to mimic the vacuolar environment (from 7.2 to 6.5). In addition to the MetRS(Δ 132) form already identified, a second lower form appeared in this assay, and deletion of Pep4 did not abolish completely the formation of this proteolytic product. When examining deletion of other proteases, it appears that (i) *cps1* Δ deletion mutant exhibits less cleavage than for WT strain, and (ii) *yps1* Δ strain shows less production of the additional lower form (**Figure R-34C**). It would be interesting to delete these two genes in the *pep4* Δ strain expressing MetRS-V5 to see if the cleavage is decreased or abolished.

II.8.3. Cleavage of MetRS is fluctuant depending on yeast clones

When Immunoblotting the MetRS-V5 expressed in yeast cells, I was surprised by the diversity of cleavage intensities found in WT strains: some clones yielded 2-3 % of MetRS(Δ 132), and I isolated a clone where the cleavage was almost absent, even at high exposure (Lane 2 in **Figure R-28B** and **R-28F**, page 160). It was interesting to study this clone since this lack of cleavage could be the result of a mutation in the protease sequence or in a regulator of this cleavage. To assess the genetic causality of this phenotype, I crossed a strain presenting a high cleavage rate with the clone containing less MetRS(Δ 132) quantity (**Figure R-35A**). If the phenotype is indeed caused by a genetic mutation, the spores resulting from the diploid should present a 2:2 distribution for the cleavage (two spores with high cleavage and two with lower cleavage). I analysed nine different tetrads obtained after diploid dissection (**Figure R-35B**) by Immunoblotting total extract from each spore. The western blot globally shows an expected 2:2 distribution for each tetrad (**Figure R-35C**). Thus a gene mutation might be the cause of the deficit of MetRS cleavage, even if the cleavage is not totally abolished since a heat shock on this strain induces increase in the MetRS(Δ 132) proportion,

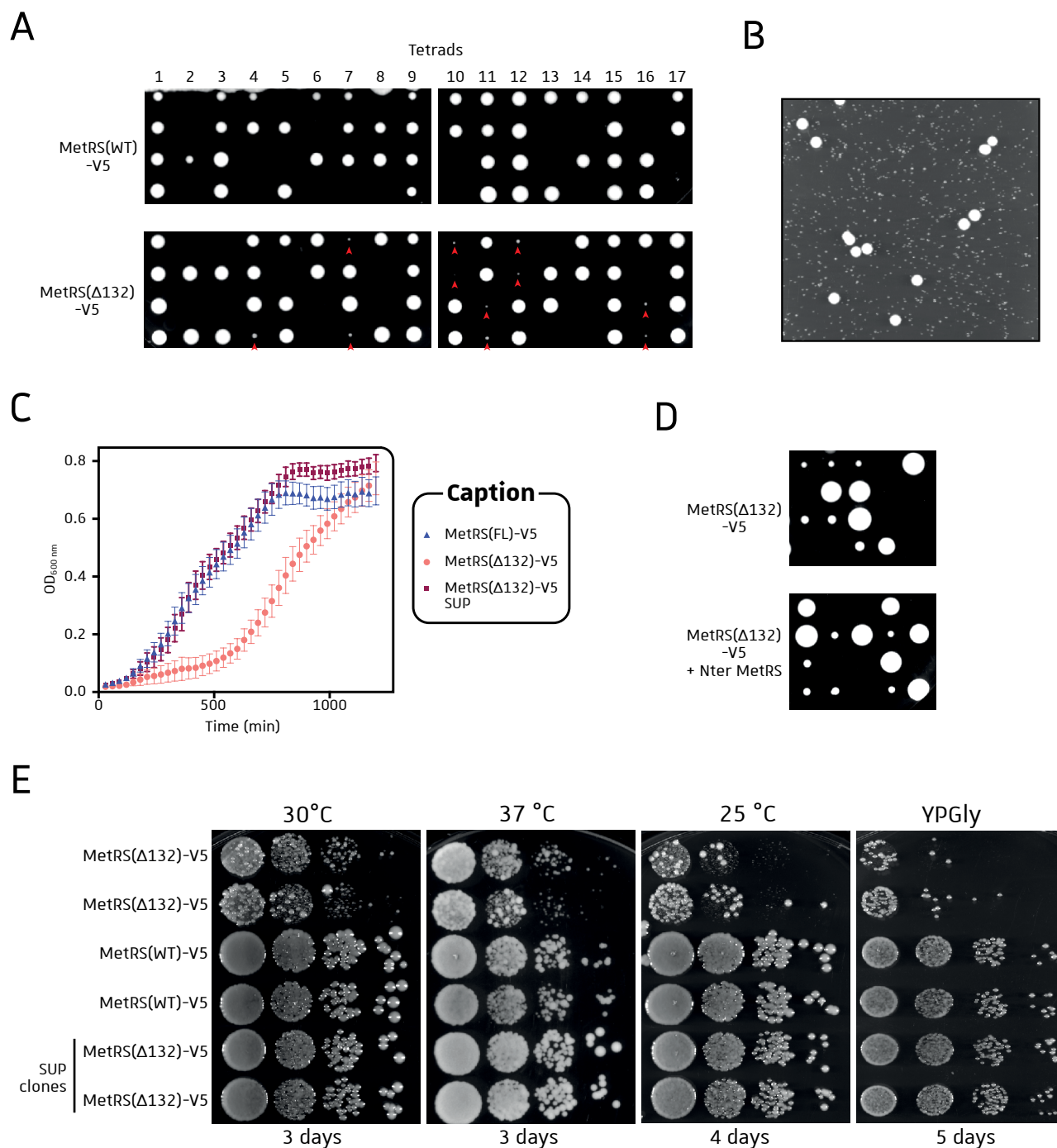


Figure R-36: Clones expressing MetRS(Δ 132)-V5 as the sole MetRS isoform displayed slow growth phenotype. **A. Dissection plates of tetrads from *mes1/MES1* diploids expressing either the MetRS(WT)-V5 or the MetRS(Δ 132)-V5 shorter form. Majority of the spores expressing the sole MetRS(Δ 132) isoform (red arrows) grows slower than WT spores. **B.** A small colony from **A** was cultured O/N at 30 °C in liquid rich medium (YPD) and spread onto an agar plate rich medium (YPD). After 4 days incubation at 30 °C, large colonies were observed among majority of small colonies. **C.** Growth curves of strains grown in YPD rich medium at 30 °C (n = 3). **D.** Dissection plates of tetrads from the *mes1/MES1* diploids expressing MetRS(Δ 132)-V5 with or without coexpression of the N-terminal domain of MetRS. **E.** Yeast spotting assay of the strains expressing the sole MetRS(WT) or MetRS(Δ 132) isoform, and suppressor clones (SUP) expressing MetRS(Δ 132). Yeast cells are spotted onto a YPD medium and incubated at either 30 °C, 37 °C or 25 °C for 3-5 days, or onto YPGly medium at 30 °C for 5 days. Other conditions have been tested in **Supplemental S7A**.**

yet with a delay compared to the strain with higher level of cleavage (**Figure R-35D**). To identify the mutation responsible for this cleavage phenotype, I performed DNA extraction on a full tetrad (tetrad 7 in **Figure R-35C**, spores a, b, c and d) and sent these four DNA samples to a high throughput DNA sequencing platform. First sequence analysis did not show any sequence differences (only Single Nucleotide Polymorphism (SNP) were checked in the analysis) and deeper analysis needs to be performed (searching for insertion/deletion for example). If we manage to find this mutation, we might be able to better understand the regulation and mode of action for this cleavage. Note that the clone exhibiting low levels of truncation has been used for the MetRS(WT)-V5 co-IP to minimize contamination of the MetRS(Δ 132) in the sample and to better distinguish interactions specific for the full-length and the cleaved MetRS. Such clone-dependent discrepancies might also explain the absence of visualized cleavage in the K11A and S10D mutant strains analysed in the previous PhD work by Dr. D. Laporte (**Figure R-20E**, page 144). Thus confirmation of MetRS cleavage requires the analysis of several clones to confirm the absence of truncation depending on a specific genetic background.

II.8.4. Clarifying the role of the truncated MetRS

I have identified heat shock as the major trigger of MetRS cleavage, and we have seen that the truncated MetRS(Δ 132) was more soluble than its WT counterpart at high temperatures (**Figure R-33**, page 170). However, I did not find a precise functionally different role for this truncated form. I made an intriguing observation while dissecting diploid cells expressing the MetRS(Δ 132)-V5. The truncated MetRS can sustain cell viability without presence of the full-length, but the majority of the spores expressing the shorter form was growing slower than the other clones (**Figure R-36A**, red arrows). Yet this slow growth was not systematic since some tetrads were composed of four spores with similar size. After growing these small colonies in liquid medium overnight (O/N) and plating on a rich medium, it appeared that majority of plated cells formed small colonies but some were forming larger clones (**Figure R-36B**). Spontaneous apparition of these larger clones (still expressing only the shorter form) was intriguing and meant that a certain adaptation was necessary for cells to normally grow. Indeed, these larger clones (called MetRS(Δ 132) SUP) are growing similarly to the WT strain (**Figure R-36C**). As expected, the small clone MetRS(Δ 132) started to grow slowly but reached a higher dividing speed after 10 hours, time needed for apparition of a SUP phenotype. We thought that these SUP clones originated from mutations in the genome (called suppressor mutation) allowing the cell to adapt its growth with only the MetRS(Δ 132) isoform.

Table R-3: Kinetic parameter (Km) of tRNA^{Met} transcripts for aminoacylation by MetRS isoforms. Aminoacylation reactions were performed at 25 °C with 10 nM enzymes.

	tRNA _i ^{Met}	tRNA _e ^{Met}
MetRS(WT)	3.2 μM	0.6 μM
MetRS(Δ132)	7.4 μM	1 μM

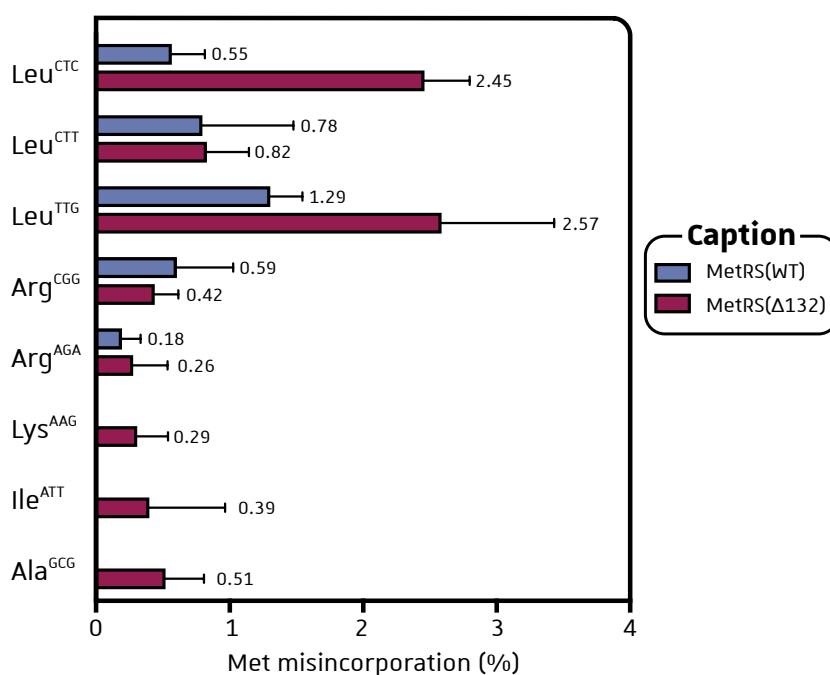


Figure R-37: Strains expressing MetRS(Δ132) presents higher Met misincorporation levels than the WT strains. Eight strains of the BFP library generated in the RS453 WT background (MetRS(WT)) or overexpressing MetRS(Δ132) were analysed by epifluorescence microscopy. Cells were grown in rich YPD medium and harvested in logarithmic phase before observation under the microscope. Quantification is performed as described in **Figure R-10**. Means and standard deviations are obtained on more than 100 cells analysed.

Thus I prepared genomic DNA of these strains (small MetRS(Δ 132) clones and their associated SUP clones) and sent them to high throughput DNA sequencing platform to identify potential mutation. Despite high quality of sequencing, the SNP profiles were identical, but some differences in the gene Copy Number Variant (CNV) were identified for some genes (listed in **Table S3**, page 202). Among these genes, apart from retrotransposons and genes with unknown functions, most of the genes are localized in the plasma membrane or the cell wall.

In the meantime, I tried to find particular conditions in which strains expressing only the truncated MetRS would present a growth phenotype different from the MetRS(WT) strains. Thus I followed the growth of these strains on solid medium (drop tests) in different conditions including thermal and nutritional stresses, since the cleavage was more present for these conditions (**Figure R-36E** and **Supplemental S7A**, page 203). In all conditions tested the SUP strains expressing MetRS(Δ 132) displayed a similar growth than WT strains. In contrast, and as expected, the MetRS(Δ 132) strains with no suppressive mutation exhibited a slow growth for all conditions, with some SUP clones growing faster. However, it appears that these strains have more difficulties to grow at lower temperatures, since tiny clones were observed at 25 °C compared to 30 °C (**Figure R-36E**). Maybe, this truncated form is more adapted to higher temperature, and would explain a higher cleavage during heat stress. However, first preliminary results have shown no better survival for the MetRS(Δ 132) strain compared to the WT strains during heat stress (**Supplemental S7B**, page 203), and comparison of *in vitro* aminoacylation activities between the two recombinant MetRSs did not show significant differences when temperature was raising (**Supplemental S8**, page 204).

II.8.5. Truncated MetRS and mismethionylation

For a long time we presumed that the shorter MetRS would be the major form for mismethionylation. Indeed, since loss of its N-terminal domain prevents its binding to Arc1, MetRS(Δ 132) is more prone to tRNA mismethionylation. First aminoacylation assays have shown that the K_m of the MetRS(Δ 132) for the tRNA^{Met} transcripts was similar than for the MetRS(WT) (**Table R-3**). Taking advantage of my work on the first project and the development of the dual-fluorescent reporter, I expressed some of my BFP reporters into the *mes1* Δ strain expressing only the MetRS(Δ 132)-V5 form (this strain appeared to be a SUP strain). As seen in **Figure R-37**, the MetRS(Δ 132) strain seems to yield more Met misincorporation events than the WT strain. Indeed, positive signals are observed for BFP(Lys^{AAG}), BFP(Ile^{ATT}) and BFP(Ala^{GCG}), whereas no Met misincorporation event was observed for these three codons in a WT strain. This result correlates with a truncated MetRS(Δ 132) more error

prone due to its incapacity to bind to Arc1. We need to confirm this first observation and to analyse the whole BFP library with the MetRS(Δ 132) strain. If confirmed, this result is interesting since heat stress has already been associated with oxidative stress response (Davidson *et al.*, 1996; Davidson and Schiestl, 2001b, 2001a; Ayer *et al.*, 2013).

II.8.6. Concluding remarks

Studying the dynamic of the MetRS(Δ 132) appeared to be more complex than expected. The Pep4-mediated proteolytic cleavage was observed *ex vivo* but not *in vivo*, showing a higher complexity in cells, probably due to MetRS post-translational modifications or cell compartmentalization. Finding a non-cleavable form of MetRS was also challenging, and the overproduction of MetRS(Δ 132) observed in several mutants of the N-ter domain indicates a finely tuned regulation of the MetRS cleavage. This MetRS N-terminal domain seems to be highly regulated in terms of structure and posttranslational modifications and might be intrinsically disordered since the full-length MetRS has never been crystallized. Our data suggest that the MetRS(Δ 132) produced in response to heat stress but its exact role still needs to be clarified. The bottleneck in the identification of the role of MetRS(Δ 132) resides in the extreme difficulty if not the impossibility to a non-cleavable MetRS mutant. If we could obtain such a mutant MetRS, we would be able to see whether this MetRS(Δ 132) is essential or not and if this essentiality is related to heat stress or to another physiological condition. Another possibility is that the role of MetRS(Δ 132) is to regulate transcription of a subset of genes (involved or not in the heat response) since MetRS(Δ 132) is the isoform that is found inside the nucleus. In summary, all the results I have accumulated during my study of the MetRS system unambiguously show the presence of a new truncated isoform of MetRS that potentially has a role in the response of yeast to stress whether heat-, oxidative- or some other kind of stress.



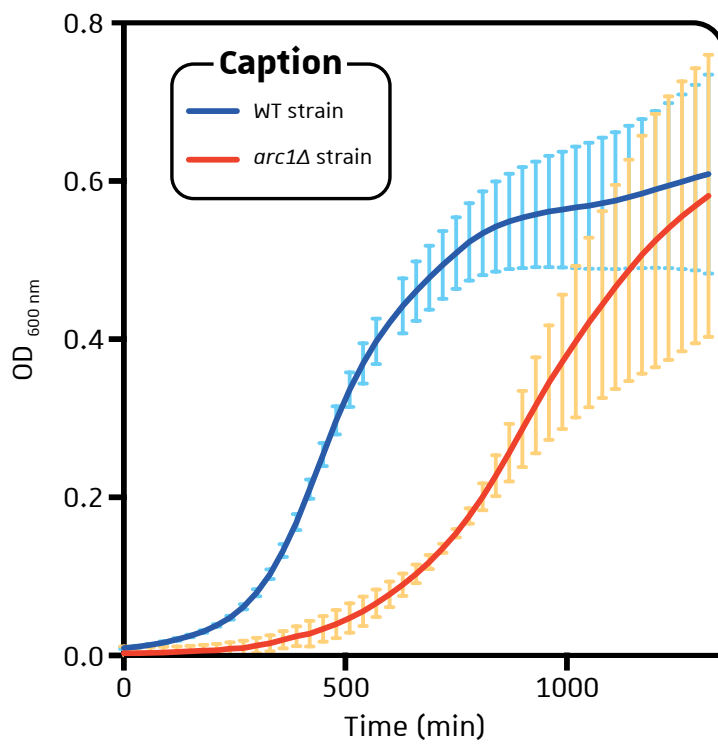


Figure R-38: The *arc1Δ* strain displays a growth phenotype. Growth curves of WT and *arc1Δ* strains grown in YPD rich medium at 30 °C.

III. Study of the mitochondrial role of Arc1 protein

III.1. Context of the study

We have seen in the introduction that Arc1 is related to a myriad of different functions: nuclear tRNA export, aminoacylation co-factor (by tRNA and aaRS binding) and potential cargo for relocation of the AME complex to the vacuolar membrane (**Figure I-23B**, page 76). Expression of this protein is also down-regulated during the diauxic shift from fermentation to respiration condition, allowing the two associated aaRS to relocate into the nucleus for MetRS and in mitochondria for the GluRS (Frechin *et al.*, 2014). This synchronized release of the two aaRS ensures the expression of both nuclear and mitochondrial-encoded subunits of the ATPase complex essential for accurate mitochondrial ATP production. Deletion of *ARC1* is not lethal and *arc1Δ* strain displays a slow growth phenotype both in liquid (**Figure R-38**) and solid rich fermenting media. Growth of this deletion strain was never tested on respiratory medium since the level of the Arc1 protein decreases during respiration suggesting that the two aaRSs might be constitutively present in their respective organelle, leading to synchronous expression of ATPase subunits and growth on respiratory medium. When I was testing strains for growth phenotype associated with MetRS(Δ 132), I also tested the growth of *arc1Δ* strains in different media, including the respiratory medium. Depending on the genetic background, the growth efficiency was different, but most of the time, absence of Arc1 correlated with an absence of growth in respiratory medium. This “petite” phenotype, associated with a blockage in the aerobic respiratory chain pathway, had never been described in the literature. Hence, I started to analyse into more details this phenotype to try to understand the role of Arc1 in respiration.

III.2. Arc1 is dual-localized in the cytosol and mitochondria

The *arc1Δ* strain available in the lab was derived from a BY4742 strain. It appeared that this genetic background was not suitable for respiratory growth since growth onto glycerol (a non-fermentable carbon source) was impaired even for the WT strain (**Figure R-39A**). Thus, it was difficult to compare the effect of *ARC1* deletion in such strain. During my PhD I engineered an *arc1Δ* deletion strain in the RS453 genetic background. The WT RS453 strain displayed an efficient respiratory growth, and subsequent deletion of *ARC1* induced a loss of growth on glycerol medium, but not on galactose medium, a fermentable substrate that does not elicit repression of mitochondrial

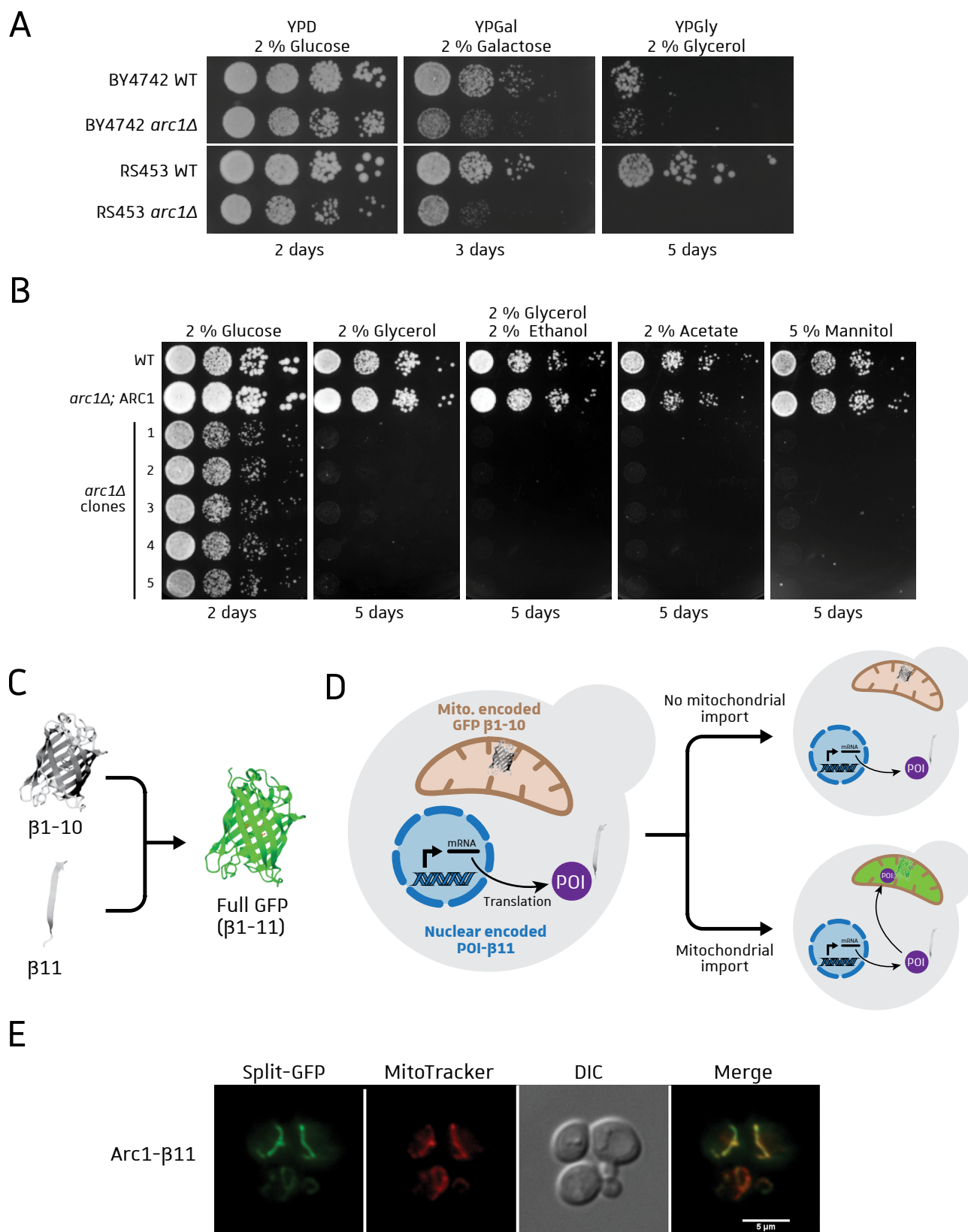


Figure R-39: Dual-localization of Arc1 both in cytosol and mitochondria. A. Yeast spotting assay for BY4742 and RS453 strains (WT and *arc1Δ*) in fermentative (glucose and galactose) or respiratory (glycerol) rich media. **B.** Yeast spotting assay of RS453 strains on fermentative (glucose) or respiratory media. **C.** The split-GFP system relies on physical interaction between the two non-fluorescent peptides β 1-10 barrel and β 11 strand. **D.** The β 11 tag protein of interest (POI) is nuclear-encoded, whereas the GFP β 1-10 is encoded into the mitochondrial genome. The green fluorescence is restored by translocation of the β 11-POI into the mitochondria. **E.** Observation by epifluorescence of a strain expressing the Arc1- β 11 fusion protein. The GFP signal colocalizes with MitoTracker, a specific dye for mitochondria staining (from Bader *et al.*, 2019 in submission).

function (**Figure R-39A**, lanes 3 and 4). The “petite” phenotype observed in the RS453 *arc1Δ* strain was confirmed for several clones and respiratory media (**Figure R-39B**). The overexpression of Arc1 restored the respiratory growth and confirmed the role of Arc1 in mitochondrial functions (**Figure R-39B**, lane 2). Despite a reduced growth rate observed for the *arc1Δ* strain compared to WT, in fermentable medium (glucose), incubation on a respiratory medium totally impaired the growth since no clones were visible after several days of culture. This was the first evidence of a mitochondrial role for Arc1, different from the synchronous aaRSs release previously demonstrated. This was surprising since Arc1 was described as a cytosolic protein with nuclear relocalization and was never observed inside mitochondria.

In the meantime, another PhD student in the lab (Dr. Gaétan Bader) was engineering a fluorescent molecular tool used to assess the mitochondrial localization of proteins previously described as cytosolic (Bader *et al.*, 2019 (in submission)). This technique relies on the use of the split-GFP molecule, with the β 1-10 GFP barrel encoded in the mitochondrial genome, and the missing β 11 strand of the GFP fused to the nuclear-encoded protein of interest (**Figure R-39C and R-39D**). Each part of the GFP molecule is not fluorescent, and reconstitution of the full-GFP by protein interaction restores the green fluorescence. Since the β 1-10 fragment is encoded by the mitochondrial genome, green fluorescence is only observed when the β 11-tag protein relocates into this organelle without any green cytosolic background (**Figure R-39D**). Intracellular localization of Arc1 using fluorescence microscopy with conventional GFP tagging had always shown cytosolic localization, even with confocal microscopy (Galani *et al.*, 2001). When Arc1 was fused to β 11-tag, a green fluorescent signal was observed, and colocalized with the mitochondria specific dye MitoTracker (**Figure R-39E**, from Bader *et al.*, 2019 (in submission)). Hence this observation confirmed for the first time the role of Arc1 in mitochondrial activity.

III.3. Respiratory deficiency can be suppressed spontaneously

We found that absence of *ARC1* gene correlated with a strong growth deficiency in respiratory rich medium. However, I noticed that after 5 days of growth on non-fermentable carbon source, some *arc1Δ* clones were starting to grow in the yeast drop tests (**Figure R-39B**, small clones observed in glycerol, acetate and mannitol plates) with absence of *ARC1* expression in these clones (**Supplemental 9**, strains *arc1* SUP, page 205). These clones were thought to be suppressors of the *arc1Δ* phenotype arising by one (or more) mutation in a gene called suppressor gene. To confirm

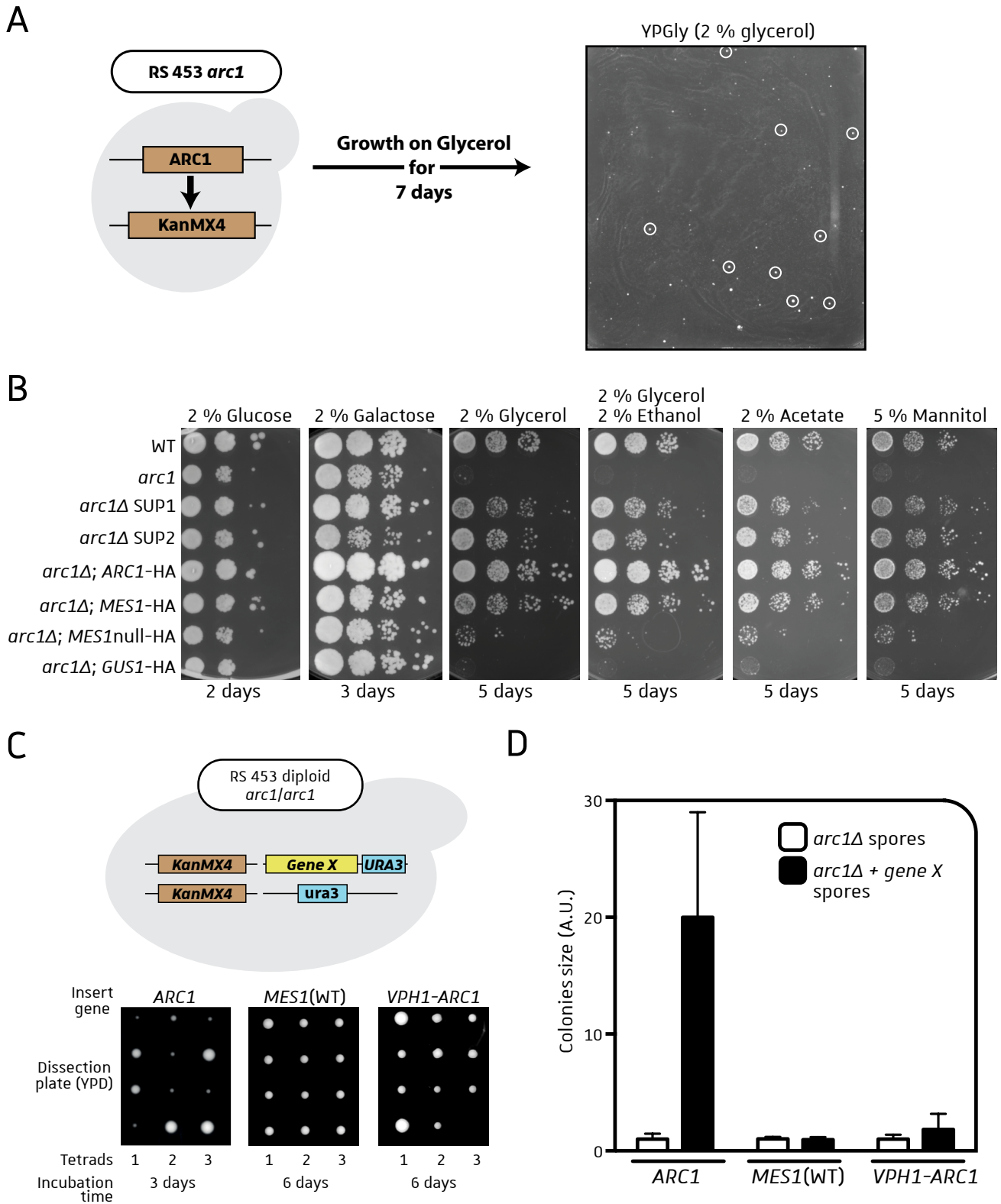


Figure R-40: Spontaneous growth of *arc1Δ* strains on respiratory medium. **A.** An *arc1Δ* strain (*ARC1* gene replaced by *KanMX4* cassette) was spread onto a glycerol agar plate and incubated at 30 °C for 7 days. Spontaneous growth of clones (called *arc1Δ* SUP) was observed (white circles). **B.** Yeast spotting assay of RS453 strains on fermentative (glucose and galactose) or respiratory media. *MES1null*: catalytic null MetRS. **C.** Gene insertion in the *arc1Δ/arc1Δ* diploid strain genome of either *ARC1*, *MES1(WT)* or *VPH1-ARC1* gene by yeast transformation (upper panel). Dissection plate for all three diploid strains is shown (lower panel). **D.** Quantification of colonies size on each dissection plate shown in D. Size for *arc1Δ* spores was set to 1 for each diploid. n = 30 spores minimum.

the observation from the yeast drop test, I spread a freshly grown (in glucose medium) *arc1Δ* strain onto a glycerol plate (YPGly). After seven days of incubation at 30 °C, several suppressor clones were observed (**Figure R-40A**, white circles) and called *arc1* SUP. Some of them were isolated and tested again for respiratory growth on a new drop test (**Figure R-40B**, *arc1* SUP1 and SUP2, and **Supplemental S10**, page 205). These two SUP strains displayed a respiratory growth that appears slightly slower than the WT strain and the *arc1Δ* strain overexpressing Arc1-HA. Thus, spontaneous mutation(s) in the *arc1Δ* genome can restore almost completely the WT growth phenotype under respiratory growth.

In the meantime, I was engineering some haploid stains by yeast crossing. I generated a diploid strain *arc1Δ/ARC1* expressing two MetRSs: one controlled by its endogenous promoter *pMES1* and the other by the constitutive and strong *GPD* promoter (*pGPD*) (**Supplemental S11A**, page 206). Sporulation of this diploid strain produced *ARC1* clones and *arc1Δ* haploids with either the endogenous MetRS (red circles) or the ectopic MetRS controlled by the *GPD* promoter (yellow circles). As shown in Supplemental S11A, all *arc1Δ* spores with the ectopic MetRS were able to grow under respiratory condition (2 % glycerol), whereas all the *arc1Δ* clones with the endogenous MetRS presented a “petite” phenotype. The only difference between them was the promoter, and *pGPD* appeared to be stronger both in fermentative (YPD) and respiratory (YPGly) conditions (**Supplemental S11B**). This observation led me to engineer *arc1Δ* strains that overexpressed the components of the AME complex (**Figure R-40B**). As a positive control, overexpression of Arc1 did restore the growth in respiration. In the same way, overexpression of the MetRS had the same impact, whereas overexpressing the GluRS was not beneficial for the growth in respiratory media. Interestingly, overexpression of the catalytic null MetRS had positive effect on the respiratory growth, but with a lower effect than the active WT MetRS (**Figure R-40B**). The overexpression of the MetRS had an effect on respiratory growth, but not on fermentative growth, since *arc1Δ* spores overexpressing the MetRS had the same size on the dissection plate (YPD medium) (**Figure R-40C and 40D**). I also try to determine if the mitochondrial localization of Arc1 was essential for respiratory growth: I engineered a strain where Arc1 is fused to the Vph1 protein, a vacuolar ATPase embedded in the vacuolar membrane with both its N- and C-termini facing the cytosol. After sporulation and dissection of the diploid expressing this Vph1-Arc1 fusion protein, the *arc1Δ* spores with vacuolar Arc1 were slightly larger than the *arc1Δ* strains (**Figure R-40D**) and were able to grow on respiratory medium (not shown). Thus, mitochondrial localization of Arc1 is not essential for growth in respiratory conditions.

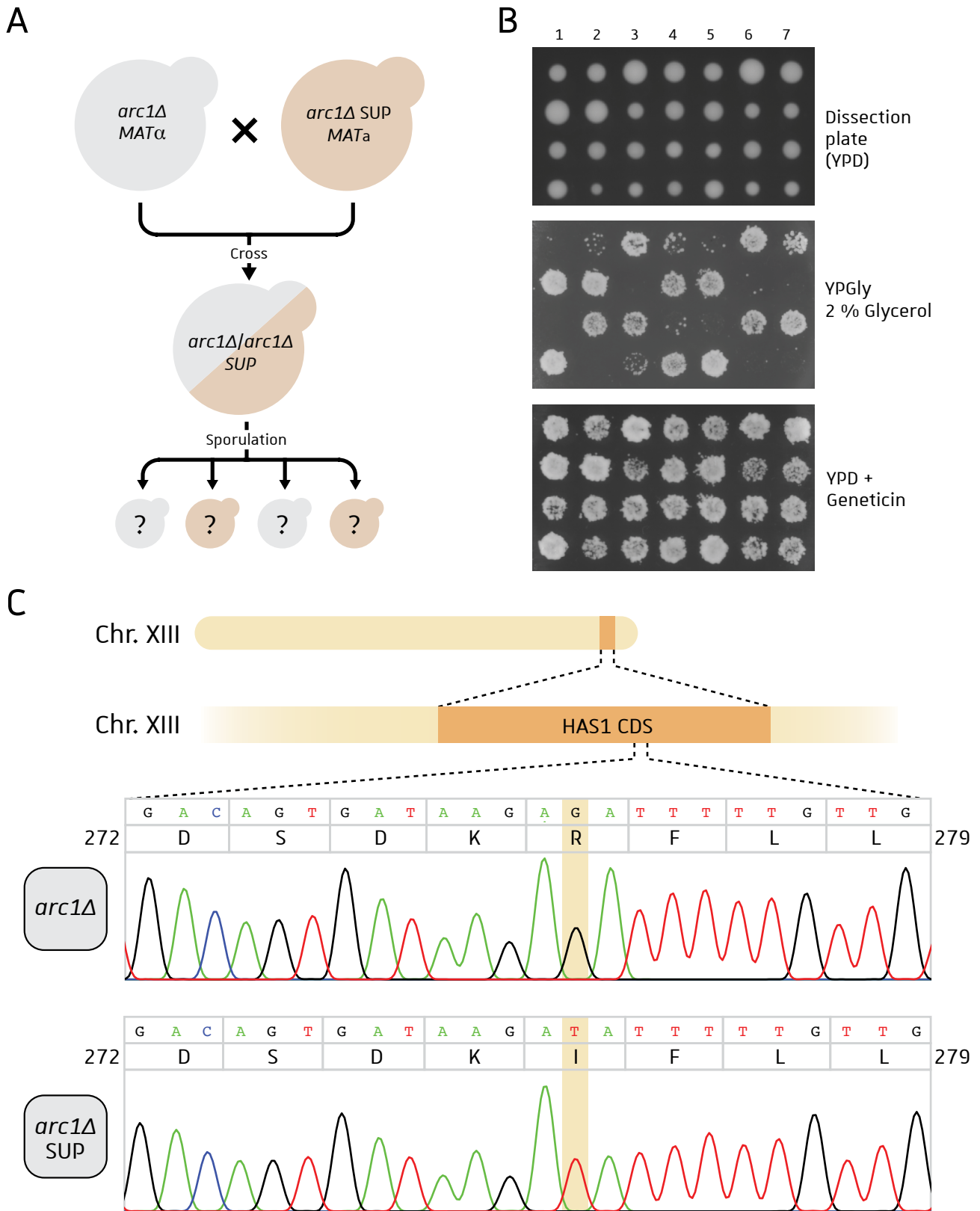


Figure R-41: The *arc1* SUP strain contains a single substitution in *HAS1* gene. **A.** Growth phenotype on glycerol plate of the cross between *arc1Δ* and *arc1* SUP strains. **B.** Dissection plate of the tetrads generated from the cross shown in A (upper panel). Growth of each spore in glycerol medium (middle) and YPD + geneticin (lower) is shown. All spores grow on YPD + geneticin, showing that all clones are deleted for *ARC1* gene (gene disruption with *KanMX4* sequence). **C.** Position of the *HAS1* gene in chromosome XIII and R276I substitution identified in Has1 protein from *arc1* SUP strain.

III.4. Identification of the suppressive mutation in *arc1Δ* SUP genome

After finding that *arc1Δ* SUP clones were able to grow in respiration, we wanted to localize the mutation(s) leading to this suppression phenotypes. Since overexpression of the MetRS appeared to recover the growth phenotype, *MES1* gene has been sequenced in both *arc1Δ* and *arc1* SUP, but no differences in sequences have been observed (data not shown). First, we wanted to know if only one or several gene were mutated in the *arc1* SUP genome. To answer this question, I crossed an *arc1Δ* strain with an *arc1* SUP strain, and I analysed the phenotype of each spore from a tetrad after sporulation (**Figure R-41A**). It appears that all tetrad were composed of two spores growing on glycerol (respiratory medium), and two with a “petite” phenotype, meaning that the suppression phenotype arises from only one mutation in one gene (or at least few mutations on a single locus) (**Figure R-41B**). To identify the mutated gene, the genome of *arc1Δ* strain as well as of *arc1* SUP have been extracted and analysed by a high throughput DNA sequencing platform. So far only the SNVs have been analysed, and a single variant has been identified in the coding region of the *HAS1* gene (YMR290C) (**Figure R-41C**). The G827T mutation in the DNA sequence gives rise to a R276I substitution in the protein sequence. The Has1 protein is a DEAD-box RNA helicase that binds and unwinds pre-rRNAs for subsequent maturation by the small nucleolar RNPs (snoRNPs) (Dembowski, Kuo and Woolford, 2013; Brüning *et al.*, 2018). Thus, Has1 regulates maturation and assembly of the 60S ribosomal subunits. It is still unclear if this protein is really implicated in *arc1* SUP phenotype, and we are currently analysing the correlation between this genetic mutation and the respiration deficiency phenotype.

III.5. Discussion: Arc1 as a co-folding partner for mitochondrial relocation?

By anchoring the two cytosolic yeast aaRSs MetRS and GluRS, Arc1 is a known aaRSs co-factor and a platform that retains the two aaRSs in the cytosolic fraction (Frechin *et al.*, 2010). Its role in respiration was elucidated few years ago by its dynamic during the diauxic shift: Arc1 is downregulated when yeast cells are shifting from fermentation to respiration, allowing the synchronous relocation of both released MetRS and GluRS (Frechin *et al.*, 2014). Mitochondrial relocation of the cytosolic GluRS during respiration is crucial since it allows the production of mitochondrial Glu-tRNA^{Gln} and the subsequent formation of Gln-tRNA^{Gln} by transamidation. This synchronous release of the

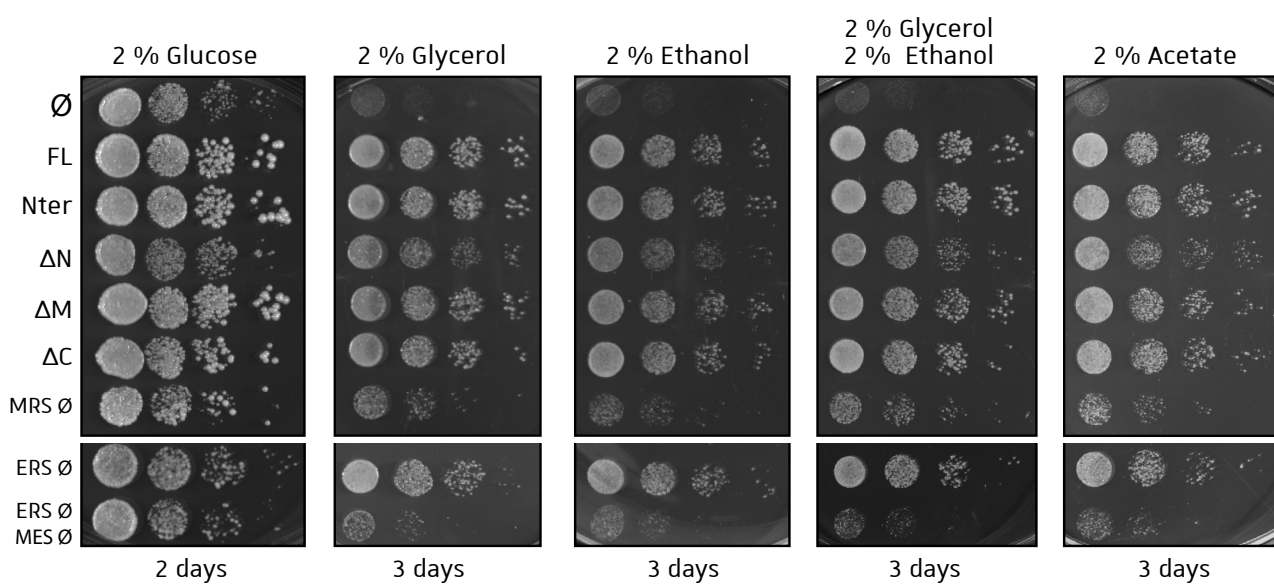


Figure R-42: Loss of interaction with GluRS and MetRS induces deficient respiratory growth. Yeast spotting assay of *arc1Δ* strain (Ø) overexpressing full length (FL) or truncated Arc1 isoforms in rich media with glucose or respiratory carbon sources. Nter: Arc1 N-terminal domain, ΔN: Arc1(ΔN-terminal domain), ΔM: Arc1(ΔMiddle domain), ΔC: Arc1(ΔC-terminal domain), MRSØ : A26R S33A mutant (loss of MetRS interaction), ERSØ : T55R R100A Y104A mutant (loss of GluRS interaction), ERSØ MRSØ : A26R S33A T55R R100A Y104A mutant (loss of both MetRS and GluRS interaction).

two cytosolic aaRSs was thought to be essential for accurate growth upon respiration. However, deletion of *ARC1* gene, equivalent to a continuous release of the two aaRSs, was not viable on non-fermentable carbon sources, and revealed a more complex role for Arc1. Note that growth deficiency in respiratory medium for *arc1Δ* strain might be dependent on the genetic background tested, since a BY4742 *arc1Δ* strain can slowly grow on glycerol (**Figure R-39A** and personal observations).

For the first time we have shown that Arc1 is actually a dual-localized protein in both the cytosol and mitochondria, partly explaining the respiratory deficiency in an *arc1Δ* strain. However, according to our results, accurate growth can be restored by overexpressing the MetRS, but not the GluRS (**Figure R41-B**). This was really surprising, since no mitochondrial connections have been found for the yeast cytosolic MetRS in the literature. One of our hypotheses was that the cytosolic GluRS was not able to reach mitochondria by its own, and that interaction with Arc1 was essential to carry the aaRS for mitochondrial translocation. To go further into details, I used *arc1Δ* strain to overexpress several mutants of Arc1 (**Figure R-42**): either the N-terminal domain of Arc1, some deletion mutants (ΔN , ΔM or ΔC), or Arc1 mutants unable to interact with either the MetRS (MRS \emptyset); the GluRS (ERS \emptyset), or both (ERS \emptyset MRS \emptyset). Figure R-42 shows that the N-terminal domain of Arc1, the ΔM and ΔC mutants are able to completely restore respiratory growth, showing that the N-ter of Arc1 is important for yeast respiration. Indeed, the ΔN mutant did not fully restore the growth on respiratory media, showing that loss of interaction with the GluRS by its N-ter domain was important. Similarly, loss of interaction with the MetRS, and in a lesser extent with the GluRS, did not fully restore the respiratory growth. These preliminary results need to be confirmed, especially by showing the loss of interaction *in vivo* between the different Arc1 mutants and both the GluRS and MetRS. However, this last observation led us to think about a carrier role for Arc1 that could bring the GluRS into mitochondria. This assumption was in agreement with results showing that the three components of the AME complex were co-translationally interacting with each other through their respective N-terminal domains (Shiber *et al.*, 2018). More interestingly, the two aaRSs can engage each other co-translationally, confirming the impact of MetRS overexpression on respiratory growth by interacting and folding properly the GluRS to be targeted to mitochondria. This is also in agreement with the vacuolar localization of the AME complex identified in the lab. Indeed, vacuole and mitochondria form several membrane contact sites (or vCLAMPs for vacuolar and mitochondrial patches), meaning that vacuolar AME complex is in close proximity to mitochondria and could favour GluRS translocation into mitochondria (González Montoro *et al.*, 2018; Scorrano *et al.*, 2019).

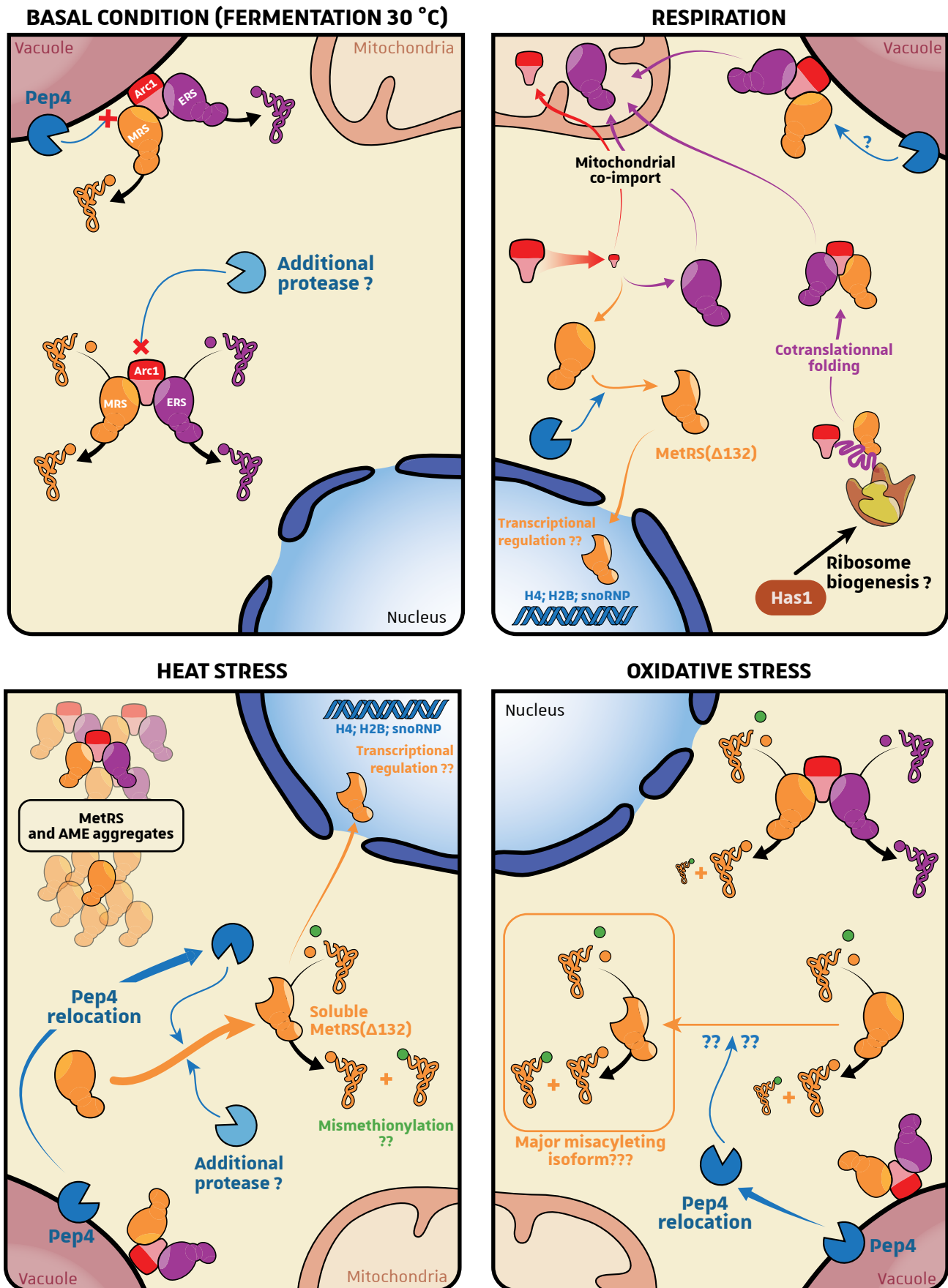


Figure R-43: Summary of results found in my thesis projects. Major regulatory events implying the MetRS and the AME complex in different growth conditions and environmental stresses. Since deletion of *PEP4* does not entirely prevent MetRS cleavage, a potential additional is shown (light blue). **X**: protection from proteolytic cleavage.

IV. General conclusion

My PhD work was essentially focusing on the study of the dynamics of the AME complex and more precisely on the potential additional functions for the yeast MetRS. These four years allowed me to gain knowledge about yeast adaptation to different environmental conditions. Yeast cells are found in a plethora of niches (soil, water, associated with plants or animals) and face a myriad of constantly changing environmental conditions (daylight, seasons...) that drive their metabolic activities. During environmental stresses, expression of stress response genes is regulated, and cellular proteome is highly dynamic. In our case, it appeared that the AME complex (and its individual components) is extremely dynamic when facing physico-chemical stress. We knew before my PhD that the source of carbon (which determines the habitat specificity for yeast cells) was crucial for the AME complex's dynamic and the subcellular relocation of its aaRSs (Frechin *et al.*, 2014). My work brought even more complexity to this system by adding regulation mechanisms during oxidative and heat stresses (**Figure R-43**). An interesting fact is the link between these two stresses: the truncated MetRS(Δ 132) was found to be highly produced during heat shock and might be a misacylating MetRS isoform. Moreover, the Pep4 protease was found to relocate from the vacuole to the cytosol during both oxidative and heat conditions. Despite the absence of link between Met misincorporation and heat stress, these preliminary results are in agreement with the yeast MetRS having a role during such environmental condition changes.

Localization of the AME complex components was also a huge issue during my PhD. In addition to the cytosolic and nuclear dual localization of the MetRS(Δ 132), we also found that the whole AME complex was tightly bound to the vacuolar membrane (results from M. Hemmerlé, PhD student, by subcellular fractionation and vacuolar split-GFP). This observation adds a new order of complexity with aaRSs being close to the vacuolar compartment which is the place of aa storage and which is bound to mitochondria through membrane contact sites. During my PhD I have started to create yeast strains with vacuolar MetRS by fusion of the aaRS to the vacuolar ATPase Vph1 embedded in the vacuolar membrane. Results have shown that the spores expressing the sole Vph1-MetRS(WT) isoform were smaller than spores expressing MetRS(WT) or both the cytosolic and the vacuolar MetRSs (**Figure R-44A and Dissection table 9**, page 216). These strains displayed also a growth deficiency in respiratory medium and were more sensitive to oxidative stress induced by H₂O₂ or paraquat (**Figure R-44B**). Thus, localization of the MetRS is essential for yeast growth and survival in

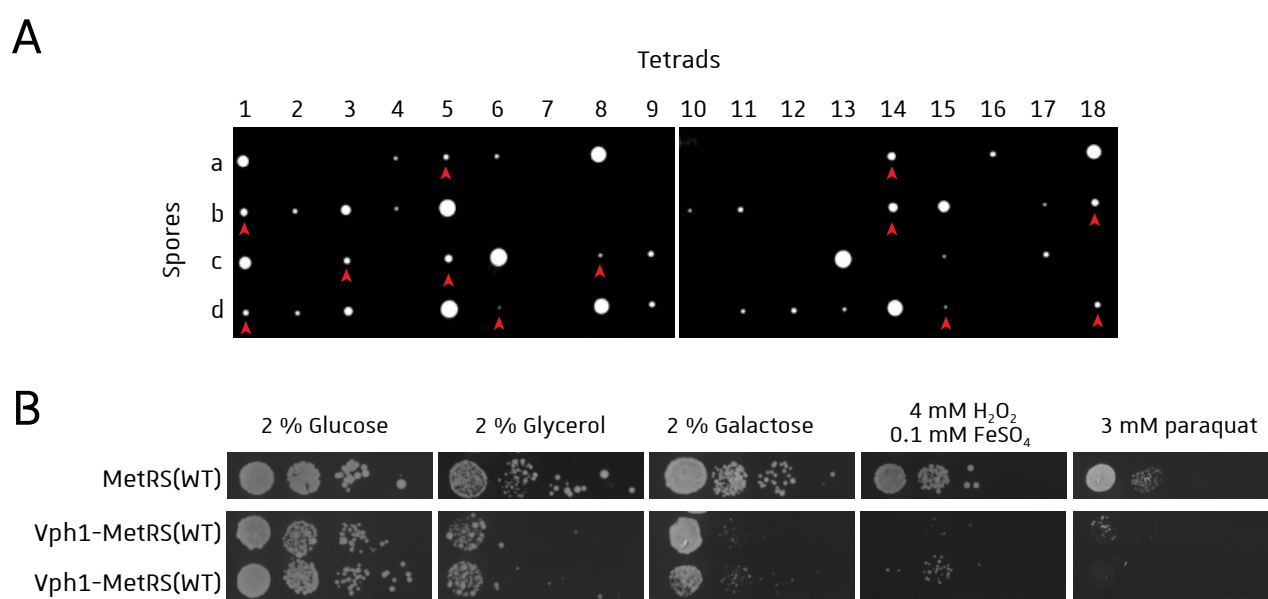


Figure R-44: Vacuolar anchored MetRS(WT) and yeast growth deficiency. A. Dissection plate of tetrads from *mes1/MES1* diploids expressing Vph1-MetRS(WT) fusion protein anchored to the vacuolar membrane. Majority of the spores expressing the sole Vph1-MetRS(WT) isoform (red arrows) grows slower than WT spores. **B.** Yeast spotting assay of strain expressing either the MetRS(WT) or the Vph1-MetRS(WT) fusion protein on several rich media.

stressed conditions. However, controls are still needed like confirming that the whole pool of MetRS is indeed attached to the vacuolar membrane through Vph1 fusion, since proteolytic cleavage could target this fusion protein, allowing the cytosolic release of the MetRS(Δ 132).

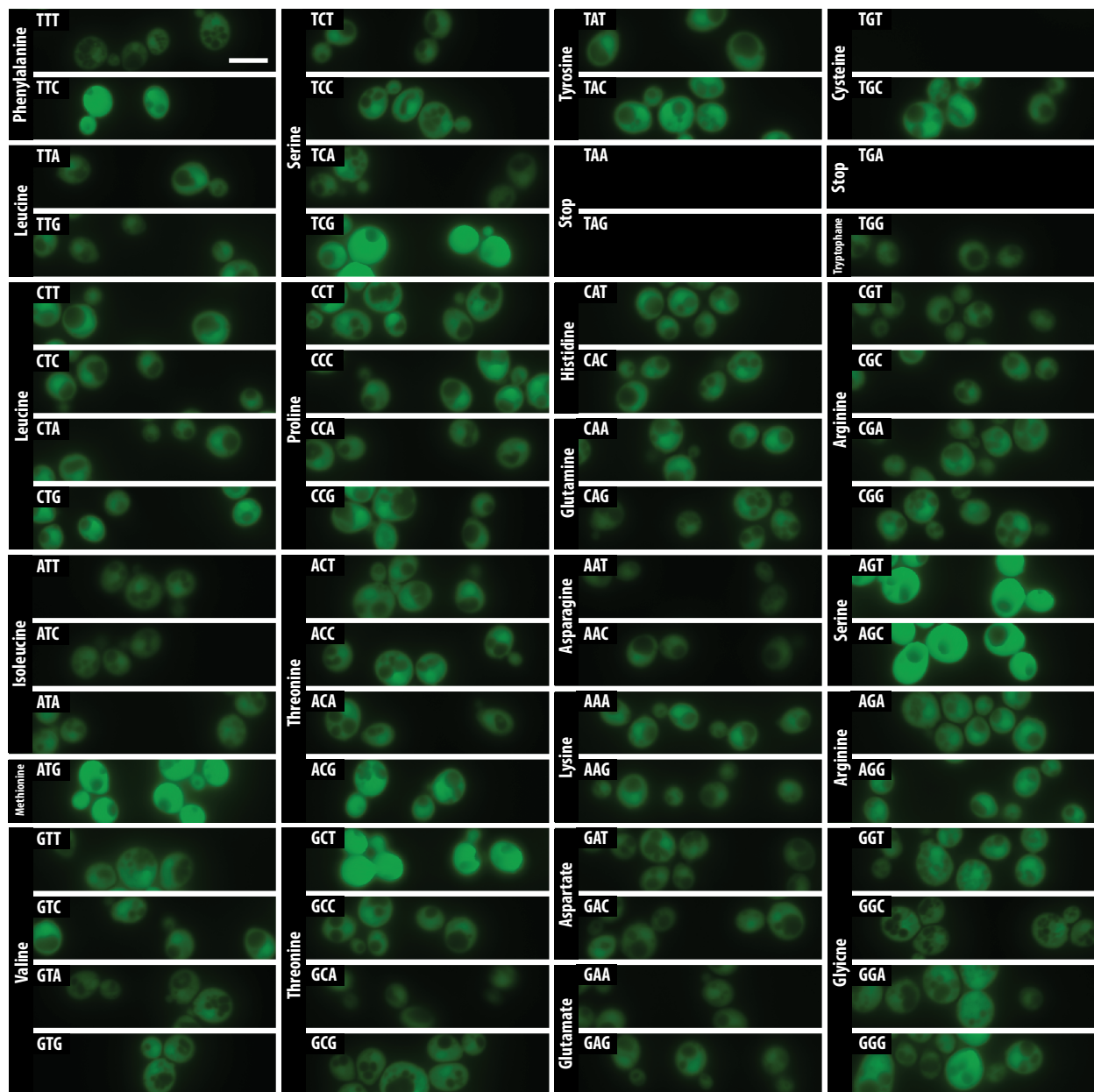
The dynamics and various roles of the yeast AME complex are far from being completely understood. Even if it represents one of the simplest eukaryotic multisynthetase complexes, its additional cellular roles are still to be discovered, and having data about the whole AME complex structure would greatly help our understanding of its structure-function relationship. The present work has unravelled part of this complexity, and further analyses will certainly highlight new essential functions for the yeast MetRS and its human ortholog.



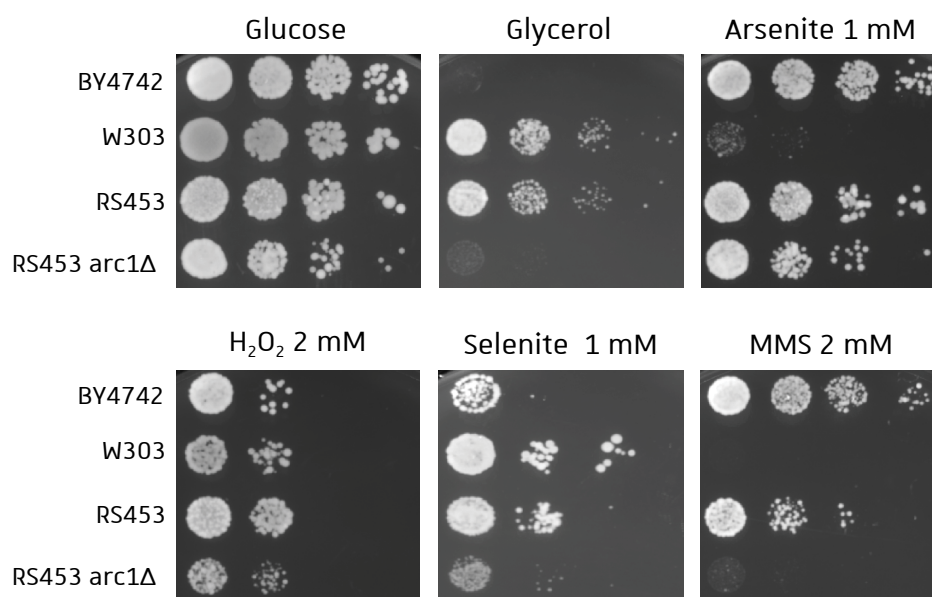
Supplemental figures and tables

Table S1: Description and photophysical properties of some fluorescent proteins (FPs). Source of data: Verkhusha *et al*, 2001; Forner and Binder, 2007; Lam *et al*, 2012; Kim and Cluzel, 2017.

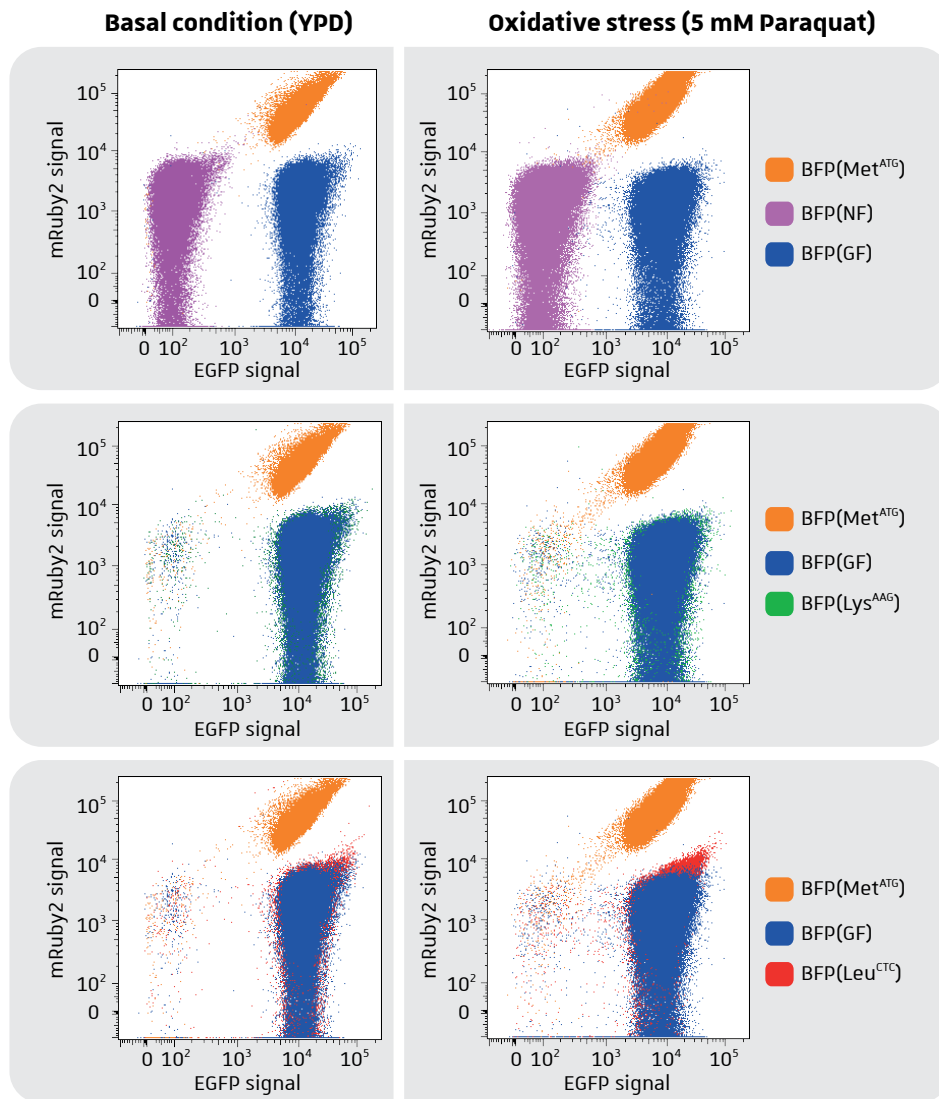
Organism of origin	Fluorescent protein	Fluorophore residues	Mutations added outside fluorophore	λ excitation (nm)	λ emission (nm)	Maturation Time t50 (min)	Relative Brightness (% EGFP)
<i>Aequorea victoria</i>	GFP (<i>Aequorea victoria</i>)	S Y G		397	475	58	48
	EGFP	T Y G	F64L	488	507	25	100
	EBFP	S H G	F64L	383	445	-	27
	ECFP	T W G	F64L	439	476	50	39
	EYFP	G Y G	T203Y	514	527	11	151
Anthozoa	DsRed	Q Y G		558	583	600	176
	mRFP1	Q Y G	DsRed with 33 aa substitutions	584	607	35	37
	mCherry	M Y G	mRFP1 with 9 substitution and Nter/Cter addition	587	610	40	47
	eqFP611 (<i>E. quadricolor</i>)	M Y G		559	611	270	106
	mRuby	M Y G	eqFP611 with 29 aa substitutions	558	605	170	117
	mRuby2	M Y G	mRuby with 4 substitutions	559	600	150	126
	mRuby3	M Y G	mRuby2 with 21 substitutions	558	592	243	170



Supplemental S1: Selection of BFP clones to create the BFP strain library. BFP library in WT BY4742 genetic background was generated by selection of clones with similar BFP expression. Selection was performed by imaging cells for green fluorescence. Stop codons were not tested with the BFP reporter (black squares). A representative picture of each BFP codon strain is shown, organized in the standard genetic code table. Bar scale, 10 μ m.



Supplemental S2: Effect of oxidants on yeast growth on solid medium. Yeast spotting assays of several WT strains (different genetic background) or RS453 *arc1*Δ strain, on YPD rich agar plate (glucose), on respiratory medium (Glycerol), or on YPD plate supplemented with the indicated oxidant.

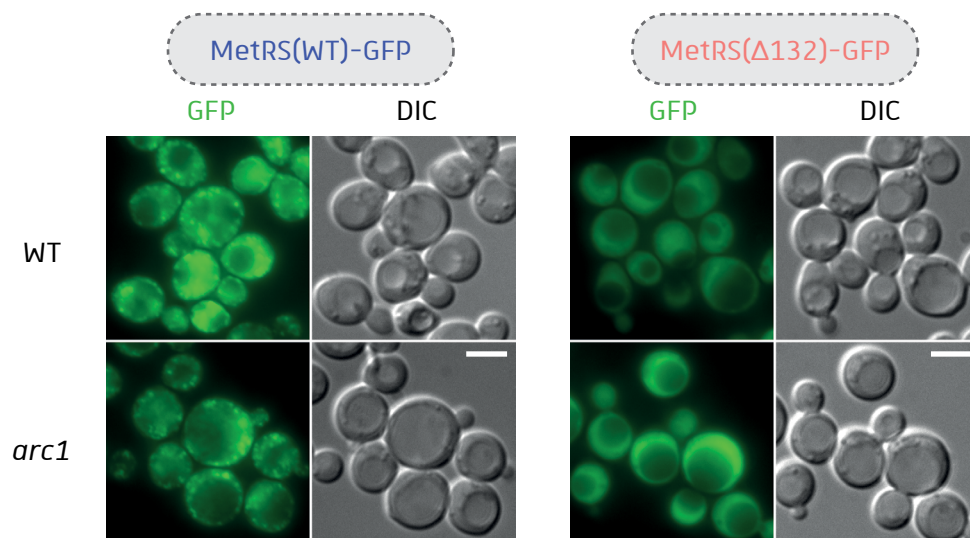


Supplemental S3: Using flow cytometry to monitor Met misincorporation with the BFP system. Flow cytometry dot-plots using EGFP and mRuby2 fluorescence. Cells are analyzed at mid-log phase in YPD (left) or after 24 h treatment with 5 mM paraquat in YPD medium. For each dot plot, the two controls BFP(Met^{ATG}) and BFP(GF) are shown forward, and either BFP(Lys^{AAG}) cells (green, middle) or BFP(Leu^{CTC}) cells (red, lower) are shown backward. Each strain is analysed on 100.000 cells.

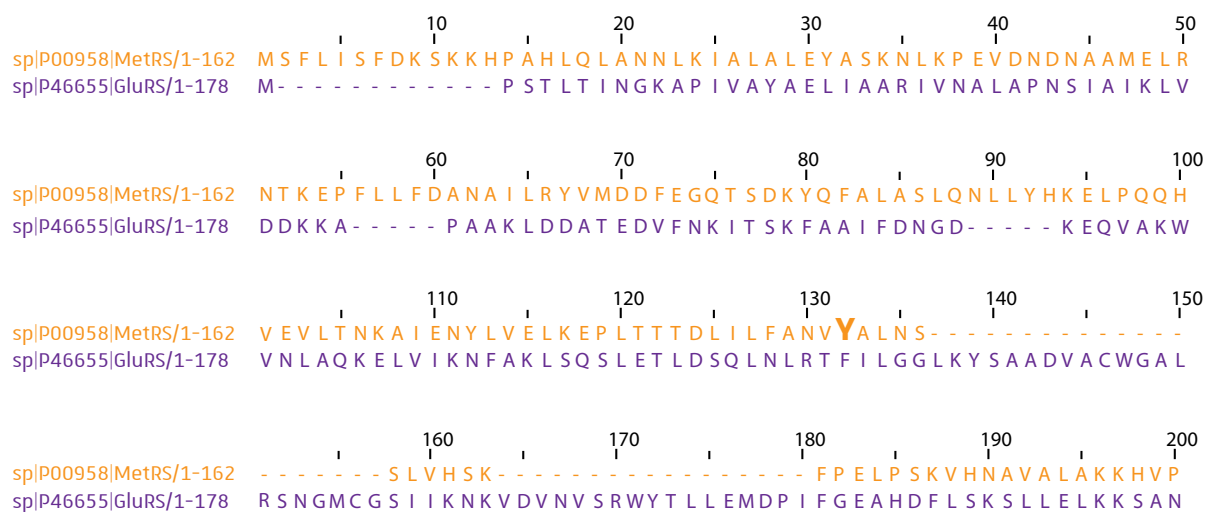
Table S2: Protein interactants found only in the MetRS(WT)-V5 (upper table) and only in the MetRS(Δ 132)-V5 (lower table) co-IP experiments.

Protein category	Uniprot Accession Number	Standard Name	Protein Description
aaRS or AIMP	P46655	GUS1 (GluRS)	GluRS
	P46672	ARC1	Arc1
Translational proteins	P39730	FUN12	Eukaryotic translation initiation factor 5B
	P05453	ERF3	Eukaryotic peptide chain release factor GTP-binding subunit
	P42846	KRI1	40S ribosome biogenesis, nucleolar processing of pre-18S rRNA
	P05744	RPL33A	60S ribosomal subunit L33-A
	P26321	RPL5	60S ribosomal protein L5
Mitochondrial proteins	P32582	CYS4	Cystathionine beta-synthase
	P19882	HSP60	Mitochondrial Heat shock protein 60
	P07149	FAS1	Fatty acid synthase subunit beta
Others	P07259	URA2	Bifunctional carbamoylphosphate synthetase/aspartate transcarbamylase
	P60010	ACT1	Actin
	Q00955	ACC1	Acetyl-CoA carboxylase
	P39986	SPF1	Manganese-transporting ATPase 1, manganese transport into the ER
PM protein	P25297	PHO84	Inorganic phosphate transporter

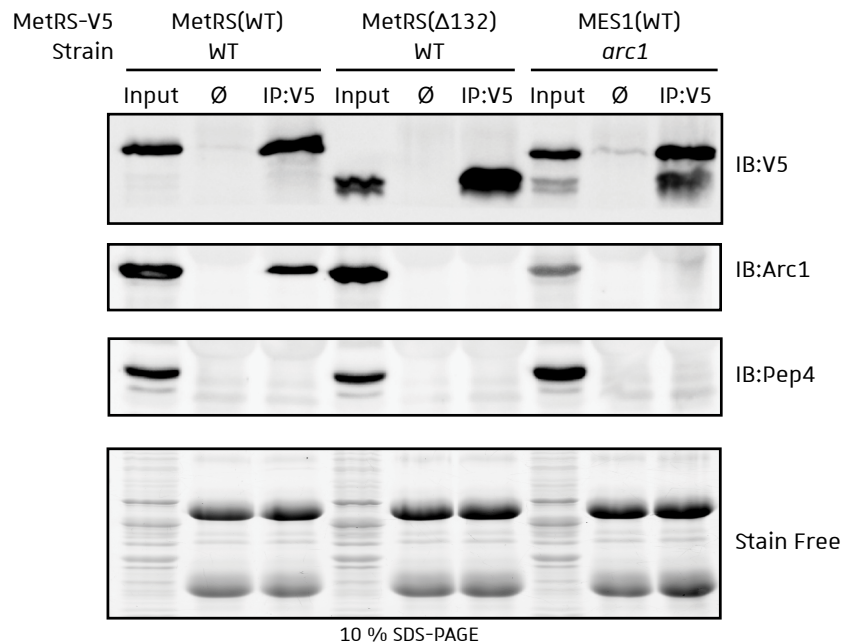
Protein category	Uniprot Accession Number	Standard Name	Protein Description
Nuclear protein	P02293	HTB1	Histone H2B.1
	P02309	HHF1	Histone H4
	P32995	NHP2	H/ACA ribonucleoprotein complex subunit NHP2 (snRNP)
Translational proteins	P04449	RPL24A	60S ribosomal protein L24-A
	P23248	RPS1B	40S ribosomal protein S1-B
	P33442	RPS1A	40S ribosomal protein S1-A
Mitochondrial protein	P00044	CYC1	Cytochrome c iso-1
	P07342	ILV2	Mitochondrial Acetolactate synthase catalytic subunit
	P38988	GGC1	Mitochondrial GTP/GDP carrier protein 1
PM protein	P38856	YAP1801	Clathrin coat assembly protein
Others	P16474	KAR2	Endoplasmic reticulum chaperone BiP
	P27614	CPS1	Carboxypeptidase S
	P03965	CPA2	Carbamoyl-phosphate synthase arginine-specific large chain



Supplemental S4: Absence of Arc1 does not prevent MetRS aggregation. Haploid *mes1Δ* strains expressing ectopic MetRS-GFP (WT or $\Delta 132$) deleted (*arc1Δ*) or not (WT) of *ARC1* gene were imaged after 9 min heat shock at 48 °C. Cytosolic foci are observed for MetRS(WT)-GFP even in the absence of Arc1. Scale bar, 5 μ m.



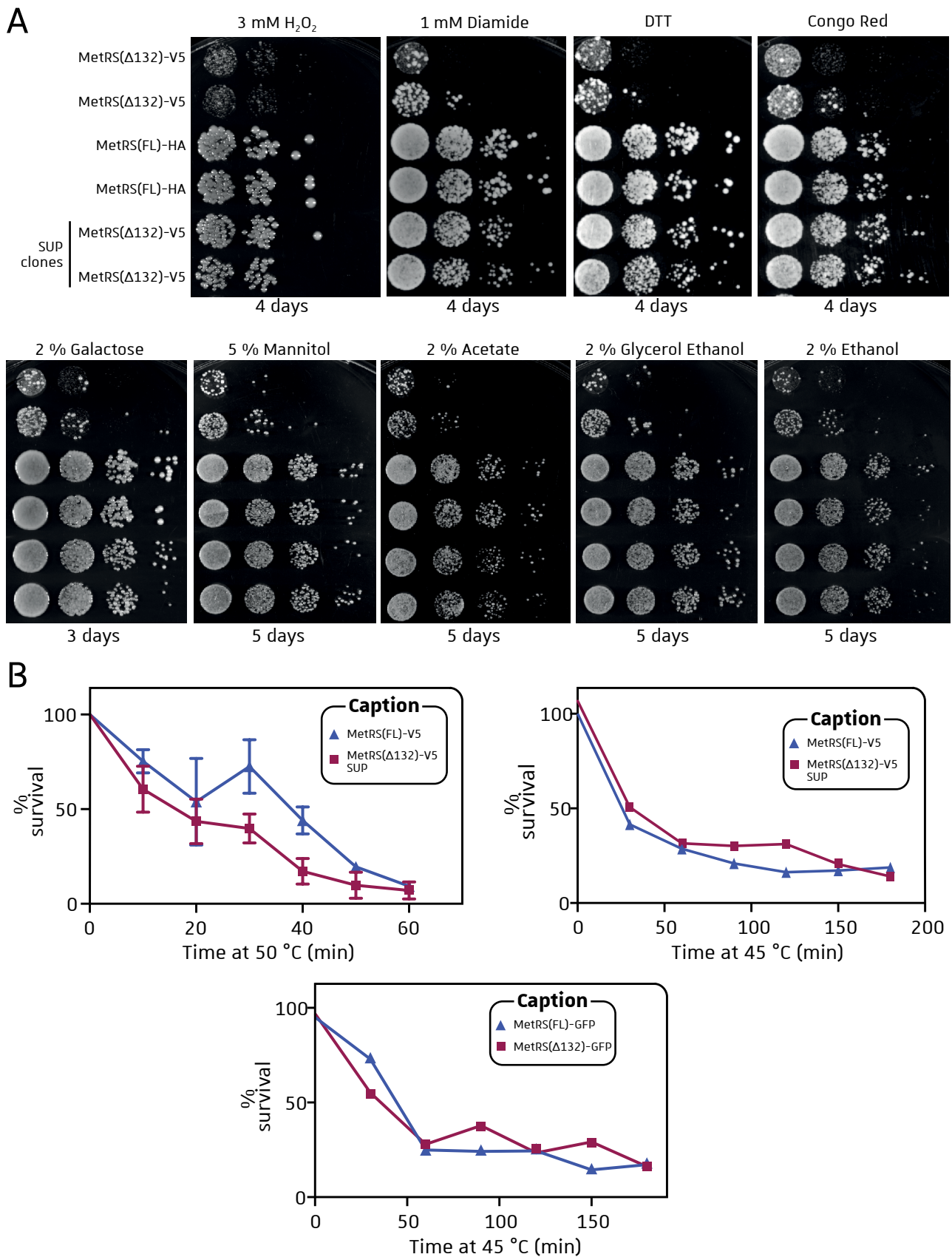
Supplemental S5: Sequence comparison of N-terminal domains of the yeast MetRS and GluRS. The N-terminal domain (1-162) of the yeast MetRS (orange) is compared with the N-terminal domain (1-178) of the yeast GluRS (purple). A pairwise sequence alignment gave only 3.6 % identity and 7.2 % similarity (EMBOSS Needle tool).



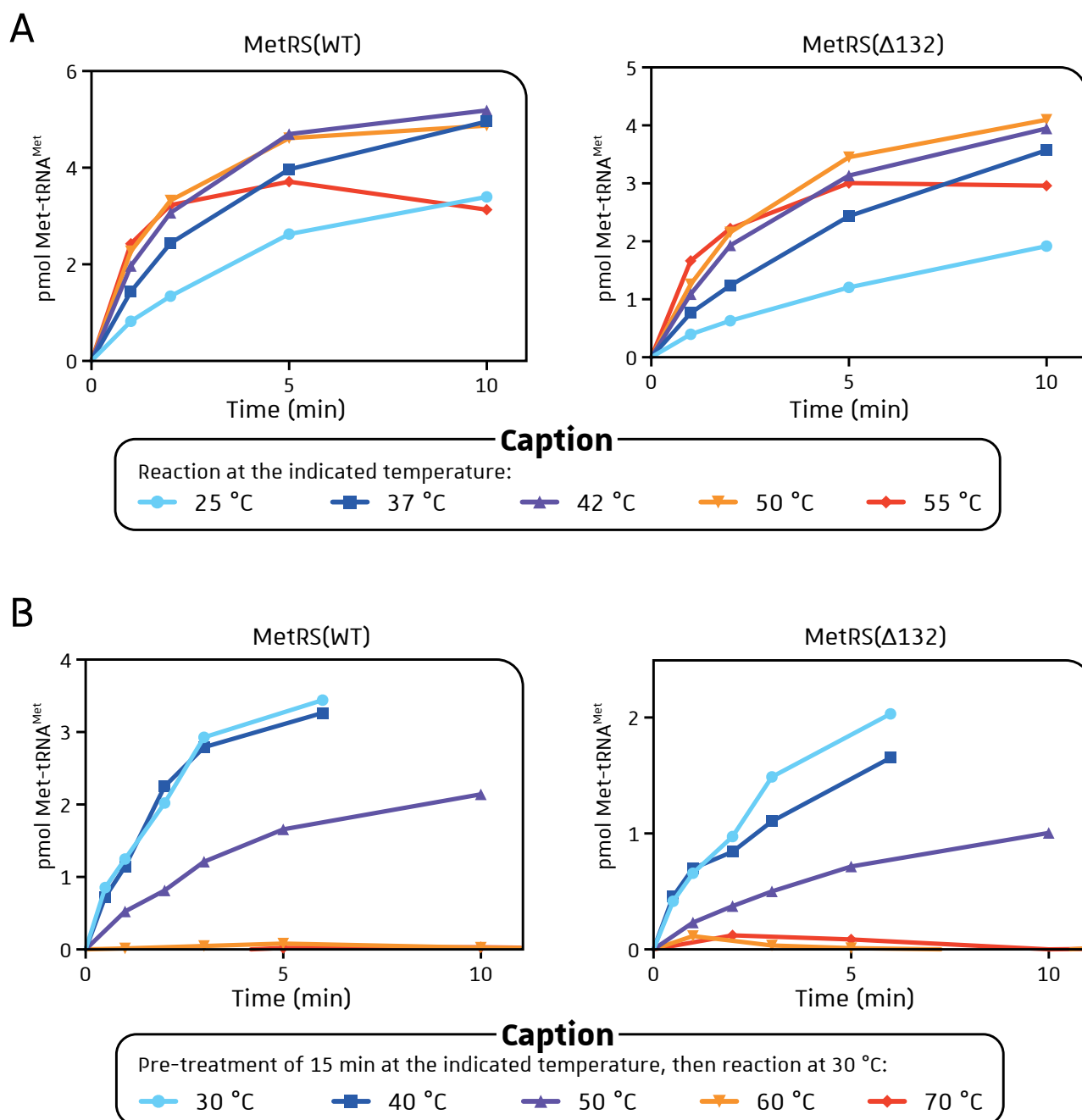
Supplemental S6: MetRS(Δ 132) does not interact with Arc1. Immunoprecipitation of MetRS-V5 with V5 antibody expressed in WT or *arc1 Δ* strain and co-immunoprecipitation of Arc1 for MetRS(WT). Input: input of total proteins loaded for the IP (5 % loaded on the gel). Ø: elution with IgG beads. IP:V5: elution with V5 antibody beads. The IP fractions were immunoblotted with V5, Arc1 and Pep4 antibodies.

Table S3: List of genes found as copy number variants (CNVs) in strains MetRS(Δ 132) and MetRS(Δ 132) SUP.

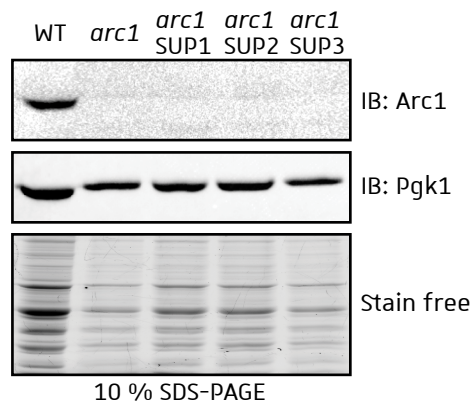
CNV loss or gain	Systematic name	Standard name	Protein description
Loss in SUP	YIR039C	YPS6	Putative GPI-anchored aspartic protease; member of the yapsin family of proteases involved in cell wall growth and maintenance
	YLR155C	ASP3-1	Cell-wall Asp3p catalyzes the conversion of L-asparagine to aspartate and ammonia. Asp3p is secreted in response to nitrogen starvation
	YDR038C	ENA5	Protein with similarity to P-type ATPase sodium pumps; member of the Na ⁺ efflux ATPase family
	YFL002W-A		Retrotransposon TYA Gag and TYB Pol genes
	YAL065C		Putative protein of unknown function, similar to FLO1 and other flocculins
Gain in SUP	YHL048W	COS8	Endosomal protein involved in turnover of plasma membrane proteins
	YBR011C	IPP1	Cytoplasmic inorganic pyrophosphatase
	YHL048C-A		Putative protein of unknown function; identified by expression profiling and mass spectrometry
	YHL049C		Putative protein of unknown function
	YHL050C		Putative protein of unknown function; potential Cdc28p substrate
	YDR261C-C		Retrotransposon TYA Gag gene co-transcribed with TYB Pol; Gag processing produces capsid proteins
	YDR261C-D		Retrotransposon TYA Gag and TYB Pol genes



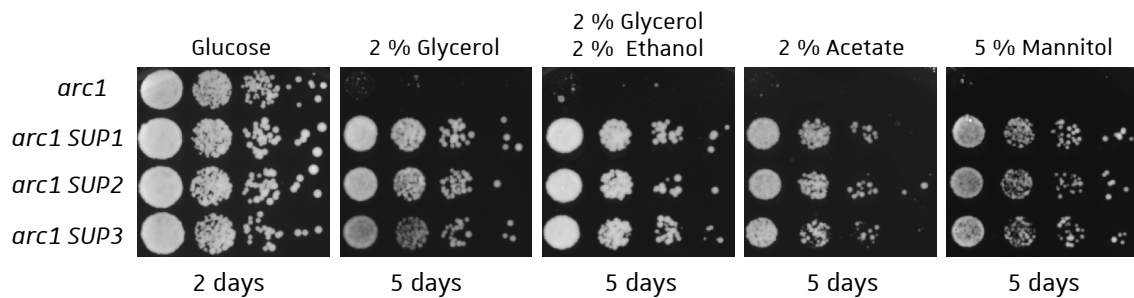
Supplemental S7: Growth and survival phenotype of strains in different stress conditions. A. Yeast spotting assay of the strains expressing the sole MetRS(WT) or MetRS(Δ132) isoform. Cells are spotted onto a YPD medium with different stress molecules (upper panel) or in different nutritional media (lower panel). **B.** Yeast survival assay after heat shock from 30 °C to 50 °C or 45 °C, in YPD liquid medium. For each time point, cells are plated on YPD agar plates and colonies are counted for survival. The number of colonies at t=0 was set at 100 %.



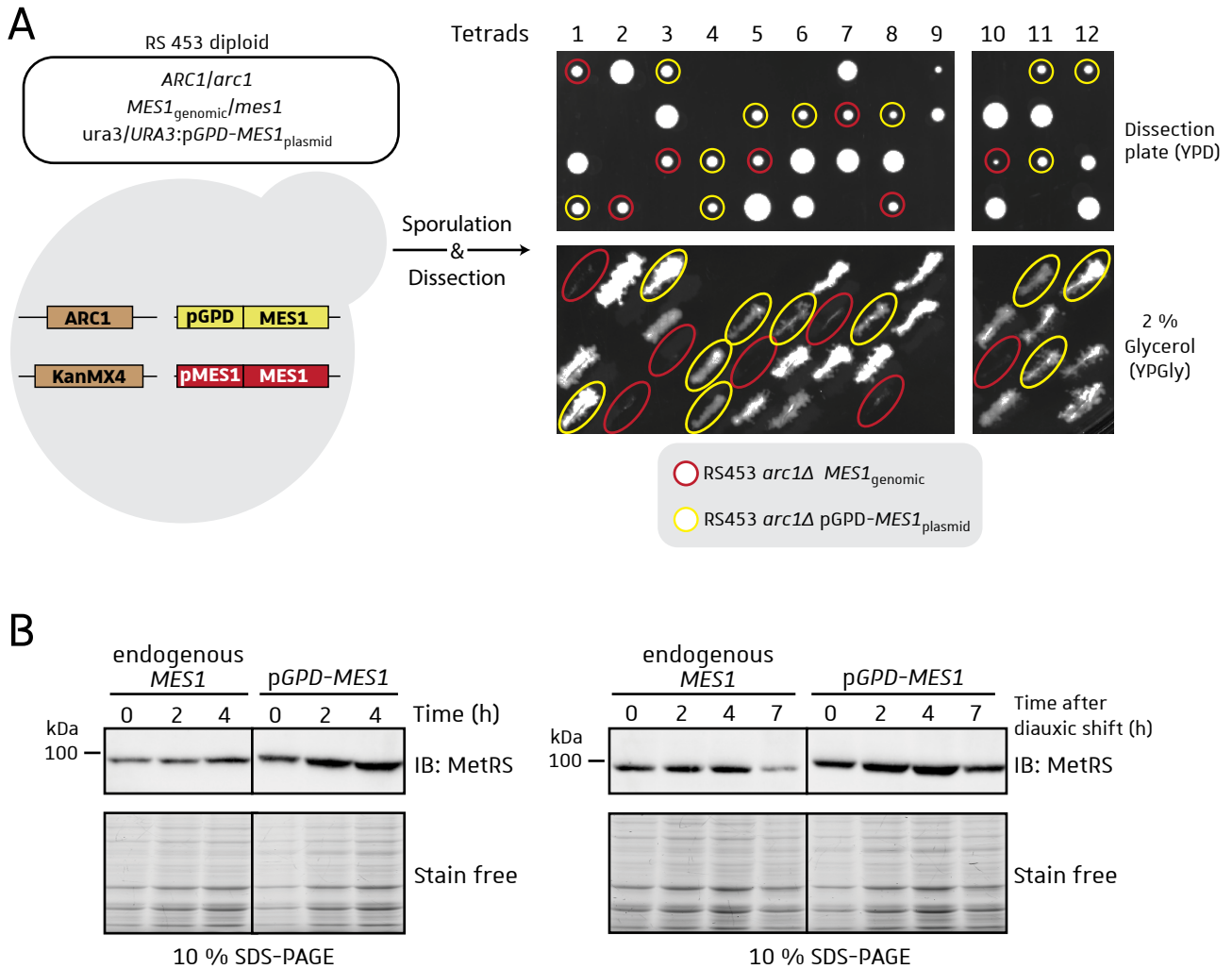
Supplemental S8: Time course of aminoacylation of yeast tRNA by the recombinant yeast MetRS(WT) and MetRS(Δ 132). **A.** Reactions were conducted at the indicated temperature for 10 min with 10 nM enzymes and 80 μ M yeast total tRNA. **B.** The enzymes were treated at the indicated temperature for 15 min before aminoacylation reaction at 30 °C with 10 nM enzymes and 80 μ M yeast total tRNA.



Supplemental S9: Confirmation of the deletion of *ARC1* gene in the *arc1* SUP strains. Western blotting of *arc1Δ* strain and the corresponding *arc1* SUP strains obtained by growth on respiratory medium (YPgly).



Supplemental S10: Growth of several *arc1Δ* strains (SUP strains) on various respiratory media. Yeast spotting assay of *arc1Δ* strain and three *arc1Δ* SUP strains in rich media with fermentative carbon source (2 % glucose) or various respiratory carbon sources.

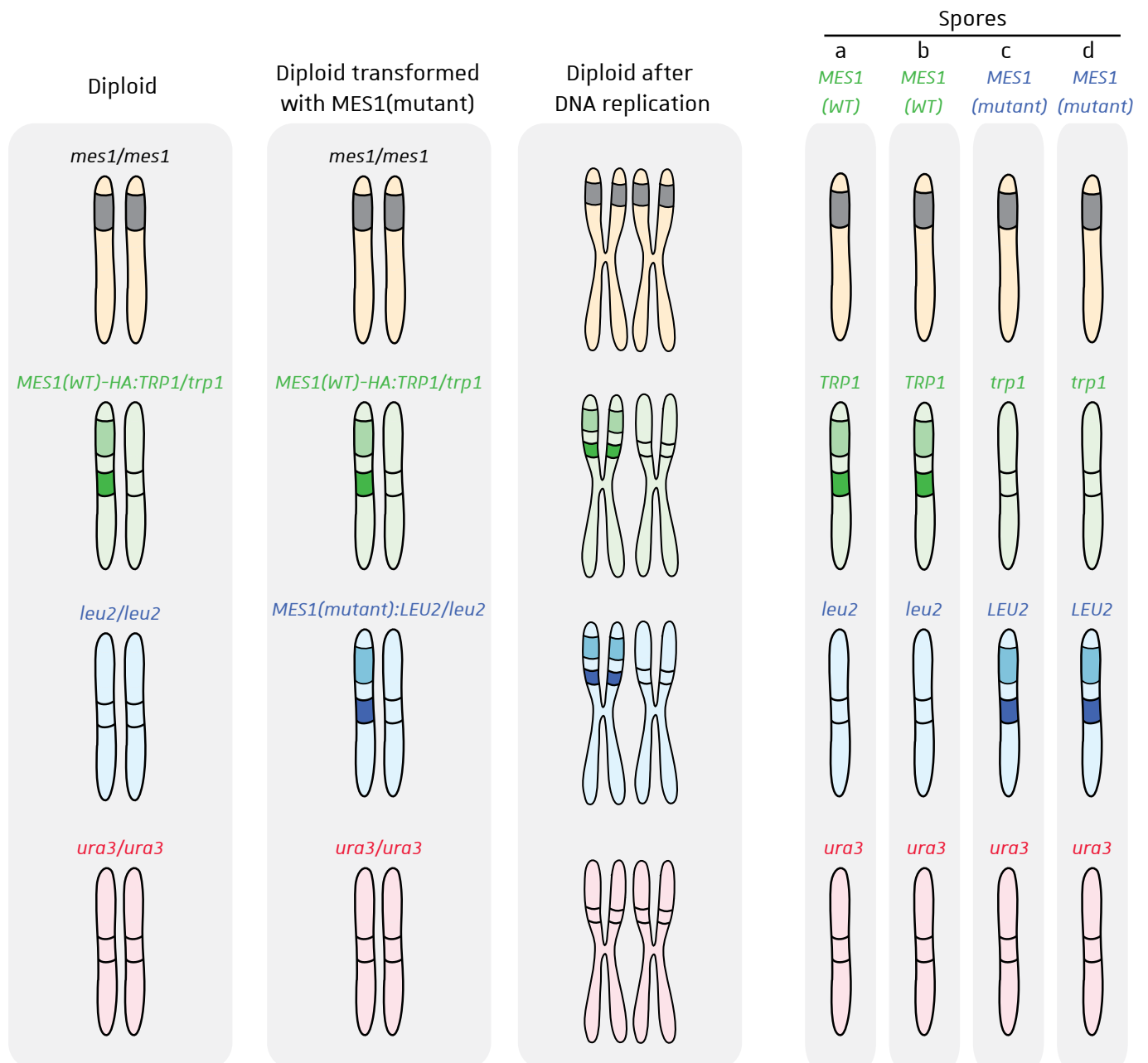


Supplemental S11: Overexpression of MetRS in *arc1Δ* strain restores growth in respiratory medium.

A. Sporulation and dissection of a diploid strain *ARC1/arc1* expressing both genomic *MES1* (with its endogenous promoter) and plasmidic *MES1* (under control *GPD* promoter). Genotype of each spore was determined, and *arc1Δ* spores with genomic *MES1* (red circles) or overexpressed plasmidic *MES1* (yellow circles). Each spore was grown on YPGly medium (glycerol, lower panel) and observed after 5 days at 30 °C. **B.** Western blotting of total protein extracts from RS453 strains expressing either the endogenous MetRS or the ectopic MetRS under control of the pGPD promoter. Yeast cells were grown in YPD rich medium. At t=0, cells were harvested and grown either in the same YPD medium (left panel) or in respiratory YPGly rich medium (right panel).

About dissection tables:

The diploid used for sporulation and dissection is a *mes1/mes1* strain expressing an ectopic *MES1(WT)-HA* at the *TRP1* locus. Dissection of tetrads from this diploid gives rise to a 2:2 segregation (Table dissection 1). To test the viability of a *MES1(mutant)* gene, this diploid is transformed with *MES1(mutant)* gene (at *LEU2* or *URA3* locus), and tetrads are analysed after dissection. If more than 2 viable spores are obtained on the dissection plate (YPD), the *MES1(mutant)* gene can supply the absence of the *MES1(WT)* gene.



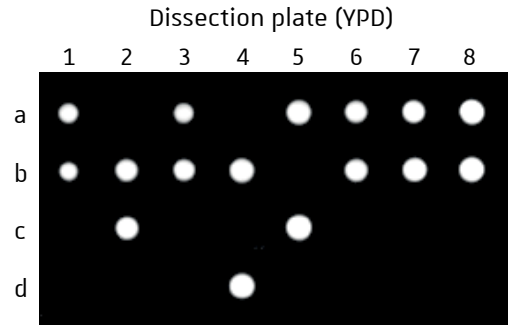
Supplemental S12: Chromosomes segregation during sporulation and spores viability. The diploid *mes1/mes1* strain is transformed with *MES1(mutant)* gene associated with *TRP1* to provide Trp auxotrophy. After DNA replication and chromosome segregation, viability of each spores is observed, and gene content is assessed by auxotrophy upon growth on minimal media. Only one combination of chromosome segregation is represented here, with two *MES1(WT)* spores and two *MES1(mutant)* spores.

Dissection Table 1:

Diploid strain
Genotype

mes1/mes1
MES1(WT)-HA:TRP1/trp1
ura3/ura3
leu2/leu2

Tetrads	Spores	YPD	YPGly	SC-His	SC-Trp	SC-Leu	SC-Ura
1	a	■	+	+	+	-	-
	b	■	+	+	+	-	-
	c						
	d						
2	a						
	b	■	+	+	+	-	-
	c	■	+	+	+	-	-
	d						
3	a	■	+	+	+	-	-
	b	■	+	+	+	-	-
	c						
	d						
4	a						
	b	■	+	+	+	-	-
	c						
	d	■	+	+	+	-	-
5	a	■	+	+	+	-	-
	b						
	c	■	+	+	+	-	-
	d						
6	a	■	+	+	+	-	-
	b	■	+	+	+	-	-
	c						
	d						
7	a	■	+	+	+	-	-
	b	■	+	+	+	-	-
	c						
	d						
8	a	■	+	+	+	-	-
	b	■	+	+	+	-	-
	c						
	d						



■ Spore grown on YPD

+ Growth on selective medium

- No growth on selective medium

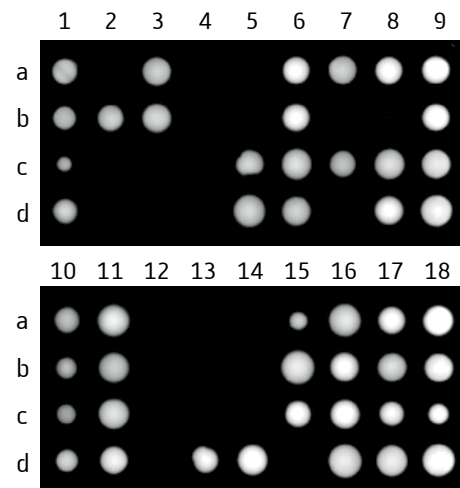
Purpose: To verify the 2:2 segregation of the diploid used for further transformations.

Dissection Table 2:

Diploid strain
Genotype*mes1/mes1*
MES1(WT)-HA:TRP1/trp1
MES1(WT)-cMyc:LEU2/leu2
URA3/ura3

Tetrads	Spores	YPD	YPGly	SC-Trp	SC-Leu	Sc-Ura
1	a		+	+	-	+
	b		+	+	-	+
	c		+	-	+	-
	d		+	-	+	-
2	a					
	b		+	+	+	+
	c					
	d					
3	a		+	+	+	+
	b		+	+	+	+
	c					
	d					
4	a					
	b					
	c					
	d					
5	a					
	b					
	c		+	+	+	+
	d		+	+	+	+
6	a		+	-	+	-
	b		+	-	+	-
	c		+	+	-	+
	d		+	+	-	+
7	a		+	+	+	+
	b					
	c		+	+	+	+
	d					
8	a		+	-	+	-
	b					
	c		+	+	-	+
	d		+	-	+	-
9	a		+	-	+	-
	b		+	-	+	-
	c		+	+	-	+
	d		+	+	-	+
10	a		+	+	-	+
	b		+	-	+	-
	c		+	+	-	+
	d		+	-	+	-
11	a		+	-	+	-
	b		+	+	-	+
	c		+	+	-	+
	d		+	-	+	-
12	a					
	b					
	c					
	d					
13	a					
	b					
	c					
	d		+	-	+	-
14	a					
	b					
	c					
	d		+	-	+	-
15	a		+	-	+	-
	b		+	+	-	+
	c		+	-	+	-
	d					
16	a		+	+	-	+
	b		+	-	+	-
	c		+	-	+	-
	d		+	+	-	+
17	a		+	-	+	-
	b		+	+	-	+
	c		+	-	+	-
	d		+	+	-	+
18	a		+	-	+	-
	b		+	+	-	+
	c		+	-	+	-
	d		+	+	-	+

Dissection plate (YPD)



- Spore grown on YPD
- + Growth on selective medium
- No growth on selective medium
- Spore with the sole *MetRS(WT)-cMyc* isoform

Purpose: Positive control to verify that the *MetRS(WT)-cMyc* sustains cell viability.

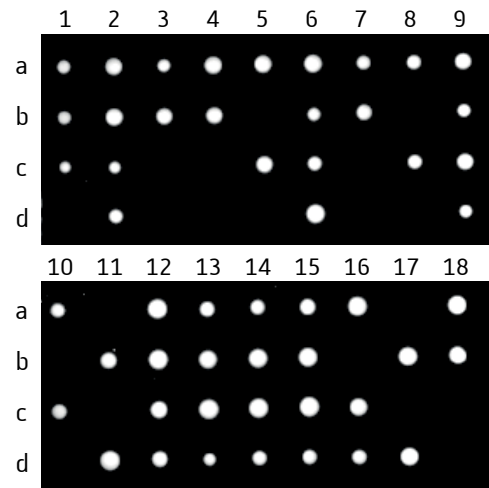
Dissection Table 4:

Diploid strain
Genotype

mes1/mes1
MES1(WT)-HA:TRP1/trp1
MES1(K11A)-cMyc:LEU2/leu2
URA3/ura3

Tetrads	Spores	YPD	YPGly	SC-Trp	SC-Leu	SC-Ura
1	a		+	+	+	+
	b		+	+	-	+
	c		+	-	+	-
	d					
2	a		+	+	-	+
	b		+	+	-	+
	c		+	-	+	-
	d		+	-	+	-
3	a		+	-	+	-
	b		+	+	-	+
	c					
	d					
4	a		+	+	+	+
	b		+	+	+	+
	c					
	d					
5	a		+	+	+	+
	b					
	c		+	+	+	+
	d					
6	a		+	+	-	+
	b		+	-	+	-
	c		+	-	+	-
	d		+	+	-	+
7	a		+	+	+	+
	b		+	+	+	+
	c					
	d					
8	a		+	+	+	+
	b					
	c		+	+	+	+
	d					
9	a		+	+	-	+
	b		+	-	+	-
	c		+	+	-	+
	d		+	-	+	-
10	a		+	+	+	+
	b					
	c		+	+	+	+
	d					
11	a					
	b		+	+	+	+
	c					
	d		+	+	+	+
12	a		+	+	-	+
	b		+	+	-	+
	c		+	-	+	-
	d		+	-	+	-
13	a		+	-	+	-
	b		+	+	-	+
	c		+	+	-	+
	d		+	-	+	-
14	a		+	-	+	-
	b		+	+	-	+
	c		+	+	-	+
	d		+	-	+	-
15	a		+	-	+	-
	b		+	+	-	+
	c		+	+	-	+
	d		+	-	+	-
16	a		+	+	-	+
	b					
	c		+	+	+	+
	d		+	-	+	-
17	a					
	b		+	+	+	+
	c					
	d		+	+	+	+
18	a		+	+	+	+
	b		+	+	+	+
	c					
	d					

Dissection plate (YPD)



Spore grown on YPD
 + Growth on selective medium
 - No growth on selective medium
 Spore with the sole
 MetRS(K11A) isoform

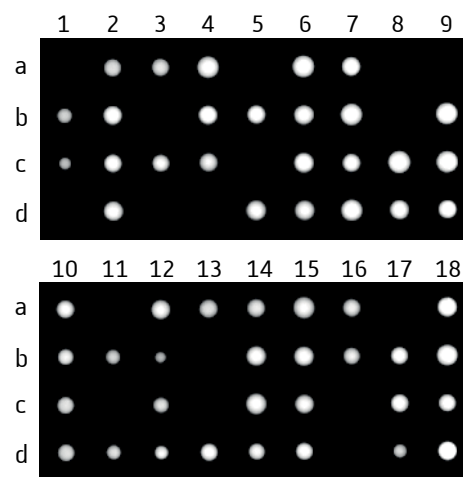
Purpose: To verify if MetRS(K11A)-cMyc mutant can sustain cell viability.

Dissection Table 5:

Diploid strain
Genotype*mes1/mes1*
MES1(WT)-HA::TRP1/trp1
MES1(S10A)-cMyc:LEU2/leu2
URA3/ura3

Tetrads	Spores	YPD	YPGly	SC-Trp	SC-Leu	SC-Ura
1	a					
	b		+	+	+	+
	c		+	+	+	+
	d					
2	a		+	+	-	+
	b		+	-	+	-
	c		+	-	+	-
	d		+	+	-	+
3	a		+	+	+	+
	b					
	c		+	+	+	+
	d					
4	a		+	+	-	+
	b		+	-	+	-
	c		+	-	+	-
	d					
5	a		+	-	+	-
	b		+	-	+	-
	c		+	-	+	-
	d		+	-	+	-
6	a		+	+	-	+
	b		+	+	-	+
	c		+	-	+	-
	d		+	-	+	-
7	a		+	-	+	-
	b		+	+	-	+
	c		+	-	+	-
	d		+	+	-	+
8	a					
	b					
	c		+	+	+	+
	d		+	+	+	+
9	a					
	b		+	+	-	+
	c		+	+	-	+
	d		+	-	+	-
10	a		+	-	+	-
	b		+	-	+	-
	c		+	+	-	+
	d		+	+	-	+
11	a					
	b		+	+	+	+
	c					
	d		+	+	+	+
12	a		+	-	+	-
	b		+	+	-	+
	c		+	+	-	+
	d		+	-	+	-
13	a		+	+	+	+
	b					
	c		+	+	+	+
	d		+	+	+	+
14	a		+	-	+	-
	b		+	-	+	-
	c		+	+	-	+
	d		+	+	-	+
15	a		+	+	-	+
	b		+	-	+	-
	c		+	+	-	+
	d		+	-	+	-
16	a		+	+	+	+
	b		+	+	+	+
	c					
	d					
17	a		+	-	+	-
	b		+	-	+	-
	c		+	-	+	-
	d		+	+	-	+
18	a		+	-	+	-
	b		+	+	-	+
	c		+	+	-	+
	d		+	-	+	-

Dissection plate (YPD)



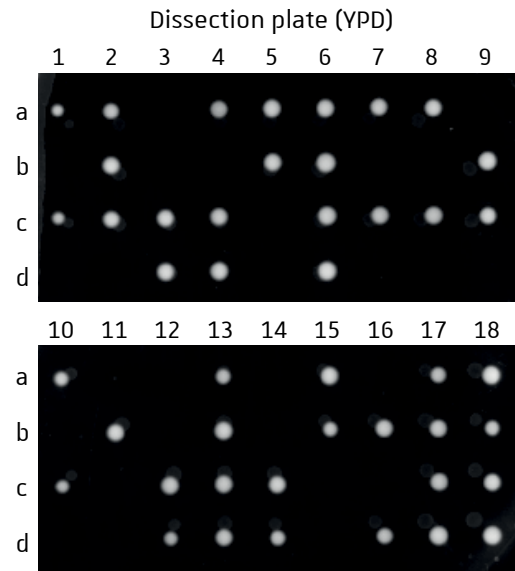
- Spore grown on YPD
- + Growth on selective medium
- No growth on selective medium
- Spore with the sole *MetRS(S10A)* isoform

Purpose: To verify if *MetRS(S10A)-cMyc* mutant can sustain cell viability.

Dissection Table 6:

Diploid strain
Genotype*mes1/mes1*
MES1(WT)-HA:TRP1/trp1
MES1(Y132A)-cMyc:LEU2/leu2
ura3/ura3

Tetrads	Spores	YPD	YPGly	SC-Trp	SC-Leu	SC-Ura
1	a	■	+	+	+	-
	b					
	c	■	+	+	+	-
	d					
2	a	■	+	+	+	-
	b	■	+	-	+	-
	c	■	+	+	-	-
	d					
3	a					
	b					
	c	■	+	+	+	-
	d		+	+	+	-
4	a	■	+	-	+	-
	b					
	c	■	+	+	-	-
	d		+	+	-	-
5	a	■	+	+	+	-
	b	■	+	+	+	-
	c					
	d					
6	a	■	+	+	-	-
	b	■	+	-	+	-
	c	■	+	+	-	-
	d	■	+	-	+	-
7	a	■	+	+	+	-
	b					
	c	■	+	+	+	-
	d					
8	a	■	+	+	+	-
	b					
	c	■	+	+	+	-
	d					
9	a					
	b	■	+	+	+	-
	c	■	+	+	+	-
	d					
10	a	■	+	+	+	-
	b					
	c	■	+	+	+	-
	d					
11	a					
	b	■	+	+	+	-
	c					
	d					
12	a					
	b					
	c	■	+	+	+	-
	d		+	+	+	-
13	a					
	b	■	+	+	-	-
	c	■	+	-	+	-
	d	■	+	+	-	-
14	a					
	b					
	c	■	+	+	+	-
	d		+	+	+	-
15	a	■	+	+	+	-
	b	■	+	+	+	-
	c					
	d					
16	a					
	b	■	+	+	+	-
	c					
	d	■	+	+	+	-
17	a	■	+	+	-	-
	b		+	+	-	-
	c	■	+	-	+	-
	d		+	-	+	-
18	a	■	+	-	-	-
	b		+	+	+	-
	c		+	+	+	-
	d		+	-	-	-



- Spore grown on YPD
- + Growth on selective medium
- No growth on selective medium
- Spore with the sole MetRS(Y132A) isoform

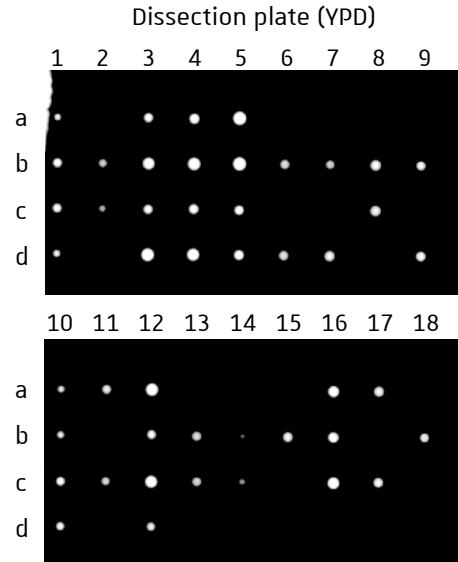
Purpose: To verify if MetRS(Y132A)-cMyc mutant can sustain cell viability.

Dissection Table 7:

Diploid strain
Genotype

mes1/mes1
MES1(WT)-HA:TRP1/trp1
leu2/leu2
MES1(Δ132)-V5:URA3/ura3

Tetrads	Spores	YPD	YPGly	SC-Trp	SC-Ura
1	a		+	+	-
	b		+	-	+
	c		+	-	+
	d		+	+	-
2	a				
	b		+	+	+
	c		+	+	+
	d				
3	a		+	+	-
	b		+	-	+
	c		+	+	-
	d		+	-	+
4	a		+	+	-
	b		+	-	+
	c		+	+	-
	d		+	-	+
5	a		+	-	+
	b		+	-	+
	c		+	+	-
	d		+	+	-
6	a				
	b		+	+	+
	c				
	d		+	+	+
7	a				
	b		+	+	+
	c				
	d		+	+	+
8	a				
	b		+	+	+
	c		+	+	+
	d				
9	a				
	b		+	+	+
	c				
	d		+	+	+
10	a		+	+	-
	b		+	+	-
	c		+	-	+
	d		+	-	+
11	a		+	+	+
	b				
	c		+	+	+
	d				
12	a		+	-	+
	b		+	+	-
	c		+	-	+
	d		+	+	-
13	a				
	b		+	+	+
	c		+	+	+
	d				
14	a				
	b		+	+	+
	c		+	+	+
	d				
15	a				
	b		+	+	+
	c				
	d				
16	a		+	+	-
	b		+	+	-
	c		+	-	+
	d				
17	a		+	+	+
	b				
	c		+	+	+
	d				
18	a				
	b		+	+	+
	c				
	d				



Spore grown on YPD
 + Growth on selective medium
 - No growth on selective medium
 Spore with the sole *MetRS(Δ142)* isoform

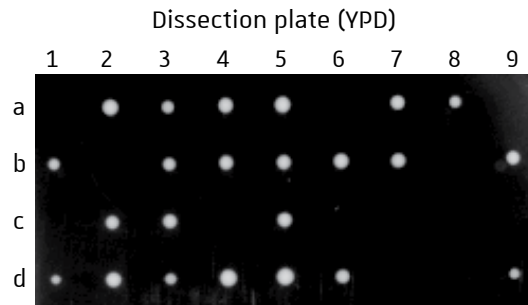
Purpose: To verify if *MetRS(Δ132)-V5* mutant can sustain cell viability.

Dissection Table 8:

Diploid strain
Genotype

mes1/mes1
MES1(WT)-HA:TRP1/trp1
MES1(Δ132)-V5:LEU2/leu2
ura3/ura3

Tetrads	Spores	YPD	YPGly	SC-Trp	SC-Leu	SC-Ura
1	a					
	b	■	+	+	+	-
	c					
	d	■	+	+	+	-
2	a	■	+	-	+	-
	b					
	c	■	+	+	+	-
	d	■	+	-	+	-
3	a	■	+	+	+	-
	b	■	+	+	+	-
	c	■	+	-	+	-
	d	■	+	-	+	-
4	a	■	+	-	+	-
	b	■	+	+	-	-
	c	■				
	d	■	+	-	+	-
5	a	■	+	-	+	-
	b	■	+	+	+	-
	c	■	+	+	+	-
	d	■	+	-	+	-
6	a					
	b	■	+	-	+	-
	c					
	d	■	+	+	-	-
7	a	■	+	+	-	-
	b	■	+	+	-	-
	c					
	d					
8	a	■	+	+	+	-
	b					
	c					
	d					
9	a					
	b	■	+	+	+	-
	c					
	d	■	+	+	+	-
10	a	■	+	+	-	-
	b					
	c					
	d					



- Spore grown on YPD
- + Growth on selective medium
- No growth on selective medium
- Spore with the sole *MetRS(Δ142)* isoform

Purpose: To verify if *MetRS(Δ132)-V5* mutant can sustain cell viability, and independently from the associated marker (*LEU2* instead of *URA3* in dissection 5).

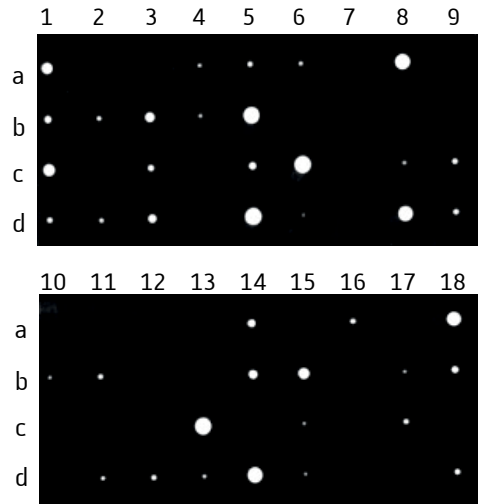
Dissection Table 9:

Diploid strain
Genotype

mes1/mes1
MES1(WT)-HA:TRP1/trp1
LEU2/leu2
MES1-VPH1-cMyc:URA3/ura3

Tetrads	Spores	YPD	YPGly	SC-Trp	SC-Leu	Sc-Ura
1	a		+	+	+	-
	b		+	-	-	+
	c		+	+	+	-
	d		+	-	-	+
2	a					
	b		+	+	+	+
	c					
	d		+	+	-	+
3	a					
	b		+	+	+	-
	c		+	-	-	+
	d		+	+	+	-
4	a		+	+	-	+
	b		+	+	-	+
	c					
	d					
5	a		+	-	+	+
	b		+	+	-	-
	c		+	-	+	+
	d		+	+	-	-
6	a		+	+	+	+
	b		+	+	+	+
	c		+	+	+	-
	d		+	-	-	+
7	a					
	b					
	c					
	d					
8	a		+	+	+	-
	b		+	+	+	-
	c		+	-	-	+
	d		+	+	+	-
9	a					
	b					
	c		+	+	+	+
	d		+	+	+	+
10	a					
	b		+	+	-	+
	c					
	d					
11	a					
	b		+	+	-	+
	c					
	d		+	+	-	+
12	a					
	b					
	c					
	d		+	+	+	+
13	a					
	b					
	c		+	+	-	-
	d		+	+	-	+
14	a		+	-	-	+
	b		+	-	-	+
	c					
	d		+	+	+	-
15	a					
	b		+	+	-	-
	c		+	+	-	+
	d		+	-	+	+
16	a		+	+	-	+
	b					
	c		+/-	+	-	+
	d					
17	a					
	b		+	+	-	+
	c		+	+	-	+
	d					
18	a		+	+	+	-
	b		+	-	+	+
	c					
	d		+	-	-	+

Dissection plate (YPD)



- Spore grown on YPD
- + Growth on selective medium
- No growth on selective medium
- Spore with the sole MetRS-Vph1 isoform





03

MATERIAL & METHODS

- I** **MOLECULAR BIOLOGY FOR GENE AMPLIFICATION AND CLONING** 221
- II** **PROCEDURE USED FOR *S. CEREVISIAE* CELLS** 229
- III** **BIOCHEMISTRY AND BIOPHYSICAL TECHNIQUES** 239
- IV** **PRIMERS, PLASMIDS AND YEAST STRAINS LISTS** 257



Table MM-1: *E. coli* competent strains used for cloning strategies

Strain	Genotype
DH5 α	F- endA1 glnV44 thi-1 recA1 relA1 gyrA96 deoR nupG Φ 80d/lacZ Δ M15 Δ (lacZYA-argF)U169 hsdR17(r _k ⁻ , m _k ⁻) λ -
XL1 Blue	endA1 gyrA96(nal ^R) thi-1 recA1 relA1 lac glnV44 F' [::Tn10 proAB+ lacI ^q lacZ Δ M15] hsdR17(r _k ⁻ , m _k ⁻) λ -

Table MM-2: Media for bacterial culture and antibiotic concentration used for selection

LB components	Concentration (g.L ⁻¹)	LB + antibiotics	Composition
Peptone	10	LB + Amp	LB composition + 100 mg.L ⁻¹ ampicilline
Yeast extract	5	LB + Kan	LB composition + 50 mg.L ⁻¹ kanamycine
NaCl	5		
Agar-agar (for solid medium)	15		

I. Molecular biology for gene amplification and cloning

I.1. Bacterial strains

Bacterial strains used to replicate plasmids derive from the K-12 strain and are listed in **Table MM-1**. They carry genomic and/or plasmid mutations that allow high plasmid yield.

I.2. Bacterial growth media

For bacterial growth, the common medium used is LB-Miller medium, a rich medium containing peptone, yeast extract and NaCl (composition detailed in **Table MM-2**). For solid medium, agar-agar is added at 15 g.L⁻¹. Liquid and solid media are autoclaved at 120 °C, 1.2 bars for 20 min. For plasmid selection during cloning, antibiotics are supplemented in solid media before pouring the plates or in liquid media before use, only when the medium has reached about 50 °C (concentrations used in **Table MM-2**). All media are stored at 4 °C.

I.3. Calcium chloride competent cell protocol

A single colony is inoculated in LB medium and incubated overnight (O/N) at 37 °C. Cells are diluted in 200–300 mL in the morning at OD_{600 nm} = 0.2 and grow at 18 °C until they reach OD_{600 nm} = 0.6. All the subsequent steps need to be realized at 4 °C, which includes cooling of the materials and solutions. After 10 min on ice, cells are centrifuged 10 min at 2,500 × *g*. Pellet is gently resuspended in 80 mL cold TBjap buffer (10 mM Na-PIPES, pH 6.7, 15 mM CaCl₂, 250 mM KCl, 55 mM MnCl₂, 2 % (v/v) DMSO). Keep the suspension on ice 10 min, then centrifuge 10 min at 2,500 × *g*, then discard supernatant and add 20 mL of TBjap buffer with 7 % (v/v) DMSO. After 10 min incubation on ice, competent cells are aliquoted (100 µL) and immediately flash-frozen in liquid nitrogen. Competent cells are stored at -80 °C.

I.4. Bacterial cell transformation

Competent cells in TBjap buffer are thawed slowly on ice for about 15 min, then the plasmid construction (from a ligation mixture or from an intact plasmid) is added to the cells (1 ng of plasmid or around 1 µg of a ligation products mixture) and incubated 20 min on ice. Cells are heat-shocked at 42 °C in a water-bath for 45 s and put back on ice for 2–3 min. Cells are then plated on a

Table MM-3: PCR protocol details according to the kit used.

		Plasmid DNA PCR	Yeast gDNA PCR	Yeast colony PCR
PCR mix composition	Enzyme (Kit)	PrimeSTAR Max [®]	Phusion [™]	Phire Plant direct Kit
	Primer Forward (μM)		0.5	
	Primer Reverse (μM)		0.5	
	Template DNA (ng)	0.5-1	10-200	a small colony
	Enzyme (or mix) (μL)	10	0.2	10
	Enzyme buffer (μL)		4	
	dNTP 10 mM (μL)		0.4	
	H ₂ O (μL)	up to 20 μL		
Cycling protocol	Initial denaturation at 98 °C (min)	2	2	5
	Denaturation time at 98 °C (s)		10	
	Annealing time at 55 °C (s)		10	
	Elongation time at 72 °C (s.kb ⁻¹)	5	30	20
	Number of cycles	16-30	30	30
	Final extension time at 72 °C (min)		2	

LB-agar plate supplemented with the appropriate antibiotics (see **Table MM-2**). For transformation with kanamycin resistance-encoding plasmids, 1 mL of LB is added on cells after the heat-shock and incubated at 37 °C for 45 min to allow the expression of the resistance protein before adding the antibiotic. LB-agar plates are then incubated O/N at 37 °C.

I.5. Plasmid extraction from bacterial cell

After O/N incubation at 37 °C, isolated bacterial colonies are incubated in 2-3 mL of LB medium supplemented with the adequate antibiotic and incubated at 37 °C O/N under shaking (Multitron, INFORS HT). Cells are then centrifuged at $6,000 \times g$ for 3 min and plasmid DNA is extracted with the EZ-10 Spin Column Plasmid DNA Miniprep kit (BIO BASIC) following supplier's instructions.

I.6. PCR amplification of DNA fragments

Fragments of interest are amplified by PCR (Polymerase Chain Reaction) using primers designed according to the cloning strategy. Depending on the DNA template used for the PCR, different enzymes and protocols are used (**Table MM-3**). All PCR reactions are performed on a thermocycler (C1000 Touch™ Thermal Cycler from Bio-Rad). Primers used to amplify yeast genomic DNA are listed in **Table-MM10** page 257.

I.7. DNA visualisation under UV light

PCR fragments or plasmids digested by restriction enzymes are loaded onto a 1-2 % (w/v) agarose gel in TAE buffer (40 mM Tris, 20 mM acetate, 1 mM EDTA) and submitted to electrophoresis in the same TAE buffer for 20-30 min at 8 V/cm. The gel is then incubated for 20-30 min in a 0.5 µg/mL ethidium bromide solution in water, washed with water and visualized with GeneTools software on an UV imaging system (G:BOX Chemi XT from Syngene).

I.8. PCR DNA clean up and gel extraction

To purify DNA from a protein-containing solution (restriction enzyme, kinase or phosphatase), the sample is either directly purified on columns with NucleoSpin® Gel and PCR Clean-up kit (Macherey-Nagel) or loaded on an agarose gel for electrophoresis then purified on gel with the same clean-up kit, following manufacturer's instructions.

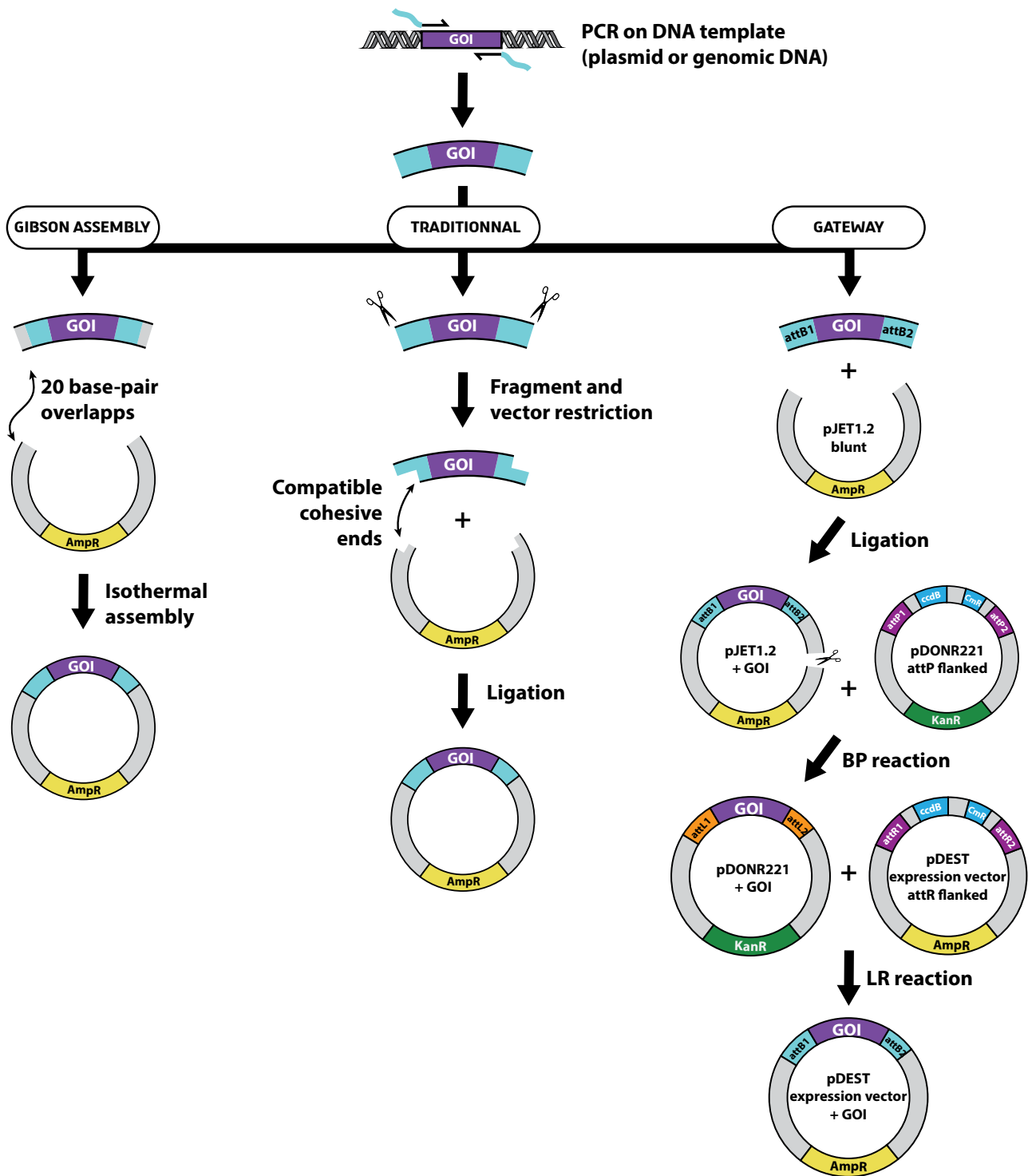


Figure MM-1: Schematic representation of the different cloning strategies used. GOI: Gene Of Interest. More descriptions are given in §1.10 in the text section.

I.9. Enzymatic restriction of plasmids

To monitor construction of recombinant plasmids, or to simply digest a plasmid in order to use it for the next cloning steps, restriction enzymes have been used (FastDigest enzymes from Thermo Scientific). Around 0.5–1 µg of plasmid (or PCR fragment) is digested with 0.5 µL of enzyme in 20 µL, with 2 µL of FD buffer 10×. Reaction is incubated at 37 °C for 15–20 min, and samples are loaded onto an agarose gel 1 % (w/v) and visualized as mentioned above.

I.10. Cloning strategies

To design expression plasmids for bacteria and/or yeast, I have used different cloning strategies, depending on the material available in the lab and the type of cloning needed. The techniques used are: traditional cloning, gateway strategy or Gibson assembly® (see **Figure MM-1** for description).

I.10.1. Traditional cloning

Gene of interest (GOI) is amplified by PCR with primers flanked by restriction sites. The corresponding restriction enzymes are used to digest the amplicon and the destination DNA plasmid vector following the restriction protocol mentioned above. The vector is also dephosphorylated in the same restriction FD buffer by addition of 1 µL of phosphatase (FastAP Thermosensitive Alkaline Phosphatase, Thermo Fisher) for 1 h at 37 °C. Both the digested PCR fragment and the dephosphorylated vector are purified on gel after electrophoresis on 1 % (w/v) agarose gel (see above for details). Concentration of each DNA sample is determined by absorption at 260 nm with a microvolume spectrophotometer NanoDrop™ 2000 (ThermoFisher). Ligation of the insert in the vector is carried out by mixing them with a ratio insert:vector of approximately 1:5, with 1 µL of PEG4000 Solution (ThermoFisher) at 65 °C for 5 min in 17 µL of reaction mixture. After 5 min at room temperature (RT), 2 µL of T4 DNA ligase and 1 µL T4 DNA ligase (ThermoFisher) are added to the mix and incubated 1 h at RT. Finally, 5 µL of the ligation mix is used to transform competent bacterial cells.

I.10.2. Gateway™ cloning

Gene of interest (GOI) is amplified by PCR with primers flanked by attB1 (for the forward primer) or attB2 (for the reverse primer). After cleaning-up, the insert is ligated into the linearized pJET1.2/blunt with the CloneJET PCR Cloning kit (Thermo Scientific, supplier protocol). After ligation, 5 µL of the mix is used to transform competent bacterial cells. After confirmation that the pJET1.2/GOI

Table MM-4: Composition of the 1 × Gibson assembly buffer.

	Components	Concentration
Buffer	Tris-HCl pH 7.5	100 mM
	MgCl ₂	10 mM
	DTT	10 mM
	NAD ⁺	1 mM
	each of the 4 dNTPs	2 mM
	PEG-8000	5% (w/v)
Enzymes	T5 exonuclease	7.5 U.mL ⁻¹
	Phusion DNA pol	25 U.ml ⁻¹
	Taq DNA ligase	200 U.ml ⁻¹

plasmid construction is as expected, 1 µg of this plasmid is linearized in a 20 µL (restriction site has to be outside the GOI sequence) restriction mixture, the restriction enzyme is inactivated by heating, then 5 µL are mixed with 150 ng of donor vector pDONR221 for BP recombination with the Gateway™ BP Clonase™ II Enzyme mix (Thermo Scientific). After O/N incubation at 25 °C, 2 µL of the recombination mix is used to transform competent bacterial cells and cells are incubated on LB agar plate supplemented with kanamycin (50 mg.L⁻¹). The resulting pDONR221/GOI vector is a shuttle vector allowing LR recombination of the GOI in any expression vector present in our gateway plasmid collection. For the LR recombination, 150 ng of each plasmid (pDONR221/GOI and expression vector) are mixed in 10 µL of LR recombinase buffer with the Gateway™ LR Clonase™ II Enzyme mix (Thermo Scientific). After 2 h of incubation at 25 °C, 2 µL of the LR recombination mix is used to transform competent bacterial cells and cells are incubated on LB agar plate supplemented with ampicillin (100 mg.L⁻¹).

I.10.3. Gibson assembly

Gene of interest (GOI) is amplified by PCR with primers flanked with sequences of 20 nucleotides overlapping sequences present in the linearized destination vector. If the GOI is amplified from a plasmid template, PCR product is digested 1 h at 37 °C with DpnI restriction enzyme to decay specifically the template and then cleaned up. The linearized plasmid is also cleaned up to remove restriction enzymes. Both cleaned up products are ligated in 20 µL of Gibson assembly buffer (see **Table MM-4** for composition). Finally, 5 µL of the ligation mixture is used to transform competent bacterial cells.

I.11. Plasmid sequence verification

To first verify the integrity of the plasmid, restriction digestion with specific restriction enzymes is performed and visualization of plasmid digestion is carried out to confirm the digestion profile. The positive plasmid clones are then sent for Sanger DNA sequencing with a specific primer (SupremeRun, GATC Biotech, Eurofins Genomics). The sequence results are analysed with ApE plasmid editor software. Specific primers used for sequencing are listed in **Table MM-11** page 258.

Table MM-5: Composition of yeast rich media

	Components	Final concentration w/v (amount per liter)	Medium description
Common components for rich media	Peptone	2 % (20 g)	Source of carbon, nitrogen, vitamins and minerals
	Yeast extract	1 % (10 g)	Supplies B-complex vitamins
	Agar-agar (for solid medium)	2 % (20 g)	
Medium name	+ carbohydrate source		
YPD	Dextrose (D-glucose)	2 % (20 g)	Fermentable carbon sources
YPGal	D-Galactose	2 % (20 g)	
YPGly	Glycerol	2 % (20 g)	Nonfermentable carbon sources
YPEtOH	Ethanol	3 % (30 g)	
YPGlyEtOH	Ethanol + Glycerol	3% each (30 g)	
YPACK	Potassium acetate	2 % (20 g)	
YPMAN	Mannitol	5 % (50 g)	

Table MM-6: Composition of yeast synthetic media

	Components	Final concentration	Medium description
Common components for synthetic media	Yeast Nitrogen Base (YNB) with ammonium sulfate	6.7 g.L ⁻¹	Source of nitrogen, vitamins, salts and trace elements
	Agar-agar (for solid medium)	2 % (20 g)	
Medium name	+ amino acids and nucleotides source		
SD	None		
SC	Complete Supplement Mixture (CSM)	0.79 g.L ⁻¹	All amino acids are present, plus adenine and uracil
SC-aa/nb	CSM - aa/nb	Depending on the CSM used	All amino acids except specific aa. Sometimes without a nitrogen base (uracil or adenine).
Medium name	+ carbohydrate source		
SD/SC	Dextrose (D-glucose)	2 % (20 g)	Fermentable carbon sources
SCGal	D-Galactose	2 % (20 g)	
SCGly	Glycerol	2 % (20 g)	Nonfermentable carbon sources

Table MM-7: Composition of yeast specific media

	Components	Final concentration	Medium description
SPM	Potassium acetate	1 % (10 g)	Sporulation medium
	Agar-agar	2 % (20 g)	
SFOA	Yeast Nitrogen Base (YNB) with ammonium sulfate	6.7 g.L ⁻¹	Used to select the loss of vectors carrying <i>URA3</i> gene.
	Dextrose (D-glucose)	2 % (20 g)	
	Complete Supplement Mixture (CSM)	0.79 g.L ⁻¹	
	5-Fluorotic Acid (SFOA)	2.5 mM	
	Agar-agar	2 % (20 g)	
YPD + G418	Peptone	2 % (20 g)	Medium used to select yeast containing the <i>KanMX4</i> allele.
	Yeast extract	1 % (10 g)	
	Dextrose (D-glucose)	2 % (20 g)	
	Geneticin (G418)	200 µg.mL ⁻¹	
	Agar-agar (for solid medium)	2 % (20 g)	
SD-N	Yeast Nitrogen Base (YNB) without ammonium sulfate	1.7 g.L ⁻¹	Nitrogen starvation medium to induce autophagy
	Dextrose (D-glucose)	2 % (20 g)	
	Agar-agar (for solid medium)	2 % (20 g)	

II. Procedures used for *S. cerevisiae* cells

II.1. Yeast growth media

All yeast media are listed in **Table MM-5** to **MM-7**. Yeast cells can be grown in either liquid medium or on solid agar plates. Two types of media can be used: minimal medium (SC, Synthetic Complete or SD, Synthetic Defined) or rich medium (YPD, Yeast extract–Peptone–Dextrose). The latter (**Table MM-5**) cannot be used for auxotrophic selection since all aa and nucleotides are present. However, this medium can be supplemented with Geneticin (G418) to select clones with the *KanMX4* allele (see **Table MM-7**). Synthetic media contain defined amounts of each component (**Table MM-6**). The use of synthetic media with all aa except specified ones allows auxotrophic selection. Depending on the carbohydrate source, yeast cells perform either fermentation or respiration. Liquid and solid media are autoclaved at 120 °C, 1.2 bars for 20 min. Geneticin is added after autoclaving, once the medium temperature has dropped to 50 °C.

II.2. Yeast growth phases and OD monitoring

In most of the experiments with yeast, cells need to be collected when they reach the mid-logarithmic (or exponential) growth phase (mid-og phase) (**Figure MM-2**). With our in house spectrophotometer (DU®730, Beckman Coulter), this phase is corresponding to an $OD_{600\text{ nm}} = 0.5 - 1.5$. On average, the doubling time (DT) of wild-type yeast strains is 90 min. To dilute yeast suspension at the right initial $OD_{600\text{ nm}}$ to be in the log phase (OD_t) after a certain time (t), the calculation is made as follow:

$$OD_0 = \frac{OD_t}{2^{\frac{t}{DT}}}$$

To verify the $OD_{600\text{ nm}}$, 1 ml of the culture is added to a polystyrene spectrophotometer cuvette and the $OD_{600\text{ nm}}$ is measured with the spectrophotometer DU®730, Beckman Coulter. If the $OD_{600\text{ nm}}$ is over 1, a 1/10 dilution is measured to be more accurate.

For growth phenotyping assay, yeast cells are diluted at initial $OD_{600\text{ nm}} = 0.05$ and inoculated into a final volume of 100 µL in a 96-well microplate. This plate is then shaken in a thermostated microplate reader (SAFAS Xenius XMA) for 48 h of orbital shaking (600 rpm) in cycle of 30 min followed by $OD_{600\text{ nm}}$ measurement.

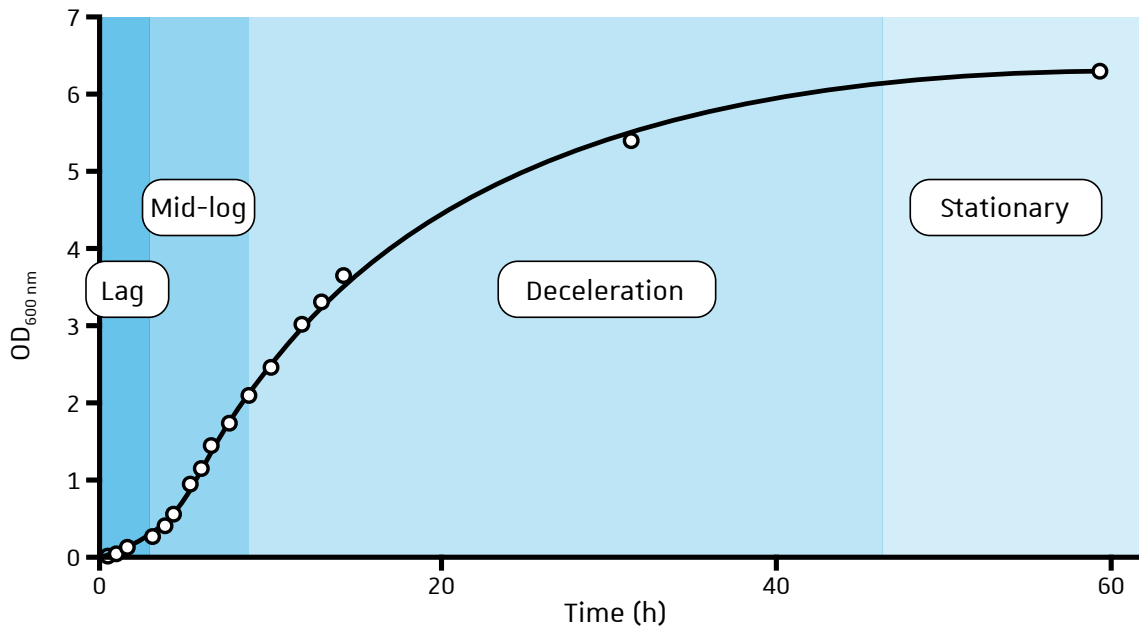


Figure MM-2: Yeast growth curve and the different growth phases. Yeast strain (RS453) was grown at 30 °C in YPD medium under constant agitation. Cells are harvested when they reach the mid-log phase.

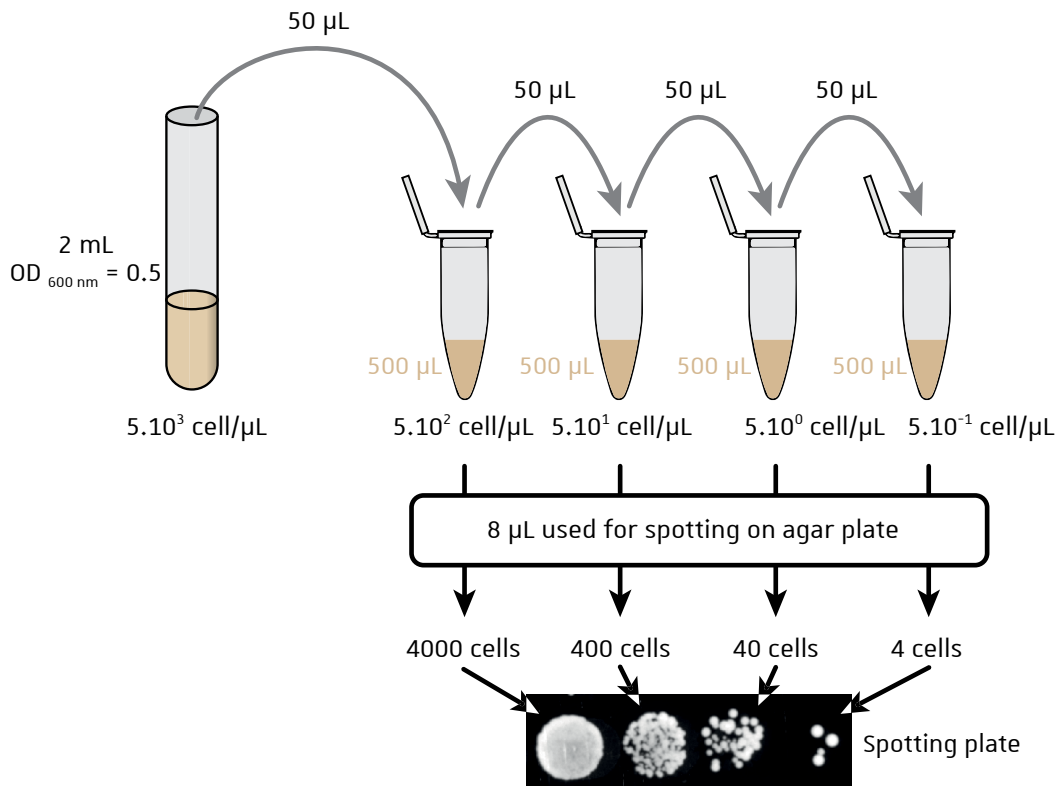


Figure MM-3: Protocol for yeast spotting assay. Freshly yeast cell suspension (mid-log phase) is adjusted to OD_{600nm} = 0.5, and ten-fold dilutions are prepared in sterile water. Then 8 μL of each dilution is spotted on the agar plate.

II.3. Yeast transformation

We used the lithium method for yeast transformation adapted from (Gietz and Woods, 2002). All steps need to be performed in a sterile environment and all buffers are sterile/sterilized. Cells are collected when the $OD_{600\text{ nm}}$ has reached the stationary phase, centrifuged at $4,500 \times g$ for 5 min, then 3 OD equivalent units are used for one transformation: cell pellet is resuspended in 50 μL of water, and 20 μL of boiled and sonicated single-stranded DNA ($10\text{ mg}\cdot\text{mL}^{-1}$) is added to cells. Then 350 μL of transformation mix (240 μL of PEG 4000, 36 μL LiAc 1M, 70 μL water) is added, cells are resuspended by vortex mixing and incubated for 45 min at $42\text{ }^\circ\text{C}$ in a water bath. The tube is then centrifuged at $10,000 \times g$ for 10 s, the supernatant is removed and 1 mL of water is added to wash cells and remove traces of LiAc. After a $10,000 \times g$ centrifugation for 10 s, cells are resuspended in 200 μL of water and spread onto the appropriate selection medium.

II.4. Serial dilution spotting assay

Drop tests are performed with fresh cells ($OD_{600\text{ nm}} = 0.5 - 1.5$) of each tested strain resuspended in sterile distilled water and adjusted to the same initial $OD_{600\text{ nm}} = 0.5$. Ten-fold serial dilutions are prepared in water (10, 100, 1,000 and 10,000; see **Figure MM-3**), and 8 μL aliquots of each dilution are spotted on appropriate agar plate vmedium. Plates are incubated at $30\text{ }^\circ\text{C}$ for several days and photographed daily.

II.5. Yeast mating procedure

Yeast mating has been used to create diploids and to determine the essentiality of a gene by using yeast sporulation. It is also convenient to introduce two different plasmids or mutations into the same host cell and can be used as an alternative to yeast co-transformation. The procedure relies on the mating of two haploids strains with different mating type (a and α).

II.5.1. Mating on agar plate

Mating on solid medium is performed when selection by at least one auxotrophic marker is possible. The two mating type strains are grown on appropriate agar medium, and then mixed on an YPD agar plate, with very small amount of the strain with the selectable marker compared to the other one. The strain mixture is incubated O/N at $30\text{ }^\circ\text{C}$, and few amount is streaked on a new appropriate medium plate allowing selection of the selectable marker. After 2-3 days incubation at $30\text{ }^\circ\text{C}$, the

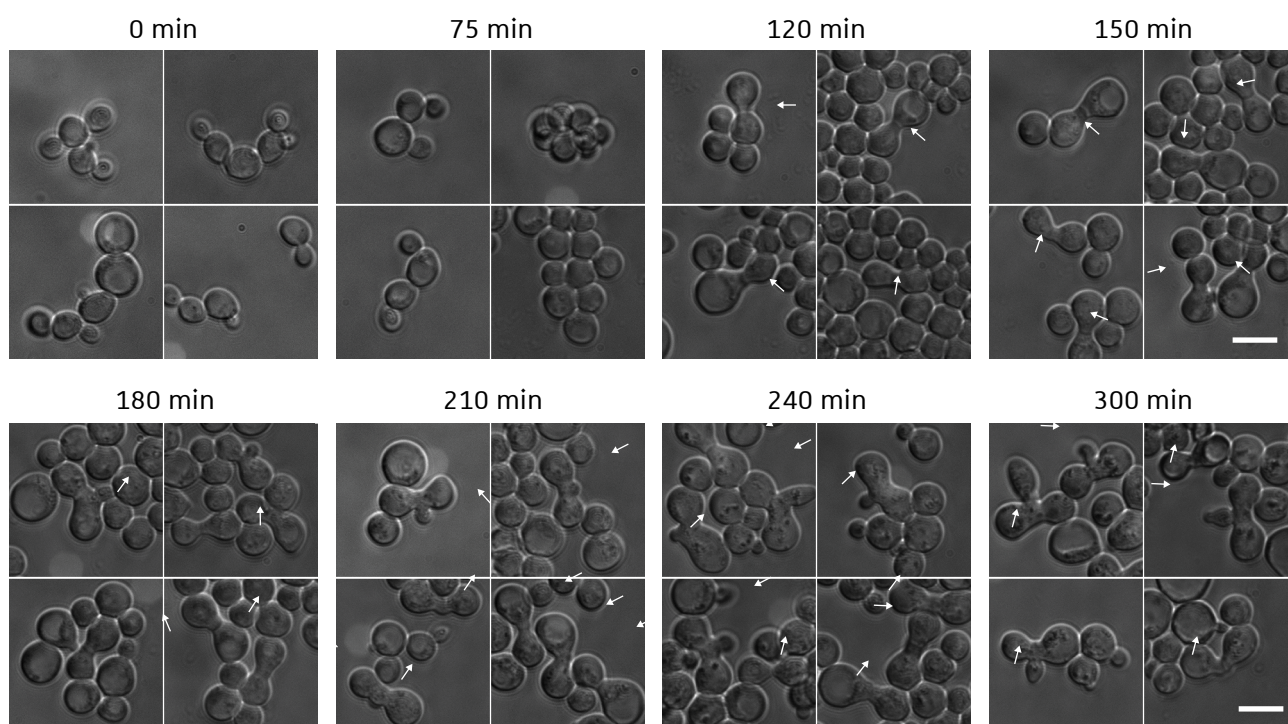


Figure MM-4: Yeast mating in liquid medium. Two mating type strains have been mixed in YPD and incubated under shaking at 30 °C. For each time point, shaking is stopped and the tube is left one minute on bench without any shaking to allow sedimentation of heavy particles, essentially diploids or shmoos. Images are taken under the microscope to observe cell mating after 120 min. White arrows indicate shmoos and diploids in cell division process. Scale bar, 10 μ m.

majority of the clones should be diploids. Diploids are then selected by double mating with control strains PT1 and PT2 on agar plates.

II.5.2. Mating in liquid medium

When no different markers are available for the diploid selection, mating can be realized in liquid medium. The two mating type strains are grown in YPD until they reach the mid-log phase. Equivalent quantities of both strains are then mixed into a single glass tube and incubated at 30 °C under shaking. Every hour, shaking is stopped and the tube is left one minute on bench without any shaking to allow sedimentation of heavy particles, essentially diploids or shmoo (see **Figure MM-4**). Then 10 µL are collected from the bottom of the tube, which should be enriched in diploids, diluted 1,000 times and spread on YPD agar plate medium. After 3–5 days of incubation at 30 °C, diploids are then selected by double mating with control strains PT1 and PT2 on agar plates.

II.5.3. Selection of diploids and/or mating type selection

To determine the mating type of a clone, or to select a diploid, we used the strains PT1 (*MAT α* , ile, hom3) and PT2 (*MAT α* , ile, hom3). These two strains are universal tester strains that can be used to determine the mating type of strains that are auxotrophic for at least one of the commonly used markers. These two strains are auxotrophic for Met, Thr and Ile only, whereas our experimental strains are prototrophic for these aa and auxotrophic for at least one different aa. Thus, none of the haploid strains are able to grow onto SD medium without any aa, but the diploid resulting from the mating between PT1/PT2 and the experimental strain is therefore auxotrophic for all aa and can grow on SD medium. Thus, the tested strain is crossed with both PT1 and PT2, incubated O/N at 30 °C on YPD and then streaked onto SD medium. Then three results can be observed on SD medium:

- growth of the strain crossed with PT1: the strain is mating type *MAT α*
- growth of the strain crossed with PT2: the strain is mating type *MAT α*
- any growth: the strain is a diploid, unable to cross with any tester strain

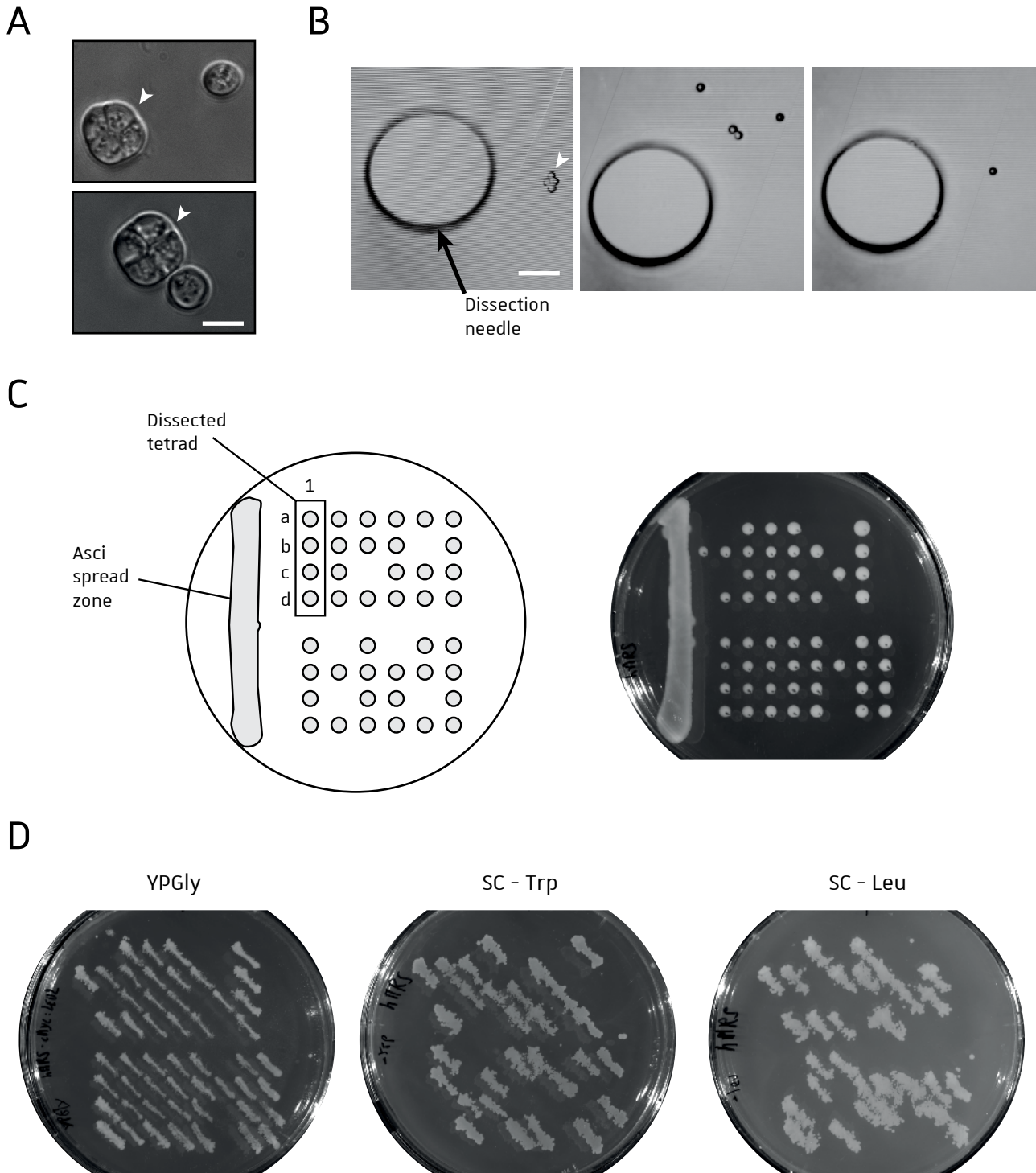


Figure MM-5: Diploid sporulation and tetrad dissection. **A.** After three days at 25 °C on a sporulation medium plate, cells were observed under the microscope with DIC optics. Asci (white arrows) were observed among non-sporulated diploids. Scale bar, 10 μ m. **B.** After zymolyase treatment, asci are dissected with a micromanipulation microscope. The ascus is isolated (white arrow) with the dissection needle, then the four spores are physically separated (middle picture) and each spore is aligned with others on the dissection plate. Scale bar, 60 μ m. **C.** After three days incubation at 30 °C, the dissection plate shows tetrads with aligned spores (a, b, c and d colonies). **D.** Each spore is restreaked onto a YPGly medium plate (left) and replica-plating on selective media (middle and right) to assess aa autotrophy and subsequent strain genotype.

II.6. Diploid sporulation and tetrad dissection

Before sporulation, the diploid strain has to be grown on a rich-medium plate (YPD) for few days, then the strain is streaked onto a sporulation medium plate and incubated at 25 °C for 2-5 days. Presence of tetrads is checked by optical microscopy by resuspending a small section of cells in water (**Figure MM-5A**). If enough tetrads are observed, cells from the sporulation plate are resuspended in 45 µL sterile water and 5 µL of zymolyase 20T (10 mg/mL) is added to the cells for 5 min at RT. Then 10 µL of liquid is gently spread in a line at the center of an YPD plate. The plate is then dried for few minutes to allow the liquid to absorb into the agar before dissection. Asci dissection was performed on a Singer MSM System 200 micromanipulation microscope (**Figure MM-5B**). After dissection (usually 18-20 ascospores are separated in four spores in one YPD plate), the plate is incubated at 30 °C for several days to observe clones' growth (**Figure MM-5C**). For replica-plating, each clone is restreaked onto a dried YPGly plate, and this plate is pressed onto a piece of velvet fabric. A new dried plate (usually a minimal medium to check aa auxotrophy) is then pressed onto the same fabric, transferring the cells onto the agar (**Figure MM-DD**).

II.7. Fluorescence microscopic observations

Living cells expressing GFP or mRuby2 fusion proteins were harvested at an $OD_{600\text{ nm}} = 0.5-1$ and resuspended in synthetic complete yeast medium before visualization. For compartment staining, the indicated yeast strain was harvested by a 500 × *g* centrifugation for 1 min, resuspended in 50 µL of YPD medium and stained with 2 µL of CMAC (200 µM) or 2 µL Hoechst (10 mg/mL) for 15 min at 30°C, prior to washing with 900 µL of YPD and followed by a second washing step in PBS. The stained cells were then observed by fluorescence microscopy.

Observation was performed with 100× objective (Zeiss, 1.45 oil, $\infty/0.17$) on a fluorescence Axio Observer D1 microscope (Zeiss) equipped with GFP, DAPI and DsRed filters, and DIC optics. Images were captured with a CoolSnap HQ2 photometrix camera (Roper Scientific) and analysed by using ImageJ (Rasband W.S., ImageJ, U. S. National Institutes of Health, Bethesda, Maryland, USA, <http://imagej.nih.gov/ij/>, 1997-2019). Microscopic panels have been created using the ImageJ plugin FigureJ (Mutterer and Zinck, 2013).

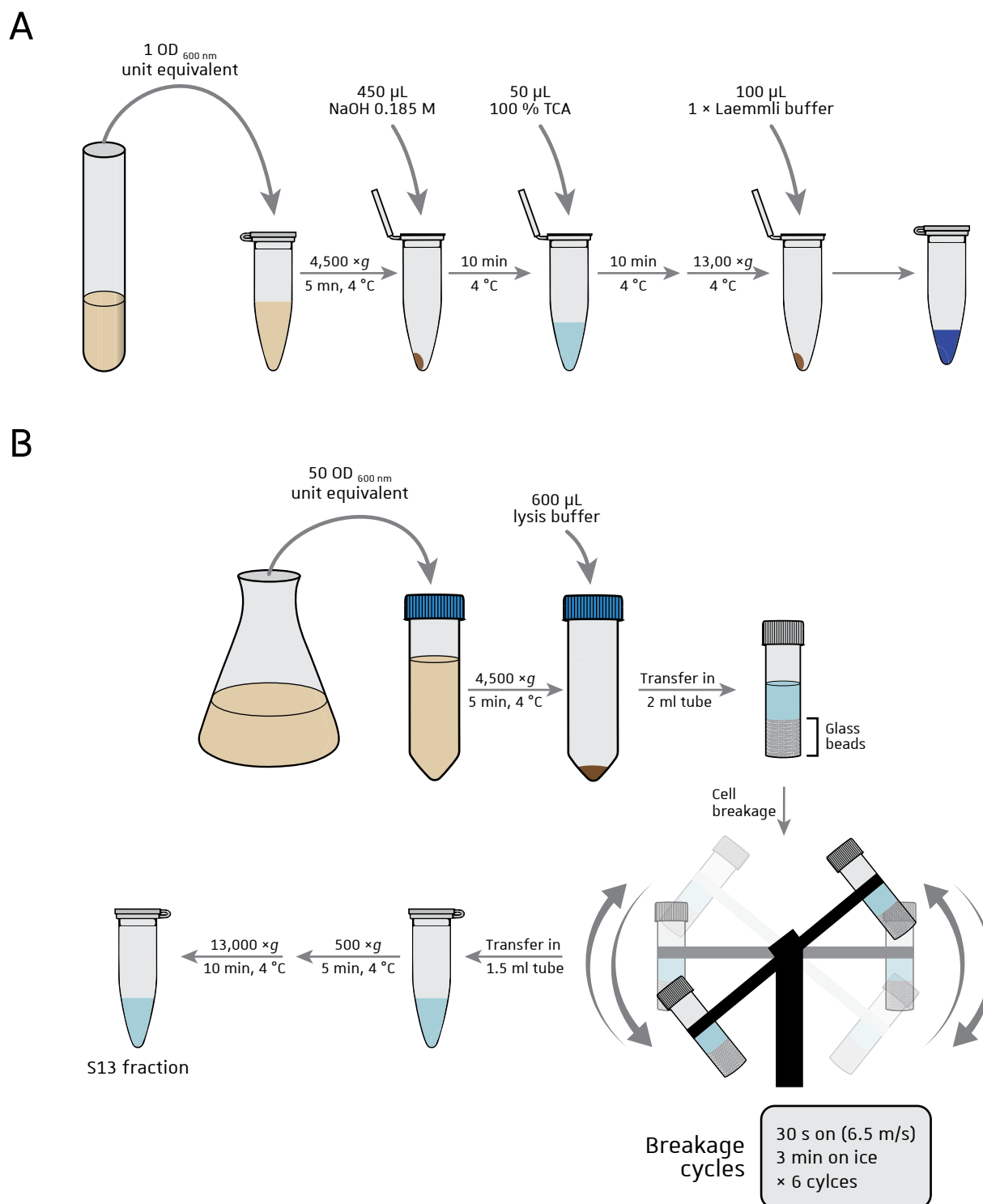


Figure MM-6: Preparation of yeast protein extracts. A. Protocol for total protein extract preparation for western blot analyses. Cells are lysed with NaOH and protein are precipitated with trichloroacetic acid (TCA). Protein pellet is directly dissolved in laemmli buffer for SDS-PAGE analysis. **B.** Protocol for soluble protein extract preparation. See the text for lysis buffer composition.

II.8. Yeast protein extract preparation

II.8.1. Total protein extract

Yeast total protein extracts were obtained by harvesting and disrupting yeast cells with 500 μL of ice cold NaOH 0.185 M for 10 min on ice (**Figure MM-6A**). Trichloroacetic acid (TCA) was added to a final concentration of 10 % (v/v), and samples were vortexed and incubated for an additional 10 min on ice. Precipitates were collected by centrifugation at $13,000 \times g$ for 10 min at 4 °C. Pellets were dissolved in 1 \times Laemmli buffer (125 mM Tris-HCl pH 6.8, 2 % (w/v) SDS, 10 % (w/v) glycerol, 2 % (v/v) β -mercaptoethanol, 0.0125 % (p/v) bromophenol blue), with 100 μL for the equivalent of 1 $\text{OD}_{600 \text{ nm}}$ unit of cells.

II.8.2. Soluble protein extract

Preparation of soluble protein extract was performed to remove membranous contaminants (**Figure MM-6B**). This was necessary before any chromatography column purification or before the *ex vivo* cleavage assay. 50 $\text{OD}_{600 \text{ nm}}$ unit of cells were harvested by a $4,500 \times g$ centrifugation for 5 min in a 50 mL Falcon™. Cells were lysed in 600 μL lysis buffer (50 mM Na-Hepes pH 7.2, 140 mM NaCl, 1 % (w/v) Triton X100, 0.1 % (w/v) deoxycholate, 0.3 % (w/v) NP40) with protease inhibitors tablet (Roche), transferred in a 2 mL tube with screw cap with 600 μL glass beads (\varnothing 0.25–0.5 mm, Roth), and broken using FastPrep®-24 homogenizer (6 \times 30 s breakage at 6.5 m/s speed, with 3 min on ice between each cycle). The extract is centrifuged once at $500 \times g$ for 5 min at 4 °C to remove cell debris, then the supernatant is centrifuged again at $13,000 \times g$ for 10 min at 4 °C. The supernatant (S13) is used for the *ex vivo* cleavage assay. An additional centrifugation at $100,000 \times g$ for 1 h at 4 °C was performed before using the soluble extract (S100) in the HPLC system for column chromatography.

II.8.3. Subcellular fractionation

For subcellular fractionation protocol, please refer to [Debard et al, 2017](#), page 283.

Table MM-8: List of antibodies used for immunoblotting (WB)

Primary antibodies	Host	Dilution for WB	Source
polyclonal anti-MetRS	Rabbit	1/1000	This lab
polyclonal anti-Arc1	Rabbit	1/1000	This lab
polyclonal anti-Pep4	Rabbit	1/1000	Gift from Dr. Friant's lab
monoclonal anti-Pgk1	Mouse	1/1000	Abcam
monoclonal anti-V5	Mouse	1/1000	Invitrogen
monoclonal anti-cMyc	Mouse	1/1000	Invitrogen
HRP-conjugate anti-GFP	Rabbit	1/1000	Life technologies
monoclonal anti-HA	Mouse	1/1000	Roche

Secondary antibodies (HRP conjugated)	Host	Dilution for WB	Source
anti-mouse IgG	Goat	1/3000	Bio-Rad
anti-rabbit IgG	Goat	1/3000	Bio-Rad

III. Biochemistry and biophysical techniques

III.1. Protein electrophoresis and immunoblotting

All protein samples are diluted in 1 × Laemmli buffer (125 mM Tris-HCl pH 6.8, 2 % (w/v) SDS, 10 % (w/v) glycerol, 2 % (v/v) β-mercaptoethanol, 0.0125 % (p/v) bromophenol blue) and heated at 95 °C for 5 min prior to loading. Usually, around 50 µg of protein are loaded onto the denaturing gel. Acrylamide gels are prepared as followed:

- the lower layer (separating gel) is composed of acrylamide:bisacrylamide (30 % 37,5:1) diluted in 375 mM Tris-HCl pH 8.8, 0.1 % (w/v) SDS. Acrylamide concentration is adjusted according to the sample to be run (common values between 8 % (v/v) and 16 % (v/v)).
- the top-most gel (stacking gel) is composed of 5 % (v/v) acrylamide:bisacrylamide (30 % 37.5:1) diluted in 125 mM Tris-HCl pH 6.8, 0.1 % (w/v) SDS.

Polymerisation of each layer is initiated by adding 1 % (w/v) of ammonium persulfate (APS) 10 % (w/v) and catalyzed by adding 0.1 % (v/v) N,N,N',N'-tetramethylethylene-diamine (TEMED, Roth). Gels are poured between two glass plates (10 × 8 cm) with 1 mm integrated spacers (Mini-PROTEAN® Spacer Plates, BioRad). Samples are loaded and electrophoresis is performed in TG-SDS running buffer (25 mM Tris, 192 mM glycine, 0.1 % (w/v) SDS, pH 8.5) at 150 V (20 mA) for 1-2h using Mini-PROTEAN® Tetra Vertical Electrophoresis Cell (BioRad).

Protein transfer onto PVDF membrane is realized using Trans-Blot Turbo™ transfer system (BioRad) for 7 min at 25 V (2.5 A). The PVDF membrane is then activated by 100 % ethanol for 1 min, washed once with TBS-Tween buffer (50 mM Tris-HCl pH 7.6, 150 mM NaCl, 0.3 % (v/v) Tween 20) and blocked at RT for 1 h with 5 % (w/v) skim milk in TBS-Tween buffer. Primary antibodies are incubated O/N at 4 °C in 5 % (w/v) skim milk in TBS-Tween buffer at a concentration of 1:1,000 (List of antibodies in **Table MM-8**). Detection was carried out using HRP-conjugated anti-rabbit or anti-mouse goat antibodies (BioRad), at a concentration of 1:3,000 (**Table MM-8**). ECL-plus reagents (Amersham) was used according to the manufacturer's instructions, and chemiluminescence detection was carried out using ChemiDoc™ imaging system (BioRad).

III.2. tRNA synthesis by *in vitro* transcription

In vitro transcription of tRNA genes allows production of high amount (μg to mg quantities) of unmodified tRNA transcripts. This protocol needs production and purification of T7 RNA polymerase (RNAP), *in vitro* transcription from DNA template, purification of tRNA by gel electrophoresis and tRNA elution from polyacrylamide gel using electrophoresis cells.

III.2.1. Purification of recombinant T7 RNA polymerase

The T7 RNAP is a single subunit of 100 kDa derived from the T7 phage of *E. coli* and highly specific for its promoter sequence. The recombinant T7 RNA polymerase used for tRNA *in vitro* transcription has been purified using vector pT7-911Q (Ichetovkin, Abramochkin and Shrader, 1997) expressing a 6×His N-terminally-tagged T7 RNA polymerase. The bacterial strain (LabCol 476) is inoculated in 3 L of LB + Amp medium at $\text{OD}_{600\text{ nm}} = 0.01$ and incubated at 37 °C until $\text{OD}_{600\text{ nm}}$ reaches 0.6, then T7 overexpression is induced by adding 100 μM final IPTG and cells are incubated 4 h at 30 °C. Cells are collected by centrifugation at 5,000 $\times g$ for 10 min at 4 °C, then stored at - 20 °C if the fraction will be used to check the overexpression by SDS-PAGE. The pellet is then thawed and dissolved in 30 mL lysis buffer (Tris-HCl 50 mM pH 8.0, NaCl 100 mM, β -Mercaptoethanol 5 mM, glycerol 5 % (v/v), imidazole 1 mM) supplemented with protease inhibitors. Cells are sonicated on ice during 10 rounds of 20 seconds (Vibra Cell bioblock), then centrifuged 15 min at 8000 $\times g$ at 4 °C. The cleared supernatant is applied onto a nickel sepharose High Performance affinity column (GE Healthcare, bed volume: 1 mL), washed with lysis buffer containing 10 mM imidazole until no more protein could be detected in the eluate. Proteins retained on the column are then eluted by 5 mL of lysis buffer containing 100 mM imidazole, then dialyzed O/N against the storage buffer (Tris-HCl 50 mM pH 7.7, EDTA 1 mM, NaCl 100 mM, Glycerol 50 % (v/v)) and kept at - 20 °C.

III.2.2. Design of the DNA template used for transcription

Synthesis of tRNA by T7 RNAP transcription requires a DNA template ending with a 3' CCA triplet and a 5' upstream T7 promoter. The polymerase is much more efficient with sequence templates beginning with G's at +1, +2 and +3, with the first two G's critical for a good transcription yield. The presence of 5'-guanosines as crucial prerequisite for effective transcription by T7 RNA polymerase limits use of *in vitro* synthesized tRNAs. However, when a tRNA sequence starts with nucleotide different from G, a *cis*-acting self-cleaving ribozyme sequence can be added in 5' that will enhance

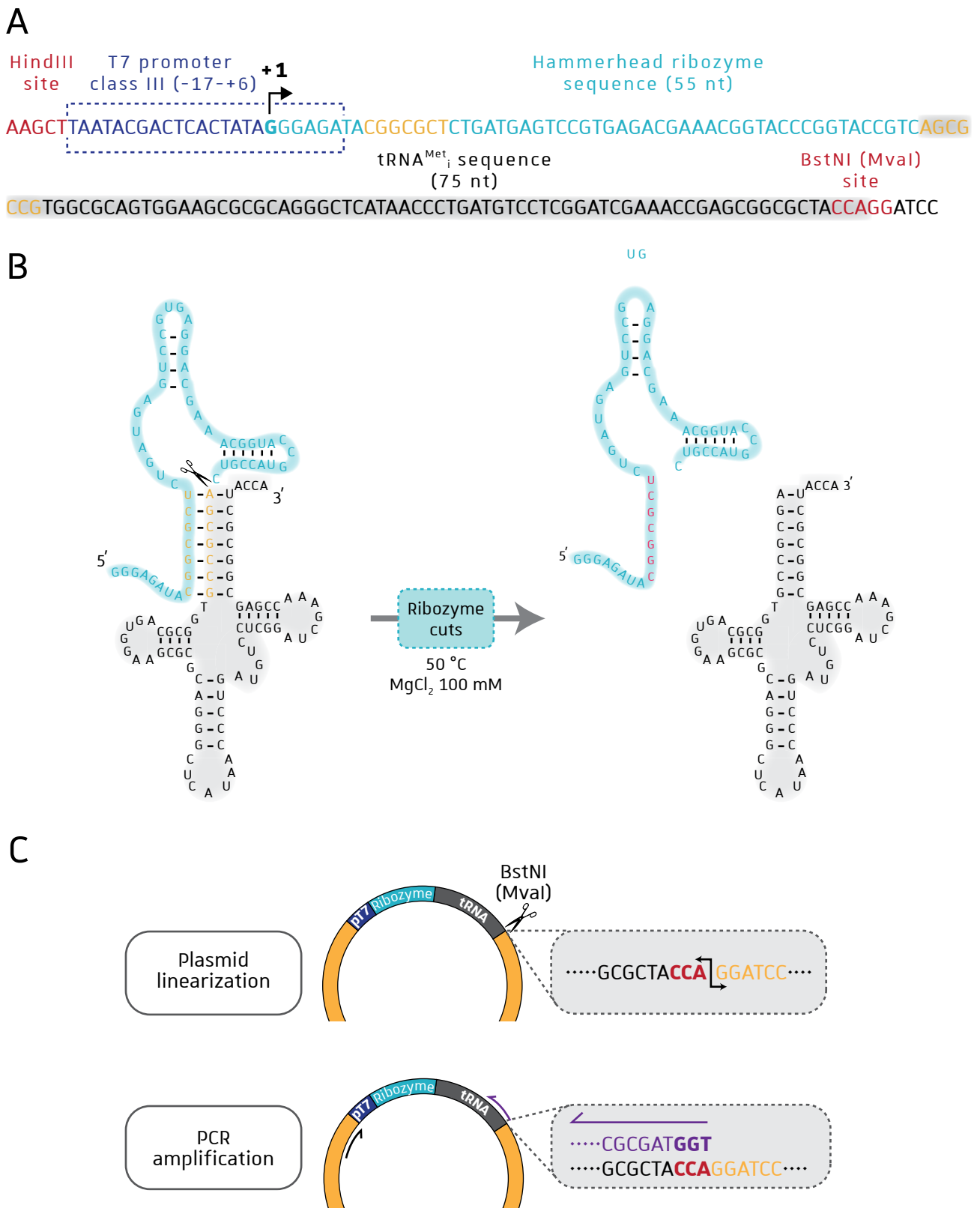


Figure MM-7: Engineering of tRNA expression plasmid for T7 *in vitro* transcription. **A.** Sequence of the T7 promoter (dark blue), the transzyme ribozyme (light blue) and the tRNA (grey, the initiator tRNA^{Met} here). **B.** Sequences complementary between the tRNA and the ribozyme (orange sequences) and self-cleavage of the ribozyme. **C.** DNA substrate for *in vitro* transcription was obtained by either (i) plasmid linearization using BstNI restriction enzyme (or the MvaI isoschizomer) (upper) or (ii) by PCR amplification of the sequence with a primer containing CCA complementary sequence (lower).

transcription efficiency because this ribozyme sequence starts with 2-3 G's. Self-cleavage of the ribozyme liberates the transcript beginning with the first tRNA nucleotide (see **Figure MM-7A and 7B**). For transcription of CCA ending tRNA, two methods have been used: linearization of plasmid using BstNI enzyme or PCR amplification of the template with specific primers (**Figure MM-7C**). These two methods produce linear DNA templates ending with 3' end CCA. Thus, termination of transcription by T7 RNAP always occurs after CCA synthesis.

III.2.3. *In vitro* transcription of tRNAs

Standard amounts of DNA template used for T7 transcription is typically either 50 µg of plasmid linearized with BstNI (or isoschizomer MvaI Fast Digest) or 20 µg of purified PCR product with 3' end CCA. Ribonucleotides Tri Phosphates (rNTPs) must be prepared at 50 mM each, pH adjusted to 8.0. GMP is added in excess to the mix to obtain 5'-monophosphate ended tRNAs. *In vitro* transcription is performed in TMSDT buffer 1 × (40 mM Tris-HCl pH 8.0, 30 mM MgCl₂, 0.01 % (v/v) Triton X100, 0.2 mM spermidine, 1 mM DTT) with 4 mM each rNTP (ATP, UTP, GTP and CTP) and 16 mM GMP in a total volume of 500 µL. Around 5 µg of T7 RNA polymerase is added to each vial and reactions are incubated at 37 °C for at least 3 h. After about 1 h, a white precipitate of magnesium pyrophosphate might appear in solution and shows T7 RNA pol activity. This precipitate can be removed by addition of 10 units of inorganic pyrophosphatase. Average rate of T7 *in vitro* transcription is 200-260 nt/s with frequency error about $6 \cdot 10^{-6}$ (Brakmann and Grzeszik, 2001). Aliquots of each reaction can be analysed by running a 2 % (w/v) agarose gel to see presence of a smear around 100-200 bp. Alternatively, a 12 % (w/v) polyacrylamide gel with 8 M urea can be ran to observe more precisely the final products.

If tRNA sequence is fused to transzyme (5' self-cleaving ribozyme), 5 volumes of transzyme buffer (20 mM MgCl₂, 50 mM Tris-HCl pH 8.0) is added to the reaction and incubated for 1 h in a water bath at 50 °C.

III.2.4. Purification of *in vitro* transcripts by gel electrophoresis

This in-gel purification allows the separation of the desired tRNA transcript from other components like the DNA sequence matrix, free nucleotides, abortive or extended transcripts or the ribozyme sequence. Transcription is stopped by phenol-chloroform (1:1) extraction followed by chloroform extraction. Nucleic acids within the aqueous phase (upper phase) are precipitated with 2.5 volumes

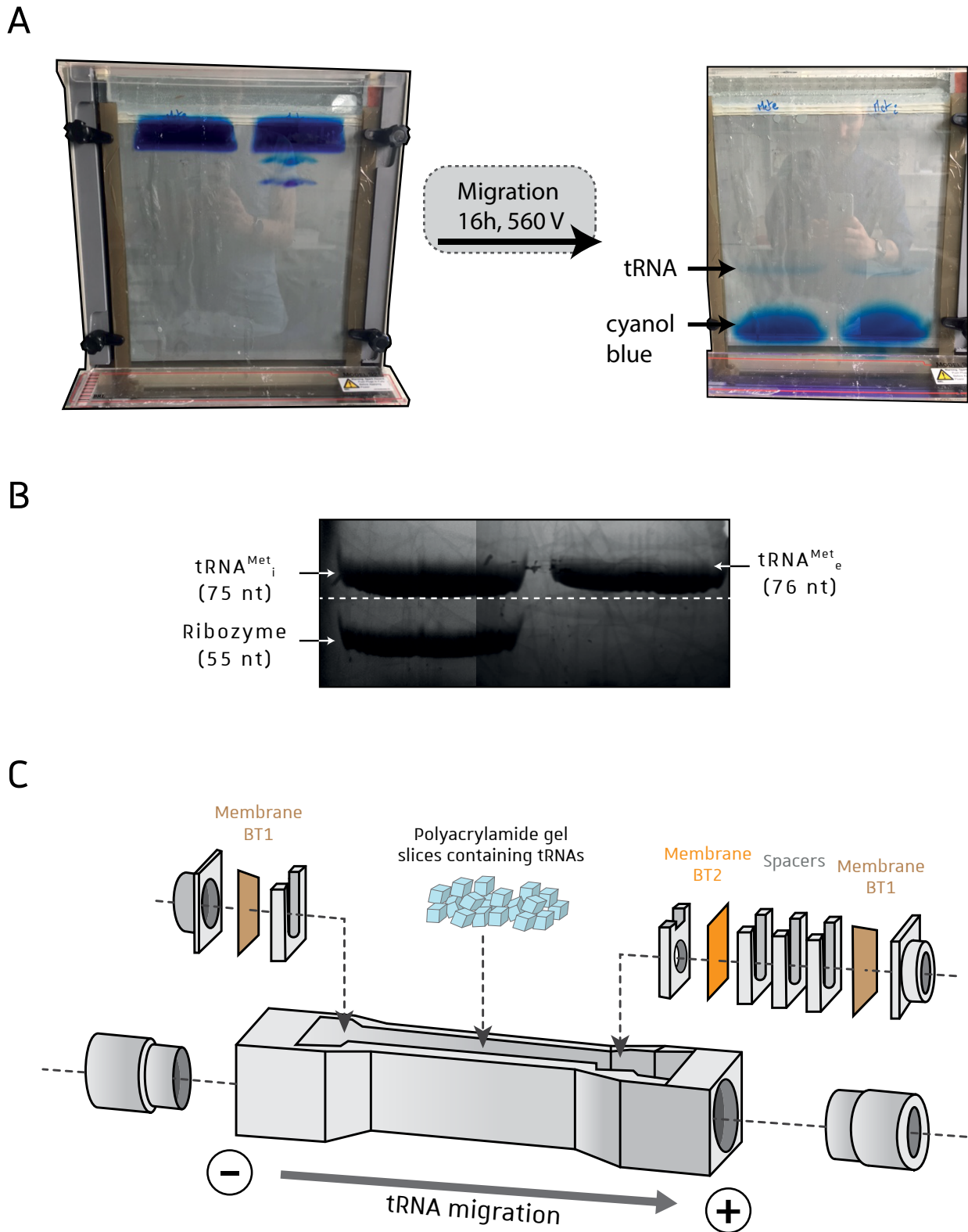


Figure MM-8: Purification of *in vitro* transcripts. **A.** Pictures of the large polyacrylamide gel used for tRNA migration. After overnight migration, the xylene cyanol is at the bottom of the gel (right). **B.** Observation of the nucleic acid bands under UV light with a phosphorescent plate. The migration allowed separation of the ribozyme sequence from the initiator tRNA^{Met}, and the one-nucleotide length difference between the two tRNAs is visible (white line). **C.** Illustration of the electroelution cell. Gel slices are placed in the middle of the device, and tRNAs migrate from the gel slices into a trap area formed by the BT1 and BT2 membranes during horizontal electrophoresis at 4 °C.

ice-cold ethanol 100 % after addition of 250 mM NaCl final concentration. After centrifugation at $13,000 \times g$ for 15 min at 4 °C, pellet is washed once with 70 % ethanol and the subsequent pellet is dried before resuspended in loading buffer (95 % formamide, 1 mM EDTA, 0.025 % (w/v) bromophenol blue and xylene cyanol). Sample is loaded on a large (33 cm \times 40 cm \times 0,2 cm) 12 % (w/v) polyacrylamide gel containing 8 M urea and ran at 550 V (75 mA) for 16 h in TBE buffer. At the end of migration, xylene cyanol blue band (light blue) should be at the bottom of the gel, and bromophenol blue (dark blue) migrated out of the gel (**Figure MM-8A**). Gel is observed under UV light with a phosphorescent plate placed under the gel (**see figure MM-8B**). The band containing the desired transcript is cut out of the gel and cut in small gel dice with a sterilized blade. Transcript is then eluted from the gel by electroelution: gel pieces are placed in an electroelution cell (Schleicher & Schüll, **Figure MM-8C**) in TBE buffer, and this cell is placed in an electroelution tank filled with TBE buffer. Electroelution is performed at 250 V (100 mA) for at least 3 h in cold room. The tRNA transcript is recovered within the compartment delimited between BT1 and BT2 membranes, and precipitated with ethanol and NaCl as described before. The pellet is then resuspended in water and stored at -20 °C.

III.3. Purification of MBP-MetRS enzymes

I used an *E. coli* strain harbouring a pMALc2 plasmid with *MES1* gene tagged with the sequence of Maltose Binding Protein (MBP) at the 5' end. Yeast MetRS purification protocol was designed previously in the lab and consists in a single step purification with amylose beads which is enough to get MetRS pure enough to be used for *ex-vivo* cleavage assay. However additional purification steps were necessary to prepare highly purified MetRS to perform aminoacylation assay.

III.3.1. Overexpression and enrichment of MBP-MetRS with amylose beads

Bacterial strain Rosetta™ 2 carrying the pMALc2 vector (**Table MM-9**) with MBP-MetRS construct is grown in 10 mL liquid LB + 100 mg.L⁻¹ Amp medium O/N at 37 °C under constant shaking. The culture is then diluted at OD_{600 nm} = 0.05 in 1 L LB + 100 mg.L⁻¹ Amp, and induction is initiated with 0.3 mM isopropyl β -D-1-thiogalactopyranoside (IPTG) added to the medium when OD_{600 nm} = 0.5. After 3.5 h at 30 °C, bacterial cells are centrifuged at $6,000 \times g$ for 5 min and washed once with PBS buffer. The pellet is suspended in ice-cold lysis buffer (250 mM Tris-HCl pH 8.0, 100 mM NaCl, 0.25 % (v/v)

Table MM-9: *E. coli* strain used for recombinant protein overexpression

Strain	Genotype
Rosetta™ 2	F- <i>ompT hsdS_B(r_B- m_B-) gal dcm</i> (DE3) pRARE2 (Cam ^R)

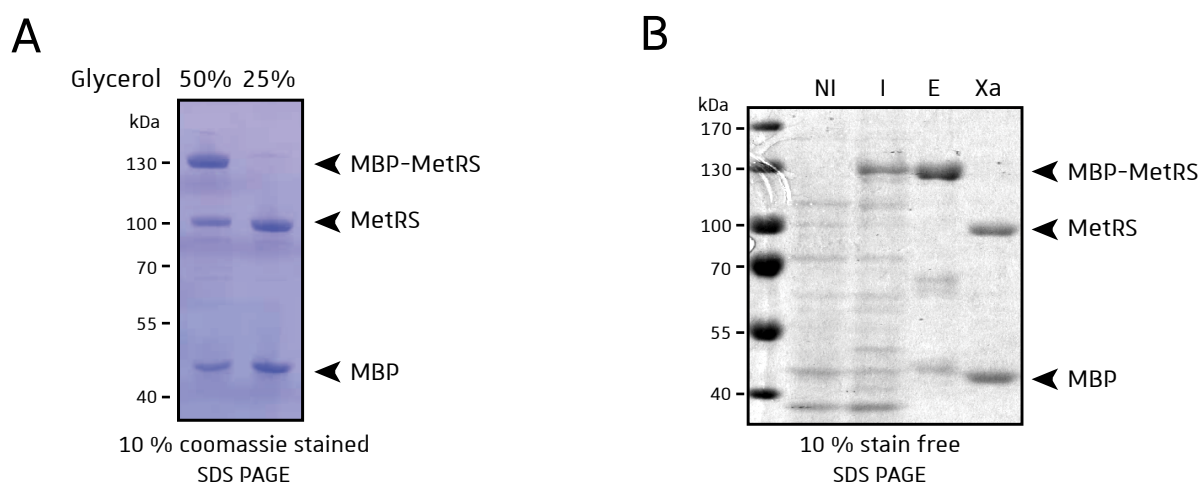


Figure MM-9: Purification of recombinant MetRS. A. Factor Xa cleavage efficiency depending on the glycerol concentration. Conditions of cleavage are described in the text section nearby. **B.** Results of recombinant MetRS(WT) purification. NI: total *E. coli* protein extract before IPTG induction. I: total *E. coli* protein extract after 3 h IPTG induction. E: elution fraction from amylose column. Xa: eluted fractions after factor Xa cleavage.

Tween20, 10 mM β -mercaptoethanol, 5 % (v/v) glycerol, 0.1 mM PMSF, 0.1 mM benzamidine, cOmplete™ protease inhibitor cocktail tablet (Roche)) in a glass cell culture tube. Sonication is performed on ice (Bioblock Scientific, VibraCell), 1 min 1 s on / 1 s off, 1 min on ice, 8 repetitions, 30 % amplitude). The lysate is then centrifuged 15 min at $10.000 \times g$ at 4 °C. Supernatant is kept and 500 μ L of amylose beads (NEB, E8021S) previously washed with lysis buffer are added and the NaCl concentration is adjusted to 300 mM. The vial is placed on rotation at 4 °C for 5 h. Beads and lysate are then poured on Poly-Prep® Chromatography Column (BioRad) and flow-through is kept. Beads retained by the column are washed with 15 mL ice-cold washing buffer (30 mM Tris-HCl pH 8.0, 300 mM NaCl, 1 mM β -mercaptoethanol, 5 % (v/v) glycerol). Elution is performed with ice-cold elution buffer (30 mM Tris-HCl pH 8.0, 100 mM NaCl, 1 mM β -mercaptoethanol, 5 % (v/v) glycerol, 1 % (w/v) maltose) collected in 500 μ L fractions. Eluted fractions can be stored at -20 °C or -80 °C supplemented with 50 % (v/v) glycerol.

III.3.2. Cleavage of MBP with factor Xa

The N-terminal MBP tag of MetRS is removed by proteolytic cleavage with factor Xa. If sample has been conserved in the storage buffer containing 50 % (v/v) glycerol, dilution to 25 % (v/v) glycerol is necessary to ensure high cleavage yield (**Figure MM-9**). *In vitro* cleavage must be performed in an Eppendorf tube (1.5 mL or 5 mL if higher volumes are needed) at 25 °C O/N with 500 mM NaCl, 30 mM Tris-HCl pH 8.0, 5 mM CaCl_2 and 5 μ g/mL Factor Xa (NEB). Note that cleavage performed in 15 mL or 50 mL Falcons™ resulted in protein precipitation for unknown reasons.

III.3.3. FPLC purification of MetRS for enzymatic characterisation

Further purification of MetRS was performed on ÄKTA™ pure chromatography system and analysed with UNICORN™ software (**Figure MM-10**). Fractions were collected in 96 deep-well plates using flexible fraction collector F9-C. All steps were performed in cold-room at 4 °C.

III.3.3.1. Heparin chromatography

The pooled fractions eluted from amylose resin in atmospheric chromatography were dialysed in 2 L buffer 1 (20 mM Tris-HCl pH 7.5, 5 % (v/v) glycerol). After dialysis, the sample is then loaded onto 5 mL HiTrap Heparin HP affinity column (GE Healthcare) previously equilibrated with buffer 1. Heparin functions as a cation exchanger due to its anionic sulfate groups. After sample

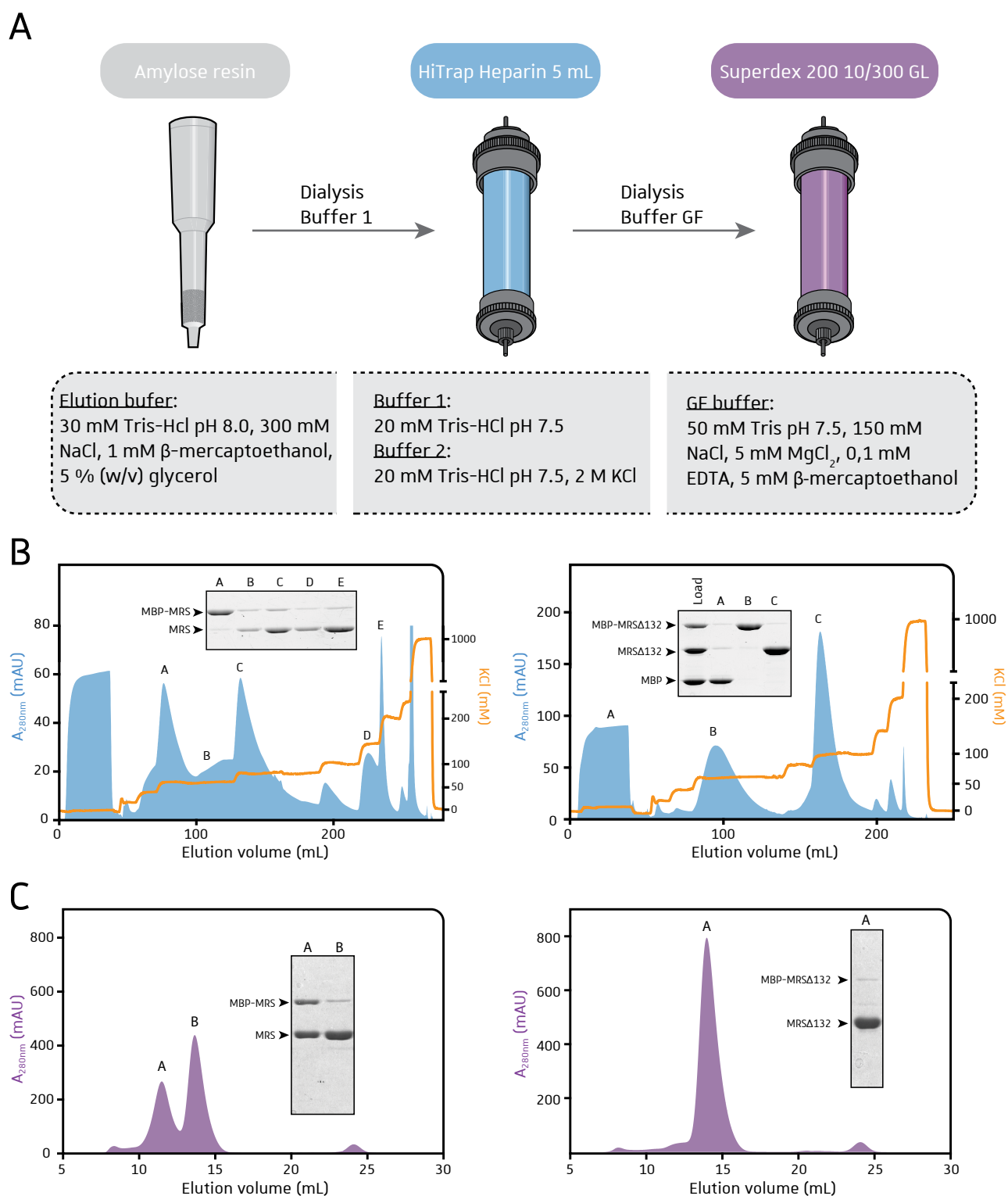


Figure MM-10: FPLC purification of recombinant MetRS. **A.** Description of the chromatography columns and buffers used for MetRS purification. **B and C.** Chromatogram from heparin (B) or gel filtration (C) chromatographies for MetRS(WT) (left) and MetRS(Δ 132) (right). Protein content of annotated fractions are shown in the inserts containing 10% stain free SDS PAGE.

loading, buffer 2 (buffer 1 + 2 M KCl) was used as elution buffer using step gradient with buffer 1 (**Figure MM-10B**). The majority of MetRS elutes at approximately 75 mM KCl, whereas MBP elutes at 40 mM KCl.

III.3.3.2. Gel filtration protocol

Pooled MetRS fractions from heparin chromatography are dialysed with GF buffer (50 mM Tris pH 7.5, 150 mM NaCl, 5mM MgCl₂, 0,1 mM EDTA, 5 mM β-mercaptoethanol) and concentrated into a 700 μL sample which is then loaded onto a Superdex 200 10/300 GL column (GE Healthcare) previously equilibrated with GF buffer. Fractions containing MetRS are collected and stored at -80 °C in GF buffer with 50 % (v/v) glycerol. Because we observed that MetRS can dimerize, the MetRS(FL) is eluted in two different peaks containing either the heterodimer MBP-MetRS(FL)•MetRS(FL) or the homodimer MetRS(FL)•MetRS(FL) (**Figure MM-10C**).

III.3.4. Sample dialysis and determination of protein concentration

The dialysis tubing I used has a 10 kDa MW cut-off. Dried dialysis tubing needs boiling preparation for 10 min in a large beaker filled with 10 mM EDTA, 10 mM sodium bicarbonate. This boiling step removes heavy metals and preservatives from the tubing. Tubing is rinsed thoroughly with water then with distilled water and stored in 50 % ethanol, 1 mM EDTA at 4 °C. Tubing is rinsed with distilled water before use to remove any trace of ethanol and soaked in dialysis buffer for 10 min. Bottom of the dialysis bag is clipped with plastic clip (Thermo Fisher) and sample is poured into the tubing. The other end of the bag is also clipped with plastic clip and length of the tubing is adjusted by cutting. Dialysis bag is suspended in ice-cold dialysis buffer under constant agitation with a stirring magnetic bar. The volume of the dialysis buffer should be at least 100 times the sample volume, and dialysis is performed for 3 h minimum.

To concentrate protein sample after dialysis, the dialysis membrane is placed in a box and covered by dry polyethylene glycol (PEG6000) at 4° C. Concentration occurs upon diffusion of buffer out of the sample and into the PEG powder. Every 15 min the dialysis bag is removed from viscous PEG and new PEG powder is added onto the bag. Concentration should last until the desired sample volume is obtained.

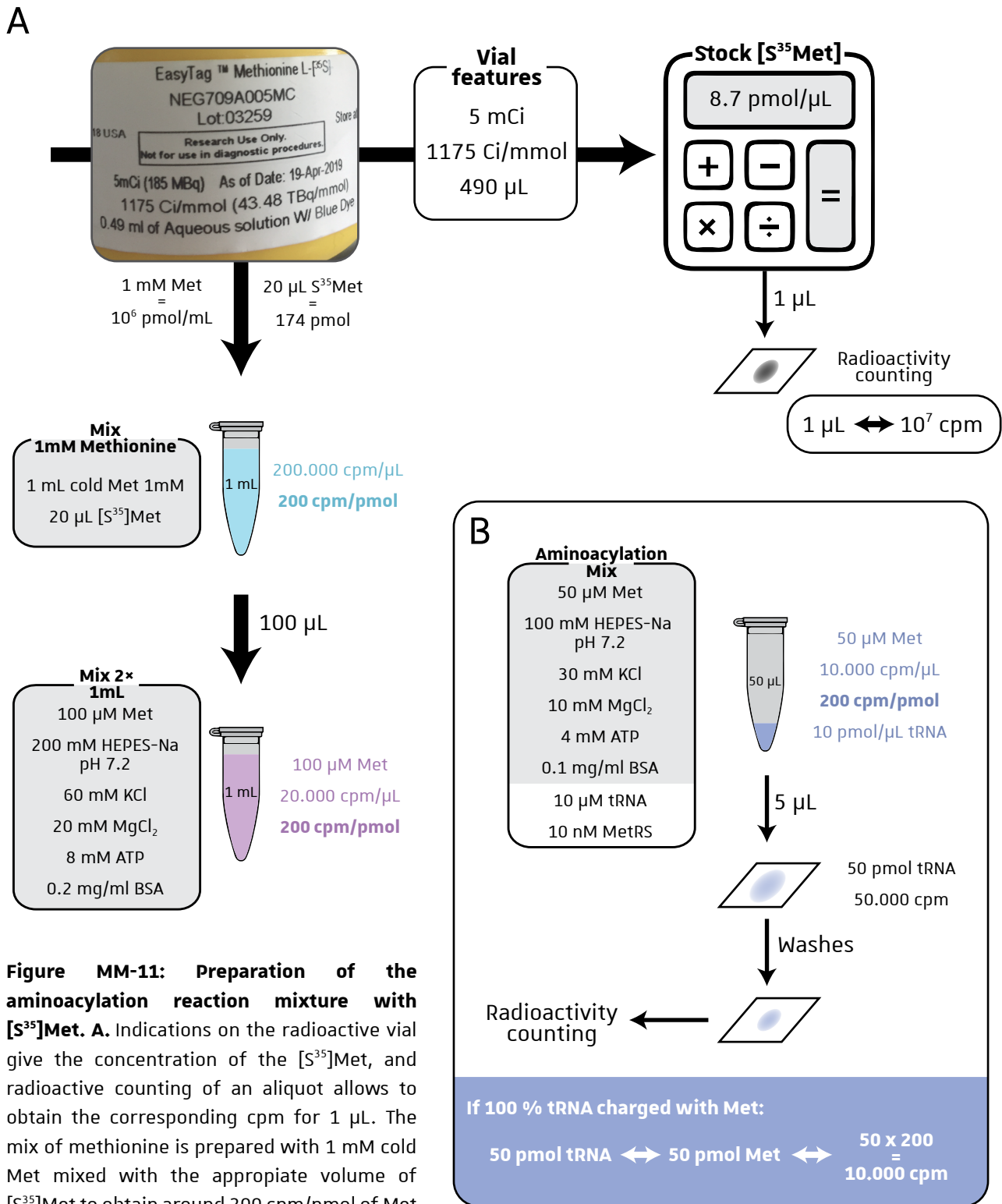


Figure MM-11: Preparation of the aminoacylation reaction mixture with [35]Met. **A.** Indications on the radioactive vial give the concentration of the [35]Met, and radioactive counting of an aliquot allows to obtain the corresponding cpm for 1 μ L. The mix of methionine is prepared with 1 mM cold Met mixed with the appropriate volume of [35]Met to obtain around 200 cpm/pmol of Met (note that this value does not change with further dilutions). Then the mix 2x is prepared with chemicals needed for the aminoacylation reaction.

B. For aminoacylation assay, the reaction mixture is prepared by adding half volume of mix 2x and the rest with tRNA, enzyme and water. The methionine working concentration is 50 μ M, still with 200 cpm/pmol of Met incorporated. If 5 μ L of reaction is sampled on a paper for counting, it represents 50 pmol of tRNA (because the working concentration is 10 μ M = 10 pmol/ μ L for tRNA). At the end, if all tRNA molecules are charged, the signal would reach 10.000 cpm, because each pmol of tRNA brings 200 cpm.

III.4. Aminoacylation assay

To determine the aminoacylation activity of purified recombinant MetRS(WT) and MetRS(Δ 132), I employed the following procedure: different concentrations of each enzyme (usually 1, 5 or 10 nM) were added to a 50 μ L reaction mixture containing 100 mM Hepes-Na (pH 7.2), 10 mM $MgCl_2$, 1 mM DTT, 5 mM ATP, 80 μ M total yeast tRNA (Roche Molecular Biochemicals) or 1–20 μ M *in vitro* transcript, and 50 μ M cold Met with L-[35 S]methionine (ICN Radiochemicals, specific activity 200 cpm/pmol), and the reaction mixture was incubated at 25 °C. Five aliquots of 15 μ L were taken at various time points (1, 2, 3, 4 and 5 min) and spotted onto Whatman paper disks presoaked in 5% (v/v) trichloroacetic acid (TCA) and 1 mM cold Met to quench the reaction. Filter papers were then washed three times with cold solution of 5% (v/v) TCA and three times with 70% (v/v) ethanol, dried and counted for radioactivity in Ultima Gold™ scintillation liquid (PerkinElmer) with LS 6500 Multi-Purpose Scintillation Counter (Beckman Coulter™). Details in sample preparation are given in **Figure MM-11**.

III.5. MetRS immunoprecipitation

The yeast MetRS (WT or Δ 132) was tagged at its C-terminus with either cMyc or V5 epitopes. Yeast protein extracts were prepared as in §II.8.2. For immunoprecipitation, the μ MACS™ Epitope Tag Protein Isolation Kits were used (Miltenyi Biotec). Equivalent of 2 mg proteins from the soluble extract were incubated with 50 μ L microbeads in 1 mL final volume at 4 °C for 30 min. Two washes were performed using the Lysis buffer (50 mM Na-Hepes pH 7.2, 140 mM NaCl, 1 % (w/v) Triton X100, 0.1 % (w/v) deoxycholate, 0.3 % (w/v) NP40), then two washes with 20 mM Tris-HCl pH 7.5. Elution was performed using 50 μ L pre-heated 1 \times Laemmli buffer (125 mM Tris-HCl pH 6.8, 2 % (w/v) SDS, 10 % (w/v) glycerol, 2 % (v/v) β -mercaptoethanol, 0.0125 % (p/v) bromophenol blue). Eluate was analysed by SDS-PAGE and by mass spectrometry analysis.

III.6. Mass spectrometry analyses

III.6.1. Procedure for co-immunoprecipitated MetRS interactants

Protein extracts were prepared as described in a previous study (Chicher *et al.*, 2015). Briefly, each sample was precipitated with 0.1 M ammonium acetate in 100 % methanol, and proteins were suspended in 50 mM ammonium bicarbonate, pH 7.8. After a reduction-alkylation step (DTT

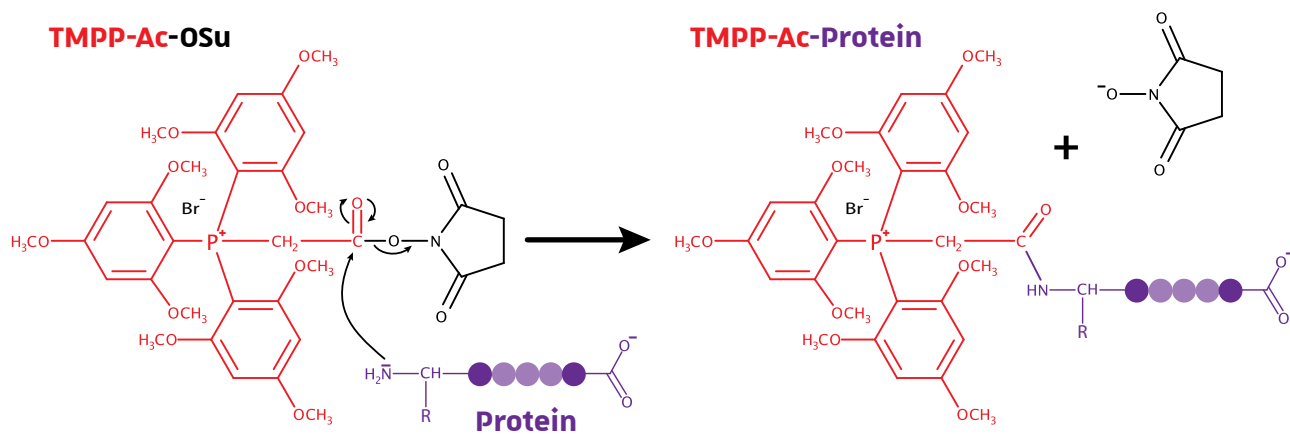


Figure MM-12: TMPP reaction performed at pH 8.2 to specifically target the N-termini amines of proteins.

5 mM, iodoacetamide 10 mM), proteins were digested O/N with sequencing-grade porcine trypsin (1:25, w/w, Promega, Fitchburg, MA, USA). The resulting vacuum-dried peptides were suspended in 25 μ L of water containing 0.1 % (v/v) formic acid (solvent A). 380 ng of the peptide mixtures were analysed by nanoLC-MS/MS an Easy-nanoLC-1000 system coupled to a Q-Exactive Plus mass spectrometer (Thermo-Fisher Scientific, USA) operating in positive mode with a nanoelectrospray source. 5 μ L of each sample were loaded on a C-18 precolumn (75 μ m ID \times 20 mm nanoViper, 3 μ m Acclaim PepMap; Thermo) coupled with the analytical C18 analytical column (75 μ m ID \times 25 cm nanoViper, 3 μ m Acclaim PepMap; Thermo). Peptides were eluted with a 160 min gradient of 0.1 % (v/v) formic acid in acetonitrile at 300 nL/min. The Q-Exactive Plus was operated in data-dependent acquisition mode (DDA) with Xcalibur software (Thermo-Fisher Scientific). Survey MS scans were acquired at a resolution of 70 K at 200 m/z (mass range 350-1250), with a maximum injection time of 100 ms and an automatic gain control (AGC) set to $3 \cdot 10^6$. Up to 10 of the most intense multiply charged ions (≥ 2) were selected for fragmentation with a maximum injection time of 100 ms, an AGC set at $1 \cdot 10^3$ and a resolution of 17.5 K. A dynamic exclusion time of 20 s was applied during the peak selection process.

MS data were searched against the Swissprot database (release 2016_07) with a decoy strategy (Database toolbox from MSDA, <https://msda.unistra.fr/>). We used the Mascot algorithm (version 2.5, Matrix Science) to perform the database search with a decoy strategy. The resulting .dat Mascot files were then imported into Proline v1.4 package (<http://proline.profiroteomics.fr/>) for further post-processing. Proteins were validated on Mascot pretty rank equal to 1 % FDR on both peptide spectrum matches (PSM) and protein sets (based on score). _YEAS* was used as typical protein during the validation process.

III.6.2. TMPP protocol for N-terminus characterization and MetRS cleavage site identification

III.6.2.1. TMPP protein labelling

The protocol used here was carried out according to the original reference paper by (Gallien *et al.*, 2009) with slight modifications. The $^{13}\text{C}_9$ -TMPP (TriMethoxyPhenyl Phosphonium) induces a mass increase of 581.21 Da instead of 572.18 Da for light TMPP on labelled peptides (**Figure MM-12**).

For the investigation of the cleavage in an *ex vivo* context, proteins were separated on a 10 % 1D SDS-PAGE (10.1 cm × 7.3 cm) on a mini PROTEAN (Bio-Rad) apparatus at 10 mA for 20 min and 100 mA until the complete migration of the blue front. After electrophoresis, gels were stained with colloidal Coomassie Blue (BioSafe coomassie stain; Bio-Rad). Gel bands corresponding to the full-length and the truncated forms of MetRS(WT) and MetRS(S10A) were excised, cut into small pieces, in-gel reduced by incubating with 10 mM tributylphosphine (TBP) for 30 min at 60 °C and 30 min at RT, and alkylated by incubating with 55 mM iodoacetamide (IAA). An equimolar solution of 0.1 M of ¹²C-TMPP-Ac-OSu and ¹³C₉-TMPP-Ac-OSu in 80 % acetonitrile (ACN) in 0.1% (v/v) formic acid (FA) was added at a 200:1 reagent:protein molar ratio, followed by 0.1 M Tris-HCl, pH 8.2 (50 µL). Selective N-terminal TMPP derivatization is achieved by a careful control of reaction pH at 8.2, exploiting the weaker basicity of the N-terminal amine relative to the ε-amino group of the lysine side chain. The reaction was maintained at RT for 1 h under agitation. Residual derivatizing reagent was quenched by adding a solution of 0.1 M hydroxylamine at RT for 30 min under agitation, in order to minimize derivatization of tyrosine residues. After extensive wash steps, proteins were finally in-gel digested O/N at 37 °C using a solution of modified porcine trypsin (Promega, Madison, WI) at a 1:50 (w/w) enzyme/protein ratio. Tryptic peptides were extracted using 60 % (v/v) ACN in 0.1 % (v/v) FA for 45 min at RT and 100 % ACN for 20 min at RT. The volume was reduced in a vacuum centrifuge and adjusted to 10 µL using 2% (v/v) ACN in 0.1 % (v/v) FA in water before nanoLC-MS/MS (nanoliquid chromatography coupled to tandem mass spectrometry) analysis.

For the validation of the cleavage site in an *in vivo* context, a similar protocol was used with the following modifications. Proteins were separated on a 10 % 1D SDS-PAGE (10.1 cm × 7.3 cm) on a mini PROTEAN (Bio-Rad) apparatus at 50 V for 35 min and 100 V until the complete migration of the blue front. After excision of the gel bands of interest, proteins were in-gel reduced and alkylated. 50 µL of a solution of 0.2 M ¹²C-TMPP-Ac-OSu in 80 % ACN diluted to a final concentration of 0.02 M with 0.1 M Tris-HCl, pH 8.2 were added. After quenching and extensive washes, proteins were in-gel digested at a 1:100 (w/w) enzyme/protein ratio, and tryptic peptides were extracted and vacuum centrifuged, before resolubilisation in 8 µL 2 % (v/v) ACN in 0.1 % (v/v) FA in water.

III.6.2.2. LC-MS/MS and data analysis

For the first investigation (from *ex vivo* assay), nanoLC-MS/MS analyses were performed on a NanoAcquity UPLC device (Waters, Milford, MA) coupled with a QToF mass spectrometer (Q-Exactive

Plus, Thermo Fisher Scientific, Bremen, Germany). The UPLC system was equipped with a Symmetry C18 precolumn (0.18 × 20 mm, 5 µm particle size, Waters) and an ACQUITY UPLC BEH130 C18 separation column (75 µm × 250 mm, 1.7 µm particle size, Waters). The solvent system consisted of 0.1 % (v/v) FA in water (solvent A) and 0.1 % (v/v) FA in acetonitrile (solvent B). Of each sample 4 µL was injected. Peptides were trapped during 3 min at 5 µL/min with 99 % A and 1 % B. Elution was performed at a flow rate of 450 nL/min, using the following gradient of solvent B: from 1 % to 6 % in 2 min, from 6 % to 50 % in 28 min, and from 50 % to 90 % in 1 min. The Q-Exactive Plus was operated in data-dependent acquisition mode by automatically switching between full MS and consecutive MS/MS acquisitions. Full-scan MS spectra were collected from 300–1,800 m/z at a resolution of 70,000 at 200 m/z with an automatic gain control target fixed at $3 \cdot 10^6$ ions and a maximum injection time of 50 ms. The top 10 precursor ions with an intensity exceeding $1.5 \cdot 10^5$ ions were selected from each MS spectrum for fragmentation by higher-energy collisional dissociation, excluding unassigned and monocharged ions. Spectra were collected at a resolution of 17,500 at 200 m/z with a fixed first mass of 100 m/z, an automatic gain control target fixed at $1 \cdot 10^5$ ions and a maximum injection time of 100 ms. Dynamic exclusion time was set to 10 s.

For the validation study, nanoLC-MS/MS analyses were performed on a NanoAcquity UPLC device (Waters) coupled with a QToF mass spectrometer (Q-Exactive HF-X, Thermo Fisher Scientific, Bremen, Germany). The same chromatographic conditions as previously described were used (except the flow rate at 0.4 µL/min and the injected sample volume of 1 µL). The Q-Exactive HF-X was operated in data-dependent acquisition mode by automatically switching between full MS and consecutive MS/MS acquisitions. Full-scan MS spectra were collected from 300–1,800 m/z at a resolution of 60,000 at 200 m/z with an automatic gain control target fixed at $3 \cdot 10^6$ ions and a maximum injection time of 50 ms. The top 10 precursor ions with an intensity exceeding $2 \cdot 10^4$ ions were selected from each MS spectrum for fragmentation by higher-energy collisional dissociation, excluding unassigned, 1+- and ≥ 7 - charged ions. Spectra were collected at a resolution of 15,000 at 200 m/z, an automatic gain control target fixed at $1 \cdot 10^5$ ions and a maximum injection time of 50 ms. Dynamic exclusion time was set to 60 s.

Peaklists in mascot generic format (.mgf) were generated using MSConvert tool from ProteomeWizard (v3.0.6090; <http://proteowizard.sourceforge.net/>), and were searched using Mascot (version 2.5.1; Matrix Science, London, UK) against an in-house database containing all *S. cerevisiae* entries extracted from UniProtKB-SwissProt (release of 03/2017, 7 902 entries), the sequence of

MetRS(S10A), trypsin, common contaminants (117 entries) and the corresponding 8,021 reverse entries. The database was generated using the database toolbox from Mass Spectrometry Data Analysis (MSDA, publicly available from <https://msda.unistra.fr>) (Carapito *et al.*, 2014). The following parameters were applied: semiTrypsin as the digestion enzyme, one permitted missed cleavage per peptide, a mass tolerance of 5 ppm for the precursor ions and 0.07 Da for the peptide fragments, carbamidomethylation of cysteine residues as a fixed modification, and oxidation of methionine residues and light (+572.18 Da) and heavy (+581.21 Da) TMPP derivatization on any N-terminal amino acid or side chain of tyrosine and lysine residues as variable modifications. Mascot result files were loaded into Proline software (<http://proline.profiroteomics.fr>; Carapito *et al.*, 2015) and proteins were validated on pretty rank equal to one, and a Mascot ion score ≥ 13 . The N-terminal peptides were validated using the "dN-TOP Validation Tool" available at <https://msda.unistra.fr>, by confirming the identification of both the light and heavy labelled peptide forms and their chromatographic co-elution.

For the validation in a *in vivo* context, peak lists were searched using Mascot against an in-house database containing all *S. cerevisiae* entries extracted from UniProtKB-SwissProt (release of 05/2017, 7 903 entries), trypsin, common contaminants (35 entries) and the corresponding 7,939 reverse entries, generated using the database toolbox from MSDA, and identifications were validated using Proline, both with the same parameters as above. Since only the light TMPP isotope was used for labelling, the previously identified N-terminal peptide was confirmed by evidencing the presence of the b1 ion on the validated MS/MS spectrum.

IV. Lists of primers, plasmids and yeast strains

I.1. Tables of primers

Only primers used for gene amplification on yeast genome and for plasmid sequencing of listed. The primers used for sequence mutagenesis and plasmid construction are not listed.

Table MM-10 : Primers used for gene amplification on DNA genome (1/2)

N°	Fw/Rv	Primer use	Primer sequence (5'→3')
P1	Fw	<i>MXR1</i> deletion checking	CCTTTGAAGCGCAGTAATCTCCC
P2	Rv	<i>MXR1</i> deletion checking	CCTCTTAAGGCAGCAGCACAAACC
P3	Fw	<i>MXR2</i> deletion checking	GCGTTTTCAAGATCCGTTCCGAGG
P4	Rv	<i>MXR2</i> deletion checking	CGCGCAGCTTCTTGGTTCACGG
P5	Fw	<i>KanMX4</i> internal primer	CCTTTTAACAGCGATCGCGTATTTCCG
P6	Rv	<i>KanMX4</i> internal primer	GGTGCACAATCTATCGATTGTATGG
P15	Fw	<i>LEU2</i> internal primer	CTGTGCGATAGCGCCCTGTGTCTCTCG
P16	Rv	<i>LEU2</i> internal primer	GAAATTACAAAATGGAATATGTTCAATAGG
P17	Fw	<i>URA3</i> internal primer	AGGTAGAGGGTGAACGTTACAGAAAAGC
P18	Rv	<i>URA3</i> internal primer	GCAGCAGCTTCTTATATGTAGCTTTCCG
P19	Fw	<i>TRP1</i> internal primer	AAATTCGTCAAAAATGCTAAGAAATAGG
P20	Rv	<i>TRP1</i> internal primer	CTGGCCCTCTCCTTTTCTTTTTCGACC
P21	Fw	<i>ADE2</i> internal primer	TGACAAATGACTCTTGTGGCATGGC
P22	Rv	<i>ADE2</i> internal primer	AATTATTCCTTGCTTCTGTACTGG
P25	Fw	<i>MXR1</i> internal primer	GCACAGCGTCAAAAAATCCGCCACC
P26	Fw	<i>MXR2</i> internal primer	GTTTACCCTCCATCTGATTGTC
P53	Fw	<i>GUS1</i> deletion with <i>KanMX4</i>	AAAGATCCAATCTCCTGTCCAATTCAGCG
P54	Rv	<i>GUS1</i> deletion with <i>KanMX4</i>	CTTCTTCTCGGATTCATCGGCCACAGCC
P74	Fw	Amplify <i>ARC1</i>	AGATGTTTTGAGACAATGAGAGTGC GG
P75	Rv	Amplify <i>ARC1</i>	TATTAGTACCATACTAGTTTCTCTGC
P97	Fw	<i>LEU2</i> upstream primer	AGAAATAGTCACTAAATAGTGGAAGC
P98	Rv	<i>LEU2</i> internal primer	CAGAATCAATCAATTGATGTTGAACC
P101	Fw	<i>URA3</i> upstream primer	AAGGATAAGTTTTGACCATCAAGAAGG
P102	Rv	<i>URA3</i> downstream primer	TAGTTCCTTTTATAAAGGCCATGAAGC
P103	Fw	<i>TRP1</i> upstream primer	GATCTAAAAGAGCTGACAGGGAATGG
P104	Rv	<i>TRP1</i> downstream primer	ATTTTCTGTACAATCAATCAAAAAGCC
P120	Fw	<i>ARC1</i> upstream primer	GACAAGGAAAGTACAGGCAAGGTATCC
P121	Rv	<i>ARC1</i> downstream primer	ATTGTTAATTGGCCAACAATTCTCGCG
P141	Fw	<i>KanMX4</i> amplification for <i>ARC1</i> deletion	ATAATGGTATGTGATAGTCATTATTAACGATTAAGCGTTTTACATGGAGGCCAGAATACC
P142	Rv	<i>KanMX4</i> amplification for <i>ARC1</i> deletion	GCGCCTTATCTGGAAGAAGGTTCCGGAGACCAAGAGGAGCCGCGTTAGTATCGAATCGAC
P143	Fw	<i>URA3</i> upstream primer	GATGTAGAAAAGGATTAAGATGCTAAG
P144	Rv	<i>URA3</i> downstream primer	CTTGATTTGTGCCCGTAAAATAC
P149	Fw	<i>KanMX4</i> amplification for <i>PEP4</i> deletion	ATTTAATCCAAATAAAATCAAAACAAAACCAAACTAACACATGGAGGCCAGAATACC
P150	Rv	<i>KanMX4</i> amplification for <i>PEP4</i> deletion	GCAGAAAAGGATAGGGCGGAGAAGTAAGAAAAGTTTAGCCGCGCTAGTATCGAATCGAC
P151	Fw	<i>PEP4</i> deletion checking	GTCTTATGCCTTCCGGGTAC
P152	Rv	<i>PEP4</i> deletion checking	ATTAGAGGTGCTCCGTATGG
P153	Fw	<i>PEP4</i> deletion checking	GCGGTTATTGAATCTATGGAGAGG
P154	Rv	<i>PEP4</i> deletion checking	CTAGTGAAGATGCAGAAATCGAC
P156	Fw	<i>pHSP26</i> amplification for cloning downstream mRuby2	CTCACTATAGGGCGAATTGGAGCTCCGTTGGACTTTTTTAAATAACCTACC
P160	Rv	<i>pHSP26</i> amplification for cloning downstream mRuby2	TTTTTTGTACAAACTTGTGATGGGGATCCGTTAATTTAGTTAGTTTGTGTTG
P158	Fw	<i>IA3</i> amplification to clone in pMALc2 vector	GGGATCGAGGGAAGGATTCAGAAATCATGAATACAGACCAACAAAAAGTGAG
P159	Rv	<i>IA3</i> amplification to clone in pMALc2 vector	CGGCCAGTGCCAAGCTTGCTGCACTACTCCTCTTATGCCCGG
P167	Fw	<i>pTRX2</i> amplification for cloning downstream mRuby2	CTCACTATAGGGCGAATTGGAGCTCTGGACACACTCAAGCGCAATTC
P168	Rv	<i>pTRX2</i> amplification for cloning downstream mRuby2	TTGTACAAACTTGTGATGGGGATCCTATTGATGTTATTTAAAGATATCGTAGACTC
P169	Fw	<i>pGPX2</i> amplification for cloning downstream mRuby2	CTCACTATAGGGCGAATTGGAGCTCGGAATGTAATGAACATTACAAAATAAATAACTG
P170	Rv	<i>pGPX2</i> amplification for cloning downstream mRuby2	TTGTACAAACTTGTGATGGGGATCCTTTGAATTTACTTTTTGTTGCTAATTTGATTC
P171	Fw	<i>pHSP12</i> amplification for cloning downstream mRuby2	CTCACTATAGGGCGAATTGGAGCTCTATGATATAGGACTTCTCTCTTTTTTTTT
P172	Rv	<i>pHSP12</i> amplification for cloning downstream mRuby2	TTGTACAAACTTGTGATGGGGATCCTGTTGATTTAGTTTTTTTTGTTTGTGAGTTG
P173	Fw	<i>pMXR1</i> amplification for cloning downstream mRuby2	CTCACTATAGGGCGAATTGGAGCTCAATATACCCATTTCTCTCAATCTCCTTTG
P174	Rv	<i>pMXR1</i> amplification for cloning downstream mRuby2	TTGTACAAACTTGTGATGGGGATCCTGCAACTGATTACTTGTAAAGTTTTTG

Table MM-10 : Primers used for gene amplification on DNA genome (2/2)

N°	Fw/Rv	Primer use	Primer sequence (5'→3')
P175	Fw	<i>pMXR2</i> amplification for cloning downstream mRuby2	CTCACTATAGGGCGAATTGGAGCTCTCCTGATCTGCTAAGTTATGTCTTTTC
P176	Rv	<i>pMXR2</i> amplification for cloning downstream mRuby2	TTGTACAAACTTGTGATGGGGATCCTTTTGGATTTGATTCCTCTTTCTCCC
P177	Fw	<i>pCTT1</i> amplification for cloning downstream mRuby2	CTCACTATAGGGCGAATTGGAGCTCTTGGCAAGTACATAGAATCCACAG
P178	Rv	<i>pCTT1</i> amplification for cloning downstream mRuby2	TTGTACAAACTTGTGATGGGGATCCTTGTGAAGCTGAGCTGATTGATC
P179	Fw	<i>pTSA2</i> amplification for cloning downstream mRuby2	CTCACTATAGGGCGAATTGGAGCTCGTAGATGAATCAAATCTATGATTAAGAACAATG
P180	Rv	<i>pTSA2</i> amplification for cloning downstream mRuby2	TTGTACAAACTTGTGATGGGGATCCGATTGGTTTTTACGTTCTTGTAAAGGC
P181	Fw	<i>pPRX1</i> amplification for cloning downstream mRuby2	CTCACTATAGGGCGAATTGGAGCTCAACCGTTGGACAGAATGATTTCTTTC
P182	Rv	<i>pPRX1</i> amplification for cloning downstream mRuby2	TTGTACAAACTTGTGATGGGGATCCCTTTGCTTCTGCTTCTTTG
P201	Fw	<i>TRP1</i> amplification for <i>PEP4</i> deletion	ATTTAATCCAAATAAAATTCAAACAAAACCAAACTAACCCAGATGGCAGTAGTGGAAAG
P202	Rv	<i>TRP1</i> amplification for <i>PEP4</i> deletion	GCAGAAAAGGATAGGGCGGAGAAGTAAGAAAAGTTTAGCCAGGCAAGTGCACAACAAT
P205	Fw	<i>KanMX4</i> amplification for <i>CPS1</i> deletion	CATCATCACATTAAGGAATCATTCTAACAATTACATTACATGGAGGCCAGAATACC
P206	Fw	<i>KanMX4</i> amplification for <i>CPS1</i> deletion	TGGCAGAAAAGGATAGGGCGGAGAAGTAAGAAAAGTTTAGCCGGCTTAGTATCGAATCG
P208	Fw	<i>HAS1</i> upstream primer	TATACACGGTACTTGTAGTACATAGC
P209	Rv	<i>HAS1</i> downstream primer	GGAAACAATGCGTCATTATTTATTGC
P213	Rv	<i>CPS1</i> deletion checking (use with P5)	CTGCCTTACGCAAGTGG
P226	Fw	<i>HAS1</i> amplification to clone into p305-HA (pSD147 digested SacI/PstI)	CTCACTATAGGGCGAATTGGAGCTCTTCAGGAGCTTGGTAGCACC
P227	Rv	<i>HAS1</i> amplification to clone into p305-HA (pSD147 digested SacI/PstI)	TAAGCTTGATATCGAATTCTGCTGCAGCTTATGAGTTTTACGTTCTTTGGTATTTGG
P228	Fw	<i>HAS1</i> amplification to clone into p414-β11 (pSD69 digested SacI/PstI)	CTAAAGGGAACAAAAGCTGGAGCTCTTCAGGAGCTTGGTAGCACC
P229	Rv	<i>HAS1</i> amplification to clone into p414-β11 (pSD69 digested SacI/PstI)	TAAGCTTGATATCGAATTCTGCTGCAGCTTATGAGTTTTACGTTCTTTGGTATTTGG
P234	Fw	<i>pTSA1</i> amplification for cloning downstream mRuby2	CTCACTATAGGGCGAATTGGAGCTCCGAGACTATCCACTTGAATG
P235	Rv	<i>pTSA1</i> amplification for cloning downstream mRuby2	TCTTACCCTTAGATACCATTGTGTATGTATGTATGTAGTTGG

Table MM-11 : Primers used for plasmid sequencing

N°	Rv/Fw	Sequenced region	Primer sequence (5'→3')
P13	Rv	5' <i>MES1</i>	GCTTAGGCAAAATTTCTGAATCCTTTGG
P14	Fw	3' <i>MES1</i>	TCCTAGAAGGACATAATATAAACAAGGC
P23	Fw	3' <i>MES1</i>	CCAGAAAAGTCAGATGCTGTTGTGCG
P24	Rv	5' <i>MES1</i>	CGTTATGCACCTTTGGATGGCAATTCTGGG
P37	Rv	5' <i>mRuby2</i> (codon 67)	GATAAAAAGAAGTTGCCAAGATATCG
P38	Fw	3' <i>mRuby2</i>	TACGGTTCAAGAACTTTTATTAAGTACC
P55	Rv	upstream attB2	ACTTTGTACAAGAAAGCTG
P71	Fw	downstream attB1	AGTTTGTACAAAAAAGCAG
P119	Fw	tRNA sequence in pUC18 vector	ATACCGCACAGATGCGTAAGG
P155	Fw	<i>PEP4</i> sequencing	CCTACCACGTAAGGGAAGAATAAC
P198	Rv	<i>MES1</i> sequence	GTTGAGCAATCTCCGTTTGC
P199	Fw	<i>MES1</i> sequence	TGACACCAAGACAATTATGTGAC
P200	Fw	<i>MES1</i> sequence	CAAGACTCTGGAATTTCTCCAAG
P207	Fw	<i>HAS1</i> sequence to check suppressor	TGTTGATTGCTACCCCTGG

Primers used for BFP plasmids mutation (5'→3')

-	Fw	GCTTTCGATATCTTGGCAACTTCTTTT(XXX) ₆₇ TACGGTTCAAGAACTTTTATTAAGTACCC
-	Rv	GGGTACTTAATAAAAGTTCTTGAACCGTA(YYY) ₆₇ AAAAGAAGTTGCCAAGATATCGAAAGC

(XXX)₆₇: one of the 60 coding codon of the standard genetic code coding for the aa in position 67 in the mRuby2 sequence

(YYY)₆₇: reverse complementary sequence from (XXX)₆₇

I.2. Tables of plasmids

Table MM-12: BFP plasmids library (Part 1/2)

BFP N°	BFP name	Vector	Promoter	Mutant codon	Enzyme for linearization
BFP 1	BFP(Met ^{ATG})	pAG304	<i>pGPD</i>	mRuby2(ATG)-EGFP	PmlI or Accl
BFP 2	BFP(Leu ^{CTC})	pAG304	<i>pGPD</i>	mRuby2(CTC)-EGFP	PmlI or Accl
BFP 3	BFP(Leu ^{CTG})	pAG304	<i>pGPD</i>	mRuby2(CTG)-EGFP	PmlI or Accl
BFP 4	BFP(Leu ^{CTT})	pAG304	<i>pGPD</i>	mRuby2(CTT)-EGFP	PmlI or Accl
BFP 5	BFP(Leu ^{CTA})	pAG304	<i>pGPD</i>	mRuby2(CTA)-EGFP	PmlI or Accl
BFP 6	BFP(Leu ^{TTA})	pAG304	<i>pGPD</i>	mRuby2(TTA)-EGFP	PmlI or Accl
BFP 7	BFP(Leu ^{TTG})	pAG304	<i>pGPD</i>	mRuby2(TTG)-EGFP	PmlI or Accl
BFP 8	BFP(Arg ^{CGG})	pAG304	<i>pGPD</i>	mRuby2(CGG)-EGFP	PmlI or Accl
BFP 9	BFP(Arg ^{CGC})	pAG304	<i>pGPD</i>	mRuby2(CGC)-EGFP	PmlI or Accl
BFP 10	BFP(Arg ^{CGA})	pAG304	<i>pGPD</i>	mRuby2(CGA)-EGFP	PmlI or Accl
BFP 11	BFP(Arg ^{CGT})	pAG304	<i>pGPD</i>	mRuby2(CGT)-EGFP	PmlI or Accl
BFP 12	BFP(Arg ^{AGG})	pAG304	<i>pGPD</i>	mRuby2(AGG)-EGFP	PmlI or Accl
BFP 13	BFP(Arg ^{AGA})	pAG304	<i>pGPD</i>	mRuby2(AGA)-EGFP	PmlI or Accl
BFP 14	BFP(Lys ^{AAG})	pAG304	<i>pGPD</i>	mRuby2(AAG)-EGFP	PmlI or Accl
BFP 15	BFP(Lys ^{AAA})	pAG304	<i>pGPD</i>	mRuby2(AAA)-EGFP	PmlI or Accl
BFP 16	BFP(GF)	pAG304	<i>pGPD</i>	mRuby2(IFA)-EGFP	PmlI or Accl
BFP 17	BFP(RF)	pAG304	<i>pGPD</i>	mRuby2(ATG)-EGFP(AFA)	PmlI or Accl
BFP 18	BFP(Asp ^{GAT})	pAG304	<i>pGPD</i>	mRuby2(GAT)-EGFP	PmlI or Accl
BFP 19	BFP(Asp ^{GAC})	pAG304	<i>pGPD</i>	mRuby2(GAC)-EGFP	PmlI or Accl
BFP 20	BFP(Glu ^{GAA})	pAG304	<i>pGPD</i>	mRuby2(GAA)-EGFP	PmlI or Accl
BFP 21	BFP(Glu ^{GAG})	pAG304	<i>pGPD</i>	mRuby2(GAG)-EGFP	PmlI or Accl
BFP 22	BFP(Ile ^{ATT})	pAG304	<i>pGPD</i>	mRuby2(ATT)-EGFP	PmlI or Accl
BFP 23	BFP(Ile ^{ATC})	pAG304	<i>pGPD</i>	mRuby2(ATC)-EGFP	PmlI or Accl
BFP 24	BFP(Ile ^{ATA})	pAG304	<i>pGPD</i>	mRuby2(ATA)-EGFP	PmlI or Accl
BFP 25	BFP(Asn ^{AAT})	pAG304	<i>pGPD</i>	mRuby2(AAT)-EGFP	PmlI or Accl
BFP 26	BFP(Asn ^{AAC})	pAG304	<i>pGPD</i>	mRuby2(AAC)-EGFP	PmlI or Accl
BFP 27	BFP(NF)	pAG304	<i>pGPD</i>	mRuby2(IFA)-EGFP(AFA)	PmlI or Accl
BFP 28	BFP(Ser ^{TCG})	pAG304	<i>pGPD</i>	mRuby2(TCG)-EGFP	PmlI or Accl
BFP 29	BFP(Ser ^{AGC})	pAG304	<i>pGPD</i>	mRuby2(AGC)-EGFP	PmlI or Accl
BFP 30	BFP(Ser ^{TCC})	pAG304	<i>pGPD</i>	mRuby2(TCC)-EGFP	PmlI or Accl
BFP 31	BFP(Ser ^{AGT})	pAG304	<i>pGPD</i>	mRuby2(AGT)-EGFP	PmlI or Accl
BFP 32	BFP(Ser ^{TCA})	pAG304	<i>pGPD</i>	mRuby2(TCA)-EGFP	PmlI or Accl
BFP 33	BFP(Ser ^{TCT})	pAG304	<i>pGPD</i>	mRuby2(TCT)-EGFP	PmlI or Accl
BFP 34	BFP(Val ^{GTG})	pAG304	<i>pGPD</i>	mRuby2(GTG)-EGFP	PmlI or Accl

Table MM-12: BFP plasmids library (Part 2/2)

BFP N°	BFP name	Vector	Promoter	Mutant codon	Enzyme for linearization
BFP 35	BFP(Val ^{GTC})	pAG304	<i>pGPD</i>	mRuby2(GTC)-EGFP	PmlI or Accl
BFP 36	BFP(Val ^{GTA})	pAG304	<i>pGPD</i>	mRuby2(GTA)-EGFP	PmlI
BFP 37	BFP(Val ^{GTT})	pAG304	<i>pGPD</i>	mRuby2(GTT)-EGFP	PmlI or Accl
BFP 38	BFP(Pro ^{CCG})	pAG304	<i>pGPD</i>	mRuby2(CCG)-EGFP	PmlI or Accl
BFP 39	BFP(Pro ^{CCC})	pAG304	<i>pGPD</i>	mRuby2(CCC)-EGFP	PmlI or Accl
BFP 40	BFP(Pro ^{CCT})	pAG304	<i>pGPD</i>	mRuby2(CCT)-EGFP	PmlI or Accl
BFP 41	BFP(Pro ^{CCA})	pAG304	<i>pGPD</i>	mRuby2(CCA)-EGFP	PmlI or Accl
BFP 42	BFP(Thr ^{ACG})	pAG304	<i>pGPD</i>	mRuby2(ACG)-EGFP	PmlI or Accl
BFP 43	BFP(Thr ^{ACC})	pAG304	<i>pGPD</i>	mRuby2(ACC)-EGFP	PmlI or Accl
BFP 44	BFP(Thr ^{ACA})	pAG304	<i>pGPD</i>	mRuby2(ACA)-EGFP	PmlI or Accl
BFP 45	BFP(Thr ^{ACT})	pAG304	<i>pGPD</i>	mRuby2(ACT)-EGFP	PmlI or Accl
BFP 46	BFP(Ala ^{GCG})	pAG304	<i>pGPD</i>	mRuby2(GCG)-EGFP	PmlI or Accl
BFP 47	BFP(Ala ^{GCC})	pAG304	<i>pGPD</i>	mRuby2(GCC)-EGFP	PmlI or Accl
BFP 48	BFP(Ala ^{GCA})	pAG304	<i>pGPD</i>	mRuby2(GCA)-EGFP	PmlI or Accl
BFP 49	BFP(Ala ^{GCT})	pAG304	<i>pGPD</i>	mRuby2(GCT)-EGFP	PmlI or Accl
BFP 50	BFP(Gly ^{GGG})	pAG304	<i>pGPD</i>	mRuby2(GGG)-EGFP	PmlI or Accl
BFP 51	BFP(Gly ^{GGC})	pAG304	<i>pGPD</i>	mRuby2(GGC)-EGFP	PmlI or Accl
BFP 52	BFP(Gly ^{GGA})	pAG304	<i>pGPD</i>	mRuby2(GGA)-EGFP	PmlI or Accl
BFP 53	BFP(Gly ^{GGT})	pAG304	<i>pGPD</i>	mRuby2(GGT)-EGFP	PmlI or Accl
BFP 54	BFP(Stop ^{TAG})	pAG304	<i>pGPD</i>	EGFP-mRuby2(TAG)	PmlI or Accl
BFP 55	BFP(Stop ^{TGA})	pAG304	<i>pGPD</i>	EGFP-mRuby2(TGA)	PmlI or Accl
BFP 56	BFP(Stop ^{TAA})	pAG304	<i>pGPD</i>	EGFP-mRuby2(TAA)	PmlI or Accl
BFP 57	BFP(His ^{CAC})	pAG304	<i>pGPD</i>	mRuby2(CAC)-EGFP	PmlI or Accl
BFP 58	BFP(His ^{CAT})	pAG304	<i>pGPD</i>	mRuby2(CAT)-EGFP	PmlI or Accl
BFP 59	BFP(Gln ^{CAG})	pAG304	<i>pGPD</i>	mRuby2(CAG)-EGFP	PmlI or Accl
BFP 60	BFP(Gln ^{CAA})	pAG304	<i>pGPD</i>	mRuby2(CAA)-EGFP	PmlI or Accl
BFP 61	BFP(Cys ^{TGC})	pAG304	<i>pGPD</i>	mRuby2(TGC)-EGFP	PmlI or Accl
BFP 62	BFP(Cys ^{TGT})	pAG304	<i>pGPD</i>	mRuby2(TGT)-EGFP	PmlI or Accl
BFP 63	BFP(Tyr ^{TAC})	pAG304	<i>pGPD</i>	mRuby2(TAC)-EGFP	PmlI or Accl
BFP 64	BFP(Tyr ^{TAT})	pAG304	<i>pGPD</i>	mRuby2(TAT)-EGFP	PmlI or Accl
BFP 65	BFP(Phe ^{TTC})	pAG304	<i>pGPD</i>	mRuby2(TTC)-EGFP	PmlI or Accl
BFP 66	BFP(Phe ^{TTT})	pAG304	<i>pGPD</i>	mRuby2(TTT)-EGFP	PmlI or Accl

Table MM-13: Mutated or modified BFP plasmids

pSD n°	Vector	Promoter	Insert-Tag	Enzyme for linearization
162	pAG304	<i>pGPD</i>	(D60K)BFP(Met ^{ATG})	PmlI
163	pAG304	<i>pGPD</i>	(A58K)BFP(Met ^{ATG})	PmlI
164	pAG304	<i>pGPD</i>	(F59K)BFP(Met ^{ATG})	PmlI
165	pAG414	<i>pGPD</i>	BFP(Met ^{ATG})	-
166	pAG414	<i>pGPX2</i>	BFP(Met ^{ATG})	-
167	pAG304	<i>pGPD</i>	(F59K)BFP(Leu ^{CTG})	PmlI
168	pAG304	<i>pGPD</i>	(F59K)BFP(Leu ^{CTG})	PmlI
169	pAG304	<i>pGPD</i>	(F59K)BFP(Arg ^{CGG})	PmlI
170	pAG304	<i>pGPD</i>	(F59K)BFP(Arg ^{CGC})	PmlI
171	pAG304	<i>pGPD</i>	(F59K)BFP(Gln ^{CAG})	PmlI
-	pAG304	<i>pMXR1</i>	BFP(Met ^{ATG})	PmlI
-	pAG304	<i>pMXR2</i>	BFP(Met ^{ATG})	PmlI
-	pAG304	<i>pCTT1</i>	BFP(Met ^{ATG})	PmlI
-	pAG304	<i>pTSA2</i>	BFP(Met ^{ATG})	PmlI
-	pAG304	<i>pGPX2</i>	BFP(Met ^{ATG})	PmlI
-	pAG304	<i>pTRX2</i>	BFP(Met ^{ATG})	PmlI

Table MM-14: Plasmids for *E. coli* overexpression (Part 1/2)

pSD n°	Vector	Insert-Tag
61	pMALc2	MBP-MES1(WT)
62	pMALc2	MBP-MES1(K11A)
63	pMALc2	MBP-MES1(Δ 142)
64	pMALc2	MBP-MES1(S10A)
65	pMALc2	MBP-MES1(S10D)
66	pMALc2	MBP-MES1(S10D K11A)
101	pMALc2	MBP-MES1(Δ 132)
106	pMALc2	MBP-MES1(Y132A)
149	pMALc2	MBP-MES1(3A)
177	pMALc2	MBP-MES1(WT)-V5
178	pMALc2	MBP-MES1(Δ 132)-V5
179	pMALc2	MBP-MES1(Y132A)-V5
180	pMALc2	MBP-MES1(AAAA)-V5
189	pMALc2	MBP-MES1(K11A)-V5
190	pMALc2	MBP-MES1(S10A)-V5

Table MM-14: Plasmids for *E. coli* overexpression (Part 2/2)

pSD n°	Vector	Insert-Tag
191	pMALc2	MBP-MES1(S10D)-V5
192	pMALc2	MBP-MES1(S10D K11A)-V5
193	pMALc2	MBP-MES1(K11A+3A)-V5
194	pMALc2	MBP-MES1(S10A+3A)-V5
195	pMALc2	MBP-MES1(S10D+3A)-V5
196	pMALc2	MBP-MES1(S10D K11A+3A)-V5
140	pMALc2	MBP-PEP4(mature from RS453)
141	pMALc2	MBP-PEP4(mature from BY4742)
133	pMALc2	MBP-HA-MES1(Y132A)-cMyc
74	pET8c	ARC1-6His

Table MM-15: Plasmid vectors for Gateway cloning

pSD n°	Vector	Promoter	Insert-Tag
7	pDONR221	-	<i>MES1</i> -WT
8	pDONR221	-	<i>MES1</i> -K11A
9	pDONR221	-	<i>MES1</i> (Δ 142)
10	pDONR221	-	mRuby2 (no stop codon)
11	pDONR221	-	<i>MES1</i> (WT)-AFSAS
12	pDONR221	-	<i>MES1</i> (K11A)-AFSAS
13	pDONR221	-	<i>MES1</i> (142T)-AFSAS
102	pDONR221	-	<i>MES1</i> (S10A)
103	pDONR221	-	<i>MES1</i> (S10D)
104	pDONR221	-	<i>MES1</i> (S10D K11A)
127	pDONR221	-	<i>ARC1</i>
116	pDONR221	-	<i>GUS1</i>
34	pAG306	<i>pGPD</i>	<i>ccdB</i> -FLAG
35	pAG304	<i>pGPD</i>	<i>ccdB</i> -FLAG
36	pAG305	<i>pGPD</i>	<i>ccdB</i> -cMyc
37	pAG304	<i>pGPD</i>	<i>ccdB</i> -cMyc
46	pAG305	<i>pGPD</i>	<i>ccdB</i> -FLAG
47	pAG306	<i>pGPD</i>	<i>ccdB</i> -Vph1-HA
48	pAG306	<i>pGPD</i>	Vph1- <i>ccdB</i> -HA
49	pAG305	<i>pGPD</i>	<i>ccdB</i> -Heh2-HA
50	pAG305	<i>pGPD</i>	Heh2- <i>ccdB</i> -HA
68	pAG414	<i>pMES1</i>	<i>ccdB</i> - β 11
75	pAG416	<i>pGPD</i>	Vph1- <i>ccdB</i> -HA
142	pAG304	<i>pMES1</i>	<i>ccdB</i> -EGFP

Table MM-16 : Plasmids with fluorescent tag

pSD n°	Vector	Promoter	Insert-Tag	Enzyme for linearization
69	pAG414	<i>pMES1</i>	<i>MES1(WT)-β11</i>	-
70	pAG414	<i>pMES1</i>	<i>MES1(Δ142)-β11</i>	-
111	pAG304	<i>pGPD</i>	<i>1-111MES1-EGFP</i>	AccI
112	pAG304	<i>pGPD</i>	<i>1-121MES1-EGFP</i>	AccI
113	pAG304	<i>pGPD</i>	<i>1-142MES1-EGFP</i>	AccI
114	pAG304	<i>pGPD</i>	<i>1-157MES1-EGFP</i>	AccI
115	pAG304	<i>pGPD</i>	<i>1-192MES1-EGFP</i>	AccI
197	pAG414	<i>pMES1</i>	<i>MES1(Δ132)-β11</i>	-
198	pAG414	<i>pMES1</i>	<i>MES1(WT)-EGFP</i>	-
199	pAG414	<i>pMES1</i>	<i>MES1(Δ132)-EGFP</i>	-
224	pAG305	<i>pMES1</i>	<i>MES1-Vph-EGFP</i>	AflII
225	pAG305	<i>pMES1</i>	<i>MES1(Δ132)-Vph-EGFP</i>	AflII
159	pAG305	<i>pMES1</i>	<i>MES1(WT)-EGFP</i>	AflII
160	pAG305	<i>pMES1</i>	<i>MES1(AAAA)-EGFP</i>	AflII
161	pAG305	<i>pMES1</i>	<i>MES1(Δ132)-EGFP</i>	AflII
148	pAG305	<i>pPEP4</i>	<i>PEP4-mRuby2</i>	AflII
71	pRS416	<i>pGPD</i>	<i>mito-roGFP</i>	-
72	pRS304	<i>pGPD</i>	<i>mito-roGFP</i>	SnaBI
73	pRS304	<i>pGPD</i>	<i>roGFP</i>	SnaBI

Table MM-17: Plasmids with cMyc tag (Part 1/2)

pSD n°	Vector	Promoter	Insert-Tag	Enzyme for linearization
82	pAG305	pGPD	<i>MES1(Δ142-AFSAS)-cMyc</i>	AflII
83	pAG305	pGPD	<i>MES1(S10A-AFSAS)-cMyc</i>	AflII
84	pAG305	pGPD	<i>MES1(S10D-AFSAS)-cMyc</i>	AflII
85	pAG305	pGPD	<i>MES1(S10D K11A-AFSAS)-cMyc</i>	AflII
40	pAG305	pGPD	<i>MES1(K11A)-cMyc</i>	AflII
41	pAG305	pGPD	<i>MES1(Δ142)-cMyc</i>	AflII
42	pAG305	pGPD	<i>MES1(S10A)-cMyc</i>	AflII
43	pAG305	pGPD	<i>MES1(S10D)-cMyc</i>	AflII
44	pAG305	pGPD	<i>MES1(S10D K11A)-cMyc</i>	AflII
45	pAG305	pGPD	<i>MES1(K11A-AFSAS)-cMyc</i>	AflII
88	pAG305	pGPD	<i>MES1(WT)-cMyc</i>	AflII
90	pAG306	pGPD	<i>Vph1-MES1(K11A)-cMyc</i>	AflII
91	pAG305	pGPD	<i>MES1(AFSAS)-cMyc</i>	AflII

Table MM-17: Plasmids with cMyc tag (Part 2/2)

pSD n°	Vector	Promoter	Insert-Tag	Enzyme for linearization
92	pAG306	pGPD	<i>Vph1-MES1(WT)-cMyc</i>	AflIII
93	pAG305	pGPD	<i>MES1(Y132A)-cMyc</i>	AflIII
97	pAG306	pGPD	<i>MES1(S10D K11A)-cMyc</i>	Nsil
98	pAG306	pGPD	<i>MES1(S10D)-cMyc</i>	Nsil
99	pAG306	pGPD	<i>Vph1-MES1(S10A)-cMyc</i>	Nsil
107	pAG306	pGPD	<i>MES1(WT)-Vph1-cMyc</i>	Nsil
108	pAG305	pGPD	<i>hMRS(WT)-cMyc</i>	AflIII
150	pAG305	pGPD	<i>MES1(AAAA)-cMyc</i>	AflIII
151	pAG305	pMES1	<i>MES1(AAAA)-cMyc</i>	AflIII
120	pAG305	pMES1	<i>MES1(WT)-cMyc</i>	AflIII
121	pAG305	pMES1	<i>MES1(K11A)-cMyc</i>	AflIII
123	pAG305	pMES1	<i>MES1(S10D K11A)-cMyc</i>	AflIII
124	pAG305	pMES1	<i>MES1(Y132A)-cMyc</i>	AflIII
134	pAG305	pGPD	<i>p43(cyto)-cMyc</i>	HpaI
135	pAG305	pGPD	<i>p43(WT)-cMyc</i>	HpaI
136	pAG305	pGPD	<i>p43(mito/c-)-cMyc</i>	HpaI

Table MM-18: Plasmids with HA tag (Part 1/2)

pSD n°	Vector	Promoter	Insert-Tag	Enzyme for linearization
14	pAG306	<i>pGPD</i>	<i>MES1(WT)-HA</i>	Nsil
22	pAG305	<i>pGPD</i>	<i>MES1(WT)-HA</i>	AflIII
30	pAG304	<i>pGPD</i>	<i>MES1(WT)-HA</i>	AccI
147	pAG305	<i>pMES1</i>	<i>MES1(WT)-HA</i>	AflIII
15	pAG306	<i>pGPD</i>	<i>MES1(K11A)-HA</i>	Nsil
23	pAG305	<i>pGPD</i>	<i>MES1(K11A)-HA</i>	AflIII
31	pAG304	<i>pGPD</i>	<i>MES1(K11A)-HA</i>	AccI
24	pAG305	<i>pGPD</i>	<i>MES1(Δ142)-HA</i>	AflIII
16	pAG306	<i>pGPD</i>	<i>MES1(Δ142)-HA</i>	Nsil
32	pAG304	<i>pGPD</i>	<i>MES1(Δ142)-HA</i>	AccI
156	pAG305	<i>pGPD</i>	<i>MES1(Δ132)-HA</i>	AflIII
158	pAG305	<i>pMES1</i>	<i>MES1(Δ132)-HA</i>	AflIII
17	pAG306	<i>pGPD</i>	<i>MES1(S10A)-HA</i>	Nsil
25	pAG305	<i>pGPD</i>	<i>MES1(S10A)-HA</i>	AflIII
18	pAG306	<i>pGPD</i>	<i>MES1(S10D)-HA</i>	Nsil
33	pAG304	<i>pGPD</i>	<i>MES1(S10D K11A)-HA</i>	AccI

Table MM-18: Plasmids with HA tag (Part 2/2)

pSD n°	Vector	Promoter	Insert-Tag	Enzyme for linearization
26	pAG305	<i>pGPD</i>	<i>MES1(S10D K11A)-HA</i>	AflIII
157	pAG305	<i>pMES1</i>	<i>MES1(AAAA)-HA</i>	AflIII
19	pAG306	<i>pGPD</i>	<i>MES1(WT-AFSAS)-HA</i>	Nsil
27	pAG305	<i>pGPD</i>	<i>MES1(WT-AFSAS)-HA</i>	Nsil
20	pAG306	<i>pGPD</i>	<i>MES1(K11A-AFSAS)-HA</i>	Nsil
28	pAG305	<i>pGPD</i>	<i>MES1(K11A-AFSAS)-HA</i>	Nsil
21	pAG306	<i>pGPD</i>	<i>MES1(Δ142-AFSAS)-HA</i>	Nsil
29	pAG305	<i>pGPD</i>	<i>MES1(Δ142-AFSAS)-HA</i>	AflIII
55	pAG306	<i>pGPD</i>	<i>Vph1-MES1(WT)-HA</i>	Nsil
56	pAG306	<i>pGPD</i>	<i>MES1(WT)-Vph1-HA</i>	Nsil
57	pAG306	<i>pGPD</i>	<i>Vph1-MES1(K11A)-HA</i>	Nsil
58	pAG306	<i>pGPD</i>	<i>MES1(K11A)-Vph1-HA</i>	Nsil
59	pAG306	<i>pGPD</i>	<i>Vph1-MES1(Δ142)-HA</i>	Nsil
60	pAG306	<i>pGPD</i>	<i>MES1(Δ142)-Vph1-HA</i>	Nsil
51	pAG305	<i>pGPD</i>	<i>mRuby2-Heh2-HA</i>	AccI or AflIII
52	pAG305	<i>pGPD</i>	<i>Heh2-mRuby2-HA</i>	AccI or AflIII
53	pAG306	<i>pGPD</i>	<i>Vph1-mRuby2-HA</i>	Nsil
54	pAG306	<i>pGPD</i>	<i>mRuby2-Vph1-HA</i>	Nsil
109	pAG306	<i>pGPD</i>	<i>ARC1-HA</i>	NcoI
110	pAG306	<i>pGPD</i>	<i>Vph1-ARC1-HA</i>	NcoI
128	pAG306	<i>pGPD</i>	<i>Δ1-132ARC1-HA</i>	NcoI
200	pRS426	<i>pGPD</i>	<i>HA-(1-132)MES1</i>	-
137	pAG305	<i>pPEP4</i>	<i>PEP4-3HA (from RS453)</i>	AccI or AflIII
138	pAG306	<i>pPEP4</i>	<i>PEP4-3HA (from RS453)</i>	Nsil
139	pAG305	<i>pPEP4</i>	<i>PEP4-3HA (from BY4742)</i>	AccI or AflIII
117	pAG306	<i>pGPD</i>	<i>GUS1-HA</i>	NcoI
131	pAG305	<i>pGPD</i>	<i>HA-MES1(Y132A)-cMyc</i>	AflIII
132	pAG305	<i>pGPD</i>	<i>HA-MES1(WT)-cMyc</i>	AflIII

Table MM-19: Plasmids with V5 tag (Part 1/3)

pSD n°	Vector	Promoter	Insert-Tag	Enzyme for linearization
86	pAG306	<i>pGPD</i>	<i>MES1(Δ142)-V5</i>	NcoI or Nsil
87	pAG306	<i>pGPD</i>	<i>MES1(Δ142-AFSAS)-V5</i>	NcoI or Nsil
89	pAG305	<i>pGPD</i>	<i>MES1(Δ142)-V5</i>	AflIII
94	pAG306	<i>pGPD</i>	<i>MES1(Δ132-AFSAS)-V5</i>	NcoI or Nsil
95	pAG306	<i>pGPD</i>	<i>MES1(Δ132)-V5</i>	NcoI or Nsil

Table MM-19: Plasmids with V5 tag (Part 2/3)

pSD n°	Vector	Promoter	Insert-Tag	Enzyme for linearization
96	pAG305	<i>pMES1</i>	<i>MES1(Δ132)-V5</i>	AflII
100	pAG306	<i>pGPD</i>	<i>Vph1-MES1(Δ142)-V5</i>	NsiI
105	pAG306	<i>pGPD</i>	<i>Vph1-MES1(Δ132)-V5</i>	NsiI
122	pAG305	<i>pMES1</i>	<i>MES1(Δ132)-V5</i>	AflII
125	pAG305	<i>pMES1</i>	<i>MES1(Δ142)-V5</i>	AflII
126	pAG306	<i>pMES1</i>	<i>MES1(Δ132)-V5</i>	NcoI or NsiI
143	pAG305	<i>pGPD</i>	<i>MES1(WT)-V5</i>	AflII
144	pAG306	<i>pGPD</i>	<i>MES1(WT)-V5</i>	NsiI
145	pAG305	<i>pMES1</i>	<i>MES1(WT)-V5</i>	AflII
146	pAG306	<i>pMES1</i>	<i>MES1(WT)-V5</i>	NsiI
152	pAG305	<i>pGPD</i>	<i>MES1(3A)-V5</i>	AflII
153	pAG306	<i>pGPD</i>	<i>MES1(3A)-V5</i>	NsiI
154	pAG305	<i>pMES1</i>	<i>MES1(3A)-V5</i>	AflII
155	pAG306	<i>pMES1</i>	<i>MES1(3A)-V5</i>	NsiI
172	pAG305	<i>pMES1</i>	<i>MES1(Y132A A133V)-V5</i>	XcmI
173	pAG305	<i>pMES1</i>	<i>MES1(Y132A)-V5</i>	XcmI
174	pAG305	<i>pMES1</i>	<i>MES1(Y132R)-V5</i>	AflII
175	pAG305	<i>pMES1</i>	<i>MES1(Y132D)-V5</i>	AflII
176	pAG305	<i>pMES1</i>	<i>MES1(Y132D A133R)-V5</i>	AflII
181	pAG305	<i>pMES1</i>	<i>MES1(K11A)-V5</i>	AflII
182	pAG305	<i>pMES1</i>	<i>MES1(S10A)-V5</i>	AflII
183	pAG305	<i>pMES1</i>	<i>MES1(S10D)-V5</i>	AflII
184	pAG305	<i>pMES1</i>	<i>MES1(S10D K11A)-V5</i>	AflII
185	pAG305	<i>pMES1</i>	<i>MES1(K11A+3A)-V5</i>	AflII
186	pAG305	<i>pMES1</i>	<i>MES1(S10A+3A)-V5</i>	AflII
187	pAG305	<i>pMES1</i>	<i>MES1(S10D+3A)-V5</i>	AflII
188	pAG305	<i>pMES1</i>	<i>MES1(S10D K11A+3A)-V5</i>	AflII
201	pAG415	<i>pMES1</i>	<i>MES1(Δ132)-V5</i>	-
202	pAG415	<i>pMES1</i>	<i>MES1(WT)-V5</i>	-
203	pAG415	<i>pMES1</i>	<i>MES1(3A)-V5</i>	-
204	pAG415	<i>pMES1</i>	<i>MES1(Y132A A133V)-V5</i>	-
205	pAG415	<i>pMES1</i>	<i>MES1(Y132A)-V5</i>	-
206	pAG415	<i>pMES1</i>	<i>MES1(Y132R)-V5</i>	-
207	pAG415	<i>pMES1</i>	<i>MES1(Y132D)-V5</i>	-
208	pAG415	<i>pMES1</i>	<i>MES1(K11A)-V5</i>	-
209	pAG415	<i>pMES1</i>	<i>MES1(S10A)-V5</i>	-
210	pAG415	<i>pMES1</i>	<i>MES1(S10D)-V5</i>	-

Table MM-19: Plasmids with V5 tag (Part 3/3)

pSD n°	Vector	Promoter	Insert-Tag	Enzyme for linearization
211	pAG415	<i>pMES1</i>	<i>MES1(S10D K11A)-V5</i>	-
212	pAG415	<i>pMES1</i>	<i>MES1(K11A+3A)-V5</i>	-
214	pAG305	<i>pMES1</i>	<i>GUS1(30-196)-MES1(136-Cter)-V5</i>	AflIII
215	pAG305	<i>pMES1</i>	<i>GUS1(30-196)-MES1(196-Cter)-V5</i>	AflIII
216	pAG305	<i>pMES1</i>	<i>MES1(F59A A63H)-V5</i>	AflIII
219	pAG305	<i>pMES1</i>	<i>HA-MES1-V5</i>	AflIII
220	pAG305	<i>pMES1</i>	<i>GUS1(30-196)-MES1(143-Cter)-V5</i>	AflIII
221	pAG305	<i>pMES1</i>	<i>GUS1(30-196)-MES1(S148-Cter)-V5</i>	AflIII
222	pAG305	<i>pMES1</i>	<i>GUS1(30-196)-MES1(K159-Cter)-V5</i>	AflIII
223	pAG305	<i>pMES1</i>	<i>MES1(196-Cter)-V5</i>	AflIII
226	pAG305	<i>pMES1</i>	<i>GUS1(30-196)-MES1(143-158)(196-Cter)-V5</i>	AflIII
227	pAG305	<i>pMES1</i>	<i>GUS1(30-196)-MES1(143-158)(171-Cter)-V5</i>	AflIII
228	pAG305	<i>pMES1</i>	<i>GUS1(30-196)-MES1(143-158)(181-Cter)-V5</i>	AflIII
229	pAG305	<i>pMES1</i>	<i>GUS1(30-196)-MES1(143-169)(181-Cter)-V5</i>	AflIII
230	pAG305	<i>pMES1</i>	<i>GUS1(30-196)-MES1(143-169)(191-Cter)-V5</i>	AflIII
231	pAG305	<i>pMES1</i>	<i>GUS1(30-196)-MES1(143-179)(191-Cter)-V5</i>	AflIII

I.3. Tables of yeast strains

Table MM-20: WT haploid yeast strains and genetic background

sSD N°	Genetic background	Genotype
113,114	RS453 MATa	<i>ade2-1 his3-11,15 leu2-3,112 trp1-1 ura3-52</i>
112	RS453 MATα	<i>ade2-1 his3-11,15 leu2-3,112 trp1-1 ura3-52</i>
100,106	RS453 MATα	<i>ADE2 his3-11,15 leu2-3,112 trp1-1 ura3-52</i>
107	RS453 MATa	<i>ADE2 his3-11,15 leu2-3,112 trp1-1 ura3-52</i>
LabCol 601	BY4741 MATa	<i>his3-Δ1 ura3-Δ0 leu2-Δ0 met15-Δ0 trp1Δ</i>
LabCol 602	BY4742 MATα	<i>his3-Δ1 ura3-Δ0 leu2-Δ0 met15-Δ0 trp1Δ</i>
	W303 MATa	<i>leu2 ura3 lys2 trp1 his3</i>
	SEV6210 MATa	<i>leu2-3,112 ura3-52 his3-Δ200 trp1-Δ901 suc2-Δ9 lys2-801</i>

Table MM-21: Haploid yeast strains (1/3)

SSD N°	Genetic background	Genotype or relevant characteristics	Strain origin
15	RS453 MATa	<i>mRuby2-VPH1-HA:URA3</i>	LabCol 549
16	BY4742 MATα		LabCol 602
17	BY4741 MATa	<i>mxr1Δ::KanMX4</i>	
18	BY4741 MAT?	<i>mxr2Δ::KanMX4</i>	
19	BY4741 MATa	<i>mxr1Δ::KanMX4 mxr2Δ::KanMX4</i>	
82	RS453 MATα	<i>mes1Δ::HIS3 MES1(S10D/K11A)-cMyc:LEU2</i>	sSD60 spore
83	RS453 MAT?		sSD60 spore
84	RS453 MATa	<i>mes1Δ::HIS3 VPH1-MES1(Δ132)-V5:URA3</i>	sSD60 spore
85	RS453 MAT?		sSD61 spore
86	RS453 MATa		-
87	RS453 MAT?	<i>mes1Δ::HIS3 ; MES1(Δ142)-V5:LEU2</i>	-
88	RS453 MATα	<i>mes1Δ::HIS3 MES1(Y132A)-cMyc:LEU2</i>	sSD54 spore
89	RS453 MAT?		sSD54 spore
90	RS453 MATα	<i>mes1Δ::HIS3 MES1(WT)-cMyc:LEU2</i>	sSD42 spore
91	RS453 MAT?		sSD42 spore
92	RS453 MATa	<i>mes1Δ::HIS3 MES1(S10D)-cMyc:LEU2</i>	sSD40 spore
93	RS453 MAT?		sSD40 spore
94	RS453 MATa	<i>mes1Δ::HIS3 MES1(WT)-Vph1-cMyc:URA3</i>	sSD71 spore
95	RS453 MAT?		sSD71 spore
96	RS453 MATα	<i>mes1Δ::HIS3 MES1(S10A)-cMyc:LEU2</i>	sSD39 spore
97	RS453 MAT?		sSD39 spore
98	RS453 MATa	<i>mes1Δ::HIS3 MES1(S10D/K11A)-cMyc:LEU2</i>	sSD41 spore
99	RS453 MAT?		sSD41 spore
101	RS453 MATa	<i>ADE2 arc1::KanMX4</i>	-
102,103	RS453 MAT?	<i>mes1Δ::HIS3 MES1(Δ142)-V5:URA3</i>	-
104,105	RS453 MAT?	<i>mes1Δ::HIS3 ; MES1(K11A)-cMyc:LEU2</i>	sSD38 spore
108,109	RS453 MATα	<i>ADE2 arc1::KanMX4</i>	-
110,111	RS453 MATa		-
115	RS453 MATα	<i>arc1::KanMX4</i>	-
116	RS453 MAT?		-
117-119	RS453 MAT?	<i>mes1Δ::HIS3 VPH1-MES1(Δ132)-cMyc:URA3</i>	sSD44 spore
120,121	RS453 MAT?	<i>arc1::KanMX4 MES1-VPH1:URA3</i>	ssSD71 spore
122,123	RS453 MAT?	<i>mes1Δ::HIS3 MES1(Δ132)-V5:URA3</i>	sSD52 spore
124,125	RS453 MAT?	<i>arc1::KanMX4 mes1Δ::HIS3 MES1(S10A)-cMyc:LEU2</i>	-
126	RS453 MATα	<i>mes1Δ::HIS3 hMRS-cMyc:LEU2</i>	-
127	RS453 MATa		-
128,129	RS453 MAT?	<i>mes1Δ::HIS3 hMRS-cMyc:LEU2</i>	-
130,131	RS453 MAT?	<i>MES1-HA:TRP1 MES1-VPH1-cMyc:URA3</i>	sSD71 spore
132,133	RS453 MAT?	<i>ADE2 mes1Δ::HIS3 arc1::KanMX4 hMRS-cMyc:LEU2</i>	-
134,135	RS453 MAT?	<i>mes1Δ::HIS3 arc1::KanMX4 hMRS-cMyc:LEU2</i>	-
144,145	RS453 MAT?	<i>ADE2 mes1Δ::HIS3 arc1::KanMX4 MES1(Y132A)-cMyc:LEU2</i>	-
146	RS453 MAT?	<i>mes1Δ::HIS3 arc1::KanMX4 MES1(Y132A)-cMyc:LEU2</i>	-
147,148	RS453 MAT?	<i>ADE2 mes1Δ::HIS3 arc1::KanMX4 MES1(S10D)-cMyc:LEU2</i>	-
149	RS453 MAT?	<i>mes1Δ::HIS3 arc1::KanMX4 MES1(S10D)-cMyc:LEU2</i>	-
150,151	RS453 MAT?	<i>ADE2 mes1Δ::HIS3 arc1::KanMX4 MES1(S10D/K11A)-cMyc:LEU2</i>	-
152	RS453 MAT?	<i>mes1Δ::HIS3 arc1::KanMX4 MES1(S10D/K11A)-cMyc:LEU2</i>	-
153	RS453 MAT?	<i>ADE2 mes1Δ::HIS3 arc1::KanMX4 MES1-VPH1-cMyc:LEU2</i>	-
154	RS453 MAT?	<i>ADE2 mes1Δ::HIS3 arc1::KanMX4 VPH1-MES1(Δ132)-cMyc:LEU2</i>	-
155	RS453 MAT?	<i>mes1Δ::HIS3 arc1::KanMX4 VPH1-MES1(Δ132)-cMyc:LEU2</i>	-

Table MM-21: Haploid yeast strains (2/3)

SSD N°	Genetic background	Genotype or relevant characteristics	Strain origin
156	RS453 MAT α	<i>ADE2 mes1Δ::HIS3 arc1::KanMX4 p(shuffle)-MES1</i>	-
157	RS453 MAT α	<i>mes1Δ::HIS3 arc1::KanMX4 p(shuffle)-MES1</i>	-
158	RS453 MAT α	<i>ADE2 arc1::KanMX4 ARC1:URA3</i>	sSD111+ pSD109
159	RS453 MAT α	<i>ADE2 arc1::KanMX4 URA3</i>	sSD111+ pSD3
165	RS453 MAT α	<i>ADE2 arc1::KanMX4 GUS1:URA3</i>	sSD111 + pSD117
166	RS453 MAT α	<i>ADE2 arc1::KanMX4 MES1(AFSAS):URA3</i>	sSD111 + pSD19
167	RS453 MAT α	<i>ADE2 arc1::KanMX4 MES1(WT):URA3</i>	sSD111 + pSD14
168	RS453 MAT α	<i>ADE2 arc1::KanMX4 MES1(WT):URA3</i>	sSD111 + pSD14
169-171	RS453 MAT α	<i>ADE2 arc1::KanMX4 SUP11 2nd generation</i>	sSD111 SUP 2 nd generation
172	RS453 MAT α	<i>ADE2 arc1::KanMX4 pAG425-ARC1-10\timesHis</i>	sSD111 + pMH10
176-179	RS453 MAT α	<i>ADE2 arc1::KanMX4 SUP11 1st generation</i>	sSD111 SUP 1 st generation
216	RS453 MAT α	<i>mes1Δ::HIS3 pMES1-MES1(WT)-cMyc:LEU2</i>	sSD180 spore
217-220	RS453 MAT α	<i>arc1Δ::KanMX4</i>	LabCo1549 <i>arc1Δ</i>
221-224	RS453 MAT α	<i>pep4Δ::KanMX4</i>	LabCo1550 <i>pep4Δ</i>
225	RS453 MAT α	<i>pep4Δ::KanMX4 pPEP4-PEP4-HA:LEU2</i>	sSD223 + pSD137
226	RS453 MAT α	<i>pep4Δ::KanMX4 pPEP4-PEP4-HA:URA3</i>	sSD221 + pSD138
227,228	RS453 MAT α	<i>mes1Δ::HIS3 pMES1-MES1(Δ132)-V5:LEU2</i>	sSD183 spore
231,232	RS453 MAT α	<i>mes1Δ::HIS3 pep4Δ::KanMX4 pMES1-MES1(WT)-cMyc:LEU2</i>	sSD230 spore
233	RS453 MAT α		sSD230 spore
235-237	RS453 MAT α	<i>mes1Δ::HIS3 ΔPEP4::KanMX4 pMES1-MES1(WT)-cMyc:LEU2 pMES1-MES1(Δ132)-V5:URA3</i>	sSD231 + pSD126
242	RS453 MAT α	<i>mes1Δ::HIS3 pMES1-MES1(WT)-V5:LEU2</i>	sSD240 spore
243	RS453 MAT α		sSD240 spore
244	RS453 MAT α	<i>mes1Δ::HIS3 pMES1-MES1(WT)-HA:LEU2</i>	sSD241 spore
245	RS453 MAT α		sSD241 spore
246	RS453 MAT α	<i>ADE2 mes1Δ::HIS3 hMRS-cMyc:LEU2</i>	sSD126 <i>ADE2</i>
247	RS453 MAT α		sSD127 <i>ADE2</i>
248	RS453 MAT α	<i>ADE2 mes1Δ::HIS3 pMES1-MES1(Δ132)-V5:LEU2</i>	sSD227 <i>ADE2</i>
249	RS453 MAT α		sSD228 <i>ADE2</i>
252	RS453 MAT α	<i>mes1Δ::HIS3 pMES1-MES1(3A)-V5:LEU2</i>	-
253	RS453 MAT α		-
254	RS453 MAT α	<i>mes1Δ::HIS3 pGPD-MES1(3A)-cMyc:LEU2</i>	-
255	RS453 MAT α		-
256	RS453 MAT α	<i>mes1Δ::HIS3 pGPD-MES1(3A)-V5:LEU2</i>	-
257	RS453 MAT α		-
258	RS453 MAT α	<i>ADE2 pPEP4-PEP4-mRuby2:LEU2</i>	-
264	RS453 MAT α	<i>mes1Δ::HIS3 pep4Δ::KanMX4 pMES1-MES1(WT)-V5:LEU2</i>	sSD251 spore
265,266	RS453 MAT α	<i>ADE2 mes1Δ::HIS3 pep4Δ::KanMX4 pMES1-MES1(WT)-V5:LEU2</i>	sSD251 spore
270	RS453 MAT α	<i>mes1Δ::HIS3 pMES1-MES1(WT)-V5:LEU2</i>	sSD269 spore
271	RS453 MAT α		sSD269 spore
272,273	RS453 MAT α	<i>mes1Δ::HIS3 pep4Δ::KanMX4 pMES1-MES1(WT)-V5:LEU2</i>	sSD270 <i>pep4Δ</i>
274,275	RS453 MAT α		sSD271 <i>pep4Δ</i>
276	RS453 MAT α	<i>ADE2 pep4Δ::KanMX4 pPEP4-PEP4-mRuby2:LEU2</i>	sSD258 <i>pep4Δ</i>
277	RS453 MAT α	<i>mes1Δ::HIS3 arc1Δ::KanMX4 pMES1-MES1(WT)-V5:LEU2</i>	sSD270 <i>arc1Δ</i>
278	RS453 MAT α		sSD271 <i>arc1Δ</i>
279	RS453 MAT α	<i>ADE2 pGPD-(F59K)mRuby2(Leu^{F5C})-EGFP:TRP1</i>	sSD106 + pSD167
280	RS453 MAT α	<i>ADE2 pGPD-(F59K)mRuby2(Leu^{F5C})-EGFP:TRP1</i>	sSD106 + pSD168
281	RS453 MAT α	<i>ADE2 pGPD-(F59K)mRuby2(Arg^{F66})-EGFP:TRP1</i>	sSD106 + pSD169
282	RS453 MAT α	<i>ADE2 pGPD-(F59K)mRuby2(Arg^{F66})-EGFP:TRP1</i>	sSD106 + pSD170
283	RS453 MAT α	<i>ADE2 pGPD-(F59K)mRuby2(Gln^{C46})-EGFP:TRP1</i>	sSD106 + pSD171

Table MM-21: Haploid yeast strains (3/3)

SSD N°	Genetic background	Genotype or relevant characteristics	Strain origin
284	RS453 MATa	<i>ADE2 arc1::KanMX4 pGPD-(F59K)mRuby2(Leu^{TC})-EGFP:TRP1</i>	SSD111 + pSD167
285	RS453 MATa	<i>ADE2 arc1::KanMX4 pGPD-(F59K)mRuby2(Leu^{TC})-EGFP:TRP1</i>	SSD111 + pSD168
286	RS453 MATa	<i>ADE2 arc1::KanMX4 pGPD-(F59K)mRuby2(Arg^{GC6})-EGFP:TRP1</i>	SSD111 + pSD169
287	RS453 MATa	<i>ADE2 arc1::KanMX4 pGPD-(F59K)mRuby2(Arg^{GC6})-EGFP:TRP1</i>	SSD111 + pSD170
288	RS453 MATa	<i>ADE2 arc1::KanMX4 pGPD-(F59K)mRuby2(Gln^{AG})-EGFP:TRP1</i>	SSD111 + pSD171
290,291	RS453 MATa	<i>mes1Δ::HIS3 arc1Δ::KanMX4 ; pep4Δ::TRP1 pMES1-MES1(WT)-V5:LEU2</i>	SSD277 pep4Δ
292	RS453 MATa	<i>mes1Δ::HIS3 pMES1-MES1(Y132A)-V5:LEU2</i>	SSD297 spore3
293	RS453 MATα		SSD297 spore3
294	RS453 MATa		SSD296 spore
295	RS453 MATα		SSD296 spore
300	RS453 MATα		<i>ADE2 pGPD-(F59K)mRuby2(Met^{AT6})-EGFP:TRP1</i>
301	RS453 MATa	<i>ADE2 arc1::KanMX4 pGPD-(F59K)mRuby2(Met^{AT6})-EGFP:TRP1</i>	SSD111 + pSD164
302,303	RS453 MAT?	<i>mes1Δ::HIS3 pMES1-MES1(WT)-EGFP:LEU2</i>	SSD267 spore
304	RS453 MATa		SSD298 spore
305,306	RS453 MAT?	<i>mes1Δ::HIS3 pMES1-MES1(Δ132)-EGFP:LEU2</i>	SSD268 spore
315	RS453 MATα	<i>mes1Δ::HIS3 arc1::KanMX pMES1-MES1(WT)-V5:LEU2</i>	SSD242 arc1Δ
316	RS453 MATa	<i>mes1Δ::HIS3 arc1::KanMX pMES1-MES1(Δ132)-V5:LEU2</i>	SSD228 arc1Δ
323	RS453 MATa	<i>mes1Δ::HIS3 pMES1-MES1(WT)-V5:LEU2</i>	SSD289 spore 7a
324	RS453 MATa		SSD289 spore 7b
325	RS453 MATα		SSD289 spore 7c
326	RS453 MATα		SSD289 spore 7d
327-330	RS453 MATa	<i>mes1Δ::HIS3 pep4Δ::URA3 pMES1-MES1(WT)-V5:LEU2</i>	SSD270 + pep4Δ
331,332	RS453 MATa	<i>mes1Δ::HIS3 arc1Δ::KanMX4 pMES1-MES1(WT)-V5:LEU2 pAG414-pARC1-ARC1(Nter)-β11</i>	SSD277 + pMH6
333,334	RS453 MATa	<i>mes1Δ::HIS3 arc1Δ::KanMX4 pMES1-MES1(WT)-V5:LEU2 pAG414-pARC1-ARC1(WT)-β11</i>	SSD277 + pMH7
335,336	RS453 MATa	<i>mes1Δ::HIS3 arc1Δ::KanMX4 pMES1-MES1(WT)-V5:LEU2 pAG414-pARC1-ARC1(ΔN)-β11</i>	SSD277 + pMH24
337,338	RS453 MATa	<i>mes1Δ::HIS3 arc1Δ::KanMX4 pMES1-MES1(WT)-V5:LEU2 pAG414-pARC1-ARC1(ΔC)-β11</i>	SSD277 + pMH30
339	RS453 MATa	<i>mes1Δ::HIS3 pMES1-MES1(WT)-V5:LEU2 pAG414-pMES1-MES1(WT)-EGFP</i>	SSD270 + pSD198
340	RS453 MATa	<i>mes1Δ::HIS3 pMES1-MES1(WT)-V5:LEU2 pAG414-pMES1-MES1(Δ132)-EGFP</i>	SSD270 + pSD199
341	RS453 MAT?	<i>mes1Δ::HIS3 pMES1-MES1(Δ132)-V5:LEU2 SUP 1c</i>	SSD183 spore SUP
342	RS453 MAT?	<i>mes1Δ::HIS3 pMES1-MES1(Δ132)-V5:LEU2 SUP 1d</i>	SSD183 spore SUP
343	RS453 MAT?	<i>mes1Δ::HIS3 pMES1-MES1(Δ132)-V5:LEU2 SUP 2a</i>	SSD183 spore SUP
344	RS453 MAT?	<i>mes1Δ::HIS3 pMES1-MES1(Δ132)-V5:LEU2 SUP 2b</i>	SSD183 spore SUP
345-348	RS453 MAT?	<i>mes1Δ::HIS3 pMES1-MES1(Δ132)-V5:LEU2 pAG426-MES1(Nter)</i>	SSD183 spore + MES1(Nter)
352	RS453 MATa	<i>mes1Δ::HIS3 pMES1-GUS1(30-196)-MES1(136-Cter)-V5:LEU2</i>	SSD349 spore
353	RS453 MATα	<i>mes1Δ::HIS3 pMES1-GUS1(30-196)-MES1(136-Cter)-V5:LEU2</i>	SSD349 spore
354	RS453 MATα	<i>mes1Δ::HIS3 pMES1-MES1(F59A A63H)-V5:LEU2</i>	SSD351 spore
355	RS453 MATa		SSD351 spore
360	RS453 MATa	<i>ADE2 arc1::KanMX4 pAG415-pMES1-MES1(WT)-10×His</i>	SSD111 + pSD217
361	RS453 MATa	<i>ADE2 arc1::KanMX4 pAG415-pMES1-MES1(Δ132)-10×His</i>	SSD111 + pSD218

Table MM-22: Diploid yeast strains (1/2)

sSD N°	Genetic background	Genotype or relevant characteristics	Strain origin
34	RS453 2n	<i>mes1Δ::HIS3/mes1Δ::HIS3 MES1-HA:TRP1</i>	LabCol1366*LabCol35
35	RS453 2n	<i>MES1/mes1Δ::HIS3 LEU2/leu2</i>	SSD34 + pSD2
36	RS453 2n	<i>MES1/mes1Δ::HIS3 URA3:ura3</i>	SSD34 + pSD3
37	RS453 2n	<i>mes1Δ/mes1Δ MES1-HA:TRP1 MES1(Δ132)-V5:URA3</i>	SSD34 + pSD95
38	RS453 2n	<i>mes1Δ/mes1Δ MES1-HA:TRP1 URA3 MES1(K11A)-cMyc:LEU2</i>	SSD36 + pSD40
39	RS453 2n	<i>mes1Δ/mes1Δ MES1-HA:TRP1 URA3 MES1(S10A)-cMyc:LEU2</i>	SSD36 + pSD42
40	RS453 2n	<i>mes1Δ/mes1Δ MES1-HA:TRP1 URA3 MES1(S10D)-cMyc:LEU2</i>	SSD36 + pSD43
41	RS453 2n	<i>mes1Δ/mes1Δ MES1-HA:TRP1 URA3 MES1(S10D K11A)-cMyc:LEU2</i>	SSD36 + pSD44
42	RS453 2n	<i>mes1Δ/mes1Δ MES1-HA:TRP1 URA3 MES1(WT)-cMyc:LEU2</i>	SSD36 + pSD88
44,45	RS453 2n	<i>mes1Δ/mes1Δ MES1-HA:TRP1 VPH1-MES1(Δ132)-V5:URA3</i>	SSD34 + pSD105
46,47	RS453 2n	<i>mes1Δ/mes1Δ MES1-HA:TRP1 MES1(Δ132)-V5:LEU2</i>	SSD34 + pSD96
48	RS453 2n	<i>mes1Δ/mes1Δ MES1-HA:TRP1 MES1(Δ132)-V5:URA3 MES1(S10D)-cMyc:LEU2</i>	SSD37 + pSD43
49	RS453 2n	<i>mes1Δ/mes1Δ MES1-HA:TRP1 MES1(Δ132)-V5:URA3 MES1(S10D K11A)-cMyc:LEU2</i>	SSD37 + pSD44
50	RS453 2n	<i>mes1Δ/mes1Δ MES1-HA:TRP1 MES1(Δ132)-V5:URA3 MES1(S10D K11A-AFSAS)-cMyc:LEU2</i>	SSD37 + pSD85
51	RS453 2n	<i>mes1Δ/mes1Δ MES1-HA:TRP1 MES1(Δ132)-V5:URA3 MES1(S10D-AFSAS)-cMyc:LEU2</i>	SSD37 + pSD84
52,53	RS453 2n	<i>mes1Δ/mes1Δ MES1-HA:TRP1 MES1(Δ132)-V5:URA3 LEU2</i>	SSD37 + pSD2
54,55	RS453 2n	<i>mes1Δ/mes1Δ MES1-HA:TRP1 URA3 MES1(Y132A)-cMyc:LEU2</i>	SSD36 + pSD93
56,57	RS453 2n	<i>mes1Δ/mes1Δ MES1-HA:TRP1 URA3 MES1(AFSAS)-cMyc:LEU2</i>	SSD36 + pSD91
58,59	RS453 2n	<i>mes1Δ/mes1Δ MES1-HA:TRP1 VPH1-MES1(Δ132)-V5:URA3 MES1(K11A)-cMyc:LEU2</i>	SSD45 + pSD40
60,61	RS453 2n	<i>mes1Δ/mes1Δ MES1-HA:TRP1 VPH1-MES1(Δ132)-V5:URA3 MES1(S10D K11A)-cMyc:LEU2</i>	SSD45 + pSD44
62	RS453 2n	<i>mes1Δ/mes1Δ MES1-HA:TRP1 VPH1-MES1(Δ132)-V5:URA3 MES1(S10A)-cMyc:LEU2</i>	SSD45 + pSD42
63,64	RS453 2n	<i>mes1Δ/mes1Δ MES1-HA:TRP1 MES1(Δ132)-V5:LEU2 VPH1-MES1(S10D)-cMyc:URA3</i>	SSD47 + pSD98
65,66	RS453 2n	<i>mes1Δ/mes1Δ MES1-HA:TRP1 MES1(Δ132)-V5:LEU2 VPH1-MES1(K11A)-cMyc:URA3</i>	SSD47 + pSD90
67,68	RS453 2n	<i>mes1Δ/mes1Δ MES1-HA:TRP1 MES1(Δ132)-V5:LEU2 VPH1-MES1(S10D K11A)-cMyc:URA3</i>	SSD47 + pSD97
69,70	RS453 2n	<i>mes1Δ/mes1Δ MES1-HA:TRP1 MES1(Δ132)-V5:LEU2 VPH1-MES1(S10A)-cMyc:URA3</i>	SSD47 + pSD99
71	RS453 2n	<i>MES1/mes1Δ::HIS3 LEU2 MES1(WT)-VPH1-cMyc:URA3</i>	SSD35 + pSD107
72,73	RS453 2n	<i>mes1Δ/mes1Δ MES1-HA:TRP1 MES1(Δ132-AFSAS)-V5:URA3</i>	SSD34 + pSD94
74,75	RS453 2n	<i>mes1Δ/mes1Δ MES1-HA:TRP1 MES1(Δ132)-V5:URA3 MES1(K11A)-cMyc:LEU2</i>	SSD37 + pSD40
76	RS453 2n	<i>mes1Δ/mes1Δ MES1-HA:TRP1 MES1(Δ132)-V5:URA3 MES1(S10A)-cMyc:LEU2</i>	SSD37 + pSD42
77	RS453 2n	<i>mes1Δ/mes1Δ MES1-HA:TRP1 MES1(Δ132)-V5:URA3 MES1(S10A-AFSAS)-cMyc:LEU2</i>	SSD37 + pSD83
78,79	RS453 2n	<i>mes1Δ/mes1Δ MES1-HA:TRP1 MES1(Δ132)-V5:URA3 MES1(Y132A)-cMyc:LEU2</i>	SSD37 + pSD93
80,81	RS453 2n	<i>mes1Δ/mes1Δ MES1-HA:TRP1 URA3 LEU2</i>	SSD36 + pSD2
160,161	RS 2n	<i>arc1Δ/arc1Δ</i>	SSD109*SSD111
162	RS 2n		SSD109*SSD110
163	RS 2n		SSD108*SSD110
164	RS 2n		SSD108*SSD111
180,181	RS453 2n	<i>mes1Δ/mes1Δ MES1-HA:TRP1 pMES1-MES1(WT)-cMyc:LEU2</i>	SSD34 + pSD120
182	RS453 2n	<i>mes1Δ/mes1Δ MES1-HA:TRP1 pMES1-MES1(K11A)-cMyc:LEU2</i>	SSD34 + pSD121
183	RS453 2n	<i>mes1Δ/mes1Δ MES1-HA:TRP1 pMES1-MES1(Δ132)-V5:LEU2</i>	SSD34 + pSD122
184	RS453 2n	<i>mes1Δ/mes1Δ MES1-HA:TRP1 pMES1-MES1(S10D K11A)-cMyc:LEU2</i>	SSD34 + pSD123
185,186	RS453 2n	<i>mes1Δ/mes1Δ MES1-HA:TRP1 pMES1-MES1(Y132A)-cMyc:LEU2</i>	SSD34 + pSD124
187	RS453 2n	<i>mes1Δ/mes1Δ MES1-HA:TRP1 pMES1-MES1(Δ142)-V5:LEU2</i>	SSD34 + pSD125
188	RS453 2n	<i>mes1Δ/mes1Δ MES1-HA:TRP1 pMES1-MES1(Δ132)-V5:URA3</i>	SSD34 + pSD126
189	RS453 2n	<i>mes1Δ/mes1Δ MES1-HA:TRP1 pGPD-MES1(WT-AFSAS)-HA:URA3</i>	SSD34 + pSD19
190	RS453 2n	<i>arc1Δ/arc1Δ URA3</i>	SSD164 + pSD3

Table MM-22: Diploid yeast strains (2/2)

sSD N°	Genetic background	Genotype or relevant characteristics	Strain origin
191,192	RS453 2n	<i>arc1Δ/arc1Δ pGPD-MES1(WT)-HA:URA3</i>	SSD164 + pSD14
193	RS453 2n	<i>arc1Δ/arc1Δ pGPD-MES1(Δ142)-HA:URA3</i>	SSD164 + pSD16
194,195	RS453 2n	<i>arc1Δ/arc1Δ pGPD-MES1(AFSAS)-HA:URA3</i>	SSD164 + pSD19
196,197	RS453 2n	<i>arc1Δ/arc1Δ pGPD-MES1(Δ132)-V5:URA3</i>	SSD164 + pSD95
198,199	RS453 2n	<i>arc1Δ/arc1Δ pGPD-MES1(WT)-VPH1-cMyc:URA3</i>	SSD164 + pSD107
200	RS453 2n	<i>arc1Δ/arc1Δ pGPD-ARC1-3HA:URA3</i>	SSD164 + pSD109
201	RS453 2n	<i>arc1Δ/arc1Δ pGPD-VPH1-ARC1-3HA:URA3</i>	SSD164 + pSD110
202	RS453 2n	<i>arc1Δ/arc1Δ pGPD-ARC1(Δ1-132)-HA:URA3</i>	SSD164 + pSD128
203,204	RS453 2n	<i>arc1Δ/arc1Δ pMES1-MES1(WT)-cMyc:LEU2</i>	SSD164 + pSD120
205,206	RS453 2n	<i>arc1Δ/arc1Δ pMES1-MES1(Δ132)-cMyc:LEU2</i>	SSD164 + pSD122
215	RS453 2n	<i>arc1Δ/arc1Δ Sup11/WT</i>	SSD115* ^s SSD176
229	RS453 2n	<i>mes1Δ/MES1 arc1Δ/ARC1 pMES1-MES1(Δ132)-V5:LEU2</i>	-
230	RS453 2n	<i>mes1Δ/MES1 Δpep4/PEP4 pMES1-MES1(WT)-cMyc:LEU2</i>	SSD216* ^s SSD221
234	RS453 2n	<i>mes1Δ/MES1 pGPD-MES1(WT)-HA:TRP1 pMES1-MES1(Δ132)-cMyc:LEU2</i>	-
238	RS453 2n	<i>mes1Δ/MES1 arc1Δ/ARC1 pMES1-MES1(WT)-cMyc:LEU2</i>	SSD216* ^s SSD219
239	RS453 2n		SSD216* ^s SSD220
240	RS453 2n	<i>mes1Δ/mes1Δ MES1-HA:TRP1 pMES1-MES1(WT)-V5:LEU2</i>	SSD34 + pSD145
241	RS453 2n	<i>mes1Δ/mes1Δ MES1-HA:TRP1 pMES1-MES1(WT)-HA:LEU2</i>	SSD34 + pSD147
250	RS453 2n	<i>mes1Δ/MES1 Δpep4/PEP4 pMES1-MES1(WT)-HA:LEU2</i>	SSD244* ^s SSD224
251	RS453 2n	<i>mes1Δ/MES1 Δpep4/PEP4 pMES1-MES1(WT)-V5:LEU2</i>	SSD242* ^s SSD223
259	RS453 2n	<i>arc1Δ/ARC1 pep4Δ/PEP4 ADE2/ade2</i>	SSD221* ^s SSD111
260	RS453 2n	<i>mes1Δ/MES1 arc1Δ/ARC1 pMES1-MES1(3A)-V5:LEU2</i>	-
261	RS453 2n	<i>mes1Δ/MES1 arc1Δ/ARC1 pMES1-MES1(WT)-V5:LEU2</i>	-
267	RS453 2n	<i>mes1Δ/mes1Δ MES1-HA:TRP1 pMES1-MES1(WT)-EGFP:LEU2</i>	SSD34 + pSD159
268	RS453 2n	<i>mes1Δ/mes1Δ MES1-HA:TRP1 pMES1-MES1(Δ132)-EGFP:LEU2</i>	SSD34 + pSD161
269	RS453 2n	<i>mes1Δ/mes1Δ MES1-HA:TRP1 pMES1-MES1(WT)-V5:LEU2</i>	SSD34 + pSD145
289	RS453 2n	<i>mes1Δ/mes1Δ pMES1-MES1(WT)-V5:LEU2/pMES1-MES1(WT)-V5:LEU2</i>	SSD242* ^s SSD270
296	RS453 2n	<i>mes1Δ/mes1Δ MES1-HA:TRP1 pMES1-MES1(Y132A A133V)-V5:LEU2</i>	SSD34 + pSD172
297	RS453 2n	<i>mes1Δ/mes1Δ MES1-HA:TRP1 pMES1-MES1(Y132A)-V5:LEU2</i>	SSD34 + pSD173
298	RS453 2n	<i>mes1Δ/mes1Δ MES1-HA:TRP1 pMES1-MES1(WT)-EGFP:LEU2</i>	SSD34 + pSD159
299	RS453 2n	<i>mes1Δ/mes1Δ MES1-HA:TRP1 pMES1-MES1(Δ132)-EGFP:LEU2</i>	SSD34 + pSD161
307	RS453 2n	<i>mes1Δ/mes1Δ MES1-HA:TRP1 pMES1-MES1(Y132R)-V5:LEU2</i>	SSD34 + pSD174
308	RS453 2n	<i>mes1Δ/mes1Δ MES1-HA:TRP1 pMES1-MES1(Y132D)-V5:LEU2</i>	SSD34 + pSD175
309	RS453 2n	<i>mes1Δ/mes1Δ MES1-HA:TRP1 pMES1-MES1(Y132D A133R)-V5:LEU2</i>	SSD34 + pSD176
310	RS453 2n	<i>mes1Δ/mes1Δ MES1-HA:TRP1 pMES1-MES1(K11A)-V5:LEU2</i>	SSD34 + pSD181
311	RS453 2n	<i>mes1Δ/mes1Δ MES1-HA:TRP1 pMES1-MES1(S10A)-V5:LEU2</i>	SSD34 + pSD182
312	RS453 2n	<i>mes1Δ/mes1Δ MES1-HA:TRP1 pMES1-MES1(S10D)-V5:LEU2</i>	SSD34 + pSD183
313	RS453 2n	<i>mes1Δ/mes1Δ MES1-HA:TRP1 pMES1-MES1(S10D K11A)-V5:LEU2</i>	SSD34 + pSD184
314	RS453 2n	<i>mes1Δ/mes1Δ MES1-HA:TRP1 pMES1-MES1(K11A+3A)-V5:LEU2</i>	SSD34 + pSD185
349	RS453 2n	<i>mes1Δ/mes1Δ MES1-HA:TRP1 promMES1-(30-196)GUS1-(136-Cter)MES1-V5:LEU2</i>	SSD34 + pSD214
350	RS453 2n	<i>mes1Δ/mes1Δ MES1-HA:TRP1 promMES1-(30-196)GUS1-(196-Cter)MES1-V5:LEU2</i>	SSD34 + pSD215
351	RS453 2n	<i>mes1Δ/mes1Δ MES1-HA:TRP1 promMES1-MES1(F59A A63H)-V5:LEU2</i>	SSD34 + pSD216
356	RS453 2n	<i>mes1Δ/mes1Δ MES1-HA:TRP1 promMES1-(30-196)GUS1-(143-Cter)MES1-V5:LEU2</i>	SSD34 + pSD220
357	RS453 2n	<i>mes1Δ/mes1Δ MES1-HA:TRP1 promMES1-(30-196)GUS1-(148-Cter)MES1-V5:LEU2</i>	SSD34 + pSD221
358	RS453 2n	<i>mes1Δ/mes1Δ MES1-HA:TRP1 promMES1-(30-196)GUS1-(159-Cter)MES1-V5:LEU2</i>	SSD34 + pSD222
359	RS453 2n	<i>mes1Δ/mes1Δ MES1-HA:TRP1 promMES1-MES1(196-Cter)-V5:LEU2</i>	SSD34 + pSD223
215	RS453 2n	<i>arc1Δ/arc1Δ Sup11/WT</i>	SSD115* ^s SSD176





PUBLICATION & POSTERS

- PUBLICATION 1** *Debard et al., Methods, 2017, 113, 91-104* **276**
- PUBLICATION 2** *Yakobov et al., BBA, 2018, 1861(4), 387-400* **292**
- POSTER 1** *26th tRNA conference, 2016, Jeju, South Korea* **308**
- POSTER 2** *11th aaRS meeting, 2017, Clearwater, Florida* **310**
- POSTER 3** *27th tRNA conference, 2018, Strasbourg, France* **312**



Publication 1

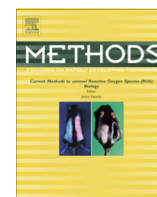
Nonconventional localizations of
cytosolic aminoacyl-tRNA synthetases
in yeast and human cells

***Methods*, 2017, 113, pp. 91-104**



Contents lists available at ScienceDirect

Methods

journal homepage: www.elsevier.com/locate/ymeth

Nonconventional localizations of cytosolic aminoacyl-tRNA synthetases in yeast and human cells

Sylvain Debard^{a,1}, Gaétan Bader^{a,1}, Johan-Owen De Craene^{a,2}, Ludovic Enkler^b, Séverine Bär^a, Daphné Laporte^a, Philippe Hamman^c, Evelyne Myslinski^a, Bruno Senger^a, Sylvie Friant^a, Hubert Dominique Becker^{a,*}

^a Université de Strasbourg, CNRS, GMGM UMR 7156, F-67000 Strasbourg, France

^b IBMC-CNRS, Evolution des ARN non codants chez la levure, Architecture et Réactivité de l'ARN, 15 rue René Descartes, Université de Strasbourg, Strasbourg, France

^c Plateforme Protéomique Strasbourg-Esplanade, Institut de Biologie Moléculaire et Cellulaire, FRC 1589, Centre National de la Recherche Scientifique, Université de Strasbourg, 67084 Strasbourg, France

ARTICLE INFO

Article history:

Received 31 July 2016

Received in revised form 27 September 2016

Accepted 30 September 2016

Available online xxx

Keywords:

aaRS
tRNA
Yeast
Human
Microscopy
Fractionation
MTS
NLS

ABSTRACT

By definition, cytosolic aminoacyl-tRNA synthetases (aaRSs) should be restricted to the cytosol of eukaryotic cells where they supply translating ribosomes with their aminoacyl-tRNA substrates. However, it has been shown that other translationally-active compartments like mitochondria and plastids can simultaneously contain the cytosolic aaRS and its corresponding organellar ortholog suggesting that both forms do not share the same organellar function. In addition, a fair number of cytosolic aaRSs have also been found in the nucleus of cells from several species. Hence, these supposedly cytosolic-restricted enzymes have instead the potential to be multi-localized. As expected, in all examples that were studied so far, when the cytosolic aaRS is imported inside an organelle that already contains its *bona fide* corresponding organellar-restricted aaRSs, the cytosolic form was proven to exert a nonconventional and essential function. Some of these essential functions include regulating homeostasis and protecting against various stresses. It thus becomes critical to assess meticulously the subcellular localization of each of these cytosolic aaRSs to unravel their additional roles. With this objective in mind, we provide here a review on what is currently known about cytosolic aaRSs multi-compartmentalization and we describe all commonly used protocols and procedures for identifying the compartments in which cytosolic aaRSs relocalize in yeast and human cells.

© 2016 The Authors. Published by Elsevier Inc. This is an open access article under the CC BY-NC-ND license (<http://creativecommons.org/licenses/by-nc-nd/4.0/>).

Contents

1. Introduction	00
2. Antibodies: A fundamental tool for aaRSs localization	00
3. Prediction and analysis of aaRSs with organellar import signal	00
3.1. Mitochondrial targeting sequence prediction	00
3.2. Nuclear localization signal prediction	00
4. Subcellular fractionation	00
4.1. Crude membranes fractionation from yeast cells	00
4.2. Purification of nuclei and preparation of nuclear protein extracts	00
4.2.1. Purification of nuclei from yeast cells	00
4.2.2. Purification of nuclei from human cells	00
4.3. Purification of mitochondria and preparation of mitochondrial protein extracts	00

* Corresponding author.

E-mail address: h.becker@unistra.fr (H.D. Becker).

¹ These authors contributed equally to this work.

² Present address: EA 2106, Biomolécules et Biotechnologies Végétales, Université François Rabelais de Tours, UFR Sciences et Techniques, Parc de Grandmont, 37200 Tours, France.

<http://dx.doi.org/10.1016/j.ymeth.2016.09.017>

1046-2023/© 2016 The Authors. Published by Elsevier Inc.

This is an open access article under the CC BY-NC-ND license (<http://creativecommons.org/licenses/by-nc-nd/4.0/>).

4.3.1.	Purification of mitochondria from yeast cells	00
4.3.2.	Obtention of mitoplasts from yeast mitochondria	00
4.3.3.	Purification of mitochondria from human cells	00
4.3.4.	Obtention of mitoplasts from human mitochondria	00
5.	Mass spectrometry analysis and identification of cytosolic aaRSs in yeast mitochondrial extracts	00
5.1.	Protein digestion solution	00
5.2.	Nano-liquid Chromatography – electrospray Ionization TripleTOF MS/MS Analysis	00
5.3.	Database search and data analysis	00
6.	Microscopy analysis and single cell localization	00
6.1.	Immunofluorescence on yeast cells	00
6.1.1.	Fixation steps	00
6.1.2.	Incubation with antibodies	00
6.2.	Immunofluorescence on human cells	00
7.	Concluding remarks	00
	Acknowledgements	00
	Appendix A. Supplementary data	00
	References	00

1. Introduction

Aminoacyl-tRNA synthetases (aaRSs) constitute a family of ubiquitous enzymes present in the three kingdoms of life and essentially known for transfer RNA (tRNA) aminoacylation. Indeed, they are required for the ligation of the 20 standard proteinogenic amino acids (aa) to their cognate tRNAs [1]. tRNA aminoacylation and protein synthesis occur in the cytosol of all organisms but unlike bacteria, eukaryotes have membrane-enclosed structures compartmentalizing their cytosol. Among these compartments, mitochondria in all eukaryotes and also chloroplasts in plants synthesize proteins by translating organellar mRNAs [2]. Hence, a compartmentalized set of the 20 aaRSs is expected in each translationally-active compartment. Since no gene encoding mitochondrial aaRSs was found in any of the mitochondrial DNA sequenced so far, the nuclear genome has to encode both full sets of cytosolic and organellar aaRSs. However, while this is true for the set of 20 cytosolic aaRSs, a full set of 20 additional separate genes encoding organellar aaRSs has never been found in any of the nuclear genomes sequenced so far [3–5]. Both sets of genes can usually be easily distinguished based on phylogenetic analyses. These studies show that a majority of the mitochondrial aaRSs are of bacterial descent but that the α -proteobacterial endosymbiotic origin of the mitochondrial aaRSs has largely been lost because of gene replacements, intranuclear gene duplications and divergence or horizontal gene transfers [6,7].

In plants, the evolution of the different aaRSs seems more complicated. Monocot and dicot have either at least 1 gene encoding a given aaRS for each protein-synthesizing compartment or 2 genes with one gene encoding the cytosolic and the second both the mitochondrial and the chloroplastic aaRS [8]. Surprisingly, both have one instance where only one gene seems to encode all 3 activities: isoleucyl-tRNA synthetase (IleRS) for monocot and glutaminyl-tRNA synthetase (GlnRS) for dicot [5,8,9]. The same is true for diatoms and brown algae in which a single gene seems to encode all 3 arginyl-tRNA synthetases (ArgRSs) [5]. In many instances, the mechanism that allows expression of the organellar aaRS from a gene that also encodes the cytosolic isoform is unknown or ill defined [10,11]. For the sake of brevity, from now on we will use the three letters code for each amino acid mentioned.

Genes encoding several mitochondrial aaRSs are also missing in metazoan and fungal genomes and various strategies are used by these organisms to produce the mitochondrial aaRS from an apparently missing gene. Many of them are encoded by the same exact gene that encodes the cytosolic form, except that the mRNA that

will be translated into the mitochondrial isoform contains an additional 5'-extension for the mitochondrial targeting sequence (MTS). The synthesis of these 2 proteins from the same gene is achieved through different mechanisms: (i) alternative transcription start as shown for the yeast ValRS and HisRS mRNAs [12,13]; (ii) alternative splicing as shown for example for the human LysRS [14]; (iii) alternative translation initiation at two different AUG start codons within the same mRNA such as for the human GlyRS [15]; or (iv) alternative transcription start at a non-canonical start codon such as for the yeast AlaRS [16]. The complete list of cytosolic and organellar aaRSs generated from a single gene is presented in Table 1.

Eukaryotes, with the exception of a few parasites that possess a mitochondrial GlnRS encoded by the same gene as the cytosolic GlnRS, use a different strategy to compensate for the ubiquitous absence of the gene encoding mitochondrial GlnRS [41]. This widespread absence of a mitochondrial GlnRS is an illustration of the evolutionary origin of mitochondria that very likely originated from an α -proteobacterial endosymbiont that was generating glutaminyl-tRNA^{Gln} (Gln-tRNA^{Gln}) not by direct charging of tRNA^{Gln} by a GlnRS but by a tRNA-dependent transamidation pathway, metazoans and fungi kept the endosymbiont's route for mitochondrial Gln-tRNA^{Gln} formation [42]. This tRNA-dependent transamidation pathway requires first glutamylation of mitochondrially-encoded tRNA^{Gln} (mttRNA^{Gln}) by a mitochondrial non-discriminating GluRS and subsequent transamidation of the charged glutamate into glutamine by a mitochondrial tRNA-dependent amidotransferase (AdT) [9,28,43,44]. However, the two enzymes that sustain this pathway seem to have species-specific features. In human cells, it is the mitochondrial GluRS that charges both the mttRNA^{Glu} and the mttRNA^{Gln} [44], whereas in the yeast *Saccharomyces cerevisiae* a pool of the cytosolic GluRS is imported into the mitochondria to carry out glutamylation of mttRNA^{Gln} [28]. Even if metazoans and fungi both belong to the opisthokonta group, their trimeric mitochondrial AdTs differ by one subunit, the classical bacterial-like GatC subunit found in metazoan AdTs is replaced by a fungi-specific GatF subunit [45].

In yeast, there is only one CysRS gene (Supp. Table 1) suggesting that it encodes both the cytosolic and mitochondrial isoforms. However, the mitochondrial CysRS has yet not been experimentally characterized. Along the same line, *S. cerevisiae* genome has two genes, *AIM10* and *YHR020W* that encode for proteins showing similarities to prokaryotic (*AIM10*) and eukaryotic (*YHR020W*) ProRSs (Supp. Table 1). While there are no experimental proofs that *AIM10* encodes a protein with ProRS activity, its deletion leads to a respiratory-deficient yeast cell showing that it required for

Table 1
List of dual-localized cytosolic aaRSs identified so far.

Organism	Localisation	aaRS	Techniques used	Mechanism	References
Hs	Mitochondrial	GlyRS	IF, CF	Alternative transcription start	[15,17]
		LysRS	FM	Alternative mRNA splicing	[14]
	Nuclear	LysRS	CM, CF, CE	Phosphorylation	[18,19]
		MetRS	FM, CE, IF, CF	Cell growth signal induced	[19,20]
		PheRS	IF	n.d.	[21]
		TrpRS	CF, IF, IEM	IFN gamma induced	[22-24]
		TyrRS	IF, CM, CF	tRNA ^{Tyr} binding	[25]
		TyrRS	CF, IF	Oxidative stress induced	[26]
Sc	Mitochondrial	AlaRS	G, CF	Non-AUG alternative translation start	[16,27]
		GluRS	FM, G, CF, CM	Arc1p released	[28,29]
		GlyRS1	G	Non-AUG alternative translation start	[30,31]
		HisRS	G, CF	Alternative transcription start	[12,32]
		ValRS	G	Alternative translation start	[13,33]
	Nuclear	MetRS	FM, CF, CM	Arc1p released	[29,34]
		TyrRS	FM, CF	NLS characterisation	[25,35]
Tb	Mitochondrial	IleRS	IF, CF	Trans-splicing	[36,37]
		GluRS	IF, CF	Trans-splicing	[37,38]
		GlnRS	IF, CF	Trans-splicing	[37,38]
		ProRS	IF	Trans-splicing	[37]
Pf	Apicoplast	AlaRS	IF	n.d.	[39]
		CysRS	FM, IF	Alternative mRNA splicing	[40]
		GlyRS	IF	n.d.	[39]
		ThrRS	IF	n.d.	[39]

aaRSs in bold are enzymes that relocalize stricto sensu from cytosol to the organellar compartment. *Hs*, *Homo sapiens*; *Sc*, *Saccharomyces cerevisiae*; *Tb*, *Trypanosoma brucei*; *Pf*, *Plasmodium falciparum*; CM, confocal microscopy; IF, immunofluorescence; CF, cell fractionation; FM, epifluorescence microscopy; CE, capillary electrophoresis; IEM, immuno-electron microscopy; G, genetic; NLS, nuclear localization signal; n.d., not determined.

mitochondria function [46]. The protein encoded by the *YHR020W* gene has been shown to retain ProRS activity, *in vitro*, and to be essential for cell survival, suggesting that it might be the cytosolic

ProRS [47]. The mitoproteome done on purified *S. cerevisiae* mitochondria (performed as described in Section 5; Fig. 1A) shows that cytosolic CysRS is found in the mitoproteome, suggesting that the

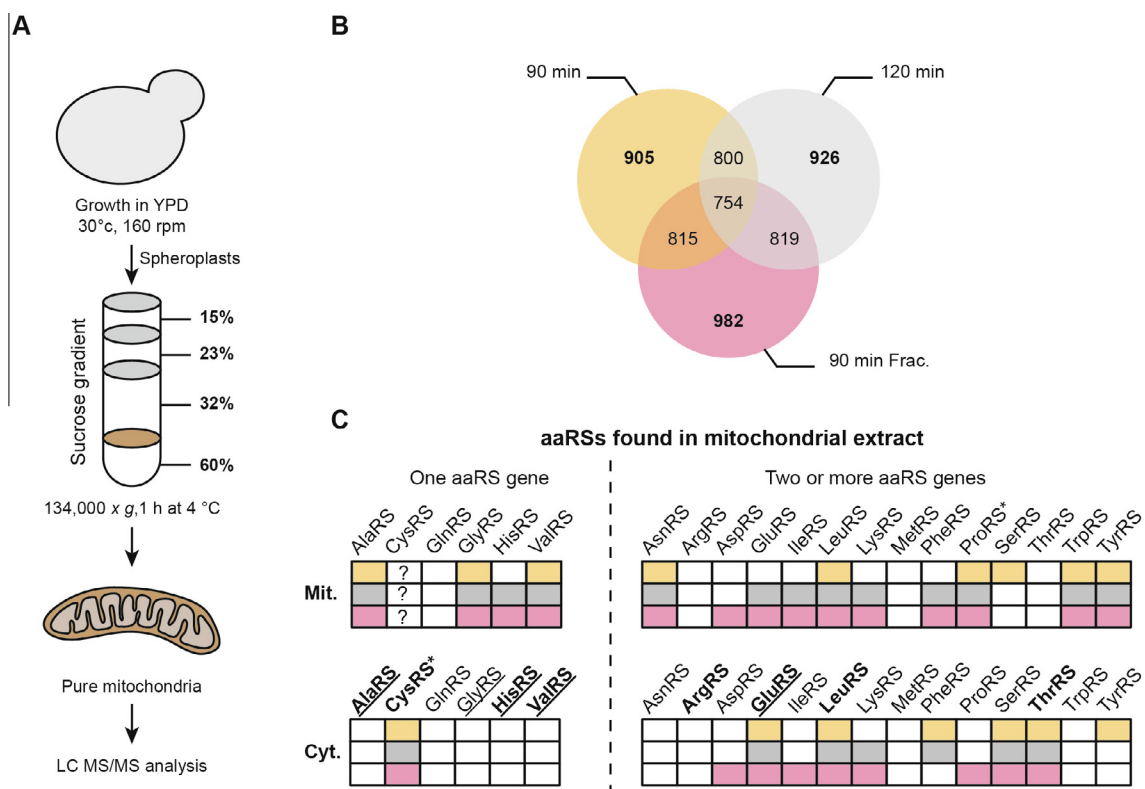


Fig. 1. Mitochondrial localization of cytosolic and mitochondrial aaRSs. (A) Schematized representation of yeast mitochondria preparation. The procedure we followed was that described by Meisinger and coworkers [48]. Mitochondria are recovered from the 60%-32% interphase. (B) LC MS/MS analysis of the mitoproteome. After separation, pure yeast mitochondria were subjected to LC MS/MS analysis with 3 different injection gradients (90 min, 120 min and 90 min Frac, see Section 5 for details). Number of total proteins identified in each samples are represented in bold. Proteins found shared between conditions are also showed. (C) Mitochondrial (top) and cytosolic (bottom) forms of aaRSs identified in mitochondrial extract by LC MS/MS analysis. Colors are corresponding to samples in panel B. Cytosolic aaRSs predicted to have an MTS by at least 1 predictor (see Table 5) are in bold. Yeast cytosolic aaRSs previously shown experimentally as mitochondria dual-localized are underlined (see Table 1). No mitochondrial specific CysRS identify in yeast. * indicates putative aaRSs. See Supplemental Table 1 for yeast aaRSs genes name.

missing mitochondrial CysRS could be compensated by mitochondrial import of the cytosolic ortholog (Fig. 1C). The *AIM10* gene product was found in the different mass-spectrometry analyses (Fig. 1C and Supp. Table 2), confirming its mitochondrial localization, but further experimental proofs that this protein is a functional ProRS are still needed. Interestingly, the *YHR020W* gene product was also found in one of the mass-spectrometry data set we obtained (Fig. 1C and Supp. Table 2), suggesting that the cytosolic ProRS might be dual-localized. In addition, depending on the sample injection time used prior to mass spectrometry, 6–8 additional other cytosolic aaRSs were found in the mitoproteome. Interestingly, each of these mitochondria-imported cytosolic aaRSs has a mitochondrial ortholog encoded by a separate gene. Nonetheless, the deletion of any of these genes encoding the *bona fide* mitochondrial aaRS leads to a respiratory deficiency (SGD website source). This means that the cytosolic aaRS orthologs, imported into mitochondria, cannot compensate for the loss of the mitochondrial ones and thus suggests that they have other roles than cognate $_{\text{mt}}$ tRNA aminoacylation.

Relocalization of cytosolic aaRSs is not restricted to compartments in which their presence is required to supply protein synthesis with aa-tRNAs. Indeed, some cytosolic aaRSs have been localized in the nucleus both in human and *S. cerevisiae* (Table 1). These and other proteins of the translation machinery were first observed while analyzing the protein content of *Xenopus* oocytes and has since also been observed in mammalian and yeast cells [20,29,49–51]. Their proposed function in the nucleus is that by charging only the mature tRNAs, these aaRSs are in charge of a quality-control step of the tRNA maturation process prior to their export to the cytoplasm [49,50]. More recent reports show other functions for these nuclear pools of human and yeast aaRSs that do not require their tRNA-charging capacities. For example, under oxidative stress a portion of the human TyrRS relocalizes to the nucleus where it activates E2F1, a transcription factor that up-regulates the expression of DNA damage repair genes [26]. Likewise, a pool of the human MetRS relocalizes into the nucleoli of

proliferating cells to regulate rRNA biogenesis [20]. In the yeast *S. cerevisiae*, a pool of MetRS relocalizes into the nucleus to regulate transcription of genes encoding subunits of respiratory complexes [29]. More broadly, a previous bioinformatics analysis identified 16 yeast cytosolic aaRSs as harboring a putative nuclear localization signal (NLS) suggesting that these enzymes could enter the nucleus to ensure additional functions other than translation [52]. However the MetRS, experimentally shown to relocalize into the nucleus was not identified by this bioinformatics study. This highlights the limits of the bioinformatics prediction algorithms to identify targeting sequences, hence the difficulties to predict in which additional compartments these aaRSs could eventually relocalize. However, the scientific community that studies these enzymes has come to the consensus that any cytosolic aaRSs could potentially be multi-localized.

Defining what we mean by multi-localized aaRSs is not an easy task given the variety of strategies that organisms use to relocalize the same protein in several compartments. In the present review, we will define a multi-localized aaRS as a cytosolic aaRS that is found in at least 2 different compartments and for which the organellar isoform is produced from the same gene as the cytosolic one through the various strategies that have been detailed in the previous paragraphs (see also Table 1).

The mechanisms regulating these multi-localizations have been mostly studied for aaRSs that belong to multi-synthetase complexes (MSCs) found in all eukaryotic species studied so far. They are composed of 2–9 cytosolic aaRSs interacting with 1–3 cytosolic anchors called aminoacyl-tRNA synthetase-interacting multifunctional proteins (AIMPs) [53–59]. It has been proposed and experimentally verified for some of the MSC-interacting cytosolic aaRSs that these MSCs are reservoirs for releasable aaRSs that can relocalize to other subcellular compartments to exert nonconventional functions [29,60,61].

In this review, we gather the various methods and procedures that have been used to address the localization of individual cytosolic aaRSs (Fig. 2). Some are biochemical (organelle purification),

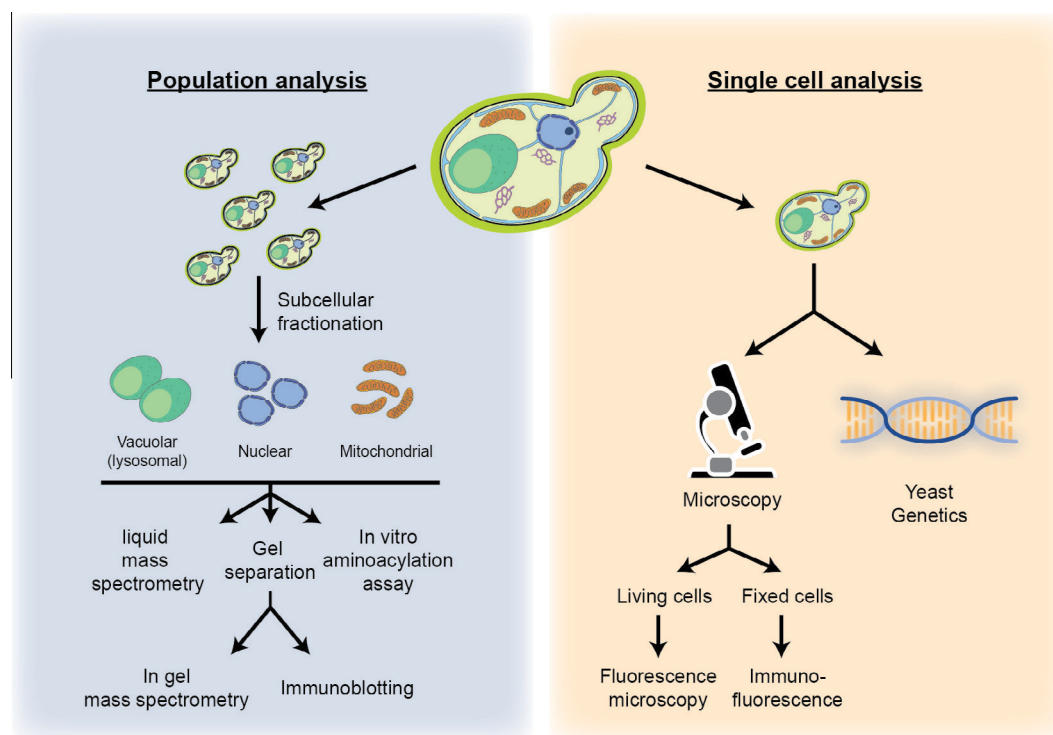


Fig. 2. Different strategies commonly used for localizing aaRSs in yeast cells. All techniques can be used on mammalian cells except those specific to yeast genetics.

genetic (isolation of mutations preventing mitochondrial import, not described in this review) and others are from cell biology (immunofluorescence on fixed cells or GFP-tagged proteins on living cells). The localization of each aaRS in various organisms together with the techniques that were used to localize them are described in Table 1. We also mention the predicted organellar import signals (MTS and NLS) that we found in yeast and human aaRSs. All the methods described in this review have their advantages and drawbacks, and the purpose of this review is to help researchers defining which techniques or procedures should be used to localize a given cytosolic aaRSs. We have focused mainly on techniques used on yeast and human cells although we mention work done on other organisms.

2. Antibodies: A fundamental tool for aaRSs localization

To ascertain the hitherto unreported localization of pools of cytosolic aaRSs pool in a compartment can be done by various methods, but immunodetection will be almost inevitable. Apart from genetics and tagging one's favorite aaRS with a fluorescent protein, all techniques rely on the use of antibodies because of their high degree of specificity and sensitivity. The key step in confirming the localization of a cytosolic aaRS in a compartment with accuracy and reproducibility is to choose the specific antibodies against the marker protein of the compartment of interest. The

number of antibodies currently available has expanded in the last years, however published articles often do not report critical parameters (such as the origin of antibodies, the immunogen used to raise the antibodies...), which sometimes compromises the reproducibility of the results. Hence there is a push to require for at least, minimal reporting standards about the use of antibodies [62,63]. In Table 2, we provide an exhaustive list of proteins that were used as compartment markers for both immunofluorescence and Western blot, in studies that report the subcellular localization of an aaRS. More controls used for yeast cells can be found in the *Current Protocols in Cell Biology* paper by Rieder and Emr [64]. Immunodetection of aaRSs, like for any other protein, has so far been done on either native and unmodified aaRS or on tagged enzymes. Table 3 lists the few antibodies that were raised against native aaRSs and that have been used to determine their subcellular localizations. Since antibodies directed against native aaRSs can unpredictably cross-react with other proteins and be less sensitive than expected, most of the immunodetections of aaRSs where performed on tagged-proteins using anti-tag antibodies that usually are highly specific and sensitive. The main limit of this approach is that adding a tag at one extremity of the aaRS can potentially influence the intracellular localization of the chimeric enzyme [65]. Table 4 lists all the tags that have been fused so far to specific aaRSs of different organisms, which extremity of the protein was tagged, which antibody and what approach were used to detect the tagged aaRSs.

Table 2
Proteins used as controls for compartment staining and for confirming organellar localization of aaRSs.

Compartment	Application	Organism	Protein	Antibody source	References
Cytosol	WB	<i>Hs</i>	Tubulin beta	n.a.	[18]
			Hsp90 alpha	c.a.	[20]
		<i>Sc</i>	Pgk1	c.a.	[29]
			Gut2	c.a.	[32]
Nucleus	WB	<i>Tb</i>	eEF1A	n.a.	[36]
		<i>Hs</i>	Lamin B1	c.a.	[18,20]
			YY1	c.a.	[20]
		<i>Sc</i>	Hta2	c.a.	[29]
Nucleolus	IF	<i>Hs</i>	Nop1	c.a.	[29]
			Nucleolin	c.a.	[20]
Mitochondria	WB	<i>Sc</i>	Por1	c.a.	[29]
			Atp2	n.a.	[32]
			Rip1	n.a.	[32]
			Cit1	n.a.	[32]
		<i>Tb</i>	mHSP70	n.a.	[36,37]
		<i>Pf</i>	ACP	h.	[39,40]

WB, western blot; IF, immunofluorescence; *Hs*, *Homo sapiens*; *Sc*, *Saccharomyces cerevisiae*; *Tb*, *Trypanosoma brucei*; *Pf*, *Plasmodium falciparum*; n.a., not available; c.a., commercially available; h., homemade.

Table 3
Antibodies used for localizing untagged aaRSs.

Organism	Application	aaRS	Antibody	aaRS antigen	References		
<i>Hs</i>	IF	ArgRS	h.: rabbit	His-tagged 72 N-terminal residues of <i>HsArgRS</i>	[20]		
		Glu-ProRS	h.: rabbit	His-tagged peptide from D677 to E884 of <i>HsEPRS</i>	[20]		
		GlnRS	h.: rabbit	His-tagged 236 N-terminal residues of <i>HsGlnRS</i>	[20]		
		LysRS	c.a.; rabbit	n.d.	[18]		
		MetRS	h.: rabbit	Full-length denatured His-tagged <i>HsMetRS</i>	[20]		
		PheRS	h.; rabbit	Endogenous PheRS from sheep liver	[21]		
		TyrRS	h.: rabbit	n.d.	[25,26]		
			WB	TyrRS	h.: rabbit	n.d.	[25,26]
				TrpRS	h.: rabbit	Full-length <i>HsTrpRS</i>	[22]
				GluRS	c.a.; rabbit	His-tagged full-length <i>ScGluRS</i>	[29]
		<i>Sc</i>	WB	HisRS	h.; mouse	Full-length <i>ScHisRS</i>	[32]
MetRS	c.a.; rabbit			His-tagged full-length <i>ScMetRS</i>	[29]		
<i>Pf</i>	WB, IF	CysRS	h.; rabbit	KLH conjugate 14 C-terminal residues of <i>PfCysRS</i>	[40]		

WB, Western Blot; IF, Immunofluorescence; *Hs*, *Homo sapiens*; *Sc*, *Saccharomyces cerevisiae*; *Pf*, *Plasmodium falciparum*; n.d., not described; c.a., commercially available; h., homemade.

Table 4
Protein-tags used for localizing aaRSs.

Organism	Tag	Tagged aaRS	Tag position	Application	Antibody	References
Hs	GFP	ArgRS	C-ter	CM		[66]
		AsnRS	C-ter	CM		[66]
		LysRS	C-ter; N-ter	CM, FM		[19,66]
		MetRS	C-ter; N-ter	CM, FM		[19,66]
Sc	V5 epitope	GlyRS	C-ter	IF, WB	c.a.	[15]
		MetRS	C-ter; N-ter	FM, CM		[29,34]
	GFP	Nter-GluRS	C-ter	CM		[28]
		GluRS	N-ter	FM, CM		[34]
		TyrRS	C-ter	FM		[35]
		GlnRS	C-ter	WB, FM	c.a.	[67]
		AlaRS	C-ter	WB	c.a.	[27]
		TyrRS	C-ter	WB	c.a.	[35]
Tb	V5 epitope	CysRS	C-ter	IF	c.a.	[37]
		GluRS	C-ter	IF	c.a.	[37]
	GFP	GlyRS	C-ter	IF	c.a.	[37]
		IleRS	C-ter	IF	c.a.	[37]
		MetRS	C-ter	IF	c.a.	[37]
		ProRS	C-ter	IF	c.a.	[37]
		SerRS	C-ter	IF	c.a.	[37]
		ValRS	C-ter	IF	c.a.	[37]
		IleRS	C-ter	IF, WB	n.d.	[36]
		AlaRS	C-ter	IF, WB	c.a.	[39]
		CysRS	C-ter	IF, WB	c.a.	[40]
		GlyRS	C-ter	IF, WB	c.a.	[40]
Pf	3× HA	ThrRS	C-ter	IF, WB	c.a.	[39]
		AlaRS	C-ter	IF, WB	c.a.	[39]
	GFP	GlyRS	C-ter	IF, WB	c.a.	[39]
		ThrRS	C-ter	IF, WB	c.a.	[39]

Hs, *Homo sapiens*; Sc, *Saccharomyces cerevisiae*; Tb, *Trypanosoma brucei*; Pf, *Plasmodium falciparum*; CM, confocal microscopy; FM, fluorescence microscopy; IF, immunofluorescence; WB, western blot; c.a., commercially available; n.d., not described.

3. Prediction and analysis of aaRSs with organellar import signal

Among the many bioinformatic predictors of protein localizations, we chose 3 to predict the presence of an MTS and 3 to predict NLSs [68]. We used these predictors regardless of the organismal origin of the aaRSs analyzed. Moreover, to gather as much information as possible we tried the “Euk-mPloc2.0” website (<http://www.csbio.sjtu.edu.cn/bioinf/euk-multi-2/>) which predicts whether an aaRS might be localized to the mitochondria, the nucleus, the cytosol or extracellularly without predicting any targeting sequence of any kind [69].

3.1. Mitochondrial targeting sequence prediction

MTS were predicted using TPpred2.0 (<http://tppred2.biocomp.unibo.it/tppred2/>) [70], TargetP1.1 (<http://cbs.dtu.dk/services/TargetP/>) [71,72] and MitoFates (<http://mitf.cbrc.jp/MitoFates/cgi-bin/top.cgi>) [73]. Query sequences should be given in the FASTA format, and depending on the MTS predictor, between 1 and 20 sequences can be analyzed at once. These predictors give back a mitochondrial probability score, the MTS sequence, the putative cleavage site that follows the MTS and the N-terminal peptide resulting from the cleavage. Additionally, MitoFates gives the mitochondrial processing enzymes responsible for maturation of the imported proteins. (Supp. Tables 3a and 3b). The MitoFates predictor was used for fungal, metazoan and plant proteins, while TargetP1.1 was used for non-plant organisms with no cut-off and with cleavage site prediction.

Submitting the yeast cytosolic aaRSs sequences to these predictors resulted in the HisRS having a strong probability of harbouring an MTS, the Cys-, Glu- and Val-RS a good probability and the Arg-, Leu- and Thr-RS only a low probability (Table 5). The predictions

have been partially validated since the relocalization of cytosolic His-, Glu- and Val-RS has been experimentally described (Table 1). The good probability of CysRS of having an MTS suggests that it is the cytosolic CysRS that aminoacylates the mitochondrial-encoded tRNA^{Cys} since there is no gene encoding a mitochondrial CysRS.

For human aaRSs, only the mitochondrial LysRS and GlyRS are encoded by the same gene as the cytosolic form. Mitochondrial LysRS originates from alternative splicing [14], and the mitochondrial GlyRS via an alternative start site [15,17]. Analyzing the remaining human aaRSs by the predictors shows that only the CysRS might contain an MTS, however, this cytosolic aaRS has never been described to localize to mitochondria (Table 5).

3.2. Nuclear localization signal prediction

To identify NLS, we used NLStradamus (<http://www.moseslab.cs.utoronto.ca/NLStradamus/>) [74], SeqNLS (<http://mleg.cse.sc.edu/seqNLS/>) [75], and NLS-Mapper (http://nls-mapper.iab.keio.ac.jp/cgi-bin/NLS_Mapper_form.cgi) [76] predictors. For all predictors, we used default settings. We added a 60 amino-acids N- or C-terminal cut-off for the predictions by NLS-Mapper since it is the only one able to predict bipartite NLSs which are usually found in the 60 first or last amino acids of a sequence. We therefore only kept bipartite NLSs of aaRSs fitting this criteria. This program is better suited for prediction purposes since instead of a simple “nuclear or not nuclear” output, it ranks protein localization on a scale from exclusively nuclear (8–10), partially nuclear (7–8), dual-localized cytosol-nucleus (3–5) or exclusively cytosolic (1–2). Supplemental Tables 3a and 3b list the results obtained with these 3 predictors for human and yeast aaRSs.

Schimmel and Wang, in their first attempt at identifying NLSs in the 20 yeast cytosolic aaRSs using the program PSORT II, showed that Ala-, Gly-, Pro-, Asn-, Asp-, Gln-, Glu-, His-, Ile-, Leu-, Lys-, Phe-, Ser-, Tyr- and Val-RS harbor at least one SV40

Table 5
Predictions of mitochondrial targeting and nuclear localization signals among *S. cerevisiae* and human cytosolic aaRSs.

Class	aaRS	MTS predictors ¹						Localization predictor		NLS predictors ²							
		TPpred2.0		TargetP1.1		MitoFates		Euk-mPloc2.0		NLStradamus		SeqNLS		NLS Mapper (Monopartite)		NLS Mapper (Bipartite)	
		Yeast	Human	Yeast	Human	Yeast	Human	Yeast	Human	Yeast	Human	Yeast	Human	Yeast	Human	Yeast	Human
Class I	ArgRS	n.p.	n.p.	n.p.	n.p.	n.p.	n.p.	C/M	C	n.p.	n.p.	n.p.	1	n.p.	n.p.	1	1
	CysRS	0.771	0.776	n.p.	n.p.	0.539	n.p.	C	C	1	1	1	2	n.p.	n.p.	1	4
	GluRS	0.896		0.357		n.p.		C	C	1	1	2		n.p.	n.p.	1	
	GlnRS	n.p.	n.p.	n.p.	n.p.	n.p.	n.p.	C	C	1	n.p.	1	2	1	n.p.	n.p.	2
	IleRS	n.p.	n.p.	n.p.	n.p.	n.p.	n.p.	C	C	1	n.p.	2	2	1	1	1	2
	LeuRS	n.p.	n.p.	0.538	n.p.	n.p.	n.p.	C	C	2	1	2	2	n.p.	n.p.	1	2
	LysRS	n.p.	n.p.	n.p.	n.p.	n.p.	n.p.	C	C	1	1	2	1	n.p.	n.p.	2	2
	MetRS	n.p.	n.p.	n.p.	n.p.	n.p.	n.p.	C	C	n.p.	1	1	1	n.p.	1	1	3
	TrpRS	n.p.	n.p.	n.p.	n.p.	n.p.	n.p.	C	C	1	n.p.	1	1	1	n.p.	1	1
	TyrRS	n.p.	n.p.	n.p.	n.p.	n.p.	n.p.	C/N	C/E	1	n.p.	2	2	1	1	2	2
Class II	ValRS	0.871	n.p.	n.p.	n.p.	0.996	n.p.	C/M	C	1	1	1	2	n.p.	n.p.	n.p.	1
	AlaRS	n.p.	n.p.	n.p.	n.p.	n.p.	n.p.	C/M	C	n.p.	n.p.	2	1	n.p.	n.p.	1	1
	AsnRS	n.p.	n.p.	n.p.	n.p.	n.p.	n.p.	C	C	1	n.p.	1	1	n.p.	2	1	2
	AspRS	n.p.	n.p.	n.p.	n.p.	n.p.	n.p.	C	C	1	n.p.	2	1	n.p.	n.p.	2	1
	GlyRS	n.p.	n.p.	n.p.	n.p.	n.p.	n.p.	C	C	n.p.	n.p.	1	2	n.p.	n.p.	n.p.	1
	HisRS	0.556	n.p.	0.846	n.p.	0.996	n.p.	C/M	C/M	1	n.p.	1	n.p.	1	n.p.	3	2
	PheRS1	n.p.	n.p.	n.p.	n.p.	n.p.	n.p.	C	C	n.p.	n.p.	1	1	n.p.	1	n.p.	2
	PheRS2	n.p.	n.p.	n.p.	n.p.	n.p.	n.p.	C	C	n.p.	n.p.	1	2	1	n.p.	1	2
	ProRS	n.p.	n.p.	n.p.	n.p.	n.p.	n.p.	C	C	n.p.	n.p.	2		n.p.	n.p.		
	SerRS	n.p.	n.p.	n.p.	n.p.	n.p.	n.p.	C	C	1	1	1	2	n.p.	1	1	1
ThrRS	n.p.	n.p.	n.p.	n.p.	n.p.	n.p.	C/M	C	n.p.	1	2	2	1	n.p.	2	3	
	GluProRS		n.p.		n.p.		n.p.	C	C		1		2		1		1

n.p.: not predicted; for NLS sequence details see [Supp. Table 3a](#).

¹ MTS scores are probabilities of the considered protein to have an MTS.

² NLS scores are numbers of NLS sequences identified in each aaRS protein. C, cytosolic; M, mitochondrial; N, nuclear; E, extracellular.

T-antigen-like NLS or bipartite NLS (aaRSs in bold type have been found both in our study and by Schimmel and Wang) [49,77]. Using the aforementioned websites, we could classify the yeast aaRSs in three groups, those with a strongly probability of having an NLS (**Asn**-, **Asp**-, **Cys**-, **Gln**-, **Glu**-, **His**-, **Ile**-, **Leu**-, **Lys**-, **Pheβ**-, **Ser**-, **Trp**- and **Tyr**-RS), those likely to have one (**Ala**-, **Met**-, **Thr**- and **Val**-RS) and those unlikely to have one (**Arg**-, **Gly**-, **Pheα**- and **Pro**-RS) (Table 5). We see a high overlap between the published results and our own suggesting the robustness of the methods used. It is noteworthy that the **MetRS** missing from the original list was predicted by NLS-Mapper and then by SeqNLS. Despite the fact that these bioinformatics studies highlight the presence of NLSs in many cytosolic aaRSs, only 2 have been experimentally confirmed: the **MetRS** [29] and the **TyrRS** (3 bioinformatically found NLSs and one confirmed [35]). This emphasizes the need to use different algorithms to identify NLSs and that they are not yet sufficiently accurate to not require experimental confirmation.

Similar NLS prediction analysis has been done on human cells (Table 5). Using the aforementioned websites, we could classify the human aaRSs in three groups, those with a strong probability of having an NLS (**Cys**-, **GluPro**-, **Leu**-, **Lys**-, **Met**-, **Pheβ**-, **Ser**-, **Thr**- and **Val**-RS), those likely to have one (**Ala**-, **Arg**-, **Asn**-, **Asp**-, **Gln**-, **Gly**-, **Ile**-, **Pheα**-, **Pheβ**-, **Trp**- and **Tyr**-RS) and the ones unlikely to have an NLS (**His**RS).

The fact that NLS predictions for yeast and human aaRSs converge seem to reinforce the hypothesis that this localization is true and not artifactual. The one notable exception is **HisRS** which is most likely nuclear in yeast and most unlikely in human. Since the nuclear localizations of the **MetRS**, **TyrRS** and **IleRS** have been determined experimentally, we can speculate that either some of their functions are shared and would have been present in their common ancestor, or that they exert different roles suggesting that the functions were acquired after the opisthokonta splitting (Table 5).

4. Subcellular fractionation

Subcellular fractionation can be divided into 3 different techniques according to the precision of the separation and the organelle that one wants to purify: crude membranes fractionation, nuclear purification and mitochondrial purification.

4.1. Crude membranes fractionation from yeast cells

This technique allows the separation of membranes from the cytosol (S100) and yields 2 separate membrane fractions (P13 and P100). To analyze the subcellular distribution of yeast aaRSs we performed a subcellular fractionation adapted from the protocol published by Bonangelino and collaborators [78].

- Yeast cells are inoculated in the morning or the previous evening depending on the generation time in the appropriate medium (YPD or SC dropout) on a rotary shaker at 200 rpm at 30 °C.
- In the evening, the cells are diluted in 100 mL of the same medium to reach an OD_{600nm} of about 0.5 in the morning. 40 units of OD_{600nm} are transferred to a 50 mL Falcon tube. From here on out, all steps are performed on ice and centrifugations are performed at 4 °C.
- The cell suspension is centrifuged for 5 min at 5250g at 4 °C to pellet the cells. For cells grown on SC dropout medium, add 1 mL of YPD to facilitate the pelleting.
- Cells are washed twice in 20 mL of ice cold fractionation buffer (20 mM Hepes/KOH, pH 6.8, 50 mM CH₃COOK, 10 mM MgCl₂, 250 mM Sorbitol, 10 mM NaN₃).
- Cells are then resuspended in 800 μL of fractionation buffer (with protease inhibitor cocktail cComplete ULTRA Tablets, EDTA-free from Roche™) and transferred into a 15 mL cold Corax®II centrifuge tube (ref. 1-8441-15) containing 650 μL of glass beads (acid washed 0.25–0.5 mm diameter beads).

- The tube is vortexed 6 times for 30 s at full speed to lyse cells.
- The lysate is transferred to a 1.5 mL microfuge tube and centrifuged at 4 °C for 5 min at 500g in a fixed-angle rotor to clarify it.
- The S5 supernatant is carefully transferred to a fresh microfuge tube and centrifuged at 4 °C for 10 min at 13,000g in a fixed-angle rotor.
- The pellet (P13), which mainly contains the plasma membrane, the endoplasmic reticulum, the nucleus, the vacuole and mitochondria, is kept on ice until the end of the experiment.
- The supernatant (S13) is transferred in a 1.5 mL ultracentrifugation microfuge tube (Beckman Coulter® ref. 357448) for further centrifugation at 4 °C for 1 h at 100,000g in an ultracentrifuge using a fixed rotor.
- The supernatant (S100), which contains cytosol and vesicles, is carefully transferred to a fresh 1.5 mL microfuge tube. The pellet (P100) contains Golgi and endosomes.
- P13 and P100 are subsequently resuspended in fractionation buffer in the same volume as the S100 fraction.

4.2. Purification of nuclei and preparation of nuclear protein extracts

Purification of nuclei needs to be performed quickly to avoid passive diffusion of small proteins through nuclear pores. Moreover, the composition of buffers is critical for maintaining osmotic balance to prevent nuclear proteins from leaving the nucleoplasm fraction.

4.2.1. Purification of nuclei from yeast cells

This method is an adaptation from the original protocol of Stephanie E. Rieder and Scott D. Emr [79].

- Yeast cells from 2 L of culture in rich or synthetic medium, depending on auxotrophic markers or studied conditions, are harvested at 0.7 OD₆₀₀ and washed once with water to ensure that all traces of medium are eliminated.
- The wet pellet is weighed (approximately 7 g/2 L of culture). Pellet is resuspended in 100 mM Tris H₂SO₄, 10 mM DTT in a volume of 2 mL/g of wet cells and incubated 20 min at 30 °C with gentle agitation. The purpose of this step is to weaken the cell wall.
- The mixture is centrifuged 4 min at 3500g and the pellet is washed with 1.1 M sorbitol to keep osmotic pressure, 100 mM K₂HPO₄/KH₂PO₄, pH 7.4 using 7 mL of buffer per g of cells and resuspended with the same buffer.
- Zymolase 20T is added to the mixture (5 mg/g of pellet) and incubated during 45 min at 30 °C with gentle agitation (80 rpm), to digest the cell wall.

All following steps are performed at 4 °C, to avoid protein degradation. Approximately 3.5 g of wet cells should be settled by falcon 50 (two falcons 50 for 2 L of culture at 0.7 OD_{600nm}). Note that all the subsequent steps are detailed for the treatment of 1 falcon 50 out of the two necessary to treat the whole 2 L culture.

- The spheroplasts (cells without their wall) are centrifuged 4 min at 3500g, gently resuspended in 1.1 M sorbitol, 100 mM K₂HPO₄/KH₂PO₄, pH 7.4 to remove the zymolase and centrifuged again 4 min at 3500g.
- The pellet is resuspended in 20 mL 1.1 M sorbitol, 100 mM K₂HPO₄/KH₂PO₄, pH 7.4 and loaded on a 6 mL cushion containing 30 mM sorbitol, 5% (v/v) ficoll 400, with protease inhibitors. The spheroplasts are centrifuged 10 min at 4000g.
- The pellet is resuspended into 15 mL of ice cold ficoll 20% (v/v), 20 mM K₂HPO₄/KH₂PO₄, pH 7.4, 1 mM MgCl₂ and protease inhibitors, and the spheroplasts are broken by osmotic shock

in potter by 20 S in maximum 5 min. The ficoll keeps the osmotic pressure between the medium and the nuclei, to avoid nuclear protein from diffusing out of the nucleus.

- The lysate is incubated 10 min on ice to let nuclei cool down prior to subsequent centrifugation during 5 min at 13,000g.
- The supernatant is collected and immediately centrifuged again 10 min at 13,000g. At this step, nuclei cannot pellet because of the viscosity of the buffer.
- The supernatant is then loaded on a ficoll gradient containing 20 mM K₂HPO₄/KH₂PO₄ pH 7.4, 1 mM MgCl₂, protease inhibitors and ficoll 50% (v/v), ficoll 40% (v/v), ficoll 30% (v/v), 6.5 g each in 25 × 89–mm ultracentrifuge tube (Beckman Coulter®, Ultra Clear Tubes, 38.5 mL, ref. 344058). Then, the gradient is ultracentrifuged 1 h at 58,000g (Beckman, SW28 rotor, 18,000 rpm).
- After the centrifugation, the 20 and 30% layers containing all the cellular debris are removed. The 40% layer and the interface 40–50% containing the nuclei are harvested by pipetting. Nuclei are also present in the interface 30–40%, but this interface layer is not harvested because it contains too many non-nuclear contaminants.
- To remove the ficoll, the samples are diluted 10 times in 20 mM K₂HPO₄/KH₂PO₄, pH 7.4, 1 mM MgCl₂ and centrifuged 10 min at 10,000g to pellet nuclei (since the ficoll is diluted, nuclei are able to pellet at 3000g).
- Nuclei are finally resuspended in 500 µL of buffer containing 100 mM Tris HCl pH 7.8, 0.1 mM EDTA, 5 mM β-Mercaptoethanol, 1 mM benzamidine, protease inhibitors, and sonicated for 80 s (1 s on/1 s off, 30% amplitude, Bioblock Vibracell) in order to disrupt the nuclear envelope.
- After a chilling step on ice to avoid foaming, nuclei are re-sonicated for 30 s (1 s on/1 s off, 30% amplitude, Bioblock Vibracell).
- The nuclear extracts are ultra-centrifuged 30 min at 100,000g to pellet nuclear membranes. The supernatant contains soluble nuclear proteins.

4.2.2. Purification of nuclei from human cells

This protocol is adapted from Jason M. Dahlman and Denis C. Guttridge [80]. Perform all steps at room temperature unless otherwise specified. Volumes are determined for the preparation of 10 samples. All centrifugation was performed in a bench top microfuge. A minimum of 1 × 10⁶ cultured cells are used for this protocol.

- Cell culture media is removed from the plates.
- Cells are gently washed twice with 1 mL of PBS (137 mM NaCl, 2.7 mM KCl, 10 mM Na₂HPO₄, 1.8 mM KH₂PO₄).
- After the addition of 1 mL of PBS, cells are removed from the polystyrene tissue culture dish using a cell scraper.
- Scraped cells (1 mL) are removed with a 1 mL pipette and placed in a 1.5 mL microcentrifuge tube.
- Cells are centrifuged at 250g for 5 min at 4 °C.
- After centrifugation, supernatants are removed and 5 pellet volumes of cytoplasmic extraction buffer (CEB: 10 mM HEPES-KOH, pH 7.6, 60 mM KCl, 1 mM EDTA, 0.25% (v/v) Tergitol-type NP-40 (Sigma-Aldrich), Complete protease inhibitor cocktail, EDTA-free (Roche)) are added to each sample.
- Cellular pellets are dissolved by flicking the tubes. It is important to minimize the amount of bubbles generated while flicking. After adding the cytoplasmic extraction buffer, let samples stand on ice for 1–3 min before resuspending and make sure that cellular pellets are completely dissolved.
- Resuspended pellets are incubated on ice for 5 min and then, centrifuged at 650g for 4 min at 4 °C.

- After centrifugation, supernatants, containing the cytoplasmic proteins, are carefully transferred to new 1.5 mL microcentrifuge tubes. While removing the supernatant, take special care not to disrupt the nuclear pellet, which now should take on an opaque appearance. The cytoplasmic extract can be either disposed of or stored at -80°C .
- 100 μL of cytoplasmic wash buffer (CWB: 10 mM HEPES-KOH, pH 7.6, 60 mM KCl, 1 mM EDTA, Complete protease inhibitor cocktail, EDTA-free (Roche)) is added to the nuclear pellets to remove the excess of NP-40. The 1.5 mL microcentrifuge tubes are gently tapped to dislodge the nuclear pellets. There is no need to resuspend the pellets.
- Centrifugation is repeated at 650g for 4 min at 4°C .
- Supernatants are carefully discarded, once again taking care not to disturb the nuclear pellets.
- 1 pellet volume of nuclear extraction buffer (NEB: 20 mM Tris HCl pH 8.0, 420 mM NaCl, 1.5 mM MgCl_2 , 0.2 mM EDTA, 25% (v/v) glycerol, Complete protease inhibitor cocktail, EDTA-free (Roche)) is added to the 1.5 mL microcentrifuge tubes containing the nuclear pellets and they are resuspended by flicking the tubes until they are completely resuspended. Try to minimize the amount of bubbles you generate while flicking.
- The resuspended nuclear pellets are incubated on ice for 10 min and mixed by flicking every 2 min.
- After the 10 min incubation, the resuspended nuclear pellets are centrifuged at 15,000g for 10 min at 4°C .
- After centrifugation, supernatants, containing the nuclear proteins, are transferred to new pre-chilled 1.5 mL microcentrifuge tubes
- Nuclear extracts are stored at -80°C .

4.3. Purification of mitochondria and preparation of mitochondrial protein extracts

4.3.1. Purification of mitochondria from yeast cells

To analyze the mitochondrial localization of aaRSs, we performed a mitochondria purification (described below) adapted from the protocol published by Meisinger and collaborators [48].

- All steps are performed at 4°C unless otherwise specified. To get enough mitochondria it is recommended to use at least 2–3 L of yeast cells grown to log-phase.
 - Yeast cells are pelleted by centrifugation at 3000g for 5 min and resuspended in distilled water.
 - Cells are pelleted again as for nuclei preparation, the wet weight is measured and the pellet is resuspended at a concentration of 2 mL/g of pellet in prewarmed at 30°C DTT buffer (100 mM Tris- H_2SO_4 , pH 9.4, 10 mM dithiothreitol (DTT)).
 - After 20 min incubation in a 30°C shaker at 80 rpm, cells are pelleted at 3000g for 5 min and resuspended in 7 mL/g of zymolyase buffer (1.2 M sorbitol, 20 mM potassium phosphate, pH 7.4), pelleted again at 3000g for 5 min and resuspended at a concentration of 7 mL/g of cells in zymolyase buffer containing 3 mg Zymolyase 20T (Seikagaku Kogyo Co., Tokyo, Japan) per gram wet weight.
 - After incubation for 45 min in 30°C shaker at 80 rpm, cells are pelleted at 3000g for 5 min and resuspended in 7 mL/g of fresh zymolyase buffer, pelleted again at 3000g for 5 min and resuspended (6.5 mL/g wet weight) in ice-cold homogenization buffer (0.6 M sorbitol, 10 mM Tris HCl, pH 7.4, 1 mM EDTA, 0.2% (w/v) BSA (Sigma-Aldrich), and 1 mM of freshly prepared PMSF).
 - From this step, it is very important to maintain the lysate, buffers and rotors at 4°C to prevent proteolysis.
 - Samples are poured in a glass Teflon homogenizer and spheroplasts are homogenized with 15 S.
 - Samples are then 2-fold diluted with ice-cold homogenization buffer and the lysate is cleared by centrifugation at 1500g for 5 min to remove cell debris and nuclei.
 - The supernatant is centrifuged at 4000g for 5 min, the pellet is discarded and the supernatant is centrifuged again at 12,000g for 15 min to isolate the mitochondrial fraction.
 - The supernatant is discarded and the mitochondrial pellet is resuspended in 0.5 to 1 mL of SEM buffer (250 mM sucrose, 1 mM EDTA, 10 mM MOPS-KOH, pH 7.2) and the protein concentration is measured using the Bradford method and adjusted to 5 mg/mL.
- In order to obtain highly purified mitochondria, firstly prepare sucrose step gradients in Beckman centrifuge tubes (Beckman Coulter®, Ultra Clear Tubes, 13.2 mL, ref. 344059):
- 1.5 mL 60% (w/v) sucrose diluted in EM buffer (1 mM EDTA, 10 mM MOPS-KOH, pH 7.2) is loaded at the bottom of the centrifuge tube.
 - Without disturbing the phases, 4 mL 32% (w/v), 1.5 mL 23% (w/v), and 1.5 mL 15% (w/v) sucrose/EM are carefully pipetted stepwise and the tubes are kept at 4°C .
 - Samples are homogenized again in a glass Teflon homogenizer (10–15 strokes) and poured (0.2 to 1 mL) to the sucrose gradient.
 - The clarified samples are then centrifuged (Beckman, SW41 Ti rotor) at 134,000g for 1 h at 4°C and the highly purified mitochondria are collected with a Pasteur pipette from the 60–32% sucrose interface.
 - Mitochondrial samples are diluted 2-fold in SEM buffer and centrifuged at 12,000g for 15 min. Repeat this step to wash the purified mitochondria.
 - Pellet can be frozen at -80°C .
- For extraction of soluble mitochondrial proteins, mitochondria are disrupted by sonication (see below) otherwise they are resuspended in SEM buffer and the concentration is adjusted as required.
- Mitochondria pellets are resuspended in 1 vol of lysis buffer (50 mM Tris-HCl, pH 7.2, 1.1 M Sorbitol, 2 mM EDTA; 5 mM β -mercaptoethanol).
 - Sonication (4 run of 10 S with a 2 s duration time, amplitude 25%; Vibracell) is performed with a small probe (2 mm diameter) on ice.
 - Broken mitochondria are then centrifuged for one hour at 105,000g at 4°C to eliminate unbroken mitochondria and disrupted membranes.
 - The supernatant which is recovered, corresponds to soluble mitochondrial proteins and can be frozen at -80°C .

4.3.2. Obtention of mitoplasts from yeast mitochondria

For generation of mitoplasts, digitonin is used to permeabilize the outer mitochondrial membrane of yeast mitochondria.

- Mitochondria are suspended at a concentration of 1 mg/ml in SEM buffer.
- 250 μg of mitochondria are incubated for 25 min on ice in 250 μL of SEM buffer containing 0.05% to 0.2% digitonin.
- The resulting mitoplasts are harvested by spinning at 14,000 rpm for 10 min and the supernatant is saved for further analysis.
- The mitoplast containing pellet is washed once again with SEM buffer.
- To determine the efficiency of digitonin treatment, 100 μg of mitochondria are treated as above with digitonin, centrifuged,

and the pellet and supernatant fractions separated by SDS-PAGE and transferred to a polyvinylidene difluoride membrane (Immobilon P, Millipore). Immunoblots are performed using antibodies specific for cytochrome *c* peroxidase (CCPO) (intermembrane space), TIM23 (inner membrane), delta-1-pyrroline-5-carboxylate dehydrogenase (Put2p) (matrix) and porin (outer membrane).

4.3.3. Purification of mitochondria from human cells

This protocol is adapted from Jason M. Dahlman and Denis C. Guttridge [80] and has been designed to extract mitochondria from HeLa cells. Volumes are adapted to cells grown in 5 flasks of 58 cm². All steps are performed on ice or at 4 °C.

- Cell culture growth media from desired cells is removed.
- Cells are gently washed twice with 5 mL of PBS (see Section 4.2.2).
- Cells are removed from the polystyrene tissue culture dish by adding 1 mL of PBS and the cells are scraped gently with a cell scraper.
- Cells are centrifuged for 5 min at 250g at room temperature
- The pellet is resuspended in 1 mL of BSA buffer (0.6 M sorbitol, 1 mM EDTA, 20 mM Hepes-KOH, pH 7.6, 300 mM NaCl, Complete protease inhibitor cocktail, EDTA-free (Roche) and 0.3% (v/v) of BSA (1 mg/mL)).
- Cells are then mechanically broken on ice by repeated (at least 80 times) aspiration/backflow using a 1 mL syringe with a G23 needle.
- The lysate is centrifuged twice at 1200g for 6 min at 4 °C.
- The supernatant is then centrifuged at 16,000g for 40 min at 4 °C.
- Pellet can be frozen at -80 °C.

4.3.4. Obtention of mitoplasts from human mitochondria

For generation of mitoplasts, digitonin is used to permeabilize the outer mitochondrial membrane of human mitochondria.

- Mitochondria-containing pellet is resuspended in 300 µL BSA buffer (0.6 M sorbitol, 1 mM EDTA, 10 mM Hepes-KOH, pH 6.7 and 0.3% (v/v) of BSA (1 mg/mL)) containing 0.2% digitonin (50 µL of a 1 mg/mL stock solution) and incubated 15 min at room temperature.
- 1 mL of BSA buffer is added and the mixture is centrifuged 20 min at 16,000g at 4 °C.
- The resulting pellet is washed two times with 1 mL BSA buffer without resuspending the mitoplasts.
- The final mitoplasts-containing pellet can be resuspended in various types of buffers depending on the subsequent analyses that will be performed (TRizol (Invitrogen) for RNA extraction, Laemmli for SDS-PAGE analysis...) or stored at -80 °C as a wet pellet.

5. Mass spectrometry analysis and identification of cytosolic aaRSs in yeast mitochondrial extracts

We performed yeast mitochondria purification as explained in the Section 4.3.1 and recovered pure mitochondria at the 32–60% interphase from a cushions gradient (Fig. 1A). In order to identify mitochondrial proteins, mitochondria were disrupted (see Section 4.3.1) and soluble proteins were subjected to mass spectrometry (see protocol below). For analysis, we carried out 3 different injections, two of 90 min (one regular and one using restricted mass ranges of 400–800 *m/z* and 800–1250 *m/z*, termed Frac.) and one of 120 min. These features allowed us to identify 905 (90 min.), 982 (90 min. Frac.) and 926 (120. min) mitochondrial proteins respectively (Fig. 1B). We describe here the detailed procedure

for protein digestion and mass spectrometry analysis as well as data analysis.

5.1. Protein digestion solution

- Proteins from mitochondrial extracts are resuspended in 50 mM ammonium bicarbonate.
- After a reduction-alkylation step (5 mM DTT and 10 mM iodoacetamide), proteins are digested overnight with 100 ng of sequencing-grade trypsin (Promega).
- After centrifugation at 12,000g, the supernatants are collected in glass inserts and vacuum dried.

5.2. Nano-liquid Chromatography – electrospray Ionization TripleTOF MS/MS Analysis

- Before injection, dried peptides are resuspended in 15 µL of 0.1% (v/v) formic acid. One third of each sample was injected on a NanoLC-2DPlus system (nanoFlexChiP module; Eksigent, ABSciex, Concord, Ontario, Canada) coupled to a TripleTOF 5600 mass spectrometer (ABSciex) operating in positive mode.
- Peptides are loaded with a trap and elute configuration on C18 reverse-phase columns (ChiP C-18 precolumn 300 µm ID × 5 mm ChromXP and ChiP C-18 analytical column 75 µm ID × 15 cm ChromXP; Eksigent).
- Peptides are eluted by using a 5–40% gradient of 0.1% (v/v) formic acid in acetonitrile for 90 or 120 min at a 300 nL/minute flow rate. The TripleTOF 5600 was operated in high-sensitivity data-dependant acquisition mode with Analyst software (v1.6, ABSciex) on a 400–1250 *m/z* range.
- To extend the sensitivity, two new injections are carried out using restricted mass ranges, 400–800 *m/z* and 800–1250 *m/z*. An external calibration is performed before each sample by monitoring 10 peptides of a beta-galactosidase trypsin digest. A discovery “Top20” method is used: up to 20 of the most intense multiply-charged ions (2+ to 5+) are selected for CID fragmentation, with a cycle time of 3.3 s.

5.3. Database search and data analysis

Raw data are first converted to Mascot Generic File format (.mgf) and searched against the yeast *S. cerevisiae* database supplemented by a decoy database (reverse sequences). The database search algorithm used is Mascot (version 2.2, Matrix Science, London, UK) through the ProteinScape 3.1 package (Bruker Daltonics, Leipzig, Germany). Peptide modifications allowed during the search are: N-acetyl (protein), carbamidomethylation(C) and oxidation (M). Mass tolerances in MS and MS/MS is set to 20 ppm and 0.5 Da, respectively. Two trypsin missed cleavages sites is allowed. Peptide identifications obtained from Mascot is validated with a protein FDR < 1%, using the Protein Assessment tool from ProteinScape. Identified proteins are assessed by spectral count.

The aaRSs identified in the mitochondrial extract analyzed by three different injections methods are presented in Fig. 1C and Supp. Table 2. Excepting the Arg-, Met- and Thr-RS (note that there are no genes encoding the mitochondrial CysRS and GlnRS in yeast), we found all the mitochondrial aaRSs in our assay. The absence of these three mitochondrial aaRSs could be due to a strong binding to the mitochondrial membrane that resulted in their loss during the protein extract preparation. Indeed, it has previously been shown that a functional aaRS could be membrane-anchored [81]. In addition to the mitochondrial aaRSs, we identified 10 cytosolic ones (Asp-, Glu-, Ile-, Leu-, Lys-, Phe-, Pro, Ser-, Thr- and Tyr-RS) of which only the cytosolic GluRS has been shown experimentally to be dual-localized [28,29]. Since there is no gene identified for the yeast mitochondrial CysRS, we assume

Table 6

List of markers for specific compartments in mammalian cells and their respective antibodies.

Compartment	Protein marker*	Antibody
Nucleus	Lamin B1	Abcam ab16048
Plasma membrane	Cadherin	Abcam ab6528
Endoplasmic Reticulum	Calnexin	Abcam ab22595
	Calreticulin	Abcam ab2907
	GRP-78	Abcam ab21685
Golgi	GM130	Abcam ab31561
	Giantin	Abcam ab80864
	TGN46	Abcam ab2809
Mitochondria	COX IV-1	Abcam ab14744
	Cytochrome c	Abcam ab13575
Endosomes	Early endosome antigen 1	Abcam ab2900
	Ras related protein Rab-5A	Abcam ab18211
	Ras related protein Rab-7a	Abcam ab126712
Lysosomes	LAMP-1	Abcam ab24170
	LAMP-2	Abcam ab18529
Autophagosomes	MAP1A/MAP1B LC3 A	Abcam ab52768
Peroxisomes	Catalase	Abcam ab16771

* Protein marker names are recommended names or short names from the UniProt database.

that the cytosolic form would also be mitochondrial; and we, indeed, found it in the mitochondrial fraction we analyzed. It is now important to confirm the mitochondrial localization of these cytosolic aaRSs and then determine their function in this other compartment.

6. Microscopy analysis and single cell localization

Unlike subcellular fractionation, microscopic analysis allows the study of aaRSs localization at the single cell scale. For more precision, a confocal microscope is needed to set only one focal plan and prevent accumulation of cytosolic fluorescence around the organelle. If the aaRS is fused to GFP, analysis can be performed directly on living cells, and aaRSs used with a GFP-tag are listed in Table 4. To control the aaRS localization on living cells, the need of compartment markers is essential, like DAPI and Mitotracker for nuclear and mitochondrial compartment, respectively. For yeast cells, some additional fluorescent dyes can also be used for fluorescent microscopy on living cells, as CellTracker Blue CMAC (ThermoFischer Scientific, ref. C2110) that is specific for vacuolar lumen (DAPI filter), or FM4-64 (ThermoFischer Scientific, ref. T3166) used in time lapse experiments to stain the plasma membrane, the endosomes and the vacuolar membrane (RFP filter) [82]. For more precision, protein markers can be targeted by specific antibodies: frequently used markers for mammalian intracellular compartments are listed in Table 6. As GFP can possibly perturb the aaRS localization due to its large size, smaller tags (listed in Table 4) have been used for immunofluorescence (IF) study. For IF, a fixation step is essential to allow antibodies penetration in the sample. Next sections present immunofluorescence protocols for both yeast and human cells.

6.1. Immunofluorescence on yeast cells

This technique allows the observation by fluorescent microscopy of the aaRSs of interest on fixed yeast cells.

6.1.1. Fixation steps

- Cells are grown overnight in 20 mL of either complete or synthetic medium (YPD or SC dropout medium) to about 1×10^7 cells/mL ($OD_{600nm} = 0.4-0.6$); 10 mL culture gives 6 samples.
- 1.25 mL of 1 M K_2HPO_4/KH_2PO_4 , pH 6.5 and 1.25 mL of 37% (v/v) formaldehyde are added to 10 mL of overnight culture

(10×10^7 cells) and incubated for 2 h at room temperature with gentle shaking every 30 min.

- Cells are centrifuged for 5 min at 3000g, washed 3 times with 10 mL SP buffer (1.2 M sorbitol, 0.1 M KPO_4 , pH 6.5) and resuspended in 1 mL SP/ME (SP, 20 mM β -mercaptoethanol).
- 10 μ L Zymolyase 20T (5 mg/mL) is added and the mixture is incubated 45 min at 30 °C (gentle shaking every 10 min); the amount of Zymolyase needed depends on the strain.
- Cells are centrifuged for 5 min at 2000g, washed 3 times with 3 mL SP buffer and resuspended in 0.1 mL SP; after the digestion of the cell wall, the resuspension has to be very gentle to avoid lysis.
- Cells are stored at 4 °C (can be kept for 1–2 weeks).

6.1.2. Incubation with antibodies

The following steps are done on a slide for immunofluorescence (HTC or epoxy, single use slides, diameter 6 mm) at room temperature.

- Slides are washed with ethanol 96% (v/v).
- 20 μ L of poly-Lysine (0.1% (w/v) in H_2O) is added to each well and incubated for 1 min.
- The liquid is removed, slides are dried and washed 3 times with 20 μ L H_2O ; all washing steps are done by adding one drop (with Pasteur pipette) and removing with vacuum without touching the slide.
- Slides are placed in a humid chamber (Petri dish with H_2O -soaked paper), 15 μ L of fixed yeast cells are added to each well and incubated for 30 min.
- The excess of liquid is removed very gently and slides are washed twice with PBS $1 \times$ (see Section 4.2.2).
- Slides are then incubated for 5 min with 15 μ L of PBT (PBS $1 \times$, Triton X-100 0.1% (v/v), NaN_3 0.1% (w/v), BSA 1% (w/v)).
- After removing the excess of liquid, slides are incubated for 30 min at room temperature with 15 μ L of primary antibody diluted in PBT, according to manufacturer indications.
- Slides are washed 10 times with PBT, followed by the incubation for 30 min in the dark and at room temperature with 15 μ L of secondary antibodies (either Cy-conjugated or Alexa Fluor®-conjugated; ThermoFischer Scientific) diluted in PBT.
- Slides are washed 10 times with PBS.
- Optional: Nuclei can be stained with 15 μ L of DAPI (10 μ g/mL) and incubated 5 min in the dark. 5 washes with PBS are needed to avoid non-specific background fluorescence.
- Finally, 3 μ L of Vectashield® (Vector laboratories) are added and slides are covered with coverslip; fix coverslip on all ends with nail polish.
- Slides can be stored at 4 °C in the dark (can be kept for months) or directly observed by fluorescence microscopy.

6.2. Immunofluorescence on human cells

This technique allows observing the subcellular localization of the aaRSs of interest in fixed mammalian cells on a single cell scale with a fluorescence microscope.

- Cells are grown in complete medium, mostly DMEM (D5796 Sigma) or MEM (M2279 Sigma), supplemented with 10% (v/v) Fetal Calf Serum (FCS).
- On day one of the experiment, the medium of the culture flask is removed, cells are washed with PBS (see Section 4.2.2.) and detached using trypsin (T4049 Sigma).
- Cells are then spotted on 10-well spotslides (Marienfeld Superior, #1216650) to a 70% confluency (for most cell types 4000–5000 cells per spot), let to attach and grown overnight in a cell culture incubator at 37 °C, 5% CO_2 .

- After removing the medium, cells are fixed by adding 50 μ L of 4% (v/v) formaldehyde (F8775 Sigma) in PBS to the spots and incubated for 20 min at room temperature.
- If Mitotracker (ThermoFisher Scientific, M7512) is used to detect mitochondria, Mitotracker staining has to be done on live cells prior to fixation. Therefore, cells are incubated for 15–45 min at 37 °C with Mitotracker diluted in pre-warmed medium (37 °C) to a concentration of 100–500 nM. Cells are then washed once in medium and once in PBS and fixed as described above.
- Cells are then washed once with PBS and permeabilized with 0.2% (v/v) Triton-X 100 (Sigma-Aldrich) in PBS for 10 min at room temperature.
- After one more wash with PBS, unspecific sites are blocked by incubation with 20% (v/v) FCS in PBS for one hour at RT.
- Cells are then incubated with the antibodies raised against the aaRS of interest and marker proteins of the different subcellular compartments in PBS-2% (v/v) FCS for two hours at room temperature or overnight at 4 °C.
- After washing five times with PBS, the fluorophore-conjugated secondary antibodies diluted in PBS-2% (v/v) FCS are added for one hour at room temperature. DAPI can be added to the secondary antibody solution at a concentration of 300 nM.
- Finally, after two final washes in PBS, a drop of pre-warmed (50 °C) elvanol (Poly(vinyl alcohol) – 341584 Sigma-Aldrich) is added to each spot and the slide sealed with a coverslip. Cells are then visualized using a confocal laser scanning microscope and fluorescence can be quantified with the ImageJ software.

7. Concluding remarks

Localizing multi-compartmental aaRSs cannot be done using a one-for-all technique. For example, using fluorescence microscopy to simultaneously visualize in a single cell, the organellar and cytosolic fractions of the same aaRS (or protein in general) is complicated since the fluorescence of the organellar pool will be masked by the fluorescence of the cytosolic portion which is usually more abundant. So far no tools have been developed to overcome this difficulty and the use of confocal microscopy is usually not sufficient when one wants to ascertain the localization of a minor organellar pool of a cytosolic aaRS. Moreover, like for any other protein putatively organellar, it is currently very difficult to distinguish between a luminal localization of an aaRS and a peripheral localization of the protein on the cytosolic side of the organelle. Being able to make these distinctions is extremely important to be able to study the nonconventional roles of these multi-localized aaRSs and identify the cellular processes to which the organellar pools of these cytosolic aaRSs participate. Also, the possibility that several cytosolic aaRSs could be peripherally associated to membrane compartments other than the mitochondria and the nucleus by interacting either with membrane proteins or directly to lipids has been overlooked so far. For all these reasons, one still has to turn to the isolation of membranes and afterwards to organelle purification to be able to ascertain the relocation inside a given compartment of a fraction of a cytosolic aaRS (summarized in Table 1).

Another difficulty to overcome when working with dual-localized aaRSs is that the cytosolic pool of these proteins is always essential for viability, rendering the study of the functions of the organellar pools of the same aaRS very difficult. In this respect, yeast is a very convenient model especially when one wants to analyze the mitochondrial activity of a cytosolic aaRSs. Since these organelles are only essential for the respiratory metabolism and not when yeast is fermenting, mutations of the cytosolic aaRS gene that lead to only a respiratory deficiency (fermentative growth is unaffected) are targeting residues essential for the mitochondrial

activity of the dual-localized aaRS without affecting its cytosolic role. This simple phenotypic screen was successfully used to identify the cryptic and nonconventional MTS of yeast cytosolic GluRS which participates to the mitochondrial transamidation pathway upon mitochondrial import [28]. It was also used to show that mitochondrial forms of His-, Val- and GlyRSs are generated through an alternative translational start [13,31,32].

If confirming that a pool of a cytosolic aaRS can relocate inside an organelle is difficult with the current technologies, identifying the import signals to study the dynamics of these proteins is even more arduous. Import signal predictors still have a low consensual predictive accuracy for these dual-localized aaRSs, mainly because they often contain nonconventional import signals. Identifying the organellar roles of dual-localized aaRSs will necessitate the reinterpretation of previous yeast mutant screens as well as establishing new mutant screens. In humans, the systematic sequencing of genes encoding cytosolic aaRSs of patients with mitochondrial-related diseases and in depth analysis of the localization, protein interactants and activity of the mutant aaRS is essential for identifying the organellar functions of dual-localized aaRSs. By doing so, it was recently shown that the mutation in the cytosolic GlyRS gene that causes type 2D Charcot-Marie-Tooth disease changes the protein binding activity of GlyRS that interferes with a signaling pathway essential for motor neuron survival [83].

These findings also raise many questions, the most important being how cells regulate the distribution of multi-compartmental cytosolic aaRS between the cytosol and the different organelles. One mechanism by which cells manage the subcellular distribution of the various pools of a cytosolic aaRS is by forming the MSCs and triggering release of each cytosolically-anchored aaRS by post-translational modification of the aaRS. Since so far, a maximum of 9 cytosolic aaRSs were found participating to MSCs, there are probably others posttranslational modifications, or other mechanisms that participate in regulating the dynamic compartmentalization of the remaining 11 potentially multi-localized aaRSs. Another important issue concerning the dynamical relocation of these aaRSs is whether a portion of an existing pool is redistributed or a fraction of the neosynthesized proteins will specifically be deviated on demand towards the organelle? Finally, while in this review we focused on the relocation of cytosolic aaRSs within the cell, it has to be noted that several human aaRSs can be secreted in the extracellular medium where they also accomplish nonconventional functions [84,85].

Acknowledgements

The work was supported by the French National Program Investissement d'Avenir administered by the "Agence Nationale de la Recherche" (ANR-France), "MitoCross" Laboratory of Excellence (Labex), funded as ANR-10-IDEX-0002-02 (to H.D.B, J-O.D.C), the University of Strasbourg (H.D.B, E.M), the CNRS (B.S, S.F), the INSERM and the Université de Strasbourg through the IDEX 2015 Attractivité (to S.B), the Agence Nationale de la Recherche – ANR-13-BSV2-0004 to S.F and AFM-Téléthon – AFM-SB/CP/2013-0133/16551 (to S.F), the Ministère de l'Éducation Nationale, de la Recherche et de l'Enseignement Supérieur (G.B, S.D), the Association pour la Recherche sur le Cancer (D.L) and the ANR [ANR-10-LABX-0036_NETRNA] (L.E, P.H).

Appendix A. Supplementary data

Supplementary data associated with this article can be found, in the online version, at <http://dx.doi.org/10.1016/j.jymeth.2016.09.017>.

References

- [1] M. Ibba, D. Söll, Aminoacyl-tRNA synthesis, *Annu. Rev. Biochem.* 69 (2000) 617–650.
- [2] D.R. Smith, P.J. Keeling, Mitochondrial and plastid genome architecture: Reoccurring themes, but significant differences at the extremes, *Proc. Natl. Acad. Sci. U.S.A.* 112 (2015) 10177–10184.
- [3] M. Sissler, J. Pütz, F. Fasiolo, C. Florentz, Mitochondrial aminoacyl-tRNA synthetases, *madame Curie Biosci. Database* [Internet]. Austin Landes Biosci. 2000–2013.
- [4] D. Diodato, D. Ghezzi, V. Tiranti, The mitochondrial aminoacyl tRNA synthetases: genes and syndromes, *Int. J. Cell Biol.* 2014 (2014) 787956.
- [5] J.L. Huot, L. Enkler, C. Megel, L. Karim, D. Laporte, H.D. Becker, A.-M. Duchêne, M. Sissler, L. Maréchal-Drouard, Idiosyncrasies in decoding mitochondrial genomes, *Biochimie* 100 (2014) 95–106.
- [6] J.R. Brown, D. Gentry, J.A. Becker, K. Ingraham, D.J. Holmes, M.J. Stanhope, Horizontal transfer of drug-resistant aminoacyl-transfer-RNA synthetases of anthrax and Gram-positive pathogens, *EMBO Rep.* 4 (2003) 692–698.
- [7] B. Brindefalk, J. Viklund, D. Larsson, M. Thollesson, S.G.E. Andersson, Origin and evolution of the mitochondrial aminoacyl-tRNA synthetases, *Mol. Biol. Evol.* 24 (2007) 743–756.
- [8] A.-M. Duchêne, A. Giritch, B. Hoffmann, V. Cognat, D. Lancelin, N.M. Peeters, M. Zaepfel, L. Maréchal-Drouard, I.D. Small, Dual targeting is the rule for organellar aminoacyl-tRNA synthetases in *Arabidopsis thaliana*, *Proc. Natl. Acad. Sci. U.S.A.* 102 (2005) 16484–16489.
- [9] C. Pujol, M. Bailly, D. Kern, L. Marechal-Drouard, H. Becker, A.-M. Duchene, Dual-targeted tRNA-dependent amidotransferase ensures both mitochondrial and chloroplastic Gln-tRNAGln synthesis in plants, *Proc. Natl. Acad. Sci. U.S.A.* 105 (2008) 6481–6485.
- [10] Y. Hirakawa, F. Burki, P.J. Keeling, Dual targeting of aminoacyl-tRNA synthetases to the mitochondrion and complex plastid in chlorarachniophytes, *J. Cell Sci.* 125 (2012) 6176–6184.
- [11] G.H. Gile, D. Moog, C.H. Slamovits, U.-G. Maier, J.M. Archibald, Dual organellar targeting of aminoacyl-tRNA synthetases in diatoms and cryptophytes, *Genome Biol. Evol.* 7 (2015) 1728–1742.
- [12] G. Natsoulis, F. Hilger, G.R. Fink, The HTS1 gene encodes both the cytoplasmic and mitochondrial histidine tRNA synthetases of *S. cerevisiae*, *Cell* 46 (1986) 235–243.
- [13] B. Chatton, P. Walter, J.P. Ebel, F. Lacroute, F. Fasiolo, The yeast VAS1 gene encodes both mitochondrial and cytoplasmic valyl-tRNA synthetases, *J. Biol. Chem.* 263 (1988) 52–57.
- [14] E. Tolkunova, H. Park, J. Xia, M.P. King, E. Davidson, The human lysyl-tRNA synthetase gene encodes both the cytoplasmic and mitochondrial enzymes by means of an unusual alternative splicing of the primary transcript, *J. Biol. Chem.* 275 (2000) 35063–35069.
- [15] J. Alexandrova, C. Paulus, J. Rudinger-Thirion, F. Jossinet, M. Frugier, Elaborate uORF/IRES features control expression and localization of human glycyl-tRNA synthetase, *RNA Biol.* 6286 (2015) 1301–1313.
- [16] H.-L. Tang, L.-S. Yeh, N.-K. Chen, T. Ripmaster, P. Schimmel, C.-C. Wang, Translation of a yeast mitochondrial tRNA synthetase initiated at redundant non-AUG Codons, *J. Biol. Chem.* 279 (2004) 49656–49663.
- [17] C.-I. Chien, Y.-W. Chen, Y.-H. Wu, C.-Y. Chang, T.-L. Wang, C.-C. Wang, Functional substitution of a eukaryotic glycyl-tRNA synthetase with an evolutionarily unrelated bacterial cognate enzyme, *PLoS One* 9 (2014) e94659.
- [18] Y. Ofir-Birin, P. Fang, S.P. Bennett, H.-M. Zhang, J. Wang, I. Rachmin, R. Shapiro, J. Song, A. Dagan, J. Pozo, S. Kim, A.G. Marshall, P. Schimmel, X.-L. Yang, H. Nechushtan, E. Razin, M. Guo, Structural switch of lysyl-tRNA synthetase between translation and transcription, *Mol. Cell.* 49 (2013) 30–42.
- [19] N. Gunasekera, S.W. Lee, S. Kim, K. Musier-Forsyth, E. Arriaga, Nuclear localization of aminoacyl-tRNA synthetases using single-cell capillary electrophoresis laser-induced fluorescence analysis, *Anal. Chem.* 76 (2004) 4741–4746.
- [20] Y.G. Ko, Y.S. Kang, E.K. Kim, S.G. Park, S. Kim, Nucleolar localization of human methionyl-tRNA synthetase and its role in ribosomal RNA synthesis, *J. Cell Biol.* 149 (2000) 567–574.
- [21] M. Mirande, D. Le Corre, D. Louvard, H. Reggio, J.-P. Pailliez, J.-P. Waller, Association of an aminoacyl-tRNA synthetase complex and of phenylalanyl-tRNA synthetase with the cytoskeletal framework fraction from mammalian cells, *Exp. Cell Res.* 156 (1985) 91–102.
- [22] M. Sajish, Q. Zhou, S. Kishi, D.M. Valdez, M. Kapoor, M. Guo, S. Lee, S. Kim, X.-L. Yang, P. Schimmel, Trp-tRNA synthetase bridges DNA-PKcs to PARP-1 to link IFN- γ and p53 signaling, *Nat. Chem. Biol.* 8 (2012) 547–554.
- [23] V.I. Popenko, N.E. Cherny, S.F. Beresten, J.L. Ivanova, V.V. Filonenko, L.L. Kisselev, Immunoelectron microscopic location of tryptophanyl-tRNA synthetase in mammalian, prokaryotic and archaeobacterial cells, *Eur. J. Cell Biol.* 62 (1993) 248–258.
- [24] E.L. Paley, V.N. Baranov, N.M. Alexandrova, L.L. Kisselev, Tryptophanyl-tRNA synthetase in cell lines resistant to tryptophan analogs, *Exp. Cell Res.* 195 (1991) 66–78.
- [25] G. Fu, T. Xu, Y. Shi, N. Wei, X.-L. Yang, TRNA-controlled nuclear import of a human tRNA synthetase, *J. Biol. Chem.* 287 (2012) 9330–9334.
- [26] N. Wei, Y. Shi, L.N. Truong, K.M. Fisch, T. Xu, E. Gardiner, G. Fu, Y.-S.O. Hsu, S. Kishi, A.I. Su, X. Wu, X.-L. Yang, Oxidative stress diverts tRNA synthetase to nucleus for protection against DNA damage, *Mol. Cell.* 56 (2014) 323–332.
- [27] H.-Y. Huang, H.-L. Tang, H.-Y. Chao, L.-S. Yeh, C.-C. Wang, An unusual pattern of protein expression and localization of yeast alanyl-tRNA synthetase isoforms, *Mol. Microbiol.* 60 (2006) 189–198.
- [28] M. Frechin, B. Senger, M. Braye, D. Kern, R.P. Martin, H.D. Becker, Yeast mitochondrial Gln-tRNAGln is generated by a GatFAB-mediated transamidation pathway involving Arc1p-controlled subcellular sorting of cytosolic GluRS, *Genes Dev.* 23 (2009) 1119–1130.
- [29] M. Frechin, L. Enkler, E. Tetaud, D. Laporte, B. Senger, C. Blancard, P. Hammann, G. Bader, S. Clauder-Münster, L.M. Steinmetz, R.P. Martin, J.-P. di Rago, H.D. Becker, Expression of nuclear and mitochondrial genes encoding ATP synthase is synchronized by disassembly of a multisynthetase complex, *Mol. Cell.* 56 (2014) 763–776.
- [30] K.-J. Chang, C.-C. Wang, Translation initiation from a naturally occurring non-AUG codon in *Saccharomyces cerevisiae*, *J. Biol. Chem.* 279 (2004) 13778–13785.
- [31] R.J. Turner, M. Lovato, P. Schimmel, One of two genes encoding glycyl-tRNA synthetase in *Saccharomyces cerevisiae* provides mitochondrial and cytoplasmic functions, *J. Biol. Chem.* 275 (2000) 27681–27688.
- [32] M.I. Chiu, T.L. Mason, G.R. Fink, HTS1 encodes both the cytoplasmic and mitochondrial histidyl-tRNA synthetase of *Saccharomyces cerevisiae*: mutations alter the specificity of compartmentation, *Genetics* 132 (1992) 987–1001.
- [33] C.-C. Wang, K.-J. Chang, H.-L. Tang, C.-J. Hsieh, P. Schimmel, Mitochondrial form of a tRNA synthetase can be made bifunctional by manipulating its leader peptide, *Biochemistry* 42 (2003) 1646–1651.
- [34] K. Galani, H. Grosshans, K. Deinert, E.C. Hurt, G. Simos, The intracellular location of two aminoacyl-tRNA synthetases depends on complex formation with Arc1p, *EMBO J.* 20 (2001) 6889–6898.
- [35] A.K. Azad, D.R. Stanford, S. Sarkar, A.K. Hopper, Role of nuclear pools of aminoacyl-tRNA synthetases in tRNA nuclear export, *Mol. Biol. Cell.* 12 (2001) 1381–1392.
- [36] J. Rettig, Y. Wang, A. Schneider, T. Ochsenreiter, Dual targeting of isoleucyl-tRNA synthetase in *Trypanosoma brucei* is mediated through alternative trans-splicing, *Nucleic Acids Res.* 40 (2012) 1299–1306.
- [37] I. Cestari, S. Kalidas, S. Monnerat, A. Anupama, M.A. Phillips, K. Stuart, A multiple aminoacyl-tRNA synthetase complex that enhances tRNA-aminoacylation in African trypanosomes, *Mol. Cell Biol.* 33 (2013) 4872–4888.
- [38] J. Rinehart, E.K. Horn, D. Wei, D. Soll, A. Schneider, Non-canonical eukaryotic glutamyl- and glutamyl-tRNA synthetases form mitochondrial aminoacyl-tRNA in *Trypanosoma brucei*, *J. Biol. Chem.* 279 (2004) 1161–1166.
- [39] K.E. Jackson, J.S. Pham, M. Kwek, N.S. De Silva, S.M. Allen, C.D. Goodman, G.I. McFadden, L. Ribas de Pouplana, S.A. Ralph, Dual targeting of aminoacyl-tRNA synthetases to the apicoplast and cytosol in *Plasmodium falciparum*, *Int. J. Parasitol.* 42 (2012) 177–186.
- [40] J.S. Pham, R. Sakaguchi, L.M. Yeoh, N.S. De Silva, G.I. McFadden, Y.-M. Hou, S.A. Ralph, A dual-targeted aminoacyl-tRNA synthetase in *Plasmodium falciparum* charges cytosolic and apicoplast tRNACys, *Biochem. J.* 458 (2014) 513–523.
- [41] M. Frechin, A.-M. Duchêne, H.D. Becker, Translating organellar glutamine codons: a case by case scenario?, *RNA Biol.* 6 (2009) 31–34.
- [42] P. López-García, D. Moreira, Open questions on the origin of eukaryotes, *Trends Ecol. Evol.* 30 (2015) 697–708.
- [43] A. Schön, C.G. Kannagara, S. Cough, D. Söll, Protein biosynthesis in organelles requires misaminoacylation of tRNA, *Nature* 331 (1988) 187–190.
- [44] A. Nagao, T. Suzuki, T. Katoh, Y. Sakaguchi, T. Suzuki, Biogenesis of glutamyl-tRNAGln in human mitochondria, *Proc. Natl. Acad. Sci. U.S.A.* 106 (2009) 16209–16214.
- [45] Y. Arais, J.L. Huot, T. Sekiguchi, M. Frechin, F. Fischer, L. Enkler, B. Senger, R. Ishitani, H.D. Becker, O. Nureki, Crystal structure of *Saccharomyces cerevisiae* mitochondrial GatFAB reveals a novel subunit assembly in tRNA-dependent amidotransferases, *Nucleic Acids Res.* 42 (2014) 6052–6063.
- [46] S. Merz, B. Westermann, Genome-wide deletion mutant analysis reveals genes required for respiratory growth, mitochondrial genome maintenance and mitochondrial protein synthesis in *Saccharomyces cerevisiae*, *Genome Biol.* 10 (2009) R95.
- [47] S. Hati, B. Ziervogel, J. Sternjohn, F.-C. Wong, M.C. Nagan, A.E. Rosen, P.G. Siliciano, J.W. Chihade, K. Musier-Forsyth, Pre-transfer editing by class II prolyl-tRNA synthetase: role of aminoacylation active site in “selective release” of noncognate amino acids *, *J. Biochem.* 281 (2006) 27862–27872.
- [48] C. Meisinger, T. Sommer, N. Pfanner, Purification of *saccharomyces cerevisiae* mitochondria devoid of microsomal and cytosolic contaminations, *Anal. Biochem.* 287 (2000) 339–342.
- [49] E. Lund, J.E. Dahlberg, Proofreading and aminoacylation of tRNAs before export from the nucleus, *Science* 282 (1998) 2082–2085.
- [50] S. Sarkar, A.K. Azad, A.K. Hopper, Nuclear tRNA aminoacylation and its role in nuclear export of endogenous tRNAs in *Saccharomyces cerevisiae*, *Proc. Natl. Acad. Sci. U.S.A.* 96 (1999) 14366–14371.
- [51] J. Dostie, F. Lejbkovicz, N. Sonenberg, Nuclear eukaryotic initiation factor 4E (eIF4E) colocalizes with splicing factors in speckles, *J. Cell Biol.* 148 (2000) 239–247.
- [52] P. Schimmel, C.-C. Wang, Getting tRNA synthetases into the nucleus, *Trends Biochem. Sci.* 24 (1999) 127–128.
- [53] A.K. Bandyopadhyay, M.P. Deutscher, Complex of aminoacyl-transfer RNA synthetases, *J. Mol. Biol.* 60 (1971) 113–122.
- [54] P. Kerjan, C. Cerini, M. Sémériva, M. Mirande, The multienzyme complex containing nine aminoacyl-tRNA synthetases is ubiquitous from *Drosophila* to mammals, *Biochim. Biophys. Acta* 1199 (1994) 293–297.

- [55] G. Simos, A. Segref, F. Fasiolo, K. Hellmuth, A. Shevchenko, M. Mann, E.C. Hurt, The yeast protein Arc1p binds to tRNA and functions as a cofactor for the methionyl- and glutamyl-tRNA synthetases, *EMBO J.* 15 (1996) 5437–5448.
- [56] S. Quevillon, M. Mirande, The p18 component of the multisynthetase complex shares a protein motif with the β and γ subunits of eukaryotic elongation factor 1, *FEBS Lett.* 395 (1996) 63–67.
- [57] S. Quevillon, J.-C. Robinson, E. Berthonneau, M. Siatecka, M. Mirande, Macromolecular assemblage of aminoacyl-tRNA synthetases: identification of protein-protein interactions and characterization of a core protein, *J. Mol. Biol.* 285 (1999) 183–195.
- [58] S.S. Kim, S.Y. Hur, Y.R. Kim, N.J. Yoo, S.H. Lee, Expression of AIMP1, 2 and 3, the scaffolds for the multi-tRNA synthetase complex, is downregulated in gastric and colorectal cancer, *Tumori J.* 97 (2011) 380–385.
- [59] D. Laporte, J.L. Huot, G. Bader, L. Enkler, B. Senger, H.D. Becker, Exploring the evolutionary diversity and assembly modes of multi-aminoacyl-tRNA synthetase complexes: Lessons from unicellular organisms, *FEBS Lett.* 588 (2014) 4268–4278.
- [60] B.S. Negrutskii, R. Stapulionis, M.P. Deuschert, Supramolecular organization of the mammalian translation system, *Biochemistry* 91 (1994) 964–968.
- [61] P.S. Ray, A. Arif, P.L. Fox, Macromolecular complexes as depots for releasable regulatory proteins, *Trends Biochem. Sci.* 32 (2007) 158–164.
- [62] C.B. Saper, A guide to the perplexed on the specificity of antibodies, *J. Histochem. Cytochem.* 57 (2009) 1–5.
- [63] J.E. Gilda, R. Ghosh, J.X. Cheah, T.M. West, S.C. Bodine, A.V. Gomes, Western blotting inaccuracies with unverified antibodies: need for a western blotting minimal reporting standard (WBMRS), *PLoS One* 10 (2015) e0135392.
- [64] S.E. Rieder, S.D. Emr, Overview of subcellular fractionation procedures for the yeast *Saccharomyces cerevisiae*, *Curr. Protoc. Cell Biol.* Chapter 3 (2001) Unit 3.7.
- [65] E. Palmer, T. Freeman, Investigation into the use of C- and N-terminal GFP fusion proteins for subcellular localization studies using reverse transfection microarrays, *Comp. Funct. Genomics* 5 (2004) 342–353.
- [66] M. Kaminska, S. Havrylenko, P. Decottignies, P. Le Maréchal, B. Negrutskii, M. Mirande, Dynamic organization of aminoacyl-tRNA synthetase complexes in the cytoplasm of human cells, *J. Biol. Chem.* 284 (2009) 13746–13754.
- [67] J. Rinehart, B. Krett, M.A.T. Rubio, J.D. Alfonso, D. Söll, *Saccharomyces cerevisiae* imports the cytosolic pathway for Gln-tRNA synthesis into the mitochondrion, *Genes Dev.* 19 (2005) 583–592.
- [68] P. Dönnies, A. Höglund, Predicting protein subcellular localization: past, present, and future, *Genomics Proteomics Bioinformatics* 2 (2004) 209–215.
- [69] K.-C. Chou, H.-B. Shen, A new method for predicting the subcellular localization of eukaryotic proteins with both single and multiple sites: Euk-mPloc 2.0, *PLoS One* 5 (2010) e9931.
- [70] C. Savojardo, P.L. Martelli, P. Fariselli, R. Casadio, TPpred2: improving the prediction of mitochondrial targeting peptide cleavage sites by exploiting sequence motifs, *Bioinformatics* 30 (2014) 2973–2974.
- [71] O. Emanuelsson, H. Nielsen, S. Brunak, G. von Heijne, Predicting subcellular localization of proteins based on their N-terminal amino acid sequence, *J. Mol. Biol.* 300 (2000) 1005–1016.
- [72] H. Nielsen, J. Engelbrecht, S. Brunak, G. von Heijne, Identification of prokaryotic and eukaryotic signal peptides and prediction of their cleavage sites, *Protein Eng.* 10 (1997) 1–6.
- [73] Y. Fukasawa, J. Tsuji, S.-C. Fu, K. Tomii, P. Horton, K. Imai, MitoFates: improved prediction of mitochondrial targeting sequences and their cleavage sites, *Mol. Cell. Proteomics* 14 (2015) 1113–1126.
- [74] A.N. Nguyen Ba, A. Pogoutse, N. Provart, A.M. Moses, NLStradamus: a simple Hidden Markov Model for nuclear localization signal prediction, *BMC Bioinformatics* 10 (2009) 202.
- [75] J. Lin, J. Hu, SeqNLS: nuclear localization signal prediction based on frequent pattern mining and linear motif scoring, *PLoS One* 8 (2013) e76864.
- [76] S. Kosugi, M. Hasebe, M. Tomita, H. Yanagawa, Systematic identification of cell cycle-dependent yeast nucleocytoplasmic shuttling proteins by prediction of composite motifs, *Proc. Natl. Acad. Sci. U.S.A.* 106 (2009) 10171–10176.
- [77] K. Nakai, P. Horton, PSORT: a program for detecting sorting signals in proteins and predicting their subcellular localization, *Trends Biochem. Sci.* 24 (1999) 34–36.
- [78] C.J. Bonangelino, N.L. Catlett, L.S. Weisman, Vac7p, a novel vacuolar protein, is required for normal vacuole inheritance and morphology, *Mol. Cell. Biol.* 17 (1997) 6847–6858.
- [79] S.E. Rieder, S.D. Emr, Isolation of subcellular fractions from the yeast *Saccharomyces cerevisiae*, *Curr. Protoc. Cell Biol.* Chapter 3 (2001) Unit 3.8.
- [80] J.M. Dahlman, D.C. Guttridge, Detection of NF- κ B activity in skeletal muscle cells by electrophoretic mobility shift analysis, *Methods Mol. Biol.* 798 (2012) 505–516.
- [81] E. Olmedo-Verd, J. Santamaría-Gómez, J.A.G. Ochoa de Alda, L. Ribas de Pouplana, I. Luque, Membrane anchoring of aminoacyl-tRNA synthetases by convergent acquisition of a novel protein domain, *J. Biol. Chem.* 286 (2011) 41057–41068.
- [82] T.A. Vida, S.D. Emr, A new vital stain for visualizing vacuolar membrane dynamics and endocytosis in yeast, *J. Cell Biol.* 128 (1995) 779–792.
- [83] W. He, G. Bai, H. Zhou, N. Wei, N.M. White, J. Lauer, H. Liu, Y. Shi, C.D. Dumitru, K. Lettieri, V. Shubayev, A. Jordanova, V. Guergueltcheva, P.R. Griffin, R.W. Burgess, S.L. Pfaff, X.-L. Yang, CMT2D neuropathy is linked to the neomorphic binding activity of glycyl-tRNA synthetase, *Nature* 526 (2015) 710–714.
- [84] M.C. Park, T. Kang, D. Jin, J.M. Han, S.B. Kim, Y.J. Park, K. Cho, Y.W. Park, M. Guo, W. He, X.-L. Yang, P. Schimmel, S. Kim, Secreted human glycyl-tRNA synthetase implicated in defense against ERK-activated tumorigenesis, *Proc. Natl. Acad. Sci. U.S.A.* 109 (2012) E640–E647.
- [85] Z. Wei, Z. Xu, X. Liu, W.-S. Lo, F. Ye, C.-F. Lau, F. Wang, J.J. Zhou, L.A. Nangle, X.-L. Yang, M. Zhang, P. Schimmel, Alternative splicing creates two new architectures for human tyrosyl-tRNA synthetase, *Nucleic Acids Res.* 44 (2016) 1247–1255.

Publication 2

Cytosolic aminoacyl-tRNA synthetases:
Unanticipated relocations for
unexpected functions

***BBA - Gene Regulatory Mechanisms*, 2018, 1861(4), pp. 387-400**



Contents lists available at ScienceDirect

BBA - Gene Regulatory Mechanisms

journal homepage: www.elsevier.com/locate/bbagrm

Cytosolic aminoacyl-tRNA synthetases: Unanticipated relocations for unexpected functions



Nathaniel Yakobov, Sylvain Debard, Frédéric Fischer, Bruno Senger, Hubert Dominique Becker*

Génétique Moléculaire, Génomique, Microbiologie, UMR 7156, CNRS, Université de Strasbourg, Institut de Botanique, 28 rue Goethe, 67083 Strasbourg Cedex, France

ARTICLE INFO

Keywords:

aaRS
tRNA
Eukaryotes
Localization
Nonconventional functions

ABSTRACT

Prokaryotic and eukaryotic cytosolic aminoacyl-tRNA synthetases (aaRSs) are essentially known for their conventional function of generating the full set of aminoacyl-tRNA species that are needed to incorporate each organism's repertoire of genetically-encoded amino acids during ribosomal translation of messenger RNAs. However, bacterial and eukaryotic cytosolic aaRSs have been shown to exhibit other essential nonconventional functions. Here we review all the subcellular compartments that prokaryotic and eukaryotic cytosolic aaRSs can reach to exert either a conventional or nontranslational role. We describe the physiological and stress conditions, the mechanisms and the signaling pathways that trigger their relocation and the new functions associated with these relocating cytosolic aaRS. Finally, given that these relocating pools of cytosolic aaRSs participate to a wide range of cellular pathways beyond translation, but equally important for cellular homeostasis, we mention some of the pathologies and diseases associated with the dis-regulation or malfunctioning of these nontranslational functions.

1. Introduction

Aminoacyl-tRNA synthetases (aaRSs) belong to a family of ubiquitous and essential enzymes. Their primary task is to supply the protein synthesis machineries (cytosolic and organellar) with the full set of aminoacyl-tRNAs (aa-tRNAs) necessary to translate all messenger RNA codons into their corresponding amino acids (aa) [1]. In theory, a given organism has to encode at least one aaRS for each genetically-encoded aa, which means that a prokaryotic species that uses for protein synthesis the standard genetic code composed of 20 aa, would need 20 genes encoding the 20 required aaRSs. However, depending on the organism's origin and genetic code repertoire, the number of aaRSs that can be found in a given organism ranges from 18 to 23 in prokaryotes [2] to nearly 45 in eukaryotes [3]. Despite their essential biochemical function the majority of prokaryotes and all eukaryotic organelles have less unique aaRSs than genetically-encoded aa, because these organisms (or compartments) can compensate the lack of an essential aaRS by alternative routes to generate the aa-tRNA species corresponding to the orphan tRNA/codon pair ([4–6] and reviewed in [7,8]). Paradoxically, prokaryotes and mainly bacteria also quasi-systematically encode more aaRSs than the necessary set for decoding the genetic code repertoire because the majority of bacterial genomes harbor more than one gene for a given aaRS [2]. Although the majority of the bacteria present one or several duplicated aaRSs (and even triplicated ones), the reason for

the presence of 2 aaRSs of the same aa and tRNA-charging specificity in a given species has rarely been studied. However, in the few cases that were studied, it was found that one of the two forms is usually expressed under specific environmental or stress conditions and that this stress-induced aaRS possesses specific catalytic traits allowing formation of the cognate aa-tRNA in these particular physiological conditions [9–14].

In eukaryotes, the presence of at least 2 different translationally-active and membrane-separated compartments, the cytosol and mitochondria, makes already the situation more complex with respect to the number of aaRSs that these organisms have to possess; and becomes even more complicated if the organism possesses additional organelles besides the mitochondria. Because the organellar and cytosolic translation machineries are of different phylogenetic origins, each eukaryote carries several compartment-specific pools of aaRSs, one for cytosolic translation and one for each organelle (reviewed in [15]). While both sets of genes are encoded by the nuclear genome and translated by the cytosolic protein synthesis machinery, the organellar pools are easily distinguishable from the cytosolic one because they are of prokaryotic origins and because these aaRSs possess, usually in the N-terminus, an organelle-specific targeting sequence that directs their import into the corresponding compartment (reviewed in [15]). However, even if in theory, a eukaryotic species using the standard 20 aa-containing genetic code and that possesses mitochondria would have to encode 40 aaRS

* Corresponding author.

E-mail address: h.becker@unistra.fr (H.D. Becker).<https://doi.org/10.1016/j.bbagrm.2017.11.004>

Received 29 September 2017; Received in revised form 13 November 2017; Accepted 14 November 2017

Available online 16 November 2017

1874-9399/ © 2017 Elsevier B.V. All rights reserved.

genes, there is not a single eukaryotic species that has been proposed so far to encode 2 complete and unique compartment-specific sets of 20 aaRSs [5,15]. Depending on the species that was studied, up to 17 mitochondria-specific aaRS genes can be missing (reviewed in [15]) from the nuclear genome in certain species. To compensate this apparent lack of mitochondrial aaRSs, eukaryotes essentially utilize two different strategies: i) they use an alternate two-steps route to generate the aa-tRNA species for which the cognate aaRS is missing [6,16,17] or ii) they import the corresponding cytosolic aaRS making this enzyme a dual-localized aaRS both cytosolic and mitochondrial (reviewed in [15,18]). When both the cytosolic and mitochondrial aaRS are encoded by a single gene, both forms are either translated from two mRNAs of different length generated through different processes (see below). While using a dual-localized aaRS encoded from a single gene makes perfect sense when the gene encoding the mitochondria-specific aaRS is missing, there are examples in higher plants and *S. cerevisiae* (*Sce*), where a cytosolic aaRS can be targeted to mitochondria even if the corresponding mitochondrial ortholog encoded by a separate gene already exists (reviewed in [15]). The rationale for having duplicated mitochondrial aaRS (one strictly organellar and one dual-localized) has been clarified in yeast [6] but has so far not been ruled out in higher plants. However, it was shown that some of these plant dual-localized aaRSs are not able to charge tRNA inside the mitochondria [19], suggesting that they might have a nonconventional role inside this compartment that has yet to be identified. Interestingly, in plants the cytosolic aaRSs that are dual-localized are strictly shared with the mitochondria and never with the chloroplast, however the majority of the mitochondrial aaRSs are dual-targeted both in the mitochondria and the chloroplasts because they harbor an ambiguous organellar targeting sequence [20].

The other common trait of eukaryotic cytosolic aaRSs that influences their subcellular localization is the capacity of some of them to form so-called Multi-Synthetase Complexes (MSCs). These complexes were found in all species studied so far ranging from fungi to mammals ([21–24] and reviewed in [25]). They are all composed of cytosolic aaRS and 1 to 3 auxiliary assembly factors also called Aminoacyl-tRNA synthetase Interacting Multifunctional Proteins (AIMPs). The number of aaRSs and AIMPs that build up these MSCs varies from 2 aaRSs and 1 AIMP in the *S. cerevisiae* AME complex to 9 aaRSs and 3 AIMPs (AIMP1, AIMP2 AIMP3 also called p43, p38 and p18 respectively) in the human, MARS complex. With the exception of the yeast AME MSC (reviewed in [26]), the association of cytosolic aaRSs into MSC does not impact the catalytic efficiency of the participating aaRSs but rather regulates the alternative subcellular localization and non-conventional function that some of them have been shown to display. The studies that have been published over the past 2 decades uniformly show that these MSCs can be considered as cytosolic retention platforms for aaRSs that can be released from these complexes under specific physiological or stress conditions to relocate into other subcellular compartments in which they can exert nonconventional functions (reviewed in [27–30]). Additionally, the AIMPs can also be released from MSCs to be targeted to other compartments (reviewed in [31]). The additional compartments that these MSC-released cytosolic aaRSs or AIMPs can reach and the repertoire of atypical physiological processes to which these proteins can participate is in constant expansion ([29], reviewed in [32]). Studies show that MSCs-released aaRSs can i) stay in the cytosol by building other non-MSC complexes, ii) be imported into mitochondria or nuclei, iii) bind to membranes or even iv) be secreted (reviewed in [18]). Once relocated, they can exert a myriad of regulatory or signaling functions that impact processes among which gene expression, angiogenesis, apoptosis, inflammation, adiposity, nutrient signaling, cell-to-cell crosstalk or even resveratrol-mediated poly(ADP-ribose) polymerase 1 (PARP1) activation (reviewed in [28–31], [33]). Their involvement in these processes is far from being trivial since in human, malfunctioning of these aaRSs' additional roles, inevitably leads to diseases [31,34].

At the molecular level, the release of an aaRS or AIMP from the MSC is usually mediated by posttranslational modification of the protein that includes chemical modification or proteolytic cleavage of the aaRSs at a specific residue [35]. More rarely, the release of an aaRS can be initiated by decreasing the quantity of the AIMP binding the aaRS [36]. There are 2 types of molecular mechanism by which these aaRSs exert their atypical function, either they bind to one or several new protein partners that deviates the aaRS from aa-tRNA formation or they accumulate a by-product or intermediate of the tRNA aminoacylation reaction (reviewed in [27–30]) or both. Note that in human and yeast some of the cytosolic aaRSs that do not belong to the MSCs have also been shown or predicted to be able to relocate to other subcellular compartments and, in some cases, their atypical role has been characterized.

In the present review we give a detailed overview of all the subcellular compartments that free-standing or MSC-participating cytosolic aaRSs can reach. We mention the mechanisms, strategies and physiological or stress conditions that trigger their relocation and the unexpected cellular processes to which relocated cytosolic aaRSs participate. We have subdivided relocating aaRSs into two categories: those who keep their canonical function in their new subcellular destination, meaning formation of an aa-tRNA intermediate or end-product that supplies the translation machinery and those who exert a non-conventional function that does not require formation of an aa-tRNA species.

2. Membrane-localized aaRSs in bacteria

Prokaryotic cells are composed of distinct compartments that differ according to their phylogenetic origin. In all cases, the cytoplasm, in which transcription and translation of genetic information occur, is engulfed by a negatively charged plasma membrane made up of various lipid species, ranging from phospholipids to hopanoids [37,38]. The structure of the outer shell of prokaryotes differs between Gram-positive [39] and Gram-negative [40] bacteria, and between phylogenetical groups of archaea [41], but to date, no aaRS has been detected outside the cytoplasm, where the 20 enzymes find their substrates (ATP, aa, tRNAs) and perform their canonical aminoacylation function. Several studies, however, have shown that aaRS can sometimes be localized at membranous structures (see below).

Central and essential biological functions depend on the integrity of plasma membranes, such as respiration, electron transport, proton translocation, mechanical stresses resistance, nutrients and exogenous molecules selection and transport, interaction with the environment or host macromolecules, etc. [37–41]. Because of their relatively uniform negative charge, bacterial membranes are targeted by and sensitive to cationic antimicrobial peptides (CAMPs) synthesized and secreted by other bacteria or fungi, or by immune cells within a host [42]. Various CAMPs exist, but they often target bacteria through charge interaction, leading to membrane disruption and ultimately to bacterial death [42]. Bacteria possess CAMPs resistance factors of various types [43,44], and among them, aminoacyl-phosphatidylglycerol synthases (aaPGSs) [45,46]. AaPGSs are composed of two separated domains, an integral membrane N-terminal domain with 2 to 14 transmembrane helices, with a phospholipid flippase activity, and a C-terminal soluble domain of the DUF2156 family that has an aa-tRNA transferase activity. AaPGSs catalyze the transfer of an aa from an aa-tRNA to a second substrate, phosphatidylglycerol (PG) or cardiolipin (CL) [45]. For example, LysPGS transfers Lys from K-tRNA^K to PG, leading to a lysylated PG (K-PG), whose overall charge is +1, in comparison to PG (–1). AaPGSs can be specific of one aa (KPGS, APGS), bispecific (A/KPGS) or multi-specific (R/A/KPGS) and transfer corresponding amino acids onto PG or CL, providing aminoacylated phospholipids with modified charge properties. Such modifications change the overall properties of membranes such as permeability to various compounds (metals, antimicrobials, etc.), rigidity and, of course, global charge. AaPGSs have

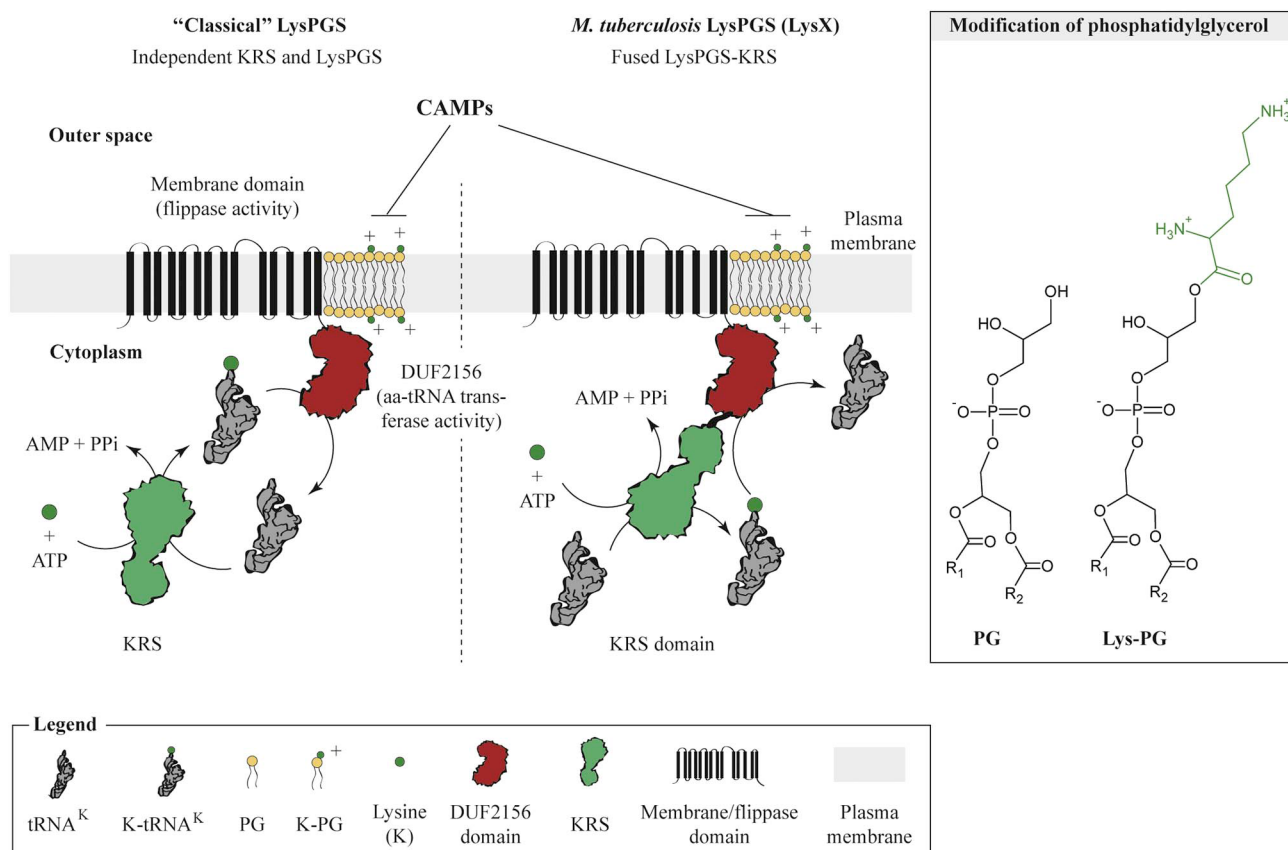


Fig. 1. Aminoacyl-phosphatidylglycerol synthases. “Classical” aaPGS, like the LysPGS from *S. aureus* is composed of an N-terminal integral membrane domain with 14 transmembrane helices (TMH, black), that targets the enzyme to the plasma membrane, and a C-terminal soluble domain, facing the cytoplasm (red), which belongs to the DUF2156 family of aa-tRNA transferases. The DUF2156 domain utilizes K-tRNA^K, produced independently by a “canonical” KRS (green), and catalyzes the transfer of K (green circle) from tRNA^K to a hydroxyl group of phosphatidylglycerol (PG). Resulting K-PG can then be transferred to the outer leaflet of the plasma membrane by the N-terminal membrane domain that displays a phospholipid flippase activity. Changes in membrane charge properties participate in resistance against CAMPs. In *M. tuberculosis*, the LysX gene product is a LysPGS-KRS fusion protein, with the N-terminal flippase/membrane (black) and middle DUF2156 (red) domains of classical aaPGSs, followed by a KRS C-terminal domain (green). This domain is responsible for the synthesis of K-tRNA^K that is subsequently used by the DUF2156 and flippase domains to produce surface exposed K-PG molecules. The aaPGS part of the protein cannot scavenge K-tRNA^K produced by the second “canonical” KRS in *M. tuberculosis*. The right panel presents structures of PG and K-PG. (For interpretation of the references to color in this figure legend, the reader is referred to the web version of this article.)

been demonstrated to increase resistance against CAMPs in various model pathogens such as *Staphylococcus aureus*, *Listeria monocytogenes*, *Pseudomonas aeruginosa* and others and have been related to virulence phenotypes. Those virulence factors have thus been named **Multiple Peptide Resistance Factors** [45,46].

In *Mycobacterium tuberculosis* and numerous Actinobacteria [45], two KRS genes are detected. One of them (*lysS*, Rv3598c) encodes a canonical KRS with an N-terminal anticodon-binding domain (ABD) and a C-terminal catalytic core, while the second (*lysX*, Rv1640c) is composed of an N-terminal MprF-like domain (flippase and DUF2156 domains) followed by a KRS domain (ABD and catalytic domains) ([47], Fig. 1 and Table 1).

This KRS localizes at the plasma membrane, through the flippase-like domain, and has been shown to be a *bona fide* KPGS [47,49]. Interestingly, the “classical” MprF part of the protein cannot scavenge K-tRNA^K synthesized by the second, canonical KRS, when deprived of the KRS appended domain, in contrast to other “classical” aaPGS. The KRS domain thus specifically synthesizes K-tRNA^K for use in membrane modification. The LysX protein is, like other aaPGSs, involved in membrane remodeling, CAMPs resistance and virulence [47].

In cyanobacteria, specialized membrane structures separated from the plasma membrane, called thylakoids, are involved in oxygenic photosynthesis, in particular in the assembly and functioning of photosystems. Proteins and protein complexes can be targeted within the thylakoid lumen, or at the surface of the organelle-like compartment, and perform various functions related to oxygenic photosynthesis. For

example, F₁F₀ ATP synthase is assembled and functions at the surface of thylakoids [50,51]. Recent work highlighted that among 279 sequenced cyanobacteria, 102 contain one or several aaRSs that are anchored to the outer leaflet of thylakoid membranes [52]. Thylakoid-specific targeting of aaRSs depends on the presence of a CAAD (for Cyanobacterial Aminoacyl-tRNA synthetases Appended Domain) domain that has been detected in 7 different aaRSs (ERS, VRS, LRS, IRS, CRS, MRS, RRS) at various positions within the protein sequences. CAAD is found at the very C-terminus of ERS, but in a C-terminal internal region in other aaRSs [52]. In all cases, no other paralogs of CAAD-containing aaRSs is found in proteomes, which suggested that they are all active in spite of unusual membrane localization [52–54]. Phylogenetic studies suggest that only cyanobacteria contain aaRSs with a CAAD domain, and that insertion of this module in aaRSs corresponds to several independent evolutionary events [52,53]. The CAAD domain shares homology with the CURT1/TMP14/PSI-P-family proteins, found in chloroplasts of plants. They are all membrane proteins involved in the organization of thylakoids and grana in chloroplasts, by influencing curvature of lipid bilayers [53]. AaRS-CAAD domains have not been shown to be involved in modulating thylakoid curvature and/or ultrastructure, but have been experimentally demonstrated to anchor aaRSs in thylakoid membranes [52,54]. It is to be noted that VRS-CAAD, that is thylakoid-bound, relocates at cell poles of mature heterocysts (specialized and differentiated cyanobacterial cells) upon nitrogen starvation [52]. A combination of *in vivo* and *in vitro* experiments showed that VRS-CAAD is active and found only in membrane fractions of cyanobacteria, while

Table 1

Non-canonical functions and relocalizations of aaRS: aaRSs that exert nontranslational functions are grouped as a function of the subcellular compartment to which they relocate: (C, cytoplasm; N, nucleus; M, mitochondria; C. mb, cytoplasmic membrane; L, lysosome; V, vacuole), or when they are extracellularly secreted (HIV, human immunodeficiency virus; RSV, Rous sarcoma virus; Exo, exosomes; EC, extracellular (secreted); S, (host) serum). Organisms or groups of organisms in which the aaRS relocalizations were reported in this review are abbreviated as follows: Mam, mammalian; Vert, vertebrates; High. Euk, higher eukaryotes; *Hsa*, *Homo sapiens*; *Sce*, *Saccharomyces cerevisiae*; *Zf*, zebrafish; *Bma*, *Brugia malayi*; *Mtu*, *Mycobacterium tuberculosis*. The schematized structural organization of each aaRS was designed based on pfam 31.0 (<http://pfam.xfam.org/>), NCBI blastp, recent reviews [29,48] and the cited references (domains are not at scale). Orange and blue boxes correspond to anticodon/tRNA binding domains and catalytic core respectively, gray boxes correspond to additional domains and green boxes to WHEP domains. Red marks indicate the position of the residue that is post-translationally modified and/or domains involved in relocalization. p, phosphorylation; ac, acetylation; n.d., not determined; Nt ext., N-terminal extension; Ct, C-terminal; Transmb, transmembrane domain; cat, Catalytic; tRNA bd, tRNA binding domain.

Comp.	Organism	aaRS	Structural organisation	(Re)loc. mec	domain(s) involved	Physiological fuction	References	
C.	<i>Hsa</i>	EPRS		pS886/pS999	WHEP	Translation regulation (GAIT element)	[32], [35], [83-87]	
	<i>Hsa, Mmu</i>	EPRS		pS990	WHEP	antiviral immunity	[88]	
	<i>Hsa</i>	QRS		MARS released	Catalytic	Anti-apoptotic	[89-92]	
	Mam	RRS		Alternative AUG	Nt. Zn finger	Protein degradation	[93-98]	
N.	<i>Hsa</i>	KRS		pS207	tRNA bd.	Transcription activation (MITF)	[103-105]	
	Mam. Zf	YRS		acK244	NLS tRNA bd.	DNA damage response	[109-112]	
	Vert.	WRS		NLS	WHEP	p53 signaling	[113-115]	
	Vert.	SRS		NLS	UNE-S	Anti-angiogenic	[28], [116], [120], [121]	
	Vert.	TRS		n.d.	not UNE-T	Anti-angiogenic	[122]	
	<i>Hsa</i>	MRS		NLS	Nt ext. (GST)	rRNA transcription	[123]	
	<i>Sce</i>	MRS		NLS	GST-like	ATP1 transcription regulation	[36]	
	<i>Sce</i>	DRS		NLS (Nt)	Nt ext.	DRS-mRNA translational regulation	[116], [125]	
	M.	<i>Sce</i>	ERS		MTS	GST-like	ATP9 translation regulation	[36]
	C. mb.	<i>Hsa</i>	KRS		pT52	ABD + ext.(1-72)	Promotes Cell-migration	[126-128]
<i>Hsa, Mmu</i>		EPRS		pS999	WHEP	Adiposity and lifespan regulation	[32]	
<i>Mtu</i>		KRS		Transmb.	Flippase, Duf2156	Virulence and cAMP resistance	[45-47]	
L.	Mam.	LRS		VPS34 (cat. site)	catalytic, UNE-L	Lysosomal mTORC1 activation	[136], [137]	
V.	<i>Sce</i>	LRS		Gtr1	editing domain	Vacuolar mTORC1 activation	[139]	
HIV	<i>Hsa</i>	KRS		pS207 / Gag	Helix H7	Primer tRNA ^K packaging	[140-144],[145]	
RSV	<i>Hsa</i>	WRS		n.d.	n.d.	Primer tRNA ^W packaging	[146]	
E.	<i>Hsa</i>	KRS		Syntenin	cleavage site, PDZ d.	TNFa and cell migration in macrophages	[147], [148]	
EC.	High. Euk.	YRS		n.d.	Mini-YRS	Pro-angiogenic (IL8 like)	[151], [152], [154-156]	
	High. Euk.	YRS		n.d.	EMAPII like Ct d.	Pro-inflammatory cytokine	[148], [153], [163]	
	High. Euk.	WRS		n.d.	Mini-WRS	Angiostatic	[153], [154] [158-162]	
	<i>Hsa</i>	WRS		n.d.	WHEP	Early immune response	[164]	
	<i>Hsa</i>	TRS		n.d.	n.d.	Endothelial cell migration	[165], [166]	
S.	<i>Hsa</i>	GRS		n.d.	n.d.	Defense against tumor formation (ERK)	[173], [174]	
S.	<i>Bma</i>	NRS		secreted	UNE-N	Host Pro Inflammatory	[167-172]	

deletion of the CAAD domain renders the protein soluble without impacting its kinetic activity. Importantly, a series of pull-down experiments coupled with LC-MS/MS characterizations conducted in *Anabaena* sp. PCC 7120 strongly support that VRS-CAAD directly interacts with the F_1F_0 -ATP synthase in thylakoid membranes in a CAAD-dependent manner. Interaction between VRS-CAAD and F_1F_0 -ATP synthase does not influence aminoacylation activity, and no impact on the overall ATP production, used as a proxy of ATP synthase activity, could be evidenced. However, authors propose several hypotheses relating CAAD-containing aaRSs and nutrient sensing (in particular nitrogen through aa sensing), or possible moonlighting functions that have yet still to be experimentally addressed [52].

3. Eukaryotic relocating aaRSs with conventional functions

The intracellular space of eukaryotic cells has a complex organization and displays more than one translationally active compartment. It is therefore questionable to ask if there is a specific aaRS for each compartment or if a single polypeptide chain can be found at multiple localizations within a cell. In this section, we examine how each translationally-active compartment is supplied with a complete set of

aa-tRNA synthesizing activities and how cytosolic aaRS are distributed throughout the cell. The latter are generally considered as soluble enzymes but it is known for decades that they may be associated with ribosomes, organelles or lipids ([55] and references therein) and nowadays a growing number of publications lead to the conclusion that cytosolic aaRSs exert their canonical functions at multiple locations within the cell.

3.1. Nuclear translocation of aaRS and tRNA nuclear export

Eukaryotic precursors tRNAs are transcribed in the nucleus and undergo several maturation steps before being fully functional for aminoacylation in the form of L-shaped and fully modified tRNAs. Those include 5' and 3' processing, CCA addition and post-transcriptional base modifications [56]. A majority of maturation steps take place within the nucleus. Classically, all tRNAs are then transported through nuclear pores to reach the cytosol where they are aminoacylated by cognate cytosolic aaRSs, and participate in ribosomal protein synthesis [57,58]. Experiments conducted in the mid-eighties surprisingly showed that a fraction of the Phenylalanyl-tRNA-synthetase pool (FRS) relocalizes into the nucleus, although its function inside the

organelle was not clearly understood [59]. The presence of an aaRS in the nucleus, where tRNAs are synthesized and processed led to the attractive hypothesis that aminoacylation of nuclear tRNAs by aaRSs could be a quality control step to assess their structural and functional integrity prior to export [60,61]. In correlation to that, aminoacylation has been experimentally demonstrated for tRNA^Y and initiator tRNA^M (tRNA_i^M) in *X. laevis* oocytes [60]. However, for a putative quality control mechanism involving aminoacylation to occur in the nucleus for all tRNAs, the corresponding aaRSs should be able to enter the nucleus as well. This hypothesis was reinforced by the detection of nuclear localization sequences (NLS) in most of these enzymes [18,62]. Incidentally, results obtained in the yeast *S. cerevisiae* showed nuclear tRNA aminoacylation activity for MRS, IRS and YRS [61,63]; and more recently 19 tRNA species have been detected in the form of aa-tRNAs in the nucleus [64]. Most of aa-tRNA are exported [65] to fuel cytosolic protein synthesis, but it has been demonstrated that 30% are retained inside the nucleus, where they might be involved in protein modification, especially in the case of R-tRNA^R, that participates in the N-end rule degradation pathway [66]. Several authors also suggested that nuclear pools of cytosolic aaRSs might assemble into molecular complexes [67,68]. Finally, nuclear relocalization of many cytosolic aaRSs seems to be a frequent feature across organisms and translocation of cytosolic aaRSs through the nuclear pores is accomplished by the classical import machinery (NLS/importins), although various other strategies to reach the nucleus [69]. Finally, their canonical function is only one of the many roles they exhibit inside this compartment.

3.2. Addressing cytosolic aaRS to mitochondria through MTS acquisition

In all organisms studied so far, no gene encoding mitochondrial aaRSs was found in any of the mitochondrial genomic DNAs. All mitochondrial aaRSs are nuclear-encoded [70,71], aside the 20 cytosolic aaRS genes. Importantly, the full set of the 20 mitochondrial aaRS genes has never been detected in any nuclear genomes so far [15,72,73]. Indeed, some aaRSs genes originating from mitochondria (or plastids in photosynthetic organisms and apicomplexans) have been lost during

evolution. Consequently, mitochondrial aminoacylation activities have to be fulfilled by other aaRS, namely the cytosolic aaRSs. In this case, mitochondrial targeting sequences (MTS) are found at the N-terminus of the mitochondrial-targeted cytosolic aaRSs (Fig. 2). Addition of MTS can be achieved through different mechanisms such as alternative splicing of the aaRS transcript (human KRS) [74] or from an alternative translation start (AUG) site within the same transcript (human GRS) [75]. Moreover, both forms can be translated from mRNA transcripts that differ only in the 5' regions. For example, the yeast *HTS1* gene, coding for the sole HRS, has two in-frame translational starts separated by an alternative transcriptional start leading, upon translation, to two isoforms of HRS, a longer (mitochondrial) and a shorter (cytosolic) one [76]. A similar strategy has been evidenced for yeast VRS [77]. Alternatively, experiments showed that the gene encoding the two isoforms of yeast ARS is translated from a single mRNA, where the mitochondrial isoform is initiated from an upstream atypical ACG start codon, and the cytoplasmic isoform from a classical AUG start codon [78]. This dual-targeting mechanism, that involves synthesis of two protein isoforms from a single mRNA seems to be the rule in multi organellar organisms like *A. thaliana* [3,79] or apicomplexan parasites [80].

3.3. Mitochondrial-cytosolic dual-localization of a single aaRS

Apart from synthesizing two protein isoforms (one with and one without an MTS) from expression of a single gene, another strategy to generate a cytosolic/mitochondrial dual-localized protein is to produce a mitochondrial protein (harboring an MTS) and to retain it within the cytosol through interaction with an anchoring protein. For example, the yeast cytosolic ERS is imported into the mitochondria even if it does not harbor an identifiable targeting signal [6]. Experiments demonstrated that mitochondrial import of cytosolic ERS compensates the absence of mitochondrial QRS. Indeed, mitochondrial Q-tRNA^Q cannot be synthesized directly, but *via* the indirect transamidation route. In this pathway, aminoacylation of mt-tRNA^Q is specifically performed by the mitochondria-localized cytosolic ERS, which produces a physiologically misacylated *E*-mt-tRNA^Q. This intermediate is further converted to

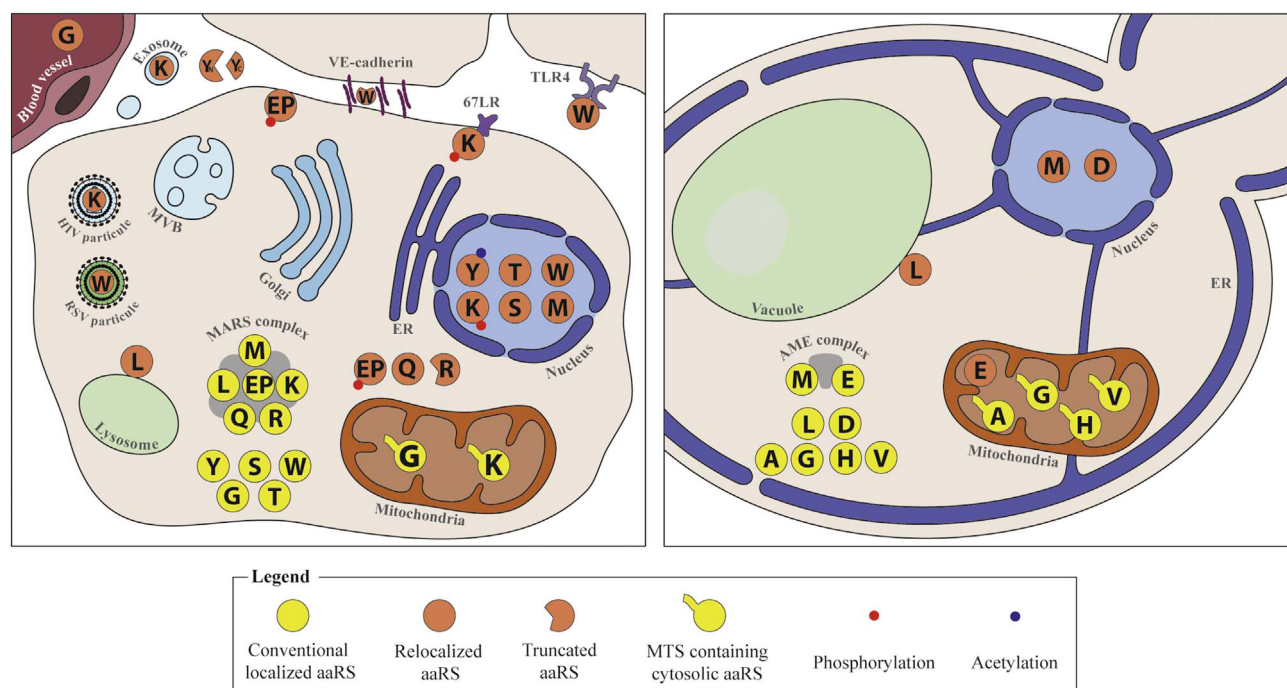


Fig. 2. Multiple subcellular localizations of mammalian (left) and yeast cytosolic aaRSs (right). Only mammalian and *S. cerevisiae* cytosolic aaRSs that relocate from the cytosol to a different compartment or that can be released from the MARS MSC and stay in the cytosol are shown. Only aaRSs that relocate to the nucleus and which are exerting non-conventional functions are represented on the figure.

$Q\text{-mttRNA}^Q$ by the tRNA-dependent GatFAB amidotransferase in yeast [6]. In *A. thaliana* and mammals [16,17], a *bona fide* mitochondrial ERS, called non-specific, produces $E\text{-mttRNA}^Q$ in addition to the cognate $E\text{-mttRNA}^E$, and the misacylated intermediate is converted to $Q\text{-mttRNA}^Q$ by the mitochondrial GatCAB amidotransferase. Mitochondrial translocation of cytosolic ERS is triggered by a non-canonical MTS located after the first 190 residues [6]. Yeast cytosolic ERS is essential in both the cytosol and mitochondria, and regulation of its localization has been proven to be crucial during diauxic shift (transition from fermentation to respiration). Both yeast ERS and MRS are associated to the cytosolic anchoring protein Arc1p [22], preventing nuclear accumulation of the two aaRSs [81]. Upon diauxic shift, levels of soluble Arc1p decrease significantly, which triggers simultaneous release of both MRS and ERS [36]. While cytosolic MRS relocates into the nucleus (see Section 4.2.7), cytosolic ERS translocates into mitochondria, where it generates $Q\text{-tRNA}^Q$ and controls the overall rate of mitochondrial protein synthesis.

4. Eukaryotic relocating cytosolic aaRSs with nonconventional functions

As mentioned in the introduction, the primary function of an aaRS is to aminoacylate its cognate isoacceptor tRNAs in the translationally active compartment where the aaRS is supposed to be localized. In eukaryotes, where several organelles and compartments are found, defining the exact subcellular localization of a given aaRS is not an easy task, since some aaRSs are free-standing enzymes while other are found in an MSC (Multi-“Synthetase” Complex), *i.e.* the human MARS-complex or the yeast AME complex. Furthermore, MSC-associated aaRSs can be released from the complex under specific physiological or stress conditions, and/or upon posttranslational modification. One of the remarkable feature of aaRSs is that they are modular enzymes. Some of them inherited additional domains, that are sometimes only be found in aaRSs, upon various evolutionary events, [29]. Some of those additional domains are necessary to ensure the specificity of the tRNA aminoacylation (“conventional”) reaction (*i.e.* Connective Peptide of the editing domains), whereas other domains are involved in “non-canonical” (and sometimes non-translational) functions that these enzymes can carry out. Interestingly, some additional domains are required for both conventional and non-canonical functions in a single aaRS.

In this context, the additional domain can harbor the non-canonical function by itself or can be the target of a post-translational modification, required for aaRS relocation. Indeed, to fulfil their non-canonical function(s), aaRSs often have to relocate from the cytoplasm (that is, their “canonical” localization) towards a new compartment. Alternatively, an MSC-associated aaRS can stay within the cytosol but be released from the MSC. In this section, we sorted the cytosolic aaRSs as a function of the subcellular compartment in which they exert their non-canonical functions. All the aaRS relocalizations reported in this section are summarized in Table 1 and Fig. 2.

4.1. aaRSs released from the MSC but staying in the cytoplasm

4.1.1. Human glutamyl-prolyl-tRNA-synthetase (EPRS) in response to $IFN\gamma$ stimulation

In higher eukaryotes and notably human, ERS is fused to PRS by a non-catalytic linker that contains 3 so-called WHEP repeats. The phylogenetic origins of these WHEP domains (present in tryptophanyl-(W) histidinyl-(H) glycylic-(G) and glutamyl-prolyl-tRNA synthetase (EP) where explored by Ray *et al.* [82] who focused their work on this unique case of fused bi-functional aaRSs called EPRS. In the human MARS complex these WHEP repeats interact with AIMP3 and lysyl-tRNA-synthetase (KRS). However, EPRS can be released from the MARS complex upon sequential bi-phosphorylation of serine residues within the WHEP domain. For instance, in myeloid cells Serine 886 (S886) is

phosphorylated by the Cyclin-dependent kinase Cdk5/p35 kinase [83] and Serine 999 (S999) is phosphorylated by the mammalian Target Of Rapamycin 1 (mTORC1) activated p70 ribosomal protein S6 kinase 1 (S6K1) [32]. These phosphorylations occur upon interferon gamma ($IFN\gamma$) stimulation and trigger the release of EPRS. The phosphorylated WHEP repeats then sequentially interact with NSAP1, GAPDH, phosphorylated ribosomal L13a and the Gamma Interferon Inhibitor of Translation (GAIT) elements that can be found in the 3'-end of some mRNAs leading to the assembly of the so-called GAIT complex. This cytoplasmic GAIT complex then interacts with the translation initiation factor eIF4G, which inhibits translation of the mRNAs targeted by the GAIT complex [35,83–86].

Because, this translation inhibition was shown to be suppressed 14–16 h after $IFN\gamma$ stimulation, Yao and coworkers [87] investigated the mechanism underlying the recovery of the translation of the mRNAs targeted by the GAIT complex. They discovered an alternative route which allows mRNAs that display GAIT-elements to be basally translated even after GAIT-complex assembly. This mechanism involves an EPRS isoform called EPRS^{N1} which is translated from a truncated EPRS mRNA. This shorter EPRS mRNA is generated through an alternative polyadenylation pathway that changes an UAU (encoding tyrosine 864) to a stop codon (UAA). This EPRS^{N1} isoform is composed of the ERS core followed by approximately two WHEP domains. Consequently, the region of the WHEP domain that can be biphosphorylated is missing in EPRS^{N1}, preventing association of this EPRS variant to the GAIT complex. However, EPRS^{N1} being still able to bind to the mRNA GAIT-elements, it competes with the GAIT-complex for binding to these mRNAs, leading to a basal expression of pro-inflammatory mRNA.

4.1.2. Human glutamyl-prolyl tRNA-synthetase (EPRS) in response to viral infection

The mitochondrial antiviral signaling protein (MAVS) is considered as a central regulator of responses to viral infections through its capacity to block virus replication. MAVS is inhibited by poly(rC)-binding protein 2 (PCBP2)-dependent ubiquitination and is activated through viral RNA genome sensors such as RIG-I and MDA5. Lee and coworkers [88] showed that following viral infection, EPRS is phosphorylated at S990 which triggers its release from the MSC and promotes its interaction with PCBP2. This interaction prevents MAVS ubiquitination and sustains in this way antiviral immunity. Thus, EPRS is also an important factor of antiviral immunity.

4.1.3. Human glutaminyl-tRNA-synthetase (QRS)

The human QRS, which participates to the MARS MSC by binding to AIMP1 and arginyl-tRNA-synthetase (RRS) has been shown to possess an anti-apoptotic action. Apoptosis can be triggered by different factors (*i.e.* Tumor Necrosis Factor (TNF), FasL, Reactive Oxygen Species (ROS)) and different pathways (*i.e.* c-Jun N-terminal kinase (JNK) and p38), and an essential factor for apoptosis is the Apoptosis Signal-regulating Kinase 1 (ASK1). To prevent apoptosis and to enhance cell survival, the QRS catalytic domain interacts directly with the ASK1 catalytic domain, in a glutamine-dependent manner. The QRS unique N-terminal domain (UNE-Q) does not seem to be involved in this aaRS-dependent anti-apoptotic pathway. Furthermore, because QRS can be released from the MARS MSC [89], Ko *et al.* [90] proposed that there is an equilibrium between the interaction of QRS with the MARS complex and with ASK1. On the opposite, Hwang *et al.* [91] showed that the translocation of ASK1 into the nucleus through its interaction with the Apoptosis-Linked Gene 2 (ALG2), also prevents apoptosis. However, no functional link between the QRS- and ALG2-dependent anti-apoptotic pathways was further revealed so far. Finally, Shao *et al.* [92] demonstrated that the microRNA miR-US4-1 encoded by the Human Cytomegalovirus (CMV) genome targets human QRS and induces cell apoptosis.

4.1.4. Mammalian RRS

During evolution, mammalian RRSs have inherited two leucine-

zippers in their N-terminal extension, and like for other aaRSs, these leucine-zippers were shown to be involved in binding with AIMP2 or other aaRSs in order to participate to the MARS complex. However, beside the full-length RRS, an alternative AUG translation start allows synthesis of a 74-residues shorter RRS isoform, in which the leucine zippers are missing [93–95]. Consequently, this isoform cannot bind to the MSC and is found in free form in the cytoplasm [96–98]. Both RRS isoforms present similar aminoacylation activities [99] but it was suggested that R-tRNA^Rs produced by the shorter isoform are rerouted from protein synthesis to provide activated arginyl moiety for the Arg-dependent protein degradation pathway (“N-end rule”) [100–102].

4.2. Cytosolic aaRSs translocating to the nucleus

4.2.1. Human lysyl-tRNA-synthetase KRS (Mast Cells)

Many non-canonical functions were discovered for cytosolic KRS this past decade. For example, mast cells are known to be implicated in allergic and anaphylaxis responses and also in some immune disorders. Through allergen recognition by the immunoglobulin E high affinity receptor, IgE-FcεRI, activated mast cells accumulate diadenosine tetraphosphate (Ap4A) also called “alarmone” or “second messenger”. This second messenger binds to Histidine triad nucleotide-binding protein 1 (Hint1) which in turn releases the Microphthalmia-associated Transcription Factor (MITF) leading to its activation and the subsequent upregulation of the transcription of subset of genes (*i.e.* tryptophan hydroxylase and mast-cell protease 5) [103–106]. Recent structural investigations revealed that the pathway that activates MITF involves the phosphorylation of KRS at S207 (located at the ABD) by the MAPK/ERK kinase which is itself activated after allergen stimulation. The subsequent KRS conformational change induces *i)* its dissociation from the MARS complex (AIMP2) *ii)* inhibition of its aminoacylation capacity and *iii)* its translocation into the nucleus. Inside the nucleus, the exposed C-terminal domain of KRS interacts with the MITF which in turn dissociates from Hint1. Furthermore, KRS synthesizes Ap4A (KRS is responsible for the synthesis of about 70–80% of cellular Ap4A) which inhibits Hint1, leading to MITF-KRS-dependent upregulation of gene transcription under allergic stimulation [107,108]. Interestingly, a very recent study reported that HIV1 infection in human cells induces similar LysRS translocation into the nucleus (see below Section 4.5.1).

4.2.2. Zebrafish and mammalian tyrosyl-tRNA-synthetase (YRS)

Such an aaRS-dependent transcription-regulation was also shown for mammalian and zebrafish YRS. Angiogenin, nicotinamide and oxidative stress were shown to trigger YRS translocation into the nucleus. This relocalization occurs through a hexapeptide NLS which is located into a tRNA binding domain which is not the Anticodon Binding Domain (ABD) of YRS [109]. Under stress conditions, resveratrol fits into the YRS active site by mimicking tyrosine and triggers *i)* inhibition of YRS's capacity to aminoacylate tRNA^Y (YRS null mutant like) [110] and *ii)* an increase in acetylation of YRS's lysine 244 (K244) by the p300/CBP-associated factor (PCAF acetylase vs. SIRT1 deacetylase) [111]. This acetylation induces a conformational change that exposes YRS's NLS and triggers its nuclear translocation. Interestingly, Fu et al., [109] showed that binding of tRNA^Y prevents nuclear relocation of YRS, which is in agreement with the fact that early acetylation occurs into the YRS tRNA-binding domain (K244). Following nuclear import, YRS binds to TRIM28 (which notably represses the transcription factor E2F1) and to its associated Histone Deacetylase 1 (HDAC1) [112]. Through acetylation, E2F1 is activated and improves expression of genes involved in DNA damage repair (*i.e.* Breast Cancer 1 BRCA1 and the recombinase RAD51). Furthermore, two studies showed that YRS is able to stimulate NAD⁺-dependent PARP1 activity which is well known for its participation to the DNA damage response [110,112]. Taken altogether, nuclear YRS seems to be an important factor to prevent DNA damages.

4.2.3. Vertebrate tryptophanyl-tRNA-synthetase (WRS)

Liu and coworkers [113] showed, in 2004, the presence of 5 WRS mRNA splice variants in human cells which are translated into 2 different WRS isoforms: the full length (residues 1 to 471) and the mini-WRS (residues 48–471). Both, WRS and mini-WRS can be further processed by extracellular elastases to produce T1-WRS (residues 71–471) and T2-WRS (residues 94–471). For instance, the full-length WRS (component of the MARS complex) harbors an additional N-terminal WHEP domain which is either in a “locked” conformation (presence of Trp~AMP into the active site) or “open” conformation (absence of W~AMP into the active site). Furthermore, WRS is a class 1 aaRS that homodimerizes (α_2) and harbors a C-terminal NLS. WRS was already shown in 1993 [114] to be imported into the nucleus and later studies [115] showed that nuclear WRS increases upon IFN- γ treatment (anti-angiogenic and anti-proliferative). Upon IFN- γ stimulation, the WHEP domain from the nuclear WRS homodimer “opens” and serves as a bridge between PARP1 and DNA-dependent protein kinase (DNA-PKc), which is essential for DNA-PKc-ADP-ribosylation by PARP1 and p53 phosphorylation (Ser15). Consequently, phosphorylated p53 triggers cell death.

4.2.4. Vertebrate seryl-tRNA-synthetase (SRS)

SRS, that belongs to class 2 aaRSs, was also shown to be imported into the nucleus [116]. This import requires a robust NLS located into a unique C-terminal domain called UNE-S [28,117] which is conserved in all vertebrate SRSs from fish to human. In human cells (HUVEC = endothelial cells, HEK293T cells), the amount of nuclear SRS was estimated to be 10% of the total SRS content [116]. In 2009, two studies [118,119] identified different SRS mutations that could lead to deletion or sequestration of the NLS (into the UNE-S domain). These mutants have deficiencies in SRS nuclear import and anomalies in angiogenesis. This phenotype was explained by an original “Yin-Yang” mechanism whereby nuclear SRS competes with c-Myc for binding to the promoter of Vascular Endothelial Growth Factor (VEGFa); c-Myc binds to the promoter of VEGFa and recruits a histone acetyltransferase which increases chromatin decondensation at VEGFa locus and its expression. Contrariwise, nuclear SRS binding to the VEGFa promoter can recruit Sirtuin 2 (SIRT2) which deacetylates histones at the VEGFa locus and represses its expression [120]. Beside this Yin-Yang mechanism that acts on the proximal *cis* regulation element (CRE) which avoids abnormal vascularization, a recent study proposed the existence of a distal CRE regulation mechanism. Notably, they demonstrated that nuclear SRS binds a transcription factor Yin-Yang1 (YY1), building a complex that represses VEGFa expression. As described for the SRS-SIRT2 complex, the recently identified SRS-YY1 complex competes with the Nuclear Factor kappa B (NFκB) which binds the same distal CRE to enhance VEGFa expression [121].

4.2.5. Vertebrates from zebrafish to human threonyl-tRNA-synthetase (TRS)

Recently Cao and coworkers [122] reported the capacity of human (HUVEC) and zebrafish TRSs to relocate to the nucleus. Based on a newly identified *taARS^{cq16}* mutant in zebrafish, they show that TRS down-regulates VEGFa expression to prevent abnormal vascular development. Interestingly, this regulatory function resembles that of the human SRS described in the previous section. The fact that *taARS^{cq16}* mutant phenotype could not be abolished by SRS mRNA injection suggests that TRS-mediated regulation of angiogenesis proceeds through a different mechanism. However, they were able to swap the Zebrafish TRS by its human ortholog, indicating that this new non-canonical regulatory function is conserved in human.

4.2.6. Human methionyl-tRNA synthetase (MRS)

MRS is another MSC-participating aaRS capable of relocating to the nucleus and more precisely to the nucleolus where ribosomal RNA (rRNA) are transcribed. Compared to prokaryotic MRSs, human MRS

possesses an N-(267 amino-acids) and a C-terminal extension, in the latter of which a NLS was found. Ko and coworkers [123] showed that nucleolar translocation of human MRS requires rRNA and RNA polymerase I activity and that this relocation upregulates rRNA biogenesis when cells are proliferating upon treatment with growth factors like insulin, Platelet-Derived Growth Factor (PDGF) or Epidermal Growth Factor (EGF). Finally, the mechanism that triggers release of MRS from the MARS complex remains unclear but Ko and coworkers anticipated that phosphorylation of the MRS N-terminal extension through casein kinase II could be the event initiating nucleolar relocation of MRS. This hypothesis is supported by the fact that this kinase is involved in cell growth and rRNA biogenesis. However, to our knowledge the exact pathway and mechanism of MRS nucleolar relocation still needs to be verified experimentally.

4.2.7. *S. cerevisiae* MRS

As mentioned above, the yeast AME composed of Arc1 ERS and MRS has been shown to constitute a cytosolic retention platform for the two participating aaRSs. In fermenting yeast cells (high glucose concentration), the majority of MRS and ERS are found bound onto Arc1 that enhances their cognate tRNA aminoacylation efficiency [22]. However, upon switch to the respiratory metabolism (low glucose concentration), *ARC1* transcription is downregulated by the Snf1/4 kinase pathway (glucose-sensing pathway), which leads to synchronous release of MRS and ERS from Arc1. Released ERS then relocates to the mitochondria and indirectly controls accumulation of the Atp9 subunit of the F₀ domain of the mitochondrial ATP synthase (ATPase). Simultaneously, dissociation of MRS from the AME complex unmasks a bipartite NLS located in the MRS N-terminus and its subsequent nuclear translocation. Nuclear MRS then regulates transcription of Atp1 subunit of the F₁ domain of ATPase. Taken together the AME complex dissociation allows a synchronous synthesis and assembly of a functional ATPase and thus mitochondrial ATP synthesis [36].

4.2.8. *S. cerevisiae* aspartyl-tRNA-synthetase (DRS)

It was first suggested that, *in vivo*, DRS could interact with its own mRNA (mRNA^{DRS}) through the 70-amino-acid N-terminal extension that contains a lysine-rich RNA binding motif [124]. A second study by Frugier and coworkers [125] confirmed the nuclear translocation of DRS through a NLS that was shown to be located in this N-terminal extension. They proposed a mechanism by which the superfluous amount of DRS that is produced by yeast cells, enters into the nucleus and binds its own mRNA thereby inhibiting its expression and stopping further accumulation of the enzyme.

4.3. Cytoplasmic aaRSs that are targeted to the cytoplasmic membrane

4.3.1. Human lysyl-tRNA synthetase (KRS)

In most human organs, laminin is found as an extracellular matrix support for surrounding cells, which interact with laminin through membranous integrins. However, in cancer cells, laminin bound to integrin induces p38-MAPK (Mitogen Activated Protein Kinase) activation which in turn phosphorylates the threonine 52 (T52) located in the N-terminal extension of KRS. T52 phosphorylation induces a conformational change of this part of KRS that triggers its release from the MARS complex and allows its interaction with the membranous 67LR laminin receptor. This interaction occurs between the KRS N-terminal domain composed of the ABD and N-terminal extension (1–72) and the C-terminal domain of the 67LR. By doing so, KRS inhibits Nedd4-mediated ubiquitination of 67LR, enhancing laminin-dependent cell migration and cell dissemination which is considered as a marker of metastasis [126]. Kim and coworkers [127] also identified a compound (BC-KYH16899) that inhibits the KRS-dependent 67LR-mediated cell migration without affecting the aminoacylation capacity of KRS. This BC-KYH16899 compound is thus a promising molecule that could selectively inhibit cancer cells dissemination without affecting the

proteinogenic role of KRS. Finally, Nam and coworkers [128] investigated the molecular steps occurring downstream this KRS – 67LR interaction and showed that KRS-dependent cell-dissemination is done through cell-cell and cell-extracellular matrix interactions.

4.3.2. Mouse and human EPRS

In higher eukaryotes, ERS is fused to PRS by a non-catalytical linker that contains 3 WHEP repeats. This bifunctional EPRS was well characterized notably in human cells in which it participates to the MARS complex by interacting with AIMP2, KRS and DRS [30,129,130]. We already described in a preceding section the non-canonical function that EPRS exhibits in myeloid cells. However, Arif *et al.* [32] recently reported another relocation for MARS-released EPRS and a new non-translational function of this aaRS. In contrast to myeloid cells in which EPRS WHEP repeats are phosphorylated at S886 by Cdk5/p35 kinase, and at S999 by S6 kinase 1 (S6K1), in adipocytes EPRS was only shown to be phosphorylated at S999 making unclear whether S886 phosphorylation is also required in this cell type. Furthermore, contrary to mast cells, in adipocytes, the mTORC1-dependent S6K1 kinase that belongs to AGC kinases, is activated under insulin stimulation (mTORC1: mammalian Target Of Rapamycin Complex 1). Phosphorylated EPRS (at S999) interacts then with the cytoplasmic Fatty Acid Transport Protein 1 (FATP1). Formation of the EPRS-FATP1 complex is followed by its relocation to plasma membrane where it induces Long Chain Fatty Acid (LCFA) uptake. Thus, in adipocytes (but not in myeloid cells), and under insulin stimulation (but not under IFN γ stimulation), EPRS regulates adiposity and lifespan in a S6K1-dependent manner.

4.4. Yeast and human cytoplasmic aaRSs that are targeted to the vacuole and the lysosome

4.4.1. Mammalian leucyl-tRNA-synthetase (LRS)

In eukaryotes, TOR complexes (TORC) were shown to be involved in many processes such as cell growth, differentiation and metabolism, but increasing evidences suggest that its regulation is far from being fully understood. Indeed, different studies showed that amino acids and especially leucine [131–133], glutamine [133–135] and arginine [131] participate to activation of mTORC1. To be activated, mTORC1 requires a combination of Rag GTPases (component of the RAGULATOR complex) that are themselves regulated by a set of Guanine nucleotide Exchange Factors (GEFs) and GTPase-Activating Proteins (GAPs). It was suggested that LRS serves as a GAP for one of these Rag GTPases [136,137]. Beside these combinations of Rag-GTPases, mTORC1 activation at the lysosomes requires phosphatidic acid which is obtained by phospholipase D1-dependent (PLD1) hydrolysis of phosphatidylcholine. PLD1 recruitment to the lysosome is done by direct interaction with phosphatidylinositol-3P (PI3P) which is synthesized at the lysosome through the vacuolar protein sorting 34 (VPS34), a class 3 PI3-kinase which phosphorylates phosphatidylinositol and which is known to be involved in autophagy [138]. Yoon and coworkers [137] demonstrated that LRS interacts directly *via* its catalytic domain with VPS34 and activates it *via* its unique C-terminal extension called UNE-L. Furthermore, leucine binding but not tRNA binding nor tRNA aminoacylation is required for mTORC1 activation. Finally, Yoon and coworkers performed immunoprecipitation assays which suggest that this non-canonical role of LRS requires the release of the enzyme from the MARS complex and its relocation at the lysosomal surface.

4.4.2. *S. cerevisiae* leucyl-tRNA synthetase (LRS)

In the Yeast *S. cerevisiae* two TOR complexes (TORC1 and TORC2) are also found and TORC1 is regulated by GTPases. Like for mammals, LRS was shown to be involved in vacuolar TORC1 regulation but this regulation is achieved through a different mechanism than the one detailed in the previous section. In yeast, LRS interacts with one of the GTPases (Gtr1) from the EGO complex (corresponding to the

mammalian RAGULATOR) *via* its non-essential connective peptide that corresponds to the editing domain (a domain involved in non-cognate aa-tRNA hydrolysis). When a non-canonical amino-acid is charged on tRNA^L, a conformational change occurs that disrupts the LRS-Gtr1 interaction and inhibits vacuolar TORC1. Bonfils and coworkers [139] proposed that in *S.cerevisiae*, LRS serves as GAP for Gtr1 GTPase and thus participates to the inactivation of TORC1.

4.5. Cytoplasmic aaRS that are targeted outside the cell

Many aaRSs were reported to be targeted/secreted outside the intracellular space. In the present section we decided to describe aaRSs that are either incorporated into viruses or secreted. For secreted aaRSs, we describe those which are secreted to the intercellular space *via* the Multi Vesicular Body MVB/exosome pathway, *via* the Endoplasmic Reticulum RE/Golgi pathway or *via* a yet unidentified pathway. Finally, we mention the aaRSs that have been found in the human serum.

4.5.1. Human KRS is encapsidated into HIV virions

During HIV1 infection, a key step for viral replication is the reverse transcription (RT) of the genomic RNA. This step requires a primer which has been shown to be the human tRNA^{Lys3} (tRK3). Cen and coworkers [140] showed that, in addition to tRK3, the human KRS is also encapsidated into HIV1 particles by interacting with the viral Gag precursor. Whereas other studies [141–143] brought evidences that tRK3 incorporation is regulated by KRS, Liu and coworkers [Anticodon-like binding of the HIV-1 tRNA-like element to human lysyl-tRNA synthetase] investigated the interaction of LysRS with the viral genome. Furthermore Dewan et al. [144] demonstrated that the H7 helix located in the class II motif 1 of human KRS, and which is responsible for KRS dimerization, is also responsible for the interaction with HIV1 Gag protein.

As mentioned in a previous section (Section 4.2.1), a very recent study [145] investigated further the implication of KRS after HIV1 infection in human cells. This study shows that following HIV1 infection, phosphorylated KRS (S207P) is released from the MSC and translocates into the nucleus. Like in mast cells, phosphorylated KRS is deprived of its capacity to aminoacylate its cognate tRNA but retains its ability to bind the tRNA. Although nuclear LysRS function was not yet clearly established, this study strongly suggests that translocation into the nucleus of the phosphorylated LysRS-tRK3 complex *i)* occurs before the reverse transcription of HIV1 genome and *ii)* is important for tRK3 packaging and for HIV1 infectivity. Finally, in agreement with the previously described EPRS antiviral function (Section 4.1.2), Duchon and coworkers could detect a low amount of released EPRS upon HIV1 infection.

4.5.2. Human WRS is encapsidated into Rous sarcoma virus (RSV)

In the previous paragraph, we reported that KRS and the tRK3 are incorporated into HIV1 particles. Cen and coworkers [146] described a similar situation concerning the Rous sarcoma virus, except that tRNA^W is used as primer for reverse transcription of the viral genomic RNA. Like for HIV1 the aaRS homologous to the tRNA species used as a primer, in this case human WRS, is also encapsidated. Interestingly, the Moloney Murine Leukemia Virus that uses tRNA^P as primer for reverse transcription of its genomic RNA, does not encapsidate the cognate PRS into the viral particles. The reason why certain viruses encapsidate a given aaRS alone or together with its cognate tRNA, has so far, not been ruled out.

4.5.3. Human KRS is secreted via exosomes

Park and coworkers [147] showed that under starvation and stimulation by Tumor Necrosis Factor α (TNF α), the human KRS can be secreted from human cells and interacts with macrophages to induce their TNF α secretion and cell migration. However, the KRS secretion pathway and its detailed molecular steps remained unclear until

recently. Kim and coworkers [148] showed that, during evolution human KRS inherited a unique N-terminal extension which harbors a Caspase 8-specific cleavage site, and a C-terminal PDZ-binding domain. Whereas many proteins that harbor a localization signal are secreted by the ER-Golgi pathway, the human KRS interacts *via* its PDZ-binding domain to syntenin which guides KRS from the MARS complex into exosomes and more precisely in their lumen, prior to its release from the cell. Note that this KRS-syntenin interaction had already been suggested previously by Meershaert and coworkers [149] and Baietti and coworkers [150]. Kim and coworkers also showed the importance of the N-terminal caspase 8-specific cleavage site in this KRS secretion pathway and proposed a mechanism in agreement with the published 3D structure of KRS [107]; KRS is a class II aaRS that forms homodimers in which the caspase 8 cleavage site that is located in the N-terminal extension of one of the monomers masks the syntenin interaction site located in the C-terminal domain from the second monomer, thus inhibiting exosomal KRS secretion. Under starvation conditions, Caspase 8 cleaves the KRS N-terminal domain which allows KRS-syntenin interaction and subsequent incorporation of the enzyme into exosomes.

4.5.4. From insect to vertebrates, the balance between mini-YRS and -WRS regulates angiogenesis

We already reported in the previous sections that nuclear imported WRS, SRS and TRS are important angiogenesis regulators. However, secreted forms of YRS and WRS are also key players of angiogenesis regulation. In comparison to prokaryotic YRS, insect and vertebrates YRS have inherited an C-terminal Endothelial-monocyte-activating polypeptide II (EMAPII) like domain that can be cleaved by extracellular proteases (elastases) from the remaining core of YRS called “mini-YRS” [151]. This mini-YRS has similarities with the CXC chemotactic factor interleukin 8 (IL8), in particular with the ELR motif (Glu-Leu-Arg) harbored by pro-angiogenic chemokines. The evolutionary close WRS can similarly be cleaved into a “mini-WRS” (where translation starts at M48 due to alternative splicing or extracellular cleavage inside the WHEP domain) but the cleaved product doesn't harbor the ELR motif. As such, it was shown that in endothelial cells (HUVEC) and in polymorphonuclear leukocytes (PMN), extracellular mini-YRS induces cell migration and angiogenesis [152], whereas extracellular WRS has opposite effects [153,154]. Extracellular mini-YRS is increased through TNF α secretion and in endothelial cells mini YRS induces phosphorylation of Src, Akt, ERK (Extracellular Signal Regulated Kinase), and VEGF-receptor 2, required for angiogenesis [155,156]. Because IL8 is known to act on the CXCR1/2 receptor, My-Nuong Vo et al., [157] verified whether this is also the case for mini-YRS. This study showed, that under low mini-YRS secreted concentrations, mini-YRS is monomeric and induces cell migration *via* CXCR1/2 whereas under high mini-YRS secreted concentrations, mini-YRS is dimeric and inhibits cell migration (antagonistic effect). On the other hand, mini-WRS exerts its angiostatic activity by binding the first extracellular (EC1) domain of VE-cadherin (vascular endothelial cadherin). Recent studies [158,159] showed that mini-WRS K153 residue binds VE-cadherin and that VE-cadherin residues W2 and W4 are docked into the empty W-AMP pocket. Through this interaction, *i)* VE-cadherin interaction with activated VEGF receptor 2 (VEGFR2) is disrupted and *ii)* the subsequent activation of Akt that, in the absence of mini-WRS leads to angiogenesis, is inhibited [160,161]. However, the mechanism by which VEGFR2 is activated by mini-YRS remains unclear and Zeng et al. [162] in human umbilical vein endothelial cells in hypoxia suggested a yet unknown trans-activation mechanism. Thus, mini-WRS and mini-YRS cytokine-like antagonistic effects belongs to a pathway that fine tunes cell migration and angiogenesis.

4.5.5. From insect to vertebrates, YRS EMAPII-like domain

Compared to their prokaryotic homologs, insects and vertebrates YRSs inherited an additional C-terminal EMAPII-like domain. When YRS is secreted, this domain is cleaved by extracellular elastases from the

remaining “mini-YRS”. This cleavage occurs during the apoptotic state and the EMAPII-like peptide will exert 2 different functions *i*) it carries chemo-attractive capacities which allows the recruitment of phagocytes to the apoptotic site and phagocytosis in order to prevent damages for surrounding cells; and *ii*) it induces TNF α secretion by leucocytes [151,153,163]. Finally, it was suggested that in the full-length YRS, EMAPII-like blocks IL-8 proangiogenic activity by preventing its recognition by IL8 receptor.

4.5.6. Secreted human full-length WRS (but not the mini-WRS) induces early innate immune response

Human WRS contains a unique 154 aa-long N-terminal domain that includes a WHEP domain (residues 8–64). Recently Ahn and coworkers [164] discovered a new function for the full-length WRS (FL-WRS) but not for the mini-WRS that we described previously. They showed that early after infection by pathogens, FL-WRS is secreted from monocytes and interacts with macrophages to induce innate immune stimulation (phagocytosis and cytokine production). Based on the available WRS crystal structure, Ahn *et al.* showed that in order to activate this type of immune response, FL-WRS binds to Toll-Like-Receptor 4 (TLR4) - MD2 complexes and probably also to TLR2 *via* its N-terminal extension. Finally, binding and activation was also showed with the 154 aa-long N-terminal domain alone.

4.5.7. Secreted human TRS regulates also angiogenesis

Similar to the above-mentioned mini-YRS angiogenic function, human TRS is also secreted under TNF α or VEGF stimulation and induces endothelial cell migration. However, it has not been elucidated if TRS cleavage or posttranslational modification is necessary for this non-canonical function [165]. Furthermore, Wellman and coworkers [166] found a link between stress-induced overexpression of TRS, angiogenesis and ovarian cancer.

4.5.8. *Brugia malayi* asparaginyl-tRNA-synthetase (NRS)

Brugia malayi is a filarial nematode which is a human parasite responsible for filariasis that causes chronic infections and elephantiasis. *Brugia malayi* NRS (BmNRS) is secreted from this intravascular worm parasite into patient's serum [167,168] and acts as immunodominant antigen. BmNRS presents a 110 aa-long N-terminal extension (compared to prokaryotic NRSs) that harbors a 80-long IL8-like domain. Different studies demonstrated that BmNRS induces several physiological responses *via* binding to 2 different types of receptors: IL8 CXCR1/2 receptors and purine receptors [168–172]. Recently Jothi and coworkers added to this list: endothelial cell proliferation, migration, ring and tube formation, vasodilation and angiogenesis which are also usually induced by VEGF.

4.5.9. Mouse and human glycyl-tRNA-synthetase GRS

Concerning GRS, Park and coworkers [173] recently showed that Fas-ligand secreted from cancer cells induces GRS secretion which can then circulate in the serum. Normally, phosphatase 2 (PP2A)-dependent ERK inhibition is blocked by its interaction to the membrane protein cadherin 6 (CDH6). However, binding of GRS to CDH6 *via* its extracellular domain, releases PP2A which inhibits ERK and provokes tumor cell death. Furthermore, this study provides *in vivo* data (mouse models) on GRS-mediated antitumor effects and suggests that this aaRS, by having this cytokine-like function, is a key player in an endogenous tumor surveillance mechanism. Finally, the mechanism by which GRS is secreted remains so far unknown, but He and coworkers [174] suggested that GRS is secreted by the exosomal pathway.

5. Concluding remarks

As described herein, the functional plasticity of relocating cytosolic aaRS is really remarkable for enzymes once considered to be restricted to the production of the ribosomes' aa-tRNA substrates. However, the

repertoire of nontranslational functions carried by these enzymes is probably even greater, especially in human, if one considers all the possible isoforms that that have been predicted to be produced by alternative splicing or initiation of translation [175]. The majority of these splice variants are catalytic nulls meaning that the alternative splicing event partially or entirely removed the functional parts responsible for aa-tRNA synthesis, leaving, usually, only domains that were added to the aaRS core in the course of evolution. These pieces of aaRSs have been found to have a tissue-specific expression profile and do not contribute or participate to the aminoacylation reaction. However, a strong selection pressure led to their conservation throughout evolution most probably because they exert a specific biological function that has nothing to do with protein synthesis but nevertheless equally essential. When tested in cell-based assay designed to check their involvement in cytoprotection, immunomodulation, acute inflammatory response, transcriptional regulation, regenerative responses, cell differentiation and cholesterol transport, almost 90% of these catalytically null pieces of aaRSs where shown to exert at least one specific biological activity. Given the type of physiological role they might be playing and their tissue-specific expression one can easily imagine that malfunctioning of their functions or a change in their expression will very likely be associated with diseases. Indeed, it has already been shown that malfunctioning of the nontranslational functions that cytosolic relocating aaRSs exert, triggers a wide spectrum of diseases in human [31,34]. The pathologies to which these aaRSs have been connected to, include for example *i*) neuronal syndromes like type-2 Charcot Mary Tooth [174,176–178] and Amyotrophic Lateral Sclerosis [179], *ii*) susceptibility to cancers [180–182], diabetes [183,184] or other abnormal metabolic conditions [32] and *iii*) autoimmune disorders [185–189]. The latter example is particularly interesting since auto-antibodies against 9 cytosolic aaRSs have been found in patients with autoimmune disorders among which inflammatory myopathies, interstitial lung diseases and rheumatic arthritis [190,191]. Despite a growing number of reports describing the clinical features of these subtypes of autoimmune diseases also called the “antisynthetase syndrome” the physiological conditions and molecular mechanism by which these aaRSs become an antigen are still unknown.

Transparency document

The <http://dx.doi.org/10.1016/j.bbagr.2017.11.004> associated with this article can be found, in online version.

Acknowledgements

The work was supported by the French National Program Investissement d'Avenir administered by the “Agence National de la Recherche” (ANR), “MitoCross” Laboratory of Excellence (Labex), funded as ANR-10-IDEX-0002-02 (to H.D.B), the University of Strasbourg (H.D.B, F.F, N.Y, G.B), the CNRS (B.S), the Ministère de l'Education Nationale, de la Recherche et de l'Enseignement Supérieur (N.Y, S.D), the Fondation Pour la Recherche Médicale (FRM DBF20160635713) (H.D.B, F.F, B.S, N.Y).

References

- [1] M. Ibba, D. Söll, Aminoacyl-tRNA synthesis, *Annu. Rev. Biochem.* 69 (2000) 617–650.
- [2] A. Chaliotis, P. Vlastaridis, D. Mossialos, M. Ibba, H.D. Becker, C. Stathopoulos, G.D. Amoutzias, The complex evolutionary history of aminoacyl-tRNA synthetases, *Nucleic Acids Res.* 45 (2017) 1059–1068.
- [3] A.-M. Duchêne, A. Giritich, B. Hoffmann, V. Cognat, D. Lancelin, N.M. Peeters, M. Zaeffel, L. Maréchal-Drouard, I.D. Small, Dual targeting is the rule for organellar aminoacyl-tRNA synthetases in *Arabidopsis thaliana*, *Proc. Natl. Acad. Sci. U. S. A.* 102 (2005) 16484–16489.
- [4] M. Wilcox, M. Nirenberg, Transfer RNA as a cofactor coupling amino acid synthesis with that of protein, *Proc. Natl. Acad. Sci. U. S. A.* 61 (1968) 229–236.
- [5] A. Schön, C.G. Kannangara, S. Cough, D. Söll, Protein biosynthesis in organelles

- requires misaminoacylation of tRNA, *Nature* 331 (1988) 187–190.
- [6] M. Frechin, B. Senger, M. Braye, D. Kern, R.P. Martin, H.D. Becker, Yeast mitochondrial Gln-tRNA^{Gln} is generated by a GatFAB-mediated transamidation pathway involving Arc1p-controlled subcellular sorting of cytosolic GluRS, *Genes Dev.* 23 (2009) 1119–1130.
- [7] K. Sheppard, J. Yuan, M.J. Hohn, B. Jester, K.M. Devine, D. Söll, From one amino acid to another: tRNA-dependent amino acid biosynthesis, *Nucleic Acids Res.* 36 (2008) 1813–1825.
- [8] M. Frechin, A.-M. Duchêne, H.D. Becker, Translating organellar glutamine codons: a case by case scenario? *RNA Biol.* 6 (2009) 31–34.
- [9] T.M. Henkin, B.L. Glass, F.J. Grundy, Analysis of the *Bacillus subtilis* tyrS gene: conservation of a regulatory sequence in multiple tRNA synthetase genes, *J. Bacteriol.* 174 (1992) 1299–1306.
- [10] J. Gilbert, C.R. Perry, B. Slocombe, High-level mupirocin resistance in *Staphylococcus aureus*: evidence for two distinct isoleucyl-tRNA synthetases, *Antimicrob. Agents Chemother.* 37 (1993) 32–38.
- [11] A. Brevet, J. Chen, F. Lévêque, S. Blanquet, P. Plateau, Comparison of the enzymatic properties of the two *Escherichia coli* lysyl-tRNA synthetase species, *J. Biol. Chem.* 270 (1995) 14439–14444.
- [12] H.D. Becker, J. Reinbolt, R. Kreutzer, R. Giegé, D. Kern, Existence of two distinct aspartyl-tRNA synthetases in *Thermus thermophilus*. Structural and biochemical properties of the two enzymes, *Biochemistry* 36 (29) (1997) 8785–8797.
- [13] S. Skouloubris, L. Ribas de Pouplana, H. De Reuse, T.L. Hendrickson, A noncognate aminoacyl-tRNA synthetase that may resolve a missing link in protein evolution, *Proc. Natl. Acad. Sci. U. S. A.* 100 (2003) 11297–11302.
- [14] M.Á. Rubio, M. Napolitano, J.A.G. Ochoa de Alda, J. Santamaría-Gómez, C.J. Patterson, A.W. Foster, R. Bru-Martínez, N.J. Robinson, I. Luque, Trans-oligomerization of duplicated aminoacyl-tRNA synthetases maintains genetic code fidelity under stress, *Nucleic Acids Res.* 43 (2015) 9905–9917.
- [15] J.L. Huot, L. Enkler, C. Megel, L. Karim, D. Laporte, H.D. Becker, A.-M. Duchêne, M. Sissler, L. Maréchal-Drouard, Idiosyncrasies in decoding mitochondrial genomes, *Biochimie* 100 (2014) 95–106.
- [16] C. Pujol, M. Bailly, D. Kern, L. Marechal-Drouard, H. Becker, A.-M. Duchene, Dual targeted tRNA-dependent amidotransferase ensures both mitochondrial and chloroplastic Gln-tRNA^{Gln} synthesis in plants, *Proc. Natl. Acad. Sci.* 105 (2008) 6481–6485.
- [17] A. Nagao, T. Suzuki, T. Katoh, Y. Sakaguchi, T. Suzuki, Biogenesis of glutamyl-mt tRNA^{Gln} in human mitochondria, *Proc. Natl. Acad. Sci.* 106 (2009) 16209–16214.
- [18] S. Debard, G. Bader, J.-O. De Craene, L. Enkler, S. Bär, D. Laporte, P. Hammann, E. Myslinski, B. Senger, S. Friant, H.D. Becker, Nonconventional localizations of cytosolic aminoacyl-tRNA synthetases in yeast and human cells, *Methods* 113 (2016) 91–104.
- [19] A.M. Duchêne, N. Peeters, A. Dietrich, A. Cosset, I.D. Small, H. Wintz, Overlapping destinations for two dual targeted glycylyl-tRNA synthetases in *Arabidopsis thaliana* and *Phaseolus vulgaris*, *J. Biol. Chem.* 276 (2001) 15275–15283.
- [20] E.G.A.K. Berglund, C. Pujol, A.M. Duchêne, Defining the determinants for dual targeting of amino acyl-tRNA synthetases to mitochondria and chloroplasts, *J. Mol. Biol.* 393 (2009) 803–814.
- [21] A.K. Bandyopadhyay, M.P. Deutscher, Complex of aminoacyl-transfer RNA synthetases, *J. Mol. Biol.* 60 (1971) 113–122.
- [22] G. Simos, A. Segref, F. Fasiolo, K. Hellmuth, A. Shevchenko, M. Mann, E.C. Hurt, The yeast protein Arc1p binds to tRNA and functions as a cofactor for the methionyl- and glutamyl-tRNA synthetases, *EMBO J.* 15 (1996) 5437–5448.
- [23] S. Havrylenko, R. Legouis, B. Negruksii, M. Mirande, *Caenorhabditis elegans* evolves a new architecture for the multi-aminoacyl-tRNA synthetase complex, *J. Biol. Chem.* 286 (2011) 28476–28487.
- [24] J.M. van Rooyen, J.-B. Murat, P.-M. Hammoudi, S. Kieffer-Jaquinod, Y. Coute, A. Sharma, H. Pelloux, H. Belrhali, M.-A. Hakimi, Assembly of the novel five-component apicomplexan multi-aminoacyl-tRNA synthetase complex is driven by the hybrid scaffold protein Tg-p43, *PLoS One* 9 (2014) e89487.
- [25] D. Laporte, J.L. Huot, G. Bader, L. Enkler, B. Senger, H.D. Becker, Exploring the evolutionary diversity and assembly modes of multi-aminoacyl-tRNA synthetase complexes: lessons from unicellular organisms, *FEBS Lett.* 588 (2014) 4268–4278.
- [26] M. Frechin, D. Kern, R.P. Martin, H.D. Becker, B. Senger, Arc1p: anchoring, routing, coordinating, *FEBS Lett.* 584 (2010) 427–433.
- [27] P.S. Ray, A. Arif, P.L. Fox, Macromolecular complexes as depots for releasable regulatory proteins, *Trends Biochem. Sci.* 32 (2007) 158–164.
- [28] M. Guo, X.-L. Yang, P. Schimmel, New functions of aminoacyl-tRNA synthetases beyond translation, *Nat. Rev. Mol. Cell Biol.* 11 (2010) 668–674.
- [29] M. Guo, X.-L. Yang, Architecture and metamorphosis, *Top. Curr. Chem.* 344 (2014) 89–118.
- [30] M. Guo, P. Schimmel, Essential nontranslational functions of tRNA synthetases, *Nat. Chem. Biol.* 9 (2013) 145–153.
- [31] S.G. Park, P. Schimmel, S. Kim, Aminoacyl tRNA synthetases and their connections to disease, *Proc. Natl. Acad. Sci. U. S. A.* 105 (2008) 11043–11049.
- [32] A. Arif, F. Terenzi, A.A. Potdar, J. Jia, J. Sacks, A. China, D. Halawani, K. Vasu, X. Li, J.M. Brown, J. Chen, S.C. Kozma, G. Thomas, P.L. Fox, EPRS is a critical mTORC1–S6K1 effector that influences adiposity in mice, *Nature* 542 (2017) 357–361.
- [33] M. Sajish, P. Schimmel, A human tRNA synthetase is a potent PARP1-activating effector target for resveratrol, *Nature* 519 (2014) 370.
- [34] P. Yao, P.L. Fox, Aminoacyl-tRNA synthetases in medicine and disease, *EMBO Mol. Med.* 5 (2013) 332–343.
- [35] A. Arif, J. Jia, R. Mukhopadhyay, B. Willard, M. Kinter, P.L. Fox, Two-site phosphorylation of EPRS coordinates multimodal regulation of noncanonical translational control activity, *Mol. Cell* 35 (2009) 164–180.
- [36] M. Frechin, L. Enkler, E. Tetaud, D. Laporte, B. Senger, C. Blancard, P. Hammann, G. Bader, S. Clauder-Münster, L.M. Steinmetz, R.P. Martin, J.-P. di Rago, H.D. Becker, Expression of nuclear and mitochondrial genes encoding ATP synthase is synchronized by disassembly of a multisynthetase complex, *Mol. Cell* 56 (2014) 763–776.
- [37] I.M. López-Lara, O. Geiger, Bacterial lipid diversity, *Biochim. Biophys. Acta* 1862 (2016) 1287–1299.
- [38] A. Caforio, A.J.M. Driessen, Archaeal phospholipids: structural properties and biosynthesis, *Biochim. Biophys. Acta* 1862 (2016) 1325–1339.
- [39] M. Rajagopal, S. Walker, Envelope structures of gram-positive bacteria, *Curr. Top. Microbiol. Immunol.*, Springer, Cham, 404 2015, pp. 1–44, http://dx.doi.org/10.1007/82_2015_5021.
- [40] J.C. Henderson, S.M. Zimmerman, A.A. Crofts, J.M. Boll, L.G. Kuhns, C.M. Herrera, M.S. Trent, The power of asymmetry: architecture and assembly of the gram-negative outer membrane lipid bilayer, *Annu. Rev. Microbiol.* 70 (2016) 255–278.
- [41] S.-V. Albers, B.H. Meyer, The archaeal cell envelope, *Nat. Rev. Microbiol.* 9 (2011) 414–426.
- [42] A. Peschel, H.-G. Sahl, The co-evolution of host cationic antimicrobial peptides and microbial resistance, *Nat. Rev. Microbiol.* 4 (2006) 529–536.
- [43] K.L. Nawrocki, E.K. Crispell, S.M. McBride, Antimicrobial peptide resistance mechanisms of gram-positive bacteria, *Antibiot. (Basel, Switzerland)* 3 (2014) 461–492.
- [44] V.I. Band, D.S. Weiss, Mechanisms of antimicrobial peptide resistance in gram-negative bacteria, *Antibiot. (Basel, Switzerland)* 4 (2015) 18–41.
- [45] R.N. Fields, H. Roy, Deciphering the tRNA-dependent lipid aminoacylation systems in bacteria: novel components and structural advances, *RNA Biol.* (2017) 1–12, <http://dx.doi.org/10.1080/15476286.2017.1356980> [Epub ahead of print].
- [46] C. Slavetinsky, S. Kuhn, A. Peschel, Bacterial aminoacyl phospholipids – biosynthesis and role in basic cellular processes and pathogenicity, *Biochim. Biophys. Acta* 1862 (2016) 1310–1318.
- [47] E. Maloney, D. Stankowska, J. Zhang, M. Fol, Q.-J. Cheng, S. Lun, W.R. Bishai, M. Rajagopalan, D. Chatterjee, M.V. Madiraju, The two-domain LysX protein of *Mycobacterium tuberculosis* is required for production of lysinylated phosphatidylglycerol and resistance to cationic antimicrobial peptides, *PLoS Pathog.* 5 (7) (2009) e1000534.
- [48] M. Mirande, The aminoacyl-tRNA synthetase complex, *Subcell. Biochem.* 83 (2017) 505–522.
- [49] E. Maloney, S. Lun, D. Stankowska, H. Guo, M. Rajagopalan, W.R. Bishai, M.V. Madiraju, Alterations in phospholipid catabolism in *Mycobacterium tuberculosis* lysX mutant, *Front. Microbiol.* 2 (2011) 19.
- [50] K.M. Frain, D. Ganj, A. Jones, J.A.Z. Zedler, C. Robinson, Protein translocation and thylakoid biogenesis in cyanobacteria, *BBA-Bioenergetics* 1857 (2016) 266–273.
- [51] J. Nickelsen, W. Zerges, Thylakoid biogenesis has joined the new era of bacterial cell biology, *Front. Plant Sci.* 4 (2013) 458.
- [52] J. Santamaría-Gómez, J.A.G. Ochoa de Alda, E. Olmedo-Verd, R. Bru-Martínez, I. Luque, Sub-cellular localization and complex formation by aminoacyl-tRNA synthetases in cyanobacteria: evidence for interaction of membrane-anchored ValRS with ATP synthase, *Front. Microbiol.* 7 (2016) 857.
- [53] I. Luque, J.A. Ochoa de Alda, CURT1, CAAD-containing aarRS, thylakoid curvature and gene translation, *Trends Plant Sci.* 19 (2014) 63–66.
- [54] E. Olmedo-Verd, J. Santamaría-Gómez, J.A.G. Ochoa de Alda, L. Ribas de Pouplana, I. Luque, Membrane anchoring of aminoacyl-tRNA synthetases by convergent acquisition of a novel protein domain, *J. Biol. Chem.* 286 (2011) 41057–41068.
- [55] L. Dimitrijevic, Intracellular localization of yeast (*Saccharomyces cerevisiae*) lysyl-tRNA synthetase, *FEBS Lett.* 79 (1977) 37–41.
- [56] T. Ohira, T. Suzuki, Precursors of tRNAs are stabilized by methylguanosine cap structures, *Nat. Chem. Biol.* 12 (2016) 648–655.
- [57] J.D. Aitchison, M.P. Rout, The yeast nuclear pore complex and transport through it, *Genetics* 190 (2012) 855–883.
- [58] M. Zaslloff, tRNA transport from the nucleus in a eukaryotic cell: carrier-mediated translocation process, *Proc. Natl. Acad. Sci. U. S. A.* 80 (1983) 6436–6440.
- [59] M. Mirande, D. Le Corre, D. Louvard, H. Reggio, J.-P. Pailliez, J.-P. Waller, Association of an aminoacyl-tRNA synthetase complex and of phenylalanyl-tRNA synthetase with the cytoskeletal framework fraction from mammalian cells, *Exp. Cell Res.* 156 (1985) 91–102.
- [60] E. Lund, J.E. Dahlberg, Proofreading and aminoacylation of tRNAs before export from the nucleus, *Science* 282 (1998) 2082–2085.
- [61] S. Sarkar, A.K. Azad, A.K. Hopper, Nuclear tRNA aminoacylation and its role in nuclear export of endogenous tRNAs in *Saccharomyces cerevisiae*, *Proc. Natl. Acad. Sci. U. S. A.* 96 (1999) 14366–14371.
- [62] P. Schimmel, C.-C. Wang, Getting tRNA synthetases into the nucleus, *Trends Biochem. Sci.* 24 (1999) 127–128.
- [63] A.K. Azad, D.R. Stanford, S. Sarkar, A.K. Hopper, Role of nuclear pools of aminoacyl-tRNA synthetases in tRNA nuclear export, *Mol. Biol. Cell* 12 (2001) 1381–1392.
- [64] M. Steiner-Mosonyi, D. Mangroo, The nuclear tRNA aminoacylation-dependent pathway may be the principal route used to export tRNA from the nucleus in *Saccharomyces cerevisiae*, *Biochem. J.* 378 (2004) 809–816.
- [65] H. Grosshans, E. Hurt, G. Simos, An aminoacylation-dependent nuclear tRNA export pathway in yeast, *Genes Dev.* 14 (2000) 830–840.
- [66] K. Rothbarth, D. Werner, Amino-acid-transfer reactions in isolated nuclei of Ehrlich ascites tumor cells, *Eur. J. Biochem.* 155 (1986) 149–156.
- [67] L. Nathanson, M.P. Deutscher, Active aminoacyl-tRNA synthetases are present in

- nuclei as a high molecular weight multienzyme complex, *J. Biol. Chem.* 275 (2000) 31559–31562.
- [68] C.L. Wolfe, J.A. Warrington, S. Davis, S. Green, M.T. Norcum, Isolation and characterization of human nuclear and cytosolic multisynthetase complexes and the intracellular distribution of p43/EMAPII, *Protein Sci.* 12 (2003) 2282–2290.
- [69] M. Christie, C.-W. Chang, G. Róna, K.M. Smith, A.G. Stewart, A.A.S. Takeda, M.R.M. Fontes, M. Stewart, B.G. Vértessy, J.K. Forwood, B. Kobe, Structural biology and regulation of protein import into the nucleus, *J. Mol. Biol.* 428 (2016) 2060–2090.
- [70] C.R. Woese, G.J. Olsen, M. Ibba, D. Söll, Aminoacyl-tRNA synthetases, the genetic code, and the evolutionary process, *Microbiol. Mol. Biol. Rev.* 64 (2000) 202–236.
- [71] B. Brindefalk, J. Viklund, D. Larsson, M. Thollesson, S.G.E. Andersson, Origin and evolution of the mitochondrial aminoacyl-tRNA synthetases, *Mol. Biol. Evol.* 24 (2007) 743–756.
- [72] D. Diodato, D. Ghezzi, V. Tiranti, The mitochondrial aminoacyl tRNA synthetases: genes and syndromes, *Int. J. Cell Biol.* 2014 (2014) 787956.
- [73] M. Sissler, L.E. González-Serrano, E. Westhof, Recent advances in mitochondrial aminoacyl-tRNA synthetases and disease, *Trends Mol. Med.* 23 (2017) 693–708.
- [74] E. Tolkunova, H. Park, J. Xia, M.P. King, E. Davidson, The human lysyl-tRNA synthetase gene encodes both the cytoplasmic and mitochondrial enzymes by means of an unusual alternative splicing of the primary transcript, *J. Biol. Chem.* 275 (2000) 35063–35069.
- [75] J. Alexandrova, C. Paulus, J. Rudinger-Thirion, F. Jossinet, M. Frugier, Elaborate uORF/IREs features control expression and localization of human glycyl-tRNA synthetase, *RNA Biol.* 12 (2015) 1301–1313.
- [76] G. Natsoulis, F. Hilger, G.R. Fink, The HTS1 gene encodes both the cytoplasmic and mitochondrial histidine tRNA synthetases of *S. cerevisiae*, *Cell* 46 (1986) 235–243.
- [77] B. Chatton, P. Walter, J.P. Ebel, F. Lacroute, F. Fasiolo, The yeast VAS1 gene encodes both mitochondrial and cytoplasmic valyl-tRNA synthetases, *J. Biol. Chem.* 263 (1988) 52–57.
- [78] H.-L. Tang, L.-S. Yeh, N.-K. Chen, T. Ripmaster, P. Schimmel, C.-C. Wang, Translation of a yeast mitochondrial tRNA synthetase initiated at redundant non-AUG codons, *J. Biol. Chem.* 279 (2004) 49656–49663.
- [79] G. Souciet, B. Menand, J. Ovesna, A. Cosset, A. Dietrich, H. Wintz, Characterization of two bifunctional Arabidopsis thaliana genes coding for mitochondrial and cytosolic forms of valyl-tRNA synthetase and threonyl-tRNA synthetase by alternative use of two in-frame AUGs, *FEBS J.* 266 (1999) 848–854.
- [80] K.G. Saman Habib, Suniti Vaishya, Translation in organelles of apicomplexan parasites, *Trends Parasitol.* 32 (2016) 939–952.
- [81] K. Galani, H. Grosshans, K. Deinert, E.C. Hurt, G. Simos, The intracellular location of two aminoacyl-tRNA synthetases depends on complex formation with Arc1p, *EMBO J.* 20 (2001) 6889–6898.
- [82] P.S. Ray, P.L. Fox, Origin and evolution of glutamyl-prolyl tRNA Synthetase WHEP domains reveal evolutionary relationships within holozoa, *PLoS One* 9 (2014) e98493.
- [83] A. Arif, J. Jia, R.A. Moodt, P.E. DiCorleto, P.L. Fox, Phosphorylation of glutamyl-prolyl tRNA synthetase by cyclin-dependent kinase 5 dictates transcript-selective translational control, *Proc. Natl. Acad. Sci. U. S. A.* 108 (2011) 1415–1420.
- [84] P. Sampath, B. Mazumder, V. Seshadri, P.L. Fox, Transcript-selective translational silencing by gamma interferon is directed by a novel structural element in the ceruloplasmin mRNA 3' untranslated region, *Mol. Cell. Biol.* 23 (2003) 1509–1519.
- [85] P. Sampath, B. Mazumder, V. Seshadri, C.A. Gerber, L. Chavatte, M. Kinter, S.M. Ting, J.D. Dignam, S. Kim, D.M. Driscoll, P.L. Fox, Noncanonical function of glutamyl-prolyl-tRNA synthetase: gene-specific silencing of translation, *Cell* 119 (2004) 195–208.
- [86] J. Jia, A. Arif, P.S. Ray, P.L. Fox, WHEP domains direct noncanonical function of glutamyl-prolyl tRNA synthetase in translational control of gene expression, *Mol. Cell* 29 (2008) 679–690.
- [87] P. Yao, A.A. Potdar, A. Arif, P.S. Ray, R. Mukhopadhyay, B. Willard, Y. Xu, J. Yan, G.M. Sidel, P.L. Fox, Coding region polyadenylation generates a truncated tRNA synthetase that counters translation repression, *Cell* 149 (2012) 88–100.
- [88] E.-Y. Lee, H.-C. Lee, H.-K. Kim, S.Y. Jang, S.-J. Park, Y.-H. Kim, J.H. Kim, J. Hwang, J.-H. Kim, T.-H. Kim, A. Arif, S.-Y. Kim, Y.-K. Choi, C. Lee, C.-H. Lee, J.U. Jung, P.L. Fox, S. Kim, J.-S. Lee, M.H. Kim, Infection-specific phosphorylation of glutamyl-prolyl tRNA synthetase induces antiviral immunity, *Nat. Immunol.* 17 (2016) 1252–1262.
- [89] E. Pahuski, M. Klekamp, T. Condon, A.E. Hampel, Altered aminoacyl-tRNA synthetase complexes in CHO cell mutants, *J. Cell. Physiol.* 114 (1983) 82–87.
- [90] Y.G. Ko, E.Y. Kim, T. Kim, H. Park, H.S. Park, E.J. Choi, S. Kim, Glutamine-dependent antiapoptotic interaction of human glutamyl-tRNA synthetase with apoptosis signal-regulating kinase 1, *J. Biol. Chem.* 276 (2001) 6030–6036.
- [91] I.-S. Hwang, Y.-S. Jung, E. Kim, Interaction of ALG-2 with ASK1 influences ASK1 localization and subsequent JNK activation, *FEBS Lett.* 529 (2002) 183–187.
- [92] Y. Shao, Y. Huang, Z. Liu, X. Guo, S. Jiang, Z. Sun, Q. Ruan, Human cytomegalovirus-encoded miR-US4-1 promotes cell apoptosis and benefits discharge of infectious virus particles by targeting QARS, *J. Biosci.* 41 (2016) 183–192.
- [93] M. Lazard, M. Mirande, Cloning and analysis of a cDNA encoding mammalian arginyl-tRNA synthetase, a component of the multisynthetase complex with a hydrophobic N-terminal extension, *Gene* 132 (1993) 237–245.
- [94] A.A. Girjes, K. Hobson, P. Chen, M.F. Lavin, Cloning and characterization of cDNA encoding a human arginyl-tRNA synthetase, *Gene* 164 (1995).
- [95] Y.-G. Zheng, H. Wei, C. Ling, M.-G. Xu, E.-D. Wang, Two forms of human cytoplasmic arginyl-tRNA synthetase produced from two translation initiations by a single mRNA, *Biochemistry* 45 (2006) 1338–1344.
- [96] M.P. Deutscher, R. Chang Ni, Purification of a low molecular weight form of rat liver arginyl-tRNA synthetase, *J. Biol. Chem.* 257 (1982) 6003–6006.
- [97] G. Vellekamp, R.K. Sihags, M.P. Deutscher, Comparison of the complexed and free forms of rat liver arginyl-tRNA synthetase and origin of the free form, *J. Biol. Chem.* 260 (1985) 9843–9847.
- [98] J.-P.W. Beyazit Cirakoglu, Multiple forms of arginyl- and lysyl-tRNA synthetases in rat liver: a re-evaluation, *Biochim. Biophys. Acta Protein Struct. Mol. Enzymol.* 829 (1985) 173–179.
- [99] M. Lazard, P. Kerjan, F. Agou, M. Mirande, The tRNA-dependent activation of arginine by arginyl-tRNA synthetase requires inter-domain communication, *J. Mol. Biol.* 302 (2000) 991–1004.
- [100] T. Tasaki, S.M. Sriram, K.S. Park, Y.T. Kwon, The N-end rule pathway, *Annu. Rev. Biochem.* 81 (2012) 261–289.
- [101] A. Varshavsky, The N-end rule pathway and regulation by proteolysis, *Protein Sci.* 20 (2011) 1298–1345.
- [102] S.V. Kyriacou, M.P. Deutscher, An important role for the multienzyme aminoacyl-tRNA synthetase complex in mammalian translation and cell growth, *Mol. Cell* 29 (2008) 419–427.
- [103] H. Nechushtan, E. Razin, The function of MITF and associated proteins in mast cells, *Mol. Immunol.* 38 (2002) 1177–1180.
- [104] E. Razin, Z.C. Zhang, H. Nechushtan, S. Frenkel, Y.N. Lee, R. Arudchandran, J. Rivera, Suppression of microphthalmia transcriptional activity by its association with protein kinase C-interacting protein 1 in mast cells, *J. Biol. Chem.* 274 (1999) 34272–34276.
- [105] I. Carmi-Levy, N. Yannay-Cohen, G. Kay, E. Razin, H. Nechushtan, Diadenosine tetraphosphate hydrolase is part of the transcriptional regulation network in immunologically activated mast cells, *Mol. Cell. Biol.* 28 (2008) 5777–5784.
- [106] Y.-N. Lee, H. Nechushtan, N. Figov, E. Razin, The function of lysyl-tRNA synthetase and Ap4A as signaling regulators of MITF activity in FcRI-activated mast cells, *Immunity* 20 (2004) 145–151.
- [107] Y. Ofir-Birin, P. Fang, S.P. Bennett, H.-M. Zhang, J. Wang, I. Rachmin, R. Shapiro, J. Song, A. Dagan, J. Pozo, S. Kim, A.G. Marshall, P. Schimmel, X.-L. Yang, H. Nechushtan, E. Razin, M. Guo, Structural switch of lysyl-tRNA synthetase between translation and transcription, *Mol. Cell* 49 (2013) 30–42.
- [108] N. Yannay-Cohen, I. Carmi-Levy, G. Kay, C.M. Yang, J.M. Han, D.M. Kemeny, S. Kim, H. Nechushtan, E. Razin, LysRS serves as a key signaling molecule in the immune response by regulating gene expression, *Mol. Cell* 34 (2009) 603–611.
- [109] G. Fu, T. Xu, Y. Shi, N. Wei, X.-L. Yang, tRNA-controlled nuclear import of a human tRNA synthetase, *J. Biol. Chem.* 287 (2012) 9330–9334.
- [110] M. Sajish, P. Schimmel, A human tRNA synthetase is a potent PARP1-activating effector target for resveratrol, *Nature* 519 (2015) 370–373.
- [111] X. Cao, C. Li, S. Xiao, Y. Tang, J. Huang, S. Zhao, X. Li, J. Li, R. Zhang, W. Yu, Acetylation promotes TyrRS nuclear translocation to prevent oxidative damage, *Proc. Natl. Acad. Sci. U. S. A.* 114 (2017) 687–692.
- [112] N. Wei, Y. Shi, L.N. Truong, K.M. Fisch, T. Xu, E. Gardiner, G. Fu, Y.-S.O. Hsu, S. Kishi, A.I. Su, X. Wu, X.-L. Yang, Oxidative stress diverts tRNA synthetase to nucleus for protection against DNA damage, *Mol. Cell* 56 (2014) 323–332.
- [113] J. Liu, E. Shue, K.L. Ewalt, P. Schimmel, A new gamma-interferon-inducible promoter and splice variants of an anti-angiogenic human tRNA synthetase, *Nucleic Acids Res.* 32 (2004) 719–727.
- [114] V.I. Popenko, N.E. Cherny, S.F. Beresten, J.L. Ivanova, V.V. Filonenko, L.L. Kisselev, Immunoelectron microscopic location of tryptophanyl-tRNA synthetase in mammalian, prokaryotic and archaeobacterial cells, *Eur. J. Cell Biol.* 62 (1993) 248–258.
- [115] M. Sajish, Q. Zhou, S. Kishi, D.M. Valdez, M. Kapoor, M. Guo, S. Lee, S. Kim, X.-L. Yang, P. Schimmel, Trp-tRNA synthetase bridges DNA-PKcs to PARP-1 to link IFN- γ and p53 signaling, *Nat. Chem. Biol.* 8 (2012) 547–554.
- [116] X. Xu, Y. Shi, H.-M. Zhang, E.C. Swindell, A.G. Marshall, M. Guo, S. Kishi, X.-L. Yang, Unique domain appended to vertebrate tRNA synthetase is essential for vascular development, *Nat. Commun.* 3 (2012) 681.
- [117] M. Guo, P. Schimmel, X.-L. Yang, Functional expansion of human tRNA synthetases achieved by structural inventions, *FEBS Lett.* 584 (2010) 434–442.
- [118] H. Fukui, R. Hanaoka, A. Kawahara, Noncanonical activity of seryl-tRNA synthetase is involved in vascular development, *Circ. Res.* 104 (2009) 1253–1259.
- [119] W. Herzog, K. Müller, J. Huisken, D.Y.R. Stainier, Genetic evidence for a non-canonical function of seryl-tRNA synthetase in vascular development, *Circ. Res.* 104 (2009) 1260–1266.
- [120] Y. Shi, X. Xu, Q. Zhang, G. Fu, Z. Mo, G.S. Wang, S. Kishi, X.-L. Yang, tRNA synthetase counteracts c-Myc to develop functional vasculature, *elife* 3 (2014) e02349.
- [121] C.-Y. Fu, P.-C. Wang, H.-J. Tsai, Competitive binding between Seryl-tRNA synthetase/YY1 complex and NFKB1 at the distal segment results in differential regulation of human vegf promoter activity during angiogenesis, *Nucleic Acids Res.* 45 (2017) 2423–2437.
- [122] Z. Cao, H. Wang, X. Mao, L. Luo, Noncanonical function of threonyl-tRNA synthetase regulates vascular development in zebrafish, *Biochem. Biophys. Res. Commun.* 473 (2016) 67–72.
- [123] Y.G. Ko, Y.S. Kang, E.K. Kim, S.G. Park, S. Kim, Nucleolar localization of human methionyl-tRNA synthetase and its role in ribosomal RNA synthesis, *J. Cell Biol.* 149 (2000) 567–574.
- [124] M. Frugier, G. Giegé, Yeast aspartyl-tRNA synthetase binds specifically its own mRNA, *J. Mol. Biol.* 331 (2003) 375–383.
- [125] M. Frugier, M. Ryckelynck, R. Giegé, tRNA-balanced expression of a eukaryal aminoacyl-tRNA synthetase by an mRNA-mediated pathway, *EMBO Rep.* 6 (2005) 860–865.
- [126] D.G. Kim, J.W. Choi, J.Y. Lee, H. Kim, Y.S. Oh, J.W. Lee, Y.K. Tak, J.M. Song,

- E. Razin, S.-H. Yun, S. Kim, Interaction of two translational components, lysyl-tRNA synthetase and p40/37LRP, in plasma membrane promotes laminin-dependent cell migration, *FASEB J.* 26 (2012) 4142–4159.
- [127] D.G. Kim, J.Y. Lee, N.H. Kwon, P. Fang, Q. Zhang, J. Wang, N.L. Young, M. Guo, H.Y. Cho, A.U. Mushtaq, Y.H. Jeon, J.W. Choi, J.M. Han, H.W. Kang, J.E. Joo, Y. Hur, W. Kang, H. Yang, D.-H. Nam, M.-S. Lee, J.W. Lee, E.-S. Kim, A. Moon, K. Kim, D. Kim, E.J. Kang, Y. Moon, K.H. Rhee, B.W. Han, J.S. Yang, G. Han, W.S. Yang, C. Lee, M.-W. Wang, S. Kim, Chemical inhibition of prometastatic lysyl-tRNA synthetase-laminin receptor interaction, *Nat. Chem. Biol.* 10 (2014) 29–34.
- [128] S.H. Nam, D. Kim, M.-S. Lee, D. Lee, T.K. Kwak, M. Kang, J. Ryu, H.-J. Kim, H.E. Song, J. Choi, G.-H. Lee, S.-Y. Kim, S.H. Park, D.G. Kim, N.H. Kwon, T.Y. Kim, J.P. Thiery, S. Kim, J.W. Lee, Noncanonical roles of membranous lysyl-tRNA synthetase in transducing cell-substrate signaling for invasive dissemination of colon cancer spheroids in 3D collagen I gels, *Oncotarget* 6 (2015) 21655–21674.
- [129] S. Bae Rho, M.J. Kim, J.S. Lee, W. Seol, H. Motegi, S. Kim, K. Shiba, Genetic dissection of protein-protein interactions in multi-tRNA synthetase complex, *Genetics* 96 (1999) 4488–4493.
- [130] M. Kaminska, S. Havrylenko, P. Decottignies, P. Le Maréchal, B. Negrutskii, M. Mirande, Dynamic organization of aminoacyl-tRNA synthetase complexes in the cytoplasm of human cells, *J. Biol. Chem.* 284 (2009) 13746–13754.
- [131] K. Hara, K. Yonezawa, Q.P. Weng, M.T. Kozlowski, C. Belham, J. Avruch, Amino acid sufficiency and mTOR regulate p70 S6 kinase and eIF-4E BP1 through a common effector mechanism, *J. Biol. Chem.* 273 (1998) 14484–14494.
- [132] Y. Sancak, T.R. Peterson, Y.D. Shaul, R.A. Lindquist, C.C. Thoreen, L. Bar-Peled, D.M. Sabatini, The rag GTPases bind raptor and mediate amino acid signaling to mTORC1, *Science* 320 (2008) 1496–1501.
- [133] P. Nicklin, P. Bergman, B. Zhang, E. Triantafellow, H. Wang, B. Nyfeler, H. Yang, M. Hild, C. Kung, C. Wilson, V.E. Myer, J.P. MacKeigan, J.A. Porter, Y.K. Wang, L.C. Cantley, P.M. Finan, L.O. Murphy, Bidirectional transport of amino acids regulates mTOR and autophagy, *Cell* 136 (2009) 521–534.
- [134] S.G. Kim, G.R. Buel, J. Blenis, Nutrient regulation of the mTOR complex 1 signaling pathway, *Mol. Cell* 35 (2013) 463–473.
- [135] R.V. Durá, W. Oppliger, A.M. Robitaille, L. Heiserich, R. Skendaj, E. Gottlieb, M.N. Hall, Glutaminolysis activates rag-mTORC1 signaling, *Mol. Cell* 47 (2012) 349–358.
- [136] J.M. Han, S.J. Jeong, M.C. Park, G. Kim, N.H. Kwon, H.K. Kim, S.H. Ha, S.H. Ryu, S. Kim, Leucyl-tRNA synthetase is an intracellular leucine sensor for the mTORC1-signaling pathway, *Cell* 149 (2012) 410–424.
- [137] M.-S. Yoon, K. Son, E. Arauz, J.M. Han, S. Kim, J. Chen, Leucyl-tRNA synthetase activates Vps34 in amino acid-sensing mTORC1 signaling, *Cell Rep.* 16 (2016) 1510–1517.
- [138] M.-S. Yoon, G. Du, J.M. Backer, M.A. Frohman, J. Chen, Class III PI-3-kinase activates phospholipase D in an amino acid-sensing mTORC1 pathway, *J. Cell Biol.* 195 (2011) 435–447.
- [139] G. Gory Bonfils, M. Jaquenoud, S.V. Bontron, C. Ostrowicz, C. Ungermann, C. De Virgilio, Leucyl-tRNA synthetase controls TORC1 via the EGO complex, *Mol. Cell* 46 (2012) 105–110.
- [140] S. Cen, A. Khorchid, H. Javanbakht, J. Gabor, T. Stello, K. Shiba, K. Musier-Forsyth, L. Kleiman, Incorporation of lysyl-tRNA synthetase into human immunodeficiency virus type 1, *J. Virol.* 75 (2001) 5043–5048.
- [141] J. Gabor, S. Cen, H. Javanbakht, M. Niu, L. Kleiman, Effect of altering the tRNA(Lys)(3) concentration in human immunodeficiency virus type 1 upon its annealing to viral RNA, GagPol incorporation, and viral infectivity, *J. Virol.* 76 (2002) 9096–9102.
- [142] F. Guo, S. Cen, M. Niu, H. Javanbakht, L. Kleiman, Specific inhibition of the synthesis of human lysyl-tRNA synthetase results in decreases in tRNA(Lys) incorporation, tRNA(3)(Lys) annealing to viral RNA, and viral infectivity in human immunodeficiency virus type 1, *J. Virol.* 77 (2003) 9817–9822.
- [143] S. Cen, H. Javanbakht, M. Niu, L. Kleiman, Ability of wild-type and mutant lysyl-tRNA synthetase to facilitate tRNA(Lys) incorporation into human immunodeficiency virus type 1, *J. Virol.* 78 (2004) 1595–1601.
- [144] V. Dewan, M. Wei, L. Kleiman, K. Musier-Forsyth, Dual role for motif 1 residues of human lysyl-tRNA synthetase in dimerization and packaging into HIV-1, *J. Biol. Chem.* 287 (2012) 41955–41962.
- [145] A.A. Duchon, C. St Gelais, N. Titkemeier, J. Hatterschide, L. Wu, K. Musier-Forsyth, HIV-1 exploits a dynamic multi-aminoacyl-tRNA synthetase complex to enhance viral replication, *J. Virol.* 91 (2017) e01240–17.
- [146] S. Cen, H. Javanbakht, S. Kim, K. Shiba, R. Craven, A. Rein, K. Ewalt, P. Schimmel, K. Musier-Forsyth, L. Kleiman, Retrovirus-specific packaging of aminoacyl-tRNA synthetases with cognate primer tRNAs, *J. Virol.* 76 (2002) 13111–13115.
- [147] S.G. Park, H.J. Kim, Y.H. Min, E.-C. Choi, Y.K. Shin, B.-J. Park, S.W. Lee, S. Kim, Human lysyl-tRNA synthetase is secreted to trigger proinflammatory response, *Proc. Natl. Acad. Sci. U. S. A.* 102 (2005) 6356–6361.
- [148] S.B. Kim, H.R. Kim, M.C. Park, S. Cho, P.C. Goughnour, D. Han, I. Yoon, Y. Kim, T. Kang, E. Song, P. Kim, H. Choi, J.Y. Mun, C. Song, S. Lee, H.S. Jung, S. Kim, Caspase-8 controls the secretion of inflammatory lysyl-tRNA synthetase in exosomes from cancer cells, *J. Cell Biol.* 216 (2017) 2201–2216.
- [149] K. Meerschaeft, E. Remue, A. De Ganc, A. Staes, C. Boucherie, K. Gevaert, J. Vandekerckhove, L. Kleiman, J. Gettemans, The tandem PDZ protein syntenin interacts with the aminoacyl tRNA synthetase complex in a lysyl-tRNA synthetase-dependent manner, *J. Proteome Res.* 7 (2008) 4962–4973.
- [150] M.F. Baietti, Z. Zhang, E. Mortier, A. Melchior, G. Degeest, A. Geeraerts, Y. Ivarsson, F. Depoortere, C. Coomans, E. Vermeiren, P. Zimmermann, G. David, Syndecan-syntenin-ALIX regulates the biogenesis of exosomes, *Nat. Cell Biol.* 14 (2012) 677–685.
- [151] K. Wakasugi, P. Schimmel, Two distinct cytokines released from a human aminoacyl-tRNA synthetase, *Science* 284 (1999) 147–151.
- [152] R. Zeng, Y. Chen, Z. Zeng, W. Liu, X. Jiang, R. Liu, O. Qiang, X. Li, Effect of mini-tyrosyl-tRNA synthetase/mini-tryptophanyl-tRNA synthetase on ischemic angiogenesis in rats: proliferation and migration of endothelial cells, *Heart Vessel.* 26 (2011) 69–80.
- [153] K. Wakasugi, B.M. Slike, J. Hood, A. Otani, K.L. Ewalt, M. Friedlander, D.A. Cheresch, P. Schimmel, A human aminoacyl-tRNA synthetase as a regulator of angiogenesis, *Proc. Natl. Acad. Sci. U. S. A.* 99 (2002) 173–177.
- [154] R. Zeng, Y. Chen, Z. Zeng, X. Liu, R. Liu, O. Qiang, X. Li, Inhibition of mini-TyrRS-induced angiogenesis response in endothelial cells by VE-cadherin-dependent mini-TrpRS, *Heart Vessel.* 27 (2012) 193–201.
- [155] Y. Greenberg, M. King, W.B. Kiosses, K. Ewalt, X. Yang, P. Schimmel, J.S. Reader, E. Tzima, The novel fragment of tyrosyl tRNA synthetase, mini-TyrRS, is secreted to induce an angiogenic response in endothelial cells, *FASEB J.* 22 (2008) 1597–1605.
- [156] P.M. Biselli, A.R. Guerzoni, M.F. de Godoy, É.C. Pavarino-Bertelli, E.M. Goloni-Bertollo, Vascular endothelial growth factor genetic variability and coronary artery disease in Brazilian population, *Heart Vessel.* 23 (2008) 371–375.
- [157] M.-N. Vo, X.-L. Yang, P. Schimmel, Dissociating quaternary structure regulates cell-signaling functions of a secreted human tRNA synthetase, *J. Biol. Chem.* 286 (2011) 11563–11568.
- [158] Q. Zhou, M. Kapoor, M. Guo, R. Belani, X. Xu, W.B. Kiosses, M. Hanan, C. Park, E. Armour, M.-H. Do, L.A. Nangle, P. Schimmel, X.-L. Yang, Orthogonal use of a human tRNA synthetase active site to achieve multifunctionality, *Nat. Struct. Mol. Biol.* 17 (2010) 57–61.
- [159] T. Nakamoto, M. Miyanokoshi, T. Tanaka, K. Wakasugi, Identification of a residue crucial for the angiostatic activity of human mini tryptophanyl-tRNA synthetase by focusing on its molecular evolution, *Sci. Rep.* 6 (2016) 24750.
- [160] E. Tzima, J.S. Reader, M. Irani-Tehrani, K.L. Ewalt, M.A. Schwartz, P. Schimmel, VE-cadherin links tRNA synthetase cytokine to anti-angiogenic function, *J. Biol. Chem.* 280 (2005) 2405–2408.
- [161] E. Tzima, P. Schimmel, Inhibition of tumor angiogenesis by a natural fragment of a tRNA synthetase, *Science* 80 (309) (2006) 1534–1539.
- [162] R. Zeng, X.-F. Jiang, Y.-C. Chen, Y.-N. Xu, S.-H. Ma, Z. Zeng, R. Liu, O. Qiang, X. Li, VEGF, not VEGFR2, is associated with the angiogenesis effect of mini-TyrRS/mini-TrpRS in human umbilical vein endothelial cells in hypoxia, *Cytotechnology* 66 (2014) 655–665.
- [163] K. Wakasugi, P. Schimmel, Highly differentiated motifs responsible for two cytokine activities of a split human tRNA synthetase, *J. Biol. Chem.* 274 (1999) 23155–23159.
- [164] Y.H. Ahn, S. Park, J.J. Choi, B.-K. Park, K.H. Rhee, E. Kang, S. Ahn, C.-H. Lee, J.S. Lee, K.-S. Inn, M.-L. Cho, S.-H. Park, K. Park, H.J. Park, J.H. Lee, J.W. Park, N.H. Kwon, H. Shim, B.W. Han, P. Kim, J.-Y. Lee, Y. Jeon, J.W. Huh, M. Jin, S. Kim, Secreted tryptophanyl-tRNA synthetase as a primary defence system against infection, *Nat. Microbiol.* 2 (2016) 16191.
- [165] T.F. Williams, A.C. Mirando, B. Wilkinson, C.S. Francklyn, K.M. Lounsbury, Secreted threonyl-tRNA synthetase stimulates endothelial cell migration and angiogenesis, *Sci. Rep.* 3 (2013) 1317.
- [166] T.L. Wellman, M. Eckenstein, C. Wong, M. Rincon, T. Ashikaga, S.L. Mount, C.S. Francklyn, K.M. Lounsbury, Threonyl-tRNA synthetase overexpression correlates with angiogenic markers and progression of human ovarian cancer, *BMC Cancer* 14 (2014) 620.
- [167] M. Kron, K. Marquard, M. Härtlein, S. Price, R. Leberman, An immunodominant antigen of *Brugia malayi* is an asparaginyl-tRNA synthetase, *FEBS Lett.* 374 (1995) 122–124.
- [168] M. Kron, M. Petridis, Y. Milev, J. Leykam, M. Härtlein, Expression, localization and alternative function of cytoplasmic asparaginyl-tRNA synthetase in *Brugia malayi*, *Mol. Biochem. Parasitol.* 129 (2003) 33–39.
- [169] B.L. Ramirez, O.M.Z. Howard, H.F. Dong, T. Edamatsu, P. Gao, M. Hartlein, M. Kron, *Brugia malayi* asparaginyl-transfer RNA synthetase induces chemotaxis of human leukocytes and activates G-protein-coupled receptors CXCR1 and CXCR2, *J. Infect. Dis.* 193 (2006) 1164–1171.
- [170] M. Kron, J. Leykam, J. Kopaczewski, I. Matus, Identification of diadenosine triphosphate in *Brugia malayi* by reverse phase high performance liquid chromatography and MALDI mass spectrometry, *J. Chromatogr. B Anal. Technol. Biomed. Life Sci.* 856 (2007) 234–238.
- [171] M.A. Kron, C. Wang, S. Vodanovic-Jankovic, O. Zack Howard, L.A. Kuhn, Interleukin-8-like activity in a filarial asparaginyl-tRNA synthetase, *Mol. Biochem. Parasitol.* 185 (2012) 66–69.
- [172] J. Jothi D., M. Dhanraj, S. Shanmugam, S. Sanjana, M. Kron, A. Dhanasekaran, *Brugia malayi* asparaginyl-tRNA synthetase stimulates endothelial cell proliferation, vasodilation and angiogenesis, *PLoS One* 11 (2016) e0146132.
- [173] M.C. Park, T. Kang, D. Jin, J.M. Han, S.B. Kim, Y.J. Park, K. Cho, Y.W. Park, M. Guo, W. He, X.-L. Yang, P. Schimmel, S. Kim, Secreted human glycyl-tRNA synthetase implicated in defense against ERK-activated tumorigenesis, *Proc. Natl. Acad. Sci. U. S. A.* 109 (2012) E640–7.
- [174] W. He, G. Bai, H. Zhou, N. Wei, N.M. White, J. Lauer, H. Liu, Y. Shi, C.D. Dumitru, K. Lettieri, V. Shubayev, A. Jordanova, V. Guerguelcheva, P.R. Griffin, R.W. Burgess, S.L. Pfaff, X.-L. Yang, CMT2D neuropathy is linked to the neomorphic binding activity of glycyl-tRNA synthetase, *Nature* 526 (2015) 710–714.
- [175] W.-S. Lo, E. Gardiner, Z. Xu, C.-F. Lau, F. Wang, J.J. Zhou, J.D. Mendlein, L.A. Nangle, K.P. Chiang, X.-L. Yang, K.-F. Au, W.H. Wong, M. Guo, M. Zhang, P. Schimmel, Human tRNA synthetase catalytic nulls with diverse functions, *Science* 345 (2014) 328–332.
- [176] K.L. Seburn, L.A. Nangle, G.A. Cox, P. Schimmel, R.W. Burgess, An active dominant mutation of glycyl-tRNA synthetase causes neuropathy in a Charcot-Marie-

- Tooth 2D mouse model, *Neuron* 51 (2006) 715–726.
- [177] A. Jordanova, J. Irobi, F.P. Thomas, P. Van Dijk, K. Meerschaert, M. Dewil, I. Dierick, A. Jacobs, E. De Vriendt, V. Guerguelcheva, C.V. Rao, I. Tournev, F.A.A. Gondim, M. D'Hooghe, V. Van Gerwen, P. Callaerts, L. Van Den Bosch, J.-P. Timmermans, W. Robberecht, J. Gettemans, J.M. Thevelein, P. De Jonghe, I. Kremensky, V. Timmerman, Disrupted function and axonal distribution of mutant tyrosyl-tRNA synthetase in dominant intermediate Charcot-Marie-Tooth neuropathy, *Nat. Genet.* 38 (2006) 197–202.
- [178] L.A. Nangle, W. Zhang, W. Xie, X.-L. Yang, P. Schimmel, Charcot-Marie-Tooth disease-associated mutant tRNA synthetases linked to altered dimer interface and neurite distribution defect, *Proc. Natl. Acad. Sci. U. S. A.* 104 (2007) 11239–11244.
- [179] C.B. Kunst, E. Mezey, M.J. Brownstein, D. Patterson, Mutations in SOD1 associated with amyotrophic lateral sclerosis cause novel protein interactions, *Nat. Genet.* 15 (1997) 91–94.
- [180] W.L. Sang, S.K. Young, K. Sunghoon, Multifunctional proteins in tumorigenesis: aminoacyl-tRNA synthetases: ingenta connect, *Curr. Proteomics* 3 (2006) 233–247.
- [181] J.P. Kushner, D. Boll, J. Quagliana, S. Dickman, Elevated methionine-tRNA synthetase activity in human colon cancer, *Proc. Soc. Exp. Biol. Med.* 153 (1976) 273–276.
- [182] E.Y. Kim, J.Y. Jung, A. Kim, K. Kim, Y.S. Chang, Methionyl-tRNA synthetase overexpression is associated with poor clinical outcomes in non-small cell lung cancer, *BMC Cancer* 17 (2017) 467.
- [183] L.M. 't Hart, T. Hansen, I. Rietveld, J.M. Dekker, G. Nijpels, G.M.C. Janssen, P.A. Arp, A.G. Uitterlinden, T. Jørgensen, K. Borch-Johnsen, H.A.P. Pols, O. Pedersen, C.M. van Duijn, R.J. Heine, J.A. Maassen, Evidence that the mitochondrial leucyl tRNA synthetase (LARS2) gene represents a novel type 2 diabetes susceptibility gene, *Diabetes* 54 (2005) 1892–1895.
- [184] E. Reiling, B. Jafar-Mohammadi, E. van 't Riet, M.N. Weedon, J.V. van Vliet-Ostapchouk, T. Hansen, R. Saxena, T.W. van Haefen, P.A. Arp, S. Das, G. Nijpels, M.J. Groenewoud, E.C. van Hove, A.G. Uitterlinden, J.W.A. Smit, A.D. Morris, A.S.F. Doney, C.N.A. Palmer, C. Guiducci, A.T. Hattersley, T.M. Frayling, O. Pedersen, P.E. Slagboom, D.M. Altshuler, L. Groop, J.A. Romijn, J.A. Maassen, M.H. Hofker, J.M. Dekker, M.I. McCarthy, L.M. 't Hart, Genetic association analysis of LARS2 with type 2 diabetes, *Diabetologia* 53 (2010) 103–110.
- [185] J.J. Zhou, F. Wang, Z. Xu, W.-S. Lo, C.-F. Lau, K.P. Chiang, L.A. Nangle, M.A. Ashlock, J.D. Mendlein, X.-L. Yang, M. Zhang, P. Schimmel, Secreted histidyl-tRNA synthetase splice variants elaborate major epitopes for autoantibodies in inflammatory myositis, *J. Biol. Chem.* 289 (2014) 19269–19275.
- [186] O.M.Z. Howard, H.F. Dong, D. Yang, N. Raben, K. Nagaraju, A. Rosen, L. Casciola-Rosen, M. Härtlein, M. Kron, D. Yang, K. Yiadom, S. Dwivedi, P.H. Plotz, J.J. Oppenheim, Histidyl-tRNA synthetase and asparaginyl-tRNA synthetase, autoantigens in myositis, activate chemokine receptors on T lymphocytes and immature dendritic cells, *J. Exp. Med.* 196 (2002) 781–791.
- [187] M.B. Mathews, R.M. Bernstein, Myositis autoantibody inhibits histidyl-tRNA synthetase: a model for autoimmunity, *Nature* 304 (1983) 177–179.
- [188] M.B. Mathews, M. Reichlin, G.R. Hughes, R.M. Bernstein, Anti-threonyl-tRNA synthetase, a second myositis-related autoantibody, *J. Exp. Med.* 160 (1984) 420–434.
- [189] L. Stojanov, M. Satoh, M. Hirakata, W.H. Reeves, Correlation of antisynthetase antibody levels with disease course in a patient with interstitial lung disease and elevated muscle enzymes, *J. Clin. Rheumatol.* 2 (1996) 89–95.
- [190] M. Mahler, F.W. Miller, M.J. Fritzler, Idiopathic inflammatory myopathies and the anti-synthetase syndrome: a comprehensive review, *Autoimmun. Rev.* 13 (2014) 367–371.
- [191] M. Cojocaru, I.M. Cojocaru, B. Chicos, New insights into antisynthetase syndrome, *Maedica (Buchar)* 11 (2016) 130–135.

POSTER 1

Significant pools of the AME
complex bind vacuolar membrane
through Arc1 shown by
biochemistry and split-GFP

**26th tRNA conference, September 4-8 2016
Jeju, South Korea**

Johan-Owen De Craene, Sylvain Debard, Gaétan Bader, Maximilian Geiger, Ludovic Enkler, Bruno Senger, and Hubert D. Becker

The University of Strasbourg - Institut de Physiologie et de Chimie Biologique - Dynamics of the Translation Machinery and Metabolic Crosstalks - UMR 7156 CNRS-UdS GMGM, Strasbourg, FRANCE

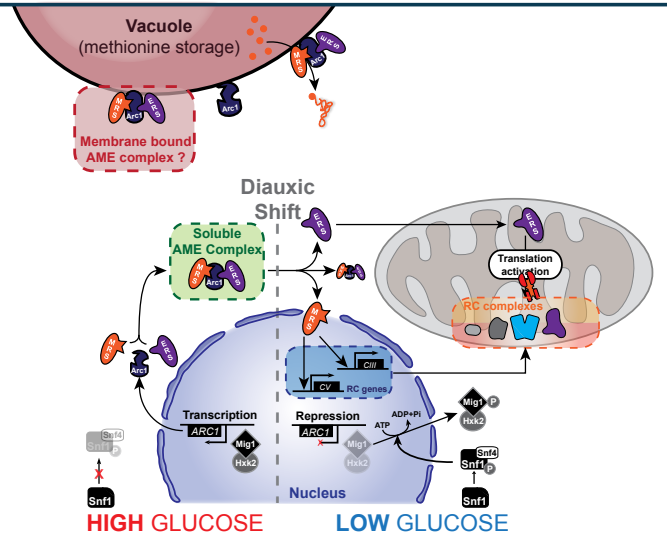


Background

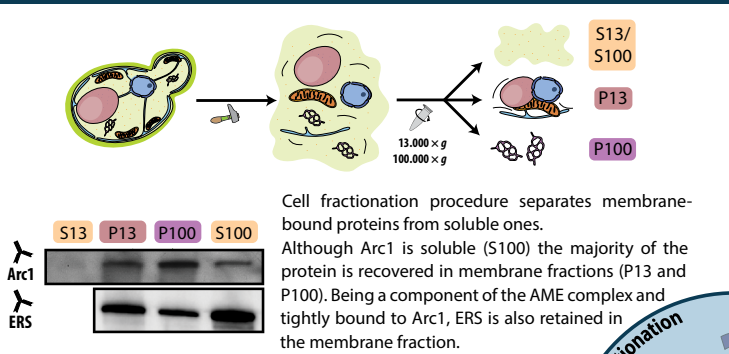
Coordinating nuclear, cytoplasmic and mitochondrial functions is essential to ensure optimal respiration. In yeast *Saccharomyces cerevisiae*, this coordination relies in part on the equilibrium between pools of cytoplasmic methionyl- (MRS) and glutamyl- (ERS) tRNA synthetases bound to Arc1 (forming the AME complex) and free MRS and ERS. Free MRS is translocated into the nucleus to regulate the expression of nuclear genes encoding subunits of F₁ domain of ATP synthase (Complex V of the respiratory chain). Free ERS is imported in the mitochondrial matrix to ensure the proper translation of mitochondrial-encoded Atp9 subunit, essential component of the F₀ domain of ATP synthase [1].

So far, the AME complex was considered to be only soluble but recently it was shown that Arc1 binds phosphoinositides *in vitro* such as PI3P and PI(3,5)P₂ [2]. Both are involved in protein sorting at endosomes and the vacuole/lysosome.

Hence, we have started the analysis of the membrane-bound Arc1 and the role of this uncharacterized pool of AME complex using biochemical approaches and a split-GFP tool for localizing specifically membrane-anchored aminoacyl-tRNA synthetases (aaRSs).



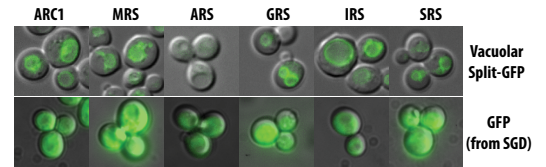
1 Subcellular fractionation confirms binding of Arc1 and ERS to membranes



Arc1 protein is predominantly binding to the vacuolar and endosomal membranes (around 75% of total) and redirects the glutamyl-tRNA synthetase to these compartments

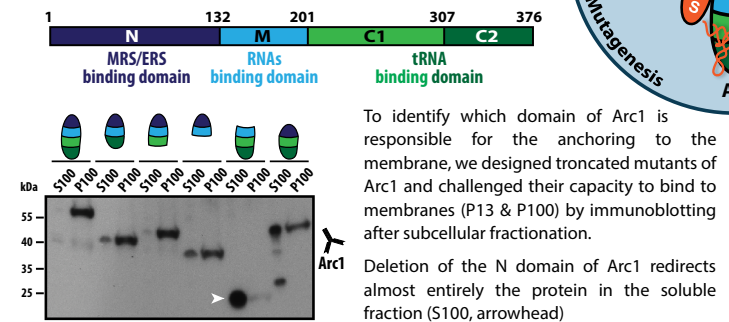
2 Split-GFP-based microscopy shows localization of Arc1, MRS but also other aaRSs to the vacuole

This system allows specific detection of the vacuolar pools of multi-localized protein through reconstitution of the GFP protein. As expected, Arc1 and MRS generate a vacuolar signal with this system (upper panel). This fraction is not visible through standard GFP tagging (lower panel). Surprisingly, pools of several other aaRSs are also found at the surface of the vacuolar membrane.



Arc1 and MRS are binding to the vacuole and vacuolar localization of cytosolic aaRSs is more frequent than expected

Modular organization of Arc1



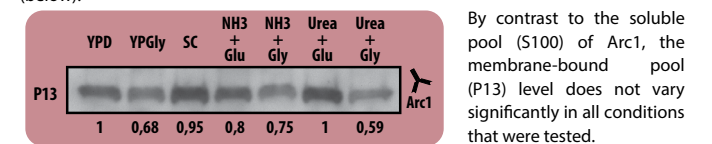
The N-terminal domain of Arc1 responsible for MRS and ERS binding is also involved in binding to phosphoinositids (PI), although Arc1 does not display any conventional PI-binding motif

3 Identification of the phosphoinositid-binding domain of Arc1

- ### Perspectives
1. What are the residues of the GST-like N-terminal domain of Arc1 involved in recognition and binding of PI ?
 2. Is vacuolar-bound AME complex activating amino acids and aminoacylating tRNAs ?
 3. Is vacuolar-bound AME complex relaying methionine availability to the translation machinery ?
 4. What pathway regulates vacuolar-bound AME complex ?

4 Membrane-anchored Arc1 level does not participate to the metabolic switch from fermentation to respiration

We have previously reported the decrease of soluble Arc1 during the metabolic shift from fermentation to respiration (right). This decrease of cytosolic Arc1 allows the organellar realisation of MRS and ERS [1]. We verified whether vacuolar-bound Arc1 is also varying under various metabolic conditions: fermentation/respiration, and nitrogen sources (below).



Unlike the soluble form of Arc1, vacuolar-bound Arc1 does not participate to the diauxic transition

References

- [1] Frechin et al., *Molecular Cell*, 2014
- [2] Fernandez-Murray et al., *FEBS Letters*, 2006



POSTER 2

Oxidative stress response and
adaptation by methionine
misincorporation in the yeast *S.*
cerevisiae

**11th aaRS meeting, Oct. 29th-Nov. 2nd 2017,
Clearwater beach, Florida, USA**

OXIDATIVE STRESS RESPONSE AND ADAPTATION BY METHIONINE MISINCORPORATION IN THE YEAST *S. CEREVISIAE*

Université de
Strasbourg

Sylvain Debard, Marion Wendenbaum and Hubert D. Becker

The University of Strasbourg - Institut de Botanique - Dynamics & Plasticity of aminoacyl-tRNA Synthetases-UMR 7156 CNRS-UdS GMGM, Strasbourg, FRANCE



Background

Cells must be able to maintain their intracellular homeostasis when confronted to environmental stresses. The oxidative stress results in an excess of electrons carried by oxidants such as Reactive Oxygen Species (ROS) and is deleterious for the cell through protein and lipid oxidation, RNA modification and DNA damage. Misincorporation of the sulphur-containing amino acid methionine has been proposed to constitute an important antioxidant defence mechanism (Figure 1). However, methionine mischarging would be relevant only if this misincorporation is not random and does not alter protein functions. It has been shown by tRNA microarrays that methionylation to non-cognate tRNAs by methionyl-tRNA synthetase (MetRS) increased under oxidative stress in human [1] and yeast [2] cells, and that some tRNAs are more likely mischarged by MetRS than others.

To confirm these results we developed a bi-fluorescent reporter system to monitor methionine misincorporation directed by the full set of codons in the yeast *Saccharomyces cerevisiae*. Using yeast as a model, we will be able to test methionine misincorporation for each codon in several growth conditions including physiological and chemically-induced oxidative stress, and to identify which of the four naturally occurring MetRS isoforms present in *S. cerevisiae* is responsible for this adaptative mismethionylation.

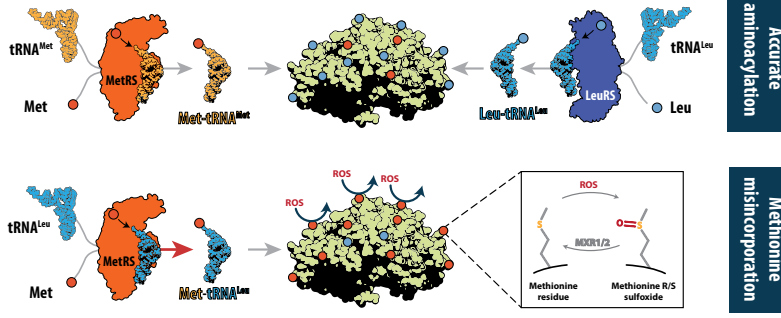


Figure 1 Mechanism and role of mismethionylation during oxidative stress

In standard conditions (top), each of the 20 cytosolic aaRSs transfer the corresponding amino acid onto its cognate tRNA. However in oxidative conditions (bottom), the methionyl-tRNA synthetase (MetRS) transfers methionine onto non-cognate tRNAs, leading to the misincorporation of methionine at specific non-AUG codons. This misincorporation would constitute a fast and general defense against ROS and oxidative stress.

1

BI-FLUORESCENT REPORTER SYSTEM

The mRuby2 fluorescence relies on Met67 in its chromophore. Mutation of the corresponding ATG codon in the mRuby2 gene turns off the red fluorescence, and methionine misincorporation at this mutated codon restores fluorescence. The downstream EGFP gene is an internal expression control.

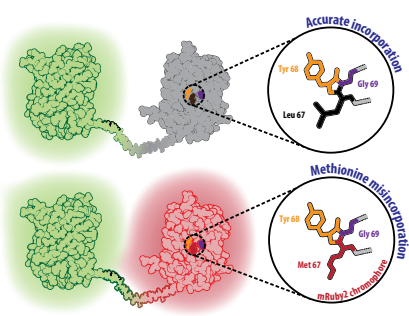
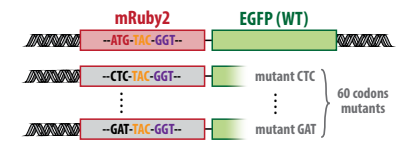


Figure 2 Principle of the Bi-fluorescent reporter

3

SELECTION OF CLONES WITH SIMILAR GFP SIGNAL

To avoid fluorescence biases due to different expression level of EGFP in cells, clones with similar EGFP intensity were selected.

Figure 4A shows a significant variation of EGFP expression among clones obtained from the same transformation. We thus selected clones with a EGFP signal compatible with quantification of fluorescence intensity signal.

A library of 61 different clones was selected. Each clone carries a mRuby2 gene in which the ATG 67 codon of chromophore was replaced by one of the 60 other combinations. The variability in GFP intensity will be normalized as described in section 4.

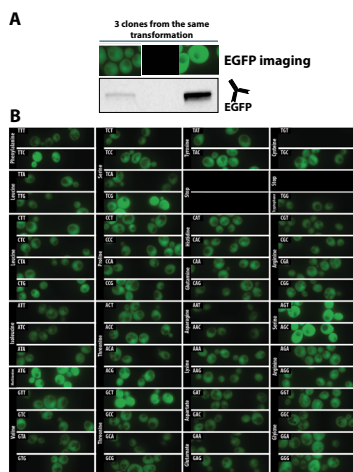


Figure 4 GFP signal variability among clones & clones selection

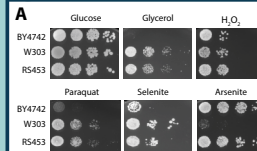
Yeast BY4742 strain has been transformed with 61 different integrative vectors, leading to 61 clones expressing each mRuby2 mutant. Selection of each mutant has been done according to their EGFP signal (A), and EGFP fluorescence intensity for all clones are shown in (B).

Perspectives

1. Find the oxidative condition that triggers most mismethionylation
2. Confirm by mass spectrometry the level of misincorporation
3. *In vitro* aminoacylation of different non-Met tRNAs by yeast MetRS
4. Explore the role of Arc1 in mismethionylation using *arc1Δ* strain and stress hypersensitive strains

2

IMPACT OF OXIDANTS ON GROWTH & PROTEIN SYNTHESIS



Depending on the oxidant used for the drop test, yeast stains do not respond equally to each oxidative molecules (3A).

Because the dual fluorescent reporter needs to be translate, the oxidant that triggers enough oxidative stress without excessively impacting growth and protein synthesis (3B), will be used.

Figure 3 Growth effects of oxidants

(A) Drop test of different yeast stains growing on YPD supplemented with oxidants. (B) Protein synthesis in RS453 strain following treatment with H₂O₂.

4

DETERMINING THE LEVEL OF MET MISINCORPORATION

We then monitored the mRuby2 signal by microscopy (5A) and by flow cytometry (not shown).

Normalization of the red signal according to GFP intensity, was calculated as follows for each clone:

$$\text{Mismethionylation score} = \frac{\text{mRuby2 signal}}{\text{EGFP signal}}$$

Results for all codons are shown in Figure 5B in percentage of misincorporation. Positive scores are only seen for leucine and glutamine codons in standard condition.

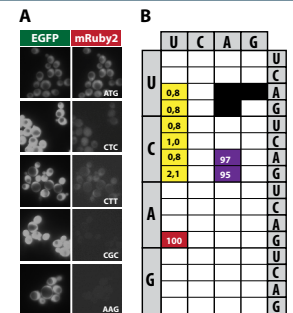


Figure 5 Quantification of mismethionylation under non-oxidative conditions

After fluorescence microscopy acquisition (A), the signal ratio mRuby2/EGFP is calculated and the percentage of misincorporation can be determined; with 100 % corresponding to MetAUG codon (in red) (B). Codon boxes without percentages correspond to codons for which red fluorescence was too low to be analyzed.

5

tRNA SEQUENCE COMPARISON AND IDENTITY ELEMENTS

tRNA sequence analysis reveals similarities between tRNA^{Met} and tRNAs^{Leu}, with A35 and A73 present in all sequences.

These tRNAs^{Leu} could be misaminoacylated by the MetRS.

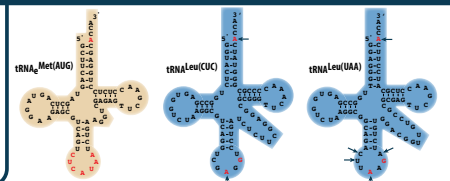


Figure 6 Comparison of identity elements between tRNA Met and Leu

Positions in red are identity elements for each tRNA. Arrows indicate tRNA Met identity elements present in other tRNAs.

References

- [1] N. Netzer, J.M. Goodenbour, A. David, K.A. Dittmar, R.B. Jones, J.R. Schneider, D. Boone, E.M. Eves, M.R. Rosner, J.S. Gibbs, A. Embry, B. Dolan, S. Das, H.D. Hickman, P. Berglund, J.R. Bennink, J.W. Yewdell, T. Pan, **Innate immune and chemically triggered oxidative stress modifies translational fidelity**, *Nature*, **462** (2009) 522–526.
- [2] E. Wiltout, J.M. Goodenbour, M. Fréchin, T. Pan, **Misacylation of tRNA with methionine in *Saccharomyces cerevisiae***, *Nucleic Acids Res.* **40** (2012) 10494–506.

École
normale
supérieure
paris-saclay



Université de
Strasbourg

POSTER 3

Oxidative stress response and
adaptation by methionine
misincorporation in the yeast *S.*
cerevisiae

27th tRNA conference, September 23-27 2018,
Strasbourg, France

OXIDATIVE STRESS RESPONSE AND ADAPTATION BY METHIONINE MISINCORPORATION IN THE YEAST *S. CEREVISIAE*

Université de
Strasbourg

Sylvain Debard, Marion Wendenbaum and Hubert D. Becker

The University of Strasbourg - Institut de Botanique - Dynamics & Plasticity of aminoacyl-tRNA Synthetases- UMR 7156 CNRS-UdS GMGM, Strasbourg, FRANCE



Background

Cells must be able to maintain their intracellular homeostasis when confronted to environmental stresses. The oxidative stress results in an excess of electrons carried by oxidants such as Reactive Oxygen Species (ROS) and is deleterious for the cell through protein and lipid oxidation, RNA modification and DNA damage. Misincorporation of the sulphur-containing amino acid methionine has been proposed to constitute an important antioxidant defence mechanism (Figure 1). However, methionine mischarging would be relevant only if this misincorporation is not random and does not alter protein functions. It has been shown by tRNA microarrays that methionylation to non-cognate tRNAs by methionyl-tRNA synthetase (MetRS) increased under oxidative stress in human [1] and yeast [2] cells, and that some tRNAs are more likely mischarged by MetRS than others.

To confirm these results we developed a bi-fluorescent reporter system to monitor methionine misincorporation directed by the full set of codons in the yeast *Saccharomyces cerevisiae*. Using yeast as a model, we will be able to test methionine misincorporation for each codon in several growth conditions including physiological and chemically-induced oxidative stress, and to identify which of the naturally occurring MetRS isoforms present in *S. cerevisiae* is responsible for this adaptative mismethionylation.

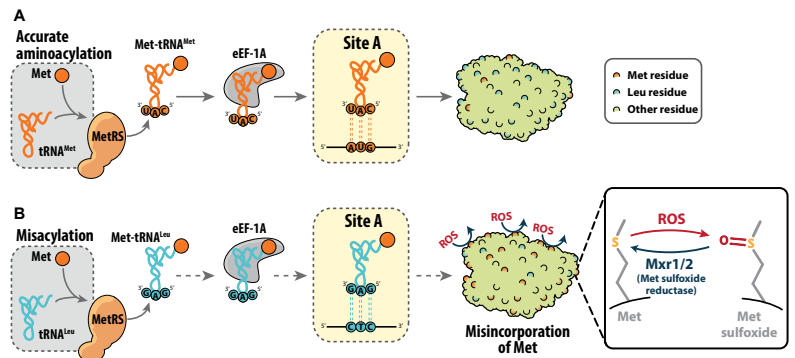
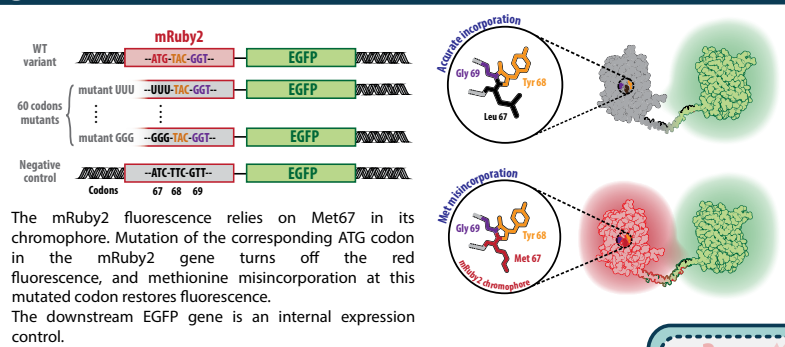


Figure 1 Mechanism and role of mismethionylation during oxidative stress

A. In standard conditions, each of the 20 cytosolic aaRS transfer the corresponding amino acid onto its cognate tRNA. **B.** However in oxidative conditions, the methionyl-tRNA synthetase (MetRS) transfers methionine onto non-cognate tRNAs, leading to the misincorporation of methionine at specific non-AUG codons. This misincorporation would constitute a fast and general defense against ROS and oxidative stress.

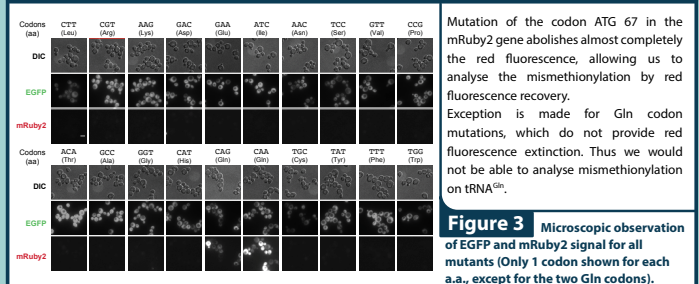
1 BI-FLUORESCENT REPORTER SYSTEM



The mRuby2 fluorescence relies on Met67 in its chromophore. Mutation of the corresponding ATG codon in the mRuby2 gene turns off the red fluorescence, and methionine misincorporation at this mutated codon restores fluorescence. The downstream EGFP gene is an internal expression control.

Figure 2 Principle of the bi-fluorescent reporter

2 FLUOROPHORE ACTIVITY FOR ALL THE REPORTER MUTANTS



Mutation of the codon ATG 67 in the mRuby2 gene abolishes almost completely the red fluorescence, allowing us to analyse the mismethionylation by red fluorescence recovery. Exception is made for Gln codon mutations, which do not provide red fluorescence extinction. Thus we would not be able to analyse mismethionylation on tRNA^{Gln}.

Figure 3 Microscopic observation of EGFP and mRuby2 signal for all mutants (Only 1 codon shown for each a.a., except for the two Gln codons).

4 EFFECT OF ARC1 PROTEIN ON tRNA MISMETHIONYLATION

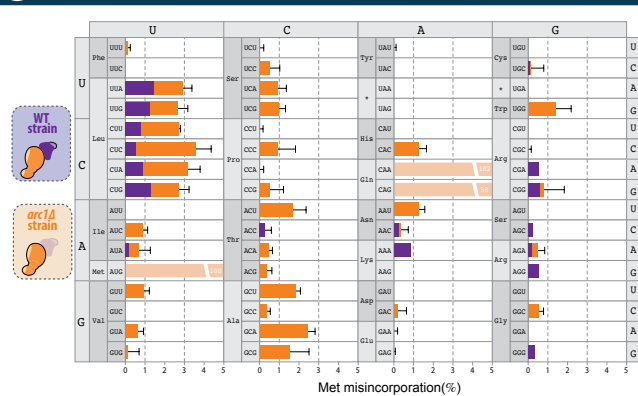


Figure 5 Impact of ARC1 deletion on Met misincorporation

We used our bi-fluorescent system on two different yeast strains: the WT strain (purple) expressing the whole AME (Arc1-MRS-ERS) complex, and the *arc1Δ* strain (orange) where the AME complex is disturbed and the MetRS is not complexed to Arc1 protein. Microscopic observation and Met misincorporation quantification show preferential misincorporation of Met at Leu codons ($\approx 1\%$) in WT context, but deletion of Arc1 protein induces misincorporation at a large subset of different codons, and an increase misincorporation at Leu codons ($\approx 3\%$). Thus Arc1 protein would have a major role in MetRS fidelity for its cognate tRNAs.

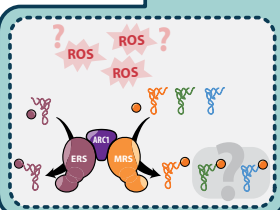
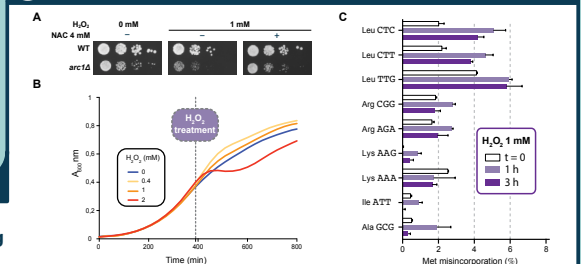


Figure 4 Effect of H_2O_2 treatment on yeast growth and mischarging of methionine.

We used H_2O_2 as oxydative molecule to measure the impact of oxydative stress on yeast translation fidelity and methionine mischarging. Determining the correct H_2O_2 concentration to use in our assay without inhibiting yeast cell growth onto solid (A) or liquid (B) medium, we quantified Met mischarging for some codons (C). We observed more than a two-fold increase in mismethionylation for CTC and CTT Leu codons, and a moderate effect on the others.

3 MISMETHIONYLATION UPON OYDATIVE STRESS



5 tRNA SEQUENCE COMPARISON AND IDENTITY ELEMENTS

tRNA sequence analysis reveals similarities between tRNA^{Met} and tRNAs^{Leu}, with A35 and A73 present in all sequences.

Thus these tRNAs^{Leu} are likely to be misaminoacylated by the MetRS, which is in correlation with our bifluorescent reporter assay.

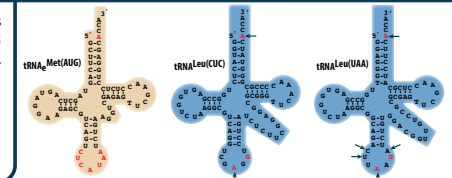


Figure 6 Comparison of identity elements between tRNA Met and Leu

Positions in red are identity elements for each tRNA. Arrows indicate tRNA Met identity elements present in other tRNAs.

Perspectives

1. Find the oxidative condition that triggers most mismethionylation
2. Confirm by mass spectrometry the level of misincorporation
3. *In vitro* aminoacylation of different non-Met tRNAs by yeast MetRS
4. Explore the dynamic and the kinetic of mismethionylation, and the role of other partners using yeast gene deletion strain.

References

- [1] N. Netzer, J.M. Goodenbour, A. David, K.A. Dittmar, R.B. Jones, J.R. Schneider, D. Boone, E.M. Eves, M.R. Rosner, J.S. Gibbs, A. Embry, B. Dolan, S. Das, H.D. Hickman, P. Berglund, J.R. Bennink, J.W. Yewdell, T. Pan, **Innate immune and chemically triggered oxidative stress modifies translational fidelity**, *Nature*. **462** (2009) 522–526.
- [2] E. Wiltrout, J.M. Goodenbour, M. Fréchin, T. Pan, **Misacylation of tRNA with methionine in *Saccharomyces cerevisiae***, *Nucleic Acids Res.* **40** (2012) 10494–506.

École
normale
supérieure
paris-saclay



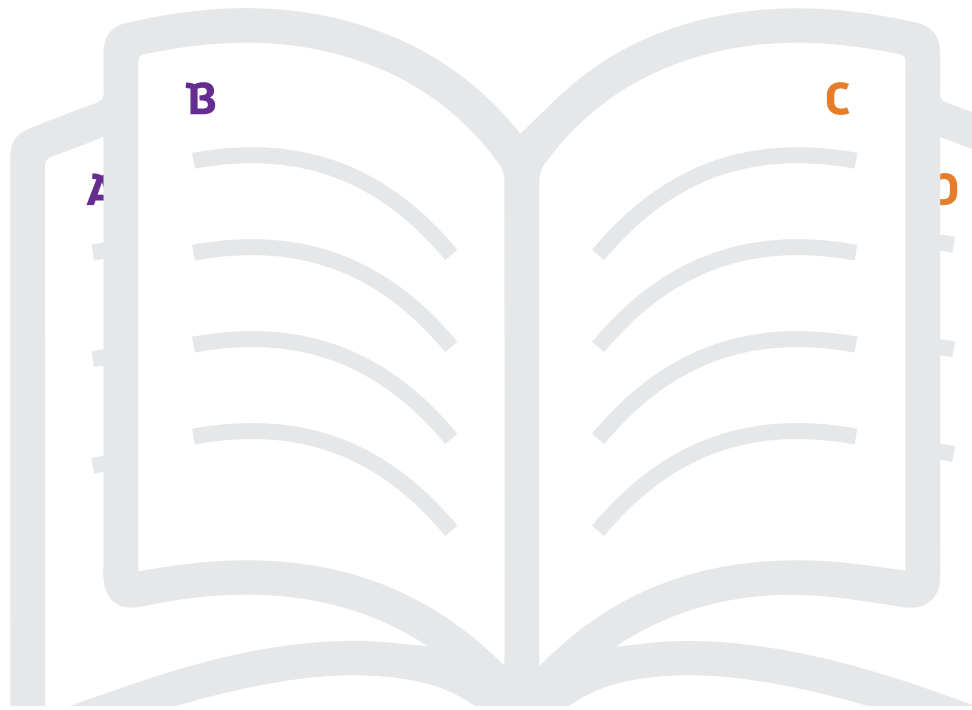
Université de
Strasbourg



05

BIBLIOGRAPHY

- I TEXT REFERENCES (ALPHABETICAL ORDER) 316
- II FIGURES AND TABLES REFERENCES (BY NUMBERS) 340



I. Text references

A

- Acker, M. G., Shin, B.-S., Nanda, J. S., Saini, A. K., Dever, T. E. and Lorsch, J. R. (2009) "Kinetic Analysis of Late Steps of Eukaryotic Translation Initiation", *Journal of Molecular Biology*, 385(2), pp. 491–506.
- Adamis, P. D. B., Mannarino, S. C., Riger, C. J., Duarte, G., Cruz, A., Pereira, M. D. and Eleutherio, E. C. A. (2009) "Lap4, a vacuolar aminopeptidase I, is involved in cadmium-glutathione metabolism", *BioMetals*, 22(2), pp. 243–249.
- Ahn, H.-C., Kim, S. and Lee, B.-J. (2003) "Solution structure and p43 binding of the p38 leucine zipper motif: coiled-coil interactions mediate the association between p38 and p43", *FEBS Letters*, 542(1–3), pp. 119–124.
- Algire, M. A., Maag, D., Savio, P., Acker, M. G., Tarun, S. Z., Sachs, A. B., Asano, K., Nielsen, K. H., Olsen, D. S., Phan, L., Hinnebusch, A. G., Lorsch, J. R. and Lorsch, J. R. (2002) "Development and characterization of a reconstituted yeast translation initiation system.", *RNA*, 8(3), pp. 382–97.
- Algire, M. A., Maag, D. and Lorsch, J. R. (2005) "Pi Release from eIF2, Not GTP Hydrolysis, Is the Step Controlled by Start-Site Selection during Eukaryotic Translation Initiation", *Molecular Cell*, 20(2), pp. 251–262.
- Ambrogelly, A., Korencic, D. and Ibba, M. (2002) "Functional annotation of class I lysyl-tRNA synthetase phylogeny indicates a limited role for gene transfer.", *Journal of bacteriology*. American Society for Microbiology Journals, 184(16), pp. 4594–600.
- Ambrogelly, A., Palioura, S. and Söll, D. (2007) "Natural expansion of the genetic code", *Nature Chemical Biology*, 3(1), pp. 29–35.
- Andersen, C. B. F., Becker, T., Blau, M., Anand, M., Halic, M., Balar, B., Mielke, T., Boesen, T., Pedersen, J. S., Spahn, C. M. T., Kinzy, T. G., Andersen, G. R. and Beckmann, R. (2006) "Structure of eEF3 and the mechanism of transfer RNA release from the E-site.", *Nature*, 443(7112), pp. 663–8.
- Anderson, J., Phan, L., Cuesta, R., Carlson, B. A., Pak, M., Asano, K., Bjork, G. R., Tamame, M. and Hinnebusch, A. G. (1998) "The essential Gcd10p-Gcd14p nuclear complex is required for 1-methyladenosine modification and maturation of initiator methionyl-tRNA", *Genes & Development*, 12(23), pp. 3650–3662.
- Araiso, Y., Huot, J. L., Sekiguchi, T., Frechin, M., Fischer, F., Enkler, L., Senger, B., Ishitani, R., Becker, H. D. and Nureki, O. (2014) "Crystal structure of *Saccharomyces cerevisiae* mitochondrial GatFAB reveals a novel subunit assembly in tRNA-dependent amidotransferases.", *Nucleic Acids Research*, 42(9), pp. 6052–63.
- Ares, M., Grate, L., Pauling, M. H. and Pauling, M. H. (1999) "A handful of intron-containing genes produces the lion's share of yeast mRNA", *RNA*, 5(9), pp. 1138–9.
- Arnér, E. S. J. (2010) "Selenoproteins—What unique properties can arise with selenocysteine in place of cysteine?", *Experimental Cell Research*, 316(8), pp. 1296–1303.
- Arnez, J. G. and Moras, D. (1997) "Structural and functional considerations of the aminoacylation reaction.", *Trends in biochemical sciences*, 22(6), pp. 211–6.

Asahara, H. and Uhlenbeck, O. C. (2005) "Predicting the Binding Affinities of Misacylated tRNAs for *Thermus thermophilus* EF-Tu·GTP", *Biochemistry*, 44(33), pp. 11254–11261.

Asano, K., Shalev, A., Phan, L., Nielsen, K., Clayton, J., Valásek, L., Donahue, T. F. and Hinnebusch, A. G. (2001) "Multiple roles for the C-terminal domain of eIF5 in translation initiation complex assembly and GTPase activation.", *The EMBO journal*, 20(9), pp. 2326–37.

Åström, S. U. and Byström, A. S. (1994) "Rit1, a tRNA backbone-modifying enzyme that mediates initiator and elongator tRNA discrimination", *Cell*. Cell Press, 79(3), pp. 535–546.

Åström, S. U., von Pawel-Rammingen, U. and Byström, A. S. (1993) "The Yeast Initiator tRNA^{Met} can Act as an Elongator tRNA^{Met} In Vivo", *Journal of Molecular Biology*, 233(1), pp. 43–58.

Aufschnaiter, A., Habernig, L., Kohler, V., Diessl, J., Carmona-Gutierrez, D., Eisenberg, T., Keller, W. and Büttner, S. (2017) "The Coordinated Action of Calcineurin and Cathepsin D Protects Against α -Synuclein Toxicity", *Frontiers in Molecular Neuroscience*. Frontiers, 10, p. 207.

Ayer, A., Sanwald, J., Pillay, B. A., Meyer, A. J., Perrone, G. G. and Dawes, I. W. (2013) "Distinct Redox Regulation in Sub-Cellular Compartments in Response to Various Stress Conditions in *Saccharomyces cerevisiae*", *PLoS ONE*. Edited by J. Rutherford, 8(6), p. e65240.

B

Balleza, E., Kim, J. M. and Cluzel, P. (2017) "Systematic characterization of maturation time of fluorescent proteins in living cells", *Nature Methods*, 15(1), pp. 47–51.

Bandyopadhyay, A. K. and Deutscher, M. P. (1971) "Complex of aminoacyl-transfer RNA synthetases", *Journal of Molecular Biology*, 60(1), pp. 113–122.

Becker, H. D., Reinbolt, J., Kreutzer, R., Giegé, R. and Kern, D. (1997) "Existence of Two Distinct Aspartyl-tRNA Synthetases in *Thermus thermophilus*. Structural and Biochemical Properties of the Two Enzymes", *Biochemistry*, 36(29), pp. 8785–8797.

Becker, H. D. and Kern, D. (1998) "Thermus thermophilus: a link in evolution of the tRNA-dependent amino acid amidation pathways.", *PNAS*, 95(22), pp. 12832–7.

Beikirch, H., von der Haar, F. and Cramer, F. (1972) "Tyrosyl-tRNA synthetase from baker's yeast. Isolation and some properties.", *European journal of biochemistry*, 26(2), pp. 182–90.

Bender, A., Hajjeva, P. and Moosmann, B. (2008) "Adaptive antioxidant methionine accumulation in respiratory chain complexes explains the use of a deviant genetic code in mitochondria.", *PNAS*, 105(43), pp. 16496–501.

Berlett, B. S. and Stadtman, E. R. (1997) "Protein oxidation in aging, disease, and oxidative stress.", *The Journal of biological chemistry*, 272(33), pp. 20313–6.

Bertaccini, D., Vaca, S., Carapito, C., Arsène-Ploetze, F., Van Dorsselaer, A. and Schaeffer-Reiss, C. (2013) "An Improved Stable Isotope N-Terminal Labeling Approach with Light/Heavy TMPP To Automate Proteogenomics Data Validation: dN-TOP", *Journal of Proteome Research*, 12(6), pp. 3063–3070.

Bertram, G., Bell, H. A., Ritchie, D. W., Fullerton, G. and Stansfield, I. (2000) "Terminating eukaryote translation: domain 1 of release factor eRF1 functions in stop codon recognition.", *RNA*, 6(9), pp. 1236–47.

Betha, A. K., Williams, A. M. and Martinis, S. A. (2007) "Isolated CP1 domain of *Escherichia coli* leucyl-tRNA synthetase is dependent on flanking hinge motifs for amino acid editing activity.", *Biochemistry*, 46(21), pp. 6258–67.

Bitter, G. A. and Egan, K. M. (1984) "Expression of heterologous genes in *Saccharomyces cerevisiae* from vectors utilizing the glyceraldehyde-3-phosphate dehydrogenase gene promoter", *Gene*, 32(3), pp. 263–274.

Black, S., Harte, E. M., Hudson, B. and Wartofsky, L. (1960) 'A Specific Enzymatic Reduction of L(-) Methionine Sulfoxide and a Related Nonspecific Reduction of Disulfides', *The Journal of biological chemistry*, 235(10), pp. 2910–16

Blight, S. K., Larue, R. C., Mahapatra, A., Longstaff, D. G., Chang, E., Zhao, G., Kang, P. T., Green-Church, K. B., Chan, M. K. and Krzycki, J. A. (2004) "Direct charging of tRNA^{CUA} with pyrrolysine in vitro and in vivo", *Nature*, 431(7006), pp. 333–335.

Boccaletto, P., Machnicka, M. A., Purta, E., Piatkowski, P., Baginski, B., Wirecki, T. K., de Crécy-Lagard, V., Ross, R., Limbach, P. A., Kotter, A., Helm, M. and Bujnicki, J. M. (2018) "MODOMICS: a database of RNA modification pathways. 2017 update.", *Nucleic Acids Research*, 46(D1), pp. D303–D307.

Böck, A., Forchhammer, K., Heider, J., Leinfelder, W., Sawers, G., Veprek, B. and Zinoni, F. (1991) "Selenocysteine: the 21st amino acid.", *Molecular microbiology*, 5(3), pp. 515–20.

Brakmann, S. and Grzeszik, S. (2001) "An Error-Prone T7 RNA Polymerase Mutant Generated by Directed Evolution", *ChemBioChem*. 2(3), pp. 212–219.

Brot, N. and Weissbach, H. (1983) "Biochemistry and physiological role of methionine sulfoxide residues in proteins", *Archives of Biochemistry and Biophysics*, 223(1), pp. 271–281.

Brunie, S., Zelwer, C. and Risler, J.-L. (1990) "Crystallographic study at 2.5 Å resolution of the interaction of methionyl-tRNA synthetase from *Escherichia coli* with ATP", *Journal of Molecular Biology*, 216(2), pp. 411–424.

Brüning, L., Hackert, P., Martin, R., Davila Gallesio, J., Aquino, G. R. R., Urlaub, H., Sloan, K. E. and Bohnsack, M. T. (2018) "RNA helicases mediate structural transitions and compositional changes in pre-ribosomal complexes", *Nature Communications*, 9(1), p. 5383.

Bult, C. J., White, O., Olsen, G. J., Zhou, L., Fleischmann, R. D., Sutton, G. G., Blake, J. A., FitzGerald, L. M., Clayton, R. A., Gocayne, J. D., Kerlavage, A. R., Dougherty, B. A., Tomb, J. F., Adams, M. D., Reich, C. I., *et al.* (1996) "Complete genome sequence of the methanogenic archaeon, *Methanococcus jannaschii*.", *Science*, 273(5278), pp. 1058–73.

Bus, J. S. and Gibson, J. E. (1984) "Paraquat: model for oxidant-initiated toxicity.", *Environmental Health Perspectives*, 55, pp. 37–46.

C

Cahuzac, B., Berthonneau, E., Birlirakis, N., Guittet, E. and Mirande, M. (2000) "A recurrent RNA-binding domain is appended to eukaryotic aminoacyl-tRNA synthetases.", *The EMBO journal*, 19(3), pp. 445–52.

- Carapito, C., Burel, A., Guterl, P., Walter, A., Varrier, F., Bertile, F. and Van Dorsselaer, A. (2014) "MSDA, a proteomics software suite for in-depth Mass Spectrometry Data Analysis using grid computing", *PROTEOMICS*, 14(9), pp. 1014–1019.
- Carapito, C., Lane, L., Benama, M., Opsomer, A., Mouton-Barbosa, E., Garrigues, L., Gonzalez de Peredo, A., Burel, A., Bruley, C., Gateau, A., Bouyssié, D., Jaquinod, M., Cianferani, S., Burlet-Schiltz, O., Van Dorsselaer, A., *et al.* (2015) "Computational and Mass-Spectrometry-Based Workflow for the Discovery and Validation of Missing Human Proteins: Application to Chromosomes 2 and 14", *Journal of Proteome Research*, 14(9), pp. 3621–3634.
- Carmona-Gutiérrez, D., Bauer, M., Ring, J., Knauer, H., Eisenberg, T., Büttner, S., Ruckenstein, C., Reisenbichler, A., Magnes, C., Rechberger, G., Birner-Gruenberger, R., Jungwirth, H., Fröhlich, K.-U., Sinner, F., Kroemer, G., *et al.* (2011) "The propeptide of yeast cathepsin D inhibits programmed necrosis", *Cell Death and Disease*, 2(5), pp. e161–e161.
- Cassio, D. and Waller, J.-P. (1971) "Modification of Methionyl-tRNA Synthetase by Proteolytic Cleavage and Properties of the Trypsin-Modified Enzyme", *European Journal of Biochemistry*, 20(2), pp. 283–300.
- Cavener, D. R. (1987) "Comparison of the consensus sequence flanking translational start sites in *Drosophila* and vertebrates.", *Nucleic Acids Research*, 15(4), pp. 1353–61.
- Chambers, I., Frampton, J., Goldfarb, P., Affara, N., McBain, W. and Harrison, P. R. (1986) "The structure of the mouse glutathione peroxidase gene: the selenocysteine in the active site is encoded by the "termination" codon, TGA.", *The EMBO journal*, 5(6), pp. 1221–7.
- Chan, P. P., Lowe, T. M. (2009) "GtRNADB: a database of transfer RNA genes detected in genomic sequence", *Nucleic Acids Research*, 37(Database issue), D93–97.
- Chang, C.-Y. C.-P., Chang, C.-Y. C.-P., Chakraborty, S., Wang, S.-W., Tseng, Y.-K. and Wang, C.-C. (2016) "Modulating the structure and function of an aminoacyl-tRNA synthetase cofactor by biotinylation.", *The Journal of biological chemistry*, 291(33), pp. 17102–11.
- Chen, J. Y., Kirchner, G., Aebi, M. and Martin, N. C. (1990) "Purification and properties of yeast ATP (CTP):tRNA nucleotidyltransferase from wild type and overproducing cells.", *The Journal of biological chemistry*, 265(27), pp. 16221–4.
- Cheong, H.-K., Park, J.-Y., Kim, E.-H., Lee, C., Kim, S., Kim, Y., Choi, B.-S. and Cheong, C. (2003) "Structure of the N-terminal extension of human aspartyl-tRNA synthetase: implications for its biological function", *The International Journal of Biochemistry & Cell Biology*, 35(11), pp. 1548–1557.
- Chicher, J., Simonetti, A., Kuhn, L., Schaeffer, L., Hammann, P., Eriani, G. and Martin, F. (2015) "Purification of mRNA-programmed translation initiation complexes suitable for mass spectrometry analysis", *PROTEOMICS*, 15(14), pp. 2417–2425.
- Cho, H. Y. H. J., Maeng, S. J., Cho, H. Y. H. J., Choi, Y. S., Chung, J. M., Lee, S., Kim, H. K., Kim, J. H., Eom, C.-Y., Kim, Y.-G., Guo, M., Jung, H. S., Kang, B. S. and Kim, S. (2015) "Assembly of Multi-tRNA Synthetase Complex via Heterotetrameric Glutathione Transferase-homology Domains", *The Journal of biological chemistry*, 290(49), pp. 29313–29328.
- Cigan, A. M., Feng, L. and Donahue, T. F. (1988) "tRNA_i(met) functions in directing the scanning ribosome to the start site of translation.", *Science*, 242(4875), pp. 93–7.

Cooper, J. F. (1982) "Nitrogen metabolism in *Saccharomyces cerevisiae*", in Strathern, J. N., Jones, E. W., and Broach, J. R. (eds) *The Molecular Biology of the Yeast Saccharomyces: Metabolism and Gene Expression*. Cold Spring, pp. 39–100.

Copeland, P. R., Fletcher, J. E., Carlson, B. A., Hatfield, D. L. and Driscoll, D. M. (2000) "A novel RNA binding protein, SBP2, is required for the translation of mammalian selenoprotein mRNAs.", *The EMBO journal*, 19(2), pp. 306–14.

Crepin, T., Peterson, F., Haertlein, M., Jensen, D., Wang, C., Cusack, S. and Kron, M. (2011) "A Hybrid Structural Model of the Complete *Brugia malayi* Cytoplasmic Asparaginyl-tRNA Synthetase", *Journal of Molecular Biology*, 405(4), pp. 1056–1069.

Crick, F. H. C. (1966) "Codon–anticodon pairing: The wobble hypothesis", *Journal of Molecular Biology*, 19(2), pp. 548–555.

Crick, F. H. C. (1968) "The origin of the genetic code", *Journal of Molecular Biology*, 38(3), pp. 367–379.

Crooks, G. E., Hon, G., Chandonia, J.-M. and Brenner, S. E. (2004) "WebLogo: A Sequence Logo Generator", *Genome research*, 14, pp. 1188–1190.

Curnow, A. W., Hong, K. -w., Yuan, R., Kim, S. -i., Martins, O., Winkler, W., Henkin, T. M. and Soll, D. (1997) "Glu-tRNA^{Gln} amidotransferase: A novel heterotrimeric enzyme required for correct decoding of glutamine codons during translation", *PNAS*, 94(22), pp. 11819–11826.

Cusack, S., Berthet-Colominas, C., Härtlein, M., Nassar, N. and Leberman, R. (1990) "A second class of synthetase structure revealed by X-ray analysis of *Escherichia coli* seryl-tRNA synthetase at 2.5 Å", *Nature*, 347(6290), pp. 249–255.

Cvetesic, N., Semanjski, M., Soufi, B., Krug, K., Gruic-Sovulj, I. and Macek, B. (2016) "Proteome-wide measurement of non-canonical bacterial mistranslation by quantitative mass spectrometry of protein modifications", *Scientific Reports*, 6(1), p. 28631.

D

Davidson, J. F., Whyte, B., Bissinger, P. H. and Schiestl, R. H. (1996) "Oxidative stress is involved in heat-induced cell death in *Saccharomyces cerevisiae*.", *PNAS*, 93(10), pp. 5116–5121.

Davidson, J. F. and Schiestl, R. H. (2001a) "Cytotoxic and Genotoxic Consequences of Heat Stress Are Dependent on the Presence of Oxygen in *Saccharomyces cerevisiae*", *Journal of Bacteriology*, 183(15), pp. 4580–4587.

Davidson, J. F. and Schiestl, R. H. (2001b) "Mitochondrial Respiratory Electron Carriers Are Involved in Oxidative Stress during Heat Stress in *Saccharomyces cerevisiae*", *Molecular and Cellular Biology*, 21(24), pp. 8483–8489.

Debard, S., Bader, G., De Craene, J.-O., Enkler, L., Bär, S., Laporte, D., Hammann, P., Myslinski, E., Senger, B., Friant, S. and Becker, H. D. (2016) "Nonconventional localizations of cytosolic aminoacyl-tRNA synthetases in yeast and human cells", *Methods*, 113, pp. 91–104.

Deinert, K., Fasiolo, F., Hurt, E. C. and Simos, G. (2001) "Arc1p Organizes the Yeast Aminoacyl-tRNA Synthetase Complex and Stabilizes Its Interaction with the Cognate tRNAs^{*}", *The Journal of biological chemistry*, 276(23), pp. 6000–6008.

Dembowski, J. A., Kuo, B. and Woolford, J. L. (2013) "Has1 regulates consecutive maturation and processing steps for assembly of 60S ribosomal subunits", *Nucleic Acids Research*, 41(16), pp. 7889–7904.

Despons, L., Walter, P., Senger, B., Ebel, J. P. and Fasiolo, F. (1991) "Identification of potential amino acid residues supporting anticodon recognition in yeast methionyl-tRNA synthetase.", *FEBS letters*, 289(2), pp. 217–20.

Dever, T. E., Kinzy, T. G. and Pavitt, G. D. (2016) "Mechanism and Regulation of Protein Synthesis in *Saccharomyces cerevisiae*", *Genetics*, 203(1).

Dintziz, H. M. (1961) "Assembly of the peptide chains of hemoglobin.", *PNAS*, 47(3), pp. 247–61.

Dong, J., Qiu, H., Garcia-Barrio, M., Anderson, J. and Hinnebusch, A. G. (2000) "Uncharged tRNA activates GCN2 by displacing the protein kinase moiety from a bipartite tRNA-binding domain.", *Molecular cell*, 6(2), pp. 269–79.

Dong, J., Munoz, A., Kolitz, S. E., Saini, A. K., Chiu, W., Rahman, H., Lorsch, J. R. and Hinnebusch, A. G. (2014) "Conserved residues in yeast initiator tRNA calibrate initiation accuracy by regulating preinitiation complex stability at the start codon", *Genes & Development*, 28(5), pp. 502–520.

Doubl e, S., Bricogne, G., Gilmore, C. and Carter, C. W. (1995) "Tryptophanyl-tRNA synthetase crystal structure reveals an unexpected homology to tyrosyl-tRNA synthetase.", *Structure (London, England : 1993)*, 3(1), pp. 17–31.

Dreyer, T. (1989) "Substrate specificity of proteinase yscA from *Saccharomyces cerevisiae*", *Carlsberg Res. Commun*, 54(3), pp. 85–97.

Drummond, D. A. and Wilke, C. O. (2009) "The evolutionary consequences of erroneous protein synthesis.", *Nature reviews. Genetics*, 10(10), pp. 715–24.

E

Enkler, L. (2014) '*Le complexe multisynth etasiq ue AME de levure : Dynamique de l' edifice et r oles non canoniques de ces composants*'. PhD thesis, University Of Strasbourg.

Eriani, G., Delarue, M., Poch, O., Gangloff, J. and Moras, D. (1990) "Partition of tRNA synthetases into two classes based on mutually exclusive sets of sequence motifs", *Nature*, 347(6289), pp. 203–206.

Evans, D., Marquez, S. M. and Pace, N. R. (2006) "RNase P: interface of the RNA and protein worlds", *Trends in Biochemical Sciences*, 31(6), pp. 333–341.

F

Fagegaltier, D., Hubert, N., Yamada, K., Mizutani, T., Carbon, P. and Krol, A. (2000) "Characterization of mSelB, a novel mammalian elongation factor for selenoprotein translation.", *The EMBO journal*, 19(17), pp. 4796–805.

Farruggio, D., Chaudhuri, J., Maitra, U. and RajBhandary, U. L. (1996) "The A1 x U72 base pair conserved in eukaryotic initiator tRNAs is important specifically for binding to the eukaryotic translation initiation factor eIF2.", *Molecular and Cellular Biology*, 16(8), pp. 4248–56.

- Fernández-Murray, J. P. and McMaster, C. R. (2006) "Identification of novel phospholipid binding proteins in *Saccharomyces cerevisiae*", *FEBS Letters*, 580(1), pp. 82–86.
- Finarov, I., Moor, N., Kessler, N., Klipcan, L. and Safro, M. G. (2010) "Structure of Human Cytosolic Phenylalanyl-tRNA Synthetase: Evidence for Kingdom-Specific Design of the Active Sites and tRNA Binding Patterns", *Structure*, 18(3), pp. 343–353.
- Finkel, T. and Holbrook, N. J. (2000) "Oxidants, oxidative stress and the biology of ageing", *Nature*, 408(6809), pp. 239–247.
- Firczuk, H., Kannambath, S., Pahle, J., Claydon, A., Beynon, R., Duncan, J., Westerhoff, H., Mendes, P. and McCarthy, J. E. (2013) "An in vivo control map for the eukaryotic mRNA translation machinery.", *Molecular systems biology*, 9, p. 635.
- Forchhammer, K., Leinfelder, W. and Böck, A. (1989) "Identification of a novel translation factor necessary for the incorporation of selenocysteine into protein", *Nature*, 342(6248), pp. 453–456.
- Forner, J. and Binder, S. (2007) "The red fluorescent protein eqFP611: application in subcellular localization studies in higher plants.", *BMC plant biology*. BioMed Central, 7, p. 28.
- Forney-Stevens, K. M., Bogner, R. H. and Pikal, M. J. (2016) "Addition of Amino Acids to Further Stabilize Lyophilized Sucrose-Based Protein Formulations: I. Screening of 15 Amino Acids in Two Model Proteins", *Journal of Pharmaceutical Sciences*, 105(2), pp. 697–704.
- Fournier, G. P., Andam, C. P., Alm, E. J. and Gogarten, J. P. (2011) "Molecular Evolution of Aminoacyl tRNA Synthetase Proteins in the Early History of Life", *Origins of Life and Evolution of Biospheres*. Springer Netherlands, 41(6), pp. 621–632.
- Francin, M., Kaminska, M., Kerjan, P. and Mirande, M. (2002) "The N-terminal domain of mammalian Lysyl-tRNA synthetase is a functional tRNA-binding domain.", *The Journal of biological chemistry*, 277(3), pp. 1762–9.
- Francis, M. A. and Rajbhandary, U. L. (1990) "Expression and function of a human initiator tRNA gene in the yeast *Saccharomyces cerevisiae*", *Molecular and Cellular Biology*, 10(9), pp. 4486–94.
- Frantz, J. D. and Gilbert, W. (1995) "A novel yeast gene product, G4p1, with a specific affinity for quadruplex nucleic acids.", *The Journal of biological chemistry*, 270(35), pp. 20692–7.
- Frechin, M., Senger, B., Braye, M., Kern, D., Martin, R. P. and Becker, H. D. (2009) "Yeast mitochondrial Gln-tRNA^{Gln} is generated by a GatFAB-mediated transamidation pathway involving Arc1p-controlled subcellular sorting of cytosolic GluRS", *Genes & Development*, 23(9), pp. 1119–1130.
- Frechin, M., Kern, D., Martin, R. P., Becker, H. D. and Senger, B. (2010) "Arc1p: Anchoring, routing, coordinating", *FEBS Letters*, 584(2), pp. 427–433.
- Frechin, M., Enkler, L., Tetaud, E., Laporte, D., Senger, B., Blancard, C., Hammann, P., Bader, G., Clauder-Münster, S., Steinmetz, L. M., Martin, R. P., di Rago, J.-P. and Becker, H. D. (2014) "Expression of Nuclear and Mitochondrial Genes Encoding ATP Synthase Is Synchronized by Disassembly of a Multisynthetase Complex", *Molecular Cell*, 56(6), pp. 763–776.
- Frugier, M., Moulinier, L. and Giegé, R. (2000) "A domain in the N-terminal extension of class IIb eukaryotic aminoacyl-tRNA synthetases is important for tRNA binding", *The EMBO Journal*, 19(10), pp. 2371–2380.

Fu, Y., Kim, Y., Jin, K. S., Kim, H. S., Kim, J. H., Wang, D., Park, M., Jo, C. H., Kwon, N. H., Kim, D., Kim, M. H., Jeon, Y. H., Hwang, K. Y., Kim, S. and Cho, Y. (2014) "Structure of the ArgRS-GlnRS-AIMP1 complex and its implications for mammalian translation.", *PNAS*, 111(42), pp. 15084–9.

Fukui, H., Hanaoka, R. and Kawahara, A. (2009) "Noncanonical activity of seryl-tRNA synthetase is involved in vascular development.", *Circulation research*, 104(11), pp. 1253–9.

G

Galani, K., Großhans, H., Deinert, K., Hurt, E. C. and Simos, G. (2001) "The intracellular location of two aminoacyl-tRNA synthetases depends on complex formation with Arc1p", *The EMBO Journal*. EMBO Press, 20(23), pp. 6889–6898.

Galani, K., Hurt, E. and Simos, G. (2005) "The tRNA aminoacylation co-factor Arc1p is excluded from the nucleus by an Xpo1p-dependent mechanism", *FEBS Letters*. 579(5), pp. 969–975.

Gallien, S., Perrodou, E., Carapito, C., Deshayes, C., Reyrat, J.-M., Van Dorselaer, A., Poch, O., Schaeffer, C. and Lecompte, O. (2009) "Ortho-proteogenomics: multiple proteomes investigation through orthology and a new MS-based protocol.", *Genome research*, 19(1), pp. 128–35.

Giegé, R., Sissler, M. and Florentz, C. (1998) "Universal rules and idiosyncratic features in tRNA identity", *Nucleic Acids Research*, 26(22).

Gietz, D. R. and Woods, R. A. (2002) "Transformation of yeast by lithium acetate/single-stranded carrier DNA/polyethylene glycol method", *Methods in Enzymology*, 350, pp. 87–96.

Godard, P., Urrestarazu, A., Vissers, S., Kontos, K., Bontempi, G., van Helden, J. and Andre, B. (2007) "Effect of 21 Different Nitrogen Sources on Global Gene Expression in the Yeast *Saccharomyces cerevisiae*", *Molecular and Cellular Biology*, 27(8), pp. 3065–3086.

Godinic-Mikulcic, V., Jaric, J., Greber, B. J., Franke, V., Hodnik, V., Anderluh, G., Ban, N. and Weygand-Durasevic, I. (2014) "Archaeal aminoacyl-tRNA synthetases interact with the ribosome to recycle tRNAs", *Nucleic Acids Research*, 42(8), pp. 5191–5201.

Gomes, A. N. A. C., Kordala, A. J., Strack, R., Wang, X., Geslain, R., Delaney, K., Clark, W. C., Keenan, R. and Pan, T. A. O. (2016) "A dual fluorescent reporter for the investigation of methionine mistranslation in live cells", *RNA*, 22, pp. 1–10.

González Montoro, A., Auffarth, K., Hönscher, C., Bohnert, M., Becker, T., Warscheid, B., Reggiori, F., van der Laan, M., Fröhlich, F. and Ungermann, C. (2018) "Vps39 Interacts with Tom40 to Establish One of Two Functionally Distinct Vacuole-Mitochondria Contact Sites.", *Developmental cell*, 45(5), pp. 621–636.e7.

Graindorge, J.-S., Senger, B., Tritch, D., Simos, G. and Fasiolo, F. (2005) "Role of Arc1p in the Modulation of Yeast Glutamyl-tRNA Synthetase Activity^{††}", *Biochemistry*, 44(4), pp. 1344–1352.

Grosshans, H., Hurt, E. and Simos, G. (2000) "An aminoacylation-dependent nuclear tRNA export pathway in yeast.", *Genes & development*, 14(7), pp. 830–40.

Gu, W., Jackman, J. E., Lohan, A. J., Gray, M. W. and Phizicky, E. M. (2003) "tRNA^{His} maturation: an essential yeast protein catalyzes addition of a guanine nucleotide to the 5' end of tRNA^{His}.", *Genes & development*, 17(23), pp. 2889–901.

Gunasekera, N., Lee, S. W., Kim, S., Musier-Forsyth, K. and Arriaga, E. (2004) "Nuclear localization of aminoacyl-tRNA synthetases using single-cell capillary electrophoresis laser-induced fluorescence analysis.", *Analytical chemistry*, 76(16), pp. 4741–6.

Guo, M., Schimmel, P. and Yang, X.-L. (2010) "Functional expansion of human tRNA synthetases achieved by structural inventions", *FEBS Letters*. 584(2), pp. 434–442.

Guo, M. and Yang, X.-L. (2014) "Architecture and metamorphosis.", *Topics in current chemistry*, 344, pp. 89–118.

von der Haar, T. (2008) "A quantitative estimation of the global translational activity in logarithmically growing yeast cells.", *BMC systems biology*. BioMed Central, 2, p. 87.

H

Hamilton, R., Watanabe, C. K. and de Boer, H. A. (1987) "Compilation and comparison of the sequence context around the AUG startcodons in *Saccharomyces cerevisiae* mRNAs.", *Nucleic Acids Research*, 15(8), pp. 3581–93.

Hao, B., Gong, W., Ferguson, T. K., James, C. M., Krzycki, J. A. and Chan, M. K. (2002) "A new UAG-encoded residue in the structure of a methanogen methyltransferase.", *Science*, 296(5572), pp. 1462–6.

Harris, C. L. (1987) "An aminoacyl-tRNA synthetase complex in *Escherichia coli*.", *Journal of bacteriology*, 169(6), pp. 2718–23.

Hauenstein, S. I., Hou, Y.-M. and Perona, J. J. (2008) "The homotetrameric phosphoseryl-tRNA synthetase from *Methanosarcina mazei* exhibits half-of-the-sites activity.", *The Journal of biological chemistry*, 283(32), pp. 21997–2006.

Hausmann, C. D. and Ibba, M. (2008) "Aminoacyl-tRNA synthetase complexes: molecular multitasking revealed.", *FEMS microbiology reviews*, 32(4), pp. 705–21.

Havrylenko, S. and Mirande, M. (2015) "Aminoacyl-tRNA synthetase complexes in evolution.", *International journal of molecular sciences*. Multidisciplinary Digital Publishing Institute (MDPI), 16(3), pp. 6571–94.

Holley, R. W., Apgar, J., Everett, G. A., Madison, J. T., Marquisee, M., Merrill, S. H., Penswick, J. R. and Zamir, A. (1965) "Structure of a Ribonucleic Acid", *Science*, 147(3664), pp. 1462–1465.

Hong, K. W., Ibba, M., Weygand-Durasevic, I., Rogers, M. J., Thomann, H. U. and Söll, D. (1996) "Transfer RNA-dependent cognate amino acid recognition by an aminoacyl-tRNA synthetase.", *The EMBO journal*, 15(8), pp. 1983–91.

Hossain, A. and Kallenbach, N. R. (1974) "Purification and subunit structure of tryptophanyl tRNA synthetase (TRS) from baker's yeast", *FEBS Letters*, 45(1), pp. 202–5.

Housman, D., Jacobs-Loreana, M., Rajbhandary, U. L. and Lodish, H. F. (1970) "Initiation of Haemoglobin Synthesis by Methionyl-tRNA", *Nature*, 227(5261), pp. 913–918.

Hubert, N., Sturchler, C., Westhof, E., Carbon, P. and Krol, A. (1998) "The 9/4 secondary structure of eukaryotic selenocysteine tRNA: More pieces of evidence", *RNA*, 4(9), pp. 1029–33.

I

Ibba, M., Losey, H. C., Kawarabayasi, Y., Kikuchi, H., Bunjun, S. and Söll, D. (1999) "Substrate recognition by class I lysyl-tRNA synthetases: a molecular basis for gene displacement.", *PNAS*, 96(2), pp. 418–23.

Ibba, M., Curnow, A. W. and Söll, D. (1997) "Aminoacyl-tRNA synthesis: divergent routes to a common goal.", *Trends in biochemical sciences*, 22(2), pp. 39–42.

Ichetovkin, I. E., Abramochkin, G. and Shrader, T. E. (1997) "Substrate Recognition by the Leucyl/Phenylalanyl-tRNA-protein Transferase", *Journal of Biological Chemistry*, 272(52), pp. 33009–33014.

Iizuka, N., Najita, L., Franzusoff, A. and Sarnow, P. (1994) "Cap-dependent and cap-independent translation by internal initiation of mRNAs in cell extracts prepared from *Saccharomyces cerevisiae*.", *Molecular and Cellular Biology*, 14(11), pp. 7322–30.

Ilan, Y. A., Czapski, G. and Meisel, D. (1976) "The one-electron transfer redox potentials of free radicals". *Biochimica et Biophysica Acta*, 430, pp. 209–224.

Inoue, M., Sato, E. F., Nishikawa, M., Park, A.-M., Kira, Y., Imada, I. and Utsumi, K. (2003) "Mitochondrial generation of reactive oxygen species and its role in aerobic life.", *Current medicinal chemistry*, 10(23), pp. 2495–505.

J

Jackman, J. E. and Alfonzo, J. D. (2013) "Transfer RNA modifications: nature's combinatorial chemistry playground.", *Wiley interdisciplinary reviews. RNA*, 4(1), pp. 35–48.

Jacob, F. and Monod, J. (1961) "Genetic regulatory mechanisms in the synthesis of proteins", *Journal of Molecular Biology*, 3(3), pp. 318–356.

Jia, J., Arif, A., Ray, P. S. and Fox, P. L. (2008) "WHEP domains direct noncanonical function of glutamyl-Prolyl tRNA synthetase in translational control of gene expression.", *Molecular cell*, 29(6), pp. 679–90.

Jones, T. E., Alexander, R. W. and Pan, T. (2011) "Misacylation of specific nonmethionyl tRNAs by a bacterial methionyl-tRNA synthetase", *PNAS*, 108(17).

K

Kaminska, M., Shalak, V. and Mirande, M. (2001) "The Appended C-Domain of Human Methionyl-tRNA Synthetase Has a tRNA-Sequestering Function", *Biochemistry*, 40(47), pp. 14309–16.

Kao, J., Ryan, J., Brett, G., Chen, J., Shen, H., Fan, Y. G., Godman, G., Familletti, P. C., Wang, F. and Pan, Y. C. (1992) "Endothelial monocyte-activating polypeptide II. A novel tumor-derived polypeptide that activates host-response mechanisms.", *The Journal of biological chemistry*, 267(28), pp. 20239–47.

Kapp, L. D., Kolitz, S. E. and Lorsch, J. R. (2006) "Yeast initiator tRNA identity elements cooperate to influence multiple steps of translation initiation", *RNA*, 12(5), pp. 751–764.

Kapp, L. D. and Lorsch, J. R. (2004) "GTP-dependent recognition of the methionine moiety on initiator tRNA by translation factor eIF2.", *Journal of molecular biology*, 335(4), pp. 923–36.

Karanasios, E., Simader, H., Panayotou, G., Suck, D. and Simos, G. (2007) "Molecular Determinants of the Yeast Arc1p–Aminoacyl-tRNA Synthetase Complex Assembly", *Journal of Molecular Biology*, 374(4), pp. 1077–1090.

Karim, A. S., Curran, K. A. and Alper, H. S. (2013) "Characterization of plasmid burden and copy number in *Saccharomyces cerevisiae* for optimization of metabolic engineering applications", *FEMS yeast research*, 13(1), pp. 107–116.

Kavran, J. M., Gundllapalli, S., O'Donoghue, P., Englert, M., Soll, D. and Steitz, T. A. (2007) "Structure of pyrrolysyl-tRNA synthetase, an archaeal enzyme for genetic code innovation", *PNAS*, 104(27), pp. 11268–11273.

Kerjan, P., Cerini, C., Sémériva, M. and Mirande, M. (1994) "The multienzyme complex containing nine aminoacyl-tRNA synthetases is ubiquitous from *Drosophila* to mammals.", *Biochimica et biophysica acta*, 1199(3), pp. 293–7.

Kern, D. and Lapointe, J. (1979) "Glutamyl transfer ribonucleic acid synthetase of *Escherichia coli*. Study of the interactions with its substrates", *Biochemistry*, 18(26), pp. 5809–5818.

Khoshnevis, S., Gross, T., Rotte, C., Baierlein, C., Ficner, R. and Krebber, H. (2010) "The iron-sulphur protein RNase L inhibitor functions in translation termination", *EMBO reports*, 11(3), pp. 214–219.

Kim, H. S., Hoja, U., Stolz, J., Sauer, G. and Schweizer, E. (2004) "Identification of the tRNA-binding protein Arc1p as a novel target of in vivo biotinylation in *Saccharomyces cerevisiae*.", *The Journal of biological chemistry*, 279(41), pp. 42445–52.

Kim, S. H., Quigley, G. J., Suddath, F. L., McPherson, A., Sneden, D., Kim, J. J., Weinzierl, J. and Rich, A. (1973) "Three-Dimensional Structure of Yeast Phenylalanine Transfer RNA: Folding of the Polynucleotide Chain", *Science*, 179(4070), pp. 285–288.

Kitamoto, K., Yoshizawa, K., Ohsumi, Y. and Anraku, Y. (1988) "Dynamic aspects of vacuolar and cytosolic amino acid pools of *Saccharomyces cerevisiae*.", *Journal of bacteriology*. American Society for Microbiology Journals, 170(6), pp. 2683–6.

Klionsky, D. J., Herman, P. K. and Emr, S. D. (1990) "The fungal vacuole: composition, function, and biogenesis.", *Microbiological reviews*. American Society for Microbiology Journals, 54(3), pp. 266–92.

Ko, Y. G., Kang, Y. S., Kim, E. K., Park, S. G. and Kim, S. (2000) "Nucleolar localization of human methionyl-tRNA synthetase and its role in ribosomal RNA synthesis.", *The Journal of cell biology*. The Rockefeller University Press, 149(3), pp. 567–74.

Kolitz, S. E. and Lorsch, J. R. (2010) "Eukaryotic initiator tRNA: finely tuned and ready for action.", *FEBS letters*, 584(2), pp. 396–404.

Kondo, H., Shibano, Y., Amachi, T., Cronin, N., Oda, K. and Dunn, B. M. (1998) "Substrate Specificities and Kinetic Properties of Proteinase A from the Yeast *Saccharomyces cerevisiae* and the Development of a Novel Substrate", *Journal of Biochemistry*, 124(1), pp. 141–147.

Koonin, E. V, Mushegian, A. R., Tatusov, R. L., Altschul, S. F., Bryant, S. H., Bork, P. and Valencia, A. (1994) "Eukaryotic translation elongation factor 1 gamma contains a glutathione transferase domain--study of a diverse, ancient protein superfamily using motif search and structural modeling.", *Protein science : a publication of the Protein Society*, 3(11), pp. 2045–54.

Kosower, N. S. and Kosower, E. M. (1995) '*Diamide: An oxidant probe for thiols*', *Methods in enzymology*.

Kozak, M. (1986) "Point mutations define a sequence flanking the AUG initiator codon that modulates translation by eukaryotic ribosomes.", *Cell*, 44(2), pp. 283–92.

Kramer, E. B., Vallabhaneni, H., Mayer, L. M. and Farabaugh, P. J. (2010) "A comprehensive analysis of translational missense errors in the yeast *Saccharomyces cerevisiae*.", *RNA*, 16(9), pp. 1797–808.

Krassowski, T., Coughlan, A. Y., Shen, X.-X., Zhou, X., Kominek, J., Opulente, D. A., Riley, R., Grigoriev, I. V., Maheshwari, N., Shields, D. C., Kurtzman, C. P., Hittinger, C. T., Rokas, A. and Wolfe, K. H. (2018) "Evolutionary instability of CUG–Leu in the genetic code of budding yeasts.", *Nature communications*, 9(1), p. 1887.

Kunkel, T. A. and Bebenek, K. (2000) "DNA Replication Fidelity", *Annual Review of Biochemistry*, 69(1), pp. 497–529.

L

Lam, A. J., St-Pierre, F., Gong, Y., Marshall, J. D., Cranfill, P. J., Baird, M. A., McKeown, M. R., Wiedenmann, J., Davidson, M. W., Schnitzer, M. J., Tsien, R. Y. and Lin, M. Z. (2012) "Improving FRET dynamic range with bright green and red fluorescent proteins.", *Nature methods*, 9(10), pp. 1005–12.

Lapointe, J., Duplain, L. and Proulx, M. (1986) "A single glutamyl-tRNA synthetase aminoacylates tRNA^{Glu} and tRNA^{Gln} in *Bacillus subtilis* and efficiently misacylates *Escherichia coli* tRNA^{Gln1} in vitro.", *Journal of bacteriology*, 165(1), pp. 88–93.

Laporte, D., Huot, J. L., Bader, G., Enkler, L., Senger, B. and Becker, H. D. (2014) "Exploring the evolutionary diversity and assembly modes of multi-aminoacyl-tRNA synthetase complexes: Lessons from unicellular organisms", *FEBS Letters*, 588(23), pp. 4268–4278.

Laporte, D. (2016) '*Découverte et caractérisation d'une nouvelle forme de MetRS nucléaire chez la levure S. cerevisiae*', PhD thesis, University of Strasbourg

LaRiviere, F. J., Wolfson, A. D. and Uhlenbeck, O. C. (2001) "Uniform Binding of Aminoacyl-tRNAs to Elongation Factor Tu by Thermodynamic Compensation", *Science*, 294(5540), pp. 165–168.

Larson, E. T., Kim, J. E., Zucker, F. H., Kelley, A., Mueller, N., Napuli, A. J., Verlinde, C. L. M. J., Fan, E., Buckner, F. S., Van Voorhis, W. C., Merritt, E. A. and Hol, W. G. J. (2011) "Structure of Leishmania major methionyl-tRNA synthetase in complex with intermediate products methionyladenylate and pyrophosphate.", *Biochimie*, 93(3), pp. 570–82.

Laursen, B. S., Sørensen, H. P., Mortensen, K. K. and Sperling-Petersen, H. U. (2005) "Initiation of protein synthesis in bacteria.", *Microbiology and molecular biology reviews : MMBR*, 69(1), pp. 101–23.

Lee, B. J., Worland, P. J., Davis, J. N., Stadtman, T. C. and Hatfield, D. L. (1989) '*Identification of a Selenocysteyl-tRNA^{Ser} in Mammalian Cells That Recognizes the Nonsense Codon, UGA*', *The journal of biological chemistry*, 264(17), pp. 9724–7

Lee, H. J., Cho, H. Y. and Kang, B. S. (no date) "The crystal structure of human cytosolic methionyl-tRNA synthetase in complex with methionine", *To be published*.

- Lee, J. Y., Kim, D. G., Kim, B., Yang, W. S., Hong, J., Kang, T., Oh, Y. S., Kim, K. R., Han, B. W., Hwang, B. J., Kang, B. S., Kang, M. and Kim, M. (2014) "Promiscuous methionyl-tRNA synthetase mediates adaptive mistranslation to protect cells against oxidative stress", *Journal of cell science*, 127(19), pp. 4234–4245.
- Lee, P. S., Zhang, H.-M., Marshall, A. G., Yang, X.-L. and Schimmel, P. (2012) "Uncovering of a short internal peptide activates a tRNA synthetase procytokine.", *The Journal of biological chemistry*, 287(24), pp. 20504–8.
- Lei, H.-Y., Zhou, X.-L., Ruan, Z.-R., Sun, W.-C., Eriani, G. and Wang, E.-D. (2015) "Calpain Cleaves Most Components in the Multiple Aminoacyl-tRNA Synthetase Complex and Affects Their Functions", *Journal of Biological Chemistry*, 290(43), pp. 26314–26327.
- Leinfelder, W., Zehelein, E., MandrandBerthelot, M. and Bock, A. (1988) "Gene for a novel tRNA species that accepts L-serine and cotranslationally inserts selenocysteine", *Nature*, 331(6158), pp. 723–725.
- Levine, R. L., Mosoni, L., Berlett, B. S. and Stadtman, E. R. (1996) "Methionine residues as endogenous antioxidants in proteins", *PNAS*, 93(December), pp. 15036–15040.
- Li, S. C. and Kane, P. M. (2009) "The yeast lysosome-like vacuole: endpoint and crossroads.", *Biochimica et biophysica acta*, 1793(4), pp. 650–63.
- Lim, J. C., You, Z., Kim, G. and Levine, R. L. (2011) "Methionine sulfoxide reductase A is a stereospecific methionine oxidase", *PNAS*, 108(26), p. 10472.
- Lim, V. I. and Curran, J. F. (2001) "Analysis of codon:anticodon interactions within the ribosome provides new insights into codon reading and the genetic code structure.", *RNA*, 7(7), pp. 942–57.
- Limbach, P. A., Crain, P. F. and McCloskey, J. A. (1994) "Summary: the modified nucleosides of RNA", *Nucleic Acids Research*, 22(12), pp. 2183–2196.
- Ling, C. and Ermolenko, D. N. (2016) "Structural insights into ribosome translocation.", *Wiley interdisciplinary reviews. RNA*. Wiley-Blackwell, 7(5), pp. 620–36.
- Ling, J., Reynolds, N. and Ibba, M. (2009) "Aminoacyl-tRNA Synthesis and Translational Quality Control", *Annual Review of Microbiology*, 63(1), pp. 61–78.
- Ljungdahl, P. O. (2009) "Amino-acid-induced signalling via the SPS-sensing pathway in yeast.", *Biochemical Society transactions*. Portland Press Limited, 37(Pt 1), pp. 242–7.
- Ljungdahl, P. O. and Daignan-Fornier, B. (2012) "Regulation of Amino Acid, Nucleotide, and Phosphate Metabolism in *Saccharomyces cerevisiae*", *Genetics*, 190(3), pp. 885–929.
- Lourenço Dos Santos, S., Petropoulos, I. and Friguet, B. (2018) "The Oxidized Protein Repair Enzymes Methionine Sulfoxide Reductases and Their Roles in Protecting against Oxidative Stress, in Ageing and in Regulating Protein Function.", *Antioxidants*, 7(12).
- Low, S. C. and Berry, M. J. (1996) "Knowing when not to stop: selenocysteine incorporation in eukaryotes.", *Trends in biochemical sciences*, 21(6), pp. 203–8.
- Lund, E. and Dahlberg, J. E. (1998) "Proofreading and aminoacylation of tRNAs before export from the nucleus.", *Science*, 282(5396), pp. 2082–5.

Luo, S. and Levine, R. L. (2009) "Methionine in proteins defends against oxidative stress.", *FASEB journal : official publication of the Federation of American Societies for Experimental Biology*. The Federation of American Societies for Experimental Biology, 23(2), pp. 464–72.

M

Mailu, B. M., Li, L., Arthur, J., Nelson, T. M., Ramasamy, G., Fritz-Wolf, K., Becker, K. and Gardner, M. J. (2015) "Plasmodium Apicoplast Gln-tRNA^{Gln} Biosynthesis Utilizes a Unique GatAB Amidotransferase Essential for Erythrocytic Stage Parasites.", *The Journal of biological chemistry*, 290(49), pp. 29629–41.

Majumdar, R., Bandyopadhyay, A. and Maitra, U. (2003) "Mammalian translation initiation factor eIF1 functions with eIF1A and eIF3 in the formation of a stable 40 S preinitiation complex.", *The Journal of biological chemistry*, 278(8), pp. 6580–7.

Marck, C. and Grosjean, H. (2002) "tRNomics: analysis of tRNA genes from 50 genomes of Eukarya, Archaea, and Bacteria reveals anticodon-sparing strategies and domain-specific features.", *RNA*, 8(10), pp. 1189–232.

Marques, M., Mojzita, D., Amorim, M. A., Almeida, T., Hohmann, S., Moradas-Ferreira, P. and Costa, V. (2006) "The Pep4p vacuolar proteinase contributes to the turnover of oxidized proteins but PEP4 overexpression is not sufficient to increase chronological lifespan in *Saccharomyces cerevisiae*", *Microbiology*, 152, pp. 3595–3605.

Mason, D. A., Shulga, N., Undavai, S., Ferrando-May, E., Rexach, M. F. and Goldfarb, D. S. (2005) "Increased nuclear envelope permeability and Pep4p-dependent degradation of nucleoporins during hydrogen peroxide-induced cell death", *FEMS yeast research*, 5, pp. 1237–1251.

Mateyak, M. K. and Kinzy, T. G. (2010) "eEF1A: thinking outside the ribosome.", *The Journal of biological chemistry*, 285(28), pp. 21209–13.

Matz, M. V., Fradkov, A. F., Labas, Y. A., Savitsky, A. P., Zaraisky, A. G., Markelov, M. L. and Lukyanov, S. A. (1999) "Fluorescent proteins from nonbioluminescent Anthozoa species", *Nature Biotechnology*, 17(10), pp. 969–973.

McLeod, T., Abdullahi, A., Li, M. and Brogna, S. (2014) "Recent studies implicate the nucleolus as the major site of nuclear translation", *Biochemical Society Transactions*. Portland Press Limited, 42(4), pp. 1224–1228.

Mehler, A. H. and Mjtra, S. K. (1967) 'The Activation of Arginyl Transfer Ribonucleic Acid Synthetase by Transfer Ribonucleic Acid', *The Journal of biological chemistry*, 242(23), pp. 5495–9

Mellot, P., Mechulam, Y., Le Corre, D., Blanquet, S. and Fayat, G. (1989) "Identification of an amino acid region supporting specific methionyl-tRNA synthetase: tRNA recognition", *Journal of Molecular Biology*, 208(3), pp. 429–443.

Mer, A. S. and Andrade-Navarro, M. A. (2013) "A novel approach for protein subcellular location prediction using amino acid exposure", *BMC Bioinformatics*, 14(1), p. 342.

Messenguy, F., Colin, D. and Have, J.-P. TEN (1980) "Regulation of Compartmentation of Amino Acid Pools in *Saccharomyces cerevisiae* and Its Effects on Metabolic Control", *European Journal of Biochemistry*. 108(2), pp. 439–447.

Meyerovich, M., Mamou, G. and Ben-Yehuda, S. (2010) "Visualizing high error levels during gene expression in living bacterial cells.", *PNAS*, 107(25), pp. 11543–8.

Min Han, J., Jae Jeong, S., Chul Park, M., Kim, G., Hoon Kwon, N., Kyoung Kim, H., Hoon Ha, S., Ho Ryu, S., Kim, S., Han, J. M. M., Jeong, S. J. J., Park, M. C. C., Kim, G., Kwon, N. H. H., Kim, H. K. K., *et al.* (2012) "Leucyl-tRNA Synthetase Is an Intracellular Leucine Sensor for the mTORC1-Signaling Pathway", *Cell*, 149(2), pp. 410–424.

Miranda, I., Silva-Dias, A., Rocha, R., Teixeira-Santos, R., Coelho, C., Gonçalves, T., Santos, M. A. S., Pina-Vaz, C., Solis, N. V., Filler, S. G. and Rodrigues, A. G. (2013) "Candida albicans CUG mistranslation is a mechanism to create cell surface variation.", *MBio*, 4(4), pii: e00285-13.

Mirande, M. (2017) "The Aminoacyl-tRNA Synthetase Complex", in *Sub-cellular biochemistry*, pp. 505–522.

Mitra, S. K. and Mehler, A. H. (1966) 'The Role of Transfer Ribonucleic Acid in the Pyrophosphate Exchange Reaction of Arginine-Transfer Ribonucleic Acid Synthetase', *The Journal of biological chemistry*, 241, 5161-5162

Mohler, K. and Ibba, M. (2017) "Translational fidelity and mistranslation in the cellular response to stress", *Nature Microbiology*, 2(9), p. 17117.

Morano, K. A., Grant, C. M. and Moye-Rowley, W. S. (2012) "The Response to Heat Shock and Oxidative Stress in *Saccharomyces cerevisiae*", *Genetics*, 190(4).

Mörl, M. and Marchfelder, A. (2001) "The final cut. The importance of tRNA 3'-processing.", *EMBO reports*. EMBO Press, 2(1), pp. 17–20.

Mukai, T., Lajoie, M. J., Englert, M. and Söll, D. (2017) "Rewriting the Genetic Code.", *Annual review of microbiology*, 71, pp. 557–577.

Muller, F., Laboratory, F. M. and Kramer, D. M. (2000) 'The nature and mechanism of superoxide production by the electron transport chain: its relevance to aging', *J. Amer. Aging Assoc.*

MUTTERER, J. and ZINCK, E. (2013) "Quick-and-clean article figures with FigureJ", *Journal of Microscopy*. 252(1), pp. 89–91.

N

Nagao, A., Suzuki, T., Katoh, T., Sakaguchi, Y. and Suzuki, T. (2009) "Biogenesis of glutaminyl-mt tRNA^{Gln} in human mitochondria", *PNAS*, 106(38), pp. 16209–16214.

Negrutskii, B. S., Shalak, V. F., Kerjan, P., El'skaya, A. V and Mirande, M. (1999) "Functional interaction of mammalian valyl-tRNA synthetase with elongation factor eEF1Alpha in the complex with EF-1H.", *The Journal of biological chemistry*, 274(8), pp. 4545–50.

Netzer, N., Goodenbour, J. M., David, A., Dittmar, K. A., Jones, R. B., Schneider, J. R., Boone, D., Eves, E. M., Rosner, M. R., Gibbs, J. S., Embry, A., Dolan, B., Das, S., Hickman, H. D., Berglund, P., *et al.* (2009) "Innate immune and chemically triggered oxidative stress modifies translational fidelity", *Nature*, 462(7272), pp. 522–526.

Niederberger, P., Miozzari, G. and Hütter, R. (1981) "Biological role of the general control of amino acid biosynthesis in *Saccharomyces cerevisiae*.", *Molecular and Cellular Biology*, 1(7), pp. 584–93.

Nirenberg, M. W. and Matthaei, J. H. (1961) "The dependence of cell-free protein synthesis in *E. coli* upon naturally occurring or synthetic polyribonucleotides.", *PNAS*, 47(10), pp. 1588–602.

Nirenberg, M. W., Matthaei, J. H. and Jones, O. W. (1962) "An intermediate in the biosynthesis of polyphenylalanine directed by synthetic template RNA.", *PNAS*, 48(1), pp. 104–9.

Normanly, J., Ollick, T. and Abelson, J. (1992) "Eight base changes are sufficient to convert a leucine-inserting tRNA into a serine-inserting tRNA.", *PNAS*, 89(12), pp. 5680–4.

O

Obara, K., Noda, T., Niimi, K. and Ohsumi, Y. (2008) "Transport of phosphatidylinositol 3-phosphate into the vacuole via autophagic membranes in *Saccharomyces cerevisiae*", *Genes to Cells*, 13(6), pp. 537–547.

Ohira, T. and Suzuki, T. (2016) "Precursors of tRNAs are stabilized by methylguanosine cap structures", *Nature Chemical Biology*, 12(8), pp. 648–655.

Orgel, L. E. (1963) "The maintenance of the accuracy of protein synthesis and its relevance to ageing.", *PNAS*, 49(4), pp. 517–21.

Ou, X., Cao, J., Cheng, A., Peppelenbosch, M. P. and Pan, Q. (2019) "Errors in translational decoding: tRNA wobbling or misincorporation?", *PLoS genetics*, 15(3), p. e1008017.

P

Parenteau, J., Durand, M., Véronneau, S., Lacombe, A.-A., Morin, G., Guérin, V., Cecez, B., Gervais-Bird, J., Koh, C.-S., Brunelle, D., Wellinger, R. J., Chabot, B. and Abou Elela, S. (2008) "Deletion of many yeast introns reveals a minority of genes that require splicing for function.", *Molecular biology of the cell*, 19(5), pp. 1932–41.

Park, S. G., Kim, H. J., Min, Y. H., Choi, E.-C., Shin, Y. K., Park, B.-J., Lee, S. W. and Kim, S. (2005) "Human lysyl-tRNA synthetase is secreted to trigger proinflammatory response.", *PNAS*, 102(18), pp. 6356–61.

Parr, C. L., Keates, R. A. B., Bryksa, B. C., Ogawa, M. and Yada, R. Y. (2007) "The structure and function of *Saccharomyces cerevisiae* proteinase A", *Yeast*, 24(6), pp. 467–480.

Pawel-Rammingen, U. von, Aström, S. and Byström, A. S. (1992) "Mutational analysis of conserved positions potentially important for initiator tRNA function in *Saccharomyces cerevisiae*", *Molecular and Cellular Biology*, 12(4), p. 1432.

Perona, J. J. and Gruic-Sovulj, I. (2013) "Synthetic and Editing Mechanisms of Aminoacyl-tRNA Synthetases", in *Topics in current chemistry*, pp. 1–41.

Perona, J. J. and Hadd, A. (2012) "Structural Diversity and Protein Engineering of the Aminoacyl-tRNA Synthetases", *Biochemistry*, 51(44), pp. 8705–8729.

Peskin, A. V and Winterbourn, C. C. (2001) "Kinetics of the reactions of hypochlorous acid and amino acid chloramines with thiols, methionine, and ascorbate.", *Free radical biology & medicine*, 30(5), pp. 572–9.

Pestova, T. V., Lomakin, I. B., Lee, J. H., Choi, S. K., Dever, T. E. and Hellen, C. U. T. (2000) "The joining of ribosomal subunits in eukaryotes requires eIF5B", *Nature*, 403(6767), pp. 332–335.

Phizicky, E. M. and Hopper, A. K. (2010) "tRNA biology charges to the front.", *Genes & development*, 24(17), pp. 1832–60.

Phizicky, E. M., Schwartz, R. C. and Abelson, J. (1986) "Saccharomyces cerevisiae tRNA ligase. Purification of the protein and isolation of the structural gene", *Journal of Biological Chemistry*, 261(6), pp. 2978–2986.

Pisarev, A. V., Skabkin, M. A., Pisareva, V. P., Skabkina, O. V., Rakotondrafara, A. M., Hentze, M. W., Hellen, C. U. T. and Pestova, T. V. (2010) "The Role of ABCE1 in Eukaryotic Posttermination Ribosomal Recycling", *Molecular Cell*, 37(2), pp. 196–210.

Prat, L., Heinemann, I. U., Aerni, H. R., Rinehart, J., O'Donoghue, P. and Söll, D. (2012) "Carbon source-dependent expansion of the genetic code in bacteria.", *PNAS*, 109(51), pp. 21070–5.

Pujol, C., Bailly, M., Kern, D., Maréchal-Drouard, L., Becker, H., Duchêne, A.-M., Marechal-Drouard, L., Becker, H. and Duchene, A.-M. (2008) "Dual-targeted tRNA-dependent amidotransferase ensures both mitochondrial and chloroplastic Gln-tRNA^{Gln} synthesis in plants", *PNAS*, 105(17), pp. 6481–6485.

R

Raina, M., Elgamal, S., Santangelo, T. J. and Ibba, M. (2012) "Association of a multi-synthetase complex with translating ribosomes in the archaeon Thermococcus kodakarensis", *FEBS Letters*, 586(16), pp. 2232–2238.

Rajkowitsch, L., Vilela, C., Berthelot, K., Ramirez, C. V. and McCarthy, J. E. G. (2004) "Reinitiation and Recycling are Distinct Processes Occurring Downstream of Translation Termination in Yeast", *Journal of Molecular Biology*, 335(1), pp. 71–85.

Rauhut, R., Green, P. R. and Abelson, J. (1990) "Yeast tRNA-splicing endonuclease is a heterotrimeric enzyme.", *The Journal of biological chemistry*, 265(30), pp. 18180–4.

Ravel, J. M., Wang, S.-F., Heinemeyer, C. and Shive, W. (1965) 'Glutamyl and Glutamyl Ribonucleic Acid Synthetases of Escherichia coli W', *The Journal of biological chemistry*, 240, pp. 432–8.

Reddy, V. Y., Desorchers, P. E., Pizzo, S. V., Gonias, S. L., Sahakian, J. A., Levine, R. L. and Weiss, S. J. (1994) "Oxidative dissociation of human alpha 2-macroglobulin tetramers into dysfunctional dimers.", *The Journal of biological chemistry*, 269(6), pp. 4683–91.

Renault, L., Kerjan, P., Pasqualato, S., Ménétrey, J., Robinson, J. C., Kawaguchi, S., Vassylyev, D. G., Yokoyama, S., Mirande, M. and Cherfils, J. (2001) "Structure of the EMAPII domain of human aminoacyl-tRNA synthetase complex reveals evolutionary dimer mimicry.", *The EMBO journal*, 20(3), pp. 570–8.

Rho, S. B., Lee, K. H., Kim, J. W., Shiba, K., Jo, Y. J. and Kim, S. (1996) "Interaction between human tRNA synthetases involves repeated sequence elements.", *PNAS*, 93(19), pp. 10128–33.

Ribas de Pouplana, L. and Schimmel, P. (2001) "Two classes of tRNA synthetases suggested by sterically compatible dockings on tRNA acceptor stem.", *Cell*, 104(2), pp. 191–3.

Robb, E. L., Hall, A. R., Prime, T. A., Eaton, S., Szibor, M., Viscomi, C., James, A. M., Michael, X. and Murphy, P. (2018) "Control of mitochondrial superoxide production by reverse electron transport at complex I", *JBC*, 293(25), pp. 9869–9879.

Rodnina, M. V and Wintermeyer, W. (2009) "Recent mechanistic insights into eukaryotic ribosomes", *Current Opinion in Cell Biology*, 21(3), pp. 435–443.

Rosenberger, R. F. and Hilton, J. (1983) "The frequency of transcriptional and translational errors at nonsense codons in the lacZ gene of *Escherichia coli*", *MGG Molecular & General Genetics*. Springer-Verlag, 191(2), pp. 207–212.

Rould, M. A., Perona, J. J., Söll, D. and Steitz, T. A. (1989) "Structure of *E. coli* glutamyl-tRNA synthetase complexed with tRNA^{Gln} and ATP at 2.8 Å resolution.", *Science*, 246(4934), pp. 1135–42.

Ruan, B., Palioura, S., Sabina, J., Marvin-Guy, L., Kochhar, S., Larossa, R. A. and Söll, D. (2008) "Quality control despite mistranslation caused by an ambiguous genetic code.", *PNAS*, 105(43), pp. 16502–7.

Ryckelynck, M., Giegé, R. and Frugier, M. (2003) "Yeast tRNA^{Asp} charging accuracy is threatened by the N-terminal extension of aspartyl-tRNA synthetase.", *The Journal of biological chemistry*, 278(11), pp. 9683–90.

S

Sajish, M., Zhou, Q., Kishi, S., Valdez, D. M., Kapoor, M., Guo, M., Lee, S., Kim, S., Yang, X.-L., Schimmel, P. and Schimmel, P. (2012) "Trp-tRNA synthetase bridges DNA-PKcs to PARP-1 to link IFN- γ and p53 signaling.", *Nature chemical biology*, 8(6), pp. 547–54.

Salmon, T. B., Evert, B. A., Song, B. and Doetsch, P. W. (2004) "Biological consequences of oxidative stress-induced DNA damage in *Saccharomyces cerevisiae*", *Nucleic Acids Research*, 32(12), pp. 3712–3723.

Sarkar, S., Azad, A. K. and Hopper, A. K. (1999) "Nuclear tRNA aminoacylation and its role in nuclear export of endogenous tRNAs in *Saccharomyces cerevisiae*." *PNAS*, 96(25), pp. 14366–71.

Sauerwald, A., Zhu, W., Major, T. A., Roy, H., Palioura, S., Jahn, D., Whitman, W. B., Yates, J. R., Ibba, M. and Söll, D. (2005) "RNA-Dependent Cysteine Biosynthesis in Archaea", *Science*, 307(5717), pp. 1969–72.

Schindeldecker, M. and Moosmann, B. (2015) "Protein-borne methionine residues as structural antioxidants in mitochondria", *Amino Acids*, 47(7), pp. 1421–1432.

Schmitt, E., Meinel, T., Blanquet, S. and Mechulam, Y. (1994) "Methionyl-tRNA Synthetase Needs an Intact and Mobile 332KMSKS336 Motif in Catalysis of Methionyl Adenylate Formation", *Journal of Molecular Biology*, 242(4), pp. 566–577.

Schulman, L. H. and Goddard, J. P. (1973) "Loss of methionine acceptor activity resulting from a base change in the anticodon of *Escherichia coli* formylmethionine transfer ribonucleic acid.", *The Journal of biological chemistry*, 248(4), pp. 1341–5.

Schulman, L. H. and Pelka, H. (1983) 'Anticodon loop size and sequence requirements for recognition of formylmethionine tRNA by methionyl-tRNA synthetase', *PNAS*, 80(22), pp. 6755–59.

Schulman, L. H. and Pelka, H. (1988) "Anticodon switching changes the identity of methionine and valine transfer RNAs.", *Science*, 242(4879), pp. 765–8.

Schwartz, M. H., Waldbauer, J. R., Zhang, L. and Pan, T. (2016) "Global tRNA misacylation induced by anaerobiosis and antibiotic exposure broadly increases stress resistance in *Escherichia coli*.", *Nucleic Acids Research*, 44(21), pp. 10292–10303.

Schwartz, M. H. and Pan, T. (2016) "Temperature dependent mistranslation in a hyperthermophile adapts proteins to lower temperatures", *Nucleic Acids Research*, 44(1), pp. 294–303.

Scorrano, L., De Matteis, M. A., Emr, S., Giordano, F., Hajnóczky, G., Kornmann, B., Lackner, L. L., Levine, T. P., Pellegrini, L., Reinisch, K., Rizzuto, R., Simmen, T., Stenmark, H., Ungermann, C. and Schuldiner, M. (2019) "Coming together to define membrane contact sites", *Nature Communications*, 10(1), p. 1287.

Sekine, S., Shichiri, M., Bernier, S., Chênevert, R., Lapointe, J. and Yokoyama, S. (2006) "Structural Bases of Transfer RNA-Dependent Amino Acid Recognition and Activation by Glutamyl-tRNA Synthetase", *Structure*. Cell Press, 14(12), pp. 1791–1799.

Senger, B., Despons, L., Walter, P. and Fasiolo, F. (1992) "The anticodon triplet is not sufficient to confer methionine acceptance to a transfer RNA", *Biochemistry*, 89(22), pp. 10768–10771.

Senger, B., Despons, L., Walter, P., Jakubowski, H. and Fasiolo, F. (2001) "Yeast cytoplasmic and mitochondrial methionyl-tRNA synthetases: two structural frameworks for identical functions", *Journal of Molecular Biology*, 311(1), pp. 205–216.

Senger, B. and Fasiolo, F. (1996) "Yeast tRNA^{Met} recognition by methionyl-tRNA synthetase requires determinants from the primary, secondary and tertiary structure: a review", *Biochimie*, 78(7), pp. 597–604.

Sengupta, S. and Higgs, P. G. (2015) "Pathways of Genetic Code Evolution in Ancient and Modern Organisms", *Journal of Molecular Evolution*, 80(5–6), pp. 229–243.

Shah, P., Ding, Y., Niemczyk, M., Kudla, G. and Plotkin, J. B. (2013) "Rate-limiting steps in yeast protein translation.", *Cell*, 153(7), pp. 1589–601.

Shechter, Y., Burstein, Y. and Patchornik, A. (1975) "Selective oxidation of methionine residues in proteins.", *Biochemistry*, 14(20), pp. 4497–503.

Shenton, D., Smirnova, J. B., Selley, J. N., Carroll, K., Hubbard, S. J., Pavitt, G. D., Ashe, M. P. and Grant, C. M. (2006) "Global translational responses to oxidative stress impact upon multiple levels of protein synthesis.", *The Journal of biological chemistry*, 281(39), pp. 29011–21.

Sheppard, K., Yuan, J., Hohn, M. J., Jester, B., Devine, K. M., Söll, D. and Soll, D. (2008) "From one amino acid to another: tRNA-dependent amino acid biosynthesis", *Nucleic Acids Research*, 36(6), pp. 1813–1825.

Shiber, A., Döring, K., Friedrich, U., Klann, K., Merker, D., Zedan, M., Tippmann, F., Kramer, G. and Bukau, B. (2018) "Cotranslational assembly of protein complexes in eukaryotes revealed by ribosome profiling", *Nature*, 561(7722), pp. 268–272.

Shin, B.-S., Kim, J.-R., Walker, S. E., Dong, J., Lorsch, J. R. and Dever, T. E. (2011) "Initiation Factor eIF2 γ Promotes eIF2-GTP-Met-tRNA_i^{Met} Ternary Complex Binding to the 40S Ribosome", *Nature Structural & Molecular Biology*, 18(11), pp. 1227–34.

Shoemaker, C. J. and Green, R. (2011) "Kinetic analysis reveals the ordered coupling of translation termination and ribosome recycling in yeast", *PNAS*, 108(51), pp. E1392–E1398.

da Silva, E. C., de Albuquerque, M. B., Azevedo Neto, A. D. de and Silva Junior, C. D. da (2013) "Drought and Its Consequences to Plants – From Individual to Ecosystem", in *Responses of Organisms to Water Stress*, pp. 17–47.

Simader, H., Hothorn, M., Köhler, C., Basquin, J., Simos, G., Suck, D., J., S., J.M., R., A.-M., M. and C.-M., C. (2006) "Structural basis of yeast aminoacyl-tRNA synthetase complex formation revealed by crystal structures of two binary sub-complexes", *Nucleic Acids Research*, 34(14), pp. 3968–3979.

Simos, G., Segref, A., Fasiolo, F., Hellmuth, K., Shevchenko, A., Mann, M. and Hurt, E. C. (1996) "The yeast protein Arc1p binds to tRNA and functions as a cofactor for the methionyl- and glutamyl-tRNA synthetases.", *The EMBO journal*, 15(19), pp. 5437–48.

Simos, G., Sauer, A., Fasiolo, F. and Hurt, E. C. (1998) "A Conserved Domain within Arc1p Delivers tRNA to Aminoacyl-tRNA Synthetases", *Molecular Cell*, 1(2), pp. 235–242.

Skowronek, E., Grzechnik, P., Späth, B., Marchfelder, A. and Kufel, J. (2014) "tRNA 3' processing in yeast involves tRNase Z, Rex1, and Rrp6.", *RNA*, 20(1), pp. 115–30.

Smith, A. E. and Marcker, K. A. (1970) "Cytoplasmic Methionine Transfer RNAs from Eukaryotes", *Nature*, 226(5246), pp. 607–610.

Sprinzi, M., Horn, C., Brown, M., Ioudovitch, A. and Steinberg, S. (1998) "Compilation of tRNA sequences and sequences of tRNA genes.", *Nucleic Acids Research*, 26(1), pp. 148–53.

Sprinzi, M. (2006) "Chemistry of aminoacylation and peptide bond formation on the 3' terminus of tRNA.", *Journal of biosciences*, 31(4), pp. 489–96.

Sprinzi, M. and Cramer, F. (1973) "Accepting Site for Aminoacylation of tRNA^{Phe} from Yeast", *Nature New Biology*, 245(140), pp. 3–5.

Sprinzi, M. and Cramer, F. (1975) "Site of aminoacylation of tRNAs from *Escherichia coli* with respect to the 2'- or 3'-hydroxyl group of the terminal adenosine.", *PNAS*, 72(8), pp. 3049–53.

Srinivasan, G., James, C. M. and Krzycki, J. A. (2002) "Pyrrolysine Encoded by UAG in Archaea: Charging of a UAG-Decoding Specialized tRNA", *Science*, 296(5572), pp. 1459–1462.

Stadtman, E. R., Moskovitz, J., Berlett, B. S. and Levine, R. L. (2002) "Cyclic oxidation and reduction of protein methionine residues is an important antioxidant mechanism.", *Molecular and cellular biochemistry*, 234–235(1–2), pp. 3–9.

Starkov, A. A. (2008) "The role of mitochondria in reactive oxygen species metabolism and signaling.", *Annals of the New York Academy of Sciences*, 1147, pp. 37–52.

Swairjo, M. A., Morales, A. J., Wang, C. C., Ortiz, A. R. and Schimmel, P. (2000) "Crystal structure of trbp111: a structure-specific tRNA-binding protein.", *The EMBO journal*, 19(23), pp. 6287–98.

T

Taiji, M., Yokoyama, S. and Miyazawa, T. (1983) "Transacylation rates of (aminoacyl)adenosine moiety at the 3'-terminus of aminoacyl transfer ribonucleic acid.", *Biochemistry*, 22(13), pp. 3220–5.

Takatori, S. and Fujimoto, T. (2016) "A novel imaging method revealed phosphatidylinositol 3,5-bisphosphate-rich domains in the endosome/lysosome membrane.", *Communicative & integrative biology*, 9(2), p. e1145319.

Takehige, K. (1992) "Autophagy in yeast demonstrated with proteinase-deficient mutants and conditions for its induction", *The Journal of Cell Biology*, 119(2), pp. 301–311.

Tanaka, K. (2009) "The proteasome: overview of structure and functions.", *Proceedings of the Japan Academy. Series B, Physical and biological sciences*. The Japan Academy, 85(1), pp. 12–36.

Tarrago, L., Kaya, A., Weerapana, E., Marino, S. M. and Gladyshev, V. N. (2012) "Methionine Sulfoxide Reductases Preferentially Reduce Unfolded Oxidized Proteins and Protect Cells from Oxidative Protein Unfolding", *The Journal of Biological Chemistry*, 287(29), p. 24448.

Tarun, S. 2 and Sachsl, A. B. (1995) "A common function for mRNA 5' and 3' ends in translation initiation in yeast", *Genes & Development*, 9, pp. 2997–3007.

Teichert, I. (2018) "Adenosine to inosine mRNA editing in fungi and how it may relate to fungal pathogenesis", *PLoS Pathogens*, 14(9), p. e1007231.

Théobald-Dietrich, A., Giegé, R. and Rudinger-Thirion, J. (2005) "Evidence for the existence in mRNAs of a hairpin element responsible for ribosome dependent pyrrolysine insertion into proteins", *Biochimie*, 87(9–10), pp. 813–817.

Thompson, M., Haeusler, R. A., Good, P. D. and Engelke, D. R. (2003) "Nucleolar clustering of dispersed tRNA genes.", *Science*, 302(5649), pp. 1399–401.

Triana-Alonso, F. J., Chakraborty, K. and Nierhaus, K. H. (1995) "The elongation factor 3 unique in higher fungi and essential for protein biosynthesis is an E site factor.", *The Journal of biological chemistry*, 270(35), pp. 20473–8.

Trotta, C. R., Miao, F., Arn, E. A., Stevens, S. W., Ho, C. K., Rauhut, R. and Abelson, J. N. (1997) "The yeast tRNA splicing endonuclease: a tetrameric enzyme with two active site subunits homologous to the archaeal tRNA endonucleases.", *Cell*, 89(6), pp. 849–58.

Tumbula, D. L., Becker, H. D., Chang, W. and Söll, D. (2000) "Domain-specific recruitment of amide amino acids for protein synthesis", *Nature*, 407(6800), pp. 106–110.

Turrens, J. F. (2003) "Mitochondrial formation of reactive oxygen species.", *The Journal of physiology*. Wiley-Blackwell, 552(Pt 2), pp. 335–44.

V

Vasil'eva, I. A. and Moor, N. A. (2007) "Interaction of aminoacyl-tRNA synthetases with tRNA: general principles and distinguishing characteristics of the high-molecular-weight substrate recognition.", *Biochemistry*, 72(3), pp. 247–63.

Verkhusha, V. V, Akovbian, N. A., Efremenko, E. N., Varfolomeyev, S. D. and Vrzheschch, P. V (2001) "Kinetic analysis of maturation and denaturation of DsRed, a coral-derived red fluorescent protein.", *Biochemistry*, 66(12), pp. 1342–51.

Vidoni, C., Follo, C., Savino, M., Melone, M. A. B. and Isidoro, C. (2016) "The Role of Cathepsin D in the Pathogenesis of Human Neurodegenerative Disorders", *Medicinal Research Reviews*, 36(5), pp. 845–870.

W

Wada, M. and Ito, K. (2014) "A genetic approach for analyzing the co-operative function of the tRNA mimicry complex, eRF1/eRF3, in translation termination on the ribosome", *Nucleic Acids Research*, 42(12), pp. 7851–7866.

Wagner, D. S., Salari, A., Gage, D. A., Leykam, J., Fetter, J., Hollingsworth, R. and Watson, J. T. (1991) "Derivatization of peptides to enhance ionization efficiency and control fragmentation during analysis by fast atom bombardment tandem mass spectrometry", *Biological Mass Spectrometry*, 20(7), pp. 419–425.

Wakasugi, K. and Schimmel, P. (1999) "Two distinct cytokines released from a human aminoacyl-tRNA synthetase.", *Science*, 284(5411), pp. 147–51.

Wallace, E. W. J., Kear-Scott, J. L., Pilipenko, E. V., Schwartz, M. H., Laskowski, P. R., Rojek, A. E., Katanski, C. D., Riback, J. A., Dion, M. F., Franks, A. M., Airoidi, E. M., Pan, T., Budnik, B. A. and Drummond, D. A. (2015) "Reversible, Specific, Active Aggregates of Endogenous Proteins Assemble upon Heat Stress", *Cell*, 162(6), pp. 1286–1298.

Walter, P., Gangloff, J., Bonnet, J., Boulanger, Y., Ebel, J. P. and Fasiolo, F. (1983) "Primary structure of the *Saccharomyces cerevisiae* gene for methionyl-tRNA synthetase.", *PNAS*, 80(9), pp. 2437–41.

Walter, P., Weygand-Durasevic, I., Sanni, A., Ebel, J. P. and Fasiolo, F. (1989) "Deletion analysis in the amino-terminal extension of methionyl-tRNA synthetase from *Saccharomyces cerevisiae* shows that a small region is important for the activity and stability of the enzyme.", *The Journal of biological chemistry*, 264(29), pp. 17126–30.

Wang, X. and Pan, T. (2016) "Stress Response and Adaptation Mediated by Amino Acid Misincorporation during Protein Synthesis", *Advances in Nutrition: An International Review Journal*. American Society for Nutrition, 7(4), pp. 773S–779S.

Watson, T. G. (1976) 'Amino-acid Pool Composition of *Saccharomyces cerevisiae* as a Function of Growth Rate and Amino-acid Nitrogen Source', *Journal of General Microbiology*, 96(2), pp. 263–8.

Weissbach, H., Resnick, L. and Brot, N. (2005) "Methionine sulfoxide reductases: history and cellular role in protecting against oxidative damage", *Biochimica et Biophysica Acta (BBA) - Proteins and Proteomics*, 1703(2), pp. 203–212.

Wells, S. E., Hillner, P. E., Vale, R. D. and Sachs, A. B. (1998) "Circularization of mRNA by Eukaryotic Translation Initiation Factors", *Molecular Cell*, 2(1), pp. 135–140.

Wen Lee, L., Ravel, J. M. and Shive, W. (1967) "A General Involvement of Acceptor Ribonucleic Acid in the Initial Activation Step of Glutamic Acid and Glutamine", *Archives of Biochemistry and Biophysics*, 121, pp. 614–618.

Wiedenmann, J., Schenk, A., Röcker, C., Girod, A., Spindler, K.-D. and Nienhaus, G. U. (2002) "A far-red fluorescent protein with fast maturation and reduced oligomerization tendency from *Entacmaea quadricolor* (Anthozoa, Actinaria)", *PNAS*, 99(18), pp. 11646–11651.

Wiemken, A. and Dürr, M. (1974) "Characterization of amino acid pools in the vacuolar compartment of *Saccharomyces cerevisiae*", *Archives of Microbiology*, 101(1), pp. 45–57.

Wilson, D. N. and Doudna Cate, J. H. (2012) "The structure and function of the eukaryotic ribosome.", *Cold Spring Harbor perspectives in biology*, 4(5).

Wilttrout, E., Goodenbour, J. M., Fréchin, M., Pan, T., Wilttrout, E., Goodenbour, J. M. and Fre, M. (2012) "Misacylation of tRNA with methionine in *Saccharomyces cerevisiae*", *Nucleic Acids Research*, 40(20), pp. 10494–10506.

Wong, H.-S., Dighe, P. A., Mezera, V., Monternier, P.-A. and Brand, M. D. (2017) "Production of superoxide and hydrogen peroxide from specific mitochondrial sites under different bioenergetic conditions.", *The Journal of biological chemistry*, 292(41), pp. 16804–16809.

Wood, P. M. (1981) "The redox potential for dimethyl sulphoxide reduction to dimethyl sulphide", *FEBS Letters*. 124(1), pp. 11–14.

Woolford, C. A., Daniels, L. B., Park, F. J., Jones, E. W., Van Arsdell, J. N. and Innis², M. A. (1986) "The PEP4 Gene Encodes an Aspartyl Protease Implicated in the Posttranslational Regulation of *Saccharomyces cerevisiae* Vacuolar Hydrolases", *Molecular and Cellular Biology*, 6(7), pp. 2500–2510.

Wu, G. (2013) '*Amino acids : biochemistry and nutrition*. CRC Press'.

Wu, L., Yi, H. and Zhang, H. (2013) "Reactive oxygen species and Ca²⁺ are involved in sodium arsenite-induced cell killing in yeast cells", *FEMS Microbiology Letters*. 343(1), pp. 57–63.

X

Xu, X., Shi, Y., Zhang, H.-M., Swindell, E. C., Marshall, A. G., Guo, M., Kishi, S. and Yang, X.-L. (2012) "Unique domain appended to vertebrate tRNA synthetase is essential for vascular development.", *Nature communications*, 3, p. 681.

Y

Yakovov, N., Debard, S., Fischer, F., Senger, B. and Becker, H. D. H. D. (2018) "Cytosolic aminoacyl-tRNA synthetases: Unanticipated relocations for unexpected functions", *Biochimica et Biophysica Acta (BBA) - Gene Regulatory Mechanisms*, 1861(4), pp. 387–400.

Yarian, C., Townsend, H., Czestkowski, W., Sochacka, E., Malkiewicz, A. J., Guenther, R., Miskiewicz, A. and Agris, P. F. (2002) "Accurate translation of the genetic code depends on tRNA modified nucleosides.", *The Journal of biological chemistry*, 277(19), pp. 16391–5.

Young, D. J., Guydosh, N. R., Zhang, F., Hinnebusch, A. G. and Green, R. (2015) "Rli1/ABCE1 Recycles Terminating Ribosomes and Controls Translation Reinitiation in 3'UTRs In Vivo.", *Cell*, 162(4), pp. 872–84.

Yuan, J., Palioura, S., Salazar, J. C., Su, D., O'Donoghue, P., Hohn, M. J., Cardoso, A. M., Whitman, W. B. and Söll, D. (2006) "RNA-dependent conversion of phosphoserine forms selenocysteine in eukaryotes and archaea.", *PNAS*, 103(50), pp. 18923–7.

Yuan, J., Sheppard, K. and Söll, D. (2008) "Amino acid modifications on tRNA", *Acta biochimica et biophysica Sinica*, 40(7), p. 539.

Z

Zeng, R., Chen, Y., Zeng, Z., Liu, W., Jiang, X., Liu, R., Qiang, O. and Li, X. (2011) "Effect of mini-tyrosyl-tRNA synthetase/mini-tryptophanyl-tRNA synthetase on ischemic angiogenesis in rats: proliferation and migration of endothelial cells", *Heart and Vessels*, 26(1), pp. 69–80.

Zenklusen, D., Larson, D. R. and Singer, R. H. (2008) "Single-RNA counting reveals alternative modes of gene expression in yeast", *Nature Structural & Molecular Biology*, 15(12), pp. 1263–1271.

Zhang, Y. and Gladyshev, V. N. (2007) "High content of proteins containing 21st and 22nd amino acids, selenocysteine and pyrrolysine, in a symbiotic deltaproteobacterium of gutless worm *Olavius algarvensis*.", *Nucleic Acids Research*, 35(15), pp. 4952–63.

Zinoni, F., Birkmann, A., Stadtman, T. C. and Böck, A. (1986) "Nucleotide sequence and expression of the selenocysteine-containing polypeptide of formate dehydrogenase (formate-hydrogen-lyase-linked) from *Escherichia coli*.", *PNAS*, 83(13), pp. 4650–4.

II. Figures and tables references

- [1] S. Kadaba, A. Krueger, T. Trice, A.M. Krecic, A.G. Hinnebusch, J. Anderson, Nuclear surveillance and degradation of hypomodified initiator tRNA^{Met} in *S. cerevisiae*, *Genes Dev.* 18 (2004) 1227–1240.
- [2] S. Kadaba, X. Wang, J.T. Anderson, Nuclear RNA surveillance in *Saccharomyces cerevisiae*: Trf4p-dependent polyadenylation of nascent hypomethylated tRNA and an aberrant form of 5S rRNA., *RNA.* 12 (2006) 508–21.
- [3] B. Senger, S. Auxilien, U. Englisch, F. Cramer, F. Fasiolo, The Modified Wobble Base Inosine in Yeast tRNA^{Ile} Is a Positive Determinant for Aminoacylation by Isoleucyl-tRNA Synthetase , *Biochemistry.* 36 (1997) 8269–8275.
- [4] A. Gerber, H. Grosjean, T. Melcher, W. Keller, Tad1p, a yeast tRNA-specific adenosine deaminase, is related to the mammalian pre-mRNA editing enzymes ADAR1 and ADAR2, *EMBO J.* 17 (1998) 4780–4789.
- [5] G.R. Bjork, A primordial tRNA modification required for the evolution of life?, *EMBO J.* 20 (2001) 231–239.
- [6] M.E. Dihanich, D. Najarian, R. Clark, E.C. Gillman, N.C. Martin, A.K. Hopper, Isolation and characterization of MOD5, a gene required for isopentenylation of cytoplasmic and mitochondrial tRNAs of *Saccharomyces cerevisiae*., *Mol. Cell. Biol.* 7 (1987) 177–84.
- [7] M. Srinivasan, P. Mehta, Y. Yu, E. Prugar, E. V Koonin, A.W. Karzai, R. Sternglanz, The highly conserved KEOPS/EKC complex is essential for a universal tRNA modification, t6A, *EMBO J.* 30 (2011) 873–881.
- [8] F. V Murphy, V. Ramakrishnan, A. Malkiewicz, P.F. Agris, The role of modifications in codon discrimination by tRNA^{Lys}UUU, *Nat. Struct. Mol. Biol.* 11 (2004) 1186–1191
- [9] S.E. Kolitz, J.R. Lorsch, Eukaryotic initiator tRNA: finely tuned and ready for action., *FEBS Lett.* 584 (2010) 396–404.
- [10] O. Nureki, T. Niimi, T. Muramatsu, H. Kanno, T. Kohno, C. Florentz, R. Giegé, S. Yokoyama, Molecular Recognition of the Identity-determinant Set of Isoleucine Transfer RNA from *Escherichia coli*, *J. Mol. Biol.* 236 (1994) 710–724.
- [11] M.-C. Daugeron, T.L. Lenstra, M. Frizzarin, B. El Yacoubi, X. Liu, A. Baudin-Baillieu, P. Lijnzaad, L. Decourty, C. Saveanu, A. Jacquier, F.C.P. Holstege, V. de Crécy-Lagard, H. van Tilbeurgh, D. Libri, Gcn4 misregulation reveals a direct role for the evolutionary conserved EKC/KEOPS in the t6A modification of tRNAs, *Nucleic Acids Res.* 39 (2011) 6148–6160.
- [12] S.U. Åström, A.S. Byström, Rit1, a tRNA backbone-modifying enzyme that mediates initiator and elongator tRNA discrimination, *Cell.* 79 (1994) 535–546.
- [13] B.-S. Shin, J.-R. Kim, S.E. Walker, J. Dong, J.R. Lorsch, T.E. Dever, Initiation factor eIF2 γ promotes eIF2-GTP-Met-tRNAi(Met) ternary complex binding to the 40S ribosome., *Nat. Struct. Mol. Biol.* 18 (2011) 1227–34.

- [14] M.L. Wilkinson, S.M. Crary, J.E. Jackman, E.J. Grayhack, E.M. Phizicky, The 2'-O-methyltransferase responsible for modification of yeast tRNA at position 4, *RNA*. 13 (2007) 404–413.
- [15] K.L. Tkaczuk, Trm13p, the tRNA:Xm4 modification enzyme from *Saccharomyces cerevisiae* is a member of the Rossmann-fold MTase superfamily: prediction of structure and active site, *J. Mol. Model.* 16 (2010) 599–606.
- [16] J.M. Whipple, E.A. Lane, I. Chernyakov, S. D'Silva, E.M. Phizicky, The yeast rapid tRNA decay pathway primarily monitors the structural integrity of the acceptor and T-stems of mature tRNA, *Genes Dev.* 25 (2011) 1173–1184.
- [17] S. D'Silva, S.J. Haider, E.M. Phizicky, A domain of the actin binding protein Abp140 is the yeast methyltransferase responsible for 3-methylcytidine modification in the tRNA anti-codon loop, *RNA*. 17 (2011) 1100–1110.
- [18] A. Noma, S. Yi, T. Katoh, Y. Takai, T. Suzuki, T. Suzuki, Actin-binding protein ABP140 is a methyltransferase for 3-methylcytidine at position 32 of tRNAs in *Saccharomyces cerevisiae*, *RNA*. 17 (2011) 1111–1119.
- [19] Y. Chen, H. Sierzputowska-Gracz, R. Guenther, K. Everett, P.F. Agris, 5-Methylcytidine is required for cooperative binding of magnesium(2+) and a conformational transition at the anticodon stem-loop of yeast phenylalanine tRNA, *Biochemistry*. 32 (1993) 10249–10253.
- [20] Y. Motorin, H. Grosjean, Multisite-specific tRNA:m5C-methyltransferase (Trm4) in yeast *Saccharomyces cerevisiae*: identification of the gene and substrate specificity of the enzyme., *RNA*. 5 (1999) 1105–18.
- [21] L. Pintard, F. Lecointe, J.M. Bujnicki, C. Bonnerot, H. Grosjean, B. Lapeyre, Trm7p catalyses the formation of two 2'-O-methylriboses in yeast tRNA anticodon loop., *EMBO J.* 21 (2002) 1811–20.
- [22] M.P. Guy, B.M. Podyma, M.A. Preston, H.H. Shaheen, K.L. Krivos, P.A. Limbach, A.K. Hopper, E.M. Phizicky, Yeast Trm7 interacts with distinct proteins for critical modifications of the tRNA^{Phe} anticodon loop, *RNA*. 18 (2012) 1921–1933.
- [23] J.E. Jackman, Identification of the yeast gene encoding the tRNA m1G methyltransferase responsible for modification at position 9, *RNA*. 9 (2003) 574–585.
- [24] J. Pütz, C. Florentz, F. Bensele, R. Giegé, A single methyl group prevents the mischarging of a tRNA., *Nat. Struct. Biol.* 1 (1994) 580–2.
- [25] S.K. Purushothaman, J.M. Bujnicki, H. Grosjean, B. Lapeyre, Trm11p and Trm112p Are both Required for the Formation of 2-Methylguanosine at Position 10 in Yeast tRNA, *Mol. Cell. Biol.* 25 (2005) 4359–4370.
- [26] S.R. Ellis, M.J. Morales, J.M. Li, A.K. Hopper, N.C. Martin, Isolation and characterization of the TRM1 locus, a gene essential for the N2,N2-dimethylguanosine modification of both mitochondrial and cytoplasmic tRNA in *Saccharomyces cerevisiae*., *J. Biol. Chem.* 261 (1986) 9703–9.
- [27] J. Edqvist, K. Blomqvist, K. Straaby, Structural Elements in Yeast tRNAs Required for Homologous Modification of Guanosine-26 into Dimethylguanosine-26 by the Yeast Trm1

- tRNA-Modifying Enzyme, *Biochemistry*. 33 (1994) 9546–9551.
- [28] A. Alexandrov, I. Chernyakov, W. Gu, S.L. Hiley, T.R. Hughes, E.J. Grayhack, E.M. Phizicky, Rapid tRNA Decay Can Result from Lack of Nonessential Modifications, *Mol. Cell*. 21 (2006) 87–96.
- [29] J. Cavaille, F. Chetouani, J.P. Bachellerie, The yeast *Saccharomyces cerevisiae* YDL112w ORF encodes the putative 2'-O-ribose methyltransferase catalyzing the formation of Gm18 in tRNAs., *RNA*. 5 (1999) 66–81.
- [30] W.F. Waas, Z. Druzina, M. Hanan, P. Schimmel, Role of a tRNA Base Modification and Its Precursors in Frameshifting in Eukaryotes, *J. Biol. Chem.* 282 (2007) 26026–26034.
- [31] A.G. Bruce, O.C. Uhlenbeck, Enzymic replacement of the anticodon of yeast tRNA^{Phe}, *Biochemistry*. 21 (1982) 855–861.
- [32] F. Xing, M.R. Martzen, E.M. Phizicky, A conserved family of *Saccharomyces cerevisiae* synthases effects dihydrouridine modification of tRNA., *RNA*. 8 (2002) 370–81.
- [33] F. Xing, S.L. Hiley, T.R. Hughes, E.M. Phizicky, The Specificities of Four Yeast Dihydrouridine Synthases for Cytoplasmic tRNAs, *J. Biol. Chem.* 279 (2004) 17850–17860.
- [34] J. Dalluge, T. Hashizume, A.E. Sopchik, J.A. McCloskey, D.R. Davis, Conformational flexibility in RNA: the role of dihydrouridine, *Nucleic Acids Res.* 24 (1996) 1073–1079.
- [35] G. Simos, H. Tekotte, H. Grosjean, A. Segref, K. Sharma, D. Tollervey, E.C. Hurt, Nuclear pore proteins are involved in the biogenesis of functional tRNA., *EMBO J.* 15 (1996) 2270–84.
- [36] I. Behm-Ansmant, C. Branlant, Y. Motorin, The *Saccharomyces cerevisiae* Pus2 protein encoded by YGL063w ORF is a mitochondrial tRNA: 27/28-synthase, *RNA*. 13 (2007) 1641–1647.
- [37] F. Lecointe, G. Simos, A. Sauer, E.C. Hurt, Y. Motorin, H. Grosjean, Characterization of Yeast Protein Deg1 as Pseudouridine Synthase (Pus3) Catalyzing the Formation of Ψ_{38} and Ψ_{39} in tRNA Anticodon Loop, *J. Biol. Chem.* 273 (1998) 1316–1323.
- [38] H. Becker, Y. Motorin, R.J. Planta, H. Grosjean, The yeast gene YNL292w encodes a pseudouridine synthase (Pus4) catalyzing the formation of psi55 in both mitochondrial and cytoplasmic tRNAs, *Nucleic Acids Res.* 25 (1997) 4493–4499.
- [39] I. Ansmant, Y. Motorin, S. Massenet, H. Grosjean, C. Branlant, Identification and Characterization of the tRNA: Ψ_{31} -Synthase (Pus6p) of *Saccharomyces cerevisiae*, *J. Biol. Chem.* 276 (2001) 34934–34940.
- [40] I. BEHM-ANSMANT, A. Urban, X. Ma, Y.-T. Yu, Y. Motorin, C. Branlant, The *Saccharomyces cerevisiae* U2 snRNA:pseudouridine-synthase Pus7p is a novel multisite-multisubstrate RNA: -synthase also acting on tRNAs, *RNA*. 9 (2003) 1371–1382.
- [41] L.A. Bare, O.C. Uhlenbeck, Specific substitution into the anticodon loop of yeast tyrosine transfer RNA, *Biochemistry*. 25 (1986) 5825–5830.
- [42] I. Behm-Ansmant, H. Grosjean, S. Massenet, Y. Motorin, C. Branlant, Pseudouridylation at Position 32 of Mitochondrial and Cytoplasmic tRNAs Requires Two Distinct Enzymes in *Saccharomyces cerevisiae*, *J. Biol. Chem.* 279 (2004) 52998–53006.

- [43] L. Kotelawala, E.J. Grayhack, E.M. Phizicky, Identification of yeast tRNA^{Um44} 2'-O-methyltransferase (Trm44) and demonstration of a Trm44 role in sustaining levels of specific tRNA^{Ser} species, *RNA*. 14 (2007) 158–169.
- [44] M.J.O. Johansson, A.S. Byström, Dual function of the tRNA(m(5)U54)methyltransferase in tRNA maturation., *RNA*. 8 (2002) 324–35.
- [45] A. Patil, C. Chan, M. Dyavaiah, J.P. Rooney, P. Dedon, T.J. Begley, Translational infidelity-induced protein stress results from a deficiency in Trm9-catalyzed tRNA modifications, *RNA Biol*. 9 (2012) 990–1001.
- [46] W. Deng, I.R. Babu, D. Su, S. Yin, T.J. Begley, P.C. Dedon, Trm9-Catalyzed tRNA Modifications Regulate Global Protein Expression by Codon-Biased Translation, *PLoS Genet*. 11 (2015) e1005706.
- [47] M.P. Guy, E.M. Phizicky, Conservation of an intricate circuit for crucial modifications of the tRNA^{Phe} anticodon loop in eukaryotes, *RNA*. 21 (2015) 61–74.
- [48] P. Studte, S. Zink, D. Jablonowski, C. Bär, T. von der Haar, M.F. Tuite, R. Schaffrath, tRNA and protein methylase complexes mediate zymocin toxicity in yeast, *Mol. Microbiol*. 69 (2008) 1266–1277.
- [49] V.A.N. Rezgui, K. Tyagi, N. Ranjan, A.L. Konevega, J. Mittelstaet, M. V. Rodnina, M. Peter, P.G.A. Pedrioli, tRNA tKUUU, tQUUG, and tEUUC wobble position modifications fine-tune protein translation by promoting ribosome A-site binding, *Proc. Natl. Acad. Sci*. 110 (2013) 12289–12294.
- [50] G.R. Björk, B. Huang, O.P. Persson, A.S. Byström, A conserved modified wobble nucleoside (mcm5s2U) in lysyl-tRNA is required for viability in yeast., *RNA*. 13 (2007) 1245–55.
- [51] B. HUANG, M.J.O. Johansson, A.S. Byström, An early step in wobble uridine tRNA modification requires the Elongator complex, *RNA*. 11 (2005) 424–436.
- [52] F. V Murphy, V. Ramakrishnan, Structure of a purine-purine wobble base pair in the decoding center of the ribosome, *Nat. Struct. Mol. Biol*. 11 (2004) 1251–1252.
- [53] A.G. Torres, D. Piñeyro, L. Filonava, T.H. Stracker, E. Batlle, L. Ribas de Pouplana, A-to-I editing on tRNAs: Biochemical, biological and evolutionary implications, *FEBS Lett*. 588 (2014) 4279–4286.
- [54] C.T.Y.Y. Chan, Y.L.J. Pang, W. Deng, I.R. Babu, M. Dyavaiah, T.J. Begley, P.C. Dedon, Reprogramming of tRNA modifications controls the oxidative stress response by codon-biased translation of proteins., *Nat. Commun*. 3 (2012) 937.
- [55] U.L. RajBhandary, S.H. Chang, A. Stuart, R.D. Faulkner, R.M. Hoskinson, H.G. Khorana, Studies on polynucleotides, LXVIII the primary structure of yeast phenylalanine transfer RNA, *Proc. Natl. Acad. Sci*. 57 (1967) 751–758.
- [56] Z. Szweykowska-Kulinska, B. Senger, G. Keith, F. Fasiolo, H. Grosjean, Intron-dependent formation of pseudouridines in the anticodon of *Saccharomyces cerevisiae* minor tRNA^{Ile}., *EMBO J*. 13 (1994) 4636–4644.

- [57] V.I. Lim, Analysis of Action of Wobble Nucleoside Modifications on Codon-Anticodon Pairing within the Ribosome, *J. Mol. Biol.* 240 (1994) 8–19.
- [58] S. Kurata, A. Weixlbaumer, T. Ohtsuki, T. Shimazaki, T. Wada, Y. Kirino, K. Takai, K. Watanabe, V. Ramakrishnan, T. Suzuki, Modified Uridines with C5-methylene Substituents at the First Position of the tRNA Anticodon Stabilize U·G Wobble Pairing during Decoding, *J. Biol. Chem.* 283 (2008) 18801–18811.
- [59] S. Yokoyama, S. Nishimura, tRNA: structure, biosynthesis and function, *Modif. Nucleosides Codon Recognit.* (1995) 207–223.
- [60] S. Yokoyama, T. Watanabe, K. Murao, H. Ishikura, Z. Yamaizumi, S. Nishimura, T. Miyazawa, Molecular mechanism of codon recognition by tRNA species with modified uridine in the first position of the anticodon., *Proc. Natl. Acad. Sci.* 82 (1985) 4905–4909.
- [61] R.B. Loftfield, The Frequency of Errors in Protein Biosynthesis., *Biochem. J.* 89 (1963) 82–92.
- [62] R.B. Loftfield, D. Vanderjagt, The Frequency of Errors in Protein Biosynthesis, *Biochem. J.* 128 (1972) 1353–1356..
- [63] P. Edelman, J. Gallant, Mistranslation in *E. coli.*, *Cell.* 10 (1977) 131–7.
- [64] J. Parker, J.D. Friesen, “Two out of three” codon reading leading to mistranslation in vivo., *Mol. Gen. Genet.* 177 (1980) 439–45.
- [65] F. Bouadloun, D. Donner, C.G. Kurland, Codon-specific missense errors in vivo., *EMBO J.* 2 (1983) 1351–6.
- [66] K. Khazaie, J.H. Buchanan, R.F. Rosenberger, The accuracy of Q beta RNA translation. 1. Errors during the synthesis of Q beta proteins by intact *Escherichia coli* cells., *Eur. J. Biochem.* 144 (1984) 485–9.
- [67] P. Londei, S. Altamura, J.L. Sanz, R. Amils, Aminoglycoside-induced mistranslation in thermophilic archaeobacteria, *Mol. Gen. Genet.* 214 (1988) 48–54.
- [68] T.L. Calderone, R.D. Stevens, T.G. Oas, High-level Misincorporation of Lysine for Arginine at AGA Codons in a Fusion Protein Expressed in *Escherichia coli*, *J. Mol. Biol.* 262 (1996) 407–412.
- [69] B. Ruan, S. Palioura, J. Sabina, L. Marvin-Guy, S. Kochhar, R.A. Larossa, D. Söll, Quality control despite mistranslation caused by an ambiguous genetic code., *Proc. Natl. Acad. Sci. U. S. A.* 105 (2008) 16502–7.
- [70] I. Miranda, A. Silva-Dias, R. Rocha, R. Teixeira-Santos, C. Coelho, T. Gonçalves, M.A.S. Santos, C. Pina-Vaz, N. V Solis, S.G. Filler, A.G. Rodrigues, *Candida albicans* CUG mistranslation is a mechanism to create cell surface variation., *MBio.* 4 (2013) e00285-13.
- [71] Z. Zhang, B. Shah, P. V. Bondarenko, G/U and Certain Wobble Position Mismatches as Possible Main Causes of Amino Acid Misincorporations, *Biochemistry.* 52 (2013) 8165–8176.
- [72] K. Mohler, R. Mann, T.J. Bullwinkle, K. Hopkins, L. Hwang, N.M. Reynolds, B. Gassaway, H.-R. Aerni, J. Rinehart, M. Polymenis, K. Faull, M. Ibba, Editing of misaminoacylated tRNA controls the sensitivity of amino acid stress responses in *Saccharomyces cerevisiae*, *Nucleic Acids Res.* 45 (2017) 3985–3996.

- [73] M.J. Toth, E.J. Murgola, P. Schimmel, Evidence for a unique first position codon-anticodon mismatch in vivo, *J. Mol. Biol.* 201 (1988) 451–454.
- [74] I. Stansfield, K.M. Jones, P. Herbert, A. Lewendon, W. V Shaw, M.F. Tuite, Missense translation errors in *Saccharomyces cerevisiae*, *J. Mol. Biol.* 282 (1998) 13–24.
- [75] T. Inaoka, K. Kasai, K. Ochi, Construction of an in vivo nonsense readthrough assay system and functional analysis of ribosomal proteins S12, S4, and S5 in *Bacillus subtilis*, *J. Bacteriol.* 183 (2001) 4958–63.
- [76] L.A. Nangle, C.M. Motta, P. Schimmel, Global Effects of Mistranslation from an Editing Defect in Mammalian Cells, *Chem. Biol.* 13 (2006) 1091–1100.
- [77] E.B. Kramer, P.J. Farabaugh, The frequency of translational misreading errors in *E. coli* is largely determined by tRNA competition., *RNA.* 13 (2007) 87–96.
- [78] M. Meyerovich, G. Mamou, S. Ben-Yehuda, Visualizing high error levels during gene expression in living bacterial cells., *Proc. Natl. Acad. Sci. U. S. A.* 107 (2010) 11543–8.
- [79] B. Javid, F. Sorrentino, M. Toosky, W. Zheng, J.T. Pinkham, N. Jain, M. Pan, P. Deighan, E.J. Rubin, Mycobacterial mistranslation is necessary and sufficient for rifampicin phenotypic resistance., *Proc. Natl. Acad. Sci. U. S. A.* 111 (2014) 1132–7.
- [80] A.N.A.C. Gomes, A.J. Kordala, R. Strack, X. Wang, R. Geslain, K. Delaney, W.C. Clark, R. Keenan, T.A.O. Pan, A dual fluorescent reporter for the investigation of methionine mistranslation in live cells, *RNA.* 22 (2016) 1–10.
- [81] K.S. Hoffman, M.D. Berg, B.H. Shilton, C.J. Brandl, P. O'Donoghue, Genetic selection for mistranslation rescues a defective co-chaperone in yeast., *Nucleic Acids Res.* 45 (2017) 3407–3421.
- [82] J.T. Lant, M.D. Berg, D.H.W. Sze, K.S. Hoffman, I.C. Akinpelu, M.A. Turk, I.U. Heinemann, M.L. Duennwald, C.J. Brandl, P. O'Donoghue, Visualizing tRNA-dependent mistranslation in human cells, *RNA Biol.* 15 (2018) 567–575.
- [83] M. Frugier, L. Moulinier, R. Giegé, A domain in the N-terminal extension of class IIb eukaryotic aminoacyl-tRNA synthetases is important for tRNA binding, *EMBO J.* 19 (2000) 2371–2380.
- [84] M. Ryckelynck, R. Giegé, M. Frugier, Yeast tRNA^{ASP} charging accuracy is threatened by the N-terminal extension of aspartyl-tRNA synthetase., *J. Biol. Chem.* 278 (2003) 9683–90.
- [85] V.S. Reed, D.C. Yang, Characterization of a novel N-terminal peptide in human aspartyl-tRNA synthetase. Roles in the transfer of aminoacyl-tRNA from aminoacyl-tRNA synthetase to the elongation factor 1 alpha., *J. Biol. Chem.* 269 (1994) 32937–41.
- [86] M. Francin, M. Kaminska, P. Kerjan, M. Mirande, The N-terminal domain of mammalian Lysyl-tRNA synthetase is a functional tRNA-binding domain., *J. Biol. Chem.* 277 (2002) 1762–9.
- [87] M. Francin, M. Mirande, Functional Dissection of the Eukaryotic-specific tRNA-interacting Factor of Lysyl-tRNA Synthetase, *J. Biol. Chem.* 278 (2003) 1472–1479.

- [88] S. Cen, H. Javanbakht, M. Niu, L. Kleiman, Ability of wild-type and mutant lysyl-tRNA synthetase to facilitate tRNA^{Lys} incorporation into human immunodeficiency virus type 1., *J. Virol.* 78 (2004) 1595–601.
- [89] D.G. Kim, J.W. Choi, J.Y. Lee, H. Kim, Y.S. Oh, J.W. Lee, Y.K. Tak, J.M. Song, E. Razin, S.-H. Yun, S. Kim, Interaction of two translational components, lysyl-tRNA synthetase and p40/37LRP, in plasma membrane promotes laminin-dependent cell migration., *FASEB J.* 26 (2012) 4142–59.
- [90] H.-C. Ahn, S. Kim, B.-J. Lee, Solution structure and p43 binding of the p38 leucine zipper motif: coiled-coil interactions mediate the association between p38 and p43, *FEBS Lett.* 542 (2003) 119–124.
- [91] C.-P. Chang, G. Lin, S.-J. Chen, W.-C. Chiu, W.-H. Chen, C.-C. Wang, Promoting the formation of an active synthetase/tRNA complex by a nonspecific tRNA-binding domain., *J. Biol. Chem.* 283 (2008) 30699–706.
- [92] B.S. Negrutskii, V.F. Shalak, P. Kerjan, A. V El'skaya, M. Mirande, Functional interaction of mammalian valyl-tRNA synthetase with elongation factor eEF1Alpha in the complex with EF-1H., *J. Biol. Chem.* 274 (1999) 4545–50.
- [93] C.-Y. Chang, C.-I. Chien, C.-P. Chang, B.-C. Lin, C.-C. Wang, A WHEP Domain Regulates the Dynamic Structure and Activity of *Caenorhabditis elegans* Glycyl-tRNA Synthetase., *J. Biol. Chem.* 291 (2016) 16567–75.
- [94] W. He, H.-M. Zhang, Y.E. Chong, M. Guo, A.G. Marshall, X.-L. Yang, Dispersed disease-causing neomorphic mutations on a single protein promote the same localized conformational opening., *Proc. Natl. Acad. Sci. U. S. A.* 108 (2011) 12307–12.
- [95] M. Jura, L. Rychlewski, J. Barciszewski, Comprehensive insight into human aminoacyl-tRNA synthetases as autoantigens in idiopathic inflammatory myopathies., *Crit. Rev. Immunol.* 27 (2007) 559–72.
- [96] A. Martin, M.J. Shulman, F.W. Tsui, Epitope studies indicate that histidyl-tRNA synthetase is a stimulating antigen in idiopathic myositis., *FASEB J.* 9 (1995) 1226–1233.
- [97] M. Sajish, Q. Zhou, S. Kishi, D.M. Valdez, M. Kapoor, M. Guo, S. Lee, S. Kim, X.-L. Yang, P. Schimmel, P. Schimmel, Trp-tRNA synthetase bridges DNA-PKcs to PARP-1 to link IFN- γ and p53 signaling., *Nat. Chem. Biol.* 8 (2012) 547–54.
- [98] K. Wakasugi, B.M. Slike, J. Hood, A. Otani, K.L. Ewalt, M. Friedlander, D.A. Cheresch, P. Schimmel, A human aminoacyl-tRNA synthetase as a regulator of angiogenesis., *Proc. Natl. Acad. Sci. U. S. A.* 99 (2002) 173–7.
- [99] T. Crepin, E. Schmitt, S. Blanquet, Y. Mechulam, Structure and Function of the C-Terminal Domain of Methionyl-tRNA Synthetase[†], *Biochemistry.* 41 (2002) 13003–13011.
- [100] G. Simos, A. Segref, F. Fasiolo, K. Hellmuth, A. Shevchenko, M. Mann, E.C. Hurt, The yeast protein Arc1p binds to tRNA and functions as a cofactor for the methionyl- and glutamyl-tRNA synthetases., *EMBO J.* 15 (1996) 5437–48.
- [101] S. Quevillon, J.-C. Robinson, E. Berthonneau, M. Siatecka, M. Mirande, Macromolecular assemblage of aminoacyl-tRNA synthetases: identification of protein-protein interactions and characterization of a core protein, *J. Mol. Biol.* 285 (1999) 183–195.

- [102] M. Kaminska, V. Shalak, M. Mirande, The Appended C-Domain of Human Methionyl-tRNA Synthetase Has a tRNA-Sequestering Function, *Biochemistry*. 40 (2001) 14309–16.
- [103] E. V Koonin, A.R. Mushegian, R.L. Tatusov, S.F. Altschul, S.H. Bryant, P. Bork, A. Valencia, Eukaryotic translation elongation factor 1 gamma contains a glutathione transferase domain--study of a diverse, ancient protein superfamily using motif search and structural modeling., *Protein Sci.* 3 (1994) 2045–54.
- [104] P.S. Ray, J.C. Sullivan, J. Jia, J. Francis, J.R. Finnerty, P.L. Fox, Evolution of function of a fused metazoan tRNA synthetase., *Mol. Biol. Evol.* 28 (2011) 437–47.
- [105] J. Jia, A. Arif, P.S. Ray, P.L. Fox, WHEP domains direct noncanonical function of glutamyl-Prolyl tRNA synthetase in translational control of gene expression., *Mol. Cell.* 29 (2008) 679–90.
- [106] S.B. Rho, J.S. Lee, E.-J. Jeong, K.-S. Kim, Y.G. Kim, S. Kim, A Multifunctional Repeated Motif Is Present in Human Bifunctional tRNA Synthetase, *J. Biol. Chem.* 273 (1998) 11267–11273.
- [107] T.D. Grant, E.H. Snell, J.R. Luft, E. Quartley, S. Corretore, J.R. Wolfley, M. Elizabeth Snell, A. Hadd, J.J. Perona, E.M. Phizicky, E.J. Grayhack, Structural conservation of an ancient tRNA sensor in eukaryotic glutamyl-tRNA synthetase, *Nucleic Acids Res.* 40 (2012) 3723–3731.
- [108] T.D. Grant, J.R. Luft, J.R. Wolfley, M.E. Snell, H. Tsuruta, S. Corretore, E. Quartley, E.M. Phizicky, E.J. Grayhack, E.H. Snell, The Structure of Yeast Glutamyl-tRNA Synthetase and Modeling of Its Interaction with tRNA, *J. Mol. Biol.* 425 (2013) 2480–2493.
- [109] I. Finarov, N. Moor, N. Kessler, L. Klipcan, M.G. Safro, Structure of Human Cytosolic Phenylalanyl-tRNA Synthetase: Evidence for Kingdom-Specific Design of the Active Sites and tRNA Binding Patterns, *Structure*. 18 (2010) 343–353.
- [110] K. Wakasugi, P. Schimmel, Two distinct cytokines released from a human aminoacyl-tRNA synthetase., *Science*. 284 (1999) 147–51.
- [111] P.S. Lee, H.-M. Zhang, A.G. Marshall, X.-L. Yang, P. Schimmel, Uncovering of a short internal peptide activates a tRNA synthetase procytokine., *J. Biol. Chem.* 287 (2012) 20504–8.
- [112] H. Fukui, R. Hanaoka, A. Kawahara, Noncanonical activity of seryl-tRNA synthetase is involved in vascular development., *Circ. Res.* 104 (2009) 1253–9.
- [113] X. Xu, Y. Shi, H.-M. Zhang, E.C. Swindell, A.G. Marshall, M. Guo, S. Kishi, X.-L. Yang, Unique domain appended to vertebrate tRNA synthetase is essential for vascular development., *Nat. Commun.* 3 (2012) 681.
- [114] S.B. Rho, K.H. Lee, J.W. Kim, K. Shiba, Y.J. Jo, S. Kim, Interaction between human tRNA synthetases involves repeated sequence elements., *Proc. Natl. Acad. Sci. U. S. A.* 93 (1996) 10128–33.
- [115] G. Gory Bonfils, M. Jaquenoud, S.V. Bontron, C. Ostrowicz, C. Ungermann, C. De Virgilio, Leucyl-tRNA Synthetase Controls TORC1 via the EGO Complex, *Mol. Cell.* 46 (2012) 105–110.
- [116] J. Min Han, S. Jae Jeong, M. Chul Park, G. Kim, N. Hoon Kwon, H. Kyoung Kim, S. Hoon Ha, S. Ho Ryu, S. Kim, J.M.M. Han, S.J.J. Jeong, M.C.C. Park, G. Kim, N.H.H. Kwon, H.K.K. Kim, S.H.H. Ha, S.H.H. Ryu, S. Kim, Leucyl-tRNA Synthetase Is an Intracellular Leucine Sensor for the mTORC1-Signaling Pathway, *Cell*. 149 (2012) 410–424.

- [117] C. Ling, Y.-N. Yao, Y.-G. Zheng, H. Wei, L. Wang, X.-F. Wu, E.-D. Wang, The C-terminal appended domain of human cytosolic leucyl-tRNA synthetase is indispensable in its interaction with arginyl-tRNA synthetase in the multi-tRNA synthetase complex., *J. Biol. Chem.* 280 (2005) 34755–63.
- [118] L. Guigou, V. Shalak, M. Mirande, The tRNA-Interacting Factor p43 Associates with Mammalian Arginyl-tRNA Synthetase but Does Not Modify Its tRNA Aminoacylation Properties †, *Biochemistry.* 43 (2004) 4592–4600.
- [119] J.Y. Kim, Y.-S. Kang, J.-W. Lee, H.J. Kim, Y.H. Ahn, H. Park, Y.-G. Ko, S. Kim, p38 is essential for the assembly and stability of macromolecular tRNA synthetase complex: Implications for its physiological significance, *Proc. Natl. Acad. Sci.* 99 (2002) 7912–7916.
- [120] S. Bae Rho, M.J. Kim, J.S. Lee, W. Seol, H. Motegi, S. Kim, K. Shiba, Genetic dissection of protein–protein interactions in multi-tRNA synthetase complex, *Genetics.* 96 (1999) 4488–4493.
- [121] B.-J. Park, J.W. Kang, S.W. Lee, S.-J. Choi, Y.K. Shin, Y.H. Ahn, Y.H. Choi, D. Choi, K.S. Lee, S. Kim, The Haploinsufficient Tumor Suppressor p18 Upregulates p53 via Interactions with ATM/ATR, *Cell.* 120 (2005) 209–221.
- [122] H. Simader, M. Hothorn, C. Köhler, J. Basquin, G. Simos, D. Suck, S. J., R. J.M., M. A.-M., C. C.-M., Structural basis of yeast aminoacyl-tRNA synthetase complex formation revealed by crystal structures of two binary sub-complexes, *Nucleic Acids Res.* 34 (2006) 3968–3979.
- [123] G. Simos, A. Sauer, F. Fasiolo, E.C. Hurt, A Conserved Domain within Arc1p Delivers tRNA to Aminoacyl-tRNA Synthetases, *Mol. Cell.* 1 (1998) 235–242.
- [124] K. Galani, The intracellular location of two aminoacyl-tRNA synthetases depends on complex formation with Arc1p, *EMBO J.* 20 (2001) 6889–6898.
- [125] S.G. Park, K.L. Ewalt, S. Kim, Functional expansion of aminoacyl-tRNA synthetases and their interacting factors: new perspectives on housekeepers, *Trends Biochem. Sci.* 30 (2005) 569–574.
- [126] H.Y.H.J. Cho, S.J. Maeng, H.Y.H.J. Cho, Y.S. Choi, J.M. Chung, S. Lee, H.K. Kim, J.H. Kim, C.-Y. Eom, Y.-G. Kim, M. Guo, H.S. Jung, B.S. Kang, S. Kim, Assembly of Multi-tRNA Synthetase Complex via Heterotetrameric Glutathione Transferase-homology Domains, *J. Biol. Chem.* 290 (2015) 29313–29328.
- [127] S. Havrylenko, R. Legouis, B. Negrutskii, M. Mirande, *Caenorhabditis elegans* evolves a new architecture for the multi-aminoacyl-tRNA synthetase complex., *J. Biol. Chem.* 286 (2011) 28476–87.
- [128] I. Cestari, S. Kalidas, S. Monnerat, A. Anupama, M.A. Phillips, K. Stuart, A multiple aminoacyl-tRNA synthetase complex that enhances tRNA-aminoacylation in African trypanosomes., *Mol. Cell. Biol.* 33 (2013) 4872–88.
- [129] J.M. van Rooyen, J.-B. Murat, P.-M. Hammoudi, S. Kieffer-Jaquinod, Y. Coute, A. Sharma, H. Pelloux, H. Belrhali, M.-A. Hakimi, Assembly of the novel five-component apicomplexan multi-aminoacyl-tRNA synthetase complex is driven by the hybrid scaffold protein Tg-p43., *PLoS One.* 9 (2014) e89487.

- [130] M. Raina, S. Elgamal, T.J. Santangelo, M. Ibba, Association of a multi-synthetase complex with translating ribosomes in the archaeon *Thermococcus kodakarensis*, *FEBS Lett.* 586 (2012) 2232–2238.
- [131] R.S.A. Lipman, J. Chen, C. Evilia, O. Vitseva, Y.-M. Hou, Association of an Aminoacyl-tRNA Synthetase with a Putative Metabolic Protein in Archaea, *Biochemistry.* 42 (2003) 7487–7496.
- [132] J.P. Oza, K.R. Sowers, J.J. Perona, Linking Energy Production and Protein Synthesis in Hydrogenotrophic Methanogens, *Biochemistry.* 51 (2012) 2378–2389.
- [133] M. Praetorius-Ibba, C.D. Hausmann, M. Paras, T.E. Rogers, M. Ibba, Functional Association between Three Archaeal Aminoacyl-tRNA Synthetases, *J. Biol. Chem.* 282 (2006) 3680–3687.
- [134] C.D. Hausmann, M. Praetorius-Ibba, M. Ibba, An aminoacyl-tRNA synthetase:elongation factor complex for substrate channeling in archaeal translation., *Nucleic Acids Res.* 35 (2007) 6094–102
- [135] V. Godinic-Mikulcic, J. Jaric, B.J. Greber, V. Franke, V. Hodnik, G. Anderluh, N. Ban, I. Weygand-Durasevic, Archaeal aminoacyl-tRNA synthetases interact with the ribosome to recycle tRNAs, *Nucleic Acids Res.* 42 (2014) 5191–5201.
- [136] Y. Goldgur, M. Safro, Aminoacyl-tRNA synthetases from *Haloarcula marismortui*: an evidence for a multienzyme complex in a procaryotic system., *Biochem. Mol. Biol. Int.* 32 (1994) 1075–83.
- [137] C.L. Harris, An aminoacyl-tRNA synthetase complex in *Escherichia coli.*, *J. Bacteriol.* 169 (1987) 2718–23.
- [138] S. An, K. Musier-Forsyth, Trans-editing of Cys-tRNA^{Pro} by *Haemophilus influenzae* YbaK Protein, *J. Biol. Chem.* 279 (2004) 42359–42362.
- [139] S. An, K. Musier-Forsyth, Cys-tRNA^{Pro} editing by *Haemophilus influenzae* YbaK via a novel synthetase.YbaK.tRNA ternary complex., *J. Biol. Chem.* 280 (2005) 34465–72.
- [140] B. Ruan, D. Söll, The Bacterial YbaK Protein Is a Cys-tRNA^{Pro} and Cys-tRNA^{Cys} Deacylase, *J. Biol. Chem.* 280 (2005) 25887–25891.
- [141] E. Maloney, D. Stankowska, J. Zhang, M. Fol, Q.-J. Cheng, S. Lun, W.R. Bishai, M. Rajagopalan, D. Chatterjee, M. V. Madiraju, The Two-Domain LysX Protein of *Mycobacterium tuberculosis* Is Required for Production of Lysinylated Phosphatidylglycerol and Resistance to Cationic Antimicrobial Peptides, *PLoS Pathog.* 5 (2009) e1000534.
- [142] M. Bailly, M. Blaise, B. Lorber, H.D. Becker, D. Kern, The Transamidosome: A Dynamic Ribonucleoprotein Particle Dedicated to Prokaryotic tRNA-Dependent Asparagine Biosynthesis, *Mol. Cell.* 28 (2007) 228–239.
- [143] M.R. Buddha, K.M. Keery, B.R. Crane, An unusual tryptophanyl tRNA synthetase interacts with nitric oxide synthase in *Deinococcus radiodurans.*, *Proc. Natl. Acad. Sci. U. S. A.* 101 (2004) 15881–6.

- [144] J. Santamaría-Gómez, J.A.G. Ochoa de Alda, E. Olmedo-Verd, R. Bru-Martínez, I. Luque, Sub-Cellular Localization and Complex Formation by Aminoacyl-tRNA Synthetases in Cyanobacteria: Evidence for Interaction of Membrane-Anchored ValRS with ATP Synthase., *Front. Microbiol.* 7 (2016) 857.
- [145] J. Santamaria-Gomez, V. Mariscal, I. Luque, Mechanisms for Protein Redistribution in Thylakoids of *Anabaena* During Cell Differentiation, *Plant Cell Physiol.* 59 (2018) 1860–1873.
- [146] S. Rocak, I. Landeka, I. Weygand-Durasevic, Identifying Pex21p as a protein that specifically interacts with yeast seryl-tRNA synthetase, *FEMS Microbiol. Lett.* 214 (2002) 101–106.
- [147] V. Godinic, M. Mocibob, S. Rocak, M. Ibba, I. Weygand-Durasevic, Peroxin Pex21p interacts with the C-terminal noncatalytic domain of yeast seryl-tRNA synthetase and forms a specific ternary complex with tRNA^{Ser}, *FEBS J.* 274 (2007) 2788–2799.
- [148] M. Mocibob, I. Weygand-Durasevic, The proximal region of a noncatalytic eukaryotic seryl-tRNA synthetase extension is required for protein stability in vitro and in vivo, *Arch. Biochem. Biophys.* 470 (2008) 129–138.
- [149] A. Dagkessamanskaia, H. Martin-Yken, F. Basmaji, P. Briza, J. Francois, Interaction of Knr4 protein, a protein involved in cell wall synthesis, with tyrosine tRNA synthetase encoded by *TYS1* in *Saccharomyces cerevisiae*, *FEMS Microbiol. Lett.* 200 (2001) 53–58.
- [150] S.S. Ivakhno, A.I. Kornelyuk, Bioinformatic analysis of changes in expression level of tyrosyl-tRNA synthetase during sporulation process in *Saccharomyces cerevisiae*., *Mikrobiol. Z.* 67 (2005) 37–49.
- [151] C.J. Herbert, M. Labouesse, G. Dujardin, P.P. Slonimski, The NAM2 proteins from *S. cerevisiae* and *S. douglasii* are mitochondrial leucyl-tRNA synthetases, and are involved in mRNA splicing., *EMBO J.* 7 (1988) 473–83.
- [152] S.B. Rho, S.A. Martinis, The b14 group I intron binds directly to both its protein splicing partners, a tRNA synthetase and maturase, to facilitate RNA splicing activity., *RNA.* 6 (2000) 1882–94.
- [153] M. Frugier, R. Giegé, Yeast Aspartyl-tRNA Synthetase Binds Specifically its Own mRNA, *J. Mol. Biol.* 331 (2003) 375–383.
- [154] M. Frugier, M. Ryckelynck, R. Giegé, tRNA-balanced expression of a eukaryal aminoacyl-tRNA synthetase by an mRNA-mediated pathway., *EMBO Rep.* 6 (2005) 860–5.
- [155] C. Magrath, L.E. Hyman, A mutation in *GRS1*, a glycyl-tRNA synthetase, affects 3'-end formation in *Saccharomyces cerevisiae*., *Genetics.* 152 (1999) 129–41.
- [156] K. Johanson, T. Hoang, M. Sheth, L.E. Hyman, *GRS1*, a yeast tRNA synthetase with a role in mRNA 3' end formation., *J. Biol. Chem.* 278 (2003) 35923–30.
- [157] M. Frechin, L. Enkler, E. Tetaud, D. Laporte, B. Senger, C. Blancard, P. Hammann, G. Bader, S. Clauder-Münster, L.M.M. Steinmetz, R.P.P. Martin, J.-P. di Rago, H.D.D. Becker, J.-P. di Rago, H.D.D. Becker, J.-P. di Rago, H.D.D. Becker, J.-P. di Rago, H.D.D. Becker, Expression of Nuclear and Mitochondrial Genes Encoding ATP Synthase Is Synchronized by Disassembly of a Multisynthetase Complex, *Mol. Cell.* 56 (2014) 763–776.

- [158] M. Frechin, B. Senger, M. Braye, D. Kern, R.P. Martin, H.D. Becker, Yeast mitochondrial Gln-tRNA^{Gln} is generated by a GatFAB-mediated transamidation pathway involving Arc1p-controlled subcellular sorting of cytosolic GluRS, *Genes Dev.* 23 (2009) 1119–1130.
- [159] Z. Cao, H. Wang, X. Mao, L. Luo, Noncanonical function of threonyl-tRNA synthetase regulates vascular development in zebrafish, *Biochem. Biophys. Res. Commun.* 473 (2016) 67–72.
- [160] Y. Chen, Z.-R. Ruan, Y. Wang, Q. Huang, M.-Q. Xue, X.-L. Zhou, E.-D. Wang, A threonyl-tRNA synthetase-like protein has tRNA aminoacylation and editing activities., *Nucleic Acids Res.* 46 (2018) 3643–3656.
- [161] W. Herzog, K. Müller, J. Huisken, D.Y.R. Stainier, Genetic evidence for a noncanonical function of seryl-tRNA synthetase in vascular development., *Circ. Res.* 104 (2009) 1260–6.
- [162] Y. Shi, X. Xu, Q. Zhang, G. Fu, Z. Mo, G.S. Wang, S. Kishi, X.-L. Yang, tRNA synthetase counteracts c-Myc to develop functional vasculature., *Elife.* 3 (2014) e02349.
- [163] G. Fu, T. Xu, Y. Shi, N. Wei, X.-L. Yang, tRNA-controlled nuclear import of a human tRNA synthetase., *J. Biol. Chem.* 287 (2012) 9330–4.
- [164] Y. Greenberg, M. King, W.B. Kiosses, K. Ewalt, X. Yang, P. Schimmel, J.S. Reader, E. Tzima, The novel fragment of tyrosyl tRNA synthetase, mini-TyrRS, is secreted to induce an angiogenic response in endothelial cells., *FASEB J.* 22 (2008) 1597–605.
- [165] R. Zeng, M. Wang, G. You, R. Yue, Y. Chen, Z. Zeng, R. Liu, O. Qiang, L. Zhang, Effect of Mini-Tyrosyl-tRNA Synthetase/Mini-Tryptophanyl-tRNA Synthetase on Angiogenesis in Rhesus Monkeys after Acute Myocardial Infarction, *Cardiovasc. Ther.* 34 (2016) 4–12.
- [166] E. Tzima, J.S. Reader, M. Irani-Tehrani, K.L. Ewalt, M.A. Schwartz, P. Schimmel, VE-cadherin links tRNA synthetase cytokine to anti-angiogenic function., *J. Biol. Chem.* 280 (2005) 2405–8.
- [167] E. Tzima, P. Schimmel, Inhibition of tumor angiogenesis by a natural fragment of a tRNA synthetase, *Science.* 309 (2006) 1534–1539.
- [168] C.M. Guzzo, D.C.H. Yang, Lysyl-tRNA synthetase interacts with EF1 α , aspartyl-tRNA synthetase and p38 in vitro, *Biochem. Biophys. Res. Commun.* 365 (2008) 718–723.
- [169] X.-L. Yang, F.J. Otero, K.L. Ewalt, J. Liu, M.A. Swairjo, C. Köhrer, U.L. RajBhandary, R.J. Skene, D.E. McRee, P. Schimmel, Two conformations of a crystalline human tRNA synthetase-tRNA complex: implications for protein synthesis, *EMBO J.* 25 (2006) 2919–2929.
- [170] Y.G. Ko, E.Y. Kim, T. Kim, H. Park, H.S. Park, E.J. Choi, S. Kim, Glutamine-dependent antiapoptotic interaction of human glutamyl-tRNA synthetase with apoptosis signal-regulating kinase 1., *J. Biol. Chem.* 276 (2001) 6030–6.
- [171] Y.G. Ko, Y.S. Kang, E.K. Kim, S.G. Park, S. Kim, Nucleolar localization of human methionyl-tRNA synthetase and its role in ribosomal RNA synthesis., *J. Cell Biol.* 149 (2000) 567–74.
- [172] G. Fu, T. Xu, Y. Shi, N. Wei, X.-L. Yang, tRNA-controlled nuclear import of a human tRNA synthetase., *J. Biol. Chem.* 287 (2012) 9330–4.

- [173] M. Sajish, P. Schimmel, A human tRNA synthetase is a potent PARP1-activating effector target for resveratrol, *Nature*. 519 (2015) 370–375.
- [174] X. Cao, C. Li, S. Xiao, Y. Tang, J. Huang, S. Zhao, X. Li, J. Li, R. Zhang, W. Yu, Acetylation promotes TyrRS nuclear translocation to prevent oxidative damage., *Proc. Natl. Acad. Sci. U. S. A.* 114 (2017) 687–692.
- [175] V.I. Popenko, N.E. Cherny, S.F. Beresten, J.L. Ivanova, V. V Filonenko, L.L. Kisselev, Immunoelectron microscopic location of tryptophanyl-tRNA synthetase in mammalian, prokaryotic and archaeobacterial cells., *Eur. J. Cell Biol.* 62 (1993) 248–58.
- [176] H. Nechushtan, E. Razin, The function of MITF and associated proteins in mast cells, *Mol. Immunol.* 38 (2002) 1177–1180.
- [177] E. Razin, Z.C. Zhang, H. Nechushtan, S. Frenkel, Y.N. Lee, R. Arudchandran, J. Rivera, Suppression of microphthalmia transcriptional activity by its association with protein kinase C-interacting protein 1 in mast cells., *J. Biol. Chem.* 274 (1999) 34272–6.
- [178] I. Carmi-Levy, N. Yannay-Cohen, G. Kay, E. Razin, H. Nechushtan, Diadenosine tetraphosphate hydrolase is part of the transcriptional regulation network in immunologically activated mast cells., *Mol. Cell. Biol.* 28 (2008) 5777–84.
- [179] S.G. Park, H.J. Kim, Y.H. Min, E.-C. Choi, Y.K. Shin, B.-J. Park, S.W. Lee, S. Kim, Human lysyl-tRNA synthetase is secreted to trigger proinflammatory response., *Proc. Natl. Acad. Sci. U. S. A.* 102 (2005) 6356–61.
- [180] S.B. Kim, H.R. Kim, M.C. Park, S. Cho, P.C. Goughnour, D. Han, I. Yoon, Y. Kim, T. Kang, E. Song, P. Kim, H. Choi, J.Y. Mun, C. Song, S. Lee, H.S. Jung, S. Kim, Caspase-8 controls the secretion of inflammatory lysyl-tRNA synthetase in exosomes from cancer cells., *J. Cell Biol.* 216 (2017) 2201–2216.
- [181] M.C. Park, T. Kang, D. Jin, J.M. Han, S.S.B. Kim, Y.J.Y.W. Park, K. Cho, Y.J.Y.W. Park, M. Guo, W. He, X.-L. Yang, P. Schimmel, S.S.B. Kim, Secreted human glycyl-tRNA synthetase implicated in defense against ERK-activated tumorigenesis., *Proc. Natl. Acad. Sci. U. S. A.* 109 (2012) e640-7.
- [182] M.-S. Yoon, K. Son, E. Arauz, J.M. Han, S. Kim, J. Chen, Leucyl-tRNA Synthetase Activates Vps34 in Amino Acid-Sensing mTORC1 Signaling., *Cell Rep.* 16 (2016) 1510–1517.
- [183] A. Arif, F. Terenzi, A.A. Potdar, J. Jia, J. Sacks, A. China, D. Halawani, K. Vasu, X. Li, J.M. Brown, J. Chen, S.C. Kozma, G. Thomas, P.L. Fox, EPRS is a critical mTORC1–S6K1 effector that influences adiposity in mice, *Nature*. 542 (2017) 357–361.
- [184] P. Sampath, B. Mazumder, V. Seshadri, P.L. Fox, Transcript-selective translational silencing by gamma interferon is directed by a novel structural element in the ceruloplasmin mRNA 3' untranslated region., *Mol. Cell. Biol.* 23 (2003) 1509–19.
- [185] P. Sampath, B. Mazumder, V. Seshadri, C.A. Gerber, L. Chavatte, M. Kinter, S.M. Ting, J.D. Dignam, S. Kim, D.M. Driscoll, P.L. Fox, Noncanonical Function of Glutamyl-Prolyl-tRNA Synthetase: Gene-Specific Silencing of Translation, *Cell*. 119 (2004) 195–208.

- [186] P.S. Ray, A. Arif, P.L. Fox, P.L.F. P.S. Ray, A. Arif, Macromolecular complexes as depots for releasable regulatory proteins, *Trends Biochem. Sci.* 32 (2007) 158–164.
- [187] E.-Y. Lee, H.-C. Lee, H.-K. Kim, S.Y. Jang, S.-J. Park, Y.-H. Kim, J.H. Kim, J. Hwang, J.-H. Kim, T.-H. Kim, A. Arif, S.-Y. Kim, Y.-K. Choi, C. Lee, C.-H. Lee, J.U. Jung, P.L. Fox, S. Kim, J.-S. Lee, M.H. Kim, Infection-specific phosphorylation of glutamyl-prolyl tRNA synthetase induces antiviral immunity., *Nat. Immunol.* 17 (2016) 1252–1262.
- [188] F. Guo, S. Cen, M. Niu, H. Javanbakht, L. Kleiman, Specific inhibition of the synthesis of human lysyl-tRNA synthetase results in decreases in tRNA^{Lys} incorporation, tRNA(3)^{Lys} annealing to viral RNA, and viral infectivity in human immunodeficiency virus type 1., *J. Virol.* 77 (2003) 9817–22.
- [189] J. Ptacek, G. Devgan, G. Michaud, H. Zhu, X. Zhu, J. Fasolo, H. Guo, G. Jona, A. Breitskreutz, R. Sopko, R.R. McCartney, M.C. Schmidt, N. Rachidi, S.-J. Lee, A.S. Mah, L. Meng, M.J.R. Stark, D.F. Stern, C. De Virgilio, M. Tyers, B. Andrews, M. Gerstein, B. Schweitzer, P.F. Predki, M. Snyder, Global analysis of protein phosphorylation in yeast, *Nature.* 438 (2005) 679–684.
- [190] A.A. Duchon, C. St Gelais, N. Titkemeier, J. Hatterschide, L. Wu, K. Musier-Forsyth, HIV-1 Exploits a Dynamic Multi-aminoacyl-tRNA Synthetase Complex To Enhance Viral Replication., *J. Virol.* 91 (2017) e01240-17.
- [191] B.J. Kovalski, R. Kennedy, M.K. Hong, S.A. Datta, L. Kleiman, A. Rein, K. Musier-Forsyth, *In Vitro* Characterization of the Interaction between HIV-1 Gag and Human Lysyl-tRNA Synthetase, *J. Biol. Chem.* 281 (2006) 19449–19456.
- [192] S. Dhandayuthapani, M.W. Blaylock, C.M. Bebear, W.G. Rasmussen, J.B. Baseman, Peptide Methionine Sulfoxide Reductase (MsrA) Is a Virulence Determinant in *Mycoplasma genitalium* Downloaded from, *J. Bacteriol.* 183 (2001) 5645–5650.
- [193] J.-P. Madeira, B.M. Alpha-Bazin, J. Armengaud, C. Duport, Methionine Residues in Exoproteins and Their Recycling by Methionine Sulfoxide Reductase AB Serve as an Antioxidant Strategy in *Bacillus cereus*., *Front. Microbiol.* 8 (2017) 1342.
- [194] Y.Y. Pang, J. Schwartz, S. Bloomberg, J.M. Boyd, A.R. Horswill, W.M. Nauseef, Methionine sulfoxide reductases protect against oxidative stress in *Staphylococcus aureus* encountering exogenous oxidants and human neutrophils., *J. Innate Immun.* 6 (2014) 353–64.
- [195] V.K. Singh, J. Moskovitz, B.J. Wilkinson, R.K. Jayaswal, Molecular characterization of a chromosomal locus in *Staphylococcus aureus* that contributes to oxidative defence and is highly induced by the cell-wall-active antibiotic oxacillin, *Microbiology.* 147 (2001) 3037–3045.
- [196] T.M. Wizemann, J. Moskovitz, B.J. Pearce, D. Cundell, C.G. Arvidson, M. Sot, H. Weissbacht, N. Brott, H.R. Masure, Peptide methionine sulfoxide reductase contributes to the maintenance of adhesins in three major pathogens, *Proc. Natl. Acad. Sci. U. S. A.* 93 (1996) 7985–90.
- [197] J. Moskovitz, M.A. Rahman, Jeffrey Strassman, S.O. Yancey, S.R. Kushner, N. Brot, H. Weissbach, *Escherichia coli* Peptide Methionine Sulfoxide Reductase Gene: Regulation of Expression and Role in Protecting Against Oxidative Damage, *J. Bacteriol.* 177 (1995) 502–7.

- [198] G. St John, N. Brot, J. Ruan, H. Erdjument-Bromage, P. Tempst, H. Weissbach, C. Nathan, Peptide methionine sulfoxide reductase from *Escherichia coli* and *Mycobacterium tuberculosis* protects bacteria against oxidative damage from reactive nitrogen intermediates, *Proc. Natl. Acad. Sci. U. S. A.* 98 (2001) 9901-6.
- [199] J. Moskovitz, B.S. Berlett, J.M. Poston, E.R. Stadtman, The yeast peptide-methionine sulfoxide reductase functions as an antioxidant in vivo., *Proc. Natl. Acad. Sci. U. S. A.* 94 (1997) 9585-9.
- [200] L. Tarrago, A. Kaya, E. Weerapana, S.M. Marino, V.N. Gladyshev, Methionine Sulfoxide Reductases Preferentially Reduce Unfolded Oxidized Proteins and Protect Cells from Oxidative Protein Unfolding, *J. Biol. Chem.* 287 (2012) 24448.
- [201] J. Moskovitz, S. Bar-Noy, W.M. Williams, J. Requena, B.S. Berlett, E.R. Stadtman, Methionine sulfoxide reductase (MsrA) is a regulator of antioxidant defense and lifespan in mammals, 2001.
- [202] A.B. Salmon, V.I. Pérez, A. Bokov, A. Jernigan, G. Kim, H. Zhao, R.L. Levine, A. Richardson, Lack of methionine sulfoxide reductase A in mice increases sensitivity to oxidative stress but does not diminish life span., *FASEB J.* 23 (2009) 3601-8.
- [203] J.I. Kim, S.H. Choi, K.-J. Jung, E. Lee, H.-Y. Kim, K.M. Park, Protective role of methionine sulfoxide reductase A against ischemia/reperfusion injury in mouse kidney and its involvement in the regulation of trans-sulfuration pathway., *Antioxid. Redox Signal.* 18 (2013) 2241-50.
- [204] J.W. Lee, N.V. Gordiyenko, M. Marchetti, N. Tserentsoodol, D. Sagher, S. Alam, H. Weissbach, M. Kantorow, I.R. Rodriguez, Gene structure, localization and role in oxidative stress of methionine sulfoxide reductase A (MSRA) in the monkey retina, *Exp. Eye Res.* 82 (2006) 816-827.
- [205] M. Kantorow, J.R. Hawse, T.L. Cowell, S. Benhamed, G.O. Pizarro, V.N. Reddy, J.F. Hejtmancik, Methionine sulfoxide reductase A is important for lens cell viability and resistance to oxidative stress, *PNAS* 101 (2004) 9654-59.
- [206] M.A. Marchetti, W. Lee, T.L. Cowell, T.M. Wells, H. Weissbach, M. Kantorow, Silencing of the methionine sulfoxide reductase A gene results in loss of mitochondrial membrane potential and increased ROS production in human lens cells, *Exp. Eye Res.* 83 (2006) 1281-6.
- [207] J. Moskovitz, E. Flescher, B.S. Berlett, J. Azare, J.M. Poston, E.R. Stadtman, Overexpression of peptide-methionine sulfoxide reductase in *Saccharomyces cerevisiae* and human T cells provides them with high resistance to oxidative stress, *Proc. Natl. Acad. Sci.* 95 (1998) 14071-14075.
- [208] H. Ruan, D. Tang, M.-L. Chen, M.-L.A. Joiner, S.¶ Guangrong, N. Brot, H. Weissbach, S.H. Heinemann, L. Iverson, C.-F. Wu, T. Hoshi, High-quality life extension by the enzyme peptide methionine sulfoxide reductase, *Proc. Natl. Acad. Sci.* 99 (2002) 2748-53.
- [209] O. Vermolaieva, R. Xu, C. Schinstock, N. Brot, H. Weissbach, S.H. Heinemann, T. Hoshi, Methionine sulfoxide reductase A protects neuronal cells against brief hypoxia/reoxygenation, *Proc. Natl. Acad. Sci.* 101 (2004) 1159-1164.
- [210] H.M. Prentice, I.A. Moench, Z.T. Rickaway, C.J. Dougherty, K.A. Webster, H. Weissbach, MsrA protects cardiac myocytes against hypoxia/reoxygenation induced cell death, *Biochem. Biophys. Res. Commun.* 366 (2008) 775-778.

- [211] C.R. Picot, I. Petropoulos, M. Perichon, M. Moreau, C. Nizard, B. Friguet, Overexpression of MsrA protects WI-38 SV40 human fibroblasts against H₂O₂-mediated oxidative stress, *Free Radic. Biol. Med.* 39 (2005) 1332–1341.
- [212] T.E. Jones, R.W. Alexander, T. Pan, Misacylation of specific nonmethionyl tRNAs by a bacterial methionyl-tRNA synthetase, *Proc. Natl. Acad. Sci. U. S. A.* 108 (2011).
- [213] M.H. Schwartz, J.R. Waldbauer, L. Zhang, T. Pan, Global tRNA misacylation induced by anaerobiosis and antibiotic exposure broadly increases stress resistance in *Escherichia coli.*, *Nucleic Acids Res.* 44 (2016) 10292–10303.
- [214] M.H. Schwartz, T. Pan, tRNA Misacylation with Methionine in the Mouse Gut Microbiome in Situ, *Microb. Ecol.* 74 (2017) 10–14.
- [215] M.H. Schwartz, T. Pan, Temperature dependent mistranslation in a hyperthermophile adapts proteins to lower temperatures, *Nucleic Acids Res.* 44 (2016) 294–303.
- [216] E. Wiltrout, J.M. Goodenbour, M. Fréchin, T. Pan, Misacylation of tRNA with methionine in *Saccharomyces cerevisiae.*, *Nucleic Acids Res.* 40 (2012) 10494–506.
- [217] N. Netzer, J.M. Goodenbour, A. David, K.A. Dittmar, R.B. Jones, J.R. Schneider, D. Boone, E.M. Eves, M.R. Rosner, J.S. Gibbs, A. Embry, B. Dolan, S. Das, H.D. Hickman, P. Berglund, J.R. Bennink, J.W. Yewdell, T. Pan, Innate immune and chemically triggered oxidative stress modifies translational fidelity, *Nature.* 462 (2009) 522–526.
- [218] J.Y. Lee, D.G. Kim, B. Kim, W.S. Yang, J. Hong, T. Kang, Y.S. Oh, K.R. Kim, B.W. Han, B.J. Hwang, B.S. Kang, M. Kang, M. Kim, Promiscuous methionyl-tRNA synthetase mediates adaptive mistranslation to protect cells against oxidative stress, *J. Cell Sci.* 127 (2014) 4234–4245.
- [219] X. Wang, T. Pan, Methionine Mistranslation Bypasses the Restraint of the Genetic Code to Generate Mutant Proteins with Distinct Activities., *PLoS Genet.* 11 (2015) e1005745.



UNIVERSITE DE STRASBOURG

RESUME DE LA THESE DE DOCTORAT

Discipline : **Sciences de la Vie et de la Santé**

Spécialité (facultative) : **Aspects Moléculaires et Cellulaires de la Biologie**

Présentée par : **DEBARD Sylvain**

Titre : **Dynamique moléculaire de la méthionyl-ARNt-synthétase et ses nouvelles fonctions non canoniques chez la levure *S. cerevisiae*.**

Unité de Recherche : **UMR7156 – Dynamiques et Plasticité des Synthétases**

Directeur de Thèse : **Pr. BECKER Hubert, Professeur des Universités**

Localisation : **Institut de Physiologie et Chimie Biologique (IPCB), campus Université Strasbourg**

ECOLE DOCTORALE : ED 414 – Sciences de la vie et de la santé

Résumé de thèse

DEBARD Sylvain

UMR7156, Dynamique et plasticité des synthétases

Dynamique moléculaire de la méthionyl-ARNt-synthétase et ses nouvelles fonctions non-canoniques chez la levure *S. cerevisiae*.

1. Etude de la mésincorporation de méthionine chez *S. cerevisiae*

1.1 Introduction

Une fonction commune des enzymes Methionyl-ARNt-synthétase cytoplasmiques (cMRS) Humaine et de Levure est leur participation au mécanisme de défense contre les dommages créés par les espèces réactives de l'oxygène (ROS). En effet, chez ces 2 organismes, il a été observé une mésincorporation élevée de méthionines dans les protéines en réponse au stress oxydatif. Cet accroissement du contenu en méthionines dans les protéines est dû à une augmentation de l'activité de "mischarging" de la cMRS ; c'est-à-dire la charge additionnelle d'espèces d'ARNt autres que l'ARNt^{Met} par cette enzyme. Cette mésincorporation encore appelée "traduction adaptative" permet de dégénérer le protéome de l'organisme face à une condition de stress afin de modifier les propriétés des protéines traduites et leur permettre d'assurer leurs fonctions ou de nouvelles dans les conditions de stress. Dans le cas du stress oxydatif, la mésincorporation de méthionines à la surface des protéines permettrait de lutter contre les espèces oxydantes car son atome de soufre, pouvant être oxydé par un mécanisme réversible, "pompe" les ROS formés et permet la diminution du stress oxydatif. Chez la Levure et l'Homme il semblerait que seules certaines espèces bien précises d'ARNt puissent être mischargées pour alimenter ce phénomène de traduction adaptative. Néanmoins, quelle forme de cMRS, nucléaire, cytosolique, nucléaire entière ou tronquée de son domaine N-terminal, est responsable de ce "mischarging" anti-oxydant reste encore à être élucidé. De plus, aucun système n'a été créé pour suivre la mésincorporation de Met dans les protéines de façon systématique pour chaque espèce d'ARNt mésacylée. L'objectif de ce projet été de construire un outil qui permette la quantification de mésincorporation de Met chez la levure *S. cerevisiae* au niveau de l'ensemble des codons codants du code génétique.

1.2 Outil développé et résultats

La stratégie utilisée pendant ma thèse pour observer la mésincorporation de Met repose sur la conception d'un nouvel outil de biologie : la protéine fluorescente mRuby2 (dérivée de la

RFP) présente une méthionine indispensable dans son fluorophore Cette méthionine (M67) est incorporée dans la séquence sauvage par le codon AUG en position 67. La substitution de ce codon en position 67 permet de générer une protéine mRuby2 mutante possédant un autre acide aminé en position 67 et dont la fluorescence rouge est abolie. S'il y a effectivement mésincorporation de méthionine en position 67, la fluorescence rouge de cette protéine mutante est rétablie. Afin de normaliser et quantifier cette fluorescence rouge émise par la protéine mRuby2 suite à la mésincorporation de Met, le gène sauvage de la protéine EGFP a été cloné en 3' du gène de la mRuby2. Le gène mRuby2 sauvage (contenant le codon ATG67) a été obtenu par synthèse de gène GenScript, flanqué par les séquences attB1/attB2 dans le vecteur pUC57. Par clonage Gateway, la séquence du gène a été clonée dans un vecteur pRS304-ccdB-EGFP qui permet l'expression de la protéine de fusion (ou rapporteur bifluorescent) de façon homogène dans toutes les cellules puisque le gène est intégré au génome. Le promoteur choisi pour l'expression de ce rapporteur bifluorescent est le promoteur du gène TDH3, promoteur constitutif et fort permettant une expression suffisante du rapporteur pour détecter de faibles signaux de fluorescence.

Afin d'obtenir toutes les constructions mutantes pour le codon 67 (soit 61 différentes constructions pour les 61 codons testés), une mutagenèse par PCR a été effectuée et m'a permis l'obtention d'une banque de 61 plasmides. Des constructions contrôles ont également été réalisées afin de normaliser la fluorescence : un contrôle EGFP seul en mutant les trois résidus du fluorophore de mRuby2 ; un contrôle mRuby2 en mutant la triade du fluorophore de l'EGFP, et le double mutant négatif en mutant les deux fluorophores. L'ensemble de ces constructions ont été exprimées dans plusieurs souches de *S. cerevisiae* et la quantification de cette mésincorporation de Met a été réalisée en microscopie à épifluorescence, et pour une partie des souches en cytométrie de flux. L'étude systématique des 61 codons sur différentes souches de *S. cerevisiae* (souche de levure RS453 et W303 adaptées à la respiration, ou BY4742 dont la croissance est ralentie en milieu respiratoire et qui peut présenter un déficit de défense en milieu oxydatif) a permis d'identifier une mésincorporation de Met en conditions basales (milieu riche) essentiellement en lieu et place du résidu leucine à hauteur de 2-3 % de mésincorporation.

La protéine Arc1 joue un rôle majeur de plateforme et de cofacteur enzymatique pour la cMRS en augmentant considérablement son activité catalytique. La souche RS453 *arc1Δ* a été transformée par la banque de plasmides et présente un taux de mésincorporation de Met plus important à la place du résidu leucine (5-6 %) mais aussi à la place de plusieurs autres résidus d'aa, ce qui constitue une preuve élégante du rôle d'Arc1 dans la fidélité d'aminoacylation de la cMRS.

L'observation microscopique sera validée par une analyse de spectrométrie de masse en collaboration avec le laboratoire du Dr. Christine Carapito à l'IPHC Cronenbourg (UMR 7178) en cours de réalisation. J'ai également mené une étude bioinformatique en collaboration avec le département iCube (Dr. Poch et L. Moulinier) afin de trouver une correspondance entre la position

d'un acide aminé dans une structure protéique (en surface ou enfoui) et le codon codant pour cet acide aminé.

2. Caractérisation d'une forme clivée de la cMRS

2.1 Introduction

J'ai également mené une étude sur le rôle potentiel du clivage de la cMRS. En effet, il a été trouvé par le laboratoire une forme tronquée de la cMRS d'environ 70 kDa (la protéine entière présente une masse de 100 kDa) dans les levures en fermentation qui n'avait jusqu'alors jamais été caractérisée. La présence d'une forme clivée de la cMRS révèle un rôle potentiel différent de celui de la cMRS entière. Il est important de connaître le mécanisme de clivage de la cMRS afin de trouver ce rôle.

2.2 Résultats et discussion

Les expériences menées sur des mutants de clivage pour la cMRS ont montré :

- que ce clivage est effectivement post traductionnel et donc protéolytique. J'ai mis au point un test de clivage *ex vivo* de la cMRS par addition d'un extrait de levure sur la protéine cMRS recombinante purifiée d'*E. coli*. Après fractionnement d'un extrait total de levure par chromatographies successives, chaque fraction a été testée pour identifier une activité de clivage et les fractions positives ont été analysées en spectrométrie de masse (collaboration Dr. Carapito, UMR7178).
- la protéase identifiée est une aspartyl-protéase codée par le gène *PEP4*. Il s'agit de l'homologue de la cathepsine D humaine, présente au niveau vacuolaire. La délétion du gène *PEP4* dans une souche de levure supprime l'activité de clivage de la cMRS dans le test *ex vivo*.
- Ce clivage est inhibé par l'interaction de la cMRS avec Arc1p (ajout de Arc1 recombinant purifié au test de clivage *in vitro*). De plus, la délétion du gène *ARC1* dans une souche de levure augmente considérablement le clivage de la cMRS *in vivo*, passant de 2-3 % de forme clivée dans une souche sauvage à 15 % pour une souche *Arc1Δ*.
- La purification de la forme tronquée de cMRS puis l'analyse de son extrémité N-terminale par spectrométrie de masse ont permis d'identifier le site de clivage entre le résidu tyrosyl en position 132 et le résidu alanyl en position 133.
- La levure est capable de survivre en présence de la seule forme tronquée de cMRS. Cependant la croissance de l'organisme est ralentie.

Des études pour comprendre le rôle de la cMRS- Δ 132 ont été menées chez la levure. J'ai pu montrer par microscopie à épifluorescence que cette forme clivée était présente dans le

noyau alors que la cMRS sauvage est exclue de cet organite en grande majorité. De plus, des premières analyses de co-immunoprécipitation suivies par spectrométrie de masse ont permis d'identifier des interactants nucléaires seulement avec la cMRS- Δ 132.

Cette forme clivée est générée rapidement dans les cellules suite à un choc thermique principalement, mais peut également apparaître suite à un stress nutritionnel (passage d'un milieu riche à un milieu pauvre en nutriments) ou métabolique (passage de glucose à glycérol comme source de carbone). L'observation des souches de cMRS étiquetées avec la GFP a révélé que la cMRS sauvage forme des agrégats cellulaires pour de hautes températures à partir de 40 °C, tandis que la forme clivée ne présente aucune agrégation cellulaire pour ces hautes températures. Il semblerait donc que la délétion du domaine N-terminal de la cMRS permette une meilleure stabilité de la protéine lors d'un stress thermique.

3. Projet annexe:

La protéine Arc1 joue un rôle majeur de plateforme pour la cMRS et la cERS, et augmente considérablement les activités catalytiques de ces dernières. En plus d'un rôle structural et enzymatique, cette protéine est également impliquée dans l'export nucléaire des ARNt aminoacylés. Au laboratoire nous avons découvert que la protéine Arc1 était présente également dans les mitochondries en respiration, et semble donc importante pour la fonction respiratoire. J'ai confirmé cette observation par un test phénotypique en milieu respiratoire (YPGlycérol) qui révèle l'absence de croissance de souches délétées pour le gène *ARC1*. Cependant, après plusieurs jours sur milieu respiratoire, la souche *arc1 Δ* présente des clones capables à nouveau de se diviser sur YPGlycérol, appelés clones suppresseurs. Ces clones ont effectivement retrouvés la capacité de croissance en milieu respiratoire. Des mutants ont été caractérisés et séquencés pour comprendre le rôle de Arc1 au niveau mitochondrial. Un gène responsable de la suppression du phénotype de déficience respiratoire a été identifié et reste à être confirmé.

4. Articles scientifiques (publiés ou en préparation)

- [1] **S. Debard**, G. Bader, J.-O. De Craene, L. Enkler, S. Bär, D. Laporte, P. Hammann, E. Myslinski, B. Senger, S. Friant, H.D. Becker, Nonconventional localizations of cytosolic aminoacyl-tRNA synthetases in yeast and human cells, *Methods*. 113 (2016) 91–104.
- [2] N. Yakobov, **S. Debard**, F. Fischer, B. Senger, H.D. Becker, Cytosolic aminoacyl-tRNA synthetases: Unanticipated relocations for unexpected functions, *Biochim. Biophys. Acta - Gene Regul. Mech.* (2017).
- [3] **S. Debard**, M. Wendenbaum, D. Laporte, H.D. Becker, Identification of a new truncated form of yeasts CMRS essential in response to several stresses, En cours de rédaction.

5. Communications Orales

- [1] **S. Debard**, M. Wendenbaum, H.D. Becker, Oxidative stress response and adaptation by methionine misincorporation during protein synthesis, Journée LabEX MitoCross, 5 octobre 2016, Campus Strasbourg.
- [2] **S. Debard**, D. Laporte, H.D. Becker, Existence of two essential and functionally distinct nuclear methionyl-tRNA synthetases in *S. cerevisiae*, 9 décembre 2016, Journée UMR, Strasbourg.
- [3] **S. Debard**, D. Laporte, M. Wendenbaum, H.D. Becker, Unravelling the role of a newly characterized aminoacyl-tRNA synthetase truncated form in the yeast *S. cerevisiae*, 29 mars 2018, Séminaire de Microbiologie de Strasbourg, Phaculté de Pharmacie, Illkirch.
- [4] [Flash talk] **S. Debard**, M. Wendenbaum, H.D. Becker, Oxidative stress response and adaptation by tRNAs mismethionylation and methionine misincorporation in the yeast *S. cerevisiae*, 25 septembre 2018, 27th tRNA conference, Strasbourg.

6. Présentation de posters

- [1] **S. Debard**, M. Wendenbaum, H.D. Becker, Oxidative stress response and adaptation by tRNAs mismethionylation and methionine misincorporation in the yeast *S. cerevisiae*, 23-27 septembre 2018, 27th tRNA conference, Strasbourg.
- [2] **S. Debard**, M. Wendenbaum, H.D. Becker, Oxidative stress response and adaptation by methionine misincorporation in the yeast *S. cerevisiae*, 29 octobre - 2 novembre 2017, 11th aaRS meeting, Clearwater, Floride, USA.
- [3] **S. Debard**, J. De Craene, G. Bader, M. Geiger, L. Enkler, B. Senger, H.D. Becker, Significant pool of the AME complex bind vacuolar membrane through Arc1 shown by biochemistry and split-GFP, 4-8 septembre 2016, 26th tRNA conference, Jeju, Corée du Sud.

DEBARD Sylvain

Dynamique moléculaire de la méthionyl-ARNt synthetase et ses nouvelles fonctions non-canoniques chez la levure *S. cerevisiae*.

Résumé

Les aminoacyl-ARNt synthétases (aaRSs) sont des enzymes essentielles et ubiquitaires dont la fonction canonique est de catalyser la formation des aminoacyl-ARNt (aa-ARNt) utilisés dans la synthèse protéique. Cependant leur rôle ne se limite pas à cette seule fonction enzymatique : les aaRSs ont acquis la capacité à former des complexes multi-protéiques leur conférant de multiples fonctions additionnelles. La levure *S. cerevisiae* possède le plus petit complexe multisynthétasique eucaryote qui est formé de la méthionyl-ARNt synthétase (MetRS) et la glutamyl-ARNt synthétase (GluRS), toutes deux associées à la protéine d'ancrage cytosolique Arc1. Ce complexe (nommé AME) présente une dynamique importante dépendant des conditions nutritionnelles dans lesquelles se trouve la levure, et les deux aaRSs associées présentent des fonctions additionnelles essentielles à la survie cellulaire. Dans cette thèse, trois caractéristiques de la MetRS ont été étudiées : (i) j'ai élaboré un outil moléculaire bifluorescent permettant de quantifier le taux de misméthionylation endogène médié par la MetRS chez la levure. J'ai également (ii) caractérisé une isoforme tronquée de la MetRS observée *in vivo*, et (iii) analysé l'importance de Arc1 lors du passage de la levure de fermentation en respiration.

Mots clés: méthionyl-ARNt synthétase, *S. cerevisiae*, misméthionylation, protéase, Arc1, respiration

Summary

Aminoacyl-tRNA synthetases (aaRSs) are essential and ubiquitous enzymes catalyzing formation of aminoacyl-tRNAs (aa-tRNAs) during protein synthesis. However, aaRSs are not limited to aa-tRNAs formation. Indeed, they evolved to form multi-protein complexes that acquired additional functions. *S. cerevisiae* contains the simplest eukaryotic multi-synthetase complex which is formed by the association of methionyl-tRNA synthetase (MetRS) and glutamyl-tRNA synthetase (GluRS) to the cytosolic anchoring protein Arc1. This complex (named AME) is highly dynamic depending on the nutritional conditions that the cells are facing, and the two associated aaRSs harbor additional functions that are essential for cell survival. In this PhD thesis, I have studied three different aspect of the yeast MetRS: (i) I created a new bifluorescent reporter to quantify endogenous mismethionylation mediated by the yeast MetRS. I also (ii) characterized a new truncated yeast MetRS isoform produced *in vivo*, and (iii) I analysed the relative importance of Arc1 for cell surviving during the diauxic shift from fermentation to respiration.

Keywords: methionyl-tRNA synthetase, *S. cerevisiae*, mismethionylation, protease, Arc1, respiration